Thèse de Doctorat
de l'Université Pierre et Marie Curie

Spécialité

Physique Théorique

(École Doctorale 107)

Présentée par
Fabien Nugier

Pour obtenir le grade de
Docteur de l'Université Pierre et Marie Curie

Sujet de thèse

Moyennes sur le Cône de Lumière et Cosmologie de Précision

Lightcone Averaging and Precision Cosmology

Soutenue le
4 Septembre 2013

devant le jury composé de :

Pr. Gabriele Veneziano	Directeur de Thèse	Collège de France
Pr. Costas Bachas	Invité	École Normale Supérieure
Pr. Luca Amendola	Rapporteur	Université de Heidelberg
Pr. Dominik Schwarz	Rapporteur	Université de Bielefeld
Pr. Ruth Durrer	Examinatrice	Université de Genève
Pr. David Langlois	Examinateur	Université Paris Diderot
Pr. Jean-Philippe Uzan	Examinateur	Univ. Pierre et Marie Curie

---

Cette thèse a été préparée
au sein du LPT ENS

Laboratoire de Physique Théorique
École Normale Supérieure
24 rue Lhomond
75231 Paris Cedex 05

ainsi qu'au
Collège de France

Collège de France
3 rue d'Ulm
75005 Paris

Pour me contacter :
`fabien.nugier@lpt.ens.fr` ou `fabien.nugier@etu.upmc.fr`
(jusque fin Septembre 2013)
`fabien.nugier@googlemail.com`
(ultérieurement, sinon voir autre adresse professionnelle)

Moyennes sur le Cône de Lumière et Cosmologie de Précision

Lightcone Averaging and Precision Cosmology

Fabien NUGIER

This thesis was written in LaTeX.
A donation for trees plantation was done to compensate for my PhD printings.
May these trees grow tall and old.

Contents

Page

Notations **1**

1 Introduction, motivations and outline of this thesis **3**
1.1 Cosmology today . . . 3
1.2 Homogeneous cosmology . . . 4
1.3 Type Ia supernovae . . . 8
1.4 The large scale structure . . . 15
1.5 Dealing with the inhomogeneous Universe . . . 18
1.6 Introduction & Outline of this thesis . . . 20

2 Gauge-invariant spatial & lightcone averaging **25**
2.1 Covariant spatial averaging . . . 25
2.2 Light-cone averaging . . . 35
2.3 Buchert-Ehlers commutation rules on the light-cone . . . 39
2.4 The FLRW Universe . . . 41

3 The GLC metric and its properties **43**
3.1 Observational coordinates . . . 43
3.2 The geodesic light-cone gauge . . . 44
3.3 Redshift in the GLC metric . . . 47
3.4 Luminosity distance in the GLC gauge . . . 48
3.5 Relations of the GLC gauge with other metrics . . . 50
3.6 Applications to the lightcone average . . . 54

4 The luminosity-redshift relation at second order **59**
4.1 From Poisson to GLC gauge at second order . . . 59
4.2 Detailed expression for $d_L(z, \theta^a)$ . . . 63

5 Combining light-cone and stochastic averaging **71**
5.1 Recalling the first order equations . . . 71
5.2 Combining lightcone and ensemble averages . . . 74
5.3 Averaging the luminosity flux at second order . . . 83

6 Effect of inhomogeneities on cosmological observables **95**
6.1 Induced backreaction in CDM and IR & UV convergence . . . 95
6.2 Full calculation for the CDM model . . . 99
6.3 The ΛCDM model : power spectrum in the linear regime . . . 103
6.4 The ΛCDM model : power spectrum in the non-linear regime . . . 108

7 Summary and conclusions **115**

Appendices

Appendix A Complementary topics **121**
A.1 ADM formalism (Arnowitt-Deser-Misner) 121
A.2 Linear theory of structure formation 126
A.3 Gauge invariance and perturbation theory 132
A.4 The power spectrum in the linear regime 144
A.5 The HaloFit model 146
A.6 Distance modulus for a Milne model 153

Appendix B Résumé (en français) **155**
B.1 Introduction, motivations et plan de la thèse 155
B.2 Moyennes sur le cône de lumière 161
B.3 Jauge géodésique sur le cône de lumière (GLC) 165
B.4 La distance de luminosité au second ordre en perturbations 168
B.5 Moyenne stochastique sur le cône de lumière 170
B.6 Résultats pour le spectre non-linéaire et un Univers ΛCDM 178
B.7 Résumé et Conclusions 188

PhD publications **197**

Bibliography **199**

Glossary **206**

À ma mère, Annick.
À mon père Frédéric
et à ma soeur Anaïs.

Je vous aime.

Ceux qui vivent, ce sont ceux qui luttent.
Victor Hugo

Acknowledgements

The first person I would like to thank here is Gabriele Veneziano. I am very grateful to him for accepting me as his student and for proposing me a very interesting subject of research. I have learned a lot from his incredible knowledge and his great human qualities. Thank you ! I would also like to thank Costas Bachas for accepting the codirection of my thesis, and his kindness, and Costas Kounnas for accepting me in the Laboratoire de Physique Théorique de l'E.N.S.

On the funding side, this thesis work has been financed by a Contrat Doctoral with the Université Pierre et Marie Curie (UPMC). I am very thankful with respect to the Ecole Doctorale 107, the UPMC, the French Ministry of Research for supporting my researches during these three years and I hope they will continue to finance projects in this field. I am also grateful to the Ecole Normale Supérieure (E.N.S.) and the Collège de France (CdF) which offered me a place to work.

There couldn't be this work without special thanks to my collaborators during this thesis, Giovanni Marozzi for his scientific support during the first two years of my PhD, and the moments of great laugh we had at the Collège de France, Maurizio Gasperini for his constant kindness and sense of compromise, Ido Ben-Dayan for our discussions and his constant checks in our considerations. I am also thankful to the other people I have met during these years and with whom I have learned about physics. In particular, I would like to thank the different labs I had the occasion to visit : the ICTP in Trieste, the Univ. of Geneva, the ITP of Zurich, the CCPP in New York, the DAS in Princeton, the CPC at UPenn, the Univ. Joseph Fourier in Les Houches, the APC and IAP in Paris. I also want to thank particularly Ed Copeland, and again Gabriele and Maurizio, for the many letters they sent on my behalf for postdoctoral applications. I'm sorry that I bothered you so much with that.

Having worked as a teaching assistant at the UPMC, I would like to thank all the great people I have met in the teaching teams. I have been impressed by their courage and motivation of every day by associating research with lectures, despite the numerous complications. I am particularly grateful to Bruno Sicardy, Stéphane Boucard, Jean Hare, Benoit Semelin, Nicolas Rambaux, Michel Capderou, Philippe Lopez, and all the other teachers that I have met. I also want to thank the students that came into my classes for they were always nice and often very interesting people.

Evolving during four years in the ENS has been an enriching experience for me. I cannot deny that I would have seek for more interaction with people there but this is not so easy. I have nevertheless to sincerely thank several people. I would like to thank the researchers that I had the most interactions with : C. Bachas, P. Fayet, J. Troost, A. Kashani-Poor, M.-T. Jaekel, G. Policastro. Outside LPT ENS, I particularly want to thank people in the Cosmology group of the LPNHE (UPMC) for our very interesting discussions : J. Guy, P. Astier, C. Balland, D. Hardin and R. Pain. A big thank you also to Béatrice Fixois, Viviane Sebille, Christelle Cagniart (ENS), and Anna Koczorowski (CdF) for their great administrative support, to Nicole Ribet for her moral help, and their perpetual good spirit.

Lots of people have crossed my world line during these three years, sometimes only for few minutes, sometimes during hours, and I would like to forget none of them. I want to thank my colleagues of the ENS for our good moments : Benjamin Assel, Noé Lahaye, Konstantina Kontoudi, Valentina Pozzoli, Alexander Dobrinevski, Swann Piatecki, Sophie Rosay, Bruno Ribstein, Pauline Maury, Evgeni Sobko, Giuseppe Fanizza, Bruno Le Floch, Paweł Laskoś-Grabowski, Marine Remaud...

Outside ENS I have to thank my long-time friends that I have spent my studies with and who gave me a wonderful support when I was sometimes losing my motivation : Rudy Romain, Noé, Panayotis Akridas-Morel, Pierre-Élie Larré, Nicolas Viens, Benoit Fleury. I like you very much guys ! I hope that our future light-cones will continue to intersect each other as often as possible.

Respect is the primary principle in all human activities which seek for a better world. I have probably missed to thank a lot of people who deserve to be thanked. At the end, even a smile or a nice word from a stranger can bring a new hope in a cloudy day and all our lives are linked in a certain way. I want to thank all the people I have met and spent nice time with. I hope that I have been as kind with you as you have been with me, and I apologize for not putting your names.

Determination is maybe my only gift and I own it from the support I always got from the closest human beings of my life. I want to thank my mother Annick Nugier for her support all along my life and during these three years of hard work, deceptions and excitations, confidence and doubts. There wouldn't be this thesis under the whole Heavens without her help of every day. I also want to thank my father, Frédéric, and my sister, Anaïs, for their support during this writing. You are the beings I love the most on Earth !

Notations

For the comfort of the reader, we summarize here the different conventions used in this thesis.

We will adopt the convention of Weinberg [1,2] and Misner, Thorne & Wheeler [3] for the signature of the 4-dimensional metric, namely we will take it to be $(-,+,+,+)$. As a consequence, the line element defined in the 4-dimensional Minkowski spacetime (sometimes denoted by $\mathcal{M}_4$), will be $ds^2 = -(cdt)^2 + \delta_{ij}dx^i dx^j$ and we will take the usual convention $c = 1$. Latin indices will denote the spatial values $1, 2, 3$ and greek indices will correspond to spacetime indices $0, 1, 2, 3$ (where 0 will denote the time component). The flat metric will be written as $\eta_{\mu\nu} = \eta^{\mu\nu} = \mathrm{diag}(-1, 1, 1, 1)$ and we will adopt the usual convention that repeated indices are summed over. For example, $x_\mu x^\mu$ will denote $\eta_{\mu\nu}x^\mu x^\nu = -(x^0)^2 + (x^1)^2 + (x^2)^2 + (x^3)^2$ in $\mathcal{M}_4$ and $g_{\mu\nu}x^\mu x^\nu$ in a more general spacetime. The angles over an homogeneous sphere will be denoted by θ^a (with $a = 1, 2$) or (θ, ϕ).

For 3-dimensional spatial vectors, we will use bold letters instead of putting arrows over them. As an example, we will find $\mathbf{x}$ instead of $\vec{x}$ (except for the null vector that we will denote by $\vec{0}$ and the usual nabla operator $\vec{\nabla} \equiv \partial_i$). The scalar products of two such vectors will be denoted by a dot : $\mathbf{x} \cdot \mathbf{k} = x^1k^1 + x^2k^2 + x^3k^3$. Bold letters will also be used to denote tensorial quantities in their general form. The variable dependence (x) will designate $(t, x^i) \equiv (t, \mathbf{x})$.

The covariant derivative with respect to a coordinate x^μ in a 4-dimensional spacetime will be denoted by ∇_μ and sometimes denoted by a semi-colon, e.g. $\nabla_\mu Q \equiv Q_{;\mu}$. We will denote by $\partial_\mu Q \equiv \partial Q/\partial x^\mu \equiv Q_{,\mu}$ the partial x^μ-derivative of a quantity Q. We will also encounter the covariant derivation of a quantity with respect to the 3-dimensional spatial metric in a 4-dimensional spacetime. We will use a vertical stroke for a simple space-derivative : $\partial_i Q \equiv Q_{|i}$; and a double stroke for the covariant derivative : ${}^{(3)}\nabla_i Q \equiv Q_{||i}$. The simple time derivation with respect to t, the cosmic time or the synchronous gauge time, will often be denoted by a dot : $\partial_t(\dots) \equiv (\dots)^{\bullet}$. The partial derivative with respect to the conformal time η will be denoted sometimes by a prime : $\partial_\eta(\dots) \equiv (\dots)'$.

As it will be defined later, we will use an overline to denote the stochastic average over inhomogeneities : $\overline{(\dots)}$. The spacetime averages, in their different forms, will be denoted by angle brackets : $\langle\dots\rangle$ (where the literature, e.g. [4], usually employs that symbol for the stochastic average).

Let us remark that several quantities are described by the same symbol. This is the case for ϕ which describes the Bardeen potential (Φ, $\phi^{(2)}$), the luminosity flux (Φ and $\Phi^{(0),(1),(2)}$), the second angle on the sphere (ϕ, $\widetilde{\phi}$), the inflaton field (ϕ) and the morphon field ($\Phi_{\mathcal{D}}$). Note also that Θ is used for the expansion scalar and for the Heaviside step function. Symbols (θ,$\widetilde{\theta}$) are the first angle on the sphere. δ is used for the matter density contrast and δ_{D} for the Dirac delta function. No confusion can be made between these different notations and it will be precised only when ambiguous.

Last, we will use sometimes shortcuts of the English language, using "LHS" and "RHS" for *left* and *right hand side* or "w.r.t." for *with respect to*, or from Latin (like i.e., e.g.). Sometimes also acronyms will be used to lighten the discussions, most of them are summarized in the glossary of this thesis.

Chapter 1

Introduction, motivations and outline of this thesis

1.1 Cosmology today

Cosmology is by far one of the oldest fields of research and at the same time, maybe one of the youngest. Indeed, human beings have always observed the sky to measure time and seasons and wondered about its composition. Nevertheless, most of the breakthroughs in the field have been done thanks to new ways to observe the sky, and only recently we have been able to gather enough knowledge to build up what we now call the standard model of cosmology (SMC).

We know from the cosmic microwave background (CMB) that the Universe is almost flat today and that it was created about 13.7 $Gyrs$ ago. The precise mechanism behind its creation is not known, but we do know that its temperature was very high and its size very small at this time. We also know that a process of rapid expansion, the so-called inflation mechanism, must have occured to make our Universe so flat and so close to homogeneity on large angular scales. This period was then followed by a phase where photons were tightly coupled to baryonic matter (the *radiation dominated era*) and no matter structure formed. But after some time, expansion cooling down the Universe, neutrons and protons decoupled from light and started to form atoms, and progressively gave birth to stars, heavier elements, galaxies and guys who live in. This is called the *matter dominated era*. We know indeed that matter is nowadays organized in galaxies, regrouped in clusters and superclusters (which size [1] is $2-10$ Mpc) and these last entities are linked by filaments made of galaxies. All these structures are separated by voids which have a size of about $10-80$ Mpc and we observe a statistical homogeneity above a scale of about $100-150$ Mpc (the value of this scale being still debated). One amazing fact about this structure that we observe around us, the *large scale structure*, is that it has evolved from tiny quantum fluctuations in the early stages of the Universe (when it has a size of the order of the Planck length $\sim 10^{-33}$cm), which have been stretched out by inflation.

Unfortunately, or fortunately for scientists, this standard model of cosmology still has some dark clouds making us unsatisfied. The biggest clouds in this picture are the true nature of dark matter and dark energy. These two parts of the energy content of the Universe are dark as we cannot observe them directly but only through indirect ways. The first one, dark matter (DM), was discovered by measurements of the velocity of stars in rotating galaxies. Scientists discovered indeed that stars had a much higher velocity than they should have from the measurement of the mass of their galaxy by light emission. It was thus necessary to add about five times more matter than we could infer from light observations to explain these profiles. Dark matter was also needed actually to explain the rapid formation of structures in simulations compared to the structures we observed, and lately became also needed in the measurements of dark energy. Though we still do not know the nature of dark matter, a lot of scientists believe that we may soon enough discover one or more particles (the so-called weakly interacting massive particles, or WIMPS) to explain it.

1. We recall that 1pc ~ 3.26 ly (light years) with 1 $ly = 0.9461\ 10^{16}$m.

On the other hand, dark energy (DE) is a complete mistery. It was first discovered experimentaly in 1998 by the observation of Type Ia supernovae (SNe Ia) as the fact that the expansion of the Universe seemed to be accelerating. In its simplest version, this exotic type of energy which has a tendency of repulsion under gravity could be simply a term proportional to the metric authorized by Einstein's equations, but we don't understand why its value is so small and comparable to the energy amount of dark+baryonic matter (this is the so-called coincidence problem). This type of energy could also be a new particle following a certain potential, a bit like the particle believed to create inflation (the *inflaton*). This scalar field is certainly possible and there has been a very great number of such solutions proposed in the literature (see e.g. the review of [5]). We never directly observed a scalar particle yet, but the discovery at the Large Hadron Collider of a good candidate for the Higgs particle is a strong indication that they may indeed be present in nature. The new game to explain dark energy, when we assume the existence of such a particle, is to lead the expansion of our Universe as it is observed today. We can search for a good potential to explain the evolution of the field (such as in quintessence) or try to couple the field with others, such as matter itself (like with the chameleon field). Direct modifications of the theory of general relativity are another alternative which, in some cases, can be related to theses particle models. A lot of involved computations has been done in this direction and especially to learn how we can accommodate these extensions with data.

Theoretical physicists have thus developed a lot of different proposals to explain this wonderful 15-years old discovery of dark energy, but observations have not yet reached enough precision to test these different models and distinguish among them. In science, having a good model to describe a phenomenon is always a good thing. Having two good models is always bad, because it means that we still do not understand something. And when we have tenths of relatively close models to explain this phenomenon, it is natural to start looking for completely new ideas. It is also what happened to dark energy for several reasons. One thing that we should know about dark energy is that it made the expansion of the Universe to accelerate only a few billion years ago ($\sim 5\ Gyrs$), and this is close to the time when the large scale structure has formed. Some researchers thus came to the idea that the formation of structure, in other words the content of the Universe, could be responsible for this late time evolution, that is to say with this particular dynamics. In fact this isn't a stupid guess at all, Einstein himself told us that the geometry was no different from its content, that energy influence spacetime. So why matter could not "mimic" the role of a dark energy ? This idea was even made more exciting from the emphasize by George Ellis, in the 80's, that looking at an inhomogeneous spacetime and its smoothed out equivalent doesn't lead to the same evolution prediction. Another branch of explanations of dark energy has thus been developed, and it has been regrouped in a maybe not so well adapted term of "backreaction", with the idea behind that word being that small inhomogeneities may backreact on spacetime and create a real or an appearant acceleration of the expansion.

1.2 Homogeneous cosmology

1.2.1 Cosmological principles

Cosmology is a particular branch of physics where the experiment – our whole observable Universe itself – is not reproducible. It thus imposes to make reasonable but philosophical assumptions to interpret our observations and get reliable predictions. Let us present some of these assumptions.

The usual assumption made in cosmology, and more generally in physics, is the Copernican principle. This principle states that the place of experiment, e.g. the solar system, is in no privileged position in the Universe. In the elaboration of cosmological models, one can derive another principle from the Copernican one, which is the cosmological principle. In [6], this hypothesis on our position in the Universe, and consequently on the data that we gather, is declined in two versions. The *strong cosmological principle* assumes that the Universe is homogeneous and isotropic at all scales. It is the combination between the Copernican principle and the isotropy assumption which leads to the global homogeneity. This principle is stricto sensu not satisfied in Nature and we have to assume the more realistic version of it, the *weak cosmological principle*, which says that we live in a Universe having an homogeneity scale and which is almost isotropic on distances above that scale. In any case, we

should remark that the cosmological principle is more strict than the Copernican one as it implies also assumptions on the non-observable parts of our Universe.

We should notice that, though the Copernican principle has proved to be very useful for all physics experiments so far, it may not be true on cosmological scales. Indeed, one cannot contradict the fact that we are, up to a certain degree, *privileged observers*. What we mean by this degree is that human beings couldn't have been born outside a galaxy, and so in parts of the Universe where the density constrast cannot be random. Moreover, the observations that we have at our disposal to understand our past are all so far light signals on our past lightcone (a 2+1 spacetime hypersurface) and few geological observations giving information on our past timelike world line. These facts must be kept in mind when building up realistic cosmological models and they are important for the discussions of inhomogeneous cosmologies.

1.2.2 Evolution equations

Let us present the general approach of the standard model of cosmology, based on the cosmological principle. The most general form of the line element of a free falling observer that observes an isotropic and homogeneous universe around him is given by the Friedmann-Lemaître-Robertson-Walker (FLRW) line element, which in cosmic time t and spherical coordinates $(\mathbf{x}) = (\chi, \theta, \phi)$ reads:

$$\begin{aligned} ds^2_{\text{FLRW}} &= -dt^2 + a^2(t)\gamma_{ij}(|\mathbf{x}|)dx^i dx^j \\ &= -dt^2 + a^2(t)\left[d\chi^2 + \left(\frac{1}{\sqrt{K}}\sin\left(\sqrt{K}\chi\right)\right)^2 d\Omega^2\right] \quad , \\ \text{with} \qquad d\Omega^2 &= d\theta^2 + (\sin\theta)^2 d\phi^2 \quad , \end{aligned} \tag{1.1}$$

and where K is a constant setting the geometry of spacelike hypersurfaces: $K \in \{-1, 0, 1\}$ in the cases of a { open, flat, closed } Universe [2]. We call $a(t)$ the scale factor in cosmic time and γ_{ij} is the 3-dimensional metric describing the Universe on a given spatial hypersurface. In this metric, $a(t)$ has the dimension of a distance. We can also use the so-called conformal time η such that $d\eta = dt/a(t)$. Defining now a new radial coordinate r such that

$$r = \sin\left(\sqrt{K}\chi\right)/\sqrt{K} \quad , \tag{1.2}$$

one can show that the FLRW line element is simply written as

$$ds^2_{\text{FLRW}} = -dt^2 + a(t)^2\left(\frac{1}{1-Kr^2}dr^2 + r^2 d\Omega^2\right) \quad , \tag{1.3}$$

where $a(t)$ can be considered as a dimensionless quantity if r is now expressed in units of a distance (in which case K has the dimension of r^{-2}).

Considering the form of the metric presented here, we can compute the Christoffel symbols which are at the basis of the connection in general relativity and that have for general definition:

$$\Gamma_{\sigma\mu\nu} = \frac{1}{2}(\partial_\mu g_{\sigma\nu} + \partial_\nu g_{\sigma\mu} - \partial_\sigma g_{\mu\nu}) \qquad \text{and} \qquad \Gamma^\alpha{}_{\mu\nu} = g^{\alpha\sigma}\Gamma_{\sigma\mu\nu} \quad . \tag{1.4}$$

These symbols are easily computed for this FLRW metric in spherical form and read

$$\Gamma^0{}_{ij} = Ha^2\gamma_{ij} \quad , \quad \Gamma^i{}_{j0} = H\delta^i_j \quad , \quad \Gamma^i{}_{jk} = {}^{(3)}\Gamma^i{}_{jk} \quad , \tag{1.5}$$

2. Indeed, the notation conventionally used in the literature is

$$\gamma_{ij}(|\mathbf{x}|)dx^i dx^j = d\chi^2 + f_K^2(\chi)d\Omega^2 \quad \text{with} \quad f_K(\chi) \equiv \begin{cases} \sin\left(\sqrt{K}\chi\right)/\sqrt{K} & \text{for } K = 1 \\ \chi & \text{for } K = 0 \\ \sinh\left(\sqrt{-K}\chi\right)/\sqrt{-K} & \text{for } K = -1 \end{cases} \quad ,$$

but $f_K(\chi)$ is correctly captured by the unique equality $f_K(\chi) = \sin\left(\sqrt{K}\chi\right)/\sqrt{K}$ if we authorize the square root to receive negative arguments, given that $\sqrt{-K} = i\sqrt{K}$, and by considering the complex expression of the sine function.

where we have defined the Hubble parameter $H \equiv \dot{a}/a$ (with the dot denoting the derivative w.r.t. the cosmic time t). The ${}^{(3)}\Gamma^i{}_{jk}$ are the Christoffel symbols associated to the spatial metric γ_{ij}. They define the connection inside the spatial hypersurfaces parametrized by the spherical coordinates $\{x^i\}$.

The Riemann tensor is generally defined as:

$$R^\delta{}_{\alpha\beta\gamma} = \partial_\alpha \Gamma^\delta_{\beta\gamma} - \partial_\beta \Gamma^\delta_{\alpha\gamma} + \Gamma^\delta_{\alpha\epsilon}\Gamma^\epsilon_{\beta\gamma} - \Gamma^\delta_{\beta\epsilon}\Gamma^\epsilon_{\alpha\gamma} \tag{1.6}$$

and has the following properties [3]:

$$R_{\alpha\beta\gamma\delta} = -R_{\beta\alpha\gamma\delta} = -R_{\alpha\beta\delta\gamma} = R_{\gamma\delta\alpha\beta} \quad . \tag{1.7}$$

We then obtain the Ricci tensor from the contraction of two indices in the Riemann tensor:

$$R_{\mu\nu} \equiv R^\lambda{}_{\mu\lambda\nu} = \partial_\mu \Gamma^\lambda_{\nu\lambda} - \partial_\lambda \Gamma^\lambda_{\mu\nu} + \Gamma^\eta_{\mu\lambda}\Gamma^\lambda_{\nu\eta} - \Gamma^\lambda_{\lambda\eta}\Gamma^\eta_{\mu\nu} \quad . \tag{1.8}$$

In the FLRW metric, this leads to the non-zero components

$$R_{00} = -3\frac{\ddot{a}}{a} \quad , \quad R_{ij} = \left(2H^2 + \frac{\ddot{a}}{a} + 2\frac{K}{a^2}\right) a^2 \gamma_{ij} \quad . \tag{1.9}$$

The final quantity that we can derive is the 4-dimensional scalar curvature, which is

$$R \equiv R^\mu{}_\mu = 6\left(H^2 + \frac{\ddot{a}}{a} + \frac{K}{a^2}\right) \quad . \tag{1.10}$$

In this geometry, we then get the Einstein tensor:

$$G_{\mu\nu} \equiv R_{\mu\nu} - \frac{R}{2} g_{\mu\nu} \quad , \tag{1.11}$$

with the following non-zero components

$$G_{00} = 3\left(H^2 + \frac{K}{a^2}\right) \quad , \quad G_{ij} = -\left(H^2 + 2\frac{\ddot{a}}{a} + \frac{K}{a^2}\right) a^2 \gamma_{ij} \quad . \tag{1.12}$$

The assumption of isotropy and homogeneity of the Universe, as seen from an observer in geodesic motion, imposes the stress energy tensor to have the following components:

$$T^{00} = \rho(t) \quad , \quad T^{0i} = T_{0i} = 0 \quad , \quad T^{ij} = p(t) a^{-2}(t) \delta_{ij} \quad , \tag{1.13}$$

where $\rho(t)$ and $p(t)$ are respectively the energy density and pressure of the background fluid of matter. Expressing this tensor in terms of the velocity of an observer u^μ which can be taken as $u^\mu = (1, \vec{0})$ in a local coming frame, we obtain:

$$T^{\mu\nu} = (\rho + p) u^\mu u^\nu + p\, g^{\mu\nu} \quad , \tag{1.14}$$

and this is the general expression of the stress energy tensor of a perfect fluid. Finally, the Einstein equations in the presence of a cosmological constant (see e.g. [7, 8]), given by:

$$G_{\mu\nu} + \Lambda g_{\mu\nu} \equiv R_{\mu\nu} - \frac{R}{2} g_{\mu\nu} + \Lambda g_{\mu\nu} = 8\pi G\, T_{\mu\nu} \quad , \tag{1.15}$$

3. Other properties of the Riemann tensor are given by the symmetries of its indices and the Bianchi identities:

$$\begin{aligned} R_{\alpha\beta\gamma\delta} &= R_{[\alpha\beta]\gamma\delta} \text{ and } R_{\alpha\beta\gamma\delta} = R_{\alpha\beta[\gamma\delta]} \quad , \\ 3R_{\alpha[\beta\gamma\delta]} &= R_{\alpha\beta\gamma\delta} + R_{\alpha\gamma\delta\beta} + R_{\alpha\delta\beta\gamma} = 0 \quad (1^{st} \text{ Bianchi Id.}) \quad , \\ 3R_{\alpha\beta[\mu\nu;\tau]} &= R_{\alpha\beta\mu\nu;\tau} + R_{\alpha\beta\nu\tau;\mu} + R_{\alpha\beta\tau\mu;\nu} = 0 \quad (2^{nd} \text{ Bianchi Id.}) \quad , \end{aligned}$$

with the definition of symmetrized and anti-symmetrized tensors:

$$T_{[\mu_1\mu_2\ldots\mu_n]} = \frac{1}{n!}\epsilon_{\mu_1\mu_2\ldots\mu_n} \sum_{permutations} T_{\mu_1\mu_2\ldots\mu_n} \quad , \quad T_{(\mu_1\mu_2\ldots\mu_n)} = \frac{1}{n!} \sum_{permutations} T_{\mu_1\mu_2\ldots\mu_n} \quad .$$

and where $\epsilon_{\mu_1\mu_2\ldots\mu_n} = \pm 1$ depending on the parity (non-parity) of permutations from $(1, 2, \ldots, n)$ to $(\mu_1, \mu_2, \ldots, \mu_n)$.

take a very simple form given by the $(0,0)$ and (i,j) components, known as the Friedmann equations :

$$H^2(t) = \frac{8\pi G}{3}\rho - \frac{K}{a^2} + \frac{\Lambda}{3} \quad , \tag{1.16}$$

$$\frac{\ddot{a}}{a}(t) = -\frac{4\pi G}{3}(\rho + 3p) + \frac{\Lambda}{3} \quad . \tag{1.17}$$

We should add, to these two equations above, the equation of conservation of the fluid given by $\nabla_\mu T^{\mu\nu} = 0$, which reads :

$$\dot{\rho} + 3H(\rho + p) = 0 \quad . \tag{1.18}$$

We remark that only two out of these three equations are independent.

We can also define a density for the cosmological constant and a pressure in order to have the same dependence as matter on the RHS of these equations. We have

$$\rho_\Lambda = \frac{\Lambda}{8\pi G} \quad , \quad p_\Lambda = -\frac{\Lambda}{8\pi G} \quad \text{imposing that} \quad w_\Lambda \equiv \frac{p_\Lambda}{\rho_\Lambda} = -1 \quad . \tag{1.19}$$

It is a well-known result that the equation of state w for a cosmological constant is -1 and that makes the cosmological constant the most simple explanation for the acceleration of the Universe expansion. Nevertheless, we don't have an explanation for the smallness of this constant, a problem referred to as the *cosmological constant problem* in cosmology [4]. It could be that the cosmological constant is smaller than expected, or even (almost) exactly zero, and that the true explanation for the acceleration of the Universe comes from a particle (in most of the models a scalar field). In that case the equation of state w_{DE} of dark energy can differ from -1 and even evolve with time.

We can also recast the first Friedmann equation (1.16) by the introduction of the energy density parameters :

$$\Omega_m = \frac{8\pi G\,\rho}{3H^2} \quad , \quad \Omega_\Lambda = \frac{\Lambda}{3H^2} \quad , \quad \Omega_K = -\frac{K}{H^2 a^2} \quad , \tag{1.20}$$

where here ρ accounts for both dark and baryonic matter. In these notations, this equation (1.16) is simply written as :

$$\Omega_m + \Omega_\Lambda + \Omega_K \equiv \Omega_{\text{tot}} + \Omega_K = 1 \quad . \tag{1.21}$$

To this equation we could add a radiation contribution Ω_r which has the same definition as Ω_m (with ρ_r replacing ρ). This contribution is important during the radiation dominated stage of the Universe but is subleading after decoupling. We thus neglect this contribution which is irrelevant for our work. Let us notice also that for a barotropic fluid with a constant equation of state $w = p/\rho$, the Eq. (1.18) is easily solved and gives the following dependence of the density parameters :

$$\Omega_m(z) = \Omega_{m0}\left(\frac{a}{a_0}\right)^{-3(1+w)}\left(\frac{H_0}{H(z)}\right)^2 \quad . \tag{1.22}$$

For a dust (i.e pressureless) fluid for which $w = 0$, one sees that the density decays as $\sim a^{-3}$. For a cosmological constant, one has a similar relation giving $\Omega_\Lambda \sim a^0$.

In conformal time η, one can similarly show that the Friedmann equations are written as :

$$\mathcal{H}^2 = \frac{8\pi G}{3}\rho a^2 - K + \frac{\Lambda}{3}a^2 \quad , \tag{1.23}$$

$$\mathcal{H}' = -\frac{4\pi G}{3}(\rho + 3p)a^2 + \frac{\Lambda}{3}a^2 \quad , \tag{1.24}$$

$$0 = \rho' + 3\mathcal{H}(\rho + p) \quad , \tag{1.25}$$

where we have used the conformal Hubble parameter $\mathcal{H} \equiv a(\eta)'/a(\eta) = aH$. These equations, which we emphasize have only two independent equations, describe the evolution of the density ρ and pressure p of a fluid. In a ΛCDM model, one then has a specific expression for the Hubble parameter H (or $\mathcal{H}$) and an explicit form for ρ and p in terms of the parameters of the model Ω_{m0} and $\Omega_{\Lambda 0}$.

4. Indeed, the consideration of the energy of the vacuum in quantum field theory predicts a density of energy wich is about 120 orders of magnitude greater that the observed density of dark energy (see [5]).

1.3 Type Ia supernovae

The idea of dark energy, in its minimal version of a cosmological constant, had been proposed by Albert Einstein in order to make the Universe static and was forgotten after the discovery of Hubble that the Universe was expanding [9]. The acceleration of the expansion of the Universe, or broadly speaking the existence of dark energy (DE), was not considered until 1998 when two different groups of experimentalists studying supernovae (SNe) arrived to the same conclusion that most of the Universe content was of an exotic nature. These groups were the High-z Supernova Search Team [10] and the Supernova Cosmology Project [11] and they recently received the Nobel Prize in physics (in 2011).

1.3.1 Main features

First of all, one should think about supernovae as really rare events happening only a few times every thousand years per galaxy. They are phenomena emerging after the explosion of a star which is not completely understood. The best explanation we have is that they consist in the result of matter accretion by a white dwarf (a star made of a plasma of unbound nuclei and electrons) in a binary system (i.e. where a star is feeding up the white dwarf) and up to the point where it reaches a mass of $1.4 - 1.5$ $M_\odot$, the Chandrasekhar mass [5]. This second star can also be a white dwarf. A consequence of this nature of supernovae is seen in their chemical composition, as we will see in Fig. 1.2. What is important in this process is that supernovae are believed to have all roughly the same mass, and that makes them be *standard candels*. Indeed, above the Chandrasekhar mass, the pressure from gravitation is stronger than the electron degeneracy pressure inside the star and that leads to a collapse up to a certain radius fixed by the nuclear degeneracy pressure of the star. We then assist to a violent increase in temperature and the conversion of ^{12}C and ^{16}O into ^{56}Ni, starting a thermonuclear explosion and the ejection of external cores of the star. The amount of energy emitted by this explosion (and though 99% of it is formed of neutrinos and 1% only by light) is so large that a supernova can be more brilliant than its host galaxy, reaching $\sim 10^{10} L_\odot$. As a consequence, supernovea can be seen from really far distances, making them useful for cosmology.

Another important point is that SNe must be observed at their peak in luminosity to be standardized and thus to be used. We hence need to detect them at an early stage of their explosive life. Indeed, we observe supernovae in different wavelength bands called U, V, B, R and I (other photometric systems can be used) and we follow their intensity, or their magnitude m_B, in the B-band as they are brighter in this band. We see that their intensity follows a growing time period during 15-20 days and is followed by a more or less slow decrease of ~ 2 months (corresponding to the radioactive decay of ^{56}Ni into ^{56}Co, decaying itself into ^{56}Fe). This is what we call the *light curve* of a supernova and it has been noticed that the brighter the supernova, the longer the decreasing time. As a consequence, we have classified SNe in different types from their light curves, as can be seen in Fig. 1.1. The main two types are I and II, and we split them in subtypes. These different types are actually confirmed by spectroscopy, showing that supernovae also differ significantly in their composition and that is originating from the variety of physical phenomena giving rise to the explosion. The main feature of SNe Ia is that, like white dwarfs, they do not present any trace of hydrogen in their composition. Their second important feature is that they contain silicon (see Fig. 1.2).

1.3.2 Observations and standardization

Supernovae have been studied during many years now and their frequency of detection has significantly grown during the last decade with the advance of fast computing and automatic detection surveys (cf. the *rolling search* method of SNLS [13]). The automatic coverage of the sky (or part of it) has greatly enhanced the number of detected SNe. Spectra are also fundamental in the current use of SNe Ia and the reason for that is because they furnish the composition of the star, necessary to confirm its type. They also determine the redshift of the star (by a direct measurement of the

5. We define the solar mass $M_\odot$ by $1\ M_\odot \equiv \frac{4\pi^2 \times (1\ a.u.)^3}{G \times (1\ \text{year})^2} \simeq 1.98\ 10^{30}\ kg$ where $a.u.$ denotes the astronomical unit (equal to the Sun-Earth distance). The solar luminosity is about $L_\odot \simeq 3.84\ 10^{26}\ W = 3.84\ 10^{33}\ erg\ s^{-1}$.

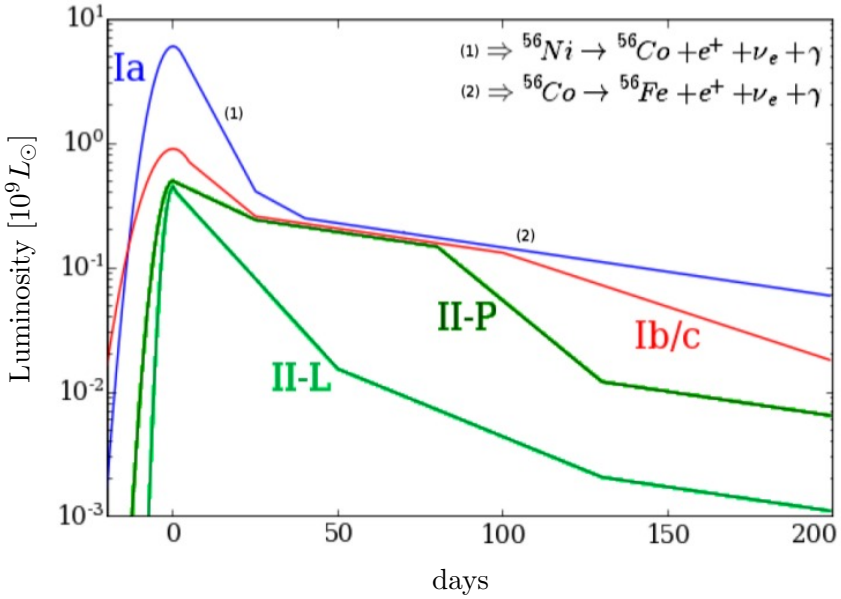

Figure 1.1: Idealized light curves for different types of supernovæ. We notice that SNe Ia are the brightest and the longest lasting case. Time is given in the rest frame of the supernovae (which for a redshift $z \sim 1$ corresponds to the one half of the observed time on Earth). Figure taken from [12].

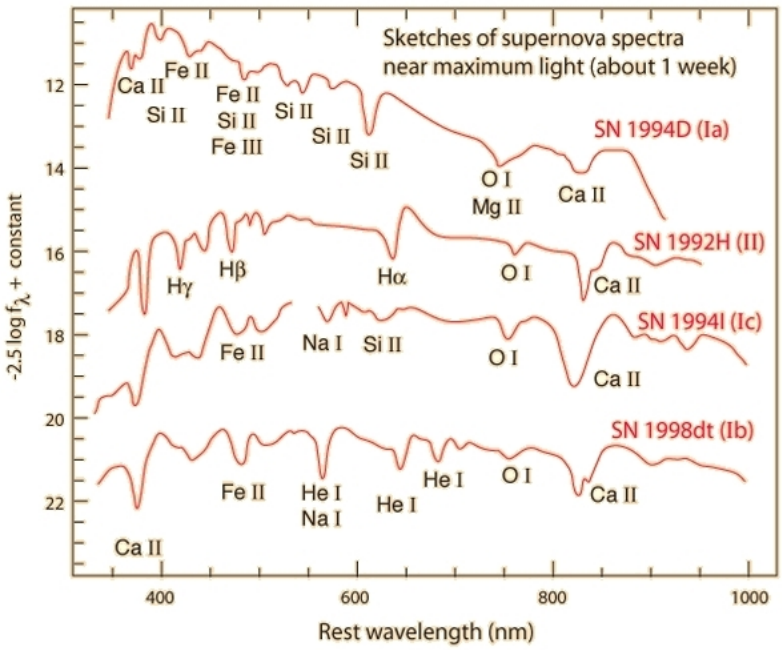

Figure 1.2: Spectra of different types of supernovæ. We can remark the absence of hydrogen and the presence of Si-II for the type Ia. Spectra are shown in the rest frame of the supernovae, i.e. corrected from redshift. It is actually such kind of Si-II absorption bands which are used [13] to estimate the redshift of the star. Spectra are usually taken near the light curve maximum for a better accuracy. This figure is taken from [14].

wavelengths of absorption bands). Note however that spectroscopy measurements are very costly in terms of observational time, limiting seriously the number of SNe Ia detections. To cure this problem and prepare the next generation of surveys (such as the Large Synoptic Survey, the Dark Energy Survey, or Pan-STAARS), the SNLS and SDSS experiments have tried to include the estimation of the redshift in the fitting process from photometry only [15]. Indeed, a supernova which is highly

redshifted is more luminous in low frenquency spectral bands. We can thus estimate – though less accurately but very fast – their redshift by the comparison of their magnitude in these different bands, i.e. from the color itself instead of spectroscopy.

The light curve of a SN is a very important source of information and it is used to calibrate the SNe and standardize them. Several methods have been used for their standardization, one can cite particularly the *Multicolor Light Curve Shape* (MLCS) and *Spectral Adaptative Lightcurve Template* (SALT, see e.g. [12, 16]). From these analyses of the light curves, we can extract two parameters of major importance : the stretch factor s and the color parameter c. The first one is linked to the lapse in time of the SNe light curve and the second one is a parameter in the SALT fit of the light curves. We can see in Fig. 1.3 that the different light curves of SNe Ia can be reshaped by applying to them the simple stretch factor to significantly reduce their dispersion. The color parameter is more precisely the excess of color between the averaged color of the supernova and its maximal color :

$$c \equiv (B-V)_{\rm max} - {\rm Moy}[B-V] \quad . \tag{1.26}$$

We also observe the magnitude of the supernova in different frequency bands and the total luminosity is thus obtained by reconstruction. For this, the magnitude in the B band is used to correct the measurements from the stretch and color parameters. A relation of the following type is used :

$$m_B^{\rm corr} = m_B - \alpha\,(s-1) + \beta\, c \quad , \tag{1.27}$$

where α and β are two parameters evaluated to reduce the dispersion between the light curves of different SNe Ia. When one considers these corrections, we get a reduction from $\sim 40\%$ to $\sim 15\%$ on the dispersion of the distance modulus, i.e. directly on the Hubble diagram.

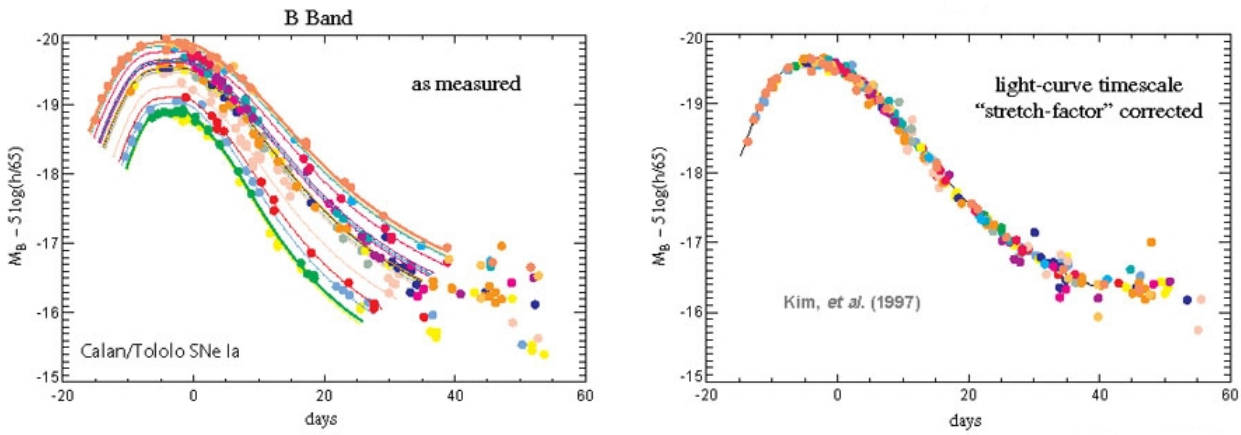

Figure 1.3: SNe Ia light curves of the Calán-Tololo survey. Left : as directly measured in the B-band, replacing them in their supernova rest-frame. Right : same light curves after applying the stretch correction. We note the significant reduction in dispersion induced by this correction. Figures borrowed from [17].

1.3.3 Magnitudes

Magnitudes are widely used in astronomy. Let us first consider a non-expanding Universe to explain this notion. One defines the *apparent magnitude* m of a star at the actual distance d_L(a.u.) (expressed in arbitrary units a.u.) in terms of its *luminosity flux* Φ (using the same distance units) by

$$m = -2.5\log_{10}(\Phi) + {\rm cst} \equiv -2.5\log_{10}\left(\frac{\Phi({\rm a.u.})}{\Phi_{\rm ref}({\rm a.u.})}\right) \quad . \tag{1.28}$$

The constant cst $\equiv 2.5\log_{10}\left(\Phi_{\rm ref}({\rm a.u.})\right)$ appearing in this expression makes dimensionless the apparent magnitude. That also means that measuring a luminosity flux is useless if one cannot compare it to a

reference source (being another star or a calibration of the apparatus used for the measurement). We also define the *absolute magnitude* which is the apparent magnitude for the observed star if we were at a distance of 10 pc, in that case we denote it by M, and we have

$$M = -2.5 \log_{10} \left(\frac{\Phi(10\,\mathrm{pc})}{\Phi_{\mathrm{ref}}(\mathrm{pc})} \right) \quad . \tag{1.29}$$

Using now the relationship between flux and distance, at a distance expressed in a.u., in a homogeneous Universe :

$$\Phi(\mathrm{a.u.}) = \frac{L}{4\pi d_L(\mathrm{a.u.})^2} \quad , \tag{1.30}$$

where L is the intrinsic luminosity of the source (assumed to be constant), we obtain that

$$m - M = 5 \log_{10} \left(\frac{d_L(\mathrm{a.u.})}{10\,\mathrm{pc}} \right) \quad . \tag{1.31}$$

This combination that we call the *distance modulus* $\mu \equiv m - M$, is thus explicitly dependent on the unit used for the distance d_L. It can be written as :

$$\mu(\mathrm{pc}) = -5 + 5 \log_{10}(d_L(\mathrm{pc})) \qquad \text{or} \qquad \mu(\mathrm{Mpc}) = 25 + 5 \log_{10}(d_L(\mathrm{Mpc})) \quad . \tag{1.32}$$

Let us now see how this relation is changed in an expanding Universe. In the case of an expanding homogeneous and flat Universe, the luminosity distance can be written in terms of the redshift $z = a(t_0)/a(t) - 1$ and it can be written as

$$d_L(z) = (1+z) a(t_0) r(z) \quad , \tag{1.33}$$

where $r(z)$ is the conformal distance from the source to the observer. Chosing a radial lightcone geodesic reaching the observer, the trajectory of light is given by $ds^2 = -dt^2 + a(t)^2 dr^2 = 0$ and we simply have the naïve relation[6] $dr = -a(t)^{-1} dt$ that describes the propagation of the photon. This gives

$$r = -\int_{t_0}^{t} \frac{dt}{a(t)} = \int_{a(t)}^{a(t_0)} \frac{da}{a^2 H(a)} = a_0^{-1} \int_0^z \frac{dz'}{H(z')} \quad , \tag{1.34}$$

where t_0 is "today" (and $a_0 \equiv a(t_0)$) and we used $dt/a = da/(a^2 H(a))$ and $dz = -a_0\, da/a^2 = -(a_0 H/a)\, dt$. In a general Universe which contains different fluids, all in a pure homogenous state, the function $H(z)$ is not simple (see e.g. Eq. (1.47)).

Staying at relatively short observable distances, more precisely in a regime where $z \ll 1$, we can expand $H(z)$ in perturbations of z. The Taylor expansion gives

$$H(z) = H_0 + \left(\frac{dH}{dz} \right)_{t=t_0} z + \mathcal{O}(z^2) \quad , \tag{1.35}$$

where we can use

$$\frac{dH}{dz} = -\frac{1}{(1+z)H(z)} \frac{dH(t)}{dt} = -\frac{1}{(1+z)H(z)} \left(\frac{\ddot{a}}{a} - H^2 \right) \quad , \tag{1.36}$$

which at the observer position (today) is

$$\left(\frac{dH}{dz} \right)_{t=t_0} = -H_0 \left(\frac{a\ddot{a}}{\dot{a}^2} - 1 \right)_{t=t_0} \equiv H_0(1+q_0) \quad , \tag{1.37}$$

and where we have introduced the so-called *deceleration parameter* q_0 :

$$q_0 \equiv -\left(\frac{a\ddot{a}}{\dot{a}^2} \right)_{t=t_0} = \left(1 + \frac{\dot{H}}{H^2} \right)_{t=t_0} \quad . \tag{1.38}$$

6. t being future directed and the system of coordinates centered on the observer, that explains the minus sign here.

We thus obtain that

$$H(z) = H_0\big[1 + (1+q_0)z + \mathcal{O}(z^2)\big] \tag{1.39}$$

which, after being introduced into Eq. (1.34), implies the following perturbative expression for the conformal distance r

$$r(z) = (a_0 H_0)^{-1}\left(z - (1+q_0)\frac{z^2}{2} + \mathcal{O}(z^3)\right) \quad . \tag{1.40}$$

This gives at the end, from Eq. (1.33), the perturbative expression of the luminosity distance

$$d_L(z) = H_0^{-1}\left[z + (1-q_0)\frac{z^2}{2} + \mathcal{O}(z^3)\right] \quad . \tag{1.41}$$

We notice in passing that a stationary (i.e. constantly evolving) Milne Universe implies $r(z) = (a_0 H_0)^{-1} z$ and thus $d_L^{\rm Milne}(z) = z(1+z/2)H_0^{-1}$ (see Sec. A.6). We then have $d_L > d_L^{\rm Milne}$ if $q_0 > -1$.

We can now come back on the definition of the distance modulus and write a definition which involves the product $H_0 d_L$ in order to have a function of redshift only. This is done by writing:

$$\mu(z) = \mathcal{M} + 5\log_{10}(H_0 d_L(z)) \quad \text{with} \quad \mathcal{M}(\text{Mpc}) \equiv 25 - 5\log_{10}(H_0) \quad , \tag{1.42}$$

and where $d_L(z)$ is still in Mpc and H_0 is expressed in Mpc^{-1}. More correctly:

$$H_0 \equiv h\ 100\ km\ s^{-1}\ \text{Mpc}^{-1} = 3.33\ 10^{-4}\ h\ c\,\text{Mpc}^{-1} \quad , \tag{1.43}$$

where we have used the speed of light $c = 299792,458\ km\ s^{-1}$ which is taken to be $c = 1$ when everything is expressed in Mpc (like here). For $h = 0.7$, we get $-5\log_{10}(H_0) \simeq 18.16$, leading to

$$\mu(\text{Mpc}) = 43.16 + 5\log_{10}\big(H_0(\text{Mpc}^{-1})d_L(\text{Mpc})\big) \quad . \tag{1.44}$$

We remark that this expression is very well adapted to SNe observations which are sensitive to the product $H_0 d_L$ rather that d_L itself.

1.3.4 The Hubble diagram

Let us first recall that the luminosity distance d_L of a source at redshift z is related to the angular distance d_A of this source (as seen from the observer) by the Etherington law (or reciprocity law) [18]:

$$d_L = (1+z)^2 d_A \quad . \tag{1.45}$$

This relation is valid in any geometry as it relies on the reversibility of light trajectories. In the particular case of an unperturbed, spatially flat FLRW background, and for a source with redshift z_s, the angular distance d_A is simply given by

$$d_A^{\rm FLRW}(z_s) = a_s\, r_s = a_s(\eta_o - \eta_s) \quad , \tag{1.46}$$

where $a_s \equiv a(\eta_s)$, while $\eta_o - \eta_s \equiv \Delta\eta$ denotes the conformal time interval between the emission and observation of the light signal.

For an unperturbed metric also we have $1 + z = a_0/a(t)$, and $d\eta = dt/a = -a_0^{-1}dz/H$, where $H = d(\ln a)/dt$. Hence, using the standard (spatially flat) Friedmann equation for H from Eq. (1.16), assuming that the homogeneous model has perfect fluid sources with present fractions of the critical density Ω_{n0} and barotropic parameters $w_n = p_n/\rho_n = \text{cst}$ as given by Eq. (1.22), i.e. using:

$$H^2(z) = H_0^2\left[\sum_n \Omega_{n0}(1+z)^{3(1+w_n)}\right] \quad , \tag{1.47}$$

we get the general expression [7] in terms of the redshift of a source z_s :

$$\begin{aligned} d_L^{\rm FLRW}(z_s) &= (1+z_s)a_0 \int_{\eta_s}^{\eta_o} d\eta = (1+z_s)\int_0^{z_s} \frac{dz}{H(z)} \\ &= \frac{1+z_s}{H_0}\int_0^{z_s} dz \left[\sum_n \Omega_{n0}(1+z)^{3(1+w_n)}\right]^{-1/2} \quad . \end{aligned} \tag{1.48}$$

Expanding in the limit $z_s \to 0$ we also obtain the expression

$$\begin{aligned} d_L^{\rm FLRW}(z_s) &\simeq \frac{1}{H_0}\left[z_s + \frac{1}{4}\left(1 - 3\sum_n w_n\,\Omega_{n0}\right) z_s^2 + O(z_s^3)\right] \\ &\equiv \frac{1}{H_0}\left[z_s + \frac{1}{2}(1-q_0)z_s^2 + O(z_s^3)\right] \quad , \end{aligned} \tag{1.49}$$

which shows the well-known sensitivity of the term quadratic in z_s to the composition of the cosmic fluid through the deceleration parameter q_0 (see Eq. (1.38)).

If we assume a flat (i.e. $K = 0$) FLRW model with only matter and a cosmological constant, we get the theoretical luminosity distance :

$$d_L^{\Lambda\rm CDM}(z_s) = \frac{1+z_s}{H_0}\int_0^{z_s} \frac{dz'}{[\Omega_{\Lambda 0} + \Omega_{m0}(1+z')^3]^{1/2}} \quad . \tag{1.50}$$

This relation is not trivially integrable when its two parameters $\Omega_{\Lambda 0}$ and Ω_{m0} are non-zero. One thus has to integrate it numerically until we find its best fit with the data. Measuring magnitudes of SNe Ia with their corresponding redshifts, one can plug the result of Eq. (1.50) into Eq. (1.31) and plot the so-called *Hubble diagram*, as shown in Fig. 1.4 (see [19] for a short history). From the binned data points, we get that $\Omega_{\Lambda 0}$ is about 73% of the total energy content in the Universe and that Ω_{m0} is about 27% (including baryons) [8]. The densities of radiation and curvature are negligible today. This is such a fit which led to the discovery of dark energy. We can see in Fig. 1.4 that the data dispersion is very important. That shows that SNe are very complex objects which are difficult to interpret even after being standardized by a long procedure.

To improve the estimation of cosmological parameters, we usually use the combination of SNe Ia observations with two other probes which give a precise estimation of the parameters in this homogeneous context. These two other probes are the cosmic microwave background (Cosmic Microwave Background (CMB)) and the baryonic acoustic oscillations (Baryonic Acoustic Oscillations (BAO)). One can indeed see in Fig. 1.5 the crossing of their different predictions and its great increase in the precision of the estimation of $\Omega_{\Lambda 0}$ and Ω_{m0}. We also remark that these data support a Universe very close to be spatially flat.

7. Actually, the most general expression that we can obtain when we consider a non-flat FLRW model with dark matter and a general form of dark energy, i.e. non-necessarily a cosmological constant, is :

$$d_L(z_s) = \frac{c\,(1+z_s)}{H_0\sqrt{|\Omega_{K0}|}} S_K\left(\sqrt{|\Omega_{K0}|}\int_0^{z_s} \frac{dz}{\left[\Omega_{m0}(1+z)^3 + \Omega_{K0}(1+z)^2 + \Omega_{DE,0}\exp\left(3\int_0^z \frac{1+w_{DE}(z')}{1+z'}dz'\right)\right]^{1/2}}\right) \quad ,$$

with the possible addition in the RHS of $\Omega_r \equiv 8\pi G\,\rho_r/3H^2$ the density parameter of radiation (for which $w_r = 1/3$), and where we used $\Omega_{DE} \equiv 8\pi G\,\rho_{DE}/3H^2$. The exponential contribution is obtained by considering the conservation of the dark matter fluid : $\rho_{DE} + 3H(\rho_{DE} + p_{DE}) = 0$ with a general (time dependent) equation of state such that $p_{DE} = w_{DE}(\rho_{DE})\,\rho_{DE}$. We used $S_K(x) = \sin(x), x, \sinh(x)$ depending on the sign of the curvature $K > 0$, $= 0$, < 0 .

8. See however the new reevaluation of these parameters by the Planck satellite first release [20].

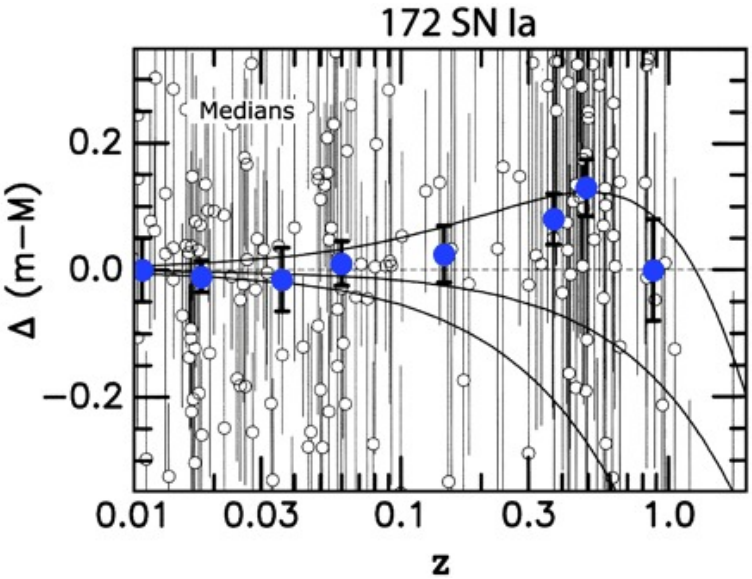

Figure 1.4: Hubble diagram with 172 SNe Ia with median values in 8 redshift bins. Solid lines (from bottom to top) correspond to the evaluation from Eq. (1.50) with $(\Omega_{m0}, \Omega_{\Lambda 0}) \simeq (1, 0)$, $(\Omega_{m0}, \Omega_{\Lambda 0}) \simeq (0.3, 0)$ and $(\Omega_{m0}, \Omega_{\Lambda 0}) \simeq (0.3, 0.7)$. The increase at large redshift in the binned data points shows the existence of a dark energy component. Figure taken from [19].

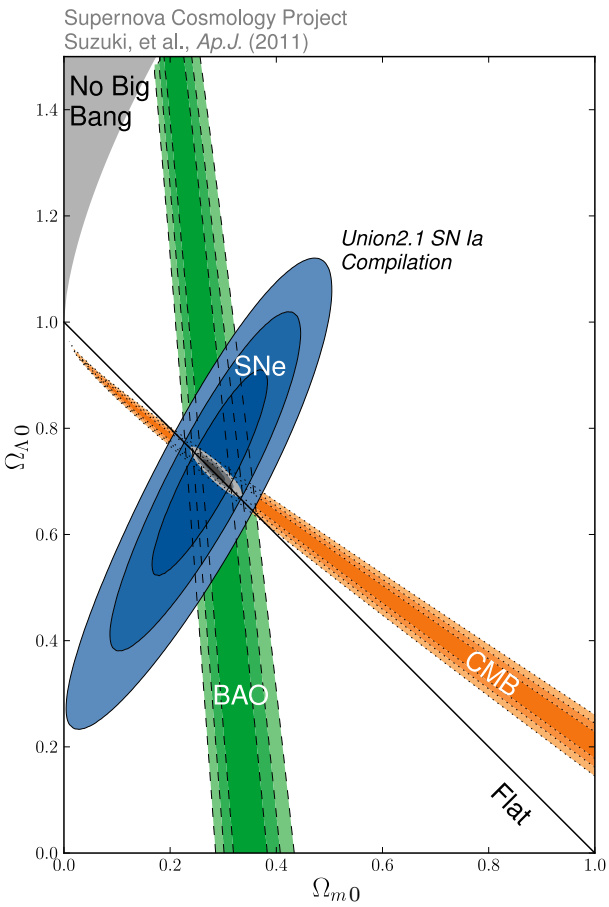

Figure 1.5: Cross plot from the Union2 data set and other probes. One can notice (within the 68%, 95%, and 99.7% confidence regions) the nice combination of the different observables which are SNe Ia, the CMB and BAOs. The predicted values, with the highest confidence, are $(\Omega_{m0}, \Omega_{\Lambda 0}) \simeq (0.27, 0.73)$. Credit : Supernova Cosmology Project (adapted from `supernova.lbl.gov/Union/`), see also [21].

1.4 The large scale structure

1.4.1 Observations

The SDSS (Sloan Digital Sky Survey) and 2dFGRS (Two degree field galaxy redshift survey) are major surveys. SDSS covered about one quarter of the sky and observed millions of objects, with more that a million of galaxies and their distances. On the other hand the 2dFGRS observed a very narrow part of the sky with 250 000 galaxies and their redshift up to ~ 0.3. As one can see on Fig. 1.6, matter is organized in a filamentous structure which looks relatively homogeneous at large scales.

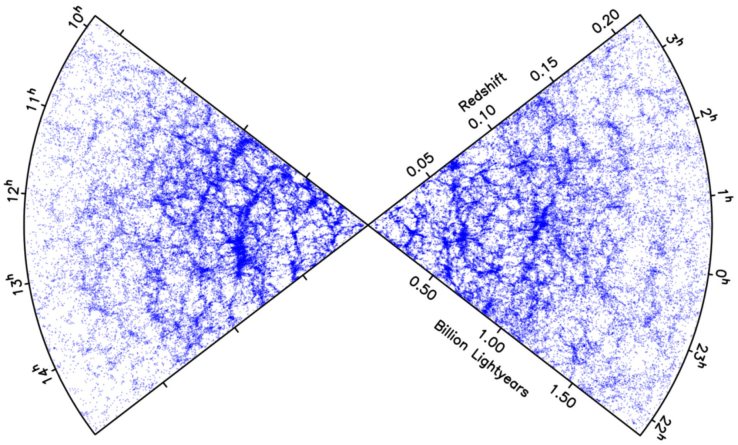

Figure 1.6: The 2dF Galaxy Redshift Survey (2dFGRS). Two narrow bands on the sky are represented. Data has been stacked in the thin ($\sim 4°$) angular direction of the survey to get a two dimensional picture. One can see the homogeneity of structures at large scales. Credit : 2dFGRS (adapted from www2.aao.gov.au/∼TDFgg/).

Nevertheless, several complications must be addressed to obtain a real picture of the matter distribution in the Universe. First, what we observe is light coming from our past lightcone, so we can only probe the galaxy distribution, not the true matter distribution containing dark baryonic objects as well as cold dark matter itself. The link between the galaxy distribution and the true matter distribution is not trivial and struggles with our lack of understanding of the galaxies formation. The density contrast of galaxies $\delta_{\rm gal}$ is related to the density contrast of matter by

$$\delta_{\rm gal}(t,\mathbf{x}) = b\,\delta(t,\mathbf{x}) \qquad \text{with} \qquad \delta(t,\mathbf{x}) = \frac{\rho(t,\mathbf{x})-\rho(t)}{\rho(t)} \equiv \frac{\delta\rho(t,\mathbf{x})}{\rho(t)} \quad , \tag{1.51}$$

where $\rho(t)$ is the background homogeneous density field and $\rho(t,\mathbf{x})$ the true matter field. The "parameter" $b(t,\mathbf{x})$ is called the bias and has been extensively studied in the literature, including its possible spacetime dependence and the complications involved in the non-linear regime.

One other complication is that galaxies are not observed in the real spacetime, namely by two angles on the sky and a spacetime combination as $\eta - r$ on the past lightcone, but are observed in the redshift space, i.e. that radial distances are measured thought the change in light frenquency. As a consequence, velocity and position are entangled in the measurements (like in the so-called *fingers of God* effect). Nevertheless, several methods have been confronted to describe matter and evaluate its power spectrum. For example, measurements from weak lensing are free from bias effects as they measure the real distribution of matter.

Considering these effects, one can measure the matter density spectrum $\delta(t,\mathbf{x})$ and go in Fourier space. By assuming an ergodic principle, one can take the volume average of the 2-point correlation functions and consider that this measurement is equal to the stochastic average $\overline{\delta_{\mathbf{k}}\delta^*_{\mathbf{k}}}$. One then obtains the definition of the dimensionless matter power spectrum by the definition :

$$\Delta^2(t,\mathbf{k}) = \frac{k^3}{2\pi^2}|\delta_{\mathbf{k}}(t)|^2 \quad . \tag{1.52}$$

From this expression it is possible to plot the experimental power spectrum of Fig. 1.7. We notice the variety of probes composing this incredible measurement over five orders of magnitude in scales.

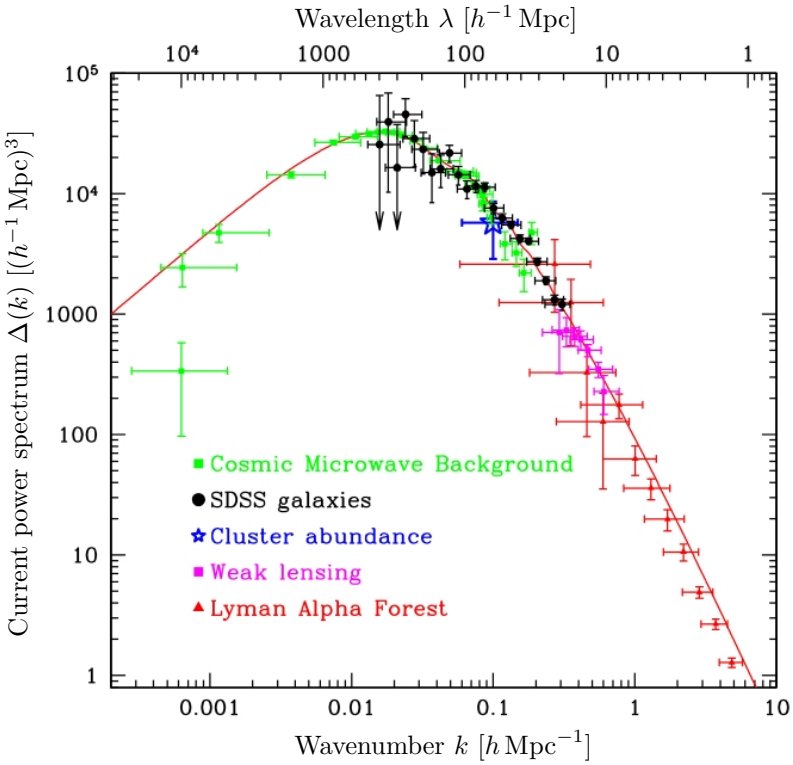

Figure 1.7: The matter power spectrum as measured from different sources. We notice that the linear part of the spectrum at large scales (small k) is reconstructed from CMB. Similarly, the linear spectrum shown at small scales (large k) is a reconstruction from the non-linear spectrum (as one observes the total, non-linear, spectrum) and is thus model dependent (see Sec. 1.4.3). Figure adapted from [22].

1.4.2 The linear power spectrum

What we will be interested by is the computation of the power spectrum for the gravitational potential in its linear and non-linear regimes. The reason for this is that metric perturbations, that we will study later, are expressed in terms of the gravitational potential and not the matter density. As a consequence, one of the most important equation for us will be the Poisson equation which links the two quantities. In synchronous gauge (see Sec. A.3.3), this equation is written as :

$$\nabla^2\psi(x) = 4\pi G\rho(t)\ \delta(x) \quad , \tag{1.53}$$

where $x = (t, \mathbf{x})$, and $\rho(t)$ is the background matter density. Taking the Fourier transform of this expression brings $k^2\psi_k \sim H_0^2\Omega_{m0}\,\delta_k$, where δ_k is the spectral function associated to the matter density contrast $\delta(x)$ and ψ_k the spectral function associated to the gravitational (Bardeen) potential $\psi(x)$ (at first order in perturbations) that we will define in Chapter 4.

The 2-point correlation function of the gravitational (Bardeen) potential, written as $\overline{\psi(x)\psi(x)}$ with the overbar denoting a statistical (or stochastic) average [9], is a dimensionless quantity. Taking its Fourier transform teaches us that $[|\psi_k|^2] = [k^{-3}]$ (where square brackets denote the dimension of the quantity). Thus, $|\delta_k|^2$ has the same dimension as $|\psi_k|^2$ when we set $c = 1$ (in that case $[k] = [H_0]$). More precisely, the relation between $|\delta_k|^2$ and $|\psi_k|^2$ is :

$$|\psi_k|^2 = \left(\frac{3}{2}\right)^2 \frac{\Omega_m^2(z)\mathcal{H}^4}{k^4}|\delta_k|^2 \quad , \tag{1.54}$$

9. In textbooks, the stochastic average is usually denoted by $\langle\ldots\rangle$. In our work this notation denotes sky-average and for that reason we prefer the notation $\overline{(\ldots)}$ to denote stochastic averaging.

where for a CDM flat FLRW Universe we have $\mathcal{H} = aH = 2/\eta$ (with η the conformal time, $a(\eta) = C\eta^2$) and hence $\mathcal{H}^4 = \left(\frac{a_0}{a(\eta)}\right)^2 \mathcal{H}_0^4$.

In a more general context (independent from the Universe model), we have seen in Sec. 1.2.2 that the equation of conservation for a perfect fluid of matter, satisfying $p = w\ \rho$ with $w = \text{cst}$, gives rise to the solution of Eq. (1.22). Using that $\mathcal{H} = Ha$, this relation becomes:

$$\Omega_m(z) = \Omega_{m0}(1+z)\left(\frac{\mathcal{H}_0}{\mathcal{H}}\right)^2 \quad , \tag{1.55}$$

and we get, in Fourier space, the Poisson equation at an arbitrary redshift:

$$|\psi_k(z)|^2 = \left(\frac{3}{2}\right)^2 \frac{\Omega_{m0}^2 \mathcal{H}_0^4}{k^4}(1+z)^2 |\delta_k(z)|^2 \quad . \tag{1.56}$$

We notice that there is an easy one-to-one relation between η and z in the case of a CDM flat FLRW Universe (where $\Omega_{m0} = 1$). In the case of a ΛCDM model, the relation $\eta(z)$ is in some way degenerated as it depends on the values of $(\Omega_{m0}, \Omega_{\Lambda 0})$ (see Sec. 1.3.4).

Moreover, the dimensionless power spectrum $\mathcal{P}_\psi(k)$ is related to $|\psi_k|^2$ by its definition:

$$\mathcal{P}_\psi(k,\eta) \equiv \frac{k^3}{2\pi^2}|\psi_k(\eta)|^2 \quad , \tag{1.57}$$

where the time dependence has been written explicitly (but can be expressed in terms of z).

The (linear) power spectrum $\mathcal{P}_\psi(k,z)$ is first obtained from the inflationary spectrum (i.e. sourced by perturbations at the end of the inflationary era) where its expression is $\left(\frac{3}{5}\right)^2 \Delta_{\mathcal{R}}^2$, with:

$$\Delta_{\mathcal{R}}^2 = A\left(\frac{k}{k_0}\right)^{n_s - 1} \quad \text{and} \quad A = 2.45\ 10^{-9} \quad , \quad n_s = 0.96 \quad , \quad k_0/a_0 = 0.002\ \text{Mpc}^{-1} \quad . \tag{1.58}$$

We remark that the value of the spectral index n_s can be related to the slow-roll parameters ϵ and η of the single field inflation model (see Sec. A.2.1, Eq. (A.55)) by

$$n_s - 1 = -6\epsilon + 2\eta \quad . \tag{1.59}$$

We have to add a transfer function $T(k)$ to describe the sub-horizon evolution of the different modes re-entering during the radiation-dominated era (see Sec. A.2.4 and A.4.2 for explicit forms). We also add a growth factor $g(z)$ which takes into account the evolution of ψ_k during the dark energy era (assuming here a ΛCDM Universe). Finally, the expression of the linear power spectrum is:

$$\mathcal{P}_\psi(k) = \left(\frac{3}{5}\right)^2 \Delta_{\mathcal{R}}^2 T^2(k)\left(\frac{g(z)}{g_\infty}\right)^2 \quad . \tag{1.60}$$

1.4.3 Short insight in the non-linear regime

At small scales, matter is organized in structures and the density contrast can take values which are more important than on cosmological scales. As opposed to the last section, we cannot work here solely in terms of the gravitational potential and we need to go through the matter density spectrum to estimate the non-linear regime. The justification for this change is that the non-linear regime has been studied by N-body simulations in which the density is the direct measurable quantity.

So we define what is called the fractional density variance per unit $\ln k$, namely $\Delta^2(k)$, by:

$$\Delta^2(k) = \frac{d\sigma^2}{d\ln k} \qquad \text{or equivalently:} \qquad \sigma^2 = \int \Delta^2(k)\ d\ln k \tag{1.61}$$

with the definition of the density variance:

$$\sigma^2 \equiv \overline{\delta(x)\delta(x)} = \int \frac{d^3k}{(2\pi)^3}|\delta_{\mathbf{k}}|^2 = \int \frac{k^2 dk}{2\pi^2}|\delta_k|^2 \quad . \tag{1.62}$$

Here the quantities depend on time (or redshift) and the overbar denotes again the usual stochastic averaging. These two expressions bring the simple relation between their integrands :

$$\Delta^2(k,z) = \frac{k^3}{2\pi^2}|\delta_k(z)|^2 \quad , \tag{1.63}$$

and confirms that $\Delta^2(k,z)$ is a dimensionless quantity. Besides this, [23] defines another dimensionless power spectrum, $P(k)$, which is called the "initial power spectrum" (in the sense of structure formation simulations) and is taken to be a simple power law :

$$P(k) = \mathcal{A}\ k^n \ . \tag{1.64}$$

This spectrum is linked to $\Delta^2(k)$ through the expression (see Eq. (5) in [23]) :

$$\Delta^2_{\rm L}(k) = \frac{V}{(2\pi)^3}4\pi k^3 P(k) \qquad , \qquad \text{i.e.} \qquad \Delta^2_{\rm L}(k) \sim k^{n+3} \qquad , \tag{1.65}$$

now taken at the linear level and where the so-called V factor is a normalization volume.

Nevertheless, this is not the approach that we will take here. A very first reason for this is that these quantities are only adapted to simulations (e.g. we have no a priori criterion to choose V). Furthermore, what we are interested in, here, is the non-linear power spectrum obtained from the linear power spectrum. Both should hence match at large scales. For this reason, the linear power spectrum that we will use is the one from Eq. (1.60), and we will now call it $\mathcal{P}^{\rm L}_\psi(k)$. We should also recall that the Poisson equation is valid both in the linear and non-linear regimes, so that we have :

$$\mathcal{P}^{\rm L,NL}_\psi(k) = \frac{9}{4}\frac{\Omega^2_{m0}\mathcal{H}^4_0}{k^4}(1+z)^2\Delta^2_{\rm L,NL}(k) \ . \tag{1.66}$$

We will thus obtain the linear density spectrum using the Poisson equation at the linear level :

$$\Delta^2_{\rm L}(k) = \frac{4}{9}\frac{k^4}{\Omega^2_{m0}\mathcal{H}^4_0(1+z)^2}\mathcal{P}^{\rm L}_\psi(k) = \frac{4}{25}\frac{A\Omega^{-2}_{m0}\mathcal{H}^{-4}_0}{(1+z)^2}\frac{k^{n_s+3}}{k_0^{n_s-1}}\left(\frac{g(z)}{g_0}\right)^2 T^2(k) \ . \tag{1.67}$$

We will then use the HaloFit model, as presented in Sec. A.4 and A.5, to generate from $\Delta^2_{\rm L}(k)$ the density power spectrum in the non-linear regime, i.e. $\Delta^2_{\rm NL}(k)$. And as a last step, we will use the Eq. (1.66) again, in the non-linear regime, to obtain the desired quantity $\mathcal{P}^{\rm NL}_\psi(k)$.

1.5 Dealing with the inhomogeneous Universe

1.5.1 Real nature of the Universe

As we have seen, the analysis of the standard model of cosmology takes place within a homogeneous context. The low precision of observations not so far in the past has justified this approach and yet brought amazingly consistent results. This is mainly due to the relative smallness of inhomogeneities as supported by the CMB. Nevertheless, we can notice that SNe Ia observations suffer from a very large dispersion which make their discovery of dark energy not straightforward. On the other hand the true nature of the Universe is inhomogeneous as revealed by the large scale structure below a certain scale. It is thus natural to ask to which extent observations, and in particular SNe Ia, are free from a contamination by the presence of matter (and thus gravitational) inhomogeneities. At the end, these probes are local astrophysical objects in virialized domains of our Universe and light signals that we receive from them propagate over very large distances, encountering possibly a large number of sources of dispersion [10]. We also know that SNe Ia measurements can be equally well fitted by a LTB model (see e.g. [25]) in which we are close to the center of a less dense region of matter.

10. Another problem is the one of curvature as the Universe is mostly filled by voids and thus photons prapagating in it are sensitive to the Weyl curvature instead of the Riemann curvature (see [24]). We will not address this here.

However, experimental constraints on our position inside this underdensity make us unreasonnably close to the center, disproving this possibility. Nevertheless, the question is still there and one can wonder how big is the effect of inhomogeneities and whether or not they could explain (partially maybe) the observation of the acceleration in the expansion. The possibility to explain dark energy with the inhomogeneous Universe is very tempting as it is the most concervative explanation at our disposal, assuming no extra physics, and only reconsidering our interpretation of general relativity. It has also the advantage to solve the coincidence problem, by linking the formation of structures with the appearance of dark energy, and the smallness of the dark energy density.

1.5.2 The backreaction problem

In relation to the problem of inhomogeneity of our Universe, different questions related to the non-linear nature of general relativity are still unsolved [26]. The question of how to average small-scales, or coarse-graine structures, to describe their large-scale geometry and dynamics, is called the *averaging problem* of cosmology. The effect of inhomogeneities on the large-scale dynamics of the Universe is difficult to evaluate. Solving this problem is also solving the *backreaction problem* which can be illustrated by the following reasoning. Imagine that we know exactly the metric $g_{\mu\nu}^{(loc)}$ at a (local) subgalactic scale. By the knowledge of a correct smoothing procedure, we could average this metric to get the metric at a larger scale, like the galactic scale : $g_{\mu\nu}^{(\mathrm{loc})} \to g_{\mu\nu}^{(\mathrm{gal})}$. Let us imagine also that this smoothing procedure is applicable to the stress energy tensor so that we have : $T_{\mu\nu}^{(\mathrm{loc})} \to T_{\mu\nu}^{(\mathrm{gal})}$. Assuming that the Einstein equations at the local scale were :

$$G_{\mu\nu}^{(\mathrm{loc})} = 8\pi G \; T_{\mu\nu}^{(\mathrm{loc})} \quad , \tag{1.68}$$

the non-linear nature of the Einstein equations, i.e. the fact that $G \sim \Gamma^2$, $\partial\Gamma \sim (g\partial g)^2$, $\partial(g\partial g)$ (in crude notations), makes that these previous equations will become at galactic scales :

$$G_{\mu\nu}^{(\mathrm{gal})} = 8\pi G \; T_{\mu\nu}^{(\mathrm{gal})} + E_{\mu\nu}^{(\mathrm{gal})} \quad . \tag{1.69}$$

In this expression, the extra contribution $E_{\mu\nu}^{(\mathrm{gal})} \neq 0$ will emerge from the non-commutation between the averaging procedure of $g_{\mu\nu}^{(\mathrm{loc})}$ and the non-linear aspect of Einstein's equations. By repeating this procedure up to the large scale structure and cosmic scales, we will ideally reach an homogeneous description where the effect of inhomogeneities have been properly taken into account.

These two problems are also related to the *fitting problem*, i.e. the question of how to relate observations made from a lumpy environment to an idealized model with a (not really existing) "backgound" geometry. We still do not know, nowadays, how to match an inhomogeneous Universe (what we really observe) with an homogeneous FLRW model (used to interpret the data), as illustrated in Fig. 1.8.

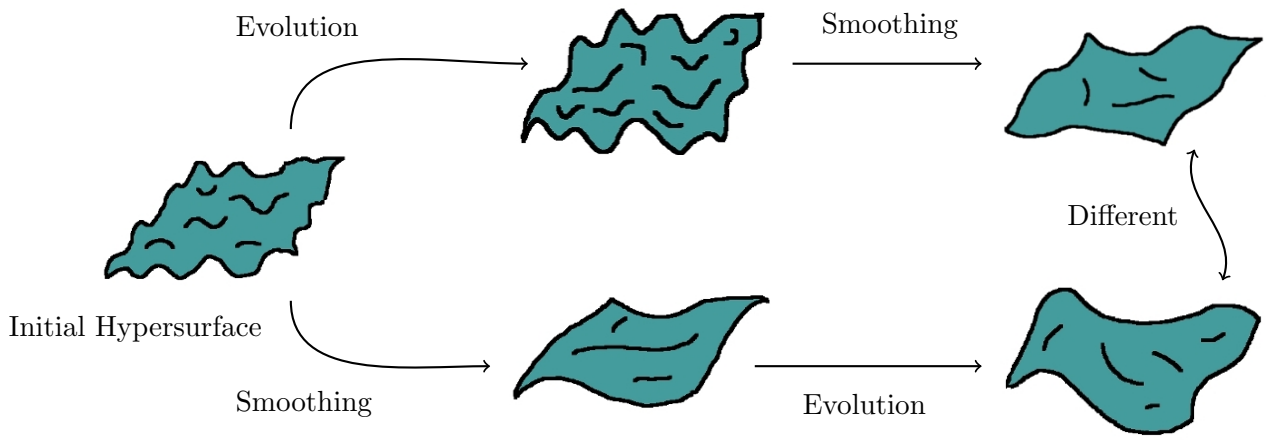

Figure 1.8: Illustration of the backreaction problem : we see the non-commutation between the smoothing, or averaging, and time evolution. This is related to the non-linearity of Einstein's equations.

1.6 Introduction & Outline of this thesis

The so-called concordance (or ΛCDM) model is based on a suitable combination of dark matter, dark energy and baryons for an overall critical density and has become the reference paradigm for the late, i.e. post-equality epoch, evolution of our Universe (see e.g. [27]). It accounts equally well for the CMB data, the Large Scale Structure and, even more significantly, for the supernovae data in terms of a cosmic acceleration [10, 11]. However, these three tests of the concordance model are not strictly speaking at the same level of theoretical rigor. While the first two have to do, by definition, with the inhomogeneities present in our Universe, the third is based on an ideal homogeneous and isotropic Friedmann-Lemaître-Robertson-Walker (FLRW) geometry. It is thus a very amazing fact that these three probes finally give a very consistent picture and this especially as we still lack of a satisfying theoretical explanation for the real nature of dark energy. Establishing the existence of this unknown component and determining its parameters is thus one of the central issues in modern cosmology.

As we said, the analysis of SNe Ia (taken as standard candels) is usually made in the simplified context of a homogeneous and isotropic (FLRW) cosmology. The issue has then been raised about whether inhomogeneities may affect the conclusion of such a theoretically naive assumption. Inhomogeneous models in which we occupy a privileged position in the Universe, for instance, can mimic dark energy (as first pointed out in [25]), but look both unrealistic and highly fine-tuned. Nevertheless, we cannot deny that the Hubble diagram is affected by a large dispersion on the data, some SNe Ia being so faint that they look to contradict the reasonable condition $\Omega_{\Lambda 0} \leq 1$. This kind of effect is certainly related to the non-standard nature of some supernovae, but we can still wonder how much is the contamination coming from the inhomogeneous aspect of our Universe. At the end, cosmology can be summarized as the study of two things : the content of the Universe and the dynamics of this content. It is thus a very important question to ask how much structures affect the measurement of distances. It is also clear that, at least for the sake of precision, a better treatment of cosmic acceleration should take inhomogeneities into account, and this at least in the presence of stochastically isotropic and homogeneous perturbations of the kind predicted by inflation. Only when this is done we can establish in a convincing way whether ΛCDM gives a simultaneous consistent description of the above-mentioned body of cosmological data.

In additions, it is by now well-known (see e.g. [28]) that averaging solutions of the full inhomogeneous Einstein equations leads, in general, to different results from those obtained by solving the averaged (i.e. homogeneous) Einstein equations. In particular, the averaging procedure does not commute with the non-linear differential operators appearing in the Einstein equations. As a result, the dynamics of the averaged geometry is affected by so-called "backreaction" terms, originating from the inhomogeneities present in the geometry and in the various components of the cosmic fluid. Following the discovery of cosmic acceleration on large scales, interest in the possible effects of inhomogeneities for interpreting the data themselves has considerably risen (see [6,26,29,30] for recent reviews). Indeed, though there is by now general agreement that super-horizon perturbations cannot mimic dark-energy effects [31–33], the impact of sub-horizon perturbations is by contrast still unsettled [34–37], owing to the appearance of ultraviolet divergences while computing their "backreaction" on certain classes of large-scale averages [36, 37]. The possibility that these effects may simulate a substantial fraction of dark energy, or that they may at least play some role in the context of near-future precision cosmology, has to be seriously considered. According to some authors [38–44] present inhomogeneities might explain, by themselves, cosmic acceleration without any need for dark-energy contributions, thereby providing an elegant solution to the well-known "coincidence problem". According to others [31, 33–35, 45, 46] the effect of inhomogeneities is, instead, completely negligible. The truth may lie somewhere in between, in the sense that a quantitative understanding of inhomogeneities effects could be important in order to put precise constraints on dark-energy parameters, such as the critical fraction of dark-energy density, Ω_Λ, and the evolution of its effective equation of state, $w_\Lambda(z)$.

If inhomogeneities do have an important impact, the actual observations must also correspond in some way to the measurement of averaged quantities. As a consequence of this, and because of the backreaction issue, much work has been done in these last few years on trying to formulate a suitable "averaged" description of inhomogeneous cosmologies. In most of these works, following

Buchert's seminal papers [47–50], the effective geometry emerging after the smoothing-out of local inhomogeneities has been determined by integrating over three-dimensional spacelike hypersurfaces and computing the ensuing "backreaction" on the averaged geometry. However, as pointed out long ago [51,52], a phenomenological reconstruction of the spacetime metric and of its dynamic evolution on a cosmological scale – revealed through the experimental study of the luminosity-distance to redshift relation [10,11] – is necessarily based on past light-cone observations (since most of the relevant signals travel with the speed of light). Hence, the averaging procedure should be possibly referred to a null hypersurface coinciding with a past light-cone rather than to some fixed-time spacelike hypersurface. Nonetheless, such a light-cone averaging procedure, whose importance has been repeatedly stressed in the specialized literature (see e.g. [6, 51–57]), has never been implemented in practice.

In this thesis we introduce a general gauge invariant prescription for averaging scalar quantities on null hypersurfaces, solving thus the long-standing problem of lightcone averaging. We apply it to the past light-cone of a generic observer in the context of an inhomogeneous cosmological metric, and provide the analog of the Buchert-Ehlers commutation rule [58] for the derivatives of light-cone averaged quantities. We also take advantage of the gauge invariance of our formalism by introducing an adapted system of coordinates (defining what we call a "geodesic light-cone (GLC) frame", which can be seen as a particular specification of the "observational coordinates" introduced in [51, 59]). In these coordinates our averaging prescription greatly simplifies while keeping all the required degrees of freedom for applications to general inhomogeneous metric backgrounds. These GLC coordinates turn out to have other interesting properties for calculations on the past light-cone. In particular, the expression of the redshift z and the luminosity distance d_L are very simple and easy to interpret in this system of coordinates.

We then turn our attention to the case of a flat FLRW model filled by scalar perturbations of primordial (inflationary) origin. It is both a realistic model for observations and a simple enough case to authorize an analytical approach. Such perturbations are often conveniently parametrized in the longitudinal (or Newtonian) gauge [60], we thus derive the transformation of coordinates between the GLC gauge and the Newtonian gauge. As a stochastic average is necessary to obtain a prediction which is independent from a given realization of inhomogeneities and because these latter give an effect from the second order in perturbations, we compute the luminosity distance up to that order. The tranformation of coordinates must then be pushed to second order. This transformation authorizes us then to compute the expression of the distance-redshift relation at second order in scalar perturbations. This very general result [11] has an interest on its own (i.e. irrespectively of its subsequent application to light-cone/ensemble averaging) and can possibly find many other applications in precision cosmology. Furthermore, the result presented here for d_L is valid in general, i.e. for any given background model (except if caustics form [66], in which case the area distance is modified).

Applying these two notions that we developed, we study the average of scalar observables around the flat FLRW background and at second order in perturbations. For this we make use of an ensemble average over the inhomogeneities, inserting a realistic power spectrum of stochastic perturbations. The combination of the angular lightcone average and this stochastic average leads to characteristic contributions designated as "induced backreaction" terms, arising from a generic correlation between the inhomogeneities present in the variable we want to average (e.g. the luminosity distance) and those appearing in the covariant integration measure [12]. Applying this developments to scalar quantites such as the luminosity flux or distance of a light source lying on our past light-cone, we compute the effects of a stochastic background of inhomogeneities on the determination of dark-energy parameters in precision cosmology. Unlike the analyses in [36, 37], made on spatial hypersurfaces, we find a result always free from ultraviolet divergences and with no significant infrared contributions either. Nevertheless, the induced backreaction terms are not accounting for all the effets engendered by

11. Following the pioneering work of [61,62], d_L has been already computed to first order in the longitudinal gauge (for a CDM model in [63], CDM and ΛCDM in [64]), and to second order in synchronous gauge, but only for a dust-dominated Universe, in [42]. See also [65].

12. This integration measure will also induce "backreaction" terms of the type usually discussed in the literature [47,48], namely terms that arise from (generalized) commutation rules between differential operators and averaging integrals.

inhomogeneities and a full calculation, including all the second order terms, is made.

Proceeding with the simple model of CDM, we find in particular that the energy flux $\Phi \sim d_L^{-2}$ is practically unaffected by inhomogeneities, while the most commonly used variables (like d_L or the distance modulus $\mu \sim 5 \log_{10} d_L$) receive much larger corrections (much bigger than we could have naïvely expected). This shows that there are (at least in principle) intrinsic ambiguities in the measurement of the dark-energy parameters, unless the backreaction of stochastic inhomogeneities is properly taken into account. Actually, the advantages of flux averaging for minimizing biases on dark-energy parameters was first pointed out in [67], where it was shown how the binning of data in appropriate redshift intervals can reduce the bias due to systematic effects such as weak lensing. It is intriguing that the preferred role played by the flux variable also comes out in this work where we perform a completely different averaging procedure, *at fixed redshift*. Our conclusions are not due to a binning of data, but to an application of our covariant spacetime average to different functions of the luminosity distance. It is thus safe to believe that this interesting property of the flux is to be related to the conservation of light along the past lightcone.

Our first conclusions of that analysis, based on the use of a perturbation spectrum valid in the linear regime in a CDM model [68], are as follows. On the one hand, such kind of perturbations cannot simulate a substantial fraction of dark energy : their contribution to the averaged flux-redshift relation is both too small (at large values of the redshift z) and has the wrong z-dependence. On the other hand, stochastic fluctuations add a new and relatively important dispersion with respect to the prediction of the homogeneous and isotropic FLRW cosmology. This dispersion is independent of the experimental apparatus, of the observational procedure, of the intrinsic fluctuations in absolute luminosity, and may prevent a determination of the dark-energy parameter $\Omega_\Lambda(z)$ down to the percent level – at least if we are using the luminosity-redshift relation alone. Another important conclusion is that (light-cone averages of) different functions of the same observable get biased in different ways, with the energy flux sticking out as the observable which gets minimally affected by inhomogeneities, irrespectively of the redshift binning utilized. We should recall here that other possible sources of uncertainty, bias and scatter in the Hubble diagram have been studied in many previous papers (see e.g. [69–73]).

The power spectrum used in this first study is valid in the linear perturbative regime. We also extend our treatment by considering a ΛCDM model, by adding the effect of baryons, and by considering two parametrizations of the HaloFit model [23,74], describing the density power spectrum in the non-linear regime. It is thus possible, by this choice, to attain a higher level of accuracy by considering the effect from small scale inhomogeneities. We hence use the power spectrum in ΛCDM to compute the effect of inhomogeneities as in the previous study and restricting ourself to the so-called "enhanced terms" (i.e the dominant ones in the relevant range of z), already identified in the CDM case. We find that the effect of inhomogeneities is enhanced at large redshifts because of the dominant (lensing) term involved. Despite this increase in the size of the effect, inhomogeneities are not strong enough to mimic a dark energy effect. The dispersion, however, is significantly increased and corresponds to a possible statistical deviation of $\sim 10\%$ on $\Omega_{\Lambda 0}$. This result underlines the importance of considering properly the effect of inhomogeneities on the dispersion of SNe Ia data. We find, furthermore, that this dispersion is in very good agreement with the Union2 data at small redshifts (where peculiar velocity effects are involved) but too small at large redshifts (where lensing is leading their effect). This constitutes a rigorous proof of the robustness of the standard model of cosmology, but still emphasize the non-negligible aspect of inhomogeneities. Finally, our calculations lead to a precise prediction for the size of the lensing dispersion within the Hubble diagram, a prediction which is in accordance with the recent attempts to detect this signal [75,76] and that should be confirmed in the next few years.

In this **Chapter** 1 we have presented the basic facts about homogeneous cosmology, stressing the link between the astrophysical object that the SNe Ia are and the inhomogeneous nature of the Universe they live in. We have also presented the equations of evolution of the Universe in the homogeneous case with some of their assumptions. We shall now give the outline of this thesis.

In **Chapter** 2 we treat the aspects relative to the averaging of scalars. We first recall the historical approach, à la Buchert, and present the interesting properties that emerge from this effective formalism. We then recall the notion of gauge invariance in averaging and give a more general definition of the average on spatial hypersurfaces. We then present the definition of a gauge invariant light-cone average prescription which has all the required properties to average scalars on null hypersurfaces. This allows us to derive relations analogous to the Buchert-Ehlers commutation rule. We also rigorously show that the average has, as expected, no effect on an homogeneous FLRW model. In **Chapter** 3 we introduce a system of coordinates, the "Geodesic Light-Cone" (GLC) coordinates, which is very well adapted to calculations on the past light-cone. This system corresponds to a complete gauge fixing of the (recalled) observational coordinates, but it also has characteristic differences with it. In these GLC coordinates, the redshift and the luminosity distance take a very simple form and the null geodesics that photons travel on are parametrized by only one coordinate. We also discuss the link between this system and the synchronous gauge and other of its properties. We finally make use of this GLC coordinates to express our averaging prescriptions in a simple way and consider the example of the redshift drift. The absence of averaging effets in the homogeneous case leads us to compute, in **Chapter** 4, the expression of the luminosity-redshift relation at second order in perturbations around a flat FLRW model. For this, we compute the full second order transformation between the Poisson gauge and the GLC gauge and then make use of the simple expression taken by the distance in this last coordinates. Vector and tensor perturbations are taken into account at second order (as imposed by inflation). The final result, though very involved, encloses terms with a clearly defined physical meaning. The role of **Chapter** 5 is to present the combination of the lightcone angular average with a stochastic average over inhomogeneities. We first recall the computation of the luminosity-redshift relation by staying at the first order for a better understanding of the physical terms involved. We then present the stochastic average and the power spectrum describing matter inhomogeneities. The formal combination of this average with the lightcone one gives rise to terms created by the mixing of the averaged scalar S and the measure of integration. These terms are interesting as they autorize an effect of inhomogeneities from the first order of S and they are called induced backreaction (IBR) terms. Using this recall at first order, we are able to compute the effect of inhomogeneities on the variance of d_L, an incomplete result, and rigorously derive its dispersion (depending only from first order). We then extend our analysis to the full second order calculation, reorganizing the numerous contributions, and present the calculation of the luminosity flux which turns out to be the quantity which is the least affected by inhomogenenities. We also show that vector and tensor perturbations exactly cancel within our average. We then link the averages of the flux and the distance and address the averaging of the distance modulus. We also present the computation of their respective dispersions and explain how genuine second order contributions are dealt with. The **Chapter** 6 presents the numerical computation of the terms previously derived. To that purpose we introduce an explicit form for the transfer function in the power spectrum. This simple expression allows to compute the IBR terms and gives a first estimate of the dispersion on d_L in a CDM model. It also gives an understanding of the dominant effects coming from inhomogeneities in our calculation, turning out to be the peculiar velocities at small redshift and the lensing at large ones. We also explain why our integrals over the wavenumber k of perturbations is finite both in the infrared and ultraviolet regimes. We then proceed to the calculation, still in CDM, of the contributions of the luminosity flux. This derivation gives us an insight on the dominant terms at the quadratic and genuine second orders. It also shows that this latter is always smaller for the redshifts we are interested by. We then move to the study of the realistic ΛCDM model by the introduction of a growth factor and the use of a more complete transfer function. Using the relations presented in the previous chapter, we compute also the impact of inhomogeneities on the luminosity distance and the distance modulus. Introducing an extra description of the power spectrum in its non-linear regime, through the so-called HaloFit model, we are able to study the enhanced effects from very small scales. Comments are given on the relative size of the effets and are compared with observations of the dispersion of SNe Ia. We then recall the main results and achievements of this thesis in **Chapter** 7. Further details on the ADM formalism, structure formation, gauge invariance and the HaloFit model are given in **Appendix** A.
A French Résumé of this thesis is given in **Appendix** B.

Chapter 2

Gauge-invariant spatial & lightcone averaging

This chapter is devoted to the mathematical framework of averaging scalar quantities as part of the averaging problem. We remark that no easy procedure exists at the moment to average vector and tensor quantities in general relativity. Nevertheless, it is important to stress the existence of a very general formalism, historically developed by R. Zalaletdinov and known as *Macroscopic Gravity*, which addresses the question of averaging and evolving general manifolds [77–80]. This work is intimately related to the backreaction issue and deserves a very high consideration. Nevertheless, because of its highly technical aspect and its relative distance with our approach of averaging, it will not be described in this thesis. In a first section, we recall the historical approach of volume averaging over inhomogeneous spacetimes, as mainly developed by T. Buchert [6,30,47,81] and written in synchronous gauge. We also present the notion of gauge invariant averaging and generalize the volume average to a coordinate-independent formulation. Both sections rely mainly on [82, 83]. We then present the formalism of light-cone averaging developed in this thesis and show some of its general properties. We derive in particular the generalized Buchert-Ehlers commutation rules on the light cone. As a final check, and to justify the perturbative calculation of Chapter 4, we show that the average effects disappear in the FLRW homogeneous case.

2.1 Covariant spatial averaging

2.1.1 Buchert formalism

In this formalism, we assume the weak cosmological principle in order to build up effective Friedmann equations inside a simply-connected compact domain $\mathcal{D}(t)$, in a foliated spacetime given by constant-t hypersurfaces. We also assume that the matter content of the Universe is made of a pressureless fluid (dust) and a possible cosmological constant, and we work in synchronous gauge :

$$ds^2_{\rm SG} = -dt^2 + g_{ij}dx^i dx^j \quad . \tag{2.1}$$

The volume $\mathcal{D}$, fixed in these coordinates, conserve the mass $M_{\mathcal{D}}$ inside it at all times and the average of a scalar quantity S is defined through a Riemannian (i.e. weighted by the metric) volume average :

$$\langle S(t,\mathbf{x})\rangle_{\mathcal{D}}(t) = \frac{1}{V_{\mathcal{D}}}\int_{\mathcal{D}} S(t,\mathbf{x})\, d\mu_g \quad \text{with} \quad V_{\mathcal{D}} = \int_{\mathcal{D}} d\mu_g \quad \text{and} \quad d\mu_g \equiv J\, d^3\mathbf{x} \equiv \sqrt{\det g_{ij}}\, d^3\mathbf{x} \ . \tag{2.2}$$

As g_{ij}, the measure of integration J is a function of (t, x^i). On the other hand, the volume $\mathcal{D}$ is assumed to keep the same x^i coordinates along its way. In synchronous gauge, the matter geodesics are given by $x^i = \text{cst}$ and the volume is thus comoving with the matter fluid. In that case, assumed in this section, the domain of integration is independent of time (although the measure J is not).

Within synchronous gauge and the assumptions employed here, the Einstein equations can be recast in terms of geometrical quantities such as the expansion scalar, the shear tensor and the vorticity tensor, defined as follows :

$$\Theta \equiv \nabla_\mu n^\mu \quad , \quad \sigma_{\mu\nu} \equiv h^\alpha{}_\mu h^\beta{}_\nu \left(\nabla_{(\alpha} n_{\beta)} - \frac{1}{3} h_{\alpha\beta}\Theta \right) \quad , \quad \omega_{\mu\nu} \equiv h^\alpha{}_\mu h^\beta{}_\nu \nabla_{[\alpha} n_{\beta]} \quad , \tag{2.3}$$

and where n^μ is the normal vector to these spatial hypersurfaces given by $n_\mu = (-1, \vec{0})$ and $n^\mu = (1, \vec{0})$. As we consider a fluid which is at rest in these coordinates, we can also consider n^μ to be its velocity. The tensor $h_{\mu\nu}$ presented here is the projection tensor on spatial hypersurfaces :

$$h_{\mu\nu} = g_{\mu\nu} + n_\mu n_\nu \quad , \quad h_{\mu\nu} n^\nu = 0 \quad . \tag{2.4}$$

The Einstein equations then turn into a system of two constraint and three dynamical equations given by (see Appendix A.1.3) :

$$\frac{1}{2}\mathcal{R} + \frac{1}{3}\Theta^2 - \sigma^2 - \omega^2 = 8\pi G\rho + \Lambda \quad , \tag{2.5}$$

$$\sigma^i{}_{j\,||\,i} + \omega^i{}_{j\,||\,i} = \frac{2}{3}\Theta_{|\,j} \quad , \tag{2.6}$$

$$\dot{\rho} = -\Theta\rho \quad , \tag{2.7}$$

$$(g_{ij})^\bullet = 2g_{ik}\sigma^k{}_j + 2g_{ik}\omega^k{}_j + \frac{2}{3}\Theta g_{ij} \quad , \tag{2.8}$$

$$(\sigma^i{}_j + \omega^i{}_j)^\bullet = -\Theta(\sigma^i{}_j + \omega^i{}_j) - \mathcal{R}^i{}_j + \frac{2}{3}\delta^i{}_j \left[\sigma^2 + \omega^2 - \frac{\Theta^2}{3} + 8\pi G\rho + \Lambda \right] \quad . \tag{2.9}$$

The rates of shear and vorticity appearing in these equations are defined as follows [1] :

$$\sigma^2 \equiv \frac{1}{2}\sigma^i{}_j\sigma^j{}_i \quad \text{and} \quad \omega^2 \equiv \frac{1}{2}\omega^i{}_j\omega^j{}_i \quad . \tag{2.10}$$

$\mathcal{R} \equiv \mathcal{R}^i{}_i$ is the 3-dimensional spatial curvature of constant t hypersurfaces. These new forms of the Einstein equations emerge from a more general set of equations in the ADM formalism which is presented in Appendix A.1. They are obtained by taking the extrinsic curvature tensor, describing the embedding of spatial hypersurfaces in the 4-dimensional $\mathcal{M}_4$ spacetime, as the opposite value of the expansion tensor :

$$K_{ij} = -\Theta_{ij} = -\left(\frac{1}{3}h_{ij}\Theta + \sigma_{ij} + \omega_{ij} \right) \quad . \tag{2.11}$$

It can also be defined in terms of the spatial metric by :

$$K^i{}_j = -\frac{1}{2}g^{ik}(g_{kj})^\bullet \quad . \tag{2.12}$$

From this framework we also obtain a very important equation, not independent from the system (2.5-2.9), known as the Raychaudhuri's equation :

$$\dot{\Theta} + \frac{\Theta^2}{3} + 2\,\sigma^2 + 2\,\omega^2 + 4\pi G\rho - \Lambda = 0 \quad . \tag{2.13}$$

This relation describes the evolution of the geometry of a bundle of geodesic world lines.

Inspired by these forms of the Hamiltonian constraint, Eq. (2.5), and Raychaudhuri's equation (2.13) in the ADM formalism, we define a volume scale factor and its associated Hubble parameter as

$$a_\mathcal{D}(t) \equiv \left(\frac{V_\mathcal{D}(t)}{V_\mathcal{D}(t_i)} \right)^{1/3} \quad , \quad \text{which implies} \quad \frac{\dot{V}_\mathcal{D}}{V_\mathcal{D}} = 3\frac{\dot{a}_\mathcal{D}}{a_\mathcal{D}} \equiv 3H_\mathcal{D} \quad . \tag{2.14}$$

1. Notice the difference in the literature where we sometimes define these rates as $\sigma^2 \equiv \frac{1}{2}\sigma_{ij}\sigma^{ij}$ and $\omega^2 \equiv \frac{1}{2}\omega_{ij}\omega^{ij}$. In this case, ω^{ij} being anti-symmetric, we get the opposite sign for ω^2 in the equations.

The relationship between this effective scale factor and the homogeneous scale factor is a bit hard to interpret. Indeed, one can see that $a_{\mathcal{D}}(t)$ becomes equivalent to $a(t)$ if the matter content is taken to be homogeneous, and this whatever the size and form of the domain $\mathcal{D}$, but on the other hand very different domains can give the same scale factor in an inhomogeneous Universe. One can nevertheless find equations of evolution for $a_{\mathcal{D}}$ and this is the purpose of the following considerations.

Using the quantity $J(t,\mathbf{x}) \equiv \sqrt{\det g_{ij}}$ defined in Eq. (2.2), we obviously have

$$(\ln J)^{\bullet} = \frac{1}{2} g^{ik} (g_{ki})^{\bullet} = -K \qquad \text{so that} \qquad \dot{J} = -KJ = \Theta J \quad . \tag{2.15}$$

From this last equality we obtain that

$$\langle \Theta \rangle_{\mathcal{D}} = \frac{1}{V_{\mathcal{D}}} \int_{\mathcal{D}} \frac{\dot{J}}{J} \, J \, d^3\mathbf{x} = \frac{1}{V_{\mathcal{D}}} \left(\int_{\mathcal{D}} J \, d^3\mathbf{x} \right)^{\bullet} = \frac{\dot{V}_{\mathcal{D}}}{V_{\mathcal{D}}} \quad . \tag{2.16}$$

One can see then that the Eq. (2.7) is simply written as

$$(\rho J)^{\bullet} = 0 \qquad \text{with the solution} \qquad \rho(t,\mathbf{x}) = \frac{\rho(t_0,\mathbf{x}) J(t_0,\mathbf{x})}{J(t,\mathbf{x})} \quad . \tag{2.17}$$

This identity implies that the mass contained in the domain $\mathcal{D}$ is, as requested, constant in time:

$$M_{\mathcal{D}} = \int_{\mathcal{D}} \rho J \, d^3\mathbf{x} = \text{cst} \quad , \tag{2.18}$$

and so the averaged density, starting with an initial volume $V_{\mathcal{D}_0} \equiv V_{\mathcal{D}}(t_0)$, becomes

$$\langle \rho \rangle_{\mathcal{D}} = \frac{1}{V_{\mathcal{D}}} \int_{\mathcal{D}} \rho J \, d^3\mathbf{x} = \frac{M_{\mathcal{D}}}{V_{\mathcal{D}}} = \frac{M_{\mathcal{D}}}{V_{\mathcal{D}_0} a_{\mathcal{D}}^3} \quad . \tag{2.19}$$

For all the scalar quantities S encountered, such as ρ, we can take the time derivative of its average $\langle S \rangle_{\mathcal{D}}$ and we are lead to the *commutation rule*:

$$\langle S \rangle_{\mathcal{D}}^{\bullet} - \langle \dot{S} \rangle_{\mathcal{D}} = \langle S \, \Theta \rangle_{\mathcal{D}} - \langle S \rangle_{\mathcal{D}} \langle \Theta \rangle_{\mathcal{D}} \quad . \tag{2.20}$$

This relation shows that the time derivation of S, in other words its evolution in time, does not commute with its average $\langle \ldots \rangle_{\mathcal{D}}$. This is related to the long-standing problem of backreaction, as presented by Ellis in the 80's (see [28]), and it shows that the spatially averaged quantity S does not follow, on average, the evolution of S when we have a space-dependent expansion scalar (or equivalently an extrinsic curvature).

Averaging the Einstein equations

Averaging Raychaudhuri's equation (2.13) of a pressureless fluid ($p = 0$), and using the commutation rule (2.20) with $S = \Theta$, leads to

$$\langle \Theta \rangle_{\mathcal{D}}^{\bullet} - \frac{2}{3} \langle \Theta^2 \rangle_{\mathcal{D}} + \langle \Theta \rangle_{\mathcal{D}}^2 + 2 \langle \sigma^2 \rangle_{\mathcal{D}} + 2 \langle \omega^2 \rangle_{\mathcal{D}} + 4\pi G \langle \rho \rangle_{\mathcal{D}} - \Lambda = 0 \quad , \tag{2.21}$$

which is equivalent to

$$3 \frac{\ddot{a}_{\mathcal{D}}(t)}{a_{\mathcal{D}}(t)} + 4\pi G \frac{M_{\mathcal{D}}}{V_{\mathcal{D}_0} a_{\mathcal{D}}^3} - \Lambda = \mathcal{Q}_{\mathcal{D}} \quad , \tag{2.22}$$

with the so-called *backreaction parameter*:

$$\mathcal{Q}_{\mathcal{D}} \equiv \frac{2}{3} \left[\langle \Theta^2 \rangle_{\mathcal{D}} - \langle \Theta \rangle_{\mathcal{D}}^2 \right] - 2 \langle \sigma^2 \rangle_{\mathcal{D}} - 2 \langle \omega^2 \rangle_{\mathcal{D}} \quad . \tag{2.23}$$

Using now the Hamiltonian constraint of Eq. (2.5) and taking its average, one obtains

$$\frac{1}{2} \langle \mathcal{R} \rangle_{\mathcal{D}} + \frac{1}{3} \langle \Theta^2 \rangle_{\mathcal{D}} - 8\pi G \langle \rho \rangle_{\mathcal{D}} - \Lambda = \langle \sigma^2 \rangle_{\mathcal{D}} + \langle \omega^2 \rangle_{\mathcal{D}} \quad . \tag{2.24}$$

Removing $\frac{1}{3}\left[\left\langle\Theta^2\right\rangle_{\mathcal{D}} - \langle\Theta\rangle_{\mathcal{D}}^2\right]$ on both sides, and using that $\langle\Theta\rangle_{\mathcal{D}} = 3\frac{\dot{a}_{\mathcal{D}}}{a_{\mathcal{D}}}$, one gets

$$3\left(\frac{\dot{a}_{\mathcal{D}}}{a_{\mathcal{D}}}\right)^2 + \frac{1}{2}\langle\mathcal{R}\rangle_{\mathcal{D}} - 8\pi G\frac{M_{\mathcal{D}}}{V_{\mathcal{D}_0}a_{\mathcal{D}}^3} - \Lambda = -\frac{\mathcal{Q}_{\mathcal{D}}}{2} \quad . \tag{2.25}$$

We can remark that the vorticity tensor plays a similar role as the shear tensor in these calculations.

We shall assume now that the considered fluid has no vorticity, so: $\omega_{\mu\nu} = 0 \;\; \forall\, \mu,\nu$ and $\omega = 0$. Gathering Raychaudhuri's equation and the Hamiltonian constraint, and allowing both for a constant curvature $K_{\mathcal{D}_i}$ of a FLRW model, one gets the general expressions:

$$3\frac{\ddot{a}_{\mathcal{D}}(t)}{a_{\mathcal{D}}(t)} = -4\pi G\langle\rho\rangle_{\mathcal{D}} + \mathcal{Q}_{\mathcal{D}} + \Lambda \quad , \tag{2.26}$$

$$3H_{\mathcal{D}}^2 = 8\pi G\langle\rho\rangle_{\mathcal{D}} - \frac{3K_{\mathcal{D}_i}}{a_{\mathcal{D}}^2} - \frac{1}{2}\left(\mathcal{W}_{\mathcal{D}} + \mathcal{Q}_{\mathcal{D}}\right) + \Lambda \quad . \tag{2.27}$$

We defined here the deviation of the curvature from the constant curvature by the quantity:

$$\mathcal{W}_{\mathcal{D}} = \langle\mathcal{R}\rangle_{\mathcal{D}} - 6\,\frac{K_{\mathcal{D}_i}}{a_{\mathcal{D}}^2} \quad . \tag{2.28}$$

As in the classical Friedmann derivation, these two equations and the conservation equation

$$\langle\rho\rangle_{\mathcal{D}}^{\bullet} + 3H_{\mathcal{D}}\langle\rho\rangle_{\mathcal{D}} = 0 \tag{2.29}$$

only form two independent ones. Differentiating Eq. (2.27) with respect to the cosmic time t and then making use of Eqs. (2.26) and (2.29), one gets the consistency relation – or so-called *integrability condition* – involving only geometrical quantities:

$$\dot{\mathcal{Q}}_{\mathcal{D}} + 6H_{\mathcal{D}}\mathcal{Q}_{\mathcal{D}} + \dot{\mathcal{W}}_{\mathcal{D}} + 2H_{\mathcal{D}}\mathcal{W}_{\mathcal{D}} = 0 \iff a_{\mathcal{D}}^{-6}\left(a_{\mathcal{D}}^6\mathcal{Q}_{\mathcal{D}}\right)^{\bullet} + a_{\mathcal{D}}^{-2}\left(a_{\mathcal{D}}^2\mathcal{W}_{\mathcal{D}}\right)^{\bullet} = 0 \quad . \tag{2.30}$$

This condition garanties the Friedmann-like form of the above equations, especially for Eq. (2.29), and gives a dependence between the averaged 3-dimensional curvature $\langle\mathcal{R}\rangle_{\mathcal{D}}$ (an intrinsic curvature invariant) and the backreaction term $\mathcal{Q}_{\mathcal{D}}$ (an extrinsic curvature invariant) which involves expansion, shear and vorticity scalars induced by the inhomogeneous aspect of the compact domain $\mathcal{D}$.

One can see from Eq. (2.30) that $\mathcal{Q}_{\mathcal{D}} = 0$ gives $\langle\mathcal{R}\rangle_{\mathcal{D}} \propto a_{\mathcal{D}}^{-2}$. This case contains the particular one of a FLRW model where there is no structure and the spatial curvature goes like $\mathcal{R} \propto a^{-2}$. One does not encounter any backreaction also in the case where $Q_{\mathcal{D}} \propto a_{\mathcal{D}}^{-6}$. On the other hand, when none of these cases is satisfied, the relation between extrinsic and intrinsic curvatures is non-trivial. It is possible (i.e. not scientifically rejected) that small perturbations of the averaged spatial curvature and the averaged expansion rate could grow to lead finally to a global instability of the perturbed FLRW model. Our real Universe tends to be dominated by voids and we can suspect that the averaged curvature tends to be negative. It is believed that this situation, lead from the development of structures, could affect the evolution of the averaged expansion rate and, maybe, explain dark energy.

The backreaction is a profound issue which has also been addressed in N-body simulations. The problem of these approaches is that backreaction is also closely related to topological issues. Indeed, when we use a Newtonian description to study structures formation in a spatially flat background, there is no spatial curvature and there are six different orientable space forms out of which we usually take the 3-torus. The backreaction in that case is equivalent to a boundary contribution. Such a study is thus believed to directly kill any possible backreaction mechanism and cannot self-generate an acceleration of the expansion. To be fair, we should also stress that the idea of backreaction could be completely wiped out by mathematics (like a "*No-backreaction*" theorem). Indeed, the consideration of general relativity in 2+1 dimensions and the use of the Gauss-Bonnet theorem proves that the volume integral of the spatial curvature in a closed Riemannian 2-space is a topological invariant directly related to the Euler characteristic of the 2-dimensional manifold (see [6]). It follows that $\langle\mathcal{R}\rangle_{\mathcal{D}} \propto a_{\mathcal{D}}^{-2}$ and $Q_{\mathcal{D}} \propto a_{\mathcal{D}}^{-4}$ (the right exponent to have no effect in a 2+1 geometry, where the coefficient 6 in Eq. (2.30) is replaced by 4). Thus the backreaction is exactly canceled. Nevertheless, the relation between curvature and topology is more involved in 3+1 gravity, and no theorem has been proved. So backreaction is still an open question in 4-dimensional spacetimes.

Rewriting of the terms, morphon field

One can define the following cosmological-like parameters :

$$\Omega_m^{\mathcal{D}} \equiv \frac{8\pi G}{3}\frac{\langle\rho\rangle_{\mathcal{D}}}{H_{\mathcal{D}}^2} \quad , \quad \Omega_\Lambda^{\mathcal{D}} \equiv \frac{\Lambda}{3H_{\mathcal{D}}^2} \quad , \quad \Omega_K^{\mathcal{D}} \equiv -\frac{\langle\mathcal{R}\rangle_{\mathcal{D}}}{6H_{\mathcal{D}}^2} \quad , \quad \Omega_{\mathcal{Q}}^{\mathcal{D}} \equiv -\frac{\mathcal{Q}_{\mathcal{D}}}{6H_{\mathcal{D}}^2} \quad , \tag{2.31}$$

and see that the Hamiltonian constraint (to compare with Eq. (1.21)) is simply written as

$$\Omega_m^{\mathcal{D}} + \Omega_\Lambda^{\mathcal{D}} + \Omega_K^{\mathcal{D}} + \Omega_{\mathcal{Q}}^{\mathcal{D}} = 1 \quad . \tag{2.32}$$

These parameters directly depend on the domain of integration $\mathcal{D}$ and this last equation has to be interpreted with care. We can also rewrite the averaged Friedmann-like equations derived above in terms of a scalar field which has been called the morphon [2], denoted by $\Phi_{\mathcal{D}}$. One then defines the effective density and pressure for this field by :

$$\rho_{\mathcal{D}}^{\Phi} \equiv -\frac{1}{16\pi G}\left(\mathcal{Q}_{\mathcal{D}} + \mathcal{W}_{\mathcal{D}}\right) \quad , \quad p_{\mathcal{D}}^{\Phi} \equiv -\frac{1}{16\pi G}\left(\mathcal{Q}_{\mathcal{D}} - \frac{\mathcal{W}_{\mathcal{D}}}{3}\right) \quad . \tag{2.33}$$

The generalized Friedmann equations then read :

$$3\frac{\ddot{a}_{\mathcal{D}}(t)}{a_{\mathcal{D}}(t)} = -4\pi G\left(\langle\rho\rangle_{\mathcal{D}} + \rho_{\mathcal{D}}^{\Phi} + 3p_{\mathcal{D}}^{\Phi}\right) + \Lambda \quad , \tag{2.34}$$

$$3H_{\mathcal{D}}^2 = 8\pi G\,\langle\rho\rangle_{\mathcal{D}} - \frac{3K_{\mathcal{D}_i}}{a_{\mathcal{D}}^2} - \frac{1}{2}\left(\mathcal{W}_{\mathcal{D}} + \mathcal{Q}_{\mathcal{D}}\right) + \Lambda \quad , \tag{2.35}$$

and we have two equations of conservation :

$$\langle\rho\rangle_{\mathcal{D}}^{\bullet} + 3H_{\mathcal{D}}\,\langle\rho\rangle_{\mathcal{D}} = 0 \quad , \quad \rho_{\mathcal{D}}^{\Phi} + 3H_{\mathcal{D}}(\rho_{\mathcal{D}}^{\Phi} + p_{\mathcal{D}}^{\Phi}) = 0 \quad . \tag{2.36}$$

We can easily check that this last condition is equivalent to the integrability condition expressed in Eq. (2.30). It is an amazing fact to see that the field $\Phi_{\mathcal{D}}$ defined here has all the properties to effectively describe a cosmological constant.

We can also re-express these quantities by defining directly the field $\Phi_{\mathcal{D}}$ and its potential $U_{\mathcal{D}}$:

$$\rho_{\mathcal{D}}^{\Phi} = \frac{e}{2}\dot{\Phi}_{\mathcal{D}}^2 + U_{\mathcal{D}} \quad , \quad p_{\mathcal{D}}^{\Phi} = \frac{e}{2}\dot{\Phi}_{\mathcal{D}}^2 - U_{\mathcal{D}} \quad , \tag{2.37}$$

where $e = +1$ if $\Phi_{\mathcal{D}}$ is a standard scalar field and $e = -1$ if it is a phantom scalar field. One can also show the correspondence between the terms

$$\mathcal{Q}_{\mathcal{D}} = -8\pi G\left(e\dot{\Phi}_{\mathcal{D}}^2 - U_{\mathcal{D}}\right) \quad , \quad \mathcal{W}_{\mathcal{D}} = -24\pi G\,U_{\mathcal{D}} \quad , \tag{2.38}$$

and show that the integrability condition can be recast in a Klein-Gordon equation for $\Phi_{\mathcal{D}}$:

$$\ddot{\Phi}_{\mathcal{D}} + 3H_{\mathcal{D}}\dot{\Phi}_{\mathcal{D}} + e\frac{\partial U_{\mathcal{D}}}{\partial\Phi_{\mathcal{D}}}\left(\Phi_{\mathcal{D}}, \langle\rho\rangle_{\mathcal{D}}\right) = 0 \quad . \tag{2.39}$$

This equation is scale dependent through its dependence in $\mathcal{D}$. Last, we can define effective kinetic and potential energies of the morphon field by

$$E_{\mathcal{D}}^{\rm kin} = e\,\dot{\Phi}_{\mathcal{D}}^2 V_{\mathcal{D}} \quad , \quad E_{\mathcal{D}}^{\rm pot} = -U_{\mathcal{D}}V_{\mathcal{D}} \quad , \tag{2.40}$$

and we get the simple relation

$$2E_{\mathcal{D}}^{\rm kin} + E_{\mathcal{D}}^{\rm pot} = -\frac{\mathcal{Q}_{\mathcal{D}}V_{\mathcal{D}}}{8\pi G} \quad . \tag{2.41}$$

We deduce that an homogeneous Universe, for which $\mathcal{Q}_{\mathcal{D}} = 0$, is equivalent to the *virial equilibrium condition* in this effective formalism.

2. This scalar field is indeed sourced by inhomogeneities and thus captures the "morphological" signature of structures.

Kullback-Leibler relative entropy

Applying the commutation rule, Eq. (2.20), to the density of matter brings the relation :

$$\langle\rho\rangle_{\mathcal{D}}^{\bullet} - \langle\dot{\rho}\rangle_{\mathcal{D}} = \langle\rho\,\Theta\rangle_{\mathcal{D}} - \langle\rho\rangle_{\mathcal{D}}\,\langle\Theta\rangle_{\mathcal{D}} \quad . \tag{2.42}$$

To describe the relative difference between the inhomogeneous function $\rho(t, x^i)$ inside the domain $\mathcal{D}$ with respect to the homogeneous function $\langle\rho\rangle_{\mathcal{D}}$, one can use the concept of relative information given by the Kullback-Leibler entropy [30]. This entropy is defined, for the density function, as [3] :

$$\mathscr{S}_{\mathcal{D}} = \int_{\mathcal{D}} \rho \ln\left(\frac{\rho}{\langle\rho\rangle_{\mathcal{D}}}\right) \, J d^3x \quad . \tag{2.43}$$

One can then show that :

$$-\frac{\dot{\mathscr{S}}_{\mathcal{D}}}{V_{\mathcal{D}}} = -\left\langle \frac{(\rho J)^{\bullet}}{J} \ln\left(\frac{\rho}{\langle\rho\rangle_{\mathcal{D}}}\right)\right\rangle_{\mathcal{D}} - \langle\rho\rangle_{\mathcal{D}} \left\langle \left(\frac{\rho}{\langle\rho\rangle_{\mathcal{D}}}\right)^{\bullet}\right\rangle_{\mathcal{D}} \quad , \tag{2.44}$$

and use that $(\rho J)^{\bullet} = 0$, which eliminates the first term. The second one is developed, using Eq. (2.15), (2.17) and (2.29), as :

$$-\frac{\dot{\mathscr{S}}_{\mathcal{D}}}{V_{\mathcal{D}}} = -\langle\rho\rangle_{\mathcal{D}} \left\langle \frac{\dot{\rho}}{\langle\rho\rangle_{\mathcal{D}}} - \rho\frac{\langle\rho\rangle_{\mathcal{D}}^{\bullet}}{\langle\rho\rangle_{\mathcal{D}}^2}\right\rangle_{\mathcal{D}} = \langle\rho\,\Theta\rangle_{\mathcal{D}} - \langle\rho\rangle_{\mathcal{D}}\,\langle\Theta\rangle_{\mathcal{D}} \quad . \tag{2.45}$$

We thus proved that the time variation of the Kullback-Liebler entropy is proportional to the non-commutation terms linking the density of matter and the expansion scalar. One can thus understand that the definition of averaged quantities in cosmology has the first obvious consequence of a loss in information, but secondly has the drawback to introduce a difference in the evolution of averaged quantities with respect to their true non-averaged equivalents.

2.1.2 Gauge invariance

The average of a quantity naturally depends on the physical hypervolume used to define it. It should not, on the other hand, depend on the chosen coordinates. This fact, called gauge invariance, is a general concept which has some subtleties. Here we will solely present the necessary relations to understand the gauge problem that appears when we try to define averaged quantities. More details about the notion of gauge invariance are presented in Appendix A.3 .

Let us consider a spacetime $\mathcal{M}_4$ equipped with a system of coordinates $\{x^\mu\}$ and a Riemannian metric $g_{\mu\nu}$ to describe its geometry. We also consider a scalar function $S(x)$ on these coordinates. Under a General Coordinate Transformation (GCT), where h is a matrix function that we suppose invertible, we have the transformation

$$x \mapsto \hat{x} = h(x) \quad : \quad S(x) \mapsto \hat{S}(x) \qquad \text{such that} \qquad \hat{S}(\hat{x}) = S(x) = S(h^{-1}(\hat{x})) \quad . \tag{2.46}$$

A Gauge Transformation (GT) f – or "local reparametrization of the fields", supposed invertible – on the other hand consists in the evaluation of the field at the same physical point, thus being given by

$$x \mapsto \tilde{x} = f(x) \quad : \quad S(x) \mapsto \tilde{S}(x) = S(f^{-1}(x)) \quad . \tag{2.47}$$

We can remark that the evaluation of this last equality at $\tilde{x}$ gives $\tilde{S}(\tilde{x}) = S(x)$ which is equivalent to Eq. (2.46) if $f \equiv h$ (and thus $\hat{S} \equiv \tilde{S}$). Under the gauge transformation, the metric is modified in the following way :

$$g_{\mu\nu}(x) \mapsto \tilde{g}_{\mu\nu}(x) = \left[\frac{\partial x^\alpha}{\partial f^\mu}\frac{\partial x^\beta}{\partial f^\nu}\right]_{f^{-1}(x)} g_{\alpha\beta}(f^{-1}(x)) \tag{2.48}$$

3. We should notice that this relative entropy can be related to the Weyl entropy, as recently proved in [84].

where the squared brackets contain the product of inverse matrices $(\partial f/\partial x)^{-1}$ in which we finally replace x by $f^{-1}(x)$. The square root of the determinant $g \equiv \det g_{\mu\nu}$ is then transformed as

$$\sqrt{-g(x)} \to \sqrt{-\tilde{g}(x)} = \left|\frac{\partial x}{\partial f}\right|_{f^{-1}(x)} \sqrt{-g(f^{-1}(x))} \quad , \tag{2.49}$$

being thus multiplied by the inverse Jacobian determinant of the gauge transformation $x \mapsto f(x)$.

Let us consider now the integration of a scalar quantity $S(x)$ on a spacetime domain $\mathscr{D} \subset \mathcal{M}_4$ spanned by the coordinates $\{x^\mu\}$. The change of this integration under the gauge transformation $x \mapsto f(x)$, when the domain $\mathscr{D}$ is kept unchanged by this gauge transformation, is given by:

$$I(S,\mathscr{D}) = \int_{\mathscr{D}(x)} d^4x\sqrt{-g(x)}\ S(x) \ \longmapsto\ \tilde{I}(\tilde{S},\mathscr{D}) = \int_{\mathscr{D}(x)} d^4x\sqrt{-\tilde{g}(x)}\ \tilde{S}(x) \quad . \tag{2.50}$$

We can now proceed to a change of coordinates. Using $\bar{x} = f^{-1}(x)$, we write:

$$\tilde{I}(\tilde{S},\mathscr{D}) = \int_{\mathscr{D}(f(\bar{x}))} d^4\bar{x} \left|\frac{\partial f}{\partial \bar{x}}\right|_{\bar{x}} \sqrt{-\tilde{g}(f(\bar{x}))}\ \tilde{S}(f(\bar{x})) = \int_{\overline{\mathscr{D}}(\bar{x})} d^4\bar{x}\sqrt{-\tilde{g}(\bar{x})}\ S(\bar{x}) = I(S,\overline{\mathscr{D}}) \quad , \tag{2.51}$$

where we used the relations (2.49) and (2.47), and introduced at the end the new spacetime domain $\overline{\mathscr{D}}$ such that $\overline{\mathscr{D}}(\bar{x}) = \mathscr{D}(x)$. We conclude that the integral $I(S,\mathscr{D})$ is not gauge invariant if the domain $\mathscr{D}$ is unchanged under the gauge transformation. In other words, the domain of integration must be gauge-dependent and transform in a precise way to keep the integral $I(S,\mathscr{D})$ gauge invariant.

The transformation of this domain under gauge transformations can easily be found. Indeed, let us assume that the domain $\mathscr{D}$ depends on the coordinates $\{x^\mu\}$ and let us implement its shape in $\mathcal{M}_4$ by the use of a window function $W_{\mathscr{D}}(x)$ in the integral:

$$I(S,\mathscr{D}) = \int_{\mathcal{M}_4} d^4x\sqrt{-g(x)}\ W_{\mathscr{D}}(x)S(x) \quad . \tag{2.52}$$

If we assume that this function transforms as

$$W_{\mathscr{D}}(x) \ \longmapsto\ \widetilde{W}_{\mathscr{D}}(x) = W_{\mathscr{D}}(f^{-1}(x)) \quad , \tag{2.53}$$

under the gauge transformation f, we then have the new transformation of the integral:

$$I(S,\mathscr{D}) \ \longmapsto\ \tilde{I}(\tilde{S},\mathscr{D}) = \int_{\mathcal{M}_4} d^4\bar{x}\sqrt{-\tilde{g}(\bar{x})}\ W_{\mathscr{D}}(\bar{x})S(\bar{x}) = I(S,\mathscr{D}) \quad , \tag{2.54}$$

which shows the gauge invariance of the integral as expected. We can understand that if $W_{\mathscr{D}}$ is only made of scalars, such that it is still invariant under $x \mapsto f(x)$, then the gauge invariance is respected (and the GCT invariance is also satisfied). On the other hand, if $W_{\mathscr{D}}$ is not invariant, we say that the domain of integration breaks gauge invariance.

One such example that we can easily visualize is a cylindrical-type domain delimited by two spacelike hypersurfaces (i.e. defined by timelike normal vectors) $A(x) = A_1$ and $A(x) = A_2 > A_1$. In properly chosen coordinates, this hypervolume can be restricted by the addition of a timelike hypersurface $B(x) = r_0$ (defined by radial spacelike normal vectors), as we will illustrate in Fig. 2.1. $W_{\mathscr{D}}$ is then simply given in terms of Heaviside step functions by:

$$W_{\mathscr{D}}(x) = \Theta(A(x) - A_1)\Theta(A_2 - A(x))\Theta(r_0 - B(x)) \quad , \tag{2.55}$$

and we have here a domain $\mathscr{D}$ which is gauge invariant if A and B are scalars. Otherwise, the physical domain is not anymore the same after a gauge transformation and breaks gauge invariance of quantities defined on this domain (such as $I(S,\mathscr{D})$).

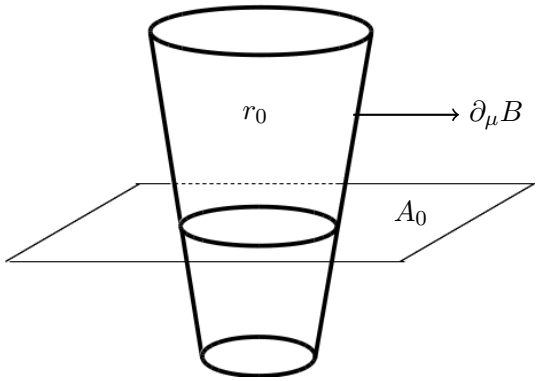

Figure 2.1: A graphic illustration of the introduction of a new parametrized hypersurface $B(x) = r_0$ to create a boundary inside the constant-A hypersurface. This newly introduced hypersurface has for spacelike gradient $\partial_\mu B$.

2.1.3 Gauge invariant generalization of Buchert's spatial average

In this section, we wish to present in a more general way the definition of an average on a spatial hypersurface, i.e. the hypersurface orthogonal to a vector n^μ which is timelike. Indeed, Buchert's definition of the average presented in Sec. 2.1 has been written in a given gauge (a synchronous gauge) and we intend to give a definition which does not depend on a gauge choice. We want to derive then the Buchert-Ehlers relation associated to this hypersurface, as it was done in [83].

Let us define a spatial hypersurface $\Sigma(A)$ whose points share the same value of a scalar field $A(x)$. This hypersurface can be defined by its (past-directed) normal vector :

$$n_\mu \equiv -\frac{\partial_\mu A}{\sqrt{-\partial_\mu A \partial^\mu A}} \tag{2.56}$$

which is a timelike vector as $n_\mu n^\mu = -1$. We choose a finite spatial domain $\mathscr{D}$ inside this hypersurface by adding up a scalar field $B(x)$ which can be defined by its spacelike vector $\propto \partial_\mu B$, see Fig. 2.1. We can then write the integration of a scalar S, as seen in Eq. (2.52), by

$$I(S; A_0, r_0) = \int_{\mathscr{D}(x)} d^4x \sqrt{-g(x)}\ S(x) \equiv \int_{\mathcal{M}_4} d^4x \sqrt{-g(x)}\ S(x) W_{\mathscr{D}}(x) \quad , \tag{2.57}$$

where the window function is

$$W_{\mathscr{D}}(x) = n^\mu \nabla_\mu \Theta(A(x) - A_0)\Theta(r_0 - B(x)) = \sqrt{-\partial_\mu A \partial^\mu A}\ \delta_{\mathrm{D}}(A(x) - A_0)\Theta(r_0 - B(x)) \quad , \tag{2.58}$$

and we have used that $n^\mu \nabla_\mu \Theta(A(x) - A_0) = n^\mu \partial_\mu A\ \delta_{\mathrm{D}}(A(x) - A_0)$. As previously shown, this integral is gauge invariant as long as A and B are gauge invariant scalars. We can thus define the gauge invariant average of a scalar $S(x)$ by the volume-weighted ratio :

$$\langle S \rangle_{A_0, r_0} = \frac{I(S; A_0, r_0)}{I(1; A_0, r_0)} \quad . \tag{2.59}$$

Let us now compute the derivative of this average with respect to the time parameter A_0 and obtain a generalization of the so-called Buchert-Ehlers commutation rules [58].

Taking the derivative of $I(S; A_0, r_0)$ with respect to the timelike parameter A_0, and using the following relation

$$\partial_{A_0} \delta(A(x) - A_0) = -\delta'_{\mathrm{D}}(A(x) - A_0) \quad , \tag{2.60}$$

we get

$$\frac{\partial I(S; A_0, r_0)}{\partial A_0} = -\int_{\mathcal{M}_4} d^4x \sqrt{-g(x)}\ \sqrt{-\partial_\mu A \partial^\mu A}\ \delta'_{\mathrm{D}}(A(x) - A_0)\Theta(r_0 - B(x))\ S(x) \quad . \tag{2.61}$$

We can then use an adapted system of coordinates such as ADM coordinates as it is done in [83]. Nevertheless, a more direct derivation is found as follows. Let us consider the identity:

$$n^\mu \nabla_\mu \delta_{\rm D}(A(x)-A_0) = \sqrt{-\partial_\mu A \partial^\mu A}\ \delta'_{\rm D}(A(x)-A_0) \quad . \tag{2.62}$$

From this we get:

$$\begin{aligned}
\frac{\partial I(S;A_0,r_0)}{\partial A_0} &= +\int_{\mathcal{M}_4} d^4x\sqrt{-g(x)}\ \delta_{\rm D}(A(x)-A_0)\nabla_\mu\left[n^\mu\ \Theta(r_0-B(x))\ S(x)\right] \\
&= \int_{\mathcal{M}_4} d^4x\sqrt{-g(x)}\ \delta_{\rm D}(A(x)-A_0)\Theta(r_0-B(x))\ \frac{n^\mu\nabla_\mu S(x)}{\sqrt{-\partial_\mu A\partial^\mu A}}\sqrt{-\partial_\mu A\partial^\mu A} \\
&\quad + \int_{\mathcal{M}_4} d^4x\sqrt{-g(x)}\ \delta_{\rm D}(A(x)-A_0)\Theta(r_0-B(x))\ \frac{\Theta(x)S(x)}{\sqrt{-\partial_\mu A\partial^\mu A}}\sqrt{-\partial_\mu A\partial^\mu A} \\
&\quad - \int_{\mathcal{M}_4} d^4x\sqrt{-g(x)}\ \delta_{\rm D}(A(x)-A_0)\ n^\mu\nabla_\mu\Theta(r_0-B(x))\ S(x) \quad ,
\end{aligned} \tag{2.63}$$

where in the first equality we used Eq. (2.62) followed by an integration by parts, with the indentity $\int_{\mathcal{M}_4} d^4x\sqrt{-g(x)}\ \nabla_\mu(\ldots) = 0$. This is true because the contribution $(\ldots)$ is zero at infinity, either from the fact that the domain of integration is rendered finite by the distributions, or simply because S can be taken to be zero at infinity. The last integral contains the following function:

$$n^\mu\nabla_\mu\Theta(r_0-B(x)) = -n^\mu\nabla_\mu\delta_{\rm D}(r_0-B(x)) = -2n^\mu\partial_\mu B\,\Theta(r_0-B(x))\delta_{\rm D}(r_0-B(x)) \quad , \tag{2.64}$$

where the factor two in the last equality can be understood from the definition of the delta-functions as the zero-width limit of a Gaussian distribution centered on zero. We understand also that this last integral is related to an integration on the boundary $\partial\mathscr{D}$ of the spatial domain $\mathscr{D}$.

Finally, using the definition of the integral in Eqs. (2.57) and (2.58), we obtain:

$$\begin{aligned}
\frac{\partial I(S;A_0,r_0)}{\partial A_0} &= I\left(\frac{\partial_\mu A\partial^\mu S(x)}{\partial_\mu A\partial^\mu A}\ ;A_0,r_0\right) + I\left(\frac{\Theta(x)S(x)}{\sqrt{-\partial_\mu A\partial^\mu A}}\ ;A_0,r_0\right) \\
&\quad -2I\left(\frac{\partial_\mu A\partial^\mu B}{\partial_\mu A\partial^\mu A}\ \delta_{\rm D}(r_0-B(x))S(x)\ ;A_0,r_0\right) \quad ,
\end{aligned} \tag{2.65}$$

where we have done trivial changes (such as $\partial^\mu A\nabla_\mu S \equiv \nabla^\mu A\nabla_\mu S = \nabla_\mu A\nabla^\mu S = \partial_\mu A\partial^\mu S$ as both A and S are scalars). Dividing now by the volume $I(1;A_0,r_0)$ and taking the limit $r_0\to\infty$, i.e. integrating over the whole spatial hypersurface fixed by $A(x)=A_0$, we have that $\langle\ldots\rangle_{A_0,r_0}\to\langle\ldots\rangle_{A_0}$ and we obtain the generalization of the Buchert-Ehlers commutation rule:

$$\frac{\partial\langle S\rangle_{A_0}}{\partial A_0} = \left\langle\frac{\partial_\mu A\partial^\mu S(x)}{\partial_\mu A\partial^\mu A}\right\rangle_{A_0} + \left\langle\frac{\Theta(x)S(x)}{\sqrt{-\partial_\mu A\partial^\mu A}}\right\rangle_{A_0} - \left\langle\frac{\Theta(x)}{\sqrt{-\partial_\mu A\partial^\mu A}}\right\rangle_{A_0}\langle S(x)\rangle_{A_0} \quad . \tag{2.66}$$

We understand the direct interpretation of this relation by going in the Arnowitt-Deser-Misner (ADM) coordinates. The spacetime $\mathcal{M}_4$ in ADM is foliated by hypersurfaces of constant time t and the line element is given by:

$$ds^2_{ADM} = -N^2dt^2 + g_{ij}(dx^i+N^idt)(dx^j+N^jdt) \quad , \tag{2.67}$$

and the normal vectors n^μ and n_μ (see Sec. A.1.1) are written as

$$n_\mu = N(-1,0,0,0) \quad , \quad n^\mu = \frac{1}{N}(1,-N^i) \quad . \tag{2.68}$$

One can then show that the volume expansion scalar $\Theta(x)$ in that case is

$$\Theta(x) = \frac{1}{N}\partial_t\ln\left(\sqrt{\det(g_{ij})}\right) \quad , \tag{2.69}$$

where g_{ij} is the spatial part of the metric $g^{ADM}_{\mu\nu}$ encoding the geometry inside the constant-t hypersurface. In those coordinates A is homogeneous on $t = \text{cst}$ hypersurfaces. So we can take $A_0 \equiv t$ and we find that the Buchert-Ehlers commutation rule of Eq. (2.20) reduces to the simple relation:

$$\frac{\partial \langle S\rangle_{A_0}}{\partial A_0} = \left\langle \frac{\partial S}{\partial A_0}\right\rangle_{A_0} + \left\langle \frac{\Theta N}{\partial_t A} S\right\rangle_{A_0} - \left\langle \frac{\Theta N}{\partial_t A}\right\rangle_{A_0} \langle S\rangle_{A_0} \quad , \tag{2.70}$$

where $S = S(A_0, \mathbf{x})$ and we have used $\partial_\mu A \partial^\mu A \equiv g^{\mu\nu}_{ADM}\partial_\mu A \partial_\nu A = g^{tt}_{ADM}(\partial_t A)^2 = -N^{-2}(\partial_t A)^2$. We used here that in ADM coordinates, where A is homogeneous, we can always choose a vanishing shift vector (and so $g^{ADM}_{tt} = -N^2$ and $g^{ADM}_{ti} = 0$) corresponding to a partial gauge fixing.

The interpretation of Eq. (2.70) is similar to the commutation rule derived in Eq. (2.20). Indeed, we see that the time derivative of the average of S is equal to the average of the time derivative of S (first term on the RHS) followed by the addition of two terms which involve the volume expansion $\Theta(x)$ and the scalar S in this schematic form: $\langle \Theta S\rangle - \langle\Theta\rangle\langle S\rangle$. If $A(x)$ is taken to be simply t and if we fix the gauge to be synchronous, i.e. $N = 1$, we get exactly the relation presented in Eq. (2.20).

2.1.4 Generalization of Friedmann equations in a gauge invariant form

Let u^μ be the fluid velocity field and n^μ the field orthonormal to the hypersurface of averaging. This vector n^μ can be seen as the peculiar velocity of the observer if this latter one is not comoving with the fluid (as assumed in Sec. 2.1.1) but is in general different from it. We define a tilt angle between these two fields by

$$u_\mu n^\mu = -[1 + \sinh^2(\alpha_T)]^{1/2} = -\cosh(\alpha_T) \quad , \tag{2.71}$$

where the sign is chosen so that we have the normalizations $u_\mu u^\mu \equiv -1$ and $n_\mu n^\mu \equiv -1$ (i.e. when $\alpha_T = 0$, we want a timelike vector). In this section the fluid of matter is assumed to be a perfect fluid of local density ρ and pressure p:

$$T_{\mu\nu} = (\rho + p)u_\mu u_\nu + p\, g_{\mu\nu} \quad . \tag{2.72}$$

From [83] we have the following contractions (ADM energy density and ADM pressure):

$$\epsilon \equiv T_{\mu\nu}n^\mu n^\nu = \rho + (\rho + p)\sinh^2(\alpha_T) \quad , \quad \pi \equiv \frac{1}{3}T_{\mu\nu}h^{\mu\nu} = p + \frac{1}{3}(\rho + p)\sinh^2(\alpha_T) \quad . \tag{2.73}$$

Here we have used the projection tensor $h_{\mu\nu}$ orthogonal to the vector n^μ, with the properties:

$$h_{\mu\nu} = g_{\mu\nu} + n_\mu n_\nu \quad , \quad h_{\mu\rho}\, h^\rho_\nu = h_{\mu\nu} \quad , \quad h_{\mu\nu}n^\nu = 0 \quad . \tag{2.74}$$

This system can be inverted and has a unique solution:

$$\begin{aligned} \rho &= \left[1 + \frac{4}{3}\sinh^2(\alpha_T)\right]^{-1}\left[\left(1 + \frac{1}{3}\sinh^2(\alpha_T)\right)\epsilon - \sinh^2(\alpha_T)\pi\right] \quad , \\ p &= \left[1 + \frac{4}{3}\sinh^2(\alpha_T)\right]^{-1}\left[-\frac{1}{3}\sinh^2(\alpha_T)\epsilon + (1 + \sinh^2(\alpha_T))\pi\right] \quad , \end{aligned} \tag{2.75}$$

that we can insert in the expression of $T_{\mu\nu}$ in Eq. (2.72). We can rewrite it by making use of

$$u_\mu h^{\mu\nu} = u^\nu - \cosh(\alpha_T)\, n^\nu \quad , \tag{2.76}$$

to get an expression depending on ϵ and π:

$$T_{\mu\nu} = \epsilon\, n_\mu n_\nu + \pi\, h_{\mu\nu} + \frac{(\epsilon + \pi)}{\left[1 + \frac{4}{3}\sinh^2(\alpha_T)\right]}\left[u_\mu u_\nu - \cosh^2(\alpha_T)n_\mu n_\nu - \frac{1}{3}\sinh^2(\alpha_T)h_{\mu\nu}\right] \quad . \tag{2.77}$$

Here the third term on the RHS gives zero when contracted with $n^\mu n^\nu$ or $h^{\mu\nu}$.

We also have the generalized Friedmann's equations for an averaged perfect fluid (i.e. in the general case where $n_\mu \neq u_\mu$, see [83]) :

$$\begin{aligned}\left(\frac{1}{\tilde{a}}\frac{\partial \tilde{a}}{\partial A_0}\right)^2 &= \frac{8\pi G}{3}\left\langle \frac{\epsilon}{[-(\partial A)^2]}\right\rangle_{A_0} - \frac{1}{6}\left\langle \frac{\mathcal{R}_S}{[-(\partial A)^2]}\right\rangle_{A_0} \\ &- \frac{1}{9}\left[\left\langle \frac{\Theta^2}{[-(\partial A)^2]}\right\rangle_{A_0} - \left\langle \frac{\Theta}{[-(\partial A)^2]^{1/2}}\right\rangle_{A_0}^2\right] + \frac{1}{3}\left\langle \frac{\sigma^2}{[-(\partial A)^2]}\right\rangle_{A_0} \quad ,\end{aligned} \tag{2.78}$$

and

$$\begin{aligned}-\frac{1}{\tilde{a}}\frac{\partial^2 \tilde{a}}{\partial {A_0}^2} &= \frac{4\pi G}{3}\left\langle \frac{\epsilon + 3\pi}{[-(\partial A)^2]}\right\rangle_{A_0} - \frac{1}{3}\left\langle \frac{\nabla^\nu(n^\mu \nabla_\mu n_\nu)}{[-(\partial A)^2]}\right\rangle_{A_0} + \frac{1}{6}\left\langle \frac{\partial_\mu A \partial^\mu[(\partial A)^2]\Theta}{[-(\partial A)^2]^{5/2}}\right\rangle_{A_0} \\ &- \frac{2}{9}\left[\left\langle \frac{\Theta^2}{[-(\partial A)^2]}\right\rangle_{A_0} - \left\langle \frac{\Theta}{[-(\partial A)^2]^{1/2}}\right\rangle_{A_0}^2\right] + \frac{2}{3}\left\langle \frac{\sigma^2}{[-(\partial A)^2]}\right\rangle_{A_0} \quad ,\end{aligned} \tag{2.79}$$

where $\tilde{a}$ is an effective scale factor defined by

$$\frac{1}{\tilde{a}}\frac{\partial \tilde{a}}{\partial A_0} \equiv \frac{1}{3I(1,A_0)}\frac{\partial I(1,A_0)}{\partial A_0} = \frac{1}{3}\left\langle \frac{\Theta}{[-(\partial A)^2]^{1/2}}\right\rangle_{A_0} \quad , \tag{2.80}$$

and where in the last equality we took the ADM coordinates and assumed that $B \subset \Sigma_{A_0}$.

In fact one can give the generalization of other quantities that have been derived in the literature. For example, we can define an effective density and an effective pressure to consider the backreaction terms as an effective scalar field. We can also generalize the integrability condition to have a gauge invariant definition of it. Nevertheless, because these expressions are really complicated, and their use very limited, we will not present them in this thesis [4].

2.2 Light-cone averaging

2.2.1 Choice of a right scalar

Let us first emphasize again the approach given in [82, 83] to gauge invariant averaging on a 3-dimensional spacelike hypersurface $\Sigma(A)$, embedded in our 4-dimensional spacetime $\mathcal{M}_4$. Assuming the hypersurface (or a spacelike foliation) to be defined by an equation involving a scalar field with timelike gradients $A(x)$:

$$A(x) - A_0 = 0 \quad , \tag{2.81}$$

4. Let us finally notice that the commutation rule for the energy density, necessary to obtain the integrability condition, is derived in [83]. This derivation makes use of the conservation of the stress-energy tensor for a perfect fluid along the geodesics of n_μ, i.e. : $n_\nu \nabla_\mu T^{\mu\nu} = 0$. Developping $T^{\mu\nu}$ from Eq. (2.72) in this equation, we get :

$$u^\mu \partial_\mu[(\rho+p)u^\rho n_\rho] + n^\mu \partial_\mu p + (\rho+p)(\nabla_\mu u^\mu)(u^\rho n_\rho) + (\rho+p)\left[n^\rho u^\mu \nabla_\mu u_\rho - u^\mu \nabla_\mu(u^\rho n_\rho)\right] = 0 \quad ,$$

where this last term can be written $-(\rho+p)u^\mu u^\rho \nabla_\mu n_\rho$. From the definition of $\Theta^{\mu\nu}$ we have:

$$\begin{aligned}-\Theta^{\mu\nu}u_\mu u_\nu &= -\Theta_{\mu\nu}u^\mu u^\nu = -({\delta_\mu}^\alpha + n_\mu n^\alpha)({\delta_\nu}^\beta + n_\nu n^\beta)(\nabla_\alpha n_\beta)u^\mu u^\nu \\ &= -u^\mu u^\nu(\nabla_\mu n_\nu) - (u^\rho n_\rho)n^\mu u^\nu \nabla_\mu n_\nu \quad ,\end{aligned}$$

where we made use of the equality $n^\mu n^\nu \nabla_\mu n_\nu = \frac{1}{2}n^\mu \nabla_\mu(n^\nu n_\nu) = 0$ (from $n^\nu n_\nu = -1$). As a consequence, the final equation we obtain is

$$u^\mu \partial_\mu[(\rho+p)u^\rho n_\rho] + n^\mu \partial_\mu p + (\rho+p)[(\nabla_\mu u^\mu)u^\rho n_\rho - \Theta^{\mu\nu}u_\mu u_\nu + (u^\rho n_\rho)n^\mu u^\nu \nabla_\mu n_\nu] = 0 \quad .$$

This last term on the LHS was missing in Eq. (2.25) of [83]. This footnote thus correct this typo.

the gauge (and hypersurface-parametrization) invariant definition of the integral of an arbitrary scalar $S(x)$ and of its average on such hypersurface is given by [5] :

$$\langle S\rangle_{A_0} = \frac{I(S;A_0)}{I(1;A_0)} \quad \text{with} \quad I(S;A_0) = \int_{\mathcal{M}_4} d^4x\sqrt{-g(x)}\ \delta_{\rm D}(A(x)-A_0)\ \sqrt{-\partial_\mu A\partial^\mu A}\ S(x) \quad . \tag{2.82}$$

Here the spatial hypersurface has no boundary, it goes to infinity. However, as shown in [82, 83], a possible spatial boundary can be added through the following extension of the previous integral :

$$I(S;A_0;r_0) = \int_{\mathcal{M}_4} d^4x\sqrt{-g(x)}\,\delta_{\rm D}(A(x)-A_0)\Theta(r_0-B(x))\sqrt{-\partial_\mu A\partial^\mu A}\ S(x) \quad , \tag{2.83}$$

and similarly for the corresponding average (Θ is the Heaviside step function, and B is a positive function of the coordinates, with spacelike gradient). As already discussed in Sec. 2.1.3 (see also [82, 86]), and as illustrated in Fig. 2.1, this is still a gauge invariant expression if $B(x)$ transforms as a scalar, while it gives violations of gauge invariance if B is not a scalar and keeps the same form in different coordinate systems. Even in that case, however, gauge invariance violations go to zero when we choose r_0 in such a way that the size of the spatial region goes to infinity [82, 86].

The above procedure unfortunately fails if $A(x) = A_0$ defines a null (light-like) hypersurface, since in that case $\partial_\mu A\partial^\mu A = 0$. In order to circumvent this problem let us start with a spacetime integral where the four-dimensional integration region is bounded by two hypersurfaces, one spacelike and the other one null (corresponding e.g. to the past light-cone of some observer). Let us choose, in particular, the region inside the past light-cone of the observer bounded in the past by the hypersurface $A(x) = A_0$. Clearly a gauge invariant definition of the integral of a scalar $S(x)$ over such a hypervolume can be written (in a useful notation generalizing the one used above) as

$$I(S;-;A_0,V_0) = \int_{\mathcal{M}_4} d^4x\sqrt{-g}\ \Theta(V_0-V)\Theta(A-A_0)\ S(x) \quad , \tag{2.84}$$

where $V(x)$ is a (generalized advanced-time) null scalar satisfying $\partial_\mu V\partial^\mu V = 0$ and V_0 specifies the past light cone of a given observer. The LHS symbol "$-$" denotes the absence of delta-like window functions. We should remark the analogy between the scalars V and B. Indeed, this gauge invariant definition corresponds to the replacement of the timelike hypersurface $B(x) = r_0$ by a null-like hypersurface $V(x) = V_0$.

2.2.2 Definition of the averages

Starting with this hypervolume integral we can construct gauge invariant hypersurface and surface integrals by applying to it appropriate differential operators – or, equivalently, by applying Gauss's theorem to the volume integral of a covariant divergence. An example of the latter, if we are interested by the variations of the volume averages along the flow lines normal to the reference hypersurface $\Sigma(A)$, is obtained by replacing the scalar S with the divergence of the unit normal to Σ,

$$n_\mu = -\frac{\partial_\mu A}{\sqrt{-\partial_\nu A\partial^\nu A}} \quad , \quad n_\mu n^\mu = -1 \quad , \tag{2.85}$$

and leads to the identity :

$$\begin{aligned}\int_{\mathcal{M}_4} d^4x\sqrt{-g}\ \Theta(V_0-V)\Theta(A-A_0)\nabla^\mu n_\mu &= -\int_{\mathcal{M}_4} d^4x\sqrt{-g}\,\Theta(V_0-V)\delta_{\rm D}(A-A_0)\sqrt{-\partial_\mu A\partial^\mu A} \\ &+ \int_{\mathcal{M}_4} d^4x\sqrt{-g}\,\delta_{\rm D}(V_0-V)\Theta(A-A_0)\frac{-\partial_\mu V\partial^\mu A}{\sqrt{-\partial_\nu A\partial^\nu A}} \quad .\end{aligned} \tag{2.86}$$

5. In [83] the prescription introduced in [82] is used to give a covariant and gauge invariant generalization of the effective equations presented in [49, 50]. Such a generalization has been recently used to deal with the backreaction of quantum fluctuations in an inflationary model [85].

Hence, if we start from Eq. (2.84), and we consider the variation of the average integral by shifting the light-cone $V = V_0$ along the flow lines defined by n_μ, we are led to define the hypersurface integral (with positive measure) :

$$I(1; V_0; A_0) = \int_{\mathcal{M}_4} d^4x\sqrt{-g}\,\delta_{\rm D}(V_0 - V)\Theta(A - A_0)\frac{|\partial_\mu V\partial^\mu A|}{\sqrt{-\partial_\nu A\partial^\nu A}} \quad . \tag{2.87}$$

Similarly, if we consider the variation of the average integral by shifting the hypersurface $A = A_0$ (along the same flow lines defined by n_μ), we are led to another hypersurface integral :

$$I(1; A_0; V_0) = \int_{\mathcal{M}_4} d^4x\sqrt{-g}\,\Theta(V_0 - V)\delta_{\rm D}(A - A_0)\sqrt{-\partial_\mu A\partial^\mu A} \quad . \tag{2.88}$$

In the first case, Eq. (2.87), the integration region is on the light-cone itself, and it is spanned by the variation of $\Sigma(A_0)$ along its normal, at fixed light-cone V_0 (see Fig. 2.2, (a)). In the second case of Eq. (2.88) – which gives exactly the same integral as in Eq. (2.83) with V replacing B – the hypersurface $\Sigma(A_0)$ is kept fixed, and the integration region describes the causally connected section of Σ spanned by the variation of the light-cone hypersurface (see Fig. 2.2, (b)).

Further differentiation also leads to the following invariant surface integral

$$I(1; V_0, A_0; -) = \int_{\mathcal{M}_4} d^4x\sqrt{-g}\;\delta_{\rm D}(V_0 - V)\delta_{\rm D}(A - A_0)|\partial_\mu V\partial^\mu A| \quad , \tag{2.89}$$

with a compact, 2-dimensional integration region defined by the intersection of $\Sigma(A_0)$ with the light-cone V_0 (Fig. 2.2, (c)). This integral, as well as the integrals of Eqs. (2.87), (2.88), is not only covariant and gauge invariant but also invariant under separate reparametrizations of the scalar fields $A \to \tilde{A}(A)$ and $V \to \tilde{V}(V)$. Eq. (2.89), in addition, is a particular case of an invariant integration over an arbitrary codimension-2 hypersurface defined by the conditions $A^{(n)}(x) = 0$, $n = 1, 2$. In general, and in D spacetime dimensions, such an integral can be written as

$$\int_{\mathcal{M}_{\mathcal{D}}} d^Dx\sqrt{-g}\prod_n \delta_{\rm D}(A^{(n)}(x))\sqrt{|\det \bar{g}^{pq}|} \quad \text{with} \quad \bar{g}^{pq} \equiv \partial_\mu A^{(p)}\partial_\nu A^{(q)}g^{\mu\nu} \quad , \tag{2.90}$$

(as can be shown by considering the induced metric on the $(D-2)$-hypersurface), and is invariant under the more general reparametrizations $A^{(1)} \to \tilde{A}^{(1)}\left(A^{(1)}, A^{(2)}\right)$ and $A^{(2)} \to \tilde{A}^{(2)}\left(A^{(1)}, A^{(2)}\right)$. It can be easily checked that Eq. (2.90) reduces to Eq. (2.89) if $D = 4$ and if $A^{(1)} = A - A_0$ and $A^{(2)} = V - V_0$ are scalar functions with timelike and null gradient, respectively.

In order to make contact with Eqs. (2.87), (2.88), it may be useful to remark that the integral of Eq. (2.89) can also be obtained starting from the hypervolume integral of Eq. (2.84) by considering the variation of the volume average along the flow lines normal to $\Sigma(A)$ for both $\Theta(A)$ and $\Theta(V)$, namely by using the following window function :

$$\begin{aligned} &-n^\mu\nabla_\mu\Theta(A(x) - A_0)n^\mu\nabla_\mu\Theta(V_0 - V(x)) \\ &\qquad = \sqrt{-\partial_\mu A\partial^\mu A}\,\delta_{\rm D}(A(x) - A_0)\frac{-\partial_\mu V\partial^\mu A}{\sqrt{-\partial_\mu A\partial^\mu A}}\delta_{\rm D}(V_0 - V(x)) \quad . \end{aligned} \tag{2.91}$$

We note, finally, that averages of a scalar S over different (hyper)surfaces are trivially defined, with self explanatory notation, by :

$$\langle S\rangle_{V_0,A_0} = \frac{I(S; V_0, A_0; -)}{I(1; V_0, A_0; -)} \quad , \tag{2.92}$$

$$\langle S\rangle_{V_0}^{A_0} = \frac{I(S; V_0; A_0)}{I(1; V_0; A_0)} \quad , \tag{2.93}$$

$$\langle S\rangle_{A_0}^{V_0} = \frac{I(S; A_0; V_0)}{I(1; A_0; V_0)} \quad . \tag{2.94}$$

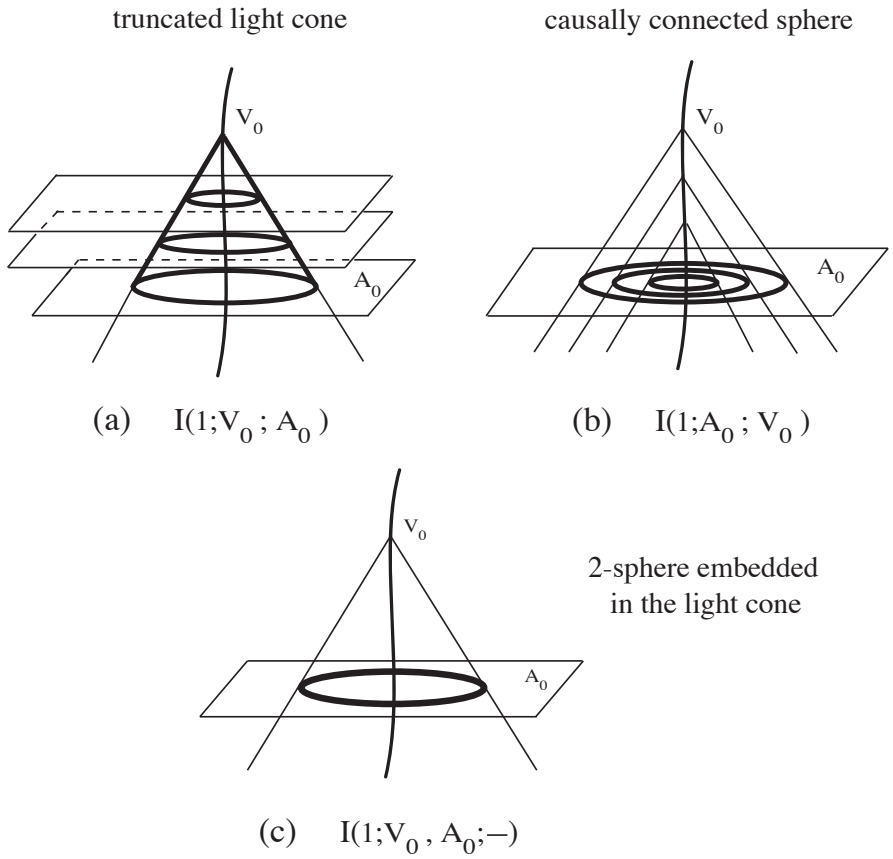

Figure 2.2: Three different light-cone averaging prescriptions. (a): the average of Eq. (2.87) on the light-cone itself starting from a given hypersurface in the past; (b): the average of Eq. (2.88) on the section of the hypersurface $A(x) = A_0$ which is causally connected with us; (c): the average of Eq. (2.89) on a 2-sphere embedded in the light-cone.

2.2.3 Compact notations

We can give a summary of the normalizations to be used in these three cases, using the general expression for the integral:

$$I[S, V_0, A_0] = \int_{\mathcal{M}_4} d^4x\sqrt{-g}\ \mathrm{D}(V_0 - V)\mathrm{D}(A - A_0)\ \mathcal{N}(V, A, \partial_\mu)\ S(x) \quad , \tag{2.95}$$

where $\mathcal{N}(V, A, \partial_\mu)$ is a normalization, $\mathrm{D}(X) = \delta_{\mathrm{D}}(X)$ or $\Theta(X)$, and we can even add a fourth case of application of this integral from Eq. (2.84), corresponding to the integration over the whole past causal volume and denoting its corresponding average as

$$\langle S\rangle^{A_0,V_0} = \frac{I(S; -; A_0, V_0)}{I(1; -; A_0, V_0)} \quad . \tag{2.96}$$

The normalization is choosen in function of the distributions being used, as shown in Table 2.1.

Table 2.1: Different normalizations to be used in Eq. (2.95) to recover the four average definitions.

Average $\overset{\Theta}{\delta_{\mathrm{D}}}$	$\langle S\rangle_{V_0}^{A_0}$	$\langle S\rangle_{A_0}^{V_0}$	$\langle S\rangle_{V_0,A_0}$	$\langle S\rangle^{V_0,A_0}$
Integral $I[S, V_0, A_0]$	$I(S; V_0; A_0)$	$I(S; A_0; V_0)$	$I(S; V_0, A_0; -)$	$I(S; -; A_0, V_0)$
$\mathcal{N}(V, A, \partial_\mu)$	$\frac{\lvert\partial_\mu V\partial^\mu A\rvert}{\sqrt{-\partial_\nu A\partial^\nu A}}$	$\sqrt{-\partial_\mu A\partial^\mu A}$	$\lvert\partial_\mu V\partial^\mu A\rvert$	1

It is interesting also to notice that we can get rid of this normalization $\mathcal{N}$ by defining new distributions that we could call "gauge invariant distributions". Indeed, Eq. (2.95) is equivalent to

$$I[S, V_0, A_0] = \int_{\mathcal{M}_4} d^4x\sqrt{-g}\ \widehat{\mathrm{D}}(V_0 - V)\widehat{\mathrm{D}}(A - A_0)\ S(x) \quad , \tag{2.97}$$

where we take

$$\widehat{\mathrm{D}}(X) \ = \ \Theta(X) \qquad \text{or} \qquad \frac{|\partial_\mu X \partial^\mu A|}{\sqrt{-\partial_\nu A \partial^\nu A}}\delta_{\mathrm{D}}(X) \tag{2.98}$$

depending on the spacetime domain we want to integrate over. We see that this definition is enough to recover the last four cases of integration : on spatial hypersurfaces, the past light cone, the embedded 2-sphere and the whole past causal volume.

2.3 Buchert-Ehlers commutation rules on the light-cone

2.3.1 Average on the embedded 2-sphere & the truncated light-cone

For the phenomenological applications of the following sections we are interested, in particular, in the derivatives of the averages defined in Eqs. (2.92) and (2.93). To this purpose, let us first consider the derivatives of $I(S; V_0, A_0; -)$ and $I(S; V_0; A_0)$ with respect to A_0 and V_0 (quantities that, like the starting integrals themselves, are covariant and gauge invariant).

We will use the identities (here $k_\mu \equiv \partial_\mu V$) :

$$\delta'_{\mathrm{D}}(A - A_0) = \frac{k^\mu \partial_\mu \delta_{\mathrm{D}}(A - A_0)}{k^\nu \partial_\nu A} \quad , \quad \delta_{\mathrm{D}}(A - A_0) = \frac{k^\mu \partial_\mu \Theta(A - A_0)}{k^\nu \partial_\nu A} \quad , \tag{2.99}$$

$$\delta'_{\mathrm{D}}(V - V_0) = \frac{\partial^\mu A\, \partial_\mu \delta_{\mathrm{D}}(V - V_0)}{k^\nu \partial_\nu A} \quad , \quad \delta_{\mathrm{D}}(V - V_0) = \frac{\partial^\mu A\, \partial_\mu \Theta(V - V_0)}{k^\nu \partial_\nu A} \quad , \tag{2.100}$$

and the relation $k^\mu \partial_\mu \delta_{\mathrm{D}}(V - V_0) = k^\mu k_\mu \delta'_{\mathrm{D}}(V - V_0) = 0$. Integrating by parts, we then obtain

$$\begin{aligned} \frac{\partial}{\partial A_0} I(S; V_0, A_0; -) \ &= \ I\left(\frac{k \cdot \partial S}{k \cdot \partial A}; V_0, A_0; -\right) + I\left(\frac{\nabla \cdot k}{k \cdot \partial A} S; V_0, A_0; -\right) \quad , \\ \frac{\partial}{\partial A_0} I(S; V_0; A_0) \ &= \ I\left(\frac{k \cdot \partial S}{k \cdot \partial A}; V_0; A_0\right) + I\left(\left[\nabla \cdot k - \frac{1}{2}\frac{k^\mu \partial_\mu \left((\partial A)^2\right)}{(\partial A)^2}\right]\frac{S}{k \cdot \partial A}; V_0; A_0\right) \quad , \end{aligned} \tag{2.101}$$

where, to simplify notations, we have introduced the following definitions :

$$\begin{aligned} k^\mu \partial_\mu S = k \cdot \partial S \quad , \quad k^\mu \partial_\mu A = k \cdot \partial A \quad , \quad \partial_\mu A \partial^\mu S = \partial A \cdot \partial S \quad , \\ \partial_\mu A \partial^\mu A = (\partial A)^2 \quad , \quad \nabla_\mu k^\mu = \nabla \cdot k \quad , \quad \Box = \nabla^\mu \nabla_\mu \quad . \end{aligned} \tag{2.102}$$

Using these results we can write a generalized version of the Buchert-Ehlers commutation rule [58] for light-cone averages. For averages defined over the integration domain of Eq. (2.89) we find :

$$\frac{\partial}{\partial A_0}\langle S\rangle_{V_0,A_0} = \left\langle \frac{k \cdot \partial S}{k \cdot \partial A}\right\rangle_{V_0,A_0} + \left\langle \frac{\nabla \cdot k}{k \cdot \partial A} S\right\rangle_{V_0,A_0} - \left\langle \frac{\nabla \cdot k}{k \cdot \partial A}\right\rangle_{V_0,A_0} \langle S\rangle_{V_0,A_0} \quad , \tag{2.103}$$

while for 3-dimensional averages over the domain of Eq. (2.87) we obtain :

$$\begin{aligned} \frac{\partial}{\partial A_0}\langle S\rangle_{V_0}^{A_0} \ &= \ \left\langle \frac{k \cdot \partial S}{k \cdot \partial A}\right\rangle_{V_0}^{A_0} + \left\langle \left[\nabla \cdot k - \frac{1}{2}\frac{k^\mu \partial_\mu \left((\partial A)^2\right)}{(\partial A)^2}\right]\frac{S}{k \cdot \partial A}\right\rangle_{V_0}^{A_0} \\ &\quad - \left\langle \left[\nabla \cdot k - \frac{1}{2}\frac{k^\mu \partial_\mu \left((\partial A)^2\right)}{(\partial A)^2}\right]\frac{1}{k \cdot \partial A}\right\rangle_{V_0}^{A_0} \langle S\rangle_{V_0}^{A_0} \quad . \end{aligned} \tag{2.104}$$

Following a similar procedure we can also evaluate the generalization of the Buchert-Ehlers commutation rule for the derivative of $I(S;V_0,A_0;-)$ and $I(S;V_0;A_0)$ with respect to V_0. As we shall see in Sec. 3.6.3, such derivatives, together with the previous ones, may be useful in evaluating an averaged version of the "redshift drift" parameter. After some calculations we are led to

$$\begin{aligned}\frac{\partial}{\partial V_0}\langle S\rangle_{V_0,A_0} &= \left\langle \frac{\partial A\cdot\partial S}{k\cdot\partial A}\right\rangle_{V_0,A_0} - \left\langle k\cdot\partial S\frac{(\partial A)^2}{(k\cdot\partial A)^2}\right\rangle_{V_0,A_0} \\ &+\left\langle\left[\Box A-\nabla_\mu\left(k^\mu\frac{(\partial A)^2}{k\cdot\partial A}\right)\right]\frac{S}{k\cdot\partial A}\right\rangle_{V_0,A_0} \\ &-\left\langle\left[\Box A-\nabla_\mu\left(k^\mu\frac{(\partial A)^2}{k\cdot\partial A}\right)\right]\frac{1}{k\cdot\partial A}\right\rangle_{V_0,A_0}\langle S\rangle_{V_0,A_0}\ ,\end{aligned} \tag{2.105}$$

and

$$\begin{aligned}\frac{\partial}{\partial V_0}\langle S\rangle_{V_0}^{A_0} &= \left\langle \frac{\partial A\cdot\partial S}{k\cdot\partial A}\right\rangle_{V_0}^{A_0} - \left\langle k\cdot\partial S\frac{(\partial A)^2}{(k\cdot\partial A)^2}\right\rangle_{V_0}^{A_0} \\ &+\left\langle\left[\Box A-\partial^\mu A\partial_\mu\ln\left((\partial A)^2\right)\right]\frac{S}{k\cdot\partial A}\right\rangle_{V_0}^{A_0} \\ &-\left\langle\left[\nabla\cdot k\frac{(\partial A)^2}{(k\cdot\partial A)^2}+\frac{1}{2}k^\mu\partial_\mu\left(\frac{(\partial A)^2}{(k\cdot\partial A)^2}\right)\right]S\right\rangle_{V_0}^{A_0} \\ &-\left\langle\left[\Box A-\partial^\mu A\partial_\mu\ln\left((\partial A)^2\right)\right]\frac{1}{k\cdot\partial A}\right\rangle_{V_0}^{A_0}\langle S\rangle_{V_0}^{A_0} \\ &+\left\langle\left[\nabla\cdot k\frac{(\partial A)^2}{(k\cdot\partial A)^2}+\frac{1}{2}k^\mu\partial_\mu\left(\frac{(\partial A)^2}{(k\cdot\partial A)^2}\right)\right]\right\rangle_{V_0}^{A_0}\langle S\rangle_{V_0}^{A_0}\ .\end{aligned} \tag{2.106}$$

These expressions will take a simpler form when we consider their averages in the GLC coordinates presented in Chapter 3. We will show these simplified expressions of the Buchert-Ehlers rules on the lightcone in Sec. 3.6.2.

2.3.2 Average on the causally connected sphere

We have not presented in this last subsection the derivatives of the average $\langle S\rangle_{A_0}^{V_0}$, namely the Buchert-Ehlers relations for the causally connected sphere case. Let us give these general expressions here and we will check in Sec. 3.6.2 that their expressions make us recover the usual average on spatial hypersurfaces.

Starting with the definition of the integral $I(1;A_0;V_0)$ presented in Eq. (2.88) we get the derivative with respect to A_0 of the average (2.94) :

$$\begin{aligned}\partial_{A_0}\langle S\rangle_{A_0}^{V_0} &= \left\langle\frac{\nabla\cdot k}{k\cdot\partial A}S\right\rangle_{A_0}^{V_0}+\left\langle\frac{k^\mu}{\sqrt{-(\partial A)^2}}\nabla_\mu\left[\frac{\sqrt{-(\partial A)^2}}{k\cdot\partial A}S\right]\right\rangle_{A_0}^{V_0} \\ &-\langle S\rangle_{A_0}^{V_0}\left\langle\frac{k^\mu}{\sqrt{-(\partial A)^2}}\nabla_\mu\left[\frac{\sqrt{-(\partial A)^2}}{k\cdot\partial A}\right]\right\rangle_{A_0}^{V_0}\ ,\end{aligned} \tag{2.107}$$

and with respect to the null parameter V_0, the derivation gives :

$$\begin{aligned}\partial_{V_0}\langle S\rangle_{A_0}^{V_0} &= \left\langle\frac{1}{\sqrt{-(\partial A)^2}}\nabla_\mu\left[\left(\partial^\mu A-k^\mu\frac{(\partial A)^2}{k\cdot\partial A}\right)\frac{\sqrt{-(\partial A)^2}}{k\cdot\partial A}S\right]\right\rangle_{A_0}^{V_0} \\ &-\langle S\rangle_{A_0}^{V_0}\left\langle\frac{1}{\sqrt{-(\partial A)^2}}\nabla_\mu\left[\left(\partial^\mu A-k^\mu\frac{(\partial A)^2}{k\cdot\partial A}\right)\frac{\sqrt{-(\partial A)^2}}{k\cdot\partial A}\right]\right\rangle_{A_0}^{V_0}\ .\end{aligned} \tag{2.108}$$

2.4 The FLRW Universe

In order to prepare the calculation of Chapter 4, we shall proceed to the consistency check that no backreaction occurs in a general homogeneous FLRW Universe. We will use the general average over spatial hypersurfaces (see Sec. 2.1.3) but this result can also be verified with lightcone averages.

Taking the FLRW metric in cosmic time such as the one defined in Eq. (1.1), we can recast it in an ADM-metric form (see Eq. (2.67)) by $N = 1$, $N^i = 0$ and $g_{ij} = a^2(t)\gamma_{ij}(|\mathbf{x}|)$. We thus have the expansion scalar from Eq. (2.69):

$$\Theta(t,\mathbf{x}) = \partial_t \ln\left(a^3(t)\sqrt{\det\gamma_{ij}(|\mathbf{x}|)}\right) = 3\frac{\dot{a}(t)}{a(t)} \equiv 3H(t) \quad . \tag{2.109}$$

Taking $A(x) \equiv t$ imposes then that the non-commutation terms in Eq. (2.70) cancel out:

$$\left\langle \frac{\Theta N}{\partial_t A} S\right\rangle_{A_0} - \left\langle \frac{\Theta N}{\partial_t A}\right\rangle_{t_0} \langle S\rangle_{t_0} = \langle 3H(t)S\rangle_{t_0} - \langle 3H(t)\rangle_{t_0}\langle S\rangle_{t_0} = 0 \quad . \tag{2.110}$$

Thus, no backreaction is present in the homogeneous FLRW model. In fact, the condition for Eq. (2.70) to exibit a non-commutation form is that $\det(g_{ij})$ must be a function of $(t,\mathbf{x})$ which is non-factorizable as $f(t)\times g(\mathbf{x})$. This is the case of perturbed spacetimes where perturbations of the spatial metric are generally $(t,\mathbf{x})$-dependent. As a consequence, backreaction occurs in many types of inhomogeneous geometries.

Let us now consider the generalization of the Friedmann equations in the context of backreaction, Eq. (2.78) and (2.79), and show that they reduce to the usual Friedmann equation in the homogeneous limit. We know in that case that we can use the ADM formalism with $N^i = 0$ and $N = 1$ and that directly lead to $n_\mu = (-1,\vec{0})$ and $n^\mu = (1,\vec{0})$. We also have that $A(t) \equiv t$ which gives the same result. In that case we find that the expansion scalar is

$$\Theta \equiv \nabla_\mu n^\mu = \partial_\mu n^\mu + \Gamma^\mu_{\mu\rho} n^\rho = \Gamma^\mu_{\mu 0} = H\delta^i_i = 3H(t) \quad . \tag{2.111}$$

We thus find that the effective scale factor reduces to the usual one:

$$\frac{1}{\tilde{a}}\frac{\partial\tilde{a}}{\partial A_0} \equiv \frac{1}{3}\left\langle \frac{\Theta}{[-(\partial A)^2]^{1/2}}\right\rangle_{A_0} = \frac{1}{3}\langle 3H(t)\rangle_{t_0} = H(t) \equiv \frac{\partial_t a(t)}{a(t)} \quad . \tag{2.112}$$

We can also see that the system of Eqs. (2.78,2.79) greatly simplifies. Indeed, the facts that $\Theta = 3H(t)$, $A(t) \equiv t$ and $\langle\ldots\rangle = \langle\ldots\rangle_{t_0}$ cancel the variance $\langle\Theta^2\rangle_{A_0} - \langle\Theta\rangle^2_{A_0}$, lead to:

$$\left(\frac{1}{\tilde{a}}\frac{\partial\tilde{a}}{\partial A_0}\right)^2 = \frac{8\pi G}{3}\langle\epsilon\rangle_{A_0} - \frac{1}{6}\langle\mathcal{R}_S\rangle_{A_0} + \frac{1}{3}\langle\sigma^2\rangle_{A_0} \quad , \tag{2.113}$$

$$-\frac{1}{\tilde{a}}\frac{\partial^2\tilde{a}}{\partial {A_0}^2} = \frac{4\pi G}{3}\langle\epsilon + 3\pi\rangle_{A_0} - \frac{1}{3}\langle\nabla^\nu(n^\mu\nabla_\mu n_\nu)\rangle_{A_0} + \frac{1}{6}\langle(\partial_\mu A\partial^\mu[(\partial A)^2])\Theta\rangle_{A_0} + \frac{2}{3}\langle\sigma^2\rangle_{A_0} \tag{2.114}$$

We can remark that $(\partial A)^2 = -1$, so $\partial_\mu A\partial^\mu[(\partial A)^2] = 0$. In a FLRW model, we have the projection tensor on the spatial hypersurfaces which is

$$h_{\mu\nu} = \delta^i_\mu\delta^j_\nu a^2\gamma_{ij} \quad , \quad h^{\mu\nu} = \delta^\mu_i\delta^\nu_j a^2\gamma^{ij} \quad , \quad h_{i\mu}h^{\mu j} = \delta^j_i \quad . \tag{2.115}$$

We thus find that the shear tensor defined in Eq. (2.3) is zero:

$$\begin{aligned}\sigma_{\mu\nu} &= h^\alpha{}_\mu h^\beta{}_\nu\left(\nabla_{(\alpha}n_{\beta)} - \frac{1}{3}h_{\alpha\beta}\nabla_\gamma n^\gamma\right) = \delta^\alpha_\mu\delta^\beta_\nu\left(-\Gamma^0_{\alpha\beta} - \frac{h_{\alpha\beta}}{3}3H(t)\right)\\ &= -\delta^i_\mu\delta^j_\nu\Gamma^0_{ij} - (a^2\gamma_{ij}\delta^i_\mu\delta^j_\nu)H(t) = 0 \quad ,\end{aligned} \tag{2.116}$$

and so the shear scalar $\sigma \equiv \sqrt{\frac{1}{2}\sigma_i{}^j\sigma_j{}^i}$ is zero. We can also show that the vorticity tensor is null:

$$\omega_{\mu\nu} = h^\alpha{}_\mu h^\beta{}_\nu\frac{1}{2}(\nabla_\alpha n_\beta - \nabla_\beta n_\alpha) = 0 \quad \text{as} \quad \nabla_\alpha n_\beta = \Gamma^\lambda_{\alpha\beta}n_\lambda = -\Gamma^0_{\alpha\beta} = \nabla_\beta n_\alpha \quad . \tag{2.117}$$

And we see that $\nabla^\nu(n^\mu\nabla_\mu n_\nu) = \nabla^0(n^0\nabla_0 n_0) = 0$ as $\nabla_0 n_0 = \Gamma^\lambda_{00} n_\lambda$ and $\Gamma^\lambda_{00} = 0 \ \ \forall\ \lambda$.

We thus proved that the system of equations (2.78,2.79) is equivalent to

$$\left(\frac{1}{\tilde{a}}\frac{\partial \tilde{a}}{\partial A_0}\right)^2 = \frac{8\pi G}{3}\langle\epsilon\rangle_{A_0} - \frac{1}{6}\langle\mathcal{R}_S\rangle_{A_0} \quad , \quad -\frac{1}{\tilde{a}}\frac{\partial^2 \tilde{a}}{\partial {A_0}^2} = \frac{4\pi G}{3}\langle\epsilon + 3\pi\rangle_{A_0} \quad .$$

For a perfect fluid which is homogeneous, we cannot distinguish a particuliar velocity and we can take $u_\mu = (-1, \vec{0}\,)$ and $u^\mu = (1, \vec{0}\,)$. From the definitions of ϵ and π given in Eq. (2.73), we see that the terms going as $(1 - (u^\mu n_\mu)^2)$ are zero and we simply get that $\epsilon = \rho$ and $\pi = p$. Also, one has

$$\sigma^2 = \frac{1}{2}\left(\Theta^\mu{}_\nu\Theta^\nu{}_\mu - \frac{\Theta^2}{3}\right) = 0 \quad \Rightarrow \quad \Theta^\mu{}_\nu\Theta^\nu{}_\mu = 3H^2(t) \quad , \tag{2.118}$$

$$\mathcal{R}_s + \Theta^2 - \Theta^\mu{}_\nu\Theta^\nu{}_\mu = 16\pi G\,\epsilon \quad , \tag{2.119}$$

where the second equation is obtained from Eqs. (A.24) and (A.34) (with $\Lambda = 0$). We thus have

$$\mathcal{R}_s = -6H^2 + 16\pi G\rho = \frac{6K}{a^2} \quad , \tag{2.120}$$

as expected for the 3-dimensional spatial curvature in the FLRW model.

We are left with equations which depend only on $\langle\rho\rangle_{A_0}$ and $\langle p\rangle_{A_0}$ on the RHS. These two quantities being only time dependent in the FLRW Universe, we have shown that the generalized Friedmann equations reduce to the Friedmann equations of Eqs. (1.16,1.17) in the FLRW model (where we took $\Lambda = 0$ here). Finally, we directly see that the averaged conservation equation

$$\frac{\partial\langle\rho\rangle_{A_0}}{\partial A_0} = -\left\langle\frac{\Theta\ p}{[-(\partial A)^2]^{1/2}}\right\rangle_{A_0} - \langle\rho\rangle_{A_0}\left\langle\frac{\Theta}{[-(\partial A)^2]^{1/2}}\right\rangle_{A_0} \quad , \tag{2.121}$$

simply reduces to the usual conservation equation for a perfect fluid $\dot{\rho} + 3H(\rho + p) = 0$.

We thus arrived to the conclusion that perturbations are needed to generate a backreaction effect in a FLRW model. In this spirit, we will compute in Chapter 4 the luminosity at second order in perturbations and will exploit this result in the other chapters.

Chapter 3

The GLC metric and its properties

This section is devoted to the geometrical description of a 4-dimensional spacetime in terms of a lightcone foliation. We introduce first an historical system of coordinates called the *observational coordinates* (substantially developed in [51] and [59]). We then define the *geodesic lightcone* (GLC) *coordinates* that will be a powerful tool in our subsequent calculations. These new coordinates share a large number of properties with the observational coordinates but are different on certain points. They have particularly nice features with, for example, the property to simplify the expressions of the redshift and the luminosity distance, and finally the lightcone averages.

3.1 Observational coordinates

In the observational coordinates, one considers the world line $\mathscr{C}$ of an observer and its past lightcones in a 4-dimensional spacetime. The past lightcones are set by a null coordinate $w \equiv x^0$ and a particular one is given by the condition $w = \text{cst}$. To fully fix this coordinate, we assume it to be equal to the proper time along the world line $\mathscr{C}$, i.e. $w|_{\mathscr{C}} = \tau|_{\mathscr{C}}$, and set its value to w_0 today. The null geodesic vector field describing the photon path on a lightcone is then given by

$$k^\mu = dx^\mu/dv \quad , \quad k_\mu = \partial_\mu w \quad , \quad k_\mu k^\mu = 0 \ , \tag{3.1}$$

where v is an affine parameter along this null geodesic (with the condition $v = 0$ along $\mathscr{C}$). The consequence of this definition is that k^μ is a hypersurface-orthogonal ($\nabla_\mu k_\nu = \nabla_\nu k_\mu$) null geodesic ($k^\mu \nabla_\mu k^\nu = 0$) vector field, orthogonal to the constant-w hypersurfaces ($\partial_\mu w \, k^\mu = 0$). We thus have $k_\mu u^\mu = \partial_\mu w \, u^\mu$ and $k_\mu u^\mu|_{\mathscr{C}} = 1$, where u^μ is the velocity of the observer.

The photon geodesic is a line along a past light cone that keeps the same angles $\theta \equiv x^2$ and $\phi \equiv x^3$ (i.e. $\partial_\mu \theta \, k^\mu = 0 = \partial_\mu \phi \, k^\mu$). They are properly normalized by imposing that they are spherical coordinates along $\mathscr{C}$, so:

$$\left\{ \lim_{v \to 0} \left(\frac{ds^2}{v^2} \right) \ / \ w = \text{cst}, v = \text{cst} \right\} = d\theta^2 + (\sin\theta)^2 d\phi^2 \equiv d^2\Omega \ . \tag{3.2}$$

The last coordinate used here, called $y \equiv x^1$, determines the "distance" down the null geodesic. Different choices are proposed by [59]:

1. $y = v$: the affine parameter with the conditions $v|_{\mathscr{C}} = 0$ and $u_\mu k^\mu|_{\mathscr{C}} = 1$.
2. $y = R$: the angular distance (denoted by r in [59] [1]) from $\mathscr{C}$.
3. $y = z$: the redshift observed from $\mathscr{C}$.
4. mixed y: one of the three cases above to set the distance on $w = w_0$ and then we take y to comove with the fluid, i.e. $\partial_\mu y \, u^\mu = 0$. We thus have $y = 0$ on all the world line $\mathscr{C}$.

1. For this section only we will use R to denote the angular distance. After, it will be written as d_A.

We can see that the condition $y \to 0$ is equivalent to $v \to 0$ or $R \to 0$. One should be careful with cases 2. and 3. as the angular distance and the redshift are not in general monotonic functions of the affine parameter v. This is thus the last case, number 4., which is chosen in [59]. Its comoving property also makes it easy and unambiguous. Because of the conditions $\partial_\mu w\, k^\mu = 0 = \partial_\mu \theta\, k^\mu = \partial_\mu \phi\, k^\mu$, we have:

$$k_\mu = \delta^0_\mu \quad \Rightarrow \quad k^\mu = \frac{dx^\mu}{dv} = \frac{1}{\beta}\delta^\mu_1 \quad \text{with} \quad \beta = \frac{dy}{dv} > 0 \quad . \tag{3.3}$$

The metric describing our geometry in these coordinates (w, y, θ, ϕ) is obtained as follows. From $k_\mu k^\mu = 0 = \partial_\mu w\, \partial_\nu w\, g^{\mu\nu}$ we get that $g^{00} = 0$. The condition $k^\mu = g^{\mu\nu} k_\nu$ imposes $g^{\mu 0} = (1/\beta)\delta^\mu_1$. Introducing new functions for the non-constrained components, we get the general expression of $g^{\mu\nu}$ and we can compute its inverse. We thus have, in (w, y, θ, ϕ)-coordinates:

$$g_{\mu\nu} = \begin{pmatrix} \alpha & \beta & v_2 & v_3 \\ \beta & 0 & 0 & 0 \\ v_2 & 0 & h_{22} & h_{23} \\ v_3 & 0 & h_{23} & h_{33} \end{pmatrix} \quad , \quad g^{\mu\nu} = \begin{pmatrix} 0 & 1/\beta & 0 & 0 \\ 1/\beta & \delta & \sigma_2 & \sigma_3 \\ 0 & \sigma_2 & h_{33}/h & -h_{23}/h \\ 0 & \sigma_3 & -h_{23}/h & h_{22}/h \end{pmatrix} \quad , \tag{3.4}$$

where $h = \det(h_{ab}) \equiv h_{22}h_{33} - (h_{23})^2$ (with $a, b = 2, 3$), $\delta \equiv -(\alpha + \beta(v_2\sigma_2 + v_3\sigma_3))/\beta^2$, $\sigma_2 = -(v_2 h_{33} - v_3 h_{23})/\beta h$ and $\sigma_3 = -(v_3 h_{22} - v_2 h_{23})/\beta h$. One should thus remark that the observational metric depends on seven arbitrary functions which are β, δ, σ_2, σ_3, h_{22}, h_{33} and h_{23}. The angular distance R can be defined in terms of these functions as:

$$R^4 (\sin\theta)^2 = h \equiv \det(h_{ab}) \quad . \tag{3.5}$$

The metric of Eq. (3.4) implies that the hypersurfaces $w = \text{cst}$ are null. Nevertheless, as it stands, this metric does not garantee that these null hypersurfaces are the past lightcones of the geodesic world line $\mathscr{C}$. To set this property, one has to impose some limits near the world line. When the coordinate y is taken to be v or R, these limits are:

$$\lim_{y\to 0} \alpha = -1 \quad , \quad \lim_{y\to 0} \beta = 1 \quad , \quad \lim_{y\to 0} (v_a/y^2) = 0 \quad , \quad \lim_{y\to 0} (h_{ab} dx^a dx^b/y^2) = d^2\Omega \quad , \tag{3.6}$$

where $d^2\Omega \equiv \sin\theta d\theta d\phi$ is the standard solid angle on the sphere. When this coordinate y is taken to be z or the last case 4. described above, one has a regular relation between y and v. The limits are found to be:

$$\lim_{y\to 0} \alpha = -1 \quad , \quad \lim_{y\to 0} \beta = \beta_0(w, x^i) \quad , \quad \lim_{y\to 0} (v_a) = 0 \quad , \quad \lim_{y\to 0} (h_{ab} dx^a dx^b/y^2) = \beta_0^2(w, x^i)\, d^2\Omega \quad . \tag{3.7}$$

These conditions that we described are the necessary conditions to make the null hypersurfaces be the past lightcones of the observer world line $\mathscr{C}$ and they garantee that the angular coordinates are correctly related to the angles as seen from $\mathscr{C}$. More precisely, the direction made by these angles is now based on a parallely propagated tetrad of vectors [2] along $\mathscr{C}$. We recall also that w is the proper time along $\mathscr{C}$. These properties define the so called *observational coordinates*.

3.2 The geodesic light-cone gauge

3.2.1 Presentation

One of the main virtues of using a gauge invariant formalism is the freedom of choosing a gauge particularly adapted to the problem at hand. In the case of spacelike averaging, for instance, a

2. These tetrad vectors $\mathbf{e}_\mu$ are defined through the conditions:

$$\mathbf{e}_0 = \mathbf{u} \quad , \quad \mathbf{u}\cdot\mathbf{e}_i = 0 \quad , \quad \mathbf{e}_i \cdot \mathbf{e}_j = \delta_{ij} \quad ,$$

and thus satisfy the parallel propagation along $\mathscr{C}$: $\nabla_{\mathbf{u}}\, \mathbf{e}_\mu|_{\mathscr{C}} = 0$, with $\mathbf{u}$ the velocity of the comoving geodesic observer.

convenient coordinate system corresponds to the case where we average over the constant-time hypersurfaces. Indeed, in many applications the averaging hypersurfaces are chosen to be associated to a class of geodesic observers described by the time parameter t of a synchronous gauge (see e.g. [86]). Similarly, for light-cone averages, it is convenient to identify the null hypersurfaces with those on which a null coordinate takes constant values. It is also useful to have a coordinate to describe the proper time measured by an observer in geodetic motion. For this reason we now turn to a special (adapted) coordinate system $x^\mu = (\tau, w, \tilde{\theta}^a)$, $a = 1, 2$ (with sometimes the change in notations: $\tilde{\theta}^1 \equiv \tilde{\theta}$ and $\tilde{\theta}^2 \equiv \tilde{\phi}$). These coordinates define what we have called the "geodesic light-cone" (GLC) coordinates, or gauge.

3.2.2 Mathematical definition

The GLC metric depends on six arbitrary functions: a scalar Υ, a two-dimensional "vector" U^a and a symmetric matrix γ_{ab} (with inverse γ^{ab}). Its line element takes the form:

$$ds^2_{GLC} = \Upsilon^2 dw^2 - 2\Upsilon dw d\tau + \gamma_{ab}(d\widetilde{\theta}^a - U^a dw)(d\widetilde{\theta}^b - U^b dw) \quad . \tag{3.8}$$

Clearly w is a null coordinate (i.e. $\partial_\mu w \, \partial^\mu w = 0$), and a past light-cone hypersurface is specified by the condition $w = \text{cst}$. We can also easily check that $\partial_\mu \tau$ defines a geodesic flow, i.e. that

$$(\partial^\nu \tau) \, \nabla_\nu \, (\partial_\mu \tau) = 0 \quad , \tag{3.9}$$

as a consequence of the relation $g^{\tau\tau}_{GLC} = -1$. Thus an observer defined by constant τ spacelike hypersurfaces is in geodesic motion. In matrix form, the metric and its inverse in the $(\tau, w, \widetilde{\theta}^a)$-coordinates are given by:

$$g^{GLC}_{\mu\nu} = \begin{pmatrix} 0 & -\Upsilon & \vec{0} \\ -\Upsilon & \Upsilon^2 + U^2 & -U_b \\ \vec{0}^T & -U^T_a & \gamma_{ab} \end{pmatrix} \quad , \quad g^{\mu\nu}_{GLC} = \begin{pmatrix} -1 & -\Upsilon^{-1} & -U^b/\Upsilon \\ -\Upsilon^{-1} & 0 & \vec{0} \\ -(U^a)^T/\Upsilon & \vec{0}^T & \gamma^{ab} \end{pmatrix} \quad , \tag{3.10}$$

where $\vec{0} = (0, 0)$ and $U_b = (U_1, U_2)$, while the 2×2 matrices γ_{ab} and γ^{ab} lower and raise the two-dimensional indices. We also have that:

$$\sqrt{-g} = \Upsilon \sqrt{|\gamma|} \qquad \text{with} \qquad g \equiv \det g^{GLC}_{\mu\nu} \qquad \text{and} \qquad \gamma \equiv \det \gamma_{ab} \quad . \tag{3.11}$$

This GLC metric has all the required degrees of freedom for applications to general geometries. It is also really well adapted to computations of quantities related to light signals, as we shall see in Sec. 3.3 and Sec. 3.4. We will also see in Sec. 3.6 that it greatly simplifies the so-called averages on the light cone.

In the limiting case of a spatially flat FLRW geometry, with scale factor a, cosmic time t, and conformal time parameter η such that $d\eta = dt/a$, the transformations to the GLC coordinates and the meaning of the metric components are easily found, from Eq. (3.8), to be:

$$\begin{gathered} \tau = t \quad , \quad w = r + \eta \quad , \quad \widetilde{\theta}^1 = \theta \ , \ \widetilde{\theta}^2 = \phi \ , \\ \Upsilon = a(t) \quad , \quad U^a = 0 \quad , \quad \gamma_{ab} d\tilde{\theta}^a d\tilde{\theta}^b = a^2(t) r^2 (d\theta^2 + \sin^2\theta d\phi^2) \quad . \end{gathered} \tag{3.12}$$

When we authorize a possible curvature, this limit is simply changed in w, which becomes $w = \chi + \eta$ where χ has been defined in Eq. (1.1), and the expression of $\gamma_{ab} d\tilde{\theta}^a d\tilde{\theta}^b$ is unchanged, r being defined by Eq. (1.2). We notice in passing that $\gamma_{ab} \propto a^2(t)$ in the homogeneous FLRW case (and should not be confused with the metric element γ_{ij} of Eq. (1.1)). Even though we will be mainly using the GLC gauge for a perturbed FLRW metric in the Newtonian gauge, it is important to stress that the equality between the coordinate τ and the proper time t of the synchronous gauge holds at the exact, non perturbative level. In fact, it is always possible to choose the GLC coordinates in such a way that τ and t are identified like in the above FLRW limit. As a consequence we can easily introduce with τ a family of geodetic reference observers which exactly coincide with the static ones of the synchronous gauge. We shall illustrate this point in Sec. 3.5.1.

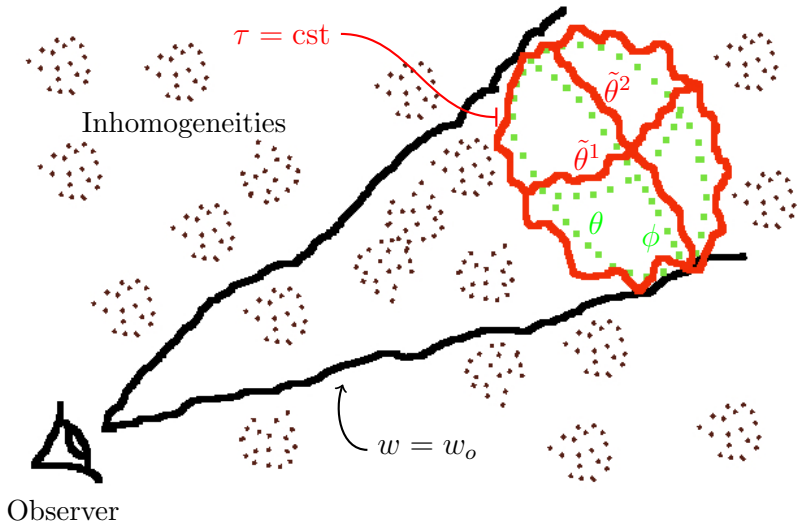

Figure 3.1: Illustration of the GLC coordinates. The observer sees the sky as the superposition of 2-spheres $\Sigma(w_o, \tau)$ embedded in the (lightcone) hypersurface $w = w_o$ at different times τ (in red). The homogeneous 2-sphere (in green) is parametrized by the angles $\theta^a = (\theta, \phi)$ whereas the presence of inhomogeneities deformes the lightcone and $\Sigma(w_o, \tau)$ is parametrized by the angles $\widetilde{\theta}^a = (\widetilde{\theta}, \widetilde{\phi})$. Photons travel at constant $(w, \widetilde{\theta}^a)$ so that a source keep the same angular coordinates along the way.

To give a more intuitive picture of these coordinates, we present a useful way to visualize the GLC coordinates in Fig. 3.1. The constant τ and constant w hypersurfaces intersect each other on a 2-dimensional surface $\Sigma(w_o, \tau_s)$ which is topologically a sphere but is deformed with respect to the standard 2-sphere in the general case. Let us notice finally that this 2-sphere can be expressed as a constant redshift hypersurface, by the use of the Eq. (3.18) that we will present later. In that case, it corresponds to the constant Υ hypersurface on the past light cone.

3.2.3 Differences with the observational coordinates

When specifying the metric in the GLC gauge, the coordinates $(\tau, w, \widetilde{\theta}^a)$ correspond to a complete gauge fixing (modulo residual transformations involving non-generic functions, i.e. not depending on all coordinates) of the so-called observational coordinates, defined e.g in [51,59,87] and recalled in Sec. 3.1. We should underline that descriptions in both systems of coodinates break down when caustics appear on the past light cones (as w becomes multivalued).

Nevertheless, several facts make the GLC metric slightly different from the observational coordinates. We note that these latter ones use the coordinates (w, y, x^2, x^3) whereas the GLC metric uses $(\tau, w, \widetilde{\theta}^a)$. The first difference is thus an inversion in the order of the first two coordinates responsible for the apparently exchanged roles of the metrics presented in Eqs. (3.4) and (3.10). This is an irrelevant difference. The second, much more serious, is that y is a spatial distance or a null distance on the past lightcone. In the GLC metric case, y is replaced by a time coordinate which is τ. This is a significant difference and it is motivated, on the GLC side, by the intention to have a system of coordinates which is both adapted to the observation of the source and the proper time of the observer. Another difference, less important, is the fact that the past lightcone on which the observations are made is set by the condition $w|_{\mathscr{C}} = \tau|_{\mathscr{C}}$ (with τ the proper time of the observer) in the observational coordinates whereas it is set by $w = \int d\tau/a(\tau) \equiv \eta$ in the GLC gauge (where $a(\tau)$ was defined as the homogeneous limit of the Υ function), i.e. from the conformal time at this local position. A very important difference as we have seen is also that the observational metric has seven arbitrary functions where the GLC metric only has six. It is in this sense, and forgetting about the other differences mentioned here, that we can say that the GLC gauge is a "further gauge fixing" of the observational coordinates.

3.3 Redshift in the GLC metric

In the GLC coordinates a past light-cone hypersurface is specified by the condition $w = w_o$, and the momentum of a photon traveling on it, being proportional to $k_\mu = \partial_\mu w$, is orthogonal both to itself ($k_\mu k^\mu = 0$) and to the 2-surface generated by ∂_{θ^a} ($\partial_\mu \theta^a k^\mu = 0$). The velocity of a generic observer defined by a scalar A can be written as :

$$n_\mu = -\frac{\partial_\mu A}{\sqrt{-\partial_\nu A \partial^\nu A}} \qquad \text{with} \qquad n_\mu n^\mu = -1 \quad , \tag{3.13}$$

and thus its scalar product with k_μ satisfies :

$$k_\mu n^\mu = \frac{1}{\Upsilon} \frac{\partial_\tau A}{\sqrt{-(\partial A)^2}} \quad . \tag{3.14}$$

For our geodesic observer, A depends only on τ and we can always set $A = \tau$, so the vector n_μ becomes $n_\mu = -\partial_\mu \tau = u_\mu$ and the above relation simplifies to :

$$k_\mu u^\mu = \Upsilon^{-1} \quad . \tag{3.15}$$

We also note for later use that, in these coordinates, the covariant divergence of k^μ takes the simple form :

$$\nabla_\mu k^\mu = -\frac{1}{\Upsilon} \partial_\tau \left(\ln \sqrt{|\gamma|} \right) \quad . \tag{3.16}$$

We also remark that, in GLC coordinates, the null geodesics connecting sources and observer are characterized by the simple tangent vector $k^\mu = g^{\mu\nu}_{GLC} \partial_\nu w = g^{\mu w}_{GLC} = -\delta^\mu_\tau \Upsilon^{-1}$, which means that photons reach the observer travelling at constant w and $\widetilde{\theta}^a$ (as it was the case in the observational coordinates). This makes the calculation of the redshift particularly easy.

Let us denote by the subscripts "o" and "s", respectively, a quantity evaluated at the observer and source spacetime position, and consider a light ray emitted by a static geodetic source lying at the intersection between the past light-cone of a static geodetic observer (defined by the equation $w = w_o$) and the spatial hypersurface $\tau = \tau_s$ where τ_s is for the moment considered as a constant parameter, the moment of source's emission. Both the observer and the source are in geodetic motion and have a velocity $u_\mu = -\partial_\mu \tau$ in the GLC gauge. They are however static in synchronous gauge. The light ray will be received by the geodetic observer at $\tau = \tau_o > \tau_s$. The redshift z_s associated with this light ray of momentum k^μ is then given by :

$$(1 + z_s) = \frac{(k^\mu u_\mu)_s}{(k^\mu u_\mu)_o} \quad . \tag{3.17}$$

Note that this object may be regarded as a bi-scalar, as it depends on the ratio of the same scalar quantity calculated in two different spacetime points. Using in particular Eq. (3.15), we get :

$$(1 + z_s) = \frac{(\partial^\mu w \partial_\mu \tau)_s}{(\partial^\mu w \partial_\mu \tau)_o} = \frac{\Upsilon(w_o, \tau_o, \widetilde{\theta}^a)}{\Upsilon(w_o, \tau_s, \widetilde{\theta}^a)} \equiv \frac{\Upsilon_o}{\Upsilon_s} \quad . \tag{3.18}$$

We should stress that the redshift, in this GLC gauge as in the FLRW case, is immediately given by an entry of the metric (evaluated at the source and observer positions). This equation will be used in Sec. 4.2.1 in connection with the redshift and luminosity distance. We shall be interested in averaging the luminosity at fixed redshift also, hence on the two-dimensional surface $\Sigma(w_o, z_s)$ (topologically a sphere) which lies on our past light-cone ($w = w_o$) and is associated with a fixed redshift ($z = z_s$, see Sec. 3.6). In terms of the τ coordinate such a surface corresponds to the equation $\tau = \tau_s(w_o, z_s, \tilde{\theta}^a)$. Hereafter τ_s will denote this (in general angle-dependent) quantity.

3.4 Luminosity distance in the GLC gauge

In a cosmological context we can define at least three different distances of physical interest (see e.g. [2]) : d_A, namely the angular distance of the source as seen from the observer (in the FLRW limit of Eq. (3.12) we have $d_A = a(t_s)\, r_s$, where r_s is the comoving radial distance of the source); d_o, namely the angular distance of the observer "as seen from" the source (in the FLRW limit we have $d_o = a(t_0)\, r_s$); and d_L, the so-called luminosity distance (as seen from the observer). These three observational distances are always related to each other, independently of the given cosmological model, by redshift factors [28, 88] :

$$d_L = (1+z)d_o = (1+z)^2 d_A \quad , \tag{3.19}$$

as a consequence of the Etherington reciprocity law [18], valid in any general spacetime.

On the other hand, in a general spacetime, we can also identify (point-by-point on the 2-sphere) the square of the angular distance of the source [89], by :

$$d_A^2 \equiv \frac{dS_s}{d^2\Omega_o} \quad , \tag{3.20}$$

where $d^2\Omega_o$ is the infinitesimal solid angle subtended by the source at the observer position, and dS_s is the area element on the surface orthogonal to both the photon momentum and to the source 4-velocity at the source's position. It is easy to check (see Sec. 3.4.2) that the surface dS_s is characterized by having constant w and τ, and that the induced 2-metric on it is nothing but γ_{ab}.

Let us now show, by two different methods, that

$$d_A^2 = \frac{d^2\tilde{\theta}\sqrt{\gamma_s}}{d^2\tilde{\theta}\sin\tilde{\theta}} = \frac{\sqrt{\gamma_s}}{\sin\tilde{\theta}} \quad , \tag{3.21}$$

where we will use the fact that photons travel at constant $\tilde{\theta}^a$ in the GLC geometry. The direct consequence of this identity gives, from Eq. (3.19), the important non-perturbative expression for d_L :

$$d_L = (1+z)^2\, \gamma_s^{1/4} \left(\sin\tilde{\theta}^1\right)^{-1/2} \quad . \tag{3.22}$$

Let us note that the averaging surface $\Sigma(w_o, z_s)$, being one of constant z, differs from the one of constant w and τ but – amusingly – the same formula holds, locally, for the area element on it, so that Eq. (3.21) will also be usable for our light-cone averages defined on $\Sigma(w_o, z_s)$.

This relation of Eq. (3.22) shows that the GLC coordinates are also very well adapted to the computation of the luminosity distance. We can indeed see that this relation involves only the determinant of a GLC metric entry, namely the 2×2 matrix γ_{ab} parametrizing the angular geometry around the source location. This fact will have important consequences on the simplicity of the expression of the averaged flux that will be presented in Sec. 5.3.1. We now present two methods proving Eq. (3.22).

3.4.1 Proof of Eq. (3.22) – method 1

In our GLC gauge we have $k^\mu = (0, -1/\Upsilon, 0, 0)$ and as already mentioned the 2-sphere embedded in the light-cone is orthogonal to the photon momentum, so that the cross-sectional area element is proportional to $\sqrt{|\gamma|}d\theta^1 d\theta^2$. Therefore, d_A^2 can be written as :

$$d_A^2(w = w_o, \tau_s, \theta^a) = \lim_{\rho\to 0}\ \rho^2 \frac{\sqrt{|\gamma_s|}}{\sqrt{|\gamma(\rho)|}} \quad , \tag{3.23}$$

where ρ is the proper radius of an infinitesimal sphere centered around the observer, $w = w_o$ defines the past light-cone connecting source and observer, and $\tau = \tau_s$ defines the spacelike hypersurface normal to n^μ at the source position. Eq. (3.23) easily reduces to $d_A = a(t_s)\, r_s$ in the FLRW case of Eq. (3.12).

Let us now discuss how the well known homogeneous result for d_L is modified when including generic inhomogeneities. We recall, to this purpose, that in a generic metric background the angular distance d_A can be computed by considering the null vector $k^\mu = dx^\mu/d\lambda$ tangent to the null ray connecting source and observer (i.e. belonging to the congruence of null geodesics forming the observer's past light-cone). Here λ is an affine parameter along the ray trajectory, chosen in such a way that $\lambda = 0$ at the observer and $\lambda = \lambda_s$ at the source position. The expansion $\hat{\Theta}$ of the congruence of null rays is then given by $\hat{\Theta} = \nabla_\mu k^\mu$, and the corresponding angular distance d_A is defined by the differential equation [59, 90]:

$$\frac{d}{d\lambda}\left(\ln d_A\right) = \frac{\hat{\Theta}}{2} = \frac{1}{2}\nabla_\mu k^\mu \quad . \tag{3.24}$$

Consider now a generic metric in the GLC gauge, and the null vector $k_\mu = \partial_\mu w$ such that $k^\mu = dx^\mu/d\lambda = -\delta^\mu_\tau \Upsilon^{-1}$. We have, in this case,

$$\nabla_\mu k^\mu = -\Upsilon^{-1}\partial_\tau\left(\ln\sqrt{\gamma}\right) = \frac{d}{d\lambda}\left(\ln\sqrt{\gamma}\right) \quad , \tag{3.25}$$

where $\gamma = \det\gamma_{ab}$, and the integration of Eq. (3.24) gives, in general,

$$d_A^2(\lambda) = c\sqrt{\gamma(\lambda)} \quad , \tag{3.26}$$

where c is independent of λ. In order to fix the constant c we may recall the boundary conditions required to guarantee that the null rays generated by k^μ belong to the past light cones centered on the world line of our observer. Considering the limit $d_A \to 0$ (or $\lambda \to 0$), and using the already mentioned fact that $\widetilde{\theta}^a$ is constant along the null geodesic, such conditions require in particular that [59]

$$\lim_{\lambda\to 0}\frac{\sqrt{\gamma}}{d_A^2} = \sin\widetilde{\theta}^1 = \sin\theta^1_o \quad , \tag{3.27}$$

where, in the last equality, we have used θ^1_o to denote the standard angle on the sphere at the observer position. This clearly fixes $c = 1/\sin\tilde{\theta}^1$, and uniquely determines the angular distance as

$$d_A(\lambda) = \gamma^{1/4}(\lambda)\left(\sin\tilde{\theta}^1\right)^{-1/2} \quad . \tag{3.28}$$

3.4.2 Proof of Eq. (3.22) – method 2

Let us remark that γ_{ab} is nothing but the induced metric on the surface $\Sigma(w_o, \tau_s)$ provided this is parametrized in terms of the two "world-sheet" coordinates $\xi^a \equiv \tilde{\theta}^a$ and otherwise given by $w = w_o$, $\tau = \tau_s(w_o, z_s, \tilde{\theta}^a)$. Using the standard definition of an induced metric:

$$\gamma^{ind}_{ab} = \frac{\partial x^\mu}{\partial\xi^a}\frac{\partial x^\nu}{\partial\xi^b}g^{GLC}_{\mu\nu}(x) \quad , \tag{3.29}$$

manifestly independent of the spacetime coordinates x^μ being used, we simply find:

$$\gamma^{ind}_{ab} = \gamma_{ab} \quad , \tag{3.30}$$

since $w = w_o$ (independently of $\tilde{\theta}^a$) and the only non-zero entry for the metric with a lower index τ is $g^{GLC}_{\tau w}$. We can also argue that the area element computed on this surface is orthogonal to the null geodesics and can therefore be identified with dS_s in Eq. (3.20). Indeed, consider the projection of the photon momentum along the constant-z_s hypersurface (which in this gauge, by Eq. (3.18), corresponds to constant Υ hypersurfaces):

$$k_{\mu\|} = k_\mu - \frac{k_\nu\partial^\nu\Upsilon}{\partial_\sigma\Upsilon\partial^\sigma\Upsilon}\partial_\mu\Upsilon \quad , \tag{3.31}$$

and the particular linear combination

$$n^{(z_s)}_\mu = \alpha\ \partial_\mu w + \beta\ \partial_\mu\Upsilon \quad , \tag{3.32}$$

defining the normal to Σ lying on the same constant-z_s hypersurface and thus satisfying :

$$n_\mu^{(z_s)}\partial^\mu\Upsilon = 0 \qquad \Rightarrow \qquad (\partial_\tau\Upsilon)\ \alpha = \Upsilon(\partial_\mu\Upsilon\partial^\mu\Upsilon)\ \beta \quad . \tag{3.33}$$

One can easily verify that $n_\mu^{(z_s)}$ is exactly parallel to $k_{\mu\|}$. Finally, using their constancy along the null geodesics, we can also identify $\widetilde{\theta}^a$ with the angular coordinates at the observer's position where, within an infinitesimal region, we can take the metric to be flat. Therefore, as promised :

$$d_A^2 = \frac{dS_s}{d^2\Omega_o} = \frac{d^2\tilde{\theta}\sqrt{\gamma_s}}{d^2\tilde{\theta}\sin\tilde{\theta}} = \frac{\sqrt{\gamma_s}}{\sin\tilde{\theta}} \quad . \tag{3.34}$$

3.5 Relations of the GLC gauge with other metrics

3.5.1 Equality between τ and synchronous gauge (SG) time t

As we stated in Sec. 3.2.2, τ generates a family of geodetic reference observers which exactly coincide with the static ones of the synchronous gauge. In order to illustrate this point let us consider an arbitrary spacetime metric written in synchronous gauge – with coordinates $X^\mu = (t, X^i)$, $i, j = 1, 2, 3$ – where the line element takes the form (already presented in Eq. (2.1)) :

$$ds_{SG}^2 = -dt^2 + g_{ij}dX^i dX^j \quad . \tag{3.35}$$

Let us impose the condition $t = \tau$, and check whether we run into any contradiction with the exact metric transformation

$$g_{SG}^{\mu\nu}(X) = \frac{\partial X^\mu}{\partial x^\rho}\frac{\partial X^\nu}{\partial x^\sigma}g_{GLC}^{\rho\sigma}(x) \quad . \tag{3.36}$$

Using Eq. (3.10) for the GLC metric, and considering the transformation for the $g_{SG}^{t\mu}$ components, we then obtain the conditions

$$g_{SG}^{t\mu} = \{-1, \vec{0}\} = -\left[\partial_\tau + \Upsilon^{-1}(\partial_w + U^a\partial_a)\right]X^\mu = u^\nu\partial_\nu X^\mu = \frac{dX^\mu}{d\lambda} \quad , \tag{3.37}$$

where $u_\mu = -\partial_\mu\tau$ is the four-velocity of the geodesic GLC observer, and λ the affine parameter along the observer world line. So the requirement $\tau = t$ boils down to the statement that along the geodesic flow of the vector field u^μ the SG coordinates X^i are constant. This clearly defines the coordinate transformation in a non-perturbative way, and also shows that the geodesic observer of the GLC gauge corresponds to a static (and geodesic) observer in synchronous gauge. It follows that the identification $t = \tau$ can always be taken for any spacetime metric, and that this simple connection between GLC and synchronous gauge has validity far beyond the particular FLRW case or its perturbed generalizations.

3.5.2 First-order transformation from synchronous to GLC gauge

We will mainly be interested in the following chapters by scalar perturbations of a conformally flat FLRW background and their expression in the Poisson gauge (see Chapter 4). It is nevertheless interesting to consider, as an example, the first-order transformation between the GLC and the synchronous gauge (SG).

The perturbed metric of a general spacetime can be written in synchronous gauge as described by Eq. (3.35). When we use cosmic time t and polar coordinates (r, θ^a) (where $\theta^a = (\theta, \phi)$)), this metric can be parametrized at first order as follows :

$$g_{SG}^{\mu\nu} = \begin{pmatrix} -1 & 0 & \vec{0} \\ 0 & a^{-2}(1+2\hat{\Psi}) & a^{-2}S^a \\ \vec{0}^T & a^{-2}(S^a)^T & a^{-2}h^{ab} \end{pmatrix} \quad , \tag{3.38}$$

where $h^{ab} = \gamma_0^{ab} + \epsilon^{ab}$ (with $a, b = 1, 2$), $\gamma_0^{ab} = r^{-2}\mathrm{diag}\left(1, \sin^{-2}\theta\right)$ and where $\hat{\Psi}$, S^a, ϵ^{ab} are first-order perturbations. These scalar perturbations can be related to the $\widetilde{\psi}$ and $\widetilde{E}$ perturbations described in Appendix A.3.3 and thus describe only two scalar degrees of freedom.

Solving perturbatively the inverse transformation of Eq. (3.36), i.e. $g^{\mu\nu}_{GLC}(x) = \frac{\partial x^\mu}{\partial X^\rho}\frac{\partial x^\nu}{\partial X^\sigma} g^{\rho\sigma}_{SG}(X)$, for the particular equations $(\mu,\nu) = (\tau,\tau)$, (w,w) and $(w,\widetilde{\theta}^a)$, we find that the coordinate transformation from SG to GLC gauge is given to first order by :

$$\tau = t \ , \tag{3.39}$$

$$w = r + \eta + \frac{1}{2}\int_{\eta_+}^{\eta_-} dx\ \hat{\Psi}(\eta_+, x, \theta^a) \ , \tag{3.40}$$

$$\widetilde{\theta}^a = \theta^a + \frac{1}{2}\int_{\eta_+}^{\eta_-} dx \left[S^a(\eta_+, x, \theta^a) + \gamma_0^{ab}\partial_b w(\eta_+, x, \theta^a)\right] \ , \tag{3.41}$$

where the first equality has been proved in the last section and we have used the zeroth order lightcone coordinates $\eta_\pm = \eta \pm r$ with the conformal time η defined as usual by $\eta = \int dt/a(t)$. From Eq. (3.40) we get the last term of Eq. (3.41) :

$$\partial_b w = \frac{1}{2}\int_{\eta_+}^{\eta_-} dy\ \partial_b\hat{\Psi}(\eta_+, y, \theta^a) \ . \tag{3.42}$$

The components Υ, U^a and γ^{ab} of the transformed GLC metric $g^{\mu\nu}_{GLC}$ are found, by the use of the $(\mu,\nu) = (\tau, w)$, $(\tau,\widetilde{\theta}^a)$ and $(\widetilde{\theta}^a,\widetilde{\theta}^b)$ equations, to be :

$$\Upsilon = a(\eta)\left[1 - \frac{1}{2}\hat{\Psi}(\eta_+,\eta_-,\theta^a) + \frac{1}{2}\hat{\Psi}(\eta_+,\eta_+,\theta^a) - \frac{1}{2}\int_{\eta_+}^{\eta_-} dx\,\partial_+\hat{\Psi}(\eta_+, x, \theta^a)\right] \ , \tag{3.43}$$

$$\begin{aligned} U^a = \frac{1}{2}\Bigg[&S^a(\eta_+,\eta_-,\theta^a) - S^a(\eta_+,\eta_+,\theta^a) + \frac{1}{2}\gamma_0^{ab}(\eta, r, \theta^a)\int_{\eta_+}^{\eta_-} dx\,\partial_b\hat{\Psi}(\eta_+, x, \theta^a) \\ &+ \int_{\eta_+}^{\eta_-} dx\,\partial_+\left(S^a(\eta_+, x, \theta^a) + \frac{1}{2}\gamma_0^{ab}(\eta_+, x, \theta^a)\int_{\eta_+}^{x} dy\,\partial_b\hat{\Psi}(\eta_+, y, \theta^a)\right)\Bigg] \ , \end{aligned} \tag{3.44}$$

$$a^2\gamma^{ab} = h^{ab} + \frac{1}{2}\gamma_0^{ac}\int_{\eta_+}^{\eta_-} dx\,\partial_c\xi^b(\eta_+,\eta_-,\theta^a) + a \leftrightarrow b \ , \tag{3.45}$$

where

$$\xi^b(\eta_+,\eta_-,\theta^a) = S^b + \frac{1}{2}\gamma_0^{bc}\int_{\eta_+}^{\eta_-} dx\,\partial_c\hat{\Psi} \ . \tag{3.46}$$

From this last equation for γ^{ab} we can easily compute also the determinant of the 2×2 matrix γ_{ab}, and we obtain :

$$\gamma^{-1} \equiv \det\gamma^{ab} = a^{-4}r^{-4}\sin\theta^{-2}\left[1 + \epsilon^c{}_c + \gamma_0^c{}_d\int_{\eta_+}^{\eta_-} dx\,\partial_c\xi^d\right]. \tag{3.47}$$

3.5.3 GLC gauge and LTB model

Let us show in this section another application of the GLC coordinates defined in Sec. 3.2. We explain how to make a link between this observer adapted system of coordinates and the usual coordinates describing the Lemaître-Tolman-Bondi (LTB) model [3]. As a first approximation we consider a Universe close to a homogeneous FLRW one and we expand our quantities only up to first order in perturbations around their FLRW limits.

The LTB model, which is a spherically symmetric exact solution of Einstein's equations with a source made of dust, is described by the following metric :

$$ds^2_{LTB} = -dt^2 + \frac{\partial_r R^2(r,t)}{1+\beta(r)}dr^2 + R(r,t)^2\left(d\theta^2 + (\sin\theta)^2 d\phi^2\right) \tag{3.48}$$

3. See [91] for a recent paper about backreaction in LTB model and [92] for a discussion involving LTB and SNe Ia.

where $R(r,t)$ is a function of the cosmic time t and of the radial coordinate r, called the *area radius*, and $\beta(r)$ is instead an arbitrary function only of the radial coordinate and is called the *energy function*. Here primes refer to derivation with respect to r and dots with respect to the proper (cosmic) time t.

In order to connect the GLC coordinates to a LTB model we restrict ourselves to the simpler case in which the metric of Eq. (3.8) has $U^a = 0$ (a=1,2). This assumption is justified from the interpretation of U^a as a shift vector made in Sec. 3.5.1 and the spherical symmetry of the LTB model. The GLC metric goes to a homogeneous FLRW Universe if we take $w = \eta + r$, $\tau = t$, $\Upsilon = a(t)$ and $\gamma_{ab} = a^2\gamma^{(0)}_{ab}$ with $\gamma^{(0)}_{ab}d\theta^a d\theta^b = r^2(d\theta^2 + (\sin\theta)^2 d\phi^2)$. In this case, the first order non-trivial perturbations around the FLRW Universe can be written in the following way:

$$\begin{aligned}
\Upsilon &= a(t)(1+\delta\Upsilon) \ , && (3.49)\\
w &= (\eta+\chi)+\delta w \ , && (3.50)\\
\tau &= t+\delta\tau \ , && (3.51)\\
\gamma_{ab} &= a(t)^2(1+\delta\gamma)\gamma^{(0)}_{ab} \ , && (3.52)
\end{aligned}$$

where $a(t)$ is the scale factor, η the conformal time, χ the radius defined in Eq. (1.2) by $\chi = \arcsin(\sqrt{K}r)/\sqrt{K}$ and $\gamma^{(0)}_{ab}$ the angular metric defined above.

On the other hand, LTB quantities g_{tt}, $R(r,t)$ and $\beta(r)$ have the following limit in the homogeneous FLRW metric: $g_{tt} = -1$, $R(r,t) = a\,r$ and $\beta(r) = -K\,r^2$. So they are expanded at first order in perturbation theory as

$$g_{tt} = -1+\delta t \ , \quad R = a(t)r\,(1+\delta R(r,t)) \ , \quad \beta(r) = -Kr^2+\delta\beta(r) \ , \tag{3.53}$$

with K the curvature of the FLRW background.

Starting from Eqs. (3.50) and (3.51) we obtain the following differential relations

$$\begin{aligned}
dw &= \frac{1}{a}(1+a\dot{\delta w})dt + (\frac{1}{\kappa}+\delta w')dr \ ,\\
d\tau &= (1+\dot{\delta\tau})dt + \delta\tau' dr \ , && (3.54)
\end{aligned}$$

where $\kappa \equiv \sqrt{1-K\,r^2}$.

Using this last equalities, writing down the two metrics in Eqs. (3.8) and (3.48) up to first order in the perturbations and comparing the results, we obtain the system of equations that links the perturbations $\delta\Upsilon$, δw, $\delta\tau$ and $\delta\gamma$ to the perturbations δR and $\delta\beta$. The system we find is

$$\begin{aligned}
-2\dot{\delta\tau} &= \delta t \ , && (3.55)\\
\delta\Upsilon + \kappa\delta w' - \frac{\kappa}{a}\delta\tau' &= \widetilde{\delta R} \ , && (3.56)\\
\delta\Upsilon + a\dot{\delta w} - \frac{1}{a}\delta\tau' &= -\frac{\delta t}{2} \ , && (3.57)\\
\delta\gamma &= 2\,\delta R \ , && (3.58)
\end{aligned}$$

with $\widetilde{\delta R} = \delta R + r\,\delta R' - \frac{1}{2}\frac{\delta\beta}{1-Kr^2}$.

To this system we could think to add the condition that w is a null-coordinate, that is to say

$$g^{\mu\nu}_{LTB}(t,r)\,\partial_\mu(\eta+r+\delta w)\,\partial_\nu(\eta+r+\delta w) = 0 \ , \tag{3.59}$$

which is equivalent to

$$a\dot{\delta w} - \kappa\delta w' = -\widetilde{\delta R} - \frac{\delta t}{2} \ . \tag{3.60}$$

Nevertheless, this condition is guaranteed by construction of the GLC metric and this is directly seen from Eqs. (3.55), (3.56) and (3.57).

We now restrict our study to the case $\delta t = 0$ and $K = 0$ (so $\kappa = 1$). From Eq. (3.55) one obtains $\delta\tau = \delta\tau(r)$ and Eq. (3.60) gives δw in terms of δR as

$$\delta w = -\frac{1}{2}\left[\int^{\eta-r}\widetilde{\delta R}(\tilde{\eta}-\tilde{r},\eta+r)\,d(\tilde{\eta}-\tilde{r})\right] + \delta\bar{w}(\eta+r) \equiv -\frac{1}{2}\left[\int^{\eta_-}\widetilde{\delta R}(\tilde{\eta}_-,\eta_+)\,d\tilde{\eta}_-\right] + \delta\bar{w}(\eta_+) \ , \tag{3.61}$$

where $\eta_+ \equiv \eta + r$, $\eta_- \equiv \eta - r$, and $\delta\bar{w}(\eta_+)$ is an integration function. This solution determines $\delta\Upsilon(r,t)$ in terms of $\widetilde{\delta R}$ by using Eq. (3.56), after a function is chosen for $\delta\tau(r)$, as:

$$\delta\Upsilon = \frac{1}{2}\left[\int^{\eta_-} \partial_+\widetilde{\delta R}(\tilde{\eta}_-,\eta_+)\,d\tilde{\eta}_- + \widetilde{\delta R}(\eta_-,\eta_+)\right] - \partial_+\delta\bar{w}(\eta_+) + \frac{1}{a}\delta\tau' \quad . \tag{3.62}$$

where we made use of the first of the two following relations

$$\begin{aligned} a\partial_t\delta w &= -\frac{1}{2}\partial_\eta\int^{\eta_-}\widetilde{\delta R}(\tilde{\eta}_-,\eta_+)\,d\tilde{\eta}_- = -\frac{1}{2}\left[\int^{\eta_-}\partial_+\widetilde{\delta R}(\tilde{\eta}_-,\eta_+)\,d\tilde{\eta}_- + \widetilde{\delta R}(\eta_-,\eta_+)\right] + \partial_+\delta\bar{w}(\eta_+) \quad , \\ \partial_r\delta w &= -\frac{1}{2}\partial_r\int^{\eta_-}\widetilde{\delta R}(\tilde{\eta}_-,\eta_+)\,d\tilde{\eta}_- = -\frac{1}{2}\left[\int^{\eta_-}\partial_+\widetilde{\delta R}(\tilde{\eta}_-,\eta_+)\,d\tilde{\eta}_- - \widetilde{\delta R}(\eta_-,\eta_+)\right] + \partial_+\delta\bar{w}(\eta_+) \quad . \end{aligned}$$

As a consequence, we have shown that when a perturbed LTB metric is given (i.e. $\delta R(r,t)$ and $\delta\beta(r)$ are given), we can match this metric with a GLC metric up to a function $\delta\tau(r)$ that we can choose at our convenience. In the case where $\delta t \neq 0$, the solution is determined by doing the replacement $\widetilde{\delta R} \to \widetilde{\delta R} + \frac{\delta t}{2}$ in the integrals. The case $K \neq 0$ is solved by introducing, instead of r, the quantity $\chi \equiv \int^r \frac{dr'}{\sqrt{1-Kr'^2}}$ already presented in Eq. (1.2), so that Eq. (3.60) is written as

$$\partial_\eta\delta w - \partial_\chi\delta w = -\widetilde{\delta R} - \frac{\delta t}{2} \quad , \tag{3.63}$$

and we then use $\eta+\chi$, $\eta-\chi$ for the variables η_+, η_- present in the previous solutions.

The results given here are expressed in terms of undetermined integrals and, to be complete, should be associated to initial boundary conditions.

3.5.4 Analogy between GLC and ADM metrics

In the ADM formalism, the Minskowski spacetime $\mathcal{M}_4$ is foliated by constant time hypersurfaces in the following way:

$$ds^2_{ADM} = -(N^2 - g_{ij}N^iN^j)dt^2 + 2g_{ij}dx^iN^jdt + g_{ij}dx^idx^j \tag{3.64}$$

with the so-called *lapse function* N and *shift vector* N^i. Physically, the lapse function sets the "distance" between two different constant-time hypersurfaces whereas N^i takes care of the change in spatial coordinates x^i when we move from a constant-time hypersurface to another.

On the other hand, the GLC line element given in Eq. (3.10) is trivially reorganized as follows:

$$ds^2_{GLC} = (\Upsilon^2 + \gamma_{ab}U^aU^b)dw^2 - 2\gamma_{ab}d\tilde{\theta}^aU^bdw + \gamma_{ab}d\widetilde{\theta}^ad\widetilde{\theta}^b - 2\Upsilon dwd\tau \quad . \tag{3.65}$$

Hence we can see that Υ acts in a way similar to the lapse function by setting the "distance" between two lightcones $w = w_0$ and $w = w_1$. We will also see in the study of the redshift drift (see Sec. 3.6.3) that $\Delta w = \Upsilon^{-1}\Delta\tau$, which clearly goes in the same line of arguments. On the other hand, U^a plays a role similar to the shift vector, though in a reduced dimensional case, taking care of the change in angular coordinates between two 2-spheres $\Sigma(w_0,\tau_0)$ and $\Sigma(w_1,\tau_1)$ (see Fig. 3.2). One can nevertheless notice a difference between the GLC metric of Eq. (3.65) and the ADM metric: it contains an extra piece $-2\Upsilon dwd\tau$ related to the fact that we are doing a foliation with both constant-w and constant-τ coordinates which are intersecting each other. This term shows that w is the coordinate acting like time here whereas τ looks more nicely comparable with a third spatial component of the ADM metric. We can again remark in this spirit that τ is playing the role of y in the observational coordinates and, if the foliation of spacetime is here seen as a foliation by null cones, the $\tau = $ cst hypersurfaces are definitely setting the radial distance along these cones.

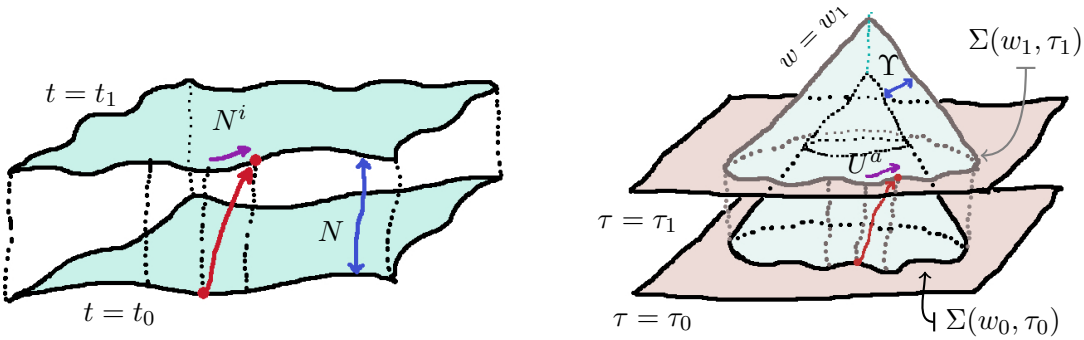

Figure 3.2: Illustration of the comparative forms of the ADM (left) and GLC (right) metrics. One can see that the GLC metric foliates $\mathcal{M}_4$ by lightcones and spatial hypersurfaces whereas the ADM metric uses only spatial hypersurfaces. Υ plays the role of a lapse function (N in ADM), U^a the role of the shift vector (N^i in ADM) that takes care of the change in angular coordinates when we go from one 2-sphere $\Sigma(w_0, \tau_0)$ to another $\Sigma(w_1, \tau_1)$. The angular part of the metric, γ_{ab} defines the geometry inside the 2-sphere (as g_{ij} in the 3-dimensional spatial volume in ADM).

3.6 Applications to the lightcone average

3.6.1 Averaging on constant redshift hypersurfaces

Let us recall here, in GLC coordinates, that the covariant average of a scalar quantity $S(\tau, w, \widetilde{\theta}^a)$ over the compact 2-dimensional surface Σ, defined by the intersection of our past light cone $w = w_o$ with the spacelike hypersurface $\tau = \tau_s$, is simply given (using $\gamma \equiv \det \gamma_{ab}$) by:

$$\begin{aligned} \langle S \rangle_{w_o,\tau_s} &= \frac{\int_\Sigma d^4x\sqrt{-g}\,\delta_{\rm D}(w-w_o)\delta_{\rm D}(\tau-\tau_s)\,|\partial_\mu\tau\partial^\mu w|\,S(\tau,w,\widetilde{\theta}^a)}{\int_\Sigma d^4x\sqrt{-g}\,\delta_{\rm D}(w-w_o)\delta_{\rm D}(\tau-\tau_s)\,|\partial_\mu\tau\partial^\mu w|} \\ &= \frac{\int d^2\widetilde{\theta}\sqrt{\gamma(w_o,\tau_s,\widetilde{\theta}^a)}\,S(w_o,\tau_s,\widetilde{\theta}^a)}{\int d^2\widetilde{\theta}\sqrt{\gamma(w_o,\tau_s,\widetilde{\theta}^a)}} \quad . \end{aligned} \tag{3.66}$$

To get an average which is still written in terms of the proper time of the geodetic observer, but corresponding to the average over the 2-sphere at constant redshift z_s, i.e. $\Sigma(w_o, z_s)$, we can express τ_s in the last equation in terms of the redshift z_s, i.e. $\tau_s = \tau_s(z_s, w_o, \widetilde{\theta}^a)$ (or in different words choosing $\tau(z, w_o, \theta^a)$ to be the solution of Eq. (3.18): $\Upsilon(w_o, \tau, \theta^a)/\Upsilon_o = 1/(1+z_s)$). We arrive at an exact expression for the light-cone average of S as a function of z_s:

$$\langle S \rangle_{w_o,z_s} = \frac{\int d^2\widetilde{\theta}\sqrt{\gamma(w_o,\tau(z_s,w_o,\widetilde{\theta}^a),\widetilde{\theta}^b)}\,S(w_o,\tau(z_s,w_o,\widetilde{\theta}^a),\widetilde{\theta}^b)}{\int d^2\widetilde{\theta}\sqrt{\gamma(w_o,\tau(z_s,w_o,\widetilde{\theta}^a),\widetilde{\theta}^b)}} \quad . \tag{3.67}$$

This average will be of great use in the next chapters as it is a well adapted expression for averaging observational quantities. To emphasize this point, let us present the effect of this change of parametrization of Σ for two physical observables related to supernovae: the luminosity distance d_L and the redshift z [4].

Using the above result of Eq. (3.66) for $S = d_L$, we obtain, for a general inhomogeneous metric background:

$$\langle d_L \rangle_{w_o,\tau_s} = \frac{\int d^2\theta\sqrt{|\gamma(w_o,\tau_s,\theta^a)|}\,\left[\Upsilon^2(w_o,\tau_o,\theta^a)/\Upsilon^2(w_o,\tau_s,\theta^a)\right]\,d_A(w_o,\tau_s,\theta^a)}{\int d^2\theta\sqrt{|\gamma(w_o,\tau_s,\theta^a)|}} \quad , \tag{3.68}$$

4. Note that their relation has been studied within a gauge invariant approach, for a linearly perturbed FLRW metric, in [61, 62].

where d_A is given by Eq. (3.28) and we used Eq. (3.18). Since our coordinates are not pathological near $w = w_o$ and $\tau = \tau_o$ we have $\lim_{\tau\to\tau_o} \Upsilon(w = w_o, \tau, \theta^a) = \Upsilon(w = w_o, \tau_o) \equiv \Upsilon_o$ independent of θ^a. Hence, in Eq. (3.68), the factor $\Upsilon(w_o, \tau_o, \theta^a) = \Upsilon_o$ behaves like a constant, leaving a well defined integral of a scalar object over the 2-sphere. In our case of interest, namely light-cone averages on surfaces of constant redshift $z = z_s$, one then obtains:

$$\langle d_L\rangle_{w_o,z_s} = (1+z_s)^2 \frac{\int d^2\widetilde{\theta}\,\sqrt{\gamma(w_o,\tau_s(z_s,w_o,\widetilde{\theta}^a),\widetilde{\theta}^b)}\,d_A(w_o,\tau_s(z_s,w_o,\widetilde{\theta}^a),\widetilde{\theta}^b)}{\int d^2\widetilde{\theta}\,\sqrt{\gamma(w_o,\tau_s(z_s,w_o,\widetilde{\theta}^a),\widetilde{\theta}^b)}} \quad . \tag{3.69}$$

This equation, being exact, can be applied in principle to any given highly inhomogeneous cosmology. It can for example be applied to a Lemaître-Tolman-Bondi (LTB) model [93–95] even in the case of a generic observer shifted away from the symmetry centre of the isotropic geometry.

Let us compare with Eq. (3.68) the average of $1+z$ on the constant τ surface, which reads:

$$\langle 1+z\rangle_{w_o,\tau_s} = \frac{\int d^2\theta\sqrt{|\gamma(w_o,\tau_s,\theta^a)|}\;\left[\Upsilon(w_o,\tau_o,\theta^a)/\Upsilon(w_o,\tau_s,\theta^a)\right]}{\int d^2\theta\sqrt{|\gamma(w_o,\tau_s,\theta^a)|}} \quad . \tag{3.70}$$

When we move to the constant z average presented in Eq. (3.67), this relation is trivially satisfied.

The above Eqs. (3.68) and (3.70) can in principle be used to see how the usual redshift to luminosity-distance relation gets affected by the inhomogeneities of the cosmological geometry. The average of the luminosity distance on constant redshift surfaces, on the other hand, corresponds to an average where the geodesic observers measuring the redshift do not coincide any longer with the "observers" associated to the flow lines of the reference hypersurface $\Sigma(z)$, chosen to specify the averaging region. In practice, this last expression of Eq. (3.67) will be the one that we will use because of its adaptation to the measured quantities in observational cosmology.

3.6.2 Simplified Buchert-Ehlers rules in the GLC gauge

In the GLC gauge the averaging integrals introduced in Sec. 2.2 greatly simplify, especially in the case where the reference hypersurface $\Sigma(A)$ defines a geodesic observer. We will concentrate on the integrals of Eqs. (2.89) and (2.87) which, setting $V = w$ and $V_0 = w_o$, are now given by:

$$I(S;w_o,A_0;-) = \int d^2\theta dw d\tau\sqrt{|\gamma|}\;\;|\partial_\tau A|\,\delta_{\rm D}(w-w_o)\delta_{\rm D}(A-A_0)S \quad , \tag{3.71}$$

$$I(S;w_o;A_0) = \int d^2\theta dw d\tau\sqrt{|\gamma|}\;\frac{|\partial_\tau A|}{\sqrt{-(\partial A)^2}}\delta_{\rm D}(w-w_o)\Theta(A-A_0)S \quad . \tag{3.72}$$

The case of the causally connected spheres of Eq. (2.88), closer to the spatial average definition, will be treated at the end of this section.

For a geodesic reference observer, with $A = \tau$ (and $A_0 = \tau_s$), we obtain by the use of the full set of GLC coordinates that the two definitions above reduce to the simple integrals:

$$I(S;w_o,\tau_s;-) = \int d^2\theta\sqrt{|\gamma(w_o,\tau_s,\theta^a)|}\;S(w_o,\tau_s,\theta^a) \quad , \tag{3.73}$$

$$I(S;w_o;\tau_s) = \int d^2\theta d\tau\sqrt{|\gamma(w_o,\tau,\theta^a)|}\;\Theta(\tau-\tau_s)S(w_o,\tau,\theta^a) \quad . \tag{3.74}$$

This has important consequences and shows one of the many reasons to use the GLC coordinates, as we also saw in Sec. 3.6.1, but let us now see how the generalized Buchert-Elhers rules introduced in Sec. 2.3.1 simplify in the GLC gauge.

Average on the 2-sphere embedded in the light cone

Let us consider separately, as before, derivatives with respect to A_0 and $V_0 = w_o$. Starting with A_0, Eq. (2.103) can now be written as

$$\partial_{A_0}\langle S\rangle_{w_o,A_0} = \left\langle\frac{\partial_\tau S}{\partial_\tau A}\right\rangle_{w_o,A_0} + \left\langle S\frac{\partial_\tau\ln\sqrt{|\gamma|}}{\partial_\tau A}\right\rangle_{w_o,A_0} - \left\langle\frac{\partial_\tau\ln\sqrt{|\gamma|}}{\partial_\tau A}\right\rangle_{w_o,A_0}\langle S\rangle_{w_o,A_0} \quad , \tag{3.75}$$

and for the special case where $\Sigma(A)$ defines a geodesic observer (i.e. $A=\tau$, $A_0=\tau_s$), it reduces to

$$\partial_{\tau_s}\langle S\rangle_{w_o,\tau_s}=\langle\partial_\tau S\rangle_{w_o,\tau_s}+\left\langle S\partial_\tau\ln\sqrt{|\gamma|}\right\rangle_{w_o,\tau_s}-\left\langle\partial_\tau\ln\sqrt{|\gamma|}\right\rangle_{w_o,\tau_s}\langle S\rangle_{w_o,\tau_s}\quad . \tag{3.76}$$

Note that, in this last case with $A=\tau$, the partial derivative with respect to A_0 reduces to a standard derivative with respect to the proper (cosmic) time if we consider the limit of a homogeneous FLRW Universe (see Sec. 3.2.1).

In the geodesic case we have also the following simplification for the derivative with respect to w_o as given in Eq. (2.105):

$$\begin{aligned}\partial_{w_o}\langle S\rangle_{w_o,\tau_s} &= \langle\partial_w S+U^a\partial_a S\rangle_{w_o,\tau_s} \\ &+\left\langle\left[\partial_w\ln\sqrt{|\gamma|}\right]S\right\rangle_{w_o,\tau_s}-\left\langle\partial_w\ln\sqrt{|\gamma|}\right\rangle_{w_o,\tau_s}\langle S\rangle_{w_o,\tau_s} \\ &+\left\langle\left[\partial_a U^a+U^a\partial_a\ln\sqrt{|\gamma|}\right]S\right\rangle_{w_o,\tau_s}-\left\langle\partial_a U^a+U^a\partial_a\ln\sqrt{|\gamma|}\right\rangle_{w_o,\tau_s}\langle S\rangle_{w_o,\tau_s}\quad .\end{aligned} \tag{3.77}$$

Average on the truncated light cone

For a generic hypersurface we cannot specify $(\partial A)^2$, and Eq. (2.104) just simplifies as

$$\partial_{A_0}\langle S\rangle_{w_o}^{A_0}=\left\langle\frac{\partial_\tau S}{\partial_\tau A}\right\rangle_{w_o}^{A_0}+\left\langle\frac{\partial_\tau\ln\sqrt{|\gamma|}-\partial_w(\partial A\cdot\partial A)}{\partial_\tau A}S\right\rangle_{w_o}^{A_0}-\left\langle\frac{\partial_\tau\ln\sqrt{|\gamma|}-\partial_w(\partial A\cdot\partial A)}{\partial_\tau A}\right\rangle_{w_o}^{A_0}\langle S\rangle_{w_o}^{A_0}\quad . \tag{3.78}$$

However, in the case where $\Sigma(A)$ defines a geodesic observer (with $A=\tau$ and $A_0=\tau_s$) one obtains:

$$\partial_{\tau_s}\langle S\rangle_{w_o}^{\tau_s}=\langle\partial_\tau S\rangle_{w_o}^{\tau_s}+\left\langle S\partial_\tau\ln\sqrt{|\gamma|}\right\rangle_{w_o}^{\tau_s}-\left\langle\partial_\tau\ln\sqrt{|\gamma|}\right\rangle_{w_o}^{\tau_s}\langle S\rangle_{w_o}^{\tau_s}\quad . \tag{3.79}$$

Comparing with Eq. (3.76) we find, for this last case, the same commutation rule independently of the averaging prescription used.

Finally, for a hypersurface $\Sigma(A)$ associated to a geodesic observer, we also have the following simplification of Eq. (2.106):

$$\begin{aligned}\partial_{w_o}\langle S\rangle_{w_o}^{\tau_s} &= \langle\partial_w S+U^a\partial_a S\rangle_{w_o}^{\tau_s}+\left\langle\left[\partial_w\ln\sqrt{|\gamma|}\right]S\right\rangle_{w_o}^{\tau_s}-\left\langle\partial_w\ln\sqrt{|\gamma|}\right\rangle_{w_o}^{\tau_s}\langle S\rangle_{w_o}^{\tau_s} \\ &+\left\langle\left[\partial_a U^a+U^a\partial_a\ln\sqrt{|\gamma|}\right]S\right\rangle_{w_o}^{\tau_s}-\left\langle\partial_a U^a+U^a\partial_a\ln\sqrt{|\gamma|}\right\rangle_{w_o}^{\tau_s}\langle S\rangle_{w_o}^{\tau_s}\quad .\end{aligned} \tag{3.80}$$

Hence, we obtain the same commutation rule (see Eq. (3.77)) for derivatives with respect to w_o.

This is one other nice property of the GLC gauge to make the very different Buchert-Ehlers relations of Eqs. (2.103), (2.104) and of (2.105), (2.106) take the same form (though keeping their own definitions of the average).

Average on the causally connected sphere

We can now consider the effect of the GLC gauge (where $V=w$ and we can choose $A=\tau$) on the integral of Eq. (2.88). In this gauge, this integral simplifies as:

$$I(1;\tau_s;w_o)=\int d^2\theta dw\Upsilon(\tau_s,w,\theta^a)\sqrt{|\gamma(\tau_s,w,\theta^a)|}\;\Theta(w_o-w)\quad . \tag{3.81}$$

One can notice by the comparison of this equation with Eq. (3.73) and (3.74) that the full metric determinant $\Upsilon\sqrt{|\gamma|}$ appears in the integral. This is a normal thing considering the fact that this average is over a 3-dimensional spatial volume whereas the integrals defined in Eq. (3.73) and (3.74) were only including the 2-sphere as part of their spatial integration. The consideration of the previous equations (2.107) and (2.108) in the GLC gauge lead to the following simplifications:

$$\partial_{\tau_s}\langle S\rangle_{\tau_s}^{w_o}=\langle\partial_\tau S\rangle_{\tau_s}^{w_o}+\left\langle S\partial_\tau\ln(\Upsilon\sqrt{|\gamma|})\right\rangle_{\tau_s}^{w_o}-\left\langle\partial_\tau\ln(\Upsilon\sqrt{|\gamma|})\right\rangle_{\tau_s}^{w_o}\langle S\rangle_{\tau_s}^{w_o}\quad , \tag{3.82}$$

$$\begin{aligned}\partial_{w_o}\langle S\rangle_{\tau_s}^{w_o} &= \langle\partial_w S+U^a\partial_a S\rangle_{\tau_s}^{w_o}+\left\langle\left[\partial_w\ln(\Upsilon\sqrt{|\gamma|})\right]S\right\rangle_{\tau_s}^{w_o}-\left\langle\partial_w\ln(\Upsilon\sqrt{|\gamma|})\right\rangle_{\tau_s}^{w_o}\langle S\rangle_{\tau_s}^{w_o} \\ &+\left\langle\left[\partial_a U^a+U^a\partial_a\ln(\Upsilon\sqrt{|\gamma|})\right]S\right\rangle_{\tau_s}^{w_o}-\left\langle\partial_a U^a+U^a\partial_a\ln(\Upsilon\sqrt{|\gamma|})\right\rangle_{\tau_s}^{w_o}\langle S\rangle_{\tau_s}^{w_o}\quad .\end{aligned} \tag{3.83}$$

We can remark the profound resemblance between these equations and those obtained in the truncated lightcone and the embedded 2-sphere, with the small difference of having replaced $\sqrt{|\gamma|}$ by $\Upsilon\sqrt{|\gamma|}$. This difference is again due to the fact that the 3-dimensional spacetime determinant of the metric is $\Upsilon\sqrt{|\gamma|}$. Considering the expression of the volume expansion Θ given by Eq. (2.69) in synchronous gauge, one can directly see that our simplified average of Eq. (3.82) gives back, after the identification $\tau = t$ valid in this gauge, the Buchert-Ehlers relation generalized in Eq. (2.70).

3.6.3 The redshift drift

The redshift drift (RD) is defined as the rate of change of the redshift of a given source with respect to the observer's proper time (see [96, 97]). Since both the observer and the source simultaneously evolve in time, the relevant hypersurfaces for the RD effect will consist of two light cones with different bases (see Fig. 3.3). Assuming that source and observer are in geodesic motion and have negligible peculiar velocities, the RD in a FLRW Universe, and in the proper-time interval Δt_0, can be simply expressed as (see e.g. [98]) :

$$\frac{\Delta z}{\Delta t_0} = (1+z)H_0 - H_s = \frac{\dot{a}_o - \dot{a}_s}{a_s} \quad , \tag{3.84}$$

where H_0 is the present value of the Hubble parameter while H_s is its value at the emission time. Clearly the RD effect is a good indicator of cosmic acceleration as a function of z which *does not* use hypothetical standard candles. Nevertheless, in practice it needs observations over several decades.

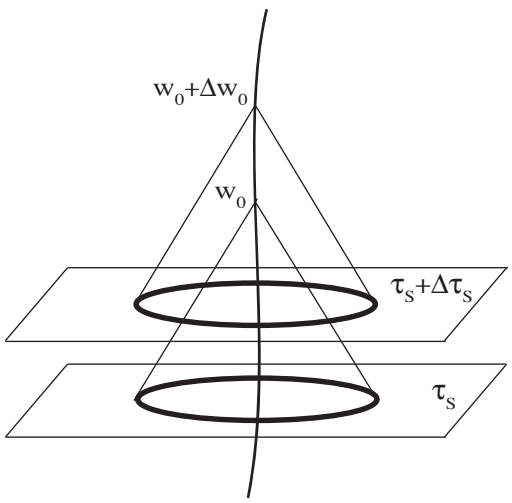

Figure 3.3: A graphic illustration of the redshift drift effect. A possible variation of the cosmological expansion rate is detected by comparing observations performed on two different past light cones.

In order to generalize this expression to a general inhomogeneous Universe (and attempt some averaging of it) let us consider again the geodesic observer of the GLC gauge, with coordinates $x^\mu = (\tau, w, \widetilde{\theta}^a)$. As shown in Eq. (3.18), z is in principle a function of seven independent variables, namely of w_o, τ_o, $\widetilde{\theta}^a_o$, τ_s and $\widetilde{\theta}^a_s$. Note that, since we are assuming that source and observer are on the same light cone $w = w_o$ at $\tau = \tau_o$, they will be both on the light cone $w = w_o + \Delta w_o$ at $\tau = \tau_o + \Delta\tau_o$, see Fig. 3.3. We can also note that Υ_o is independent of θ^a_o. As a consequence we have only five independent contributions to the variation of $1+z$, and we can write, in general :

$$\Delta(1+z) = \frac{\partial(1+z)}{\partial w_o}\Delta w_o + \frac{\partial(1+z)}{\partial \tau_o}\Delta\tau_o + \frac{\partial(1+z)}{\partial \tau_s}\Delta\tau_s + \frac{\partial(1+z)}{\partial \widetilde{\theta}^a_s}\Delta\widetilde{\theta}^a_s \quad . \tag{3.85}$$

As shown in Eq. (3.12), in the homogeneous limit the coordinate τ goes to the proper (cosmic) time t of the synchronous gauge. So, locally around our geodesic observer, we choose to evaluate the redshift drift Δz with respect to his/her time parameter τ, and we need, to this purpose, an explicit

relation between $\Delta\tau_o$ and the variation of the other coordinates involved. For a geodesic observer with $n_\mu = -\partial_\mu \tau$ we have $\dot{x}^\mu \sim n^\mu = (1/\Upsilon, 1, U^a/\Upsilon)$, so that we can express Δx^μ in terms of Δw, at all times, as:

$$\Delta\tau = \Upsilon \Delta w \quad , \quad \Delta\widetilde{\theta}^a = U^a \Delta w \quad . \tag{3.86}$$

Using Eq. (3.86) we find $\Delta w_o = \Delta\tau_o/\Upsilon_o = \Delta\tau_s/\Upsilon_s$, and the final result for the RD can be written in terms of z and its derivatives as:

$$\frac{\Delta z}{\Delta\tau_o} = (1+z)\widetilde{H}_0 + \frac{1}{\Upsilon_o}\frac{\partial}{\partial w_o}(1+z) + \frac{\partial}{\partial\tau_s}\ln(1+z) + \frac{U^a_s}{\Upsilon_o}\frac{\partial}{\partial\widetilde{\theta}^a_s}(1+z) \quad , \tag{3.87}$$

where:

$$\widetilde{H}_0 \equiv \frac{1}{\Upsilon_o}\frac{\partial\Upsilon_o}{\partial\tau_o} \quad . \tag{3.88}$$

Let us note again that ∂_{w_o} acts on both metric factors Υ contained in $(1+z)$. This result is valid for a general inhomogeneous metric, and can be compared, as a useful consistency check, with a similar result previously obtained in the particular case of a spherically symmetric geometry [99]. If we move from our coordinates to the adapted coordinates used in [99] we find that our expression of Eq. (3.87) exactly reduces to the expression for the RD reported in Eq. (5) of Ref. [99].

The quantities appearing in the above equation can now be averaged over the 2-sphere embedded, at $\tau = \tau_s$, in the light cone $w = w_o$. Using our prescription based on Eq. (3.73) we find that both Υ_o and $\widetilde{H}_0$ can be taken out from the averaging integrals (which are performed over the variables $\widetilde{\theta}^a$), and we obtain:

$$\frac{\langle\Delta z\rangle_{w_o,\tau_s}}{\Delta\tau_o} = \langle 1+z\rangle_{w_o,\tau_s}\widetilde{H}_0 + \frac{1}{\Upsilon_o}\langle\partial_w(1+z)\rangle_{w_o,\tau_s} + \langle\partial_\tau\ln(1+z)\rangle_{w_o,\tau_s} + \frac{1}{\Upsilon_o}\langle U^a\partial_a(1+z)\rangle_{w_o,\tau_s} \quad . \tag{3.89}$$

For the derivatives performed with respect to the hypersurface parameters w and τ we can now apply the Buchert-Ehlers commutation rules in the simplified form of Sec. 3.6.2. Using in particular Eqs. (3.76) and (3.77) we are lead to:

$$\frac{\langle\Delta z\rangle_{w_o,\tau_s}}{\Delta\tau_o} = \langle 1+z\rangle_{w_o,\tau_s}\widetilde{H}_0 + \frac{1}{\Upsilon_o}\partial_{w_o}\langle 1+z\rangle_{w_o,\tau_s} + \partial_{\tau_s}\langle\ln(1+z)\rangle_{w_o,\tau_s} + Q_w(z) + Q_\tau(z) \quad , \tag{3.90}$$

where

$$Q_\tau(z) = -\left\langle\ln(1+z)\partial_\tau\ln\sqrt{|\gamma|}\right\rangle_{w_o,\tau_s} + \langle\ln(1+z)\rangle_{w_o,\tau_s}\left\langle\partial_\tau\ln\sqrt{|\gamma|}\right\rangle_{w_o,\tau_s} \quad , \tag{3.91}$$

$$\begin{aligned} Q_w(z) = \frac{1}{\Upsilon_o}\Bigg\{ & -\left\langle(1+z)\partial_w\ln\sqrt{|\gamma|}\right\rangle_{w_o,\tau_s} - \left\langle(1+z)\left[\partial_a U^a + U^a\partial_a\ln\sqrt{|\gamma|}\right]\right\rangle_{w_o,\tau_s} \\ & + \langle 1+z\rangle_{w_o,\tau_s}\left[\left\langle\partial_w\ln\sqrt{|\gamma|}\right\rangle_{w_o,\tau_s} + \left\langle\partial_a U^a + U^a\partial_a\ln\sqrt{|\gamma|}\right\rangle_{w_o,\tau_s}\right]\Bigg\} \quad . \end{aligned} \tag{3.92}$$

These last terms, together with the others of Eq. (3.90) control the difference between the *averaged redshift drift* and the *drift* for the *averaged redshift* and represent a light-cone analog of the backreaction terms due to the geometric inhomogeneities, first computed by Buchert [49,50] in the context of space-like averages. Unlike Buchert's terms, however, the backreaction in this case is physically controlled by the geometry of a 2-dimensional surface, with metric γ_{ab}. Also, the possible physical meaning of these backreaction terms is in principle strongly model-dependent, and their physical effects are to be explicitly computed for any given model chosen to parametrize deviations from FLRW geometry.

For a homogeneous FLRW metric the averages disappear, and the backreaction terms Q_τ and Q_w are identically vanishing (see also Sec. 2.4). In that case $\widetilde{H}_0 = H_0$ and, using the homogeneous limit of Eq. (3.12), one also finds $\partial_w(1+z) = 0$ and $\partial_\tau\ln(1+z)_s = -H_s$, so that Eq. (3.90) gives back the result of Eq. (3.84). However, for inhomogeneous models (such as the LTB Universe [93–95], see in Sec. 3.5.3), we see that several new contributions appear. These backreaction effects may be relevant for determining the kinematics of the Universe (and the equation of state of its energy components as a function of z) from the forthcoming RD experiments (see e.g. [100]).

Chapter 4

The luminosity-redshift relation at second order

In this section, we present the computation, in the Poisson (or longitudinal) gauge, of the luminosity distance at second order in perturbations. For that we start by doing the transformation at second order between the GLC and the Poisson gauge (PG), expressing the GLC gauge coordinates in terms of the PG coordinates and metric. We then impose the condition that the sources lie on $\Sigma(w_o, z_s)$ and finally invert the second order transformation to express the luminosity distance in terms of the $\widetilde{\theta}^a$ angles. We conclude with a brief physical description of its enclosed terms. Let us notice for the reader not interested by this technical (but physically very relevant) calculation that the essential of the discussion presented here will be sketched at first order at the beginning of Chapter 5.

4.1 From Poisson to GLC gauge at second order

4.1.1 The Poisson gauge

Let us consider a non-homogeneous spacetime approximated by a spatially flat FLRW Universe plus scalar, vector and tensor perturbations. In the so-called Poisson gauge (PG) [101, 102], a generalization of the Newtonian (or longitudinal) gauge beyond first order, the corresponding metric takes the following standard form in cartesian coordinates :

$$ds^2_{PG} = a^2(\eta)\left(-(1+2\Phi)d\eta^2 + 2\omega_i\, d\eta dx^i + [(1-2\Psi)\delta_{ij} + h_{ij}]\, dx^i dx^j\right) \quad , \tag{4.1}$$

where Φ and Ψ are scalar perturbations, ω_i is a transverse vector ($\partial^i\omega_i = 0$) and h_{ij} is a transverse and traceless tensor ($\partial^i h_{ij} = 0 = h^i{}_i$). This metric depends on six arbitrary functions, hence it is completely gauge fixed. Up to second order the (generalized) Bardeen potentials Φ and Ψ are defined as follows [60] :

$$\Phi \equiv \psi + \frac{1}{2}\phi^{(2)} \quad , \quad \Psi \equiv \psi + \frac{1}{2}\psi^{(2)} \quad , \tag{4.2}$$

where we have assumed, for simplicity, that there is no (or a negligible) anisotropic stress of the matter distribution, thus setting $\Psi = \Phi = \psi$ at first order. We will consider ω_i and h_{ij} to be second order quantities as, in inflationary cosmology, first order scalar perturbations are the dominant contributions (see App. A.2.3). On the other hand vector and tensor perturbations are automatically generated from scalar perturbations at second order (see e.g. [103, 104]).

4.1.2 The second order transformation for scalar perturbations

We intend to write here the second order transformation between the GLC gauge and the PG. Before carrying on, let us mention that using the GLC approach means that we are taking many physical effects into account already at the level of the metric. In this process, the geodesic equations for the observer and light rays are solved non-perturbatively, and their solutions are expressed in terms of the τ, w coordinates. The outcome is that physical phenomena that we will describe later – such

as redshift perturbations (RP), redshift space distortions (RSD), Sachs-Wolfe effect (SW), integrated Sachs-Wolfe effect (ISW), peculiar velocities, lensing and others – are manifestly encoded in the metric, and are derived from a coordinate transformation. This is different from the usual approach, which first takes some perturbed metric, and then solves the geodesic equations order by order to construct physical observables (see, for example, [63, 105]).

Since by our assumption vector and tensor modes appear only at second order and, as a consequence, will be decoupled from scalar perturbations, we can neglect them momentarily and add them at the end. Therefore, considering only scalar perturbations in spherical coordinates $(r, \theta^a) = (r, \theta, \phi)$, the PG defined in Eq. (4.1) becomes the Newtonian gauge (NG), with inverse metric:

$$g^{\mu\nu}_{PG} = a(\eta)^{-2}\mathrm{diag}(-1 + 2\tilde{\Phi}, 1 + 2\tilde{\Psi}, (1 + 2\tilde{\Psi})\gamma_0^{ab}) \quad , \tag{4.3}$$

where

$$\gamma_0^{ab} = \mathrm{diag}\left(r^{-2}, r^{-2}\sin^{-2}\theta\right) \quad , \quad \tilde{\Phi} = \psi + \frac{1}{2}\phi^{(2)} - 2\psi^2 \quad , \quad \tilde{\Psi} = \psi + \frac{1}{2}\psi^{(2)} + 2\psi^2 \quad . \tag{4.4}$$

We compute the GLC gauge (inverse) metric through:

$$g^{\rho\sigma}_{GLC}(x) = \frac{\partial x^\rho}{\partial y^\mu}\frac{\partial x^\sigma}{\partial y^\nu} g^{\mu\nu}_{PG}(y) \quad , \tag{4.5}$$

where we indicate with $y^\mu = (\eta, r, \theta^a)$ the PG coordinates and with $x^\nu = (\tau, w, \widetilde{\theta}^a)$ the GLC ones. Let us also introduce the useful (zeroth-order) light-cone variables with corresponding derivatives:

$$\eta_\pm = \eta \pm r \quad \text{with:} \quad \partial_\eta = \partial_+ + \partial_- \quad , \quad \partial_r = \partial_+ - \partial_- \quad , \quad \partial_\pm = \frac{\partial}{\partial\eta_\pm} = \frac{1}{2}\left(\partial_\eta \pm \partial_r\right) \quad . \tag{4.6}$$

Using these variables we solve the four differential equations obtained from Eq. (4.5) for the components $g^{\tau\tau}_{GLC} = -1$, $g^{ww}_{GLC} = 0$, $g^{wa}_{GLC} = 0$, by imposing the boundary conditions that *i*) the transformation is non singular around $r = 0$, and *ii*) that the 2-dimensional spatial sections $r = \mathrm{cst}$ are locally parametrized at the observer position by standard spherical coordinates, $\widetilde{\theta}^a(0) = \theta^a = (\theta, \phi)$.

To this purpose we also introduce the following auxiliary quantities:

$$P(\eta, r, \theta^a) = \int_{\eta_{in}}^{\eta} d\eta' \frac{a(\eta')}{a(\eta)}\psi(\eta', r, \theta^a) \quad , \quad Q(\eta_+, \eta_-, \theta^a) = \int_{\eta_+}^{\eta_-} dx\ \hat{\psi}(\eta_+, x, \theta^a) \quad , \tag{4.7}$$

where, hereafter, we use a hat to denote a quantity expressed in terms of $(\eta_+, \eta_-, \theta^a)$ variables, for instance $\hat{\psi}(\eta_+, \eta_-, \theta^a) \equiv \psi(\eta, r, \theta^a)$. The sought for transformation can then be written, to second order in perturbation theory and with self-explanatory notations, as follows:

$$\begin{aligned}
\tau &= \tau^{(0)} + \tau^{(1)} + \tau^{(2)} && (4.8)\\
&\equiv \int_{\eta_{in}}^{\eta} d\eta' a(\eta') + a(\eta)P(\eta, r, \theta^a) + \int_{\eta_{in}}^{\eta} d\eta' \frac{a(\eta')}{2}\left[\phi^{(2)} - \psi^2 + (\partial_r P)^2 + \gamma_0^{ab}\ \partial_a P\ \partial_b P\right](\eta', r, \theta^a) \ , \\
w &= w^{(0)} + w^{(1)} + w^{(2)} && (4.9)\\
&\equiv \eta_+ + Q(\eta_+, \eta_-, \theta^a) + \frac{1}{4}\int_{\eta_+}^{\eta_-} dx\ \left[\hat{\psi}^{(2)} + \hat{\phi}^{(2)} + 4\hat{\psi}\partial_+ Q + \hat{\gamma}_0^{ab}\ \partial_a Q\ \partial_b Q\right](\eta_+, x, \theta^a) \quad , \\
\tilde{\theta}^a &= \tilde{\theta}^{a(0)} + \tilde{\theta}^{a(1)} + \tilde{\theta}^{a(2)} && (4.10)\\
&\equiv \theta^a + \frac{1}{2}\int_{\eta_+}^{\eta_-} dx\ \left[\hat{\gamma}_0^{ab}\partial_b Q\right](\eta_+, x, \theta^a) + \int_{\eta_+}^{\eta_-} dx\ \left[\hat{\gamma}_0^{ac}\zeta_c + \hat{\psi}\ \xi^a + \lambda^a\right](\eta_+, x, \theta^a) \quad ,
\end{aligned}$$

where η_{in} represents an early enough time when the perturbation (or better the integrand) was negligible. In other words, all the relevant integrals (i.e. for all scales of interest) are insensitive to the

actual value of η_{in}. Furthermore, we have used the following shorthand notations:

$$\begin{aligned}
\zeta_c(\eta_+,x,\theta^a) &\equiv \frac{1}{2}\partial_c w^{(2)}(\eta_+,x,\theta^a) \qquad (4.11)\\
&= \frac{1}{8}\int_{\eta_+}^{x} du\ \partial_c\left[\hat{\psi}^{(2)}+\hat{\phi}^{(2)}+4\hat{\psi}\ \partial_+Q+\hat{\gamma}_0^{ef}\ \partial_eQ\ \partial_fQ\right](\eta_+,u,\theta^a)\ ,\\
\xi^a(\eta_+,x,\theta^a) &\equiv \partial_+\tilde{\theta}^{a(1)}(\eta_+,x,\theta^a)+2\partial_x\tilde{\theta}^{a(1)}(\eta_+,x,\theta^a) \qquad (4.12)\\
&= \partial_+\left(\frac{1}{2}\int_{\eta_+}^{x} du\ [\hat{\gamma}_0^{ac}\partial_cQ](\eta_+,u,\theta^a)\right)+[\gamma_0^{ac}\partial_cQ](\eta_+,x,\theta^a)\ ,\\
\lambda^a(\eta_+,x,\theta^a) &\equiv \partial_x\tilde{\theta}^{d(1)}(\eta_+,x,\theta^a)\left(\partial_d\tilde{\theta}^{a(1)}(\eta_+,x,\theta^a)-\delta_d^a\partial_+Q(\eta_+,x,\theta^a)\right) \qquad (4.13)\\
&= \frac{1}{4}[\hat{\gamma}_0^{dc}\ \partial_cQ](\eta_+,x,\theta^a)\left(\int_{\eta_+}^{x} du\ \partial_d\left[\hat{\gamma}_0^{ae}\partial_eQ\right](\eta_+,u,\theta^a)\right)-\frac{1}{2}\left[\partial_+Q\ \hat{\gamma}_0^{ab}\partial_bQ\right](\eta_+,x,\theta^a)\ .
\end{aligned}$$

Let us now compute the various non-trivial entries of the GLC metric. Let us use on one side that $\Upsilon^{-1}=-\partial_\mu w\ \partial_\nu\tau\ g_{PG}^{\mu\nu}$ and take the following expansion:

$$\Upsilon^{-1}=\frac{1}{a(\eta)}\left(1+\epsilon^{(1)}+\epsilon^{(2)}\right)\ . \qquad (4.14)$$

In terms of quantities implicitly defined in Eqs. (4.8)-(4.9) we find:

$$\begin{aligned}
\epsilon^{(1)} &= \partial_+Q-\partial_rP\ , \qquad (4.15)\\
\epsilon^{(2)} &= \partial_\eta w^{(2)}+\frac{1}{a}(\partial_\eta-\partial_r)\tau^{(2)}-\psi\partial_\eta Q-\phi^{(2)}+2\psi^2-\partial_rP\partial_rQ-2\psi\partial_rP-\gamma_0^{ab}\partial_aP\partial_bQ\ , \qquad (4.16)
\end{aligned}$$

where

$$\begin{aligned}
\partial_+Q(\eta_+,\eta_-,\theta^a) &= -\hat{\psi}(\eta_+,\eta_+,\theta^a)+\int_{\eta_+}^{\eta_-} dx\,\partial_+\hat{\psi}(\eta_+,x,\theta^a)\ , \qquad (4.17)\\
\partial_rP(\eta,r,\theta^a) &= \int_{\eta_{in}}^{\eta} d\eta'\frac{a(\eta')}{a(\eta)}\partial_r\psi(\eta',r,\theta^a)\ , \qquad (4.18)
\end{aligned}$$

and $\hat{\psi}(\eta_+,\eta_+,\theta^a)$ denotes (at any η) the value of the perturbation potential evaluated at the tip of the light-cone connecting the origin ($r=0$) to the point $y^\mu=(\eta,r,\theta^a)$ (namely, $\hat{\psi}(\eta_+,\eta_+,\theta^a)=\psi(\eta+r,0,\theta^a)$ with $r=0$). The full explicit expression for $\epsilon^{(2)}$ can be then written as follows:

$$\begin{aligned}
\epsilon^{(2)} &= \frac{1}{4}\left(\psi^{(2)}-\phi^{(2)}\right)+\frac{\psi^2}{2}+\frac{1}{2}(\partial_rP)^2-(\psi+\partial_+Q)\,\partial_rP\\
&+ \frac{1}{4}\gamma_0^{ab}\left(2\partial_aP\,\partial_bP+\partial_aQ\,\partial_bQ-4\partial_aQ\,\partial_bP\right)\\
&+ \frac{1}{4}\ \partial_+\int_{\eta_+}^{\eta_-} dx\ \left[\hat{\psi}^{(2)}+\hat{\phi}^{(2)}+4\hat{\psi}\ \partial_+Q+\hat{\gamma}_0^{ab}\partial_aQ\,\partial_bQ\right](\eta_+,x,\theta^a)\\
&- \frac{1}{2}\int_{\eta_{in}}^{\eta} d\eta'\ \frac{a(\eta')}{a(\eta)}\partial_r\left[\phi^{(2)}-\psi^2+(\partial_rP)^2+\gamma_0^{ab}\partial_aP\,\partial_bP\right](\eta',r,\theta^a)\ , \qquad (4.19)
\end{aligned}$$

where the variables (η,r,θ^a) have been omitted for the sake of conciseness. The computation of the GLC functions U^a gives:

$$\begin{aligned}
U^a &= -\Big\{-\partial_\eta\tilde{\theta}^{a(1)}+\frac{1}{a}\gamma_0^{ab}\partial_b\tau^{(1)}-\partial_\eta\tilde{\theta}^{a(2)}+\frac{1}{a}\gamma_0^{ab}\partial_b\tau^{(2)}+\frac{1}{a}\partial_r\tau^{(1)}\partial_r\tilde{\theta}^{a(1)}\\
&+ \psi\left(\partial_\eta\tilde{\theta}^{a(1)}+\frac{2}{a}\gamma_0^{ab}\partial_b\tau^{(1)}\right)+\frac{1}{a}\gamma_0^{cd}\partial_c\tau^{(1)}\partial_d\tilde{\theta}^{a(1)}-\epsilon^{(1)}\left(-\partial_\eta\tilde{\theta}^{a(1)}+\frac{1}{a}\gamma_0^{ab}\partial_b\tau^{(1)}\right)\Big\}\ , \qquad (4.20)
\end{aligned}$$

where $\tau^{(1),(2)}$ and $\tilde{\theta}^{a(1),(2)}$ are implicitly defined in the coordinate transformations of Eqs. (4.8) and (4.10). The vector U^a is a measure of anisotropy of spacetime in GLC coordinates. Substituting in

Eq. (4.20) the explicit values of $\tau^{(1),(2)}$ and $\tilde{\theta}^{a(1),(2)}$, we obtain the explicit expression for U^a :

$$\begin{aligned} U^a &= \left\{ \gamma_0^{ab} \left(\frac{1}{2}\partial_b Q - \partial_b P \right) + \partial_+ \left(\frac{1}{2} \int_{\eta_+}^{\eta_-} dx \ \left[\hat{\gamma}_0^{ab} \ \partial_b Q \right] (\eta_+, x, \theta^a) \right) \right\} \\ &+ \left\{ -\left(\psi + \partial_+ Q\right) \partial_+ \left(\frac{1}{2} \int_{\eta_+}^{\eta_-} dx \ \left[\hat{\gamma}_0^{ab} \ \partial_b Q \right] (\eta_+, x, \theta^a) \right) + \left(-\psi + 2\partial_r P - \partial_+ Q\right) \frac{1}{2} \gamma_0^{ab} \ \partial_b Q \right. \\ &\quad -2\psi \gamma_0^{ab} \ \partial_b P - \frac{1}{2} \gamma_0^{cd} \ \partial_c P \int_{\eta_+}^{\eta_-} dx \ \partial_d \left[\hat{\gamma}_0^{ab} \ \partial_b Q \right] (\eta_+, x, \theta^a) + (\partial_+ Q - \partial_r P) \gamma_0^{ab} \partial_b P \\ &\quad -\frac{1}{2} \gamma_0^{ab} \int_{\eta_{in}}^{\eta} d\eta' \frac{a(\eta')}{a(\eta)} \partial_b \left[\phi^{(2)} - \psi^2 + (\partial_r P)^2 + \gamma_0^{cd} \partial_c P \partial_d P \right] (\eta', r, \theta^a) \\ &\quad \left. +(\partial_+ + \partial_-) \int_{\eta_+}^{\eta_-} dx \ \left[\hat{\gamma}_0^{ac} \zeta_c + \hat{\psi} \ \xi^a + \lambda^a \right] (\eta_+, x, \theta^a) \right\} \ . \end{aligned} \tag{4.21}$$

Finally, starting from $\gamma^{ab} = \frac{\partial \tilde{\theta}^a}{\partial y^\mu} \frac{\partial \tilde{\theta}^b}{\partial y^\nu} g_{PG}^{\mu\nu}(y)$, we find :

$$\begin{aligned} a(\eta)^2 \gamma^{ab} &= \gamma_0^{ab} \left(1 + 2\psi\right) + \left[\gamma_0^{ac} \partial_c \tilde{\theta}^{b(1)} + (a \leftrightarrow b) \right] \\ &+ \gamma_0^{ab} \left(\psi^{(2)} + 4\psi^2 \right) - \partial_\eta \tilde{\theta}^{a(1)} \partial_\eta \tilde{\theta}^{b(1)} + \partial_r \tilde{\theta}^{a(1)} \partial_r \tilde{\theta}^{b(1)} \\ &+ 2\psi \left[\gamma_0^{ac} \partial_c \tilde{\theta}^{b(1)} + (a \leftrightarrow b) \right] + \gamma_0^{cd} \partial_c \tilde{\theta}^{a(1)} \partial_d \tilde{\theta}^{b(1)} + \left[\gamma_0^{ac} \partial_c \tilde{\theta}^{b(2)} + (a \leftrightarrow b) \right] \ . \end{aligned} \tag{4.22}$$

More explicitly, in terms of the quantities defined in Eqs. (4.7) and (4.11)-(4.13) :

$$\begin{aligned} a(\eta)^2 \gamma^{ab} &= \gamma_0^{ab} \left(1 + 2\psi\right) + \frac{1}{2} \left\{ \gamma_0^{ad} \int_{\eta_+}^{\eta_-} dx \ \partial_d \left[\hat{\gamma}_0^{bc} \partial_c Q \right] (\eta_+, x, \theta^a) + (a \leftrightarrow b) \right\} \\ &+ \left(\psi^{(2)} + 4\psi^2 \right) \gamma_0^{ab} - \left\{ \gamma_0^{ac} \partial_c Q \ \partial_+ \left(\frac{1}{2} \int_{\eta_+}^{\eta_-} dx \ \left[\hat{\gamma}_0^{bd} \ \partial_d Q \right] (\eta_+, x, \theta^a) \right) + (a \leftrightarrow b) \right\} \\ &+ \psi \left\{ \gamma_0^{ad} \int_{\eta_+}^{\eta_-} dx \ \partial_d \left[\hat{\gamma}_0^{bc} \partial_c Q \right] (\eta_+, x, \theta^a) + (a \leftrightarrow b) \right\} \\ &+ \frac{1}{4} \gamma_0^{cd} \left(\int_{\eta_+}^{\eta_-} dx \ \partial_c \left[\hat{\gamma}_0^{ae} \partial_e Q \right] (\eta_+, x, \theta^a) \right) \left(\int_{\eta_+}^{\eta_-} d\bar{x} \ \partial_d \left[\hat{\gamma}_0^{bf} \partial_f Q \right] (\eta_+, \bar{x}, \theta^a) \right) \\ &+ \left\{ \gamma_0^{ac} \int_{\eta_+}^{\eta_-} dx \ \partial_c \left[\hat{\gamma}_0^{bd} \ \zeta_d + \hat{\psi} \ \xi^b + \lambda^b \right] (\eta_+, x, \theta^a) + (a \leftrightarrow b) \right\} \ . \end{aligned} \tag{4.23}$$

4.1.3 The second order transformation for vector and tensor perturbations

As already mentioned we can add the contributions of the tensor and vector perturbations by considering them separately. Using spherical coordinates $\{x^i\} = (r, \theta^a) \equiv (r, \theta, \phi)$, the tensor and vector part of the PG metric defined in Eq. (4.1) can be rewritten as :

$$ds_{PG}^2 = a^2(\eta) \left[-d\eta^2 + 2v_i d\eta dx^i + [(\gamma_0)_{ij} + \chi_{ij}] dx^i dx^j \right] \ , \tag{4.24}$$

corresponding to :

$$g_{PG}^{\mu\nu}(\eta, r, \theta^a) = a^{-2}(\eta) \begin{pmatrix} -1 & v^i \\ v^j & \gamma_0^{ij} - \chi^{ij} \end{pmatrix} \ , \tag{4.25}$$

and where $\gamma_0^{ij} = \mathrm{diag}(1, r^{-2}, r^{-2}(\sin\theta)^{-2})$ is the (inverse) flat 3-metric. Here v^i and χ^{ij} are the vector and tensor perturbations in spherical coordinates equivalent to the more standard definition ω^i and h^{ij} used in cartesian coordinates of Eq. (4.1). They satisfy $\nabla_i v^i = \nabla_i \chi^{ij} = 0$ and $(\gamma_0)_{ij} \chi^{ij} = 0$ with ∇_i the flat 3-dimensional covariant derivative in spherical coordinates.

Proceeding as for the scalar part of the metric, we first note that τ is not affected by vector and tensor perturbations:

$$\tau = \int_{\eta_{in}}^{\eta} d\eta' a(\eta') \quad , \tag{4.26}$$

while the light-cone coordinate w is:

$$w = \eta_+ + Q^{(\alpha)}(\eta_+, \eta_-, \theta^a) \quad , \tag{4.27}$$

and where

$$Q^{(\alpha)}(\eta_+, \eta_-, \theta^a) = \int_{\eta^+}^{\eta^-} dx\ \hat{\alpha}^r(\eta^+, x, \theta^a) \qquad \text{with} \qquad \alpha^r \equiv \frac{v^r}{2} - \frac{\chi^{rr}}{4} \quad . \tag{4.28}$$

As before, hats mean that $(\eta_+, \eta_-, \theta^a)$-coordinates are used. Finally, we find:

$$\begin{aligned} \tilde{\theta}^a &= \tilde{\theta}^{a(0)} + \tilde{\theta}^{a(2)} \\ &= \theta^a + \frac{1}{2}\int_{\eta_+}^{\eta^-} dx \left([\hat{v}^a - \hat{\chi}^{ra}](\eta_+, x, \theta^a) + \hat{\gamma}_0^{ab}(\eta_+, x, \theta^a) \int_{\eta_+}^{x} dy\ \partial_b \hat{\alpha}^r(\eta_+, y, \theta^a) \right) \quad . \end{aligned} \tag{4.29}$$

Following the same steps as for scalar perturbations, we then compute the non-trivial entries of the GLC metric:

$$a(\eta)\Upsilon^{-1} = 1 - \frac{1}{2}v^r - \frac{1}{4}\chi^{rr} + \partial_+ \int_{\eta_+}^{\eta_-} dx\ \hat{\alpha}(\eta_+, x, \theta^a) \quad , \tag{4.30}$$

$$\begin{aligned} a(\eta)^2\gamma^{ab} &= \gamma_0^{ab} - \chi^{ab} \\ &+ \left[\frac{\gamma_0^{ac}}{2} \int_{\eta_+}^{\eta_-} dx\ \partial_c \left([\hat{v}^b - \hat{\chi}^{rb}](\eta_+, x, \theta^a) + \hat{\gamma}_0^{bd}(\eta_+, x, \theta^a) \int_{\eta_+}^{x} dy\ \partial_d \hat{\alpha}^r(\eta_+, y, \theta^a) \right) + (a \leftrightarrow b) \right] \quad , \end{aligned} \tag{4.31}$$

$$\begin{aligned} U^a &= -v^a + \partial_\eta \tilde{\theta}^{a(2)} = -v^a + \partial_- \tilde{\theta}^{a(2)} + \partial_+ \tilde{\theta}^{a(2)} = \frac{1}{2}\left(-v^a - \chi^{ra} + \gamma_0^{ab} \int_{\eta_+}^{\eta^-} dx\ \partial_b \hat{\alpha}^r(\eta_+, x, \theta^a) \right) \\ &+ \frac{1}{2}\partial_+ \left(\int_{\eta_+}^{\eta^-} dx \left[[\hat{v}^a - \hat{\chi}^{ra}](\eta_+, x, \theta^a) + \hat{\gamma}_0^{ab}(\eta_+, x, \theta^a) \int_{\eta_+}^{x} dy\ \partial_b \hat{\alpha}^r(\eta_+, y, \theta^a) \right] \right) \quad , \end{aligned} \tag{4.32}$$

where, again, the variables (η, r, θ^a) have been omitted for the sake of conciseness. Of course, these vector and tensor corrections to the FLRW metric have to be added to the scalar ones of the previous subsection. We will see in Sec. 5.3.6 that these modes play a negligible role in our formalism.

4.2 Detailed expression for $d_L(z, \theta^a)$

4.2.1 The scalar contribution

We now apply the above coordinate transformations to find the final expression of the luminosity distance in terms of perturbations in the PG, of the observed redshift, and of the observer's angular coordinates beginning, once more, with the scalar contribution. From Eq. (3.22) we have:

$$d_L = (1 + z_s)^2\ \gamma^{1/4}\ (\sin\tilde{\theta})^{-1/2} \quad . \tag{4.33}$$

For a source emitting light at time η_s and radial distance r_s we obtain from Eq. (4.22):

$$\begin{aligned} \gamma^{-1} \equiv \det\gamma^{ab} &= (a_s^2 r_s^2 \sin\theta)^{-2} \Big\{ 1 + 4\psi_s + 2\partial_a \tilde{\theta}^{a(1)} + 2\psi_s^{(2)} + 12\psi_s^2 + 2\partial_a \tilde{\theta}^{a(2)} - 4\gamma_{0ab}\partial_+ \tilde{\theta}^{a(1)} \partial_- \tilde{\theta}^{b(1)} \\ &\quad + 8\psi_s \partial_a \tilde{\theta}^{a(1)} + 2\partial_a \tilde{\theta}^{a(1)} \partial_b \tilde{\theta}^{b(1)} - \partial_a \tilde{\theta}^{b(1)} \partial_b \tilde{\theta}^{a(1)} \Big\} \quad . \end{aligned} \tag{4.34}$$

We also need the expression for $\sin\tilde{\theta}$ up to second order in perturbations. This is easily given as:

$$\sin\tilde{\theta} = \sin\theta \left[1 + \cot\theta \left(\tilde{\theta}^{(1)} + \tilde{\theta}^{(2)} \right) - \frac{1}{2}\left(\tilde{\theta}^{(1)} \right)^2 \right] \quad . \tag{4.35}$$

Using Eqs. (4.34) and (4.35), the Eq. (4.33) yields:

$$d_L = (1+z_s)^2(a_s r_s)\left\{1-\psi_s - J_2 - \frac{1}{2}\psi_s^{(2)} - \frac{1}{2}\psi_s^2 - K_2 + \psi_s J_2 + \frac{1}{2}(J_2)^2 + \frac{1}{4\sin^2\theta}\left(\tilde{\theta}^{(1)}\right)^2 + (\gamma_0)_{ab}\partial_+\tilde{\theta}^{a(1)}\partial_-\tilde{\theta}^{b(1)} + \frac{1}{4}\partial_a\tilde{\theta}^{b(1)}\partial_b\tilde{\theta}^{a(1)}\right\} \quad , \tag{4.36}$$

where:

$$J_2 = \frac{1}{2}\left[\cot\theta\ \tilde{\theta}^{(1)} + \partial_a\tilde{\theta}^{a(1)}\right] \equiv \frac{1}{2}\nabla_a\tilde{\theta}^{a(1)} \quad , \quad K_2 = \frac{1}{2}\left[\cot\theta\ \tilde{\theta}^{(2)} + \partial_a\tilde{\theta}^{a(2)}\right] \equiv \frac{1}{2}\nabla_a\tilde{\theta}^{a(2)} \quad . \tag{4.37}$$

All the above quantities are evaluated at the source (apart for ψ_s we neglect the suffix s for simplicity).

At this point, for the explicit expression of the luminosity distance d_L at constant redshift, we need the first and second-order expansion of the factor $a_s r_s \equiv a(\eta_s) r_s$ appearing in Eq. (4.36). To this purpose, we start from the explicit expression for the redshift parameter z_s (see Eq. (3.18)), considered as a constant parameter localizing, together with the $w = w_o$ condition, the source on $\Sigma(w_o, z_s)$. We then look for approximate solutions for $\eta_s = \eta_s(z_s, \theta^a)$ and $r_s = r_s(z_s, \theta^a)$.

Let us first define the zero-order solution $\eta_s^{(0)}$ through the (exact) relation:

$$\frac{a(\eta_s^{(0)})}{a_o} = \frac{1}{1+z_s} \quad , \tag{4.38}$$

where $a_o \equiv a(\eta_o)$. Inserting now the result of Eq. (4.14) into Eq. (3.18) and expanding $a(\eta_s)$ and Υ^{-1} with respect to the background solutions $\eta_s^{(0)}$ and $r_s^{(0)}$ (where we define $\eta_s = \eta_s^{(0)} + \eta_s^{(1)} + \eta_s^{(2)}$ and $r_s = r_s^{(0)} + r_s^{(1)} + r_s^{(2)}$), we obtain:

$$\frac{1}{1+z_s} = \frac{a(\eta_s^{(0)})}{a(\eta_o)}\left\{1 + \left[\mathcal{H}_s\eta_s^{(1)} + \epsilon_o^{(1)} - \epsilon_s^{(1)}\right] + \left[\mathcal{H}_s\eta_s^{(2)} + (\mathcal{H}_s' + \mathcal{H}_s^2)\frac{(\eta_s^{(1)})^2}{2} + \epsilon_o^{(2)} - \epsilon_s^{(2)} - \epsilon_s^{(1\to 2)} + (\epsilon_s^{(1)})^2 - \epsilon_o^{(1)}\epsilon_s^{(1)} + \mathcal{H}_s\eta_s^{(1)}(\epsilon_o^{(1)} - \epsilon_s^{(1)})\right]\right\} \quad , \tag{4.39}$$

where $\mathcal{H}_s = a'(\eta_s^{(0)})/a(\eta_s^{(0)})$ and

$$\epsilon_o^{(1)} = \epsilon^{(1)}(\eta_o, 0, \theta^a)\ ;\ \epsilon_s^{(1)} = \epsilon^{(1)}(\eta_s^{(0)}, r_s^{(0)}, \theta^a)\ ;\ \epsilon_o^{(2)} = \epsilon^{(2)}(\eta_o, 0, \theta^a)\ ;\ \epsilon_s^{(2)} = \epsilon^{(2)}(\eta_s^{(0)}, r_s^{(0)}, \theta^a) \quad , \tag{4.40}$$

$$\epsilon_s^{(1\to 2)} = \left[\partial_\eta\epsilon^{(1)}\right](\eta_s^{(0)}, r_s^{(0)}, \theta^a)\ \eta_s^{(1)} + \left[\partial_r\epsilon^{(1)}\right](\eta_s^{(0)}, r_s^{(0)}, \theta^a)\ r_s^{(1)} \quad . \tag{4.41}$$

Similarly, in order to compute $r_s^{(1)}$ and $r_s^{(2)}$, we need to expand the $w = w_o$ constraint by writing:

$$w_o = \left\{\eta_s^{(0)} + r_s^{(0)}\right\} + \left\{\eta_s^{(1)} + r_s^{(1)} + w_s^{(1)}\right\} + \left\{\eta_s^{(2)} + r_s^{(2)} + w_s^{(2)} + w_s^{(1\to 2)}\right\} \tag{4.42}$$

and where

$$w_s^{(1)} = w^{(1)}(\eta_s^{(0)}, r_s^{(0)}, \theta^a) \quad , \quad w_s^{(2)} = w^{(2)}(\eta_s^{(0)}, r_s^{(0)}, \theta^a) \quad , \tag{4.43}$$

$$w_s^{(1\to 2)} = \left[\partial_\eta w^{(1)}\right](\eta_s^{(0)}, r_s^{(0)}, \theta^a)\ \eta_s^{(1)} + \left[\partial_r w^{(1)}\right](\eta_s^{(0)}, r_s^{(0)}, \theta^a)\ r_s^{(1)} \quad . \tag{4.44}$$

The additional terms $\epsilon_s^{(1\to 2)}$, $w_s^{(1\to 2)}$ appearing in the above equations stand for the second order contributions coming from Taylor expanding $\epsilon_s^{(1)}$, $w_s^{(1)}$, around the background source position [1]. More precisely, they come from the fact that, at first order, quantities that are already first order are

1. There is no equivalent contribution at the observer position as η_o and $r_o = 0$ are fixed quantities, with no perturbative corrections.

integrated along the *unperturbed* line of sight, while, at second order, first order terms have to be integrated along the *perturbed* line of sight.

From Eq. (4.15) we obtain:

$$\epsilon_s^{(1)} - \epsilon_o^{(1)} = J \tag{4.45}$$

with

$$J \equiv ([\partial_+ Q]_s - [\partial_+ Q]_o) - ([\partial_r P]_s - [\partial_r P]_o) \quad , \tag{4.46}$$

and where, for example, the term $[\partial_r P]_s$ denotes the expression of $\partial_r P$ with η and r replaced by $\eta_s^{(0)}$ and $r_s^{(0)}$, we also remark that $[\partial_+ Q]_o = -\psi_o$. Then, from Eqs. (4.39) and (4.42), recalling Eq. (4.9), we compute:

$$\eta_s^{(1)} = \frac{J}{\mathcal{H}_s} \quad , \quad r_s^{(0)} = \eta_o - \eta_s^{(0)} \equiv \Delta\eta \quad , \quad r_s^{(1)} = -Q_s - \frac{J}{\mathcal{H}_s} \quad . \tag{4.47}$$

We wish to note, already at this point, that the ϵ terms correspond to redshift perturbations (RP). The first order term, $\epsilon^{(1)}$, gives rise to the Doppler effect due to the peculiar velocities $\partial_r P$, and the Sachs-Wolfe effect (SW) and integrated Sachs-Wolfe effect (ISW) are combined together in $[\partial_+ Q]_s - [\partial_+ Q]_o$. Let us, in fact, recall that $\partial_r P$ can be rewritten as:

$$\partial_r P = \mathbf{v} \cdot \mathbf{n} \quad , \tag{4.48}$$

where $\mathbf{n}$ is the unit tangent vector along the null geodesic connecting source and observer, and where

$$\mathbf{v} = -\int_{\eta_{in}}^{\eta} d\eta' \frac{a(\eta')}{a(\eta)} \vec{\nabla}\psi(\eta', r, \theta^a) \tag{4.49}$$

is the *peculiar velocity* associated to a geodesic trajectory perturbed up to first order in the PG.

Let us now move to the second order quantities appearing in Eqs. (4.40), (4.41) and (4.43), (4.44). We simply have, from Eq. (4.19),

$$\begin{aligned}
\epsilon_s^{(2)} - \epsilon_o^{(2)} \;=\; & -\frac{1}{4}\left(\phi_s^{(2)} - \phi_o^{(2)}\right) + \frac{1}{4}\left(\psi_s^{(2)} - \psi_o^{(2)}\right) + \frac{1}{2}\left(\psi_s^2 - \psi_o^2\right) \\
& + \frac{1}{2}([\partial_r P]_s)^2 - \frac{1}{2}([\partial_r P]_o)^2 - (\psi_s + [\partial_+ Q]_s)\,[\partial_r P]_s \\
& + \frac{1}{4}(\gamma_0^{ab})_s\,(2\partial_a P_s\,\partial_b P_s + \partial_a Q_s\,\partial_b Q_s - 4\partial_a Q_s\,\partial_b P_s) - \frac{1}{2}\lim_{r\to 0}\left[\gamma_0^{ab}\partial_a P\,\partial_b P\right] \\
& - \frac{1}{2}\int_{\eta_{in}}^{\eta_s^{(0)}} d\eta' \frac{a(\eta')}{a(\eta_s^{(0)})}\partial_r\left[\phi^{(2)} - \psi^2 + (\partial_r P)^2 + \gamma_0^{ab}\partial_a P\,\partial_b P\right](\eta', \Delta\eta, \theta^a) \\
& + \frac{1}{2}\int_{\eta_{in}}^{\eta_o} d\eta' \frac{a(\eta')}{a(\eta_o)}\partial_r\left[\phi^{(2)} - \psi^2 + (\partial_r P)^2 + \gamma_0^{ab}\partial_a P\,\partial_b P\right](\eta', 0, \theta^a) \\
& + \frac{1}{4}\int_{\eta_s^{(0)+}}^{\eta_s^{(0)-}} dx\;\partial_+\left[\hat{\phi}^{(2)} + \hat{\psi}^{(2)} + 4\hat{\psi}\;\partial_+ Q + \hat{\gamma}_0^{ab}\,\partial_a Q\,\partial_b Q\right](\eta_s^{(0)+}, x, \theta^a) \quad ,
\end{aligned} \tag{4.50}$$

while

$$\epsilon_s^{(1\to 2)} = Q_s\left\{-[\partial_+^2 Q]_s + [\partial_+\hat{\psi}]_s + [\partial_r^2 P]_s\right\} + \frac{J}{\mathcal{H}_s}\left\{[\partial_\eta\psi]_s + \mathcal{H}_s[\partial_r P]_s + [\partial_r^2 P]_s\right\} \quad . \tag{4.51}$$

We then have:

$$w_s^{(1\to 2)} = \frac{2}{\mathcal{H}_s}\psi_s J + Q_s\left(\psi_s - [\partial_+ Q]_s\right) \quad . \tag{4.52}$$

Using Eqs. (4.39) and (4.42), and recalling again Eq. (4.9), we can now calculate η_s and r_s to second order, obtaining:

$$\begin{aligned}
\eta_s^{(2)} &= -\frac{1}{\mathcal{H}_s}\left\{(\mathcal{H}_s' + \mathcal{H}_s^2)\frac{(\eta_s^{(1)})^2}{2} + \epsilon_o^{(2)} - \epsilon_s^{(2)} - \epsilon_s^{(1\to 2)} + (\epsilon_s^{(1)})^2 - \epsilon_o^{(1)}\epsilon_s^{(1)} + \mathcal{H}_s\eta_s^{(1)}(\epsilon_o^{(1)} - \epsilon_s^{(1)})\right\} \\
&= -\frac{1}{\mathcal{H}_s}\left\{\frac{\mathcal{H}_s' + \mathcal{H}_s^2}{\mathcal{H}_s^2}\frac{J^2}{2} + \epsilon_o^{(2)} - \epsilon_s^{(2)} - \epsilon_s^{(1\to 2)} + \epsilon_s^{(1)}J - J^2\right\} \quad ,
\end{aligned} \tag{4.53}$$

and

$$\begin{aligned} r_s^{(2)} &= -\left(\eta_s^{(2)} + w_s^{(2)} + w_s^{(1\to 2)}\right) \\ &= -\frac{1}{\mathcal{H}_s}\left(\epsilon_s^{(2)} - \epsilon_o^{(2)} + \epsilon_s^{(1\to 2)}\right) - \frac{J}{\mathcal{H}_s}\left(2\psi_s + \psi_o + [\partial_r P]_o\right) + \frac{\mathcal{H}_s^2 + \mathcal{H}_s'}{2\mathcal{H}_s^3} J^2 + \left(-\psi_s + [\partial_+ Q]_s\right) Q_s \\ &\quad -\frac{1}{4}\int_{\eta_s^{(0)+}}^{\eta_s^{(0)-}} dx \ \left[\hat{\phi}^{(2)} + \hat{\psi}^{(2)} + 4\hat{\psi}\ \partial_+ Q + \hat{\gamma}_0^{ab}\ \partial_a Q\ \partial_b Q\right]\left(\eta_s^{(0)+}, x, \theta^a\right) \ . \end{aligned} \tag{4.54}$$

In the second order terms we have the expected couplings between first order terms as well as the (also expected) genuine second order SW and ISW effects such as $(\psi_s^{(2)} - \psi_o^{(2)})$ and $\int dx\ \partial_+\hat{\psi}^{(2)}$. However, at second order, new effects come into play : most notably the *tangential peculiar velocity* $\partial_a P$, the *tangential variation of the photon path* $\partial_a Q$, and a redshift space distortions (RSD) due to the *peculiar acceleration* $\partial^2 P$. The somewhat surprising appearance of tangential derivatives in $\eta_s^{(2)}$ and $r_s^{(2)}$ is simply a reflection of working on a fixed-z surface. As a consequence, redshift perturbations (RP) originating from those of τ, Eq. (4.8), feed back on η_s, r_s and eventually on $d_L(z)$.

To conclude, combining these results, we obtain :

$$\begin{aligned} \frac{a(\eta_s) r_s}{a(\eta_s^{(0)})\Delta\eta} &= 1 + \left\{\Xi_s J - \frac{Q_s}{\Delta\eta}\right\} + \left\{\Xi_s\left(\epsilon_s^{(2)} - \epsilon_o^{(2)} + \epsilon_s^{(1\to 2)}\right) - \frac{1}{\mathcal{H}_s\Delta\eta}\left(1 - \frac{\mathcal{H}_s'}{\mathcal{H}_s^2}\right)\frac{J^2}{2} - \frac{2}{\mathcal{H}_s\Delta\eta}\psi_s J\right. \\ &\quad + \Xi_s\left(\psi_o + [\partial_r P]_o\right) J + \left(-\psi_o - \psi_s + [\partial_r P]_s - [\partial_r P]_o\right)\frac{Q_s}{\Delta\eta} \\ &\quad \left. -\frac{1}{4\Delta\eta}\int_{\eta_s^{(0)+}}^{\eta_s^{(0)-}} dx \ \left[\hat{\phi}^{(2)} + \hat{\psi}^{(2)} + 4\hat{\psi}\ \partial_+ Q + \hat{\gamma}_0^{ab}\ \partial_a Q\ \partial_b Q\right]\left(\eta_s^{(0)+}, x, \theta^a\right)\right\} \ , \end{aligned} \tag{4.55}$$

where (using $\Delta\eta \equiv \eta_o - \eta_s^{(0)}$) we defined :

$$\Xi_s \equiv 1 - \frac{1}{\mathcal{H}_s\Delta\eta} \ . \tag{4.56}$$

Let us also note that in Eq. (4.36) there are two other first order terms that have to be Taylor expanded up to second order around the background solution connected to the observed redshift z_s, i.e. ψ_s and J_2. We find :

$$\psi_s = \psi_s^{(1)} + \psi_s^{(1\to 2)} = \psi(\eta_s^{(0)}, \Delta\eta, \theta^a) + \frac{J}{\mathcal{H}_s}\left[\partial_\eta\psi - \partial_r\psi\right](\eta_s^{(0)}, \Delta\eta, \theta^a) - Q_s[\partial_r\psi](\eta_s^{(0)}, \Delta\eta, \theta^a) \ , \tag{4.57}$$

$$\begin{aligned} J_2 &= J_2^{(1)} + J_2^{(1\to 2)} \qquad (4.58) \\ &= \frac{1}{\Delta\eta}\int_{\eta_s^{(0)}}^{\eta_o} d\eta' \frac{\eta' - \eta_s^{(0)}}{\eta_o - \eta'}\Delta_2\psi(\eta', \eta_o - \eta', \theta^a) - \left(\frac{J}{\mathcal{H}_s} + \frac{Q_s}{2}\right)\frac{1}{\Delta\eta^2}\int_{\eta_s^{(0)}}^{\eta_o} d\eta' \Delta_2\psi(\eta', \eta_o - \eta', \theta^a) \\ &\quad -Q_s\ \partial_+\left(\int_{\eta_s^{(0)+}}^{\eta_s^{(0)-}} dx \frac{1}{\left(\eta_s^{(0)+} - x\right)^2}\int_{\eta_s^{(0)+}}^{x} dy\ \Delta_2\hat{\psi}(\eta_s^{(0)+}, y, \theta^a)\right) \ , \end{aligned}$$

where we have used the 2-dimensional Laplacian $\Delta_2 \equiv \partial_\theta^2 + \cot\theta\,\partial_\theta + (\sin\theta)^{-2}\partial_\phi^2$.

Collecting all the results obtained up to now, and inserting them in Eq. (4.36), we write our final result on the effect of scalar perturbations in the following concise form :

$$\frac{d_L(z_s, \theta^a)}{(1+z_s)a_o\Delta\eta} = \frac{d_L(z_s, \theta^a)}{d_L^{\rm FLRW}(z_s)} = 1 + \delta_S^{(1)}(z_s, \theta^a) + \delta_S^{(2)}(z_s, \theta^a) \ , \tag{4.59}$$

where :

$$\begin{aligned} \delta_S^{(1)}(z_s, \theta^a) &= \Xi_s J - \frac{Q_s}{\Delta\eta} - \psi_s^{(1)} - J_2^{(1)} \ , \\ \delta_S^{(2)}(z_s, \theta^a) &= -\left(\Xi_s J - \frac{Q_s}{\Delta\eta}\right)\left(\psi_s^{(1)} + J_2^{(1)}\right) - \psi_s^{(1\to 2)} - J_2^{(1\to 2)} + X^{(2)} + Y^{(2)} \ . \end{aligned} \tag{4.60}$$

Here $\psi_s^{(1)}$, $\psi_s^{(1\to 2)}$, $J_2^{(1)}$ and $J_2^{(1\to 2)}$ are implicitly defined in Eqs. (4.57), (4.58) and $X^{(2)}$, $Y^{(2)}$ are the second order terms appearing in Eq. (4.36) and (4.55), namely :

$$\begin{aligned} X^{(2)} &= -\frac{1}{2}\psi_s^{(2)} - \frac{1}{2}\psi_s^2 - K_2 + \psi_s J_2 + \frac{1}{2}(J_2)^2 \\ &\quad + \frac{1}{4\sin^2\theta}\left(\tilde{\theta}^{(1)}\right)^2 + (\gamma_0)_{ab}\partial_+\tilde{\theta}^{a(1)}\partial_-\tilde{\theta}^{b(1)} + \frac{1}{4}\partial_a\tilde{\theta}^{b(1)}\partial_b\tilde{\theta}^{a(1)} \quad , \\ Y^{(2)} &= \Xi_s\left(\epsilon_s^{(2)} - \epsilon_o^{(2)} + \epsilon_s^{(1\to 2)}\right) - \frac{2}{\mathcal{H}_s\Delta\eta}\psi_s J + \Xi_s\left(\psi_o + [\partial_r P]_o\right) J + \left([\partial_r P]_s - \psi_o - \psi_s - [\partial_r P]_o\right)\frac{Q_s}{\Delta\eta} \\ &\quad - \frac{1}{\mathcal{H}_s\Delta\eta}\left(1 - \frac{\mathcal{H}_s'}{\mathcal{H}_s^2}\right)\frac{J^2}{2} - \frac{1}{4\Delta\eta}\int_{\eta_s^{(0)+}}^{\eta_s^{(0)-}} dx \ \left[\hat{\phi}^{(2)} + \hat{\psi}^{(2)} + 4\hat{\psi}\ \partial_+ Q + \hat{\gamma}_0^{ab}\ \partial_a Q\ \partial_b Q\right](\eta_s^{(0)+}, x, \theta^a) \quad . \end{aligned} \tag{4.61}$$

On the other hand, as already stressed, photons reach the observer traveling at constant $\tilde{\theta}^a$. Therefore, the observer's angles are given by the $\tilde{\theta}^a$ which coincide with θ^a at the observer position but not at the source, hence d_L should be written in terms of $\tilde{\theta}^a$ rather than of θ^a. As a consequence let us consider the inverse form of Eq. (4.10) :

$$\begin{aligned} \theta^a &= \theta^{a(0)} + \theta^{a(1)} + \theta^{a(2)} = \tilde{\theta}^a - \frac{1}{2}\int_{\eta_+}^{\eta_-} dx\ \hat{\gamma}_0^{ab}(\eta_+, x, \tilde{\theta}^a)\int_{\eta_+}^{x} dy\ \partial_b\hat{\psi}(\eta_+, y, \tilde{\theta}^a) \\ &+ \frac{1}{4}\left[\int_{\eta_+}^{\eta_-} dx\ \hat{\gamma}_0^{cb}(\eta_+, x, \tilde{\theta}^a)\int_{\eta_+}^{x} dy\ \partial_b\hat{\psi}(\eta_+, y, \tilde{\theta}^a)\right]\partial_c\left[\int_{\eta_+}^{\eta_-} dx\ \hat{\gamma}_0^{ad}(\eta_+, x, \tilde{\theta}^a)\int_{\eta_+}^{x} dy\ \partial_d\hat{\psi}(\eta_+, y, \tilde{\theta}^a)\right] \\ &- \int_{\eta_+}^{\eta_-} dx\ \left[\hat{\gamma}_0^{ac}\zeta_c + \hat{\psi}\ \xi^a + \lambda^a\right](\eta_+, x, \tilde{\theta}^a) \quad . \end{aligned} \tag{4.62}$$

The luminosity distance $\bar{d}_L(z_s, \tilde{\theta}^a)$ will then be given by Taylor expanding $d_L(z_s, \theta^a)$ around $\tilde{\theta}^a$ (we use a bar to denote that the luminosity distance is now expressed in terms of $\tilde{\theta}^a$). Using Eq. (4.62) we obtain :

$$\frac{\bar{d}_L(z_s, \tilde{\theta}^a)}{(1+z_s)a_0\Delta\eta} = \frac{\bar{d}_L(z_s, \tilde{\theta}^a)}{d_L^{\mathrm{FLRW}}(z_s)} = 1 + \bar{\delta}_S^{(1)}(z_s, \tilde{\theta}^a) + \bar{\delta}_S^{(2)}(z_s, \tilde{\theta}^a) \quad ,$$

$$\text{with} \quad \bar{\delta}_S^{(1)}(z_s, \tilde{\theta}^a) = \delta_S^{(1)}(z_s, \tilde{\theta}^a) \quad , \quad \bar{\delta}_S^{(2)}(z_s, \tilde{\theta}^a) = \delta_S^{(2)}(z_s, \tilde{\theta}^a) + \partial_b\left[\delta_S^{(1)}(z_s, \tilde{\theta}^a)\right]\theta^{b(1)} \quad . \tag{4.63}$$

Let us note the presence of two particular terms which appear in the Eqs. (4.61), (4.63) and are well-known in the literature (see e.g. [106]). The first term, present in (4.61), is called the lens-lens coupling and stands as (using Eq. (4.10)) :

$$\frac{1}{4}\partial_a\tilde{\theta}^{b(1)}\partial_b\tilde{\theta}^{a(1)} = \frac{1}{16}\partial_a\left(\int_{\eta_s^{(0)+}}^{\eta_s^{(0)-}} dx\ \left[\hat{\gamma}_0^{bc}\ \partial_c Q\right](\eta_s^{(0)+}, x, \tilde{\theta}^a)\right)\partial_b\left(\int_{\eta_s^{(0)+}}^{\eta_s^{(0)-}} d\bar{x}\ \left[\hat{\gamma}_0^{ad}\ \partial_d Q\right](\eta_s^{(0)+}, \bar{x}, \tilde{\theta}^a)\right). \tag{4.64}$$

The second, revealed in Eq. (4.63), describes the first deviations from the line of sight and is named the "first correction to the Born approximation". It is given by the term :

$$\partial_b\left[\delta_S^{(1)}(z_s, \tilde{\theta}^a)\right]\theta^{b(1)} \supset \frac{1}{2}\partial_a J_2^{(1)}\left(\int_{\eta_s^{(0)+}}^{\eta_s^{(0)-}} dx\ \left[\hat{\gamma}_0^{ab}\ \partial_b Q\right](\eta_s^{(0)+}, x, \tilde{\theta}^a)\right) \quad . \tag{4.65}$$

Equations (4.60), (4.63), supplemented with the vector and tensor contribution discussed in the next subsection, are our main result about the luminosity distance. More explicit expressions, where terms with different physical meaning are collected separately, can also be written down. Indeed, the second order corrections of $\bar{\delta}_S^{(2)}(z_s, \tilde{\theta}^a)$ appearing in Eq. (4.63) can be conveniently grouped as follows :

$$\bar{\delta}_S^{(2)}(z_s, \tilde{\theta}^a) = \bar{\delta}_{path}^{(2)} + \bar{\delta}_{pos}^{(2)} + \bar{\delta}_{mixed}^{(2)} \tag{4.66}$$

where $\bar{\delta}_{path}^{(2)}$ is for the terms concerning the photon path, $\bar{\delta}_{pos}^{(2)}$ for the terms generated by the source and observer positions, and $\bar{\delta}_{mixed}^{(2)}$ is a mixing of both effects. Their explicit expressions are :

$$
\begin{aligned}
\bar{\delta}^{(2)}_{path} &= \Xi_s \Bigg\{ -\frac{1}{4}\left(\phi^{(2)}_s - \phi^{(2)}_o\right) + \frac{1}{4}\left(\psi^{(2)}_s - \psi^{(2)}_o\right) + \frac{1}{2}\left(\psi_s - \psi_o\right)^2 - \psi_o J^{(1)}_2 \\
&+ (\psi_o - \psi_s - J^{(1)}_2)[\partial_+ Q]_s + \frac{1}{4}(\gamma^{ab}_0)_s \partial_a Q_s \partial_b Q_s + Q_s\left(-[\partial^2_+ Q]_s + [\partial_+\psi]_s\right) + \frac{1}{\mathcal{H}_s}(\psi_o + [\partial_+ Q]_s)[\partial_\eta \psi]_s \\
&- \frac{1}{2}\int_{\eta_{in}}^{\eta^{(0)}_s} d\eta' \frac{a(\eta')}{a(\eta^{(0)}_s)} \partial_r \left[\phi^{(2)} - \psi^2\right](\eta', \Delta\eta, \tilde{\theta}^a) + \frac{1}{2}\int_{\eta_{in}}^{\eta_o} d\eta' \frac{a(\eta')}{a(\eta_o)} \partial_r \left[\phi^{(2)} - \psi^2\right](\eta', 0, \tilde{\theta}^a) \\
&+ \frac{1}{4}\int_{\eta^{(0)+}_s}^{\eta^{(0)-}_s} dx\ \partial_+ \left[\hat{\phi}^{(2)} + \hat{\psi}^{(2)} + 4\hat{\psi}\ \partial_+ Q + \hat{\gamma}^{ab}_0\ \partial_a Q\ \partial_b Q\right](\eta^{(0)+}_s, x, \tilde{\theta}^a) \\
&- \frac{1}{2}\partial_a(\psi_o + \partial_+ Q_s)\left(\int_{\eta^{(0)+}_s}^{\eta^{(0)-}_s} dx\ \left[\hat{\gamma}^{ab}_0\ \partial_b Q\right](\eta^{(0)+}_s, x, \tilde{\theta}^a)\right)\Bigg\} \\
&- \frac{1}{2}\psi^{(2)}_s - \frac{1}{2}\psi^2_s - K_2 + \psi_s J^{(1)}_2 + \frac{1}{2}(J^{(1)}_2)^2 + (J^{(1)}_2 - \psi_o)\frac{Q_s}{\Delta\eta} - \frac{1}{\mathcal{H}_s \Delta\eta}\left(1 - \frac{\mathcal{H}'_s}{\mathcal{H}^2_s}\right)\frac{1}{2}(\psi_o + [\partial_+ Q]_s)^2 \\
&- \frac{2}{\mathcal{H}_s\Delta\eta}\psi_s(\psi_o + [\partial_+ Q]_s) + \frac{1}{2}\partial_a\left(\psi_s + J^{(1)}_2 + \frac{Q_s}{\Delta\eta}\right)\left(\int_{\eta^{(0)+}_s}^{\eta^{(0)-}_s} dx\ \left[\hat{\gamma}^{ab}_0\ \partial_b Q\right](\eta^{(0)+}_s, x, \tilde{\theta}^a)\right) \\
&+ \frac{1}{4}\partial_a Q_s\ \partial_+\left(\int_{\eta^{(0)+}_s}^{\eta^{(0)-}_s} dx\ \left[\hat{\gamma}^{ab}_0\ \partial_b Q\right](\eta^{(0)+}_s, x, \tilde{\theta}^a)\right) \\
&+ \frac{1}{16}\partial_a\left(\int_{\eta^{(0)+}_s}^{\eta^{(0)-}_s} dx\ \left[\hat{\gamma}^{bc}_0\ \partial_c Q\right](\eta^{(0)+}_s, x, \tilde{\theta}^a)\right)\partial_b\left(\int_{\eta^{(0)+}_s}^{\eta^{(0)-}_s} d\bar{x}\ \left[\hat{\gamma}^{ad}_0\ \partial_d Q\right](\eta^{(0)+}_s, \bar{x}, \tilde{\theta}^a)\right) \\
&- \frac{1}{4\Delta\eta}\int_{\eta^{(0)+}_s}^{\eta^{(0)-}_s} dx\ \left[\hat{\phi}^{(2)} + \hat{\psi}^{(2)} + 4\hat{\psi}\ \partial_+ Q + \hat{\gamma}^{ab}_0\ \partial_a Q\ \partial_b Q\right](\eta^{(0)+}_s, x, \tilde{\theta}^a) \\
&+ \frac{1}{\mathcal{H}_s}(\psi_o + [\partial_+ Q]_s)\left\{-[\partial_\eta\psi]_s + [\partial_r\psi]_s + \frac{1}{\Delta\eta^2}\int_{\eta^{(0)}_s}^{\eta_o} d\eta' \Delta_2\psi(\eta', \eta_o - \eta', \tilde{\theta}^a)\right\} \\
&+ Q_s\Bigg\{[\partial_r\psi]_s + \partial_+\left(\int_{\eta^{(0)+}_s}^{\eta^{(0)-}_s} dx \frac{1}{\left(\eta^{(0)+}_s - x\right)^2}\int_{\eta^{(0)+}_s}^{x} dy \Delta_2\hat{\psi}(\eta^{(0)+}_s, y, \tilde{\theta}^a)\right) \\
&+ \frac{1}{2\Delta\eta^2}\int_{\eta^{(0)}_s}^{\eta_o} d\eta' \Delta_2\psi(\eta', \eta_o - \eta', \tilde{\theta}^a)\Bigg\} + \frac{1}{16\sin^2\tilde{\theta}}\left(\int_{\eta^{(0)+}_s}^{\eta^{(0)-}_s} dx\ \left[\hat{\gamma}^{1b}_0\ \partial_b Q\right](\eta^{(0)+}_s, x, \tilde{\theta}^a)\right)^2 \quad , \qquad (4.67)
\end{aligned}
$$

$$
\begin{aligned}
\bar{\delta}^{(2)}_{pos} &= \frac{\Xi_s}{2}\Bigg\{([\partial_r P]_s - [\partial_r P]_o)^2 + (\gamma^{ab}_0)_s \partial_a P_s\, \partial_b P_s - \lim_{r\to 0}\left[\gamma^{ab}_0 \partial_a P\, \partial_b P\right] \\
&- \frac{2}{\mathcal{H}_s}\left([\partial_r P]_s - [\partial_r P]_o\right)\left(\mathcal{H}_s[\partial_r P]_s + [\partial^2_r P]_s\right) \\
&- \int_{\eta_{in}}^{\eta^{(0)}_s} d\eta' \frac{a(\eta')}{a(\eta^{(0)}_s)}\partial_r\left[(\partial_r P)^2 + \gamma^{ab}_0 \partial_a P\, \partial_b P\right](\eta', \Delta\eta, \tilde{\theta}^a) \qquad (4.68) \\
&+ \int_{\eta_{in}}^{\eta_o} d\eta' \frac{a(\eta')}{a(\eta_o)}\partial_r\left[(\partial_r P)^2 + \gamma^{ab}_0 \partial_a P\, \partial_b P\right](\eta', 0, \tilde{\theta}^a)\Bigg\} - \frac{1}{2\mathcal{H}_s\Delta\eta}\left(1 - \frac{\mathcal{H}'_s}{\mathcal{H}^2_s}\right)\left([\partial_r P]_s - [\partial_r P]_o\right)^2 \quad ,
\end{aligned}
$$

$$
\begin{aligned}
\bar{\delta}^{(2)}_{mixed} &= \Xi_s\Bigg\{\left(2\psi_o - \psi_s + \partial_+ Q_s - \frac{Q_s}{\Delta\eta}\right)[\partial_r P]_o - \left([\partial_r P]_s - [\partial_r P]_o\right)\left(\frac{1}{\mathcal{H}_s}[\partial_\eta\psi]_s - J^{(1)}_2\right) \\
&- (\gamma^{ab}_0)_s \partial_a Q_s \partial_b P_s + \frac{1}{\mathcal{H}_s}(\psi_o + [\partial_+ Q]_s)[\partial^2_r P]_s + Q_s\,[\partial^2_r P]_s \\
&+ \frac{1}{2}\partial_a([\partial_r P]_s - [\partial_r P]_o)\left(\int_{\eta^{(0)+}_s}^{\eta^{(0)-}_s} dx\ \left[\hat{\gamma}^{ab}_0\ \partial_b Q\right](\eta^{(0)+}_s, x, \tilde{\theta}^a)\right)\Bigg\} \\
&+ \frac{1}{\Delta\eta}([\partial_r P]_s - [\partial_r P]_o)\left\{\frac{1}{\mathcal{H}_s}\left(1 - \frac{\mathcal{H}'_s}{\mathcal{H}^2_s}\right)(\psi_o + [\partial_+ Q]_s) + \frac{2}{\mathcal{H}_s}\psi_s + Q_s\right\} \\
&+ \frac{1}{\mathcal{H}_s}([\partial_r P]_s - [\partial_r P]_o)\left\{[\partial_\eta\psi]_s - [\partial_r\psi]_s - \frac{1}{\Delta\eta^2}\int_{\eta^{(0)}_s}^{\eta_o} d\eta' \Delta_2\psi(\eta', \eta_o - \eta', \tilde{\theta}^a)\right\} \quad . \qquad (4.69)
\end{aligned}
$$

4.2.2 The Vector and Tensor contribution

Following the procedure just presented for scalar perturbations we start from the general expression for d_L considering now just vector and tensor perturbations [2]. We obtain:

$$d_L = (1+z_s)^2(a_s r_s)\left\{1+\frac{1}{4}[(\gamma_0)_{ab}\chi^{ab}](\eta_s, r_s, \theta^a) - J_2^{(\alpha)} - \frac{1}{4}\int_{\eta_s^+}^{\eta_s^-} dx\ \nabla_a\left[\hat{v}^a - \hat{\chi}^{ra}\right](\eta_s^+, x, \theta^a)\right\} \ , \quad (4.70)$$

where, in terms of the quantity $Q^{(\alpha)}$ defined in Eq. (4.28), we have:

$$J_2^{(\alpha)} \equiv \int_{\eta_s^+}^{\eta_s^-} dx\ \frac{1}{\left(\eta_s^{(0)+} - x\right)^2}\Delta_2 Q^{(\alpha)}(\eta_s^{(0)+}, x, \theta^a) \ , \quad (4.71)$$

and where $a_s r_s$ is a quantity that still needs to be expanded with respect to the observed redshift. In order to do that, we first write the analogue of Eq. (4.39):

$$\frac{1}{1+z_s} = \frac{a(\eta_s)}{a_o}\left\{1+\left[\frac{v^r}{2}+\frac{\chi^{rr}}{4}\right](\eta_s, r_s, \theta^a) - \left[\frac{v^r}{2}+\frac{\chi^{rr}}{4}\right](\eta_o, 0, \theta^a) - J^{(\alpha)}\right\} \ , \quad (4.72)$$

with

$$J^{(\alpha)} \equiv \int_{\eta_s^+}^{\eta_s^-} dx\ \partial_+\hat{\alpha}^r(\eta_s^+, x, \theta^a) = \hat{\alpha}_o^r + \partial_+ Q_s^{(\alpha)} \ . \quad (4.73)$$

Expanding η_s as $\eta_s = \eta_s^{(0)} + \eta_s^{(2)}$ and imposing $(1+z_s)a(\eta_s^{(0)}) = a_o$, we get

$$\eta_s = \eta_s^{(0)} + \frac{1}{\mathcal{H}_s}\left\{\left[\frac{v^r}{2}+\frac{\chi^{rr}}{4}\right](\eta_o, 0, \theta^a) - \left[\frac{v^r}{2}+\frac{\chi^{rr}}{4}\right](\eta_s^{(0)}, r_s^{(0)}, \theta^a) + J^{(\alpha)}\right\} \ . \quad (4.74)$$

Using also the transformation of w, Eq. (4.27), we get the expression of r_s:

$$r_s = \Delta\eta + \frac{1}{\mathcal{H}_s}\left\{\left[\frac{v^r}{2}+\frac{\chi^{rr}}{4}\right](\eta_s^{(0)}, r_s^{(0)}, \theta^a) - \left[\frac{v^r}{2}+\frac{\chi^{rr}}{4}\right](\eta_o, 0, \theta^a) - J^{(\alpha)}\right\} - Q^{(\alpha)} \ , \quad (4.75)$$

and finally reach the conclusion that the luminosity distance at linear order in vector and tensor perturbations (regarded themselves as second order quantities) is

$$\begin{aligned}\frac{d_L^{(V,T)}}{d_L^{\rm FLRW}} &= 1 + \delta_{V,T}^{(2)} \quad (4.76)\\ &= 1 - \frac{Q_s^{(\alpha)}}{\Delta\eta} + \Xi_s\left\{\left(\frac{v_o^r}{2}+\frac{\chi_o^{rr}}{4}\right) - \left(\frac{v_s^r}{2}+\frac{\chi_s^{rr}}{4}\right) + J^{(\alpha)}\right\} + \frac{1}{4}[(\gamma_0)_{ab}\chi^{ab}](\eta_s^{(0)}, r_s^{(0)}, \theta^a)\\ &\quad - \int_{\eta_s^{(0)+}}^{\eta_s^{(0)-}} dx\ \left\{\frac{1}{4}\nabla_a[\hat{v}^a - \hat{\chi}^{ra}](\eta_s^{(0)+}, x, \theta^a) + \frac{1}{\left(\eta_s^{(0)+} - x\right)^2}\Delta_2 Q^{(\alpha)}(\eta_s^{(0)+}, x, \theta^a)\right\} \ .\end{aligned}$$

Using the transversality and trace-free conditions on the perturbations:

$$\nabla_a v^a = -\left(\partial_r + \frac{2}{r}\right)v^r \ , \quad \nabla_a\chi^{ra} = -\left(\partial_r + \frac{3}{r}\right)\chi^{rr} \ , \quad (\gamma_0)_{ab}\chi^{ab} = -\chi^{rr} \ , \quad (4.77)$$

we finally get an expression that depends only on v^r and χ^{rr}:

$$\begin{aligned}\frac{d_L^{(V,T)}}{d_L^{\rm FLRW}} &= 1 - \frac{Q_s^{(\alpha)}}{\Delta\eta} + \Xi_s\left\{\left(\frac{v_o^r}{2}+\frac{\chi_o^{rr}}{4}\right) - \left(\frac{v_s^r}{2}+\frac{\chi_s^{rr}}{4}\right) + J^{(\alpha)}\right\} - \frac{1}{4}\chi_s^{rr}\\ &\quad + \frac{1}{4}\int_{\eta_s^{(0)+}}^{\eta_s^{(0)-}} dx\ \left[\left(\partial_r + \frac{2}{r}\right)v^r - \left(\partial_r + \frac{3}{r}\right)\chi^{rr} - \frac{1}{r^2}\Delta_2 Q^{(\alpha)}\right](\eta_s^{(0)+}, x, \theta^a) \ , \quad (4.78)\end{aligned}$$

2. Note that an expression for the contribution of vectors and tensors to d_L has been derived [105]. We can check that our results agree with this independent calculation except for a possible velocity contribution at the observer position.

where one should interpret r as $r = (\eta_s^{(0)+} - x)/2$ inside the last integral.

We note, once more, the nature of the terms appearing in Eq. (4.78). In the first line we see a SW term as well as an average (or integrated) SW effect for the vector/tensor perturbation. The second line involves frame-dragging and a "magnification" term (lensing) for vectors/tensors proportional to the Laplacian of the perturbation on the 2-sphere. Our final expression for d_L is thus:

$$\frac{\bar{d}_L(z_s, \tilde{\theta}^a)}{d_L^{\rm FLRW}(z_s)} = 1 + \bar{\delta}_S^{(1)}(z_s, \tilde{\theta}^a) + \bar{\delta}_S^{(2)}(z_s, \tilde{\theta}^a) + \bar{\delta}_{V,T}^{(2)}(z_s, \tilde{\theta}^a) \quad , \tag{4.79}$$

where we directly replaced θ^a with $\tilde{\theta}^a$ in $\delta_{V,T}^{(2)}$ to get $\bar{\delta}_{V,T}^{(2)}$ since this is already a second-order quantity.

4.2.3 Physical interpretation of terms in $\bar{d}_L(z, \widetilde{\theta}^a)$

We have obtained a "local" expression for $\bar{d}_L(z, \widetilde{\theta}^a)$, expression that can find a large number of possible applications in cosmology. The different terms appearing in $\bar{\delta}_S^{(1)}$, $\bar{\delta}_S^{(2)}$ and $\bar{\delta}_{V,T}^{(2)}$, in Eq. (4.79), can be roughly classified as follows:

- Redshift Perturbations (RP). These are the $\epsilon_s^{(2)} - \epsilon_o^{(2)}$ terms as well as the analogous vector/tensor v^r, χ^{rr} terms appearing in Eq. (4.72). As mentioned in the text, at first order they include Doppler effect of peculiar velocities ($[\partial_r P]_s - [\partial_r P]_o$), SW and ISW (in agreement with the results obtained in [63]). At second order additional effects such as the tangential peculiar velocity $\partial_a P$, the tangential variation of the photon path $\partial_a Q$, and RSD also appear. We will see that peculiar velocities are the dominant contribution at low redshift $z \lesssim 0.2$, when we average generic functions of the luminosity distance $d_L(z)$ (see Chapter 6).

- Perturbed trajectories. At second order, first order integrated quantities are evaluated along the perturbed geodesics giving rise to $(1 \to 2)$ terms.

- SW and ISW effects coming from the evaluation of the area distance. Once again, in our notation, they are simply combined as $([\partial_+ Q]_s - [\partial_+ Q]_o)$. There is also an equivalent effect in the vector/tensor contribution.

- The lensing effect. These are the magnification J_2, K_2 terms as well as the shear in $\partial_a \tilde{\theta}^{b(1)} \partial_b \tilde{\theta}^{a(1)}$. They are the most important contributions at high redshifts $z \gtrsim 0.5$, when we average generic functions of the luminosity distance $d_L(z)$.

- Frame dragging, in the vector contribution (described at the end of the last section).

We have also identified the terms that have been computed in the literature, such as the lens-lens coupling and the Born correction. The presence of these expected terms shows the validity of our calculation and clearly supports its usefulness in precision cosmology. This calculation indeed accounts for all the possible effects at second order in perturbations from scalar perturbations and in a realistic way (but effectively first order) for vector and tensor perturbations.

We will start the next chapter, in Sec. 5.1, by recalling the transformation that we presented here but keeping only the first order contributions. It will then be easier to interpret the terms that we have presented and give more details about their physical meaning.

Chapter 5

Combining light-cone and stochastic averaging

In this section, we describe how the light-cone average presented in Chapter 2 can be combined with the stochastic average over inhomogeneities. This procedure gives us a rigorous way to consider an observable (such as the luminosity flux or distance) and average it over the whole sky (to get an isotropic prediction) and over inhomogeneities (to properly consider the non-homogeneous aspect of structures). We have seen in Chapter 4 that the full computation of the luminosity distance up to second order in perturbations, around the flat FLRW Universe, was leading to a complicated expression. We can ask ourself to which extent we are able to understand the effect of inhomogeneities if we only consider the second order coming from the quadratic terms of first order. We will see that most of the physics can already be understood from this linear order because of the reduced number of dominant terms. We then address the more complicated task of a full calculation, giving a complete result that will be used in the next chapter to give numerical predictions.

5.1 Recalling the first order equations

The consideration of the transformation of coordinates, Eq. (4.5), between the geodesic light-cone gauge and the Newtonian gauge (NG) (we forget about vectors and tensors here), assuming the simplication $\Phi = \Psi = \psi$ at first order and the appropriate boundary conditions, leads to the expression for $(\tau, w, \widetilde{\theta}^a)$-coordinates (see Eqs. (4.8) to (4.10)) :

$$\tau = \int_{\eta_{in}}^{\eta} d\eta' a(\eta') \left[1 + \psi(\eta', r, \theta^a)\right] \quad , \tag{5.1}$$

$$w = \eta_+ + \int_{\eta_+}^{\eta_-} dx\, \hat{\psi}(\eta_+, x, \theta^a) \quad , \tag{5.2}$$

$$\widetilde{\theta}^a = \theta^a + \frac{1}{2}\int_{\eta_+}^{\eta_-} dx\, \hat{\gamma}_0^{ab}(\eta_+, x, \theta^a) \int_{\eta_+}^{x} dy\, \partial_b \hat{\psi}(\eta_+, y, \theta^a) \quad , \tag{5.3}$$

where $\hat{\psi}(\eta_+, \eta_-, \theta^a) \equiv \psi(\eta, r, \theta^a)$, $\hat{\gamma}^{ab}(\eta_+, \eta_-, \theta^a) \equiv \gamma^{ab}(\eta, r, \theta^a)$ and η_{in} is, as already said, an early time when the integrand of τ was negligible. Similarly, Eq. (4.5) determines the non-trivial entries of the GLC metric (see Eqs. (4.14) to (4.23)) :

$$\Upsilon = a(\eta)\left[1 + \hat{\psi}(\eta_+, \eta_+, \theta^a) - \int_{\eta_+}^{\eta_-} dx\, \partial_+ \hat{\psi}(\eta_+, x, \theta^a)\right] + \int_{\eta_{in}}^{\eta} d\eta' a(\eta') \partial_r \psi(\eta', r, \theta^a) \quad , \tag{5.4}$$

$$\begin{aligned} U^a = {} & \frac{1}{2}\hat{\gamma}_0^{ab}\int_{\eta_+}^{\eta_-} dx\, \partial_b \hat{\psi}(\eta_+, x, \theta^a) - \frac{1}{a(\eta)}\gamma_0^{ab}\int_{\eta_{in}}^{\eta} d\eta' a(\eta')\, \partial_b \psi(\eta', r, \theta^a) \\ & + \frac{1}{2}\int_{\eta_+}^{\eta_-} dx\, \partial_+ \left[\hat{\gamma}_0^{ab}(\eta_+, x, \theta^a)\int_{\eta_+}^{x} dy\, \partial_b \hat{\psi}(\eta_+, y, \theta^a)\right] - \frac{1}{2}\lim_{x\to\eta_+}\left[\hat{\gamma}_0^{ab}(\eta_+, x, \theta^a)\int_{\eta_+}^{x} dy\, \partial_b \hat{\psi}(\eta_+, y, \theta^a)\right] \quad , \end{aligned} \tag{5.5}$$

$$\gamma^{ab} = \frac{1}{a(\eta)^2}\left\{\left[1 + 2\psi(\eta, r, \theta^a)\right]\gamma_0^{ab} + \frac{1}{2}\left[\hat{\gamma}_0^{ac}\int_{\eta_+}^{\eta_-} dx\, \partial_c \left(\hat{\gamma}_0^{bd}(\eta_+, x, \theta^a)\int_{\eta_+}^{x} dy\, \partial_d \hat{\psi}(\eta_+, y, \theta^a)\right) + a \leftrightarrow b\right]\right\} \quad . \tag{5.6}$$

From Eq. (3.18) one finds that the redshift of a source in the past light-cone of the observer is:

$$1+z_s=\frac{a(\eta_o)}{a(\eta_s)}\Big[1+J(z_s,\theta^a)\Big], \tag{5.7}$$

where we defined in [107]:

$$\begin{aligned} J=I_+-I_r \qquad \text{with:} \qquad I_+ &\equiv ([\partial_+Q]_s-[\partial_+Q]_o)=\int_{\eta_s^+}^{\eta_s^-} dx\,\partial_+\hat{\psi}(\eta_s^+,x,\theta^a) \\ &= \psi_s-\psi_o-2\int_{\eta_s}^{\eta_o} d\eta'\,\partial_r\psi(\eta',\eta_o-\eta',\theta^a) \quad , \end{aligned} \tag{5.8}$$

$$\text{and:} \qquad I_r\equiv([\partial_rP]_s-[\partial_rP]_o)=\int_{\eta_{in}}^{\eta_s} d\eta'\frac{a(\eta')}{a(\eta_s)}\partial_r\psi(\eta',\eta_o-\eta_s,\theta^a)-\int_{\eta_{in}}^{\eta_o} d\eta'\frac{a(\eta')}{a(\eta_o)}\partial_r\psi(\eta',0,\theta^a) \quad . \tag{5.9}$$

and where the integrals P and Q have been defined in Eq. (4.7). We have defined $\eta_s^\pm=\eta_s\pm r_s$, $\psi_s=\psi(\eta_s,\eta_o-\eta_s,\theta^a)$, $\psi_o=\psi(\eta_o,0,\theta^a)$ and the zeroth-order light-cone condition $\eta_s^+=\eta_o^+=\eta_o$. We also used the change of coordinates:

$$x=2\eta-\eta_o \qquad \text{with:} \qquad \left\{\begin{array}{l} x=\eta_s^- \;\Leftrightarrow\; \eta=\eta_s \\ x=\eta_s^+\equiv\eta_o \;\Leftrightarrow\; \eta=\eta_o \end{array}\right. \quad , \tag{5.10}$$

and the general relation:

$$\frac{d}{d\eta}\equiv\partial_\eta+n^i\nabla_i=\partial_\eta-\partial_r \quad , \tag{5.11}$$

where n^i are the components of $\mathbf{n}$, the unit tangent vector along the null geodesic connecting source and observer (and pointing from the last to the first). It should be stressed, however, that while the integrals appearing in I_r are evaluated at constant r (namely along timelike geodesics), the integrals in I_+ are evaluated at fixed η_+ (i.e. along null geodesics on the observer's past light-cone).

The contribution associated to I_r can also be rewritten as

$$I_r=(\mathbf{v}_s-\mathbf{v}_o)\cdot\mathbf{n} \qquad \text{with} \qquad \mathbf{v}_{s,o}=-\int_{\eta_{in}}^{\eta_{s,o}} d\eta'\frac{a(\eta')}{a(\eta_{s,0})}\vec{\nabla}\psi(\eta',r,\theta^a) \quad , \tag{5.12}$$

the "peculiar velocities" of source and observer associated to a geodesic configuration perturbed up to first order in the Newtonian gauge. In a realistic situation one should add to Eq. (5.7) similar terms taking into account a possible intrinsic (non-perturbative) motion of source and observer, unless our theoretical predictions are compared with data already corrected for these latter Doppler contributions. We suppose here that these terms are zero and thus state that the source and the observer are static w.r.t. each other (apart from the peculiar velocity coming from the gravitational perturbations). The expression for the redshift, Eq. (5.7), is in full agreement with the expression obtained in Eq. (38) of [63] (where z_s is computed for the particular case of a CDM-dominated model).

To obtain the angular distance, given by Eq. (3.28), of a source emitting light at time η_s and radial distance r_s, one computes the determinant γ from Eq. (5.6), to first order [1], and we get:

$$\gamma^{-1}(\lambda_s)\equiv\det\gamma^{ab}(\lambda_s)=(a_s^2r_s^2\sin\theta)^{-2}\Big[1+4\psi_s+4\widetilde{J}_2(z_s,\theta^a)\Big] \quad , \tag{5.13}$$

where (using a simple integration by parts):

$$\begin{aligned} \widetilde{J}_2 &= \frac{1}{4}\int_{\eta_s^+}^{\eta_s^-} dx\,\hat{\gamma}_0^{ab}(\eta_s^+,x,\theta^a)\int_{\eta_s^+}^{x} dy\,\partial_a\partial_b\hat{\psi}(\eta_s^+,y,\theta^a) \\ &= \frac{1}{\eta_o-\eta_s}\int_{\eta_s}^{\eta_o} d\eta'\frac{\eta'-\eta_s}{\eta_o-\eta'}\Big[\partial_\theta^2+(\sin\theta)^{-2}\partial_\phi^2\Big]\psi(\eta',\eta_o-\eta',\theta^a) \quad . \end{aligned} \tag{5.14}$$

1. Note that $\gamma^{-1}=(\gamma_{11}\gamma_{22})^{-1}$ at first order and, for these diagonal matrix elements, ∂_b commutes with γ_0^{ab}.

We then get :

$$d_A(\lambda_s) = a_s r_s \left[1 - \psi_s - \widetilde{J}_2\right] \left(\frac{\sin\widetilde{\theta}^1}{\sin\theta}\right)^{-1/2} = a_s r_s \left[1 - \psi_s - J_2(z_s, \theta^a)\right] \quad , \tag{5.15}$$

where in the second equality we developed the term $\widetilde{\theta}^1$ from Eq. (5.3) to define J_2 as :

$$\begin{aligned} J_2 &= \frac{1}{\eta_o - \eta_s} \int_{\eta_s}^{\eta_o} d\eta \, \frac{\eta - \eta_s}{\eta_o - \eta} \left[\partial_\theta^2 + \cot\theta \, \partial_\theta + (\sin\theta)^{-2} \partial_\phi^2\right] \psi(\eta, \eta_o - \eta, \theta^a) \\ &\equiv \frac{1}{\eta_o - \eta_s} \int_{\eta_s}^{\eta_o} d\eta \, \frac{\eta - \eta_s}{\eta_o - \eta} \, \Delta_2 \psi(\eta, \eta_o - \eta, \theta^a) \quad , \end{aligned} \tag{5.16}$$

and where Δ_2 is the two-dimensional Laplacian operator on the unit two-sphere.

We finally obtain the full explicit expression of d_L by the first-order expansion of $a_s r_s \equiv a(\eta_s) r_s$ appearing in Eq. (5.15). To this purpose we start from Eq. (5.7), considering z_s as a constant parameter localising the given light source on the past light-cone ($w = w_o$) of our observer, and we look for approximate solutions for $\eta_s = \eta_s(z_s, \theta^a)$. Expanding Eq. (5.7) with respect to the parameter $\delta\eta = \eta_s - \eta_s^{(0)}$, we find :

$$\frac{1}{1 + z_s} = \frac{a(\eta_s^{(0)})}{a_0} [1 + \mathcal{H}_s \, \delta\eta - J(z_s, \theta^a)] \equiv \frac{1}{1 + z_s} [1 + \mathcal{H}_s \, \delta\eta - J(z_s, \theta^a)] \quad , \tag{5.17}$$

where $\mathcal{H}_s = d(\ln a(\eta_s^{(0)}))/d\eta_s^{(0)}$, so that $\mathcal{H}_s \, \delta\eta = J(z_s, \theta^a)$. On the other hand, applying Eq. (5.2) to the light-cone $w = w_o$ at the source position gives

$$w_o = \eta_s^+ + Q_s = \eta_o \quad , \tag{5.18}$$

where we use $\Delta\eta = \eta_o - \eta_s^{(0)}$ and Q_s is the average value of ψ along the (unperturbed) null geodesic connecting source and observer :

$$Q_s = \int_{\eta_+^s}^{\eta_-^s} dx \, \hat{\psi}(\eta_+^s, x, \theta^a) = -2 \int_{\eta_s}^{\eta_o} d\eta' \, \psi(\eta', \eta_o - \eta', \theta^a) \quad . \tag{5.19}$$

Eq. (5.18) thus brings the value of the radial coordinate $r_s(z_s, \theta^a)$ for the given redshift z_s :

$$r_s(z_s, \theta^a) = w_o - \eta_s^{(0)}(z_s) - \delta\eta - Q_s = \Delta\eta \left[1 - \frac{J(z_s, \theta^a)}{\mathcal{H}_s \Delta\eta} - \frac{Q_s}{\Delta\eta}\right] \quad , \tag{5.20}$$

and we finally obtain the value of $a_s r_s$ on the constant-z_s 2-surface :

$$[a_s r_s](z_s, \theta^a) = a(\eta_s^{(0)}) \Delta\eta \left[1 - \frac{Q_s}{\Delta\eta} + \Xi_s J(z_s, \theta^a)\right] \quad . \tag{5.21}$$

The angular distance of Eq. (5.15), for a source at redshift z_s, can now be written as [2]

$$d_A(z_s, \theta^a) = a(\eta_s^{(0)}) \Delta\eta \left[1 - \frac{Q_s}{\Delta\eta} + \Xi_s J - \psi(\eta_s, \eta_o - \eta_s, \theta^a) - J_2\right] \quad , \tag{5.22}$$

and the expression of d_L in our perturbed background is finally given, using $\psi_s \equiv \psi(\eta_s, \eta_o - \eta_s, \theta^a)$, by :

$$\frac{d_L(z_s, \theta^a)}{(1 + z_s) a_0 \Delta\eta} \equiv \frac{d_L(z_s, \theta^a)}{d_L^{\mathrm{FLRW}}(z_s)} = 1 - \psi_s - \frac{Q_s}{\Delta\eta} + \Xi_s J - J_2 \quad . \tag{5.23}$$

If we apply this general result to the particular case of a CDM-dominated Universe we find almost full agreement with the result for the luminosity distance at constant redshift computed in [63]. After

2. Let us note that in the first order terms we can always safely identify η_s with its zeroth-order value $\eta_s^{(0)}$.

several manipulations, in fact, it turns out that our d_L is equivalent to the one found in [63], modulo a term which can be written as $\mathbf{v}_o \cdot \mathbf{n}$ (in the notations of Eq. (5.12)). Such a term gives a subleading contribution to the backreaction and can be neglected with no impact on our final results.

It should be noted, however, that by expanding the above expression in the small z_s limit, and comparing the result with the analogous expansion of the homogeneous distance in Eq. (1.49), we could easily introduce a redefined value of H_0, say $H_0^{\rm ren}$, such that its inverse corresponds to the coefficient of the linear term in z_s for the perturbed relation. With such a "renormalized" Hubble parameter we have that $H_0^{\rm ren} d_L$ tends smoothly to $H_0 d_L^{\rm FLRW}$ for $z_s \to 0$, and we recover full agreement with [63] provided the same renormalization is applied there. Such a renormalization of H_0 is also suggested by (and closely related to) the first-order computation of the scalar expansion factor $\nabla_\mu u^\mu$ for the flow world lines $u_\mu = -\partial_\mu \tau$ of a local geodesic observer.

We could thus choose, for the next considerations, to take the average of $H_0^{\rm ren} d_L(z_s, \theta^a)$ instead of $d_L(z_s, \theta^a)$, computing the associated backreaction, and evaluating the corrections to the standard homogeneous relation given by $H_0 d_L^{\rm FLRW}(z_s)$. We have performed that exercise, but we have found that the contribution of the renormalization terms give large z_s-independent contributions to the variance. Furthermore, renormalizing H_0 at $z_s = 0$ could be physically incorrect since, at very small-z_s, the backreaction is dominated by short-scale inhomogeneities which are deeply inside the non-linear regime (where even the concept of a Hubble flow becomes inappropriate). We could instead try to renormalize H_0 at some small but finite z_s, e.g. at a redshift corresponding to the closest used supernovae (say $z_s \sim 0.015$, see e.g. [21]), but then the results (although much better behaved) would depend on the choice of the particular "renormalization point". Thus, it seems better to consider just the full "unrenormalized" expression of Eq. (5.23) in a limited region of z_s where one can trust the approximations made, and use that expression for a phenomenological parametrization of the backreaction effects which could possibly include a redefinition of H_0.

5.2 Combining lightcone and ensemble averages

5.2.1 Definition of the stochastic average

The simplest way to implement the ensemble average of our stochastic background of (first order) scalar perturbations ψ is to consider their Fourier decomposition in the form:

$$\psi(\eta, \mathbf{x}) = \frac{1}{(2\pi)^{3/2}} \int d^3k \, \mathrm{e}^{i\mathbf{k}\cdot\mathbf{x}} \, \psi_k(\eta) E(\mathbf{k}) \quad , \tag{5.24}$$

where, assuming that the fluctuations are statistically homogeneous, E is a unit random variable satisfying the *statistical homogeneity condition*:

$$E^*(\mathbf{k}) = E(-\mathbf{k}) \quad , \tag{5.25}$$

as well as the *ensemble-average conditions*:

$$\overline{E(\mathbf{k})} = 0 \qquad \forall \, \mathbf{k} \qquad , \qquad \overline{E(\mathbf{k}_1) E(\mathbf{k}_2)} = \delta_{\rm D}(\mathbf{k}_1 + \mathbf{k}_2) \quad . \tag{5.26}$$

These relations actually claim that two modes of different wavelengths are independent. We should keep in mind that this is true in a general FLRW model only when flatness is assumed. That is indeed the case which is taken all the way here and such a decomposition is hence justified.

In order to proceed with some qualitative and quantitative considerations it is important now to specify some of the properties of the power spectrum of ψ, denoted $\mathcal{P}_\psi(k)$, and defined in general by:

$$\mathcal{P}_\psi(k, \eta) \equiv \frac{k^3}{2\pi^2} |\psi_k(\eta)|^2 \quad . \tag{5.27}$$

Limiting ourselves to sub-horizon perturbations, and considering the standard CDM model, we can simply obtain ψ_k by applying an appropriate, time-independent transfer function to the primordial

(inflationary) spectral distribution (see e.g. [108]). The power spectrum of the Bardeen potential is then given by

$$\mathcal{P}_\psi(k) = \left(\frac{3}{5}\right)^2 \Delta^2_{\mathcal{R}} T^2(k) \quad , \quad \Delta^2_{\mathcal{R}} = A \left(\frac{k}{k_0}\right)^{n_s - 1} \quad , \tag{5.28}$$

where $T(k)$ is a time-dependent transfer function which takes into account the sub-horizon evolution of the modes re-entering during the radiation-dominated era, and $\Delta^2_{\mathcal{R}}$ is the primordial power spectrum of curvature perturbations, amplified by inflation, outside the horizon. The typical parameters of such a spectrum, namely the amplitude A, the spectral index n_s and the scale k_0, are determined by the results of WMAP observations [109]. In our computations we will use, in particular, the following approximate values :

$$A = 2.45 \times 10^{-9} \quad , \quad n_s = 0.96 \quad , \quad k_0/a_0 = 0.002\,\mathrm{Mpc}^{-1} \quad . \tag{5.29}$$

Finally, we will have to assume an explicit form of the transfer function $T(k)$. That will be done in Chapter 6 where different cases will be considered from [68], in CDM and ΛCDM models, with and without baryons.

In the next sections we will discuss the corresponding backreaction effects on $\overline{\langle d_L \rangle}$, together with its dispersion, for the scalar perturbation spectrum described by Eq. (5.28) and evaluate their spectral coefficients in order to prepare their numerical estimation in Chapter 6.

5.2.2 Combination with the lightcone average : induced backreaction terms

Let us consider that the inhomogeneous deviations from the standard FLRW quantities are sourced by a stochastic background of primordial perturbations and, according to Eq. (5.26), satisfy :

$$\overline{\psi} = 0 \quad , \quad \overline{\psi^2} \neq 0 \quad . \tag{5.30}$$

Hence, if we limit ourselves to a first-order computation of a scalar quantity S, we immediately obtain $\overline{S} = S^{\mathrm{FLRW}}$. Non-trivial effects can only be obtained from quadratic and higher-order perturbative corrections, or from the spectrum of the two-point correlation function $\overline{S(z,\theta^a)S(z',\theta'^a)}$ (as discussed in detail in [63] for $S = d_L$).

In this chapter we will consider the ensemble average not of S but of $\langle S \rangle$, where the angular brackets refer to the light-cone angular average defined in Eq. (3.67). We should notice that several studies, such as [37,110,111], considered the combination of the ensemble average with averages over spacelike hypersurfaces. However, its combination with lightcone averages has never been addressed before this work. We will see in this section that the light-cone average automatically induces quadratic (and higher-order) backreaction terms, due to the inhomogeneities present both in d_L and in the covariant integration measure [3], and since the ensemble average of such terms is non-vanishing we obtain in general that $\overline{\langle S \rangle} \neq S^{\mathrm{FLRW}}$. We will now present general considerations on how to combine lightcone and ensemble averaging, and how to isolate those terms in $\overline{\langle S \rangle}$ that we may genuinely call "backreaction" effects, i.e. effects on averaged quantities due to inhomogeneities. We shall also discuss how to estimate the variance around mean values due to such fluctuations [4].

Let us consider a typical average over the compact surface Σ (topologically equivalent to a 2-sphere) embedded on the past light-cone $w = w_o$ at constant z_s. We simply denote this average by :

$$\langle S \rangle_\Sigma = \frac{\int_\Sigma d^2\mu\, S}{\int_\Sigma d^2\mu} \quad , \tag{5.31}$$

3. This is also the case for spatial averaging. Nevertheless, the integration measure is modified and the generated terms are directly affected by this geometrical difference (see Sec. 5.2.4).

4. The importance of the cosmic variance for a precise measurement of the cosmological parameters, taking into account backreaction effects from averaging on domains embedded in a spatial hypersurface (according to [47,48]), has been recently pointed out also in [112].

where $d^2\mu$ is the appropriate measure provided by our gauge invariant prescription (see Eq. (3.67)) and S is a (possibly non local) scalar observable. We can conveniently extract, from both $d^2\mu$ and from S, a zeroth-order homogeneous contribution by defining:

$$d^2\mu = (d^2\mu)^{(0)}(1+\mu) \quad , \quad S = S^{(0)}(1+\sigma) \quad , \tag{5.32}$$

and use the possibility of rescaling both integrals in Eq. (5.31) by the same constant, in order to normalize $\int (d^2\mu)^{(0)} = 1$. We then easily get:

$$\left\langle \frac{S}{S^{(0)}} \right\rangle = \frac{\int (d^2\mu)^{(0)}(1+\mu)(1+\sigma)}{\int (d^2\mu)^{(0)}(1+\mu)} = \frac{\langle (1+\mu)(1+\sigma)\rangle_0}{1+\langle\mu\rangle_0} \quad , \tag{5.33}$$

where we have dropped, for simplicity, the subscript of the averaging region Σ, and where we have defined by $\langle\ldots\rangle_0$ averages with respect to the unperturbed measure $(d^2\mu)^{(0)}$. For simplicity, we shall even drop the subscript 0 hereafter.

Let us now perform the ensemble average, paying attention to the fact that ensemble averages do *not* factorize, i.e. $\overline{AB} \neq \overline{A}\ \overline{B}$. This simple combination leads to:

$$\overline{\langle S/S^{(0)}\rangle} = 1 + \overline{(\langle\sigma\rangle + \langle\mu\sigma\rangle)(1+\langle\mu\rangle)^{-1}} \quad . \tag{5.34}$$

This last equation is supposedly exact but, as such, pretty useless. It becomes an interesting equation, though, if we can expand the quantities μ and σ in perturbative series:

$$\mu = \sum_i \mu_i \quad , \quad \sigma = \sum_i \sigma_i \quad , \tag{5.35}$$

and we further assume that the first order quantities μ_1 and σ_1 have vanishing ensemble averages (as it is the case for typical cosmological perturbations coming from inflation). In that case we can easily expand the result and obtain, for instance:

$$\overline{\langle S/S^{(0)}\rangle} = 1 + \overline{\langle\sigma_2\rangle} + \mathrm{IBR}_2 + \overline{\langle\sigma_3\rangle} + \mathrm{IBR}_3 + \ldots \tag{5.36}$$

where

$$\mathrm{IBR}_2 = \overline{\langle\mu_1\sigma_1\rangle} - \overline{\langle\mu_1\rangle\langle\sigma_1\rangle} \quad , \tag{5.37}$$

$$\mathrm{IBR}_3 = \overline{\langle\mu_2\sigma_1\rangle} - \overline{\langle\mu_2\rangle\langle\sigma_1\rangle} + \overline{\langle\mu_1\sigma_2\rangle} - \overline{\langle\mu_1\rangle\langle\sigma_2\rangle} - \overline{\langle\mu_1\rangle\langle\mu_1\sigma_1\rangle} + \overline{\langle\mu_1\rangle\langle\mu_1\rangle\langle\sigma_1\rangle} \quad , \tag{5.38}$$

and where we have used again the non-factorization property, i.e. $\overline{\langle\mu_1\rangle\langle\sigma_1\rangle} \neq \overline{\langle\mu_1\rangle}\ \overline{\langle\sigma_1\rangle}$, and so on. We see that the result contains, to a given order, both terms that depend on expanding S to that order (but *not* on the precise averaging prescription), and induced backreaction (IBR) terms that depend on correlations between the fluctuations of S and those in the measure. These latter terms only depend on lower-order perturbations of S and the measure separately. Note also that, whenever the fluctuations of S and $d^2\mu$ are uncorrelated, all IBR effects drop out.

Let us now discuss the issue of the variance, i.e. of how broad is the distribution of values for $S/S^{(0)}$ around its mean value $\overline{\langle S/S^{(0)}\rangle}$. This dispersion is due to both the fluctuation on the averaging surface and to those due to ensemble fluctuations. Let us thus define:

$$\mathrm{Var}[S/S^{(0)}] \equiv \overline{\left\langle \left(S/S^{(0)} - \overline{\langle S/S^{(0)}\rangle}\right)^2 \right\rangle} = \overline{\langle (S/S^{(0)})^2\rangle} - \left(\overline{\langle S/S^{(0)}\rangle}\right)^2 \quad . \tag{5.39}$$

Inserting the definitions of Eq. (5.32), we get, after a little algebra:

$$\mathrm{Var}[S/S^{(0)}] = \overline{\langle\sigma^2(1+\mu)\rangle(\langle 1+\mu\rangle)^{-1}} - \left(\overline{\langle\sigma(1+\mu)\rangle(1+\langle\mu\rangle)^{-1}}\right)^2 \quad . \tag{5.40}$$

If we now make the same assumptions as before on expanding μ and σ, we find that the second term in Eq. (5.40) is at least of fourth order. Therefore, for the leading term in the variance we find the amazingly simple result (see also [112]):

$$\mathrm{Var}[S/S^{(0)}] = \overline{\langle\sigma_1^2\rangle} \quad . \tag{5.41}$$

As in the case of IBR_2 we only need to know the first-order perturbation, but this time the effect is completely independent of the averaging measure. As we shall see, for $S = d_L$ the dispersion (which is actually the square root of the variance) turns out to be larger than the averaging corrections due to IBR_2 (see Chapter 6).

We may note, at this point, that we could have also considered the dispersion of the angular average $\langle S/S^{(0)}\rangle$ due to the stochastic fluctuations, namely:

$$\mathrm{Var}'[S/S^{(0)}] \equiv \overline{\left(\langle S/S^{(0)}\rangle - \overline{\langle S/S^{(0)}\rangle}\right)^2} = \overline{\left(\langle S/S^{(0)}\rangle\right)^2} - \left(\overline{\langle S/S^{(0)}\rangle}\right)^2 \quad , \tag{5.42}$$

which, after calculations similar to the ones above, gives

$$\mathrm{Var}'[S/S^{(0)}] = \overline{\langle\sigma_1\rangle^2} \quad . \tag{5.43}$$

Such a quantity is much smaller than the previous one, as can be inferred from $S = d_L$, indicating that the main reason for the dispersion lies in the angular scatter of the data rather than in their stochastic distribution due to the ensemble (see e.g. Sec. 6.1). One can indeed understand that for an early enough time we are integrating inhomogeneities over a very large sphere $\Sigma(w_o, z_s)$ and thus the main source of dispersion, when we consider different realizations of the inhomogeneous universe, comes from the combination of lightcone and ensemble average acting on S (involving the fluctuation of S) rather than the ensemble average of $\langle S\rangle$ alone (which averages the different realizations of $\Sigma(w_o, z_s)$).

5.2.3 Application to $S = d_L$ up to the quadratic first order terms

This section will be devoted to a systematic evaluation of the various terms contributing to the induced backreaction IBR_2 defined in the previous section, as well as to the variance associated to the (angle and ensemble)-averaged value of $d_L(z_s, \theta^a)$.

Indeed, to describe the real impact of inhomogeneities on the observational data we have to consider the scalar S corresponding to the true observed quantity. In the case of the supernovae data [10, 11] this quantity is the received flux of radiation, which is proportional to d_L^{-2}. On the other hand, we can think to consider the average of d_L instead of the average of the flux. One can thus take (among others) two different ways to compute the distance, with the following expressions:

$$(\overline{\langle d_L^{-2}\rangle})^{-1/2} = d_L^{\mathrm{FLRW}}\left(1 + \overline{\langle\sigma_2\rangle} + \mathrm{IBR}_2 - \frac{3}{2}\overline{\langle\sigma_1^2\rangle}\right) \quad , \quad \overline{\langle d_L\rangle} = d_L^{\mathrm{FLRW}}\left(1 + \overline{\langle\sigma_2\rangle} + \mathrm{IBR}_2\right) \quad . \tag{5.44}$$

As we can notice, the difference between the two quantities only appears at second order. The genuine second-order contribution $\overline{\langle\sigma_2\rangle}$ cannot be determined from the first order transformation that we use here, but is only attainable through the full second order transformation that we will treat in the next section, Sec. 5.3. We remark also the interesting fact that the evaluation of μ_2, the second order contribution of the measure, is not needed for the full second order computation. We shall thus present the calculation of only IBR_2 and $\overline{\langle\sigma_1^2\rangle}$ here, i.e. the effect that comes from the above interplay of μ_1 and σ_1 or σ_1 with itself, and consider the full case later. One last remark is that the distance modulus, rather than being computed as a function of $(\overline{\langle d_L^{-2}\rangle})^{-1/2}$ or $\overline{\langle d_L\rangle}$ should be directly averaged to test its sentivity to inhomogeneities (see Sec. 5.3.3).

In such a case, from Eq. (5.23) we immediately find:

$$\sigma_1 = A_1 + A_2 + A_3 + A_4 + A_5 \quad , \tag{5.45}$$

where we have defined:

$$A_1 = -\psi_s \ , \ A_2 = -\frac{Q_s}{\Delta\eta} \ , \ A_3 = \left(1 - \frac{1}{\mathcal{H}_s\Delta\eta}\right) I_+ \ , \ A_4 = -\left(1 - \frac{1}{\mathcal{H}_s\Delta\eta}\right) I_r \ , \ A_5 = -J_2 \ . \tag{5.46}$$

On the other hand, in our particular case, the general measure $d^2\mu$ is given by Eq. (3.67):

$$d^2\mu = d^2\widetilde{\theta}\sqrt{\gamma(w_o, \tau(z_s, w_o, \tilde{\theta}^a), \tilde{\theta}^a)} \quad . \tag{5.47}$$

We need to transform the integral in $d^2\widetilde{\theta}$ (over the "2-sphere" Σ) to the standard polar coordinates $d^2\theta = d\theta d\phi$ of the Newtonian gauge. To first order, it is easy to check (by taking into account the Jacobian determinant of the transformation $\theta^a \to \widetilde{\theta}^a$, see Eq. (5.3)) that:

$$\int d^2\widetilde{\theta}\sqrt{\gamma} = \int d\phi d\theta \sin\theta \left([a_s r_s](z_s,\theta^a)\right)^2 (1-2\psi_s) \quad . \tag{5.48}$$

The normalized unperturbed measure is then given by $(d^2\mu)^{(0)} = d^2\Omega/4\pi$, where $d^2\Omega = d\phi d\theta \sin\theta$. Using now the expansion of $a_s r_s$ presented in Eq. (5.21), we obtain:

$$\mu_1 = -2\psi_s - 2\frac{Q_s}{\Delta\eta} + 2\left(1 - \frac{1}{\mathcal{H}_s\Delta\eta}\right) J(z_s,\theta^a) = 2\left(A_1 + A_2 + A_3 + A_4\right) \quad . \tag{5.49}$$

The second-order induced backreaction IBR_2, and the variance of d_L/d_L^{FLRW}, can now be obtained by inserting the results of Eqs. (5.45), (5.49) into Eqs. (5.37) and (5.41), respectively. According to these expressions, all corrections we need to compute are bilinear terms in the potential ψ, always occurring in the combination $\overline{\langle A_i A_j\rangle}$ or $\overline{\langle A_i\rangle\langle A_j\rangle}$, where the quantities A_i, A_j are defined in Eq. (5.46).

Let us illustrate a typical computation with the simplest contribution associated to $A_1 = -\psi_s$. Following previous notations, we will denote with simple angular brackets the integration over the two-surface Σ embedded on the light-cone (at $w = w_o$, $z = z_s$). The measure of integration is the unperturbed normalized one, i.e. $d^2\Omega/4\pi$. We then obtain:

$$\begin{aligned}
\overline{\langle\psi_s\psi_s\rangle} &= \int \frac{d^3k\, d^3k'}{(2\pi)^3}\overline{E(\mathbf{k})E(\mathbf{k}')} \int \frac{d^2\Omega}{4\pi}\left[\psi_k(\eta_s^{(0)})e^{ir\mathbf{k}\cdot\hat{\mathbf{x}}}\right]_{r=\eta_o-\eta_s^{(0)}}\left[\psi_{k'}(\eta_s^{(0)})e^{ir\mathbf{k}'\cdot\hat{\mathbf{x}}}\right]_{r=\eta_o-\eta_s^{(0)}} \\
&= \int \frac{d^3k}{(2\pi)^3}\,|\psi_k(\eta_s^{(0)})|^2 \int_{-1}^{1}\frac{d(\cos\theta)}{2}\left[e^{ik\Delta\eta\cos\theta}\right]\left[e^{-ik\Delta\eta\cos\theta}\right] \\
&= \int \frac{d^3k}{(2\pi)^3}\,|\psi_k(\eta_s^{(0)})|^2 = \int_0^\infty \frac{dk}{k}\,\mathcal{P}_\psi(k,\eta_s^{(0)}) \quad ,
\end{aligned} \tag{5.50}$$

$$\begin{aligned}
\overline{\langle\psi_s\rangle\langle\psi_s\rangle} &= \int \frac{d^3k\, d^3k'}{(2\pi)^3}\overline{E(\mathbf{k})E(\mathbf{k}')}\left[\int\frac{d^2\Omega}{4\pi}\psi_k(\eta_s^{(0)})e^{ir\mathbf{k}\cdot\hat{\mathbf{x}}}\right]_{r=\eta_o-\eta_s^{(0)}}\left[\int\frac{d^2\Omega'}{4\pi}\psi_{k'}(\eta_s^{(0)})e^{ir\mathbf{k}'\cdot\hat{\mathbf{x}}'}\right]_{r=\eta_o-\eta_s^{(0)}} \\
&= \int \frac{d^3k}{(2\pi)^3}\,|\psi_k(\eta_s^{(0)})|^2\left[\int_{-1}^{1}\frac{d(\cos\theta)}{2}e^{ik\Delta\eta\cos\theta}\right]\left[\int_{-1}^{1}\frac{d(\cos\theta')}{2}e^{-ik\Delta\eta\cos\theta'}\right] \\
&= \int \frac{d^3k}{(2\pi)^3}\,|\psi_k(\eta_s^{(0)})|^2\left(\frac{\sin(k\Delta\eta)}{k\Delta\eta}\right)^2 = \int_0^\infty\frac{dk}{k}\,\mathcal{P}_\psi(k,\eta_s^{(0)})\left(\frac{\sin(k\Delta\eta)}{k\Delta\eta}\right)^2 \quad ,
\end{aligned} \tag{5.51}$$

where in the second line of both equations we made use of isotropy (i.e. ψ_k only depends on $k = |\mathbf{k}|$), and defined θ and θ' as the angles between $\mathbf{k}$ and $\mathbf{x} \equiv r\hat{\mathbf{x}}$ and between $\mathbf{k}'$ and $\mathbf{x}' \equiv r\hat{\mathbf{x}}'$. We also made use of the (so-called dimensionless) power spectrum defined in Eq. (5.27). More complicated examples, that contain almost all the subtleties of these computations, are presented in Sec. 5.2.4.

In general we have many contributions like the above ones, appearing in both the induced backreaction and the variance, and generated by all the A_i terms of Eq. (5.46). Here, for a start, we only consider the particularly simple case of a CDM-dominated background geometry, with a time-independent spectral distribution of sub-horizon scalar perturbations, $\partial_\eta\psi_k = 0$. In such a case all the relevant contributions can be parameterized in the form:

$$\overline{\langle A_i A_j\rangle} = \int_0^\infty \frac{dk}{k}\,\mathcal{P}_\psi(k)\,\mathcal{C}_{ij}(k,\eta_o,\eta_s^{(0)}) \quad , \tag{5.52}$$

$$\overline{\langle A_i\rangle\langle A_j\rangle} = \int_0^\infty \frac{dk}{k}\,\mathcal{P}_\psi(k)\,\mathcal{C}_i(k,\eta_o,\eta_s^{(0)})\,\mathcal{C}_j(k,\eta_o,\eta_s^{(0)}) \quad , \tag{5.53}$$

where $\mathcal{C}_{ij}$ and $\mathcal{C}_i$ are constant spectral coefficients. This form is valid for any given model of time-independent scalar perturbation spectrum. With such a parametrization, the leading-order induced

backreaction, called IBR_2 in the expansion of Eq. (5.36), of $\overline{\langle d_L\rangle}/d_L^{\mathrm{FLRW}}$, can be written as:

$$\begin{aligned}\mathrm{IBR}_2 &= 2\sum_{i=1}^{4}\sum_{j=1}^{5}\left[\overline{\langle A_iA_j\rangle}-\overline{\langle A_i\rangle\langle A_j\rangle}\right]\\ &= \int_0^\infty\frac{dk}{k}\,\mathcal{P}_\psi(k)\times 2\sum_{i=1}^{4}\sum_{j=1}^{5}\left[\mathcal{C}_{ij}(k,\eta_o,\eta_s^{(0)})-\mathcal{C}_i(k,\eta_o,\eta_s^{(0)})\,\mathcal{C}_j(k,\eta_o,\eta_s^{(0)})\right]\quad.\end{aligned}\tag{5.54}$$

The dispersion, from Eq. (5.41), takes instead the form:

$$\begin{aligned}\left(\mathrm{Var}\left[\frac{d_L}{d_L^{\mathrm{FLRW}}}\right]\right)^{1/2} &= \sqrt{\overline{\langle\sigma_1^2\rangle}} = \left[\sum_{i=1}^{5}\sum_{j=1}^{5}\overline{\langle A_iA_j\rangle}\right]^{1/2}\\ &= \left[\int_0^\infty\frac{dk}{k}\,\mathcal{P}_\psi(k)\sum_{i=1}^{5}\sum_{j=1}^{5}\mathcal{C}_{ij}(k,\eta_o,\eta_s^{(0)})\right]^{1/2}\quad.\end{aligned}\tag{5.55}$$

The analytical values of all the required coefficients $\mathcal{C}_{ij}$, $\mathcal{C}_i$ are given in Table 5.1 for $\mathcal{C}_{ij}(k,\eta_o,\eta_s^{(0)})$, and in Table 5.2 for $\mathcal{C}_i(k,\eta_o,\eta_s^{(0)})$. In Table 5.1 we also show the small-k limit ($k\Delta\eta\ll 1$) of $\mathcal{C}_{ij}$ and of the products $\mathcal{C}_i\mathcal{C}_j$. For notational convenience we have introduced in the tables the dimensionless variable $l=k\Delta\eta$, and we have used the definition of the sine integral:

$$\mathrm{SinInt}(l)=\int_0^l dx\,\frac{\sin x}{x}\quad.\tag{5.56}$$

It should be noted that the computation of some of the terms requires the explicit expression of the scale factor $a(\eta)$. It is the case of the terms involving the integral $P(\eta,r,\widetilde{\theta}^a)$ (see Eq. (4.7)). In those cases we have assumed a dust-dominated CDM scale factor with $a(\eta)=a(\eta_o)(\eta/\eta_o)^2$, and we have defined:

$$f_{o,s}\equiv\int_{\eta_{in}}^{\eta_{o,s}}d\eta\frac{a(\eta)}{a(\eta_{o,s})}=\frac{\eta_{o,s}^3-\eta_{in}^3}{3\eta_{o,s}^2}\simeq\frac{1}{3}\eta_{o,s}\quad,\tag{5.57}$$

where we recall that η_{in} satisfies, by definition, $\eta_{in}\ll\eta_{o,s}$. Using such a CDM-dominated model also imposes the following (zeroth-order) relation between z_s and $\Delta\eta$:

$$\Delta\eta=\frac{2}{a_oH_0}\left[1-\frac{1}{\sqrt{1+z_s}}\right]\quad.\tag{5.58}$$

We can notice on this table that the difference $\overline{\langle A_iA_j\rangle}-\overline{\langle A_i\rangle\langle A_j\rangle}$ is giving spectral coefficients which are all at least of order $(k\Delta\eta)^2=l^2$. This states that the terms $\overline{\langle A_i\rangle\langle A_j\rangle}$, though negligible in general with respect to $\overline{\langle A_iA_j\rangle}$ guarantee the good behaviour of the terms in the limit $z_s\to 0$. Indeed, one can see from Eq. (5.58) that at small redshifts one has $\Delta\eta\simeq z_s/a_oH_0$, thus each of these contributions, for a fixed mode k, goes to zero in the limit $k\Delta\eta\sim z_s\to 0$. Though being clear, this nice limit property will not appear in the plots of Chapter 6 and the reason is that the turning point of this limit happens at really small redshifts ($\lesssim 10^{-4}$ depending on the modes). Looking at the l^2 dependence of the terms, one can easily see in Table 5.1 that the dominant contributions are $\overline{\langle A_4A_4\rangle}$ and $\overline{\langle A_5A_5\rangle}$ (as computed in Sec. 5.2.4). These contributions are the Doppler effect (peculiar velocities) and lensing from inhomogeneities and will play a major role in the rest of this document.

Table 5.1: The spectral coefficients $\mathcal{C}_{ij}(k,\eta_o,\eta_s^{(0)})$ for the $\overline{\langle A_i A_j\rangle}$ terms defined by Eq. (5.52). We also give the $k\Delta\eta \ll 1$ limit (up to leading order in $k\Delta\eta$) of $\mathcal{C}_{ij}$ and of the products $\mathcal{C}_i\,\mathcal{C}_j$ for the coefficients defined in Table 5.2. We have used the definition $\Xi_s \equiv \left(1-\frac{1}{\mathcal{H}_s\Delta\eta}\right)$.

$\overline{\langle A_i A_j\rangle}$	$\mathcal{C}_{ij}(k,\eta_o,\eta_s^{(0)})$	$\mathcal{C}_{ij}$, $k\Delta\eta \ll 1$	$\mathcal{C}_i\ \mathcal{C}_j$, $k\Delta\eta \ll 1$
$\overline{\langle A_1 A_1\rangle}$	1	1	$1-\frac{l^2}{3}$
$\overline{\langle A_1 A_2\rangle}$	$-\frac{2}{l}\mathrm{SinInt}(l)$	$-2+\frac{l^2}{9}$	$-2+\frac{4}{9}l^2$
$\overline{\langle A_1 A_3\rangle}$	$\Xi_s\left[1-\frac{\sin(l)}{l}\right]$	$\Xi_s\frac{l^2}{6}$	$-\Xi_s\frac{l^2}{6}$
$\overline{\langle A_1 A_4\rangle}$	$\Xi_s\frac{f_0}{\Delta\eta}[\cos l-\frac{\sin(l)}{l}]$	$-\frac{f_0}{\Delta\eta}\Xi_s\frac{l^2}{3}$	$-\frac{f_s}{\Delta\eta}\Xi_s\frac{l^2}{3}$
$\overline{\langle A_1 A_5\rangle}$	$-2\left[1-\frac{\sin(l)}{l}\right]$	$-\frac{l^2}{3}$	0
$\overline{\langle A_2 A_2\rangle}$	$\frac{8}{l^2}\left[-1+\cos l+l\mathrm{SinInt}(l)\right]$	$4-\frac{l^2}{9}$	$4-\frac{4}{9}l^2$
$\overline{\langle A_2 A_3\rangle}$	0	0	$\Xi_s\frac{l^2}{3}$
$\overline{\langle A_2 A_4\rangle}$	$2\Xi_s\frac{f_0+f_s}{\Delta\eta}[1-\frac{\sin(l)}{l}]$	$\frac{f_0+f_s}{\Delta\eta}\Xi_s\frac{l^2}{3}$	$\frac{f_s}{\Delta\eta}\Xi_s\frac{2}{3}l^2$
$\overline{\langle A_2 A_5\rangle}$	$\frac{2}{3l^2}\left[-4+(4+l^2)\cos l+l\sin l+l^3\mathrm{SinInt}(l)\right]$	$\frac{l^2}{3}$	0
$\overline{\langle A_3 A_3\rangle}$	$2\Xi_s^2\left[1-\frac{\sin(l)}{l}\right]$	$\Xi_s^2\frac{l^2}{3}$	$\Xi_s^2\frac{l^4}{36}$
$\overline{\langle A_3 A_4\rangle}$	$\Xi_s^2\frac{f_0-f_s}{\Delta\eta}\left[\cos l-\frac{\sin(l)}{l}\right]$	$-\frac{f_0-f_s}{\Delta\eta}\Xi_s^2\frac{l^2}{3}$	$\frac{f_s}{\Delta\eta}\Xi_s^2\frac{l^4}{18}$
$\overline{\langle A_3 A_5\rangle}$	$-2\Xi_s\left[1-\frac{\sin(l)}{l}\right]$	$-\Xi_s\frac{l^2}{3}$	0
$\overline{\langle A_4 A_4\rangle}$	$\Xi_s^2\left[\frac{f_0^2+f_s^2}{\Delta\eta^2}\frac{l^2}{3}-\frac{2f_0f_s}{\Delta\eta^2}\left(2\cos l+(-2+l^2)\frac{\sin l}{l}\right)\right]$	$\left(\frac{f_0-f_s}{\Delta\eta}\right)^2\Xi_s^2\frac{l^2}{3}$	$\left(\frac{f_s}{\Delta\eta}\right)^2\Xi_s^2\frac{l^4}{9}$
$\overline{\langle A_4 A_5\rangle}$	$\Xi_s\left[\frac{f_0+3f_s}{\Delta\eta}\cos l+\frac{f_0-f_s}{\Delta\eta}\frac{\sin l}{l}+\frac{(f_0+f_s)(-2+l\mathrm{SinInt}(l))}{\Delta\eta}\right]$	$\frac{f_0-f_s}{\Delta\eta}\Xi_s\frac{l^2}{3}$	0
$\overline{\langle A_5 A_5\rangle}$	$\frac{1}{15l^2}\left[-24+20l^2+(24-2l^2+l^4)\cos(l)\right.$ $\left.+l(-6+l^2)\sin(l)+l^5\mathrm{SinInt}(l)\right]$	$\frac{l^2}{3}$	0

Table 5.2: The spectral coefficients $\mathcal{C}_i$ for the $\overline{\langle A_i\rangle\langle A_j\rangle}$ terms defined by Eq. (5.53). The signs $(-1)\times$ indicated for A_1 and A_2 are emphasized as they where presented with the wrong sign in [107] (though having no consequences on the plots).

A_i	$\mathcal{C}_i(k,\eta_o,\eta_s^{(0)})$
A_1	$(-1)\times\ \frac{\sin l}{l}$
A_2	$(-1)\times\ -\frac{2}{l}\mathrm{SinInt}(l)$
A_3	$-\left(1-\frac{1}{\mathcal{H}_s\Delta\eta}\right)\left(1-\frac{\sin l}{l}\right)$
A_4	$\left(1-\frac{1}{\mathcal{H}_s\Delta\eta}\right)\frac{f_s}{\Delta\eta}\left(\cos l-\frac{\sin l}{l}\right)$
A_5	0

5.2.4 Other examples of backreaction integrals

Here we present a detailed computation of some of the terms contributing to the induced backreaction and to the dispersion associated to the light-cone average of $d_L(z_s, \theta^a)$. Such computations also explain the corresponding spectral coefficients appearing in Table 5.1 and Table 5.2. In slightly different notations and, more importantly, the consideration of all the necessary terms up to second order, it will also define the spectral coefficients presented in Sec. 5.3.4.

To give an example slightly more involved than $\overline{\langle\psi_s\psi_s\rangle} \equiv \overline{\langle A_1 A_1\rangle}$ or $\overline{\langle\psi_s\rangle\langle\psi_s\rangle} \equiv \overline{\langle A_1\rangle\langle A_1\rangle}$ of Eqs. (5.50) and (5.51), we can consider the average of a term like $\psi_s Q_s/\Delta\eta \equiv A_1 A_2$. Again we consider here the CDM case where the power spectrum has no time dependence. We get:

$$\begin{aligned}\overline{\langle A_1 A_2\rangle} &= -\frac{2}{\Delta\eta}\int\frac{d^3k d^3k'}{(2\pi)^3}\overline{E(\mathbf{k})E(\mathbf{k}')}\int\frac{d^2\Omega}{4\pi}\left[\psi_k(\eta_s^{(0)})e^{i\mathbf{k}\cdot\hat{\mathbf{x}}\Delta\eta}\int_{\eta_s^{(0)}}^{\eta_o}d\eta\,\psi_{k'}(\eta)e^{i\mathbf{k}'\cdot\hat{\mathbf{x}}(\eta_o-\eta)}\right]\\ &= -2\int_0^\infty\frac{dk}{k}\mathcal{P}_\psi(k)\frac{\mathrm{SinInt}(k\Delta\eta)}{k\Delta\eta} = \overline{\left\langle\psi_s\frac{Q_s}{\Delta\eta}\right\rangle}\ ,\end{aligned} \tag{5.59}$$

$$\begin{aligned}\overline{\langle A_1\rangle\langle A_2\rangle} &= -\frac{2}{\Delta\eta}\int\frac{d^3k d^3k'}{(2\pi)^3}\overline{E(\mathbf{k})E(\mathbf{k}')}\left[\int\frac{d^2\Omega}{4\pi}\psi_k(\eta_s^{(0)})e^{i\mathbf{k}\cdot\hat{\mathbf{x}}\Delta\eta}\right]\left[\int\frac{d^2\Omega'}{4\pi}\int_{\eta_s^{(0)}}^{\eta_o}d\eta\,\psi_{k'}(\eta)e^{i\mathbf{k}'\cdot\hat{x}'(\eta_o-\eta)}\right]\\ &= -2\int_0^\infty\frac{dk}{k}\mathcal{P}_\psi(k)\,\frac{\sin(k\Delta\eta)}{k\Delta\eta}\frac{\mathrm{SinInt}(k\Delta\eta)}{k\Delta\eta} = \overline{\langle\psi_s\rangle\left\langle\frac{Q_s}{\Delta\eta}\right\rangle}\ ,\end{aligned} \tag{5.60}$$

which indeed correspond to the results presented in Tables 5.1 and 5.2 for $\overline{\langle A_1 A_2\rangle}$ and $\overline{\langle A_1\rangle\langle A_2\rangle}$. As one can see, the angular average is making the results completely different in the two cases. We remark that the presence of the SinInt function (see Eq. (5.56)) is a direct consequence of the integration over time in Q_s. Consequently, the non-local nature of the backreaction terms is reflected in the form of the corresponding spectral coefficients.

Let us now present $\overline{\langle A_2 A_5\rangle} \propto \overline{\langle Q_s J_2/\Delta\eta\rangle}$ and $\overline{\langle A_2\rangle\langle A_5\rangle}$. These terms are interesting as they correspond to the mixing between an integrated perturbation ψ and the lensing term. Using Eqs. (5.16), (5.19), (5.46), and working in the hypothesis of time-independent ψ_k, we obtain:

$$\begin{aligned}\overline{\langle A_2 A_5\rangle} &= \int\frac{d^3k\ d^3k'}{(2\pi)^3}\overline{E(\mathbf{k})E(\mathbf{k}')}\int\frac{d^2\Omega}{4\pi}\\ &\qquad\times\left[\frac{2}{\Delta\eta}\int_{\eta_s}^{\eta_o}d\eta'\ \psi_k\,e^{i(\eta_o-\eta')\mathbf{k}\cdot\hat{\mathbf{x}}}\right]\left[-\int_{\eta_s}^{\eta_o}\frac{d\eta''}{\Delta\eta}\frac{\eta''-\eta_s}{\eta_o-\eta''}\ \Delta_2\left(\psi_{k'}\,e^{i(\eta_o-\eta'')\mathbf{k}'\cdot\hat{\mathbf{x}}}\right)\right]\\ &= \int\frac{d^3k}{(2\pi)^3}\ |\psi_k|^2\int_{-1}^{1}\frac{d(\cos\theta)}{2}\left[\frac{2}{\Delta\eta}\int_{\eta_s}^{\eta_o}d\eta'\ e^{ik(\eta_o-\eta')\cos\theta}\right]\\ &\quad\times\left[\frac{1}{\Delta\eta}\int_{\eta_s}^{\eta_o}d\eta''\frac{\eta''-\eta_s}{\eta_o-\eta''}\left(k^2(\eta_o-\eta'')^2\sin^2\theta-2ik(\eta_o-\eta'')\cos\theta\right)e^{-ik(\eta_o-\eta'')\cos\theta}\right]\\ &= \int_0^\infty\frac{dk}{k}\ \mathcal{P}_\psi(k)\\ &\qquad\times\frac{2}{3(k\Delta\eta)^2}\left[-4+(4+(k\Delta\eta)^2)\cos(k\Delta\eta)+k\Delta\eta\sin(k\Delta\eta)+(k\Delta\eta)^3\mathrm{SinInt}(k\Delta\eta)\right]\ ,\end{aligned} \tag{5.61}$$

$$\begin{aligned}\overline{\langle A_2\rangle\langle A_5\rangle} &= \int\frac{d^3k\ d^3k'}{(2\pi)^3}\overline{E(\mathbf{k})E(\mathbf{k}')}\left[\int\frac{d^2\Omega}{4\pi}\frac{2}{\Delta\eta}\int_{\eta_s}^{\eta_o}d\eta'\ \psi_k\,e^{i(\eta 0-\eta')\mathbf{k}\cdot\hat{\mathbf{x}}}\right]\\ &\qquad\times\left[-\int\frac{d^2\Omega'}{4\pi}\int_{\eta_s}^{\eta_o}\frac{d\eta''}{\Delta\eta}\frac{\eta''-\eta_s}{\eta_o-\eta''}\ \Delta_2\left(\psi_{k'}\,e^{i(\eta_o-\eta'')\mathbf{k}'\cdot\hat{\mathbf{x}}}\right)\right]\\ &= \int\frac{d^3k}{(2\pi)^3}\ |\psi_k|^2\left[\int_{-1}^{1}\frac{d(\cos\theta)}{2}\frac{2}{\Delta\eta}\int_{\eta_s}^{\eta_o}d\eta'\ e^{ik(\eta_o-\eta')\cos\theta}\right]\\ &\quad\times\left[\int_{-1}^{1}\frac{d(\cos\theta')}{2}\frac{1}{\Delta\eta}\int_{\eta_s}^{\eta_o}d\eta''\frac{\eta''-\eta_s}{\eta_o-\eta''}\left(k^2(\eta_o-\eta'')^2\sin^2\theta'-2ik(\eta_o-\eta'')\cos\theta'\right)e^{-ik(\eta_o-\eta'')\cos\theta'}\right]\\ &= \int_0^\infty\frac{dk}{k}\ \mathcal{P}_\psi(k)\left[\frac{2}{k\Delta\eta}\mathrm{SinInt}(k\Delta\eta)\right]\times 0\ =\ 0\ .\end{aligned} \tag{5.62}$$

In the second equalities of Eqs. (5.61) and (5.62) we have applied Eq. (5.26) to remove the integration over $\mathbf{k}'$, and we have used the isotropy of the scalar product $\mathbf{k}\cdot\hat{\mathbf{x}}$.

We can see that the terms presented until now are not dominant for a general power spectrum as they are, at most, going like $k\Delta\eta$. We consider now the two leading contributions given by $\overline{\langle A_4 A_4\rangle}$ and $\overline{\langle A_5 A_5\rangle}$ (and, for completeness, the associated terms $\overline{\langle A_4\rangle\langle A_4\rangle}$ and $\overline{\langle A_5\rangle\langle A_5\rangle}$). We will show in Sec. 6.1 that these are the two leading contributions to IBR_2 and to the dispersion and they correspond respectively to the "Doppler squared" and "lensing squared terms". Starting from Eq. (5.9), and using the same hypotheses as in the previous calculations, we have:

$$\begin{aligned} I_r &= \int_{\eta_{in}}^{\eta_s} d\eta' \frac{a(\eta')}{a(\eta_s)}\partial_r\psi(\eta',\eta_o-\eta_s,\theta^a) - \int_{\eta_{in}}^{\eta_o} d\eta' \frac{a(\eta')}{a(\eta_o)}\partial_r\psi(\eta',0,\theta^a) \\ &= \int \frac{d^3k}{(2\pi)^{3/2}}\left[\int_{\eta_{in}}^{\eta_s} d\eta' \frac{\eta'^2}{\eta_s^2}(ik\cos\theta)\psi_k\, e^{i\Delta\eta\,\mathbf{k}\cdot\hat{\mathbf{x}}} - \int_{\eta_{in}}^{\eta_o} d\eta' \frac{\eta'^2}{\eta_o^2}(ik\cos\theta)\psi_k\right] \\ &= \int \frac{d^3k}{(2\pi)^{3/2}}\psi_k\left(f_s e^{ik\Delta\eta\cos\theta} - f_0\right)(ik\cos\theta) \quad . \end{aligned} \tag{5.63}$$

Then, according to the definitions of Eq. (5.46) we have $\overline{\langle A_4 A_4\rangle} = \Xi_s^2\,\overline{\langle I_r I_r\rangle}$ where:

$$\begin{aligned} \overline{\langle I_r I_r\rangle} &= \int \frac{d^3k}{(2\pi)^3}\,|\psi_k|^2 \int_{-1}^{1}\frac{d(\cos\theta)}{2}\left[\left(f_s e^{ik\Delta\eta\cos\theta} - f_0\right)(ik\cos\theta)\right]\left[\left(f_s e^{-ik\Delta\eta\cos\theta} - f_0\right)(-ik\cos\theta)\right] \\ &= \int_0^\infty \frac{dk}{k}\,\frac{\mathcal{P}_\psi(k)}{3\Delta\eta^2}\left[(f_0^2+f_s^2)(k\Delta\eta)^2 - 12 f_0 f_s\cos(k\Delta\eta) - 6 f_0 f_s(-2+(k\Delta\eta)^2)\frac{\sin(k\Delta\eta)}{k\Delta\eta}\right] \quad , \end{aligned} \tag{5.64}$$

and where we have used the following exact integral result:

$$\int_{-1}^{1}\frac{d(\cos\theta)}{2}(\cos\theta)^2 e^{\pm ik\Delta\eta\cos\theta} = \frac{2k\Delta\eta\cos(k\Delta\eta) + (-2+(k\Delta\eta)^2)\sin(k\Delta\eta)}{(k\Delta\eta)^3} \quad . \tag{5.65}$$

In the same way we obtain $\overline{\langle A_4\rangle\langle A_4\rangle} = \Xi_s^2\,\overline{\langle I_r\rangle\langle I_r\rangle}$ where:

$$\begin{aligned} \overline{\langle I_r\rangle\langle I_r\rangle} &= \int \frac{d^3k}{(2\pi)^3}\,|\psi_k|^2\left[\int_{-1}^{1}\frac{d(\cos\theta)}{2}\left(f_s e^{ik\Delta\eta\cos\theta} - f_0\right)(ik\cos\theta)\right] \qquad (5.66) \\ &\quad\times\left[\int_{-1}^{1}\frac{d(\cos\theta')}{2}\left(f_s e^{-ik\Delta\eta\cos\theta'} - f_0\right)(-ik\cos\theta')\right] \\ &= \int_0^\infty \frac{dk}{k}\,\mathcal{P}_\psi(k)\left[\frac{f_s}{\Delta\eta}\left(\cos(k\Delta\eta) - \frac{\sin(k\Delta\eta)}{k\Delta\eta}\right)\right]^2 \quad , \qquad (5.67) \end{aligned}$$

and where we have used the integral

$$\int_{-1}^{1}\frac{d(\cos\theta)}{2}\,\cos\theta e^{\pm ik\Delta\eta\cos\theta} = \pm i\left(\frac{-k\Delta\eta\cos(k\Delta\eta)+\sin(k\Delta\eta)}{(k\Delta\eta)^2}\right) . \tag{5.68}$$

Following a similar procedure, Eq. (5.16) leads us to the lensing contribution:

$$\begin{aligned} \overline{\langle A_5 A_5\rangle} &= \int \frac{d^3k}{(2\pi)^3}\,|\psi_k|^2\int_{-1}^{1}\frac{d(\cos\theta)}{2} \\ &\quad\times\left[\int_{\eta_s}^{\eta_o}\frac{d\eta'}{\Delta\eta}\frac{\eta'-\eta_s}{\eta_o-\eta'}\left(k^2(\eta_o-\eta')^2\sin^2\theta + 2ik(\eta_o-\eta')\cos\theta\right)e^{ik(\eta_o-\eta')\cos\theta}\right] \\ &\quad\times\left[\int_{\eta_s}^{\eta_o}\frac{d\eta''}{\Delta\eta}\frac{\eta''-\eta_s}{\eta_o-\eta''}\left(k^2(\eta_o-\eta'')^2\sin^2\theta - 2ik(\eta_o-\eta'')\cos\theta\right)e^{-ik(\eta_o-\eta'')\cos\theta}\right] \\ &= \int_0^\infty \frac{dk}{k}\,\mathcal{P}_\psi(k)\frac{1}{15(k\Delta\eta)^2}\left[-24+20(k\Delta\eta)^2 + (24-2(k\Delta\eta)^2+(k\Delta\eta)^4)\cos(k\Delta\eta)\right. \\ &\qquad\left. -6k\Delta\eta\sin(k\Delta\eta) + (k\Delta\eta)^3\sin(k\Delta\eta) + (k\Delta\eta)^5\mathrm{SinInt}(k\Delta\eta)\right] \quad . \end{aligned} \tag{5.69}$$

Note that, for the same reason for which $\overline{\langle A_2\rangle\langle A_5\rangle} = 0$, i.e. for the fact that the integrand of A_5 gives exactly zero when averaged over the angles, we finally also obtain $\overline{\langle A_5\rangle\langle A_5\rangle} = 0$.

5.3 Averaging the luminosity flux at second order

In this section we treat the full computation of the light-cone and stochastic average of the luminosity flux $\overline{\langle\Phi\rangle} \sim \overline{\langle d_L^{-2}\rangle}$ and the luminosity distance $\overline{\langle d_L\rangle}$, including the contributions from the genuine second order. The calculations will thus rely on the full transformation of coordinates as presented in Chapter 4. We will further consider all types of perturbations, of scalar, vector and tensor kind. Because the number of terms is even more important than with the consideration of the terms generated by first-order only, namely IBR_2 and $\overline{\langle\sigma_1^2\rangle}$, we will proceed to a different regroupment of the terms.

5.3.1 Exact expression for $\langle d_L^{-2}\rangle$ in the geodesic light-cone gauge

The luminosity flux, $\Phi \sim d_L^{-2} = (1+z_s)^{-4} d_A^{-2}$, appears as an important and extremely simple observable to average over the 2-sphere $\Sigma(w_o, z_s)$ embedded in the light-cone. In fact, we have:

$$\langle d_L^{-2}\rangle(w_o, z_s) = (1+z_s)^{-4} \frac{\int dS \frac{d^2\Omega_o}{dS}}{\int dS} = (1+z_s)^{-4} \frac{\int d^2\Omega_o}{\int dS} = (1+z_s)^{-4} \frac{4\pi}{\mathcal{A}(w_o, z_s)} \quad , \tag{5.70}$$

where

$$\mathcal{A}(w_o, z_s) = \int_{\Sigma(w_o,z_s)} d^2\tilde{\theta}^a \sqrt{\gamma(w_o, \tau_s(w_o, z_s, \widetilde{\theta}^a), \widetilde{\theta}^a)} \tag{5.71}$$

is the proper area of $\Sigma(w_o, z_s)$ computed with the metric γ_{ab}, and expressed in terms of internal coordinates (w_o, z_s) parametrizing this deformed 2-sphere. One could decide to parametrize this integral by two other angular coordinates ξ^a. One would then have the same expression:

$$\mathcal{A}(w_o, z_s) = \int_{\Sigma(w_o,z_s)} d^2\xi \sqrt{\gamma(w_o, \tau_s(w_o, z_s, \widetilde{\xi}^a), \widetilde{\xi}^a)} \quad \text{with} \quad \gamma_{ab}(\xi) = \frac{\partial y^\mu}{\partial \xi^a}\frac{\partial y^\nu}{\partial \xi^b} g^{PG}_{\mu\nu}(y) = \gamma_{ab} \quad , \tag{5.72}$$

and where $\{y^\mu\}$ are, for instance, the Poisson gauge coordinates such that $y^\mu = y^\mu(w_o, \tau_s(w_o, z_s, \tilde{\xi}^a), \tilde{\xi}^b)$. In fact, one can notice that $\gamma_{ab}(\xi)$ is the metric induced by the coordinates $\{y^\mu\}$ on $\Sigma(w_o, z_s)$, so we can write $\gamma_{ab}(\xi) \equiv \gamma^{ind}_{ab}(\xi)$. From this remark and the consideration of Eq. (5.72), we can see very amusingly that $\mathcal{A}$ is similar to the reparametrization-invariant Nambu-Goto action in string theory.

The Eq. (5.70) holds non-perturbatively for any spacetime geometry and is the starting point for the computation of the average flux. It can also be written in an elegant form in which the flux of an inhomogeneous Universe is compared to that of a FLRW one:

$$\langle \Phi/\Phi^{\mathrm{FLRW}}\rangle = \frac{4\pi \left(d_A^{\mathrm{FLRW}}\right)^2}{\mathcal{A}} \quad . \tag{5.73}$$

This expression directly shows that a deviation by the presence of inhomogeneities from the standard FLRW result is related to a deformation of the 2-sphere $\Sigma(w_o, z_s)$ because of these inhomogeneities.

Coming back to the notations introduced in Chapter 4, we can in particular recast Eq. (5.70) into:

$$\langle d_L^{-2}\rangle(w_o, z_s) = (1+z_s)^{-4} \left[\int \frac{d^2\tilde{\theta}^a}{4\pi} \sqrt{\gamma(w_o, \tau_s(w_o, z_s, \tilde{\theta}^a), \tilde{\theta}^a)}\right]^{-1} \equiv \left(d_L^{\mathrm{FLRW}}\right)^{-2} I_\phi^{-1}(w_o, z_s) \quad , \tag{5.74}$$

where we have defined

$$I_\phi(w_o, z_s) \equiv \frac{\mathcal{A}(w_o, z_s)}{4\pi \left[a(\eta_s^{(0)})\Delta\eta\right]^2} \quad , \tag{5.75}$$

and where $d_L^{\mathrm{FLRW}} = (1+z_s)^2 a(\eta_s^{(0)})\Delta\eta$ is the luminosity distance for the unperturbed FLRW geometry, with scale factor $a(\eta)$. Here η is the conformal time coordinate, $\Delta\eta = \eta_o - \eta_s^{(0)}$, and we have denoted with $\eta_s^{(0)}$ the background solution of the equation for the source's conformal time $\eta_s = \eta_s(z_s, \widetilde{\theta}^a)$ (see Sec. 4.2.1). Note again that, according to the above equation, the interpretation of $I_\phi(w_o, z_s)$ is straightforward: it is simply the ratio of the area of the 2-sphere at redshift z_s on the past light-cone (deformed by inhomogeneities), over the area of the corresponding homogeneous 2-sphere.

5.3.2 Second-order expression for $\langle d_L^{-2}\rangle$ in the Poisson gauge

Let us consider a spacetime geometry that can be approximated by a spatially flat FLRW metric distorted by the presence of scalar, vector and tensor perturbations, in the Poisson gauge and as used in Chapter 4. It is important to stress that for this thesis we can safely restrict our discussion to pure scalar perturbations. In fact, it is true that at second order different perturbations get mixed : vector and tensor perturbations, ω_i and h_{ij}, are automatically generated from scalar perturbations (see e.g. [103, 104]), while second-order scalar perturbations are generated from first-order vector and tensor perturbations. However, a single vector or tensor perturbation does not contribute to our angular averages on $\Sigma(w_o, z_s)$, as it will be proved in Sec. 5.3.6. Furthermore, we treat ω_i and h_{ij} as second order quantities, i.e. we assume the first-order perturbed metric to be dominated by scalar contributions (as perturbations generated by a phase of standard slow-roll inflation, see e.g. [7, 108]).

We have established a connection between the second-order perturbative expression of the luminosity distance d_L and of the integrand of I_ϕ (controlling $\langle d_L^{-2}\rangle$), both written in terms of the PG perturbations and the observer's angles $\tilde\theta^a$ (remember that photons travel at constant $\tilde\theta^a$). In particular, recalling Eq. (4.79) where the contribution $\bar\delta^{(2)}_{V,T}$ has been forgotten (see Sec. 5.3.6), we have :

$$\frac{d_L(z_s,\tilde\theta^a)}{(1+z_s)a_o\Delta\eta} = \frac{d_L(z_s,\tilde\theta^a)}{d_L^{\rm FLRW}(z_s)} = 1 + \bar\delta_S^{(1)}(z_s,\tilde\theta^a) + \bar\delta_S^{(2)}(z_s,\tilde\theta^a) \quad , \tag{5.76}$$

$$I_\phi(z_s) = \int \frac{d^2\tilde\theta^a}{4\pi}\sin\tilde\theta\,(1+\mathcal{I}_1+\mathcal{I}_{1,1}+\mathcal{I}_2) \quad , \tag{5.77}$$

and we can show that [5] :

$$\mathcal{I}_1 = 2\bar\delta_S^{(1)} + (\text{t. d.})^{(1)} \quad , \quad \mathcal{I}_{1,1}+\mathcal{I}_2 = 2\bar\delta_S^{(2)} + (\bar\delta_S^{(1)})^2 + (\text{t. d.})^{(2)} \quad . \tag{5.78}$$

where the terms $(\text{t. d.})^{(1),(2)}$ denote total derivative terms w.r.t. the $\tilde\theta^a$ angles, giving vanishing contributions either by periodicity in $\widetilde\phi$ or by the vanishing of the integrand at $\widetilde\theta = 0, \pi$. We only recall here, for later use, the first-order total derivative :

$$(\text{t. d.})^{(1)} = 2\,J_2^{(1)} \quad , \quad J_2^{(1)} = \frac{1}{\Delta\eta}\int_{\eta_s^{(0)}}^{\eta_o} d\eta\,\frac{\eta-\eta_s^{(0)}}{\eta_o-\eta}\Delta_2\psi(\eta,\eta_o-\eta,\widetilde\theta^a) \quad , \tag{5.79}$$

where $\Delta_2 = \partial^2_{\widetilde\theta} + \cot\widetilde\theta\partial_{\widetilde\theta} + \sin^{-2}\widetilde\theta\partial^2_{\widetilde\phi}$. It is also convenient to rewrite the PG metric using spherical coordinates (but still considering that photons travel at constant $\tilde\theta^a$), and use the following quantities :

$$P(\eta,r,\widetilde\theta^a) = \textstyle\int_{\eta_{in}}^{\eta} d\eta'\frac{a(\eta')}{a(\eta)}\psi(\eta',r,\widetilde\theta^a) \quad , \quad Q(\eta_+,\eta_-,\widetilde\theta^a) = \int_{\eta_+}^{\eta_-} dx\;\hat\psi(\eta_+,x,\widetilde\theta^a) \quad ,$$
$$\Xi_s = 1 - \frac{1}{\mathcal{H}_s\Delta\eta} \quad , \quad J = ([\partial_+Q]_s - [\partial_+Q]_o) - ([\partial_rP]_s - [\partial_rP]_o) \quad , \tag{5.80}$$

which were defined in Chapter 4. We recall that the radial gradient of P is related to the Doppler effect (due to peculiar velocities of source and observer), while the gradient of Q with respect to ∂_+ represents the Sachs-Wolfe (SW) and the integrated Sachs-Wolfe (ISW) effects. The last term J corresponds to a combination of the three mentioned effects.

The results obtained in Eqs. (5.77) and (5.78) can be reported in the following form :

$$\mathcal{I}_1 = \sum_{i=1}^{3}\mathcal{T}_i^{(1)} \quad , \quad \mathcal{I}_{1,1} = \sum_{i=1}^{23}\mathcal{T}_i^{(1,1)} \quad , \quad \mathcal{I}_2 = \sum_{i=1}^{7}\mathcal{T}_i^{(2)} \quad , \tag{5.81}$$

where $\mathcal{I}_1$, $\mathcal{I}_{1,1}$, $\mathcal{I}_2$ are, respectively, the first-order, quadratic first-order, and genuine second-order contributions of our stochastic fluctuations, and where these sums are made of the terms :

$$\mathcal{T}_1^{(1)} = -2\psi(\eta_s^{(0)},r_s^{(0)},\widetilde\theta^a) \quad ; \quad \mathcal{T}_2^{(1)} = 2\Xi_s J \quad ; \quad \mathcal{T}_3^{(1)} = -\frac{2}{\Delta\eta}Q_s \quad ; \tag{5.82}$$

5. As already mentioned, the terms appearing on the RHS of Eq. (5.76) should be corrected, in principle, for the peculiar velocity of the observer. However, such a correction has no effect on the integral I_ϕ itself, since it can be compensated by a Lorentz transformation of the angular variables.

$$
\begin{aligned}
&\mathcal{T}_1^{(1,1)} = \Xi_s \left[\psi_s^2 - \psi_o^2\right] \quad ; \quad \mathcal{T}_2^{(1,1)} = \Xi_s \left(([\partial_r P]_s)^2 - ([\partial_r P]_o)^2\right) \quad ; \quad \mathcal{T}_3^{(1,1)} = -2\Xi_s \left(\psi_s + [\partial_+ Q]_s\right) [\partial_r P]_s \quad ; \\
&\mathcal{T}_4^{(1,1)} = \frac{1}{2}\Xi_s (\gamma_0^{ab})_s \left(2\partial_a P_s \partial_b P_s + \partial_a Q_s \partial_b Q_s - 4\partial_a Q_s \partial_b P_s\right) \quad ; \quad \mathcal{T}_5^{(1,1)} = -\Xi_s \lim_{r\to 0} \left[\gamma_0^{ab} \partial_a P \partial_b P\right] \quad ; \\
&\mathcal{T}_6^{(1,1)} = 2\Xi_s Q_s \left(2\partial_r \psi_o + 2\partial_\eta \psi_o - \partial_r \psi_s + 2\int_{\eta_s^{(0)}}^{\eta_o} d\eta' \partial_r^2 \psi \left(\eta', \eta_o - \eta', \widetilde{\theta}^a\right) + [\partial_r^2 P]_s\right) \quad ; \\
&\mathcal{T}_7^{(1,1)} = 2\Xi_s \frac{J}{\mathcal{H}_s} \left([\partial_\eta \psi]_s + \mathcal{H}_s [\partial_r P]_s\right) \quad ; \quad \mathcal{T}_8^{(1,1)} = 2\Xi_s \frac{J}{\mathcal{H}_s} [\partial_r^2 P]_s \quad ; \\
&\mathcal{T}_9^{(1,1)} = -\Xi_s \int_{\eta_{in}}^{\eta_s^{(0)}} d\eta' \frac{a(\eta')}{a(\eta_s^{(0)})} \partial_r \left[-\psi^2 + (\partial_r P)^2 + \gamma_0^{ab} \partial_a P \partial_b P\right] (\eta', \Delta\eta, \tilde{\theta}^a) \quad ; \\
&\mathcal{T}_{10}^{(1,1)} = \Xi_s \int_{\eta_{in}}^{\eta_o} d\eta' \frac{a(\eta')}{a(\eta_o)} \partial_r \left[-\psi^2 + (\partial_r P)^2 + \gamma_0^{ab} \partial_a P \partial_b P\right] (\eta', 0, \tilde{\theta}^a) \quad ; \\
&\mathcal{T}_{11}^{(1,1)} = 2\Xi_s \int_{\eta_s^{(0)+}}^{\eta_s^{(0)-}} dx\ \partial_+ \left[\hat{\psi}\ \partial_+ Q + \frac{1}{4} \hat{\gamma}_0^{ab} \partial_a Q \partial_b Q\right] (\eta_s^{(0)+}, x, \tilde{\theta}^a) \quad ;
\end{aligned}
$$

$$
\begin{aligned}
&\mathcal{T}_{12}^{(1,1)} = \left[\Xi_s^2 - \frac{1}{\mathcal{H}_s \Delta\eta} \left(1 - \frac{\mathcal{H}_s'}{\mathcal{H}_s^2}\right)\right] J^2 \quad ; \quad \mathcal{T}_{13}^{(1,1)} = -4\psi_s J \quad ; \quad \mathcal{T}_{14}^{(1,1)} = 2\Xi_s \left\{\psi_o + [\partial_r P]_o - \frac{Q_s}{\Delta\eta}\right\} J \quad ; \\
&\mathcal{T}_{15}^{(1,1)} = -2(J - 2\psi_s) \frac{Q_s}{\Delta\eta} \quad ; \quad \mathcal{T}_{16}^{(1,1)} = -2\left(\psi_s - \partial_+ Q_s\right) \frac{Q_s}{\Delta\eta} \quad ; \quad \mathcal{T}_{17}^{(1,1)} = \left(\frac{Q_s}{\Delta\eta}\right)^2 \quad ; \\
&\mathcal{T}_{18}^{(1,1)} = \frac{1}{\mathcal{H}_s} (\gamma_0^{ab})_s \partial_a Q_s \partial_b J \quad ; \quad \mathcal{T}_{19}^{(1,1)} = \frac{1}{2} (\gamma_0^{ab})_s \partial_a Q_s \partial_b Q_s \quad ; \quad \mathcal{T}_{20}^{(1,1)} = 2\frac{J}{\mathcal{H}_s} \left(-[\partial_\eta \psi]_s + [\partial_r \psi]_s\right) \quad ; \\
&\mathcal{T}_{21}^{(1,1)} = 2Q_s [\partial_r \psi]_s \quad ; \quad \mathcal{T}_{22}^{(1,1)} = -\frac{2}{\Delta\eta} \int_{\eta_s^{(0)+}}^{\eta_s^{(0)-}} dx\ \left[\hat{\psi}\ \partial_+ Q + \frac{1}{4} \hat{\gamma}_0^{ab}\ \partial_a Q\ \partial_b Q\right] (\eta_s^{(0)+}, x, \tilde{\theta}^a) \quad ; \\
&\mathcal{T}_{23}^{(1,1)} = \frac{1}{8\sin\tilde{\theta}} \frac{\partial}{\partial\tilde{\theta}} \left\{\cos\tilde{\theta}\ \left(\int_{\eta_s^{(0)+}}^{\eta_s^{(0)-}} dx\ [\hat{\gamma}_0^{1b}\ \partial_b Q](\eta_s^{(0)+}, x, \tilde{\theta}^a)\right)^2\right\} \quad ;
\end{aligned}
\tag{5.83}
$$

$$
\begin{aligned}
&\mathcal{T}_1^{(2)} = -\frac{1}{2}\Xi_s \left(\phi_s^{(2)} - \phi_o^{(2)}\right) \quad ; \quad \mathcal{T}_2^{(2)} = \frac{1}{2}\Xi_s \left(\psi_s^{(2)} - \psi_o^{(2)}\right) \quad ; \\
&\mathcal{T}_3^{(2)} = -\Xi_s \int_{\eta_{in}}^{\eta_s^{(0)}} d\eta' \frac{a(\eta')}{a(\eta_s^{(0)})} [\partial_r \phi^{(2)}](\eta', \Delta\eta, \tilde{\theta}^a) \quad ; \\
&\mathcal{T}_4^{(2)} = \Xi_s \int_{\eta_{in}}^{\eta_o} d\eta' \frac{a(\eta')}{a(\eta_o)} [\partial_r \phi^{(2)}](\eta', 0, \tilde{\theta}^a) \quad ; \\
&\mathcal{T}_5^{(2)} = \frac{1}{2}\Xi_s \int_{\eta_s^{(0)+}}^{\eta_s^{(0)-}} dx\ \partial_+ \left[\hat{\phi}^{(2)} + \hat{\psi}^{(2)}\right] (\eta_s^{(0)+}, x, \tilde{\theta}^a) \quad ; \\
&\mathcal{T}_6^{(2)} = -\psi_s^{(2)} \quad ; \quad \mathcal{T}_7^{(2)} = -\frac{2}{\Delta\eta} \int_{\eta_s^{(0)+}}^{\eta_s^{(0)-}} dx\ \left[\frac{\hat{\phi}^{(2)} + \hat{\psi}^{(2)}}{4}\right] (\eta_s^{(0)+}, x, \tilde{\theta}^a) \quad .
\end{aligned}
\tag{5.84}
$$

In the above equations $\gamma_0^{ab} = \mathrm{diag}(r^{-2}, r^{-2}\sin^{-2}\widetilde{\theta})$, and for $\mathcal{T}_6^{(1,1)}$ we used the following identity :

$$
-[\partial_+^2 Q]_s + [\partial_+ \hat{\psi}]_s = 2\partial_r \psi_o + 2\partial_\eta \psi_o - \partial_r \psi_s + 2\int_{\eta_s^{(0)}}^{\eta_o} d\eta' \partial_r^2 \psi \left(\eta', \eta_o - \eta', \widetilde{\theta}^a\right) \quad . \tag{5.85}
$$

This relation can be proved by first noticing that :

$$
\begin{aligned}
-\left[\partial_+^2 Q\right]_s + [\partial_+ \hat{\psi}]_s \quad = \quad & \Big\{\partial_+ \hat{\psi}(\eta_+, \eta_-, \widetilde{\theta}^a) + \partial_+ \hat{\psi}(\eta_+, \eta_+, \widetilde{\theta}^a) + \lim_{x\to\eta_+} \left[\partial_+ \hat{\psi}(\eta_+, x, \widetilde{\theta}^a)\right] \\
& - \int_{\eta_+}^{\eta_-} dx\, \partial_+^2 \hat{\psi}(\eta_+, x, \widetilde{\theta}^a)\Big\} (\eta_s^{(0)+}, \eta_s^{(0)-, \widetilde{\theta}^a}) \quad .
\end{aligned}
\tag{5.86}
$$

We then convert the integral term in an integration over the time η and convert the derivatives by the use of Eqs. (5.10) and (5.11). We can hence perform the integrations involving a total derivative and we are left with integrands at observer and source positions and integrals involving partial derivatives of ψ with respect to r. The last subtlety to consider is at the tip of the observer light cone. Indeed, the relation $\partial_+ \equiv (\partial_\eta + \partial_r)/2$ leads to :

$$\lim_{x\to\eta_s^{(0)+}} \left[\partial_+\hat{\psi}(\eta_+, x, \widetilde{\theta}^a)\right]_s = \lim_{\eta\to\eta_o} \left[\frac{1}{2}(\partial_\eta + \partial_r)\psi(\eta, \eta_o - \eta, \widetilde{\theta}^a)\right] = \frac{1}{2}\left([\partial_\eta\psi]_o + [\partial_r\psi]_o\right) \quad , \tag{5.87}$$

where the subscript "s" denotes $\eta_+ \to \eta_s^{(0)+}$, but on the other hand we have to take for the second term in the RHS of Eq. (5.86) :

$$[\partial_+\hat{\psi}(\eta_+, \eta_+, \widetilde{\theta}^a)]_s = [\partial_\eta\psi]_o \quad . \tag{5.88}$$

This last result is well understood by seeing that this derivative is a derivative at the tip of the light cone, thus acting in all angular directions, giving thus a double derivation in the η-direction and a cancelation in r-direction. After a few simplifications we recover Eq. (5.85).

Let us point out, finally, that the last term in Eq. (5.83) corresponds to a total derivative, and thus to a boundary contribution, that superficially looks non vanishing. This term is probably the result of a naive treatment of the angular coordinate transformation, which becomes singular near the poles of the 2-sphere. This contribution, indeed, has the same form as the irrelevant one coming from an overall $SO(3)$ rotation. In any case, we will see that its spectral coefficient is zero (Sec. 5.3.4).

Let us conclude this section about the flux by giving the explicit expressions for $\mathcal{I}_1$, $\mathcal{I}_{1,1}$ and $\mathcal{I}_2$. Gathering the terms from Eqs. (5.81) and (5.82), we get the explicit expression of $\mathcal{I}_1$ which is :

$$\mathcal{I}_1 \;=\; 2\left(\Xi_s J - \frac{1}{\Delta\eta}Q_s - \psi(\eta_s^{(0)}, r_s^{(0)}, \theta^a)\right) \quad . \tag{5.89}$$

This expression can be compared with the one of $\bar{\delta}_S^{(1)}$ given in Eq. (4.60). Apart from an obvious factor of two, the expression for $\mathcal{I}_1$ lacks the $J_2^{(1)}$ (lensing) term which is precisely a typical one that vanishes upon angular integration.

Still dropping irrelevant total derivatives, the two second order terms appearing in Eq. (5.77) take the following explicit form :

$$\begin{aligned}
\mathcal{I}_{1,1} \;=\; & 2\Xi_s \Bigg\{ \frac{1}{2}\left[\psi_s^2 - \psi_o^2\right] + \frac{1}{2}([\partial_r P]_s)^2 - \frac{1}{2}([\partial_r P]_o)^2 - (\psi_s + [\partial_+ Q]_s)\,[\partial_r P]_s \\
+ & \frac{1}{4}(\gamma_0^{ab})_s\,(2\partial_a P_s\,\partial_b P_s + \partial_a Q_s\,\partial_b Q_s - 4\partial_a Q_s\,\partial_b P_s) - \frac{1}{2}\lim_{r\to 0}\left[\gamma_0^{ab}\partial_a P\,\partial_b P\right] \\
+ & Q_s\left(-[\partial_+^2 Q]_s + [\partial_+\hat{\psi}]_s + [\partial_r^2 P]_s\right) + \frac{J}{\mathcal{H}_s}\left([\partial_\eta\psi]_s + \mathcal{H}_s[\partial_r P]_s + [\partial_r^2 P]_s\right) \\
- & \frac{1}{2}\int_{\eta_{in}}^{\eta_s^{(0)}} d\eta'\,\frac{a(\eta')}{a(\eta_s^{(0)})}\partial_r\left[-\psi^2 + (\partial_r P)^2 + \gamma_0^{ab}\partial_a P\,\partial_b P\right](\eta', \Delta\eta, \tilde{\theta}^a) \\
+ & \frac{1}{2}\int_{\eta_{in}}^{\eta_o} d\eta'\,\frac{a(\eta')}{a(\eta_o)}\partial_r\left[-\psi^2 + (\partial_r P)^2 + \gamma_0^{ab}\partial_a P\,\partial_b P\right](\eta', 0, \tilde{\theta}^a) \\
+ & \int_{\eta_s^{(0)+}}^{\eta_s^{(0)-}} dx\;\partial_+\left[\hat{\psi}\;\partial_+ Q + \frac{1}{4}\hat{\gamma}_0^{ab}\,\partial_a Q\,\partial_b Q\right](\eta_s^{(0)+}, x, \tilde{\theta}^a)\;\Bigg\} \\
+ & \left[\Xi_s^2 - \frac{1}{\mathcal{H}_s\Delta\eta}\left(1 - \frac{\mathcal{H}_s'}{\mathcal{H}_s^2}\right)\right]J^2 - 4\psi_s J + 2\Xi_s\left(\psi_o - \frac{Q_s}{\Delta\eta} + [\partial_r P]_o\right)J + \left(\frac{Q_s}{\Delta\eta}\right)^2 \\
+ & 2\,(\psi_s - \psi_o + [\partial_r P]_s - [\partial_r P]_o)\,\frac{Q_s}{\Delta\eta} + (\gamma_0^{ab})_s\partial_a Q_s\partial_b\left(\frac{Q_s}{2} + \frac{J}{\mathcal{H}_s}\right) - 2\frac{J}{\mathcal{H}_s}[\partial_\eta\psi]_s \\
+ & 2\left(\frac{J}{\mathcal{H}_s} + Q_s\right)[\partial_r\psi]_s - \frac{2}{\Delta\eta}\int_{\eta_s^{(0)+}}^{\eta_s^{(0)-}} dx\;\left[\hat{\psi}\;\partial_+ Q + \frac{1}{4}\hat{\gamma}_0^{ab}\;\partial_a Q\;\partial_b Q\right](\eta_s^{(0)+}, x, \tilde{\theta}^a) \\
+ & \frac{1}{8}\frac{1}{\sin\tilde{\theta}}\frac{\partial}{\partial\tilde{\theta}}\left\{\cos\tilde{\theta}\;\left(\int_{\eta_s^{(0)+}}^{\eta_s^{(0)-}} dx\;[\hat{\gamma}_0^{1b}\;\partial_b Q](\eta_s^{(0)+}, x, \tilde{\theta}^a)\right)^2\right\} \quad ,
\end{aligned} \tag{5.90}$$

$$\begin{aligned}
\mathcal{I}_2 &= 2\Xi_s \left\{ -\frac{1}{4}\left(\phi_s^{(2)} - \phi_o^{(2)}\right) + \frac{1}{4}\left(\psi_s^{(2)} - \psi_o^{(2)}\right) - \frac{1}{2}\int_{\eta_{in}}^{\eta_s^{(0)}} d\eta' \frac{a(\eta')}{a(\eta_s^{(0)})}[\partial_r \phi^{(2)}](\eta', r_s^{(0)}, \tilde{\theta}^a) \right. \\
&+ \left. \frac{1}{2}\int_{\eta_{in}}^{\eta_o} d\eta' \frac{a(\eta')}{a(\eta_o)}[\partial_r \phi^{(2)}](\eta', 0, \tilde{\theta}^a) + \frac{1}{4}\int_{\eta_s^{(0)+}}^{\eta_s^{(0)-}} dx\, \partial_+ \left[\hat{\phi}^{(2)} + \hat{\psi}^{(2)}\right](\eta_s^{(0)+}, x, \tilde{\theta}^a) \right\} \\
&- \psi_s^{(2)} - \frac{2}{\Delta\eta}\int_{\eta_s^{(0)+}}^{\eta_s^{(0)-}} dx \left[\frac{\hat{\phi}^{(2)} + \hat{\psi}^{(2)}}{4}\right](\eta_s^{(0)+}, x, \tilde{\theta}^a) \quad ,
\end{aligned} \tag{5.91}$$

where it is important to stress that all these quantities have their angular dependence expressed in terms of $\tilde{\theta}^a$. One can explicitly check (through a long but straightforward calculation) that Eq. (5.78) is indeed satisfied.

To conclude, using the results of Eqs. (5.89-5.91) in Eq. (5.77) and considering the well-known ensemble average (see e.g. [37,110,111,113]) of $\langle d_L^{-2}\rangle(w_o, z_s)$ for a stochastic spectrum of inhomogeneities, we obtained the full second order contributions of the averaged flux.

5.3.3 Combining light-cone and ensemble average for other observables

Now that we have presented the procedure to combine ensemble average with lightcone average for the quadratic first order terms (Sec. 5.2) and presented also the full calculation of the luminosity flux (Sec. 5.3.1 and 5.3.2), we can address the complete task of computing the stochastic average of the luminosity distance d_L and the distance modulus $\mu \sim 5\log_{10} d_L$. We will also recall the general necessary facts on the flux $\Phi \sim d_L^{-2}$.

Non-trivial effects on the *ensemble* average of d_L, or of a generic function of it, can only originate either from quadratic and higher-order perturbative corrections, or from the spectrum of correlation functions such as $\overline{d_L(z, \widetilde{\theta}^a) d_L(z', \widetilde{\theta}'^a)}$ (see [63]). Here, and as before, we deal with the *ensemble* average of $\langle d_L\rangle$ instead of d_L. As already stressed in Sec. 5.2.2, given the covariant (light-cone) average of a perturbed (inhomogeneous) observable S, the average of a generic function of this observable differs, in general, from the function of its average, i.e. $\overline{\langle F(S)\rangle} \neq F(\overline{\langle S\rangle})$ (as a consequence of the nonlinearity of the averaging process). Expanding the observable to second order as $S = S_0 + S_1 + S_2$, one finds:

$$\overline{\langle F(S)\rangle} = F(S_0) + F'(S_0)\overline{\langle S_1 + S_2\rangle} + F''(S_0)\overline{\langle S_1^2/2\rangle} \quad , \tag{5.92}$$

where in general $\overline{\langle S_1\rangle} \neq 0$ as a consequence of the so-called "induced backreaction" (IBR) terms, arising from the coupling between the inhomogeneity fluctuations of S and those of the integration measure (see Sec. 5.2.2). The overall correction to $\overline{\langle F(S)\rangle}$ thus depends not only on the intrinsic inhomogeneity of the observable S, but also on the covariance properties of the adopted averaging procedure. The Eq. (5.92) implies, in our case, that different functions of the luminosity distance (or of the flux) may be differently affected by the process of averaging out the inhomogeneities, and may require different "subtraction" procedures for an unbiased determination of the relevant observable quantities.

Let us consider, in particular, the lightcone averaged luminosity flux $\langle\Phi\rangle \sim \langle d_L^{-2}\rangle$ computed in Sec. 5.3.1. Performing the stochastic average of Eq. (5.74) (and using Eq. (5.77)) we have:

$$\overline{\langle d_L^{-2}\rangle}(z) = (d_L^{\rm FLRW})^{-2}\,\overline{(I_\Phi(z))^{-1}} \equiv (d_L^{\rm FLRW})^{-2}\left[1 + f_\Phi(z)\right] \quad , \tag{5.93}$$

where:

$$f_\Phi(z) \equiv \overline{\langle \mathcal{I}_1\rangle^2} - \overline{\langle \mathcal{I}_{1,1} + \mathcal{I}_2\rangle} \quad . \tag{5.94}$$

We can now apply the general result of Eq. (5.92) to the flux variable, by setting $S = \Phi$ and consider two important functions of the flux: $F(\Phi) = \Phi^{-1/2} \sim d_L$ and $F(\Phi) = -2.5\log_{10}\Phi + \text{cst} \sim \mu$ (the distance modulus). For the luminosity distance we can introduce a fractional correction f_d, in analogy with Eq. (5.93), such that:

$$\overline{\langle d_L\rangle}(z) = d_L^{\rm FLRW}\left[1 + f_d(z)\right] \quad . \tag{5.95}$$

Then, by using the general expression of Eq. (5.92), we find the important relation :

$$f_d = -\frac{1}{2} f_\Phi + \frac{3}{8} \overline{\langle (\Phi_1/\Phi_0)^2 \rangle} \quad , \tag{5.96}$$

where, in terms of the quantities defined in Eq. (5.76), we have

$$\overline{\langle (\Phi_1/\Phi_0)^2 \rangle} = 4\, \overline{\langle (\bar{\delta}_S^{(1)})^2 \rangle} \quad , \tag{5.97}$$

and where f_Φ is defined by Eq. (5.94). For the distance modulus we obtain, instead,

$$\overline{\langle \mu \rangle} - \mu^{\rm FLRW} = -1.25 (\log_{10} e) \Big[2 f_\Phi - \overline{\langle (\Phi_1/\Phi_0)^2 \rangle} \Big] \quad . \tag{5.98}$$

We can also consider, for any given averaged variable $\langle S \rangle$, the associated dispersion σ_S controlling how broad is the distribution of a perturbed observable S around its mean value $\overline{\langle S \rangle}$. This dispersion is due to both the geometric fluctuations of the averaging surface and to the statistical *ensemble* fluctuations, and is defined in general by (see Eq. (5.39)) :

$$\sigma_S \equiv \sqrt{\overline{\Big\langle \Big(S - \overline{\langle S \rangle} \Big)^2 \Big\rangle}} = \sqrt{\overline{\langle S^2 \rangle} - \Big(\overline{\langle S \rangle} \Big)^2} \quad . \tag{5.99}$$

The dispersion associated with the flux and the distance are thus given by :

$$\sigma_\Phi = \sqrt{\overline{\langle (\Phi/\Phi_0)^2 \rangle} - \Big(\overline{\langle \Phi/\Phi_0 \rangle} \Big)^2} = \sqrt{\overline{\langle (\Phi_1/\Phi_0)^2 \rangle}} \quad , \tag{5.100}$$

$$\sigma_{d_L} = \sqrt{\overline{\Big\langle \big(d_L/d_L^{\rm FLRW} \big)^2 \Big\rangle} - \Big(\overline{\langle d_L/d_L^{\rm FLRW} \rangle} \Big)^2} = \tfrac{1}{2} \sqrt{\overline{\langle (\Phi_1/\Phi_0)^2 \rangle}} \quad , \tag{5.101}$$

while for the distance modulus we find :

$$\sigma_\mu = \sqrt{\overline{\langle \mu^2 \rangle} - \Big(\overline{\langle \mu \rangle} \Big)^2} = 2.5 (\log_{10} e) \sqrt{\overline{\langle (\Phi_1/\Phi_0)^2 \rangle}} \quad . \tag{5.102}$$

The above results will be applied to the case of a realistic background of cosmological perturbations of inflationary origin in the following chapter.

Let us conclude this section by recalling the convenient spectral parametrization, slightly different from Eqs. (5.52) and (5.53), to be used for the various terms contributing to the fractional corrections of our observables. All the relevant contributions to the averaged functions of the luminosity redshift relation, at second order, can be parameterized in the form :

$$\overline{\langle X \rangle} = \int_0^\infty \frac{dk}{k}\, \mathcal{P}_\psi(k, \eta_o)\, \mathcal{C}_X(k, \eta_o, \eta_s^{(0)}) \quad , \tag{5.103}$$

$$\overline{\langle X' \rangle \langle Y' \rangle} = \int_0^\infty \frac{dk}{k}\, \mathcal{P}_\psi(k, \eta_o)\, \mathcal{C}_{X'}(k, \eta_o, \eta_s^{(0)})\, \mathcal{C}_{Y'}(k, \eta_o, \eta_s^{(0)}) \quad , \tag{5.104}$$

valid for any given model of perturbation spectrum. Here, X' and Y' (X) are first (second) order generic functions of $(\eta, r, \widetilde{\theta}^a)$, and the $\mathcal{C}$ are the associated spectral coefficients. In the particularly simple case of a CDM-dominated geometry the spectral distribution of sub-horizon scalar perturbations is time-independent ($\partial_\eta \psi_k = 0$) and, as we shall see later, all the spectral coefficients $\mathcal{C}$ can be calculated analytically. In the more general case where the power spectrum is a function of time, like for a ΛCDM model, the above equations are still satisfied but the spectral coefficients also depend on the power spectrum (usually through time integrals of it, convolved with other functions). We should also stress that when performing numerical calculations the above integration limits will be replaced by appropriate cut-off values determined by the physical range of validity of the considered spectrum.

The next three sections will present the detailed expression of the spectral coefficients for the flux, considerations relative to the genuine second order terms and the proof that vector and tensor perturbations average out under the lightcone average. The reader not interested by these technical considerations can skip this part and follow his/her reading from Chapter 6.

5.3.4 Computation of the $\mathcal{C}(\mathcal{T}_i^{(1,1)})$ spectral coefficients of $\overline{\langle\mathcal{I}_{1,1}\rangle}$

We give here the result for the $\mathcal{C}(\mathcal{T}_i^{(1,1)})$ spectral coefficients of $\overline{\langle\mathcal{I}_{1,1}\rangle}$ computed in the CDM case, using the notations $l = k\Delta\eta$ and $\mathrm{Sinc}(l) = \sin(l)/l$, and enclosing in a box the leading contributions.

$$
\begin{aligned}
\mathcal{C}(\mathcal{T}_1^{(1,1)}) &= 0 \quad , \quad \mathcal{C}(\mathcal{T}_2^{(1,1)}) = \boxed{\Xi_s \frac{f_s^2 - f_o^2}{\Delta\eta^2}\frac{l^2}{3}} \quad , \quad \mathcal{C}(\mathcal{T}_3^{(1,1)}) = 0 \ , \\
\mathcal{C}(\mathcal{T}_4^{(1,1)}) &= \boxed{2\Xi_s \frac{f_s^2}{\Delta\eta^2}\frac{l^2}{3}} + \frac{4\Xi_s}{3l^2}\left\{2 - 3l^2 + (l^2-2)\cos(l) + l\sin(l) + l^3\mathrm{SinInt}(l)\right\} \\
&\qquad + 4\Xi_s \frac{f_s}{\Delta\eta}\left(\cos l - 2 + \mathrm{Sinc}(l) + l\mathrm{SinInt}(l)\right) \ , \\
\mathcal{C}(\mathcal{T}_5^{(1,1)}) &= \boxed{-2\Xi_s \frac{f_o^2}{\Delta\eta^2}\frac{l^2}{3}} \quad , \quad \mathcal{C}(\mathcal{T}_6^{(1,1)}) = 4\Xi_s[1 - \mathrm{Sinc}(l)] - 4\Xi_s \frac{f_s}{\Delta\eta}\left(\cos(l) - \mathrm{Sinc}(l)\right) \ , \\
\mathcal{C}(\mathcal{T}_7^{(1,1)}) &= -\frac{2\Xi_s}{3}\left\{\boxed{\frac{f_s^2}{\Delta\eta^2}l^2} - 3\frac{f_s}{\Delta\eta}(\cos(l) - \mathrm{Sinc}(l)) - \frac{f_s}{\Delta\eta}\frac{2}{\mathcal{H}_0\Delta\eta}[2\cos(l) + (l^2-2)\mathrm{Sinc}(l)]\right\} \ , \\
\mathcal{C}(\mathcal{T}_8^{(1,1)}) &= \frac{2\Xi_s}{\mathcal{H}_s}\frac{f_s}{3\mathcal{H}_0\Delta\eta^3}\left\{\boxed{\mathcal{H}_0\Delta\eta\ l^2} + 2[-3\mathcal{H}_0\Delta\eta + (l^2-6)]\cos(l) - 3(2+\mathcal{H}_0\Delta\eta)(-2+l^2)\mathrm{Sinc}(l)\right\} \ , \\
\mathcal{C}(\mathcal{T}_9^{(1,1)}) &= 0 \ , \ \mathcal{C}(\mathcal{T}_{10}^{(1,1)}) = 0 \ , \\
\mathcal{C}(\mathcal{T}_{11}^{(1,1)}) &= 8\Xi_s\left\{\frac{1}{2} - \frac{1}{3l^2} + \left[\frac{1}{3l^2} - \frac{1}{6}\right]\cos(l) - \frac{1}{6}\mathrm{Sinc}(l) - \frac{l}{6}\mathrm{SinInt}(l)\right\} \ , \\
\mathcal{C}(\mathcal{T}_{12}^{(1,1)}) &= \left[\Xi_s^2 - \frac{1}{\mathcal{H}_s\Delta\eta}\left(1 - \frac{\mathcal{H}_s'}{\mathcal{H}_s^2}\right)\right]\left\{2\ [1 - \mathrm{Sinc}(l)] + 2\frac{f_o - f_s}{\Delta\eta}[cos(l) - \mathrm{Sinc}(l)]\right. \\
&\qquad \left. + \boxed{\frac{f_o^2 + f_s^2}{\Delta\eta^2}\frac{l^2}{3}} - \frac{2f_of_s}{\Delta\eta^2}[2\cos(l) + (l^2-2)\mathrm{Sinc}(l)]\right\} \ , \\
\mathcal{C}(\mathcal{T}_{13}^{(1,1)}) &= 4\left\{1 - \mathrm{Sinc}(l) + \frac{f_o}{\Delta\eta}[cos(l) - \mathrm{Sinc}(l)]\right\} \ , \\
\mathcal{C}(\mathcal{T}_{14}^{(1,1)}) &= 2\Xi_s\left\{\frac{f_o - f_s}{\Delta\eta}(\cos l - \mathrm{Sinc}(l))\right. \\
&\qquad \left. + \boxed{\frac{f_o^2}{3\Delta\eta^2}l^2} - \frac{f_of_s}{\Delta\eta^2}\left(2\cos(l) + (l^2-2)\mathrm{Sinc}(l)\right) + \left(1 + 2\frac{f_o + f_s}{\Delta\eta}\right)(1 - \mathrm{Sinc}(l))\right\} \ , \\
\mathcal{C}(\mathcal{T}_{15}^{(1,1)}) &= 4\ \Xi_s\frac{f_o + f_s}{\Delta\eta}\{1 - \mathrm{Sinc}(l)\} - \frac{8}{l}\mathrm{SinInt}(l) \ , \\
\mathcal{C}(\mathcal{T}_{16}^{(1,1)}) &= \frac{8}{l}\mathrm{SinInt}(l) \ , \ \mathcal{C}(\mathcal{T}_{17}^{(1,1)}) = \frac{8}{l^2}\{-1 + \cos(l) + l\ \mathrm{SinInt}(l)\} \ , \\
\mathcal{C}(\mathcal{T}_{18}^{(1,1)}) &= -\frac{2}{\mathcal{H}_s\Delta\eta}\left\{2 - \cos(l) - \mathrm{Sinc}(l) - l\ \mathrm{SinInt}(l)\right. \\
&\qquad \left. + \frac{2f_s}{\Delta\eta}\left(1 + \boxed{\frac{l^2}{3}} - \cos(l) - l\ \mathrm{SinInt}(l)\right) + \frac{2f_o}{\Delta\eta}[1 - \mathrm{Sinc}(l)]\right\} \ , \\
\mathcal{C}(\mathcal{T}_{19}^{(1,1)}) &= \frac{4}{3l^2}\left\{2 - 3l^2 + (l^2-2)\cos(l) + l\sin(l) + l^3\mathrm{SinInt}(l)\right\} \ , \\
\mathcal{C}(\mathcal{T}_{20}^{(1,1)}) &= -\frac{2}{\mathcal{H}_s\Delta\eta}\left\{-\cos(l) + \mathrm{Sinc}(l) + \boxed{\frac{f_s}{3\Delta\eta}l^2} - \frac{f_o}{\Delta\eta}[2\cos(l) + (l^2-2)\mathrm{Sinc}(l)]\right\} \ , \\
\mathcal{C}(\mathcal{T}_{21}^{(1,1)}) &= 4\ [1 - \mathrm{Sinc}(l)] \ , \\
\mathcal{C}(\mathcal{T}_{22}^{(1,1)}) &= -4 + \frac{4}{3l^2}\left[-2(2+3l^2) + (4+l^2)\cos(l) + l\sin(l) + l(6+l^2)\mathrm{SinInt}(l)\right] \ , \\
\mathcal{C}(\mathcal{T}_{23}^{(1,1)}) &= 0 \ . \qquad (5.105)
\end{aligned}
$$

5.3.5 Dynamical evolution of scalar perturbations up to second-order

For a full computation of the fractional correction f_Φ, what we need is the combined angular and ensemble averages of the three basic quantities, $\mathcal{I}_1$, $\mathcal{I}_{1,1}$ and $\mathcal{I}_2$. We must evaluate, in particular, the spectral coefficients $\mathcal{C}(\mathcal{T}_i^{(1)})$, $\mathcal{C}(\mathcal{T}_i^{(1,1)})$ and $\mathcal{C}(\mathcal{T}_i^{(2)})$, related to the terms of Eqs. (5.82-5.84) in terms of the first and second-order Bardeen potentials. For this we need to know the dynamical evolution of the scalar fluctuations, at first order for the computation of $\mathcal{I}_1$, $\mathcal{I}_{1,1}$ and at second order for $\mathcal{I}_2$.

Let us consider, first of all, a general model with cosmological constant and dust sources. For the evolution of the scalar degrees of freedom in the Poisson gauge we will follow the analysis performed, up to second order, in [104]. In a general ΛCDM model the linear scalar perturbation obeys the evolution equation :

$$\psi'' + 3\mathcal{H}\psi' + \left(2\mathcal{H}' + \mathcal{H}^2\right)\psi = 0 \quad . \tag{5.106}$$

Considering only the growing mode solution we can set

$$\psi(\eta, \vec{x}) = \frac{g(\eta)}{g(\eta_o)}\psi_o(\vec{x}) \quad , \tag{5.107}$$

where $g(\eta)$ is the so-called "growth-suppression factor", or – more precisely – the least decaying mode solution, and ψ_o is the present value of the gravitational potential. This "growth factor" can be expressed analytically in terms of elliptic functions [114] (see also [8]), and it is well approximated by a simple function of the critical-density parameters of non-relativistic matter Ω_m and cosmological constant Ω_Λ :

$$g(z) = \frac{5\,\Omega_m(z)/2}{\Omega_m(z)^{4/7} - \Omega_\Lambda(z) + (1+\Omega_m(z)/2)(1+\Omega_\Lambda(z)/70)}g_\infty \quad . \tag{5.108}$$

Here g_∞ represents the value of $g(\eta)$ at early enough times when the cosmological constant was negligible, and is fixed by the condition $g(\eta_o) = g(z=0) = 1$.

The second-order potentials obey a similar evolution equation containing, however, an appropriate source term. Their final expression in terms of ψ_o has been given in [104] and reads :

$$\begin{aligned}
\psi^{(2)}(\eta) &= \left(B_1(\eta) - 2g(\eta)g_\infty - \frac{10}{3}(a_{\rm nl}-1)g(\eta)g_\infty\right)\psi_o^2 + \left(B_2(\eta) - \frac{4}{3}g(\eta)g_\infty\right)\mathcal{O}^{ij}\partial_j\psi_o\partial_i\psi_o \\
&\quad + B_3(\eta)\,\mathcal{O}_3^{ij}\partial_j\psi_o\partial_i\psi_o + B_4(\eta)\,\mathcal{O}_4^{ij}\partial_j\psi_o\partial_i\psi_o \quad , \qquad (5.109)\\
\phi^{(2)}(\eta) &= \left(B_1(\eta) + 4g^2(\eta) - 2g(\eta)g_\infty - \frac{10}{3}(a_{\rm nl}-1)g(\eta)g_\infty\right)\psi_o^2 \\
&\quad + \left(B_2(\eta) + \frac{4}{3}g^2(\eta)\left(e(\eta)+\frac{3}{2}\right) - \frac{4}{3}g(\eta)g_\infty\right)\mathcal{O}^{ij}\partial_j\psi_o\partial_i\psi_o \\
&\quad + B_3(\eta)\,\mathcal{O}_3^{ij}\partial_j\psi_o\partial_i\psi_o + B_4(\eta)\,\mathcal{O}_4^{ij}\partial_j\psi_o\partial_i\psi_o \quad , \qquad (5.110)
\end{aligned}$$

where

$$\mathcal{O}^{ij} = \nabla^{-2}\left(\delta^{ij} - 3\frac{\partial^i\partial^j}{\nabla^2}\right) \quad , \quad \mathcal{O}_3^{ij} = \frac{\partial^i\partial^j}{\nabla^2} \quad , \quad \mathcal{O}_4^{ij} = \delta^{ij} \quad . \tag{5.111}$$

We have introduced the functions $B_A(\eta) = \mathcal{H}_o^{-2}\left[l(\eta_o) + 3\Omega_m(\eta_o)/2\right]^{-1}\tilde{B}_A(\eta)$, with $A = 1,2,3,4$, and the following definitions :

$$\tilde{B}_1(\eta) = \int_{\eta_m}^{\eta} d\tilde{\eta}\,\mathcal{H}^2(\tilde{\eta})(l(\tilde{\eta})-1)^2 C(\eta,\tilde{\eta}) \quad , \tag{5.112}$$

$$\tilde{B}_2(\eta) = 2\int_{\eta_m}^{\eta} d\tilde{\eta}\,\mathcal{H}^2(\tilde{\eta})\Big[2(l(\tilde{\eta})-1)^2 - 3 + 3\Omega_m(\tilde{\eta})\Big]C(\eta,\tilde{\eta}) \quad , \tag{5.113}$$

$$\tilde{B}_3(\eta) = \tfrac{4}{3}\int_{\eta_m}^{\eta} d\tilde{\eta}\left(e(\tilde{\eta}) + \tfrac{3}{2}\right)C(\eta,\tilde{\eta}) \quad , \quad \tilde{B}_4(\eta) = -\int_{\eta_m}^{\eta} d\tilde{\eta}\,C(\eta,\tilde{\eta}) \quad , \tag{5.114}$$

and with

$$C(\eta,\tilde{\eta}) = g^2(\tilde{\eta})\frac{a(\tilde{\eta})}{a(\eta_o)}\left[g(\eta)\mathcal{H}(\tilde{\eta}) - g(\tilde{\eta})\frac{a^2(\tilde{\eta})}{a^2(\eta)}\mathcal{H}(\eta)\right] \quad , \quad e(\eta) = \frac{l^2(\eta)}{\Omega_m(\eta)} \quad , \quad l(\eta) = 1 + \frac{g'}{\mathcal{H}g} \quad . \tag{5.115}$$

Here η_m denotes the time when full matter domination starts [104]. Its precise value is irrelevant since the region of integration around η_m is strongly suppressed. Finally, $a_{\rm nl}$ is the so-called non-gaussianity parameter (see [104]), which approaches unity in the standard inflationary scenario.

For further use let us now evaluate the ensemble (and angular/light-cone) average of the different operators defined in Eq. (5.111), when applied to $\partial_i\psi_o\partial_j\psi_o$. Considering first the ensemble average of $\mathcal{O}^{ij}\partial_i\psi_o\partial_j\psi_o$, and Fourier-expanding ψ_o, we get (see [115]) :

$$\overline{\mathcal{O}^{ij}\partial_i\psi_o\partial_j\psi_o} = \int \frac{d^3q\ d^3k}{(2\pi)^3}\delta^{(3)}(\mathbf{q})e^{ir\mathbf{q}\cdot\hat{\mathbf{x}}}\ \psi_{|\mathbf{k}|}\psi^*_{|\mathbf{k}-\mathbf{q}|}\left[-\frac{2(\mathbf{k}\cdot\mathbf{q})+|\mathbf{k}|^2}{|\mathbf{q}|^2}+3\frac{(\mathbf{k}\cdot\mathbf{q})^2}{|\mathbf{q}|^4}\right] \quad . \tag{5.116}$$

From this point, and up to the end of this section, we will neglect all suffixes "o" present in terms inside the integrals. By using the Taylor expansion of $\psi^*_{|\mathbf{k}-\mathbf{q}|}$ around $\mathbf{q}=\vec{0}$ we have :

$$\psi^*_{|\mathbf{k}-\mathbf{q}|} \simeq \psi^*_k - \frac{\mathbf{k}\cdot\mathbf{q}}{k}\partial_k\psi^*_k + \frac{1}{2}\left\{\left(\frac{q^2}{k}-\frac{(\mathbf{k}\cdot\mathbf{q})^2}{k^3}\right)\partial_k\psi^*_k + \frac{(\mathbf{k}\cdot\mathbf{q})^2}{k^2}\partial_k^2\psi^*_k\right\} + \mathcal{O}(q^3) \quad , \tag{5.117}$$

where $k\equiv|\mathbf{k}|$, $q\equiv|\mathbf{q}|$, and where the latter terms have been obtained by using the Hessian matrix :

$$H^{ij} = \partial_{k_i}\partial_{k_j}\psi^*_k = \partial_{k_i}\left[\frac{k^j}{k}\partial_k\psi^*_k\right] \quad . \tag{5.118}$$

Combining the last two results, writing the integral over k as $\int_0^\infty 2\pi k^2 dk \int_{-1}^{+1} d\cos\alpha\,(...)$, where $\mathbf{k}\cdot\mathbf{q} = kq\cos\alpha$, and integrating over $\cos\alpha$, we obtain :

$$\overline{\mathcal{O}^{ij}\partial_i\psi_o\partial_j\psi_o} = \int \frac{d^3q}{(2\pi)^3}\delta^{(3)}(\mathbf{q})e^{ir\mathbf{q}\cdot\hat{\mathbf{x}}}\int_0^\infty 2\pi k^2 dk\ \left[\frac{16k}{15}\ \psi_k\partial_k\psi^*_k + \frac{4k^2}{15}\ \psi_k\partial_k^2\psi^*_k\right] \quad . \tag{5.119}$$

Note that the integrand's dependence on the angle θ between $\mathbf{x}$ and $\mathbf{q}$ only arises from the exponential term $\exp(ir\mathbf{q}\cdot\hat{\mathbf{x}})$, which disappears in the presence of $\delta^{(3)}(\mathbf{q})$. As a consequence, the angular average has no impact on this particular term and we get :

$$\overline{\langle\mathcal{O}^{ij}\partial_i\psi_o\partial_j\psi_o\rangle} = \overline{\mathcal{O}^{ij}\partial_i\psi_o\partial_j\psi_o} = \int_0^\infty dk\frac{k^2}{2\pi^2}\ \left[\frac{8k}{15}\ \psi_k\partial_k\psi^*_k + \frac{2k^2}{15}\ \psi_k\partial_k^2\psi^*_k\right] \quad . \tag{5.120}$$

Let us note also that, quite generally, $\partial_k\psi_k \sim \psi_k/k$, and thus the above term is of the same order as $\overline{\langle\psi_o\psi_o\rangle}$.

By repeating exactly the same procedure for the $\mathcal{O}_3^{ij}\partial_i\psi_o\partial_j\psi_o$ term, we find :

$$\overline{\mathcal{O}_3^{ij}\partial_i\psi_o\partial_j\psi_o} = \int \frac{d^3q}{(2\pi)^3}\delta^{(3)}(\mathbf{q})e^{ir\mathbf{q}\cdot\hat{\mathbf{x}}}\int_0^\infty 4\pi k^2 dk\ \left[\frac{k^2}{3}|\psi_k|^2 + \frac{kq^2}{5}\ \psi_k\partial_k\psi^*_k + \frac{k^2q^2}{20}\ \psi_k\partial_k^2\psi^*_k\right] , \tag{5.121}$$

where the last two contributions are vanishing because of the q-integration. We are thus left with the following simple result (insensitive to the angular average, as before) :

$$\overline{\left\langle\mathcal{O}_3^{ij}\partial_i\psi_o\partial_j\psi_o\right\rangle} = \overline{\mathcal{O}_3^{ij}\partial_i\psi_o\partial_j\psi_o} = \int_0^\infty \frac{dk}{k}\ \left[\frac{k^2}{3}\mathcal{P}_\psi(k,\eta_o)\right] \quad . \tag{5.122}$$

Finally, the last term $\mathcal{O}_4^{ij}\partial_i\psi_o\partial_j\psi_o = |\vec{\nabla}\psi_o|^2$ is trivial and gives

$$\overline{\left\langle\mathcal{O}_4^{ij}\partial_i\psi_o\partial_j\psi_0\right\rangle} = \overline{\mathcal{O}_4^{ij}\partial_i\psi_o\partial_j\psi_o} = \int_0^\infty \frac{dk}{k}\ \left[k^2\mathcal{P}_\psi(k,\eta_o)\right] \quad . \tag{5.123}$$

5.3.6 Second-order vector and tensor perturbations

We have stressed in Chapter 4 that vector and tensor perturbations automatically appear, at second order, as sourced by the squared first-order perturbation terms. Hence, vector and tensor perturbations must be included in a consistent second-order computation of the luminosity distance, even if their contributions are negligible at first order (as expected, in particular, for a background of super-horizon perturbations generated by a phase of slow-roll inflation).

Working in the Poisson gauge, and moving to spherical coordinates $x^i = (r, \theta, \phi)$, the PG metric of Eq. (4.24), implying Eq. (4.25), is:

$$ds^2_{PG} = a^2 \left[-d\eta^2 + 2v_i\, d\eta dx^i\right] + a^2 \left[(\gamma_0)_{ij} + \chi_{ij}\right] dx^i dx^j \quad , \tag{5.124}$$

where $\gamma_0^{ij} = \mathrm{diag}(1, r^{-2}, r^{-2}\sin^{-2}\theta)$, and where v^i and χ^{ij} are the vector and tensor perturbations written in spherical polar coordinates. They satisfy the conditions $\nabla_i v^i = 0 = \nabla_i \chi^{ij}$ and $\gamma_0^{ij}\chi_{ij} = 0$, where ∇_i is the covariant gradient of the 3-dimensional Euclidean space in spherical coordinates.

Following the same procedure as in the scalar case we can evaluate the vector and tensor contributions to the coordinate transformation connecting Poisson and GLC gauge, and then express the perturbed GLC metric, up to second order, including the vector and tensor variables v^i and χ^{ij}. Such a detailed computation has already been performed in Sec. 4.1.3. We recall here the vector and tensor contributions to the coordinate transformation between θ and $\widetilde{\theta}$:

$$\begin{aligned} \tilde{\theta}^a &= \tilde{\theta}^{a(0)} + \tilde{\theta}^{a(2)} \\ &= \theta^a + \frac{1}{2}\int_{\eta_+}^{\eta_-} dx \left(\hat{v}^a - \hat{\chi}^{ra} + \hat{\gamma}_0^{ab}\int_{\eta_+}^{x} dy\; \partial_b \hat{\alpha}^r(\eta_+, y, \theta^a)\right)(\eta_+, x, \theta^a) \quad , \end{aligned} \tag{5.125}$$

and to the 2×2 matrix γ^{ab} appearing in the GLC metric:

$$\begin{aligned} a(\eta)^2\gamma^{ab} &= \gamma_0^{ab} - \chi^{ab} + \\ &+ \left[\frac{\gamma_0^{ac}}{2}\int_{\eta_+}^{\eta_-} dx\; \partial_c \left(\hat{v}^b - \hat{\chi}^{rb} + \hat{\gamma}_0^{bd}\int_{\eta_+}^{x} dy\; \partial_d \hat{\alpha}^r(\eta_+, y, \theta^a)\right)(\eta_+, x, \theta^a) + (a \leftrightarrow b)\right] \quad , \end{aligned} \tag{5.126}$$

where $\alpha^r \equiv (v^r/2) - (\chi^{rr}/4)$. Both results are needed, in fact, for the computation of the averaged flux as presented in Eq. (5.74).

If we take into account v^i and χ^{ij} and compute d_L, we find that the right-hand side of Eq. (5.76) has to be modified by the addition of $\delta^{(2)}_{V,T}(z_s, \widetilde{\theta}^a)$ as presented in Eq. (4.79), representing the effect of the vector and tensor part of the perturbed geometry. In fact it turns out that no modification is induced on the corresponding equation for $I_\phi(z_s)$ controlling the light-cone average of $\langle d_L^{-2}\rangle$, so that Eq. (5.77) holds even in the presence of vector and tensor perturbations. The sought average, in fact, is proportional to the proper area of the deformed 2-sphere $\Sigma(w_o, z_s)$, and is given by $I_\phi \sim \int d^2\widetilde{\theta}\sqrt{\gamma}$ (see Eq. (5.74)). Considering the vector and tensor contributions to $\gamma^{-1} = \det\gamma^{ab}$ (obtained from Eq. (5.126)), and computing from Eq. (5.125) the Jacobian determinant $|\partial\widetilde{\theta}/\partial\theta|$, we can express I_ϕ as an angular integral over the 2-sphere with unperturbed measure $d^2\Omega = \sin\theta d\theta d\phi$. In that case many terms cancel among each other, and we end up with the result:

$$I_\phi(w_o, z_s) - 1 = \frac{1}{4\pi}\int_0^\pi \sin\theta d\theta \int_0^{2\pi} d\phi\, f(\eta, r, \theta, \phi), \tag{5.127}$$

where the integrand $f(\eta, r, \theta, \phi)$ is a simple expression proportional to the components of the vector and tensor perturbations.

The above angular integrals are all identically vanishing, as we can check by expanding the perturbations in Fourier modes $v^i_{\mathbf{k}}$ and $\chi^{ij}_{\mathbf{k}}$. For each mode $\mathbf{k}$ we can choose, without loss of generality, the x^3 axis of our coordinate system aligned along the direction of $\mathbf{k}$. Considering, for instance, tensor perturbations, we can then write the most general perturbed line-element, in Cartesian coordinates (omitting, for simplicity, the Fourier index), as follows:

$$h_{ij}dx^i dx^j = h_+(\eta, x^3)(dx^1dx^1 - dx^2dx^2) + 2h_\times(\eta, x^3)dx^1dx^2 \quad . \tag{5.128}$$

We have called h_+ and $h_\times$, as usual, the two independent polarization modes. After transforming to spherical coordinates, using the standard definitions

$$x^1 = r\sin\theta\cos\phi \quad , \quad x^2 = r\sin\theta\sin\phi \quad , \quad x^3 = r\cos\theta \quad , \tag{5.129}$$

we easily obtain :

$$\begin{aligned}
\chi^{rr} &= \sin^2\theta\,(h_+\cos 2\phi + h_\times\sin 2\phi) \quad , \quad \chi^{r\theta} = \frac{\sin 2\theta}{2r}\,(h_+\cos 2\phi + h_\times\sin 2\phi) \quad , \\
\chi^{r\phi} &= \frac{1}{r}\,(-h_+\sin 2\phi + h_\times\cos 2\phi) \quad , \quad \chi^{\theta\theta} = \frac{\cos^2\theta}{r^2}\,(h_+\cos 2\phi + h_\times\sin 2\phi) \quad , \\
\chi^{\theta\phi} &= \frac{\cos\theta}{r^2\sin\theta}\,(-h_+\sin 2\phi + h_\times\cos 2\phi) \quad , \quad \chi^{\phi\phi} = -\frac{1}{r^2\sin^2\theta}\,(h_+\cos 2\phi + h_\times\sin 2\phi) \quad .
\end{aligned} \tag{5.130}$$

Since $h_+ = h_+(\eta, r\cos\theta)$ and $h_\times = h_\times(\eta, r\cos\theta)$, all perturbation components depend on ϕ only through $\cos 2\phi$ or $\sin 2\phi$, so that their contribution averages to zero when inserted into Eq. (5.127). The same is true for the case of vector perturbations, with the only difference that the ϕ dependence of v^i, in spherical coordinates, goes through $\cos\phi$ or $\sin\phi$ (corresponding to waves of helicity one instead of helicity two as in the tensor case). Also the vector contribution thus averages to zero when inserted into Eq. (5.127).

Chapter 6

Effect of inhomogeneities on cosmological observables

We now present the final results of this thesis. We first address the incomplete stage of quadratic first order terms. We see that it allows a rough estimation of the size of the effect of inhomogeneities, giving a rigorous prediction for the dispersion but leaving open the question of the average itself. We also explain why the computed effects are infrared and ultraviolet convergent, showing the robustness of our approach. We then turn our attention to the full calculation and use the power spectrum in its non-linear regime, and with a proper transfer function. We finally compute the full effect of inhomogeneities from second order perturbations, explaining the approximations made in the process to circumvent the problems of numerical calculations.

6.1 Induced backreaction in CDM and IR & UV convergence

6.1.1 The linear power spectrum of the CDM case

In order to perform the numerical computations that we intend to do, we need to insert the explicit form of the power spectrum. Limiting ourselves to sub-horizon perturbations in a CDM model, we can obtain this spectrum by applying an appropriate, time-independent, transfer function to the primordial (inflationary) spectral distribution (see e.g. [108]). The power spectrum is then given by Eq. (1.60) :

$$\mathcal{P}_\psi(k) = \left(\frac{3}{5}\right)^2 \Delta^2_{\mathcal{R}} T^2(k) \quad , \quad \Delta^2_{\mathcal{R}} = A \left(\frac{k}{k_0}\right)^{n_s-1} \quad , \tag{6.1}$$

where $T(k)$ is the transfer function which takes into account the sub-horizon evolution of the modes re-entering during the radiation-dominated era, and $\Delta^2_{\mathcal{R}}$ is the primordial power spectrum of curvature perturbations outside the horizon. The typical parameters of such a spectrum, namely the amplitude A, the spectral index n_s and the scale k_0, are determined by the results of recent WMAP observations [109]. In our computations we will use, in particular, the following approximate values :

$$A = 2.41 \times 10^{-9} \quad , \quad n_s = 0.96 \quad , \quad k_0 = 0.002\,\mathrm{Mpc}^{-1} \quad . \tag{6.2}$$

Finally, since our main purpose here is to present an illustrative example, it will be enough for our needs to approximate $T(k)$ by the effective shape of the transfer function for density perturbations without baryons, namely $T(k) = T_0(k)$, where [68]:

$$T_0(q) = \frac{L_0}{L_0 + q^2 C_0(q)} \quad , \quad L_0(q) = \ln(2e + 1.8q) \quad , \quad C_0(q) = 14.2 + \frac{731}{1 + 62.5q} \quad , \quad q = \frac{k}{13.41 k_{\mathrm{eq}}} \quad , \tag{6.3}$$

and where $k_{\mathrm{eq}} \simeq 0.07\,\Omega_{m0}\ h^2\mathrm{Mpc}^{-1}$ is the scale corresponding to matter-radiation equality, with $h \equiv H_0/(100\,\mathrm{km\,s^{-1}Mpc^{-1}})$. We can easily check that the above transfer function goes to 1 for $k \ll k_{\mathrm{eq}}$, while it falls like $k^{-2}(\log k)$ for $k \gg k_{\mathrm{eq}}$. For the numerical estimates we will use $h = 0.7$ and

we will set $a_o = 1$, $\Omega_m = 1$. In that case we obtain $k_{\rm eq} \simeq 0.036\,{\rm Mpc}^{-1}$ (see [68]), and we can more precisely define the asymptotic regimes of our transfer function as $T_0 \simeq 1$ for $k \lesssim 10^{-3}\,{\rm Mpc}^{-1}$, and $T_0 \sim k^{-2}(\log k)$ for $k \gtrsim 2.5\,{\rm Mpc}^{-1}$. This second scale is already deep inside the so-called non-linear regime, roughly corresponding to $k \gtrsim 0.1\,h\,{\rm Mpc}^{-1}$ (see e.g. [116]). Further information on the transfer function is given in the Appendix sections A.2.4 and A.4.2.

6.1.2 Dominant contributions in induced backreaction terms and convergence

Let us start by comparing the behaviour of the power spectrum with the behaviour of the coefficients in Tables 5.1 and 5.2. As shown in Table 5.1, all the coefficients $\mathcal{C}_{ij}$ and $\mathcal{C}_i\mathcal{C}_j$ will go at most as $\mathcal{O}(1)$ while their combination $\mathcal{C}_{ij} - \mathcal{C}_i\mathcal{C}_j$ will vanish at least as $\mathcal{O}(k^2\Delta\eta^2)$ in the infrared (IR) limit $k\Delta\eta \ll 1$. On the other hand the power spectrum is almost constant in this limit ($\mathcal{P}_\psi(k) \sim k^{n_s-1} \simeq k^{-0.04}$). As a consequence, the infrared part of the terms in the induced backreaction ${\rm IBR}_2$ and in the dispersion $\overline{\langle\sigma_1^2\rangle}$ will give a subleading contribution, and we can safely fix our infrared cut-off to be $k = H_0$ – i.e. we can limit ourselves to all the sub-horizon modes – without affecting the final result.

Furthermore, as can be seen in Tables 5.1 and 5.2, all the coefficients $\mathcal{C}_{ij}$ and $\mathcal{C}_i\mathcal{C}_j$ will go at most as $\mathcal{O}(k^3\Delta\eta^3)$ in the ultraviolet (UV) limit $k\Delta\eta \gg 1$. As a consequence, all the integrals involved in the induced backreaction and in the dispersion will be UV-convergent and their main contribution will come from the range $1/\Delta\eta \ll k \lesssim 2.5\,{\rm Mpc}^{-1}$. In this range, some of the backreaction coefficients grow as positive power of k while the transfer function is not yet decreasing as $k^{-2}(\log k)$. In particular, there are only two leading contributions corresponding to the integrals controlled by the coefficients : $\mathcal{C}_{44}$ and $\mathcal{C}_{55}$. This is the reason why the dispersion of the angular average of d_L, Eq. (5.43), is smaller than the one of d_L itself, Eq. (5.41). For such coefficients we have in fact the following behaviour at $k\Delta\eta \gg 1$:

$$\mathcal{C}_{44} \simeq \left(1 - \frac{1}{\mathcal{H}_s\Delta\eta}\right)^2 \frac{(f_0^2 + f_s^2)}{\Delta\eta^2}\frac{k^2\Delta\eta^2}{3} \quad , \tag{6.4}$$

$$\mathcal{C}_{55} \simeq \frac{k^3\Delta\eta^3}{15}{\rm SinInt}(k\Delta\eta) \quad . \tag{6.5}$$

From the above expressions it is easy to understand that $\overline{\langle A_4A_4\rangle}$ will give the largest contribution for $z_s \ll 1$ while $\overline{\langle A_5A_5\rangle}$ will give the largest contribution for $z_s \gg 1$ (see Fig. 6.1).

It is also clear that both the induced backreaction ${\rm IBR}_2$ and the dispersion depend in principle on the UV cut-off k_{UV} eventually used to evaluate the integrals. On the other hand, when k_{UV} is taken inside the regime where the spectrum goes like $k^{-4}(\log k)^2$, the dependence on the cut-off is not too strong. In particular the leading contribution to ${\rm IBR}_2$, given by $2\overline{\langle A_4A_4\rangle}$, depends very weakly on the particular value of k_{UV}. The leading contribution to the dispersion of Eq. (5.55), controlled by $\overline{\langle A_5A_5\rangle}$, has a somewhat stronger dependence on k_{UV} (because of the extra power of k in the integrand of $\overline{\langle A_5A_5\rangle}$). The numerical integrations of $\overline{\langle A_4A_4\rangle}$ and $\overline{\langle A_5A_5\rangle}$ are presented in Fig. 6.1, where we illustrate the magnitude of the backreaction effects as a function of the redshift (in the range of values relevant to supernovae observations), and as a function of its dependence on the cut-off (ranging from $k_{UV} = 0.1\,{\rm Mpc}^{-1}$ to $k_{UV} = +\infty$). We should emphasize that the two abovementioned contributions have a clear and distinct physical meaning in the Newtonian gauge. Going back to their explicit expressions it appears that $\overline{\langle A_4A_4\rangle}$ represents the Doppler effect while $\overline{\langle A_5A_5\rangle}$ is associated with lensing, both in qualitative agreement with previous claims in the literature [63, 90]. Note that the latter term can only appear in the variance, because it contributes to $\overline{\langle\sigma_1^2\rangle}$, while $\overline{\langle A_4A_4\rangle}$ appears also in ${\rm IBR}_2$ since A_4 is present in both μ_1 and σ_1. In the left panel of Fig. 6.1 we have also plotted the corrected leading contribution of ${\rm IBR}_2$, namely $\overline{\langle A_4A_4\rangle} - \overline{\langle A_4\rangle\langle A_4\rangle}$ (see Eq. (5.54)) : we can see that the difference from the behavior of the $\overline{\langle A_4A_4\rangle}$ term is very small, with no qualitative effect on our discussion.

It is important to stress that, although all considered backreaction contributions are (at any redshift) UV-finite, they can induce relatively big effects at the distance scales relevant for supernovae observations, provided the given spectrum is extrapolated to sufficiently large values of k. We also

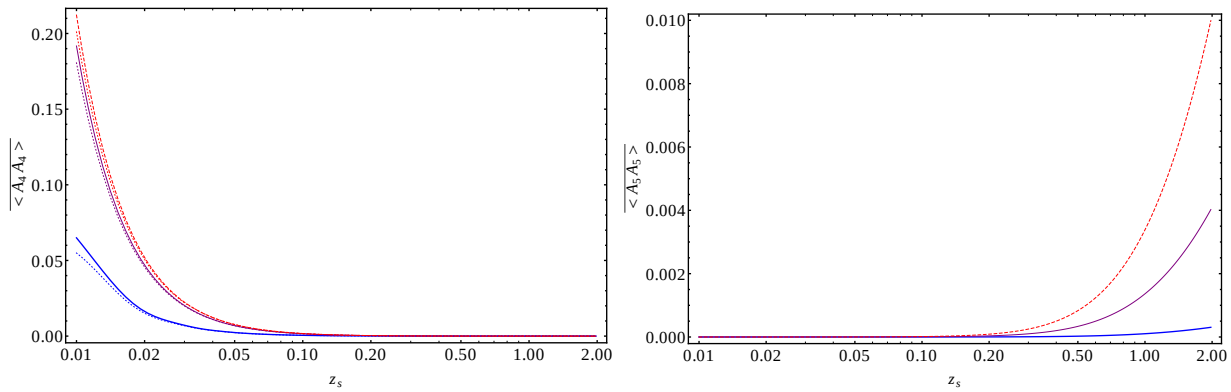

Figure 6.1: The result of the numerical integration of Eq. (5.52) for $\overline{\langle A_4 A_4\rangle}$ (*Left*) and $\overline{\langle A_5 A_5\rangle}$ (*Right*) is plotted as a function of z_s for three different values of the UV cut-off: $k = 0.1\,\mathrm{Mpc}^{-1}$ (thick blue line), $k = 1\,\mathrm{Mpc}^{-1}$ (thin purple line), $k = +\infty$ (dashed red line). *Left:* Also shown (by the corresponding dotted curves) is the plot of the IBR_2 contribution $\overline{\langle A_4 A_4\rangle} - \overline{\langle A_4\rangle\langle A_4\rangle}$.

stress that the decoupling of the small-distance (high-k) scales from the considered large-scale backreaction is due to the efficient suppression of the linear perturbation modes inside the horizon, an effect well described by the transfer function of Eq. (6.3). The overall behaviour of the integrated terms, both in the IR and UV regimes, and the crucial role of the transfer function to make them finite is illustrated in Fig. 6.2.

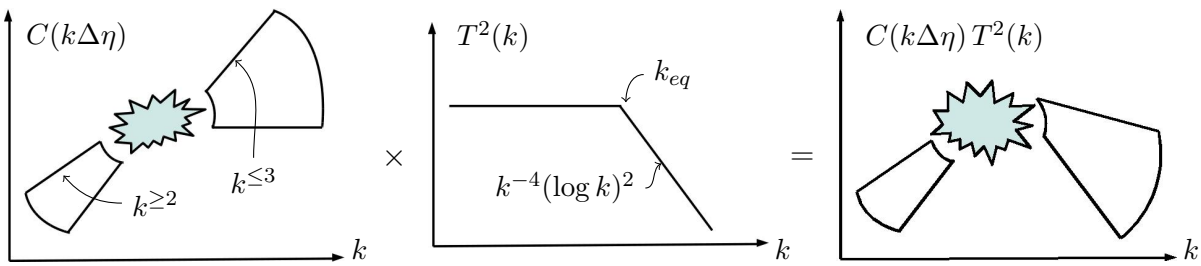

Figure 6.2: Illustration of the absence of IR and UV divergences. One can see that the functions of k which appear from the spectral coefficients of our terms, when multiplied by the transfer function, give rise to an integrand giving a finite contribution both in IR ($k \to 0$) and in UV ($k \to \infty$) regimes.

Let us now sum up all contributions to the induced backreaction IBR_2 of Eq. (5.54), and to the dispersion of Eq. (5.55), and compare the results for $\overline{\langle d_L\rangle} \pm d_L^{CDM}\sqrt{\overline{\langle\sigma_1^2\rangle}}$ with the homogeneous luminosity-distance of a pure CDM model and of a successful ΛCDM model. We include into $\overline{\langle d_L\rangle}$ only the IBR_2 contribution, namely we will set $\overline{\langle d_L\rangle} = d_L^{CDM}(1+\mathrm{IBR}_2)$. It is thus an incomplete calculation but a full computation will be presented in the next section. The extra contributions arising from second-order perturbations of d_L, like the term called $\overline{\langle\sigma_2\rangle}$ in Eq. (5.36), are a priori expected to be of the same order of $\overline{\langle\sigma_1^2\rangle}$ and we could even believe that (modulo cancellations) our computation may estimate a reliable "lower limit" on the strength of the possible corrections to the luminosity-redshift relation. The reality, as we will see in the next section, is more complexe and we will find that the answer is highly dependent of the observable which is considered.

The comparison between the homogeneous and inhomogeneous (averaged) values of d_L can be conveniently illustrated by plotting the so-called distance modulus $\mu \equiv m - M = 5\log_{10} d_L$ or, even better, by plotting the difference between the distance modulus of the considered model and that of a flat, linearly expanding Milne-type geometry, used as a reference value (see e.g. [7] and Appendix A.6). In such a case we can plot, in particular, the following quantity:

$$\Delta(m-M) \equiv \mu(\overline{\langle d_L\rangle}) - \mu^M = 5\log_{10}\left[\overline{\langle d_L\rangle}\right] - 5\log_{10}\left[\frac{(2+z_s)z_s}{2H_0}\right] \quad . \tag{6.6}$$

The results are illustrated in Fig. 6.3 for the cases of cut-off $k_{UV} = 0.1\,\mathrm{Mpc}^{-1}$ and $k_{UV} = 1\,\mathrm{Mpc}^{-1}$. The averaged luminosity-redshift relation of our inhomogeneous model is compared, in particular, with that of a pure CDM model and with that of a ΛCDM model with $\Omega_\Lambda = 0.1$ and with $\Omega_\Lambda = 0.73$. We have also explicitly shown the expected dispersion around the averaged result, by plotting the curves corresponding to $\overline{\langle d_L\rangle} \pm d_L^{CDM}\sqrt{\overline{\langle\sigma_1^2\rangle}}$ (bounding the coloured areas appearing in the figures).

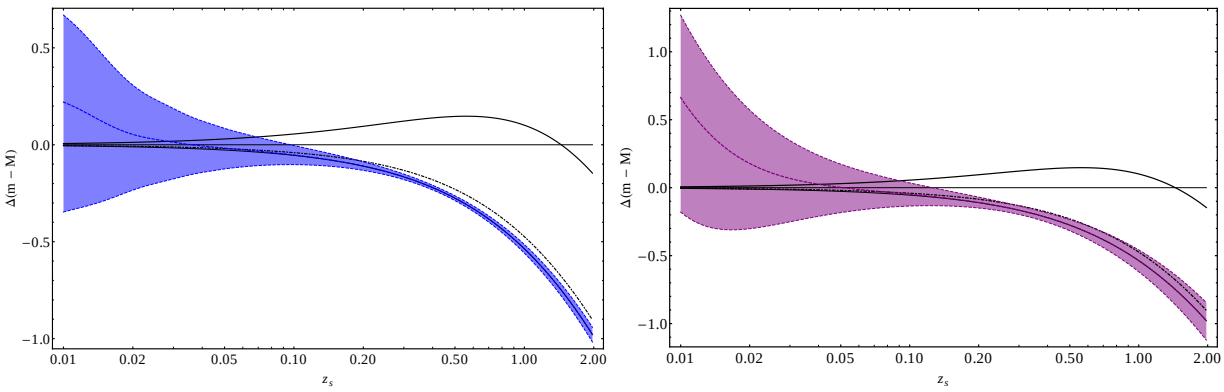

Figure 6.3: The distance-modulus difference $\mu(\overline{\langle d_L\rangle}) - \mu^M$ of Eq. (6.6) plotted for pure homogeneous models : CDM (thin line), ΛCDM with $\Omega_\Lambda = 0.73$ (thick) and $\Omega_\Lambda = 0.1$ (dashed-dot thick) ; and for a CDM model including the contribution of IBR_2 (dashed line) plus/minus the dispersion (coloured region). *Left :* We used for backreaction integrals the cut-off $k = 0.1\,\mathrm{Mpc}^{-1}$. *Right :* same with $k = 1\,\mathrm{Mpc}^{-1}$.

Let us stress again that the choice of the cut-off may affect (even if not dramatically) the final result when the values of k_{UV} are varying in the range $(0.1-1)\,\mathrm{Mpc}^{-1}$, while the precise choice becomes less important at higher values of k_{UV}. We should recall, however, that the inhomogeneous model adopted here is fully under control only in the linear perturbative regime, and that the spectrum cannot be extrapolated at scales higher than about $k \sim 1\,\mathrm{Mpc}^{-1}$ without taking into account the complicated effects of its non-linear dynamical evolution. The approximate coincidence between the above limiting value of k_{UV} and the scale marking the beginning of the non-linear perturbative regime is not only a particular consequence of the transfer function adopted here (see Eq. (6.3)), but also an avoidable property of realistic non-linear perturbations spectra (see e.g. [23]).

6.1.3 Conclusions from quadratic first order

As clearly shown by Fig. 6.3, the corrections induced by IBR_2 on the luminosity distance of a homogeneous CDM model, even taking into account the expected dispersion of values around $\overline{\langle d_L\rangle}$, cannot be used to successfully simulate realistic dark-energy effects. In the figures we have also plotted, for illustrative purposes, an example of a standard ΛCDM model with $\Omega_\Lambda = 0.1$, which seems to be compatible (within the allowed region defined by the dispersion) with the prediction of our simple CDM+IBR_2 model, at least for sufficiently high values of the cut-off scale (see *Right* figure of Fig. 6.3). However, we would be wrong to conclude that our backreaction can mimic a fraction of dark energy of the order of $\Omega_\Lambda \sim 0.1$, because a similar conclusion might be reliably reached only by averaging inhomogeneities on a background which already includes a significant amount of dark energy from the beginning. This situation will be realized in Sec. 6.3 where we will perform a calculation in a ΛCDM model.

Several arguments relative to this incomplete evaluation suggest the need of the full calculation that we are going to present in the next sections. First, as already stressed, a consistent second-order computation of the backreaction should include the contribution of $\overline{\langle\sigma_2\rangle}$. Nevertheless, we recall that from Eq. (5.44), we can believe that $\overline{\langle\sigma_2\rangle}$ could contain, among others, contributions of the type $\overline{\langle A_5 A_5\rangle}$ already computed in this section. The behaviour of this term, in the asymptotic regime $k\Delta\eta \gg 1$, is very different from the behaviour of terms like $\overline{\langle A_4 A_4\rangle}$ which give the leading contribution to IBR_2. The contribution of $\overline{\langle A_5 A_5\rangle}$, in particular, grows at large redshifts, as illustrated in Fig. 6.1. Using our

results for $\overline{\langle A_5 A_5\rangle}$, and barring an unlikely cancellation, we could suggest that a full computation of $\overline{\langle\sigma_2\rangle}$ may strongly enhance the overall backreaction effects at large z_s, with respect to the effects due to IBR$_2$ discussed previously. We will see that it is the case, $\overline{\langle\sigma_2\rangle}$ does contain this lensing contribution, but a cancellation with the $\overline{\langle\sigma_1^2\rangle}$ term does happen, miraculously, as a nice property of the luminosity flux.

Secondly, we expect to see an enhancement of the effect of inhomogeneities by the use of a reliable estimate of contributions from the non-linear regime [1]. Also, the different behaviour of the backreaction contributions, at small and large z_s, can represent an important signature to distinguish the effects due to the averaged inhomogeneities from the more conventional dynamical effects of homogeneous dark energy sources. This is another justification for an accurate and robust second order calculation.

Let us note however that although a reliable estimate of the full backreaction on the averaged luminosity distance requires a full second-order calculation, some suitable linear combinations of averages of different powers of d_L only depend on the first-order quantity σ_1 (defined by the expansion of d_L). As an example, one can show that the following equality holds at second order:

$$\overline{\left\langle \left(d_L/d_L^{\rm FLRW}\right)^\alpha\right\rangle} - \alpha\overline{\left\langle d_L/d_L^{\rm FLRW}\right\rangle} = 1-\alpha+\frac{\alpha(\alpha-1)}{2}\,\overline{\langle\sigma_1^2\rangle} \qquad \forall\,\alpha\in\mathbb{R}\ . \tag{6.7}$$

This quantity can be plotted for a given inhomogeneous model, and compared with its (deterministic) value in a ΛCDM model, for different values of α. The result is that the two models disagree for a generic α, bringing to the conclusion that realistic inhomogeneities added to CDM lead to a model that can be distinguished, in principle, from the conventional ΛCDM scenario. In practice, however, we only have a single quantity measured by SNe Ia experiments (basically the received flux of radiation), and one cannot exclude that the two models happen to give the same result for that particular observable.

6.2 Full calculation for the CDM model

In this section we evaluate the averages of the terms $\mathcal{I}_1$, $\mathcal{I}_{1,1}$ and $\mathcal{I}_2$ for the particular case of the standard CDM model, as more than a simple illustrative example. The results we will obtain shall confirm that the dominant terms are those already obtained for IBR$_2$ and $\overline{\langle\sigma_1^2\rangle}$ but within a complete study. The described dominant terms will be selected also for the discussion of the phenomenologically more relevant case, the ΛCDM model, presented in the forthcoming sections.

6.2.1 The quadratic first-order contributions $\overline{\langle\mathcal{I}_1\rangle^2}$ and $\overline{\langle\mathcal{I}_{1,1}\rangle}$

Let us now explicitly calculate the spectral coefficients for the first two backreaction terms (induced by the averaging) contributing to Eq. (5.94). The genuine second-order term $\overline{\langle\mathcal{I}_2\rangle}$ will be discussed in the next subsection. We start considering the first term $\overline{\langle\mathcal{I}_1\rangle^2}$. From Eq. (5.82) we obtain:

$$\overline{\langle\mathcal{I}_1\rangle^2} = \sum_{i=1}^{3}\sum_{j=1}^{3}\overline{\left\langle\mathcal{T}_i^{(1)}\right\rangle\left\langle\mathcal{T}_j^{(1)}\right\rangle} = \int_0^\infty\frac{dk}{k}\,\mathcal{P}_\psi(k,\eta_o)\,\sum_{i=1}^{3}\sum_{j=1}^{3}\mathcal{C}_{\mathcal{T}_i^{(1)}}(k,\eta_o,\eta_s)\,\mathcal{C}_{\mathcal{T}_j^{(1)}}(k,\eta_o,\eta_s) \tag{6.8}$$

(notice that, from now on, the background solution $\eta_s^{(0)}$ will be simply denoted by η_s). For a dust-dominated phase the spectral distribution of sub-horizon scalar perturbations is time independent, $\partial_\eta\psi_k=0$, and the scale factor $a(\eta)$ can be written as $a(\eta)=a(\eta_o)(\eta/\eta_o)^2$. We can also define

$$f_{o,s}\equiv\int_{\eta_{in}}^{\eta_{o,s}}d\eta\frac{a(\eta)}{a(\eta_{o,s})} = \frac{\eta_{o,s}^3-\eta_{in}^3}{3\eta_{o,s}^2}\ \simeq\frac{1}{3}\eta_{o,s} \tag{6.9}$$

(recall that η_{in} satisfies, by definition, $\eta_{in}\ll\eta_{o,s}$). All the spectral coefficients of Eq. (6.8) can then be easily calculated, and the result is reported in Table 6.1. This table is equivalent, within different

1. The importance of such a non-linear regime was also underlined in [24], following a different approach to describe the impact of inhomogeneities on the supernovae observations.

Table 6.1: The spectral coefficients $\mathcal{C}(\mathcal{T}_i^{(1)})$ for the $\overline{\left\langle \mathcal{T}_i^{(1)} \right\rangle \left\langle \mathcal{T}_j^{(1)} \right\rangle}$ terms.

$\mathcal{T}_i^{(1)}$	$\mathcal{C}_{\mathcal{T}_i^{(1)}}(k,\eta_o,\eta_s)$
$\mathcal{T}_1^{(1)}$	$-2\frac{\sin k\Delta\eta}{k\Delta\eta}$
$\mathcal{T}_2^{(1)}$	$-2\left(1-\frac{1}{\mathcal{H}_s\Delta\eta}\right)\left(1-\frac{\sin k\Delta\eta}{k\Delta\eta}\right)+2\left(1-\frac{1}{\mathcal{H}_s\Delta\eta}\right)\frac{f_s}{\Delta\eta}\left(\cos k\Delta\eta-\frac{\sin k\Delta\eta}{k\Delta\eta}\right)$
$\mathcal{T}_3^{(1)}$	$\frac{4}{k\Delta\eta}\mathrm{SinInt}(k\Delta\eta)$

notations, to the already presented Tab. 5.2. In a similar way, the second contribution to Eq. (5.94) can be expressed as:

$$\overline{\langle \mathcal{I}_{1,1}\rangle} = \int_0^\infty \frac{dk}{k}\, \mathcal{P}_\psi(k,\eta_o) \sum_{i=1}^{23} \mathcal{C}_{\mathcal{T}_i^{(1,1)}}(k,\eta_o,\eta_s) \quad , \tag{6.10}$$

and the explicit form of the spectral coefficients $\mathcal{C}(\mathcal{T}_i^{(1,1)})$ for CDM has been presented in Sec. 5.3.4.

Considering all contributions generated by $\mathcal{I}_1$ and $\mathcal{I}_{1,1}$, we find that the dominant ones are all contained in $\overline{\langle \mathcal{I}_{1,1}\rangle}$, not $\overline{\langle \mathcal{I}_1\rangle^2}$, and are characterized by spectral coefficients proportional to k^2. Such dominant terms have been emphasized, in Sec. 5.3.4, by enclosing them in a rectangular box. They correspond, in particular, to the terms $\mathcal{T}_i^{(1,1)}$ with $\{i = 2,4,5,7,8,12,14,18,20\}$. Including only such dominant contributions we find that, to leading order,

$$\begin{aligned}
\left[\sum_{i=1}^{23} \mathcal{C}_{\mathcal{T}_i^{(1,1)}}\right]_{\mathrm{Lead}} &= \aleph_s \frac{f_s^2+f_o^2}{3}k^2 + \frac{2(\Xi_s-3)}{\mathcal{H}_s}\frac{f_s}{3}k^2 + \Xi_s\frac{f_s^2}{3}k^2 - \Xi_s\frac{f_o^2}{3}k^2 \\
&= f_o^2k^2\left(\frac{\aleph_s}{3}-\frac{\Xi_s}{3}\right) + f_s^2k^2\left(\frac{\aleph_s}{3}+\frac{4\Xi_s}{3}-3\right) \\
&= -\frac{k^2}{\mathcal{H}_0^2}\,\widetilde{f}_{1,1}(z) \quad ,
\end{aligned} \tag{6.11}$$

where we have defined

$$\aleph_s \equiv \Xi_s^2 - \frac{1}{\mathcal{H}_s\Delta\eta}\left(1-\frac{\mathcal{H}_s'}{\mathcal{H}_s^2}\right) \quad , \tag{6.12}$$

and we have used the relation $\mathcal{H}_s \simeq 2/(3f_s)$ (valid in CDM). Also, we have included into the function $\widetilde{f}_{1,1}(z)$ all the z-dependence of these leading contributions. After some simple algebra we find:

$$\widetilde{f}_{1,1}(z) = \frac{10-12\sqrt{1+z}+5z\left(2+\sqrt{1+z}\right)}{27\,(1+z)\left(-1+\sqrt{1+z}\right)^2} \quad . \tag{6.13}$$

This function (and thus the corresponding backreaction) flips sign around $z^* = 0.205$ (as illustrated in Fig. 6.4, also visible in Fig. 6.5). It should be noted, finally, that some of the genuine second-order terms contained into $\mathcal{I}_2$ are also associated to spectral coefficients proportional to k^2. However, as we shall see in the next subsection, the corresponding contributions to Eq. (5.94) turn out to be roughly an order of magnitude smaller than the above ones, this because of approximate cancellations.

6.2.2 The genuine second-order contribution $\overline{\langle \mathcal{I}_2\rangle}$

In order to complete the calculation of $f_\Phi(z)$ we still have to consider the genuine second-order backreaction term $\overline{\langle \mathcal{I}_2\rangle}$. In particular, we must evaluate the spectral coefficients $\mathcal{C}(\mathcal{T}_i^{(2)})$, corresponding to the various contributions defined in Eq. (5.84), in terms of the first-order Bardeen potential. By using the results of Sec. 5.3.5, and starting from Eqs. (5.109) and (5.110), we can easily see that the only possible k^2-enhanced contributions arising from the coefficients $\mathcal{C}(\mathcal{T}_i^{(2)})$ (which only

contain functions of $\phi^{(2)}$ and $\psi^{(2)}$) should correspond to the terms $B_3(\eta)\nabla^{-2}\partial_i\partial^j(\partial^i\psi_o\partial_j\psi_o)$ and $B_4(\eta)\partial^i\psi_o\partial_i\psi_o$. Therefore, we should obtain $\phi^{(2)} \simeq \psi^{(2)}$ at leading order.

Let us discuss and estimate all possible contributions for the CDM model we are considering in this section. In this simple case $l(\eta) = 1$ and $B_1(\eta) = B_2(\eta) = 0$ (see Eqs. (5.112), (5.113)). Furthermore, restricting our attention to the standard inflationary scenario, we can set $a_{nl} = 1$. Eqs. (5.109) and (5.110) thus reduce to :

$$\psi^{(2)} = -2\psi_o^2 - \frac{4}{3}\,\mathcal{O}^{ij}\partial_i\psi_o\partial_j\psi_o + B_3(\eta)\,\mathcal{O}_3^{ij}\partial_i\psi_o\partial_j\psi_o + B_4(\eta)\,\mathcal{O}_4^{ij}\partial_i\psi_o\partial_j\psi_o \quad , \tag{6.14}$$

$$\phi^{(2)} = 2\psi_o^2 + 2\,\mathcal{O}^{ij}\partial_i\psi_o\partial_j\psi_o + B_3(\eta)\,\mathcal{O}_3^{ij}\partial_i\psi_o\partial_j\psi_o + B_4(\eta)\,\mathcal{O}_4^{ij}\partial_i\psi_o\partial_j\psi_o \quad . \tag{6.15}$$

Finally, we can use (as before) the scale factor $a(\eta) = a(\eta_o)\,(\eta/\eta_o)^2$, and obtain (according to Eq. (5.114)) :

$$B_3(\eta) = \frac{20}{21}\frac{1}{\mathcal{H}^2} \quad , \quad B_4(\eta) = -\frac{2}{7}\frac{1}{\mathcal{H}^2} \quad . \tag{6.16}$$

We are now in the position of evaluating the genuine second-order terms, by exploiting the results given in Eqs. (5.120), (5.122) and (5.123). Following the classification of Eq. (5.84) we can see that the first two terms $\mathcal{C}(\mathcal{T}_1^{(2)})$ and $\mathcal{C}(\mathcal{T}_2^{(2)})$ exactly cancel for the CDM case (while they cancel only at leading order for the case of a ΛCDM model). For CDM we have, in particular,

$$\mathcal{C}(\mathcal{T}_1^{(2)}) = -\mathcal{C}(\mathcal{T}_2^{(2)}) = -\frac{\Xi_s}{252}(\eta_s^2 - \eta_o^2)k^2 \quad . \tag{6.17}$$

Another interesting simplification concerns the terms $\mathcal{T}_3^{(2)}$, $\mathcal{T}_4^{(2)}$ and $\mathcal{T}_5^{(2)}$, namely those terms for which the integrand contains $\partial_r\psi^{(2)}$ or $\partial_r\phi^{(2)}$. From our previous results, in particular from Eqs. (5.120), (5.122) and (5.123), it is easy to see that the $\psi^{(2)}$ and $\phi^{(2)}$ contributions are unchanged when one averages over the 2-sphere (i.e. over θ by isotropy), since the θ-dependence is removed by the presence of $\delta^{(3)}(\mathbf{q})$. On the other hand, the presence of the r-derivative brings a further factor $|\mathbf{q}|\cos\theta$, and the q-integration gives zero, even before performing the angular average. It follows that, for a general model,

$$\mathcal{C}(\mathcal{T}_3^{(2)}) = 0 \quad , \quad \mathcal{C}(\mathcal{T}_4^{(2)}) = 0 \quad . \tag{6.18}$$

The contribution of $\mathcal{T}_5^{(2)}$, on the contrary, is non-vanishing because of the presence of the partial derivative ∂_η, acting on the $B_A(\eta)$ coefficients. For the CDM model we find, in particular,

$$\mathcal{C}(\mathcal{T}_5^{(2)}) = \frac{\Xi_s}{126}(\eta_s^2 - \eta_o^2)k^2 \quad . \tag{6.19}$$

Finally, for the last two terms $\mathcal{T}_6^{(2)}$ and $\mathcal{T}_7^{(2)}$ we obtain :

$$\mathcal{C}(\mathcal{T}_6^{(2)}) = -2 - \frac{k^2\eta_s^2}{126} + \frac{32k}{45}\frac{\psi_k\partial_k\psi_k^*}{|\psi_k|^2} + \frac{8k^2}{45}\frac{\psi_k\partial_k^2\psi_k^*}{|\psi_k|^2} \quad ,$$

$$\mathcal{C}(\mathcal{T}_7^{(2)}) = \frac{\eta_o^3 - \eta_s^3}{189\Delta\eta}k^2 + \frac{16k}{45}\frac{\psi_k\partial_k\psi_k^*}{|\psi_k|^2} + \frac{4k^2}{45}\frac{\psi_k\partial_k^2\psi_k^*}{|\psi_k|^2} \quad . \tag{6.20}$$

The sum of all contributions then leads to :

$$\sum_{i=1}^{7}\mathcal{C}(\mathcal{T}_i^{(2)}) = -2 + \frac{1}{7}\left[\frac{\Xi_s}{2}(f_s^2 - f_o^2) - \frac{f_s^2}{2} - \frac{f_s^3 - f_o^3}{\Delta\eta}\right]k^2 + \frac{16k}{15}\frac{\psi_k\partial_k\psi_k^*}{|\psi_k|^2} + \frac{4k^2}{15}\frac{\psi_k\partial_k^2\psi_k^*}{|\psi_k|^2} \quad . \tag{6.21}$$

All the above spectral coefficients are now to be numerically evaluated by using the power spectrum of the CDM model. We can easily check, however, that the leading k^2-contributions of these coefficients are given by :

$$\left[\sum_{i=1}^{7}\mathcal{C}(\mathcal{T}_i^{(2)})\right]_{\text{Lead}} = \frac{1}{7}\left[\frac{\Xi_s}{2}(f_s^2 - f_o^2) - \frac{f_s^2}{2} - \frac{f_s^3 - f_o^3}{\Delta\eta}\right]k^2 = -\frac{k^2}{\mathcal{H}_o^2}\,\widetilde{f}_2(z) \quad , \tag{6.22}$$

where :

$$\widetilde{f}_2(z) = -\frac{1}{189}\frac{2-2\sqrt{1+z}+z\left(9-2\sqrt{1+z}\right)}{(1+z)(\sqrt{1+z}-1)} \quad . \tag{6.23}$$

Such second-order contributions turn out, for redshifts $z \sim 0.1 - 2$, to be about one or two orders of magnitude smaller than the leading contributions of the squared first-order terms of Sec. 6.2.1, as can be easily checked by comparing the plots of $\widetilde{f}_{1,1}$ and $\widetilde{f}_2$ in Fig. 6.4. We can also remark that it flips sign at a value of the redshift equal to $z^* = 17.59$, a value which is much too large for impacting the observed data. Nevertheless, we can see from this plot that the genuine second order is constant at large redshift, making it more important than the quadratic first order in the early Universe. This answers the question of how large is the genuine second order term $\overline{\langle\sigma_2\rangle}$ with respect to the induced backreaction terms IBR_2.

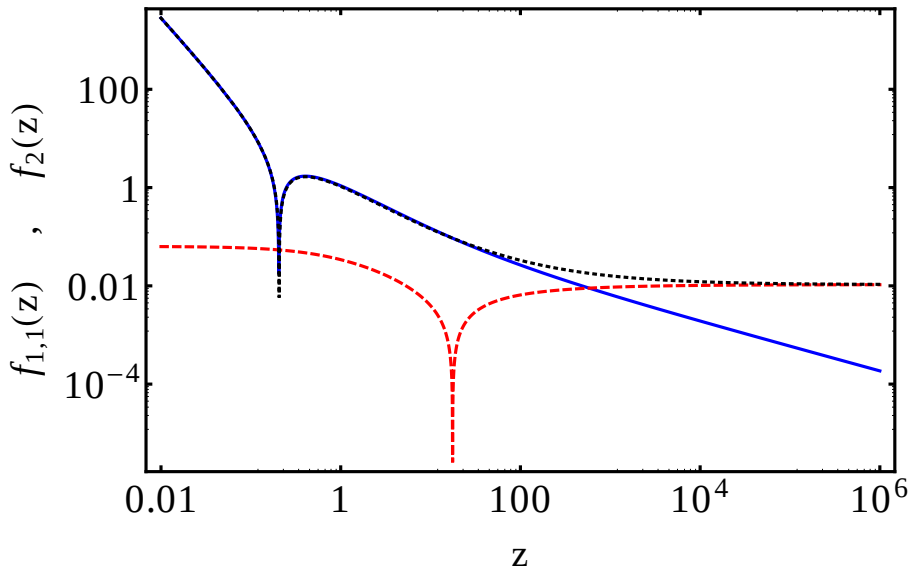

Figure 6.4: Plot of the redshift functions $\widetilde{f}_{1,1}(z)$ and $\widetilde{f}_2(z)$ for a very wide range of redshifts. One notice the different roles played by $\widetilde{f}_{1,1}(z)$ (solid blue) and $\widetilde{f}_2(z)$ (dashed red). The sum $\widetilde{f}_{1,1}(z)+\widetilde{f}_2(z)$ (dotted black) is also presented for the understanding of Eq. (6.24).

Considering the sum of these two contributions that will appear in the next section, we can deduce that there is no blowing up of the effect from inhomogeneities on the flux when we go to arbitrary early times (within the classical description employed here).

6.2.3 Full numerical results for the CDM model

We made use here of the transfer function presented in Sec. 6.1.1 to represent the CDM model. Following the results of the previous subsections, especially Eq. (5.94), we have found :

$$f_\Phi(z) = \int_0^\infty \frac{dk}{k}\,\mathcal{P}_\psi(k, z=0)\Big[f_{1,1}(k,z) + f_2(k,z)\Big] \quad , \tag{6.24}$$

where $f_{1,1}$ and f_2 are complicated – but known for the CDM case – analytic functions of their arguments. However, as already stressed, the leading contributions in the range of z relevant to dark-energy phenomenology are sourced by terms of the type $f(k,z) \sim (k/\mathcal{H}_o)^2\widetilde{f}(z)$. In that range of z we can thus write, to a very good accuracy :

$$f_\Phi(z) \simeq \Big[\widetilde{f}_{1,1}(z) + \widetilde{f}_2(z)\Big]\int_0^\infty \frac{dk}{k}\left(\frac{k}{\mathcal{H}_o}\right)^2 \mathcal{P}_\psi(k, z=0) \quad , \tag{6.25}$$

where $\widetilde{f}_{1,1}(z)$ and $\widetilde{f}_2(z)$ are given, respectively, by Eqs. (6.13) and (6.23).

To proceed, we need to insert a power spectrum as well as infrared (IR) and ultraviolet (UV) cutoffs in Eq. (6.24). The former can be identified with the present horizon $\mathcal{H}_o^{-1}$. However, considering the used spectra, larger scales give a completely negligible contribution. On the other hand, in spite of the fact that our expressions converge in the UV for any reasonable power spectrum, some mild sensitivity to the actual UV cutoff will be shown to occur in certain observables. The absolute value (and sign) of $f_\Phi(z)$ for the CDM model, obtained from both Eqs. (6.24) and (6.25), are illustrated in Fig. 6.5. We can explicitly check the accuracy of the leading order terms of Eq. (6.25). The figure also confirms that the backreaction of a realistic spectrum of stochastic perturbations induces negligible corrections to the averaged flux at large z (the larger corrections at small z, due to "Doppler terms", have been already discussed also in Sec. 6.1.2). In addition, it shows that such corrections have the wrong z-dependence (in particular, they change sign at some z) for simulating even a tiny dark-energy component.

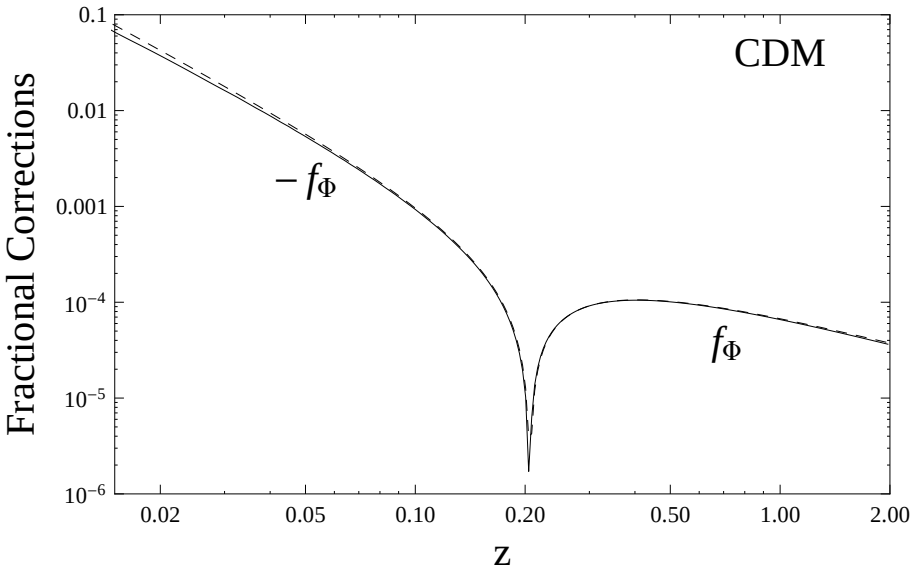

Figure 6.5: The fractional correction f_Φ of Eq. (6.24) (solid curve), compared with the same quantity given to leading order by Eq. (6.25) (dashed curve), in the context of an inhomogeneous CDM model. We have used for the spectrum the one defined in Eq. (6.1). The plotted curves refer, as an illustrative example, to an UV cutoff $k_{UV} = 1\,\mathrm{Mpc}^{-1}$.

6.3 The ΛCDM model : power spectrum in the linear regime

We will now extend the procedure of the previous section to the case of the so-called "concordance" cosmological model, using first a power spectrum computed in the linear regime, and then in Sec. 6.4, adding the effects of non-linearities following the parametrizations proposed in [23] and [74]. In both cases, we will restrict our attention only to the k^2-enhanced terms already identified in the CDM model for the light-cone average of the flux variable, as well as to the k^3-enhanced terms which, as we will see, will appear in the variance, or in the averages of other functions of $d_L(z)$. Hereafter in all numerical computations we will use, in particular, the following numerical values :

$$\Omega_{\Lambda 0} = 0.73 \quad , \quad \Omega_{m0} = 0.27 \quad , \quad \Omega_{b0} = 0.046 \quad , \quad h = 0.7 \ .$$

6.3.1 Second-order corrections to the averaged luminosity flux

The scalar power spectrum of the ΛCDM model is, in general, time-dependent. Considering for the moment only the linear regime, this spectrum can be written, starting from Eq. (5.107), as :

$$\mathcal{P}_\psi(k,\eta) = \left[\frac{g(\eta)}{g(\eta_o)}\right]^2 \mathcal{P}_\psi(k,\eta=\eta_o) \quad , \tag{6.26}$$

and in this case we can easily extend the results previously obtained for the CDM model, concerning the leading (k^2-enhanced) contributions to the averaged-flux integral I_ϕ. Using the general definitions of the $\mathcal{T}_i^{(1,1)}$ terms, we already noticed, in Eq. (6.11), that such enhanced contributions arise from the following particular (sub)-terms of Eq. (5.83) :

$$\mathcal{T}_{2,L}^{(1,1)} = \Xi_s\left(([\partial_r P]_s)^2 - ([\partial_r P]_o)^2\right) \quad ,$$

$$\mathcal{T}_{4,L}^{(1,1)} = \frac{1}{2}\Xi_s(\gamma_0^{ab})_s\,(2\partial_a P_s \partial_b P_s) \quad , \quad \mathcal{T}_{5,L}^{(1,1)} = -\Xi_s \lim_{r\to 0}\left[\gamma_0^{ab}\partial_a P \partial_b P\right] \quad ,$$

$$\mathcal{T}_{7,L}^{(1,1)} = -2\Xi_s([\partial_r P]_s)^2 \quad , \quad \mathcal{T}_{8,L}^{(1,1)} = 2\Xi_s\frac{1}{\mathcal{H}_s}\left(\psi_s - 2\int_{\eta_s}^{\eta_o} d\eta' \partial_r\psi(\eta',\eta_o-\eta',\tilde{\theta}^a)\right)[\partial_r^2 P]_s \quad ,$$

$$\mathcal{T}_{12,L}^{(1,1)} = \left[\Xi_s^2 - \frac{1}{\mathcal{H}_s\Delta\eta}\left(1-\frac{\mathcal{H}_s'}{\mathcal{H}_s^2}\right)\right]\left(([\partial_r P]_s)^2 + ([\partial_r P]_o)^2\right) \quad , \quad \mathcal{T}_{14,L}^{(1,1)} = 2\Xi_s\,([\partial_r P]_o)^2 \quad ,$$

$$\mathcal{T}_{18,L}^{(1,1)} = -\frac{1}{\mathcal{H}_s}(\gamma_0^{ab})_s\partial_a Q_s \partial_b[\partial_r P]_s \quad , \quad \mathcal{T}_{20,L}^{(1,1)} = -2\frac{1}{\mathcal{H}_s}[\partial_r P]_s[\partial_r\psi]_s \quad , \tag{6.27}$$

where we have added the suffix "L" to stress that we are reporting here only the leading terms.

In order to calculate the corresponding spectral coefficients in ΛCDM, we note that their time dependence can be factorized with respect to the k-dependence whenever the time variable does not appear in the exponential factor $\exp(i\,\mathbf{k}\cdot\mathbf{x})$ present in our integrals (see for instance the examples of Sec. 5.2.4). This is indeed the case for the terms $\mathcal{T}_{2,L}^{(1,1)}$, $\mathcal{T}_{4,L}^{(1,1)}$, $\mathcal{T}_{5,L}^{(1,1)}$, $\mathcal{T}_{7,L}^{(1,1)}$, $\mathcal{T}_{12,L}^{(1,1)}$, $\mathcal{T}_{14,L}^{(1,1)}$ and $\mathcal{T}_{20,L}^{(1,1)}$ which involve the integral $P(\eta,r,\widetilde{\theta}^a)$. In that case the previous CDM results for the leading spectral coefficients can be simply generalized to the ΛCDM case through the following procedure : (i) by inserting a factor $g(\eta_s)/g(\eta_o)$ whenever ψ_s is present in the initial term, and (ii) by replacing the $f_{o,s}$ factors (see Eq. (6.9)), arising from the presence of $P_{o,s}$ terms, by :

$$\widetilde{f}_{o,s} \equiv \int_{\eta_{in}}^{\eta_{o,s}} d\eta \frac{a(\eta)}{a(\eta_{o,s})}\frac{g(\eta)}{g(\eta_o)} \quad . \tag{6.28}$$

For the remaining two terms $\mathcal{T}_{8,L}^{(1,1)}$ and $\mathcal{T}_{18,L}^{(1,1)}$, the integrals are performed along the path $r=\eta_o-\eta$, and the time dependence cannot be fully factorized. Therefore, the evaluation of the double integrals over η and k is much more involved than in the previous cases. However, a good approximation of the exact result can be obtained by replacing $\psi(\eta',\eta_o-\eta',\tilde{\theta}^a)$, appearing in the integrands of $\mathcal{T}_{8,L}^{(1,1)}$ and $\mathcal{T}_{18,L}^{(1,1)}$, with $\psi(\eta_s,\eta_o-\eta',\tilde{\theta}^a)$. This is possible since the leading contributions to the time integral arise from a range of values of η approaching η_s. By adopting such an approximation we can follow the same procedure as before, and we obtain :

$$\mathcal{C}(\mathcal{T}_{8,L}^{(1,1)}) = \frac{2}{3}\Xi_s\frac{\widetilde{f}_s}{\mathcal{H}_s}k^2 \quad , \quad \mathcal{C}(\mathcal{T}_{18,L}^{(1,1)}) = -\frac{4}{3}\frac{\widetilde{f}_s}{\mathcal{H}_s}k^2 \quad . \tag{6.29}$$

This is formally the same result as in the CDM case (see Sec. 5.3.4 for the leading terms of $\mathcal{T}_{8,L}^{(1,1)}$ and $\mathcal{T}_{18,L}^{(1,1)}$), with the only difference that f_s is replaced by $\widetilde{f}_s$.

Let us now move to the evaluation of the leading contributions present in the genuine second-order part $\mathcal{I}_2$. The final results of Sec. 6.2.2, for the particular case of a CDM model, can be easily generalized to the ΛCDM case starting from the observation that the leading contributions can only arise from terms containing the operators $\mathcal{O}_3^{ij}$ and $\mathcal{O}_4^{ij}$ in Eqs. (5.109), (5.110) and (5.111). As a consequence, the first two terms $\mathcal{T}_1^{(2)}$ and $\mathcal{T}_2^{(2)}$ will give a subleading overall contribution, while the general result that the terms $\mathcal{T}_3^{(2)}$ and $\mathcal{T}_4^{(2)}$ give identically zero still holds. The remaining leading contributions can be easily obtained, using the results in Eqs. (5.122) and (5.123), as follows:

$$\mathcal{C}(\mathcal{T}_{5,L}^{(2)}) = -\Xi_s \left[\frac{1}{3}\left(B_3(\eta_o) - B_3(\eta_s)\right) + \left(B_4(\eta_o) - B_4(\eta_s)\right)\right] k^2 \quad , \tag{6.30}$$

$$\mathcal{C}(\mathcal{T}_{6,L}^{(2)}) = -\left(\frac{1}{3}B_3(\eta_s) + B_4(\eta_s)\right) k^2 \quad , \tag{6.31}$$

$$\mathcal{C}(\mathcal{T}_{7,L}^{(2)}) = \frac{2}{\Delta\eta}\int_{\eta_s}^{\eta_o} d\eta' \left(\frac{1}{3}B_3(\eta') + B_4(\eta')\right) k^2 \quad . \tag{6.32}$$

These leading contributions can be now evaluated using Eqs. (5.114) and (5.115) and moving to redshift space, where we can write:

$$\mathcal{H}(z) = \frac{\mathcal{H}_0}{1+z}\left[\Omega_{m0}(1+z)^3 + \Omega_{\Lambda 0}\right]^{1/2} \quad , \tag{6.33}$$

$$\Omega_m(z) = \frac{\Omega_{m0}(1+z)^3}{\Omega_{m0}(1+z)^3 + \Omega_{\Lambda 0}} \quad , \tag{6.34}$$

$$\Omega_\Lambda(z) = \frac{\Omega_{\Lambda 0}}{\Omega_{m0}(1+z)^3 + \Omega_{\Lambda 0}} \quad , \tag{6.35}$$

where the suffix "0" appended to Ω_m and Ω_Λ denotes the present value of those fractions of critical density. We note that, as in CDM, the leading genuine second-order contributions are about one to two orders of magnitude smaller than the leading squared first-order contributions, evaluated above.

We need now to insert the explicit form of the power spectrum. Considering the general solution of Eq. (5.107) we can also re-express the z-dependence of the power spectrum, in the linear regime, as follows:

$$\mathcal{P}_\psi(k,z) = \left(\frac{3}{5}\right)^2 \Delta_{\mathcal{R}}^2 T^2(k) \left(\frac{g(z)}{g_\infty}\right)^2 \quad , \tag{6.36}$$

where the previous CDM result of Eq. (6.1), based on the transfer function $T(k)$ given in [68], is modified by the presence of the factor $g(z)/g_\infty$ originating from the time dependence of the gravitational perturbations. Another modification with respect to the CDM result, implicitly contained into the transfer function $T(k)$, concerns the different numerical value of the equality scale $k_{\rm eq}$ (which now turns out to be lower because of the lower value of Ω_{m0}). The effects of such modifications are illustrated in Fig. 6.6 by comparing the ΛCDM spectrum of Eq. (6.36), at different values of z, with two z-independent spectra: the primordial spectrum of scalar perturbations $(3/5)^2\Delta_{\mathcal{R}}^2$, and the "transferred" spectrum of the CDM model, introduced in Sec. 6.1.1. Notice that, as expected, the ΛCDM and CDM spectra tend to coincide at large enough values of z. In the ΛCDM case the solid curves are obtained with a transfer function which takes into account the presence of baryonic matter, while the dashed curves correspond to the transfer function $T(k) = T_0(k)$ of Eq. (6.3) (without baryons). Here, however, we are always using a spectrum evaluated in the linear regime.

As illustrated in Fig. 6.6, the effect of neglecting the baryonic fraction of Ω_{m0} (and thus the associated Silk damping effect) may lead to an overestimation up to 40% of the corresponding transfer function for scalar perturbations, in the range $k \gtrsim 0.01\ h\,\mathrm{Mpc}^{-1}$ (see [68]). In order to take into account this baryonic contribution we have to replace the value of q used in the previous section, i.e.

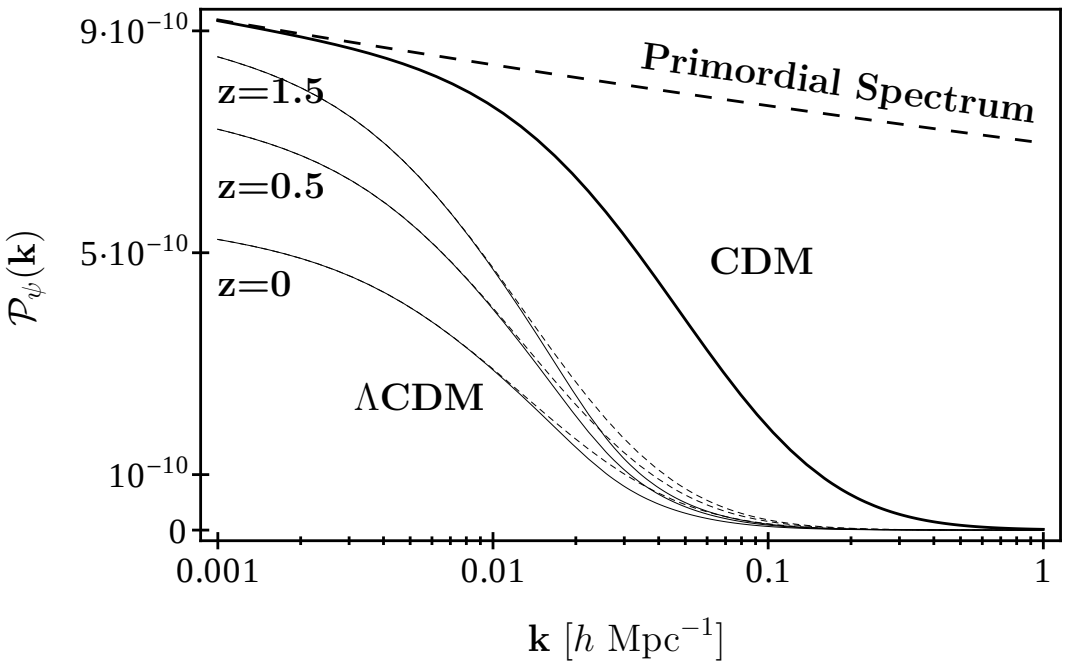

Figure 6.6: A comparison of the primordial inflationary spectrum (long-dashed curve) with the spectrum of the CDM model neglecting baryons (thick solid curve) and of a ΛCDM model (thin solid curves), at various values of z. The dotted curves for the ΛCDM case describe the spectrum obtained by neglecting the baryon contribution (hence without taking into account the Silk damping effect).

$q = k/(13.41\, k_{\rm eq})$, with the more accurate value given by [68] :

$$q = \frac{k \times \mathrm{Mpc}}{h\Gamma} \quad , \tag{6.37}$$

$$\Gamma = \Omega_{m0} h \left(\alpha_\Gamma + \frac{1-\alpha_\Gamma}{1+(0.43ks)^4} \right) \quad , \tag{6.38}$$

$$\alpha_\Gamma = 1 - 0.328 \ln(431\Omega_{m0}h^2)\frac{\Omega_{b0}}{\Omega_{m0}} + 0.38 \ln(22.3\Omega_{m0}h^2)\left(\frac{\Omega_{b0}}{\Omega_{m0}}\right)^2 \quad , \tag{6.39}$$

$$s = \frac{44.5 \ln(9.83/\Omega_{m0}h^2)}{\sqrt{1+10(\Omega_{b0}h^2)^{3/4}}}\,\mathrm{Mpc} \quad . \tag{6.40}$$

Here Ω_{b0} is the baryon density parameter, s is the sound horizon and Γ is the k-dependent effective shape parameter.

We have compared the above transfer function to the one which includes baryon acoustic oscillations (BAO) [68], and to a transfer function calculated numerically by using the so-called "code for anisotropies in the microwave background" (CAMB) [117]. We have checked, in particular, that the above simple form of transfer function is accurate to within a few percent compared to the one calculated numerically by CAMB, for all scales of interest. In addition, the effect of including BAO only produces oscillations of the spectrum around the above value. Since we are considering here integrals over a large range of k, the presence of BAO has a negligible effect on our final results, and will be neglected in the rest of the paper.

We are now in the position of computing the fractional corrections to the averaged flux variable in a perturbed ΛCDM geometry. As discussed before, there are complicated average integrals which can be performed only by using some approximations. Once this is done, the remaining integration over k can be done numerically, exactly as in the case of the CDM model. In a ΛCDM context we may generally expect smaller corrections to the averaged flux, due to the fact that the perturbation spectrum $\mathcal{P}_\psi$ is suppressed by the presence of $g(z)$. In addition (and as already stressed) the transfer function [68] turns out to be suppressed, at large k, because of a smaller value of the parameter $k_{\rm eq}$ (see Eq. (6.3)). These expectations are fully confirmed by an explicit numerical computation of $|f_\Phi|$,

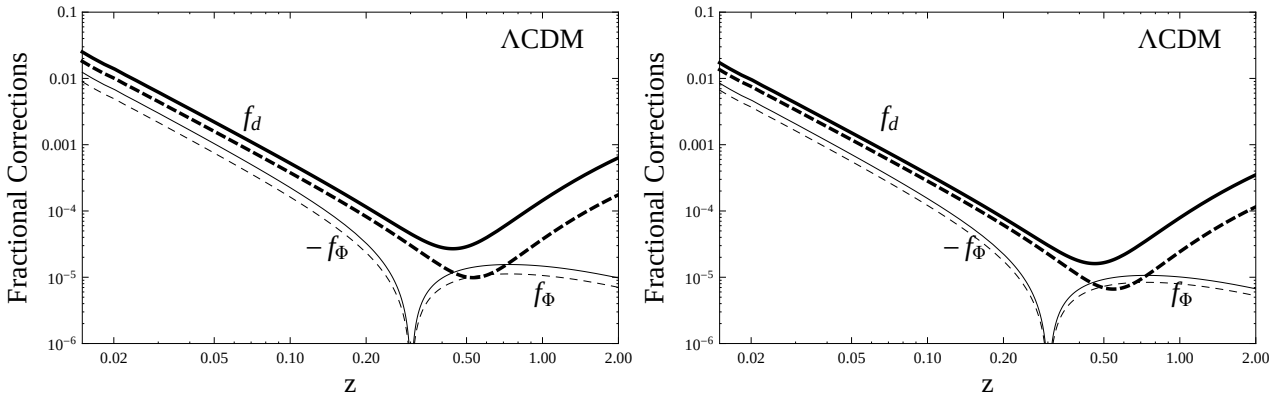

Figure 6.7: The fractional correction to the flux f_Φ of Eq. (5.94) (thin curves) is plotted together with the fractional correction to the luminosity distance f_d of Eq. (5.96) (thick curves), for a ΛCDM model with $\Omega_{\Lambda 0} = 0.73$. We have used two different cutoff values: $k_{UV} = 0.1\,\mathrm{Mpc}^{-1}$ (dashed curves) and $k_{UV} = 1\,\mathrm{Mpc}^{-1}$ (solid curves). *Left*: results obtained with a linear spectrum without baryon contributions. *Right*: effects of including baryons (we have used, in particular, $\Omega_{b0} = 0.046$).

which we have performed with and without the inclusion of the baryon contributions into the transfer function $T(k)$.

The results of such a computation are illustrated in Fig. 6.7, and a comparison with Fig. 6.5 clearly shows that $|f_\Phi|$ is smaller in the ΛCDM case than in the CDM case, and further (slightly) depressed when we take into account the presence of a small fraction of baryonic matter (see the curves presented in the right panel). In any case, the small values of $|f_\Phi|$ at relatively large z, for a realistic ΛCDM scenario, lead us to conclude that the averaged flux is a particularly appropriate quantity for extracting from the observational data the "true" cosmological parameters. As we will discuss now, the situation is somewhat different for other functions of d_L.

6.3.2 Second-order corrections to other observables and dispersions

Let us now consider other observables, beyond the flux, to see how the impact of the inhomogeneities may change. We will treat, in particular, the two important examples extensively presented in Sec. 5.3.3, namely the luminosity distance d_L and the distance modulus μ. The fractional corrections to their averages (see Eqs. (5.95–5.98)) are qualitatively different from those of the averaged flux (represented by f_Φ), because of the presence of extra contributions, unavoidable for any non-linear function of the flux and proportional to the square of the first order fluctuation $(\Phi_1/\Phi_0)^2$.

For a better understanding of such contributions let us start with the results obtained in Sec. 5.3.2, concerning the second-order perturbative expansion of the luminosity distance, $d_L = d_L^{(0)} + d_L^{(1)} + d_L^{(2)}$ (see in particular Eqs. (5.76) and (5.78)). Using those results we obtain:

$$\frac{\Phi_1}{\Phi_0} = -2\frac{d_L^{(1)}}{d_L^{(0)}} = -\mathcal{I}_1 + (\mathrm{t.d.})^{(1)} = 2\left(-\Xi_s J + \frac{Q_s}{\Delta\eta} + \psi_s + J_2^{(1)}\right) \quad . \tag{6.41}$$

In order to determine the leading corrections we first notice that, by applying the procedure of Sec. 6.2.1, and computing the averages for the CDM case, we obtain, to leading order,

$$\overline{\left\langle \left(\frac{\Phi_1}{\Phi_0}\right)^2 \right\rangle_L} = 4\left\{ \overline{\left\langle \left(J_2^{(1)}\right)^2 \right\rangle} + \Xi_s^2 \left[\overline{\langle ([\partial_r P]_s)^2 \rangle} + \overline{\langle ([\partial_r P]_o)^2 \rangle} \right] \right\} \quad . \tag{6.42}$$

Working in the context of a ΛCDM model, considering only these leading terms, and limiting ourselves to the linear regime, we find that the terms multiplying Ξ_s^2 on the right hand side of the above equation can be calculated without approximations (as seen in the previous subsection). Also, we find that their contribution is controlled by the spectral factor $k^2\mathcal{P}_\psi(k,\eta_o)$ and they correspond to the peculiar

velocity terms. The first term, on the contrary, is due to the so-called "lensing effect", dominates at large z (as already shown in Sec. 6.1.2 for a CDM model), and has leading spectral contributions of the type $k^3\mathcal{P}_\psi(k,\eta_o)$. For such term, however, the integrals over time cannot be factorized with respect to the k integrals, and we must use the approximation already introduced in the previous subsection (namely, we have to replace in the integrands $\psi(\eta',\eta_o-\eta',\tilde\theta^a)$ with $\psi(\eta_s,\eta_o-\eta',\tilde\theta^a)$). The full result for the spectral coefficient can then be finally written as follows :

$$\mathcal{C}((\Phi_1/\Phi_0)^2_L) \simeq \frac{4}{3}\Xi_s^2\left(\widetilde{f}_s^2+\widetilde{f}_o^2\right)k^2+\frac{4}{15}\left[\frac{g(\eta_s)}{g(\eta_o)}\right]^2\Delta\eta^3k^3\,\mathrm{SinInt}(k\Delta\eta)\quad . \tag{6.43}$$

Because of the new term (due to lensing) affecting the average of μ and d_L – but not of the flux Φ – we may expect larger fractional corrections for these variables, as well as for other functions of Φ, at higher redshifts. This is indeed confirmed by the plots presented in Fig. 6.7, reporting the results of an explicit numerical integration and comparing, in particular, the value of f_d with the absolute value of f_Φ. We obtain $|f_\Phi| \ll f_d$, at large values of z where the lensing term dominates, both in the presence and in the absence of the baryon contribution to the total energy density. It should be stressed, however, that also the new k^3-enhanced contributions are free from IR and UV divergences, at least for the class of models we are considering.

Let us now discuss to what extent the enhanced corrections due to the square of the first-order flux fluctuation can affect the determination of the dark-energy parameters, if quantities other than the flux are used to fit the observational data. To this purpose we may consider the much used (average of the) distance modulus given in Eq. (5.98), referring it to a homogeneous Milne model with $\mu^M = 5\log_{10}[(2+z)z/(2H_0)]$. Considering Eqs. (5.98) and (5.102), where the averaged value of the distance modulus and its dispersion are given in function of f_Φ and of $\overline{\left\langle(\Phi_1/\Phi_0)^2\right\rangle}$, we have investigated the magnitude of the effect in this case. In particular, in Fig. 6.8 we have compared the averaged value $\overline{\langle\mu\rangle}-\mu^M$ with the corresponding expression for homogeneous ΛCDM models with different values of $\Omega_{\Lambda0}$. We have also illustrated the expected dispersion around the averaged result, represented by the dispersion previously reported in Eq. (5.102) (and already computed in CDM).

We have found that the given inhomogeneities, on the average, may affect the determination of $\Omega_{\Lambda0}$ obtained from the measure of the distance modulus, at large z, only at the third decimal figure (at least if the spectral contributions are computed in the linear regime). As we can see from Fig. 6.8, the curves for $\overline{\langle\mu\rangle}$ and for the corresponding unperturbed value μ^{FLRW} (with the same $\Omega_{\Lambda0}$) practically coincide at large enough z. It should be stressed, also, that the dispersion on the distance modulus computed from Eq. (5.102) reaches, at large redshift, a value which is comparable with a change of about 2% in the dark energy parameter $\Omega_{\Lambda0}$ (cf. Sec. 6.1.2, considering however that baryonic effects have now been added in the transfer function). We shall see in the next section that this effect is enhanced by the use of non-linear power spectra.

6.4 The ΛCDM model : power spectrum in the non-linear regime

The linear spectra considered so far are sufficiently accurate only up to scales of $\sim 0.1\,h\,\mathrm{Mpc}^{-1}$. If we want to better study the effect of shorter-scale inhomogeneities on our light-cone averages we need to go beyond such linear approximation, taking into consideration the non-linear evolution of the gravitational perturbations. This can be done by using the so-called "HaloFit" model, which is known to reproduce quite accurately the results of cosmological N-body simulations. In particular, the HaloFit model of [23] and its recent upgrade of [74] provide an accurate fitting formula for the power spectrum up to a wavenumber $k \simeq 30\,h\,\mathrm{Mpc}^{-1}$.

In our previous section, Sec. 6.3, the analysis was limited to $k < 1\,\mathrm{Mpc}^{-1}$, but with the use of the non-linear power spectra we can now extend our analysis up to the maximum scale of the mentioned HaloFit models. The main difficulty with such an extension is that the time (i.e. z) dependence of the spectrum becomes more involved than in the linear case, since different scales no longer evolve independently. Hence, the need for introducing approximations in performing the integrals becomes even more essential in this case.

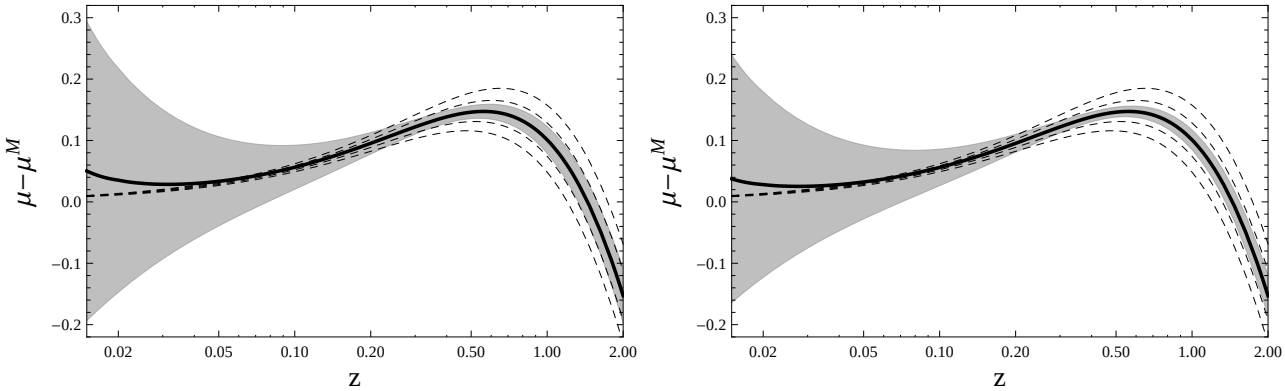

Figure 6.8: The averaged distance modulus $\overline{\langle\mu\rangle}-\mu^M$ of Eq. (5.98) (thick solid curve), and its dispersion of Eq. (5.102) (shaded region) are computed for $\Omega_{\Lambda 0} = 0.73$ and compared with the homogeneous value for the unperturbed ΛCDM models with, from bottom to top, $\Omega_{\Lambda 0} = 0.69$, 0.71, 0.73, 0.75, 0.77 (dashed curves). We have used $k_{UV} = 1\,\mathrm{Mpc}^{-1}$. The *left* panel shows the results obtained with a linear spectrum without baryon contributions. The *right* panel illustrates the effects of including baryons, with $\Omega_{b0} = 0.046$.

Let us start by recalling a few details of the HaloFit model. A more complete presentation is given in Appendix A.5. The fractional density variance per unit $\ln k$ is represented by the variable $\Delta^2(k)$, defined by [23] :

$$\sigma^2 \equiv \overline{\delta(x)\delta(x)} = \int \frac{d^3k}{(2\pi)^3}|\delta_{\vec{k}}|^2 = \int \Delta^2(k)\ d\ln k \quad , \tag{6.44}$$

which implies

$$\Delta^2(k) = \frac{k^3}{2\pi^2}|\delta_k|^2 \quad , \tag{6.45}$$

and where $\delta(x) = \delta\rho(x)/\rho(t)$ is the fractional density perturbation of the gravitational sources, and δ_k is the associated Fourier component. On the other hand, the power spectrum of scalar perturbations, $\mathcal{P}_\psi(k,z)$, is related to $\Delta^2(k,z)$ by the Poisson equation, holding at both the linear (L) and non-linear (NL) level [8] :

$$\mathcal{P}_\psi^{\mathrm{L,NL}}(k,z) = \frac{9}{4}\frac{\Omega_{m0}^2\mathcal{H}_0^4}{k^4}(1+z)^2\Delta^2_{\mathrm{L,NL}}(k,z) \quad . \tag{6.46}$$

The linear part of the spectrum is used to introduce the normalization equation, defining the non-linearity length scale $k_\sigma^{-1}(z)$, as follows :

$$\sigma^2(k_\sigma^{-1}) \equiv \int \Delta^2_{\mathrm{L}}(k,z)\ \exp(-(k/k_\sigma)^2)\ d\ln k \equiv 1 \quad . \tag{6.47}$$

It is then obvious that the non-linearity scale k_σ^{-1} is redshift-dependent. Since the non-linear power spectra obtained from the models [23] and [74] are using such a scale, they will be characterized by an implicit z-dependence which is more complicated than the one following from the usual growth factor of Eq. (5.108), and which cannot be factorized.

Besides k_σ, the linear spectrum also determines two additional parameters, important for the construction of the HaloFit model : the effective spectral index n_{eff} and the parameter C, controlling the curvature of the spectral index at the scale k_σ^{-1}. They are defined by :

$$3 + n_{\mathrm{eff}} \equiv -\left.\frac{d\ln\sigma^2(R)}{d\ln R}\right|_{R=k_\sigma^{-1}} \quad , \qquad C \equiv -\left.\frac{d^2\ln\sigma^2(R)}{d\ln R^2}\right|_{R=k_\sigma^{-1}} \quad . \tag{6.48}$$

Once the values of k_σ, n_{eff} and C are determined, they can be inserted into a given HaloFit model [23,74] to produce the non-linear power spectrum $\Delta^2_{\mathrm{NL}}(k,z)$. One finally goes back to $\mathcal{P}_\psi^{\mathrm{NL}}(k,z)$ using again the Poisson equation (6.46), as already explained in Sec. 1.4.3.

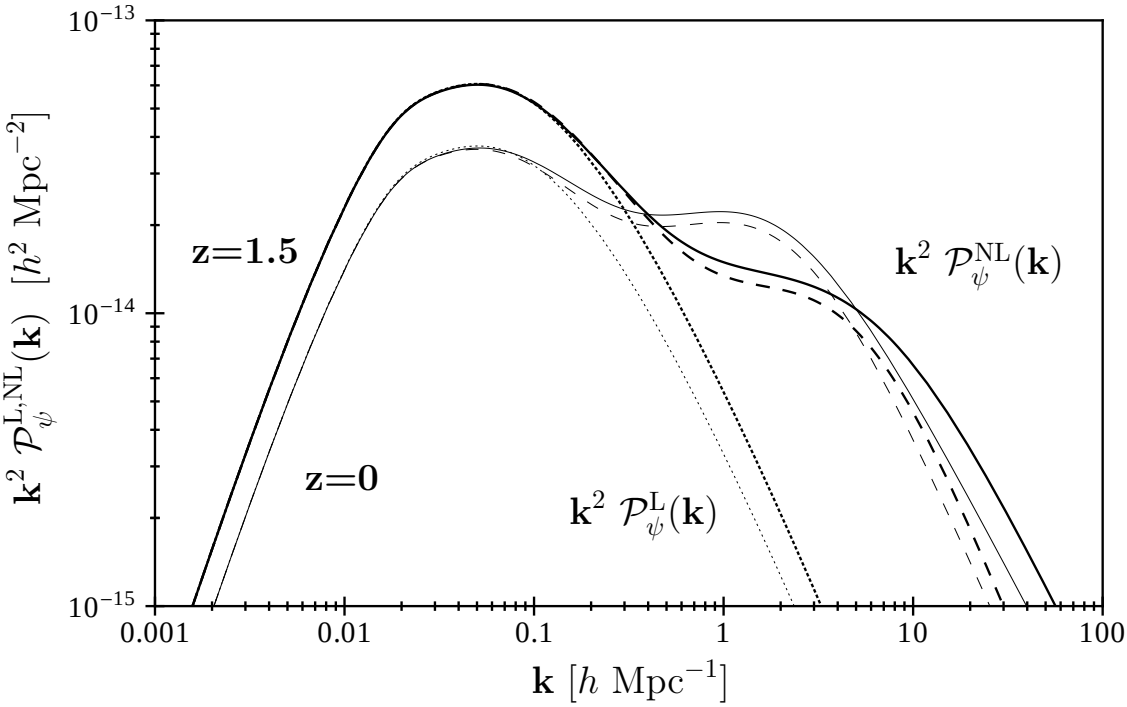

Figure 6.9: The linear spectrum $\mathcal{P}_\psi^{\mathrm{L}}$ (dotted curves) and the non-linear spectrum $\mathcal{P}_\psi^{\mathrm{NL}}$ for the HaloFit model of [23] (dashed curves) and of [74] (solid curves). In all three cases the spectrum is multiplied by k^2 (for graphical convenience) and is given for $z = 0$ (thin curves) and $z = 1.5$ (thick curves). We have included baryons with $\Omega_{b0} = 0.046$.

The non-linear spectra obtained in this way, and based on the previous linear spectrum with baryon contributions, are illustrated in Fig. 6.9 for the two HaloFit models [23] and [74]. The results are compared with the spectrum of the linear regime, for different values of the redshift ($z = 0$ and $z = 1.5$). We can see that the spectra intersect each other in the non-linear regime ($k \gtrsim 0.1\, h\,\mathrm{Mpc}^{-1}$), as a result of the intricate redshift dependence. We can also observe that the two HaloFit models lead to the same result at low values of k (including baryons, but without BAO).

6.4.1 Numerical results and comparison with the linear regime

In order to evaluate our integrals using the non-linear power spectra we need to face the additional (already mentioned) problem that the non-linear spectra – unlike the linear ones – cannot be factorized as a function of k times a function of z. In that case the full two-dimensional integration is highly non-trivial, and we have thus exploited a further approximation. In the presence of time-integrals of the mode functions (like those appearing, for instance, in the leading terms of $\overline{\langle \mathcal{I}_{1,1} \rangle}$), we have parametrized the non-linear power spectrum in a factorized form as follows :

$$\mathcal{P}_\psi^{\mathrm{NL}}(k, z) = \frac{g^2(z)}{g^2(z^*)} \mathcal{P}_\psi^{\mathrm{NL}}(k, z^*) \quad , \tag{6.49}$$

and we have chosen $z^* = z_s/2$ to try to minimize the error.

Let us briefly comment on the validity of the approximation we have introduced. Our analysis being focussed on the redshift range $0.015 \leq z \leq 2$, the above approximation is most inadequate only when we consider $z_s = 2$ (i.e. $z^* = 1$), and our mode functions are evaluated inside the integrals at the values of z most distant from z^* (namely, $z = 0.015$ and $z = 2$). In that case we are led to underestimate the spectrum by about a 40% factor for $z = 0.015$, and to overestimate it by about a 80% factor for $z = 2$. However, this only occurs in two narrow bands of k centered around the values $k = 1\, h\,\mathrm{Mpc}^{-1}$ and $k = 2\, h\,\mathrm{Mpc}^{-1}$, while, outside these bands, our approximation is good. Since these errors are limited to only a part of the region of integration, both in z and in k, we can estimate an

overall accuracy at the 10% level, at least, for the results given by the adopted approximation. We have also checked the sensitivity of the numerical results to changes in z^*, such as $z^* = z_s$, and checked that our final results are only weakly dependent (typically at the 1% level) on the choice of z^*.

Once we have established the range of validity of the parametrization (6.49), we proceed in evaluating the z (or η) integrals as we did in Sec. 6.3. The final results of this procedure are illustrated by the curves plotted in Figs. 6.10 and 6.11, computed with the non-linear power spectrum following from the HaloFit model of [74] and including baryon contributions [2]. As illustrated for instance in Fig. 6.10, the fractional correction to the luminosity distance d_L turns out to be of order of a few parts in 10^{-3} around $z = 2$, and smaller in the rest of the intermediate redshift range relevant for cosmic acceleration. On the other hand, in the same redshift range, the fractional correction to the flux is about two orders of magnitude smaller.

Comparing with the results obtained using the linear spectrum (see Figs. 6.7, 6.8), we can see that taking into account the non-linearity distortions (and using higher cut-off values) enhances the backreaction effects on the considered functions of the luminosity distance, but not enough to reach a (currently) observable level. We see in Fig. 6.11, especially on the right panel, that the average is very weakly affected by inhomogeneities. On the other hand, the dispersion, already large in the linear case, is further enhanced when non-linearities are included. In particular, the dispersion on μ due to inhomogeneities is of order 10% around $z = 2$, which implies that the predictions of homogeneous models with $\Omega_{\Lambda 0}$ ranging from 0.68 to 0.78 lie inside one standard deviation with respect to the averaged predictions of a perturbed (inhomogeneous) model with $\Omega_{\Lambda 0} = 0.73$.

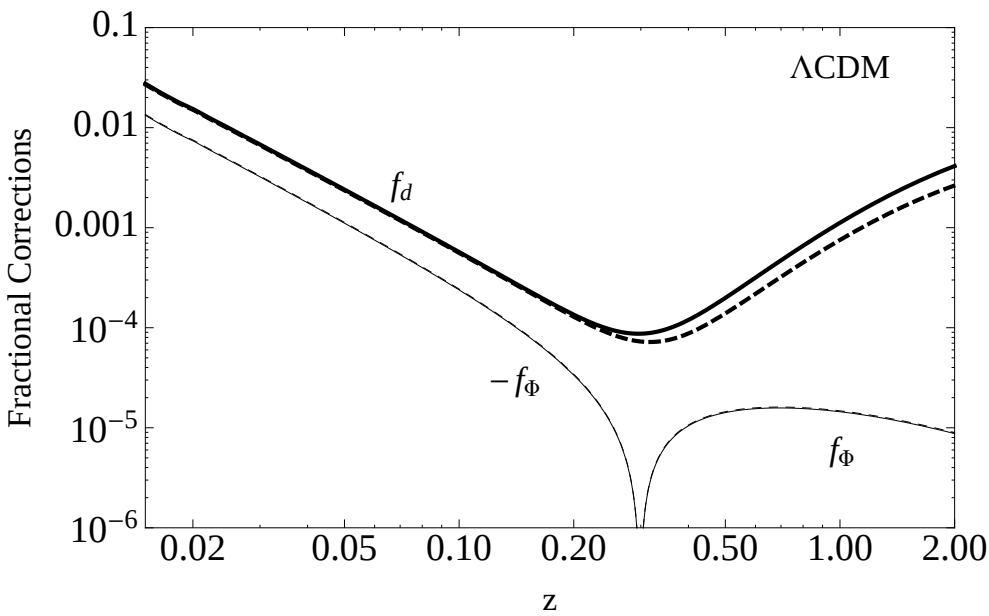

Figure 6.10: The fractional correction to the flux (f_Φ, thin curves) and to the luminosity distance (f_d, thick curves), for a perturbed ΛCDM model with $\Omega_{\Lambda 0} = 0.73$. Unlike in Fig. 6.7, we have taken into account the non-linear contributions to the power spectrum given by the HaloFit model of [74] (including baryons), and we have used the following cutoff values: $k_{UV} = 10\,h\,\mathrm{Mpc}^{-1}$ (dashed curves) and $k_{UV} = 30\,h\,\mathrm{Mpc}^{-1}$ (solid curves).

6.4.2 Comparing theory and observations via the intrinsic dispersion of data

Let us now consider in more detail our prediction for the dispersion σ_μ induced by the presence of the inflationary perturbation background, and compare it with the intrinsic dispersion of the distance modulus inferred from SNe Ia data. Our results for the dispersion are already implicitly contained in

2. The two HaloFit models quoted above give similar results, and we have chosen to present here, for simplicity, only those obtained with the parametrization of [74].

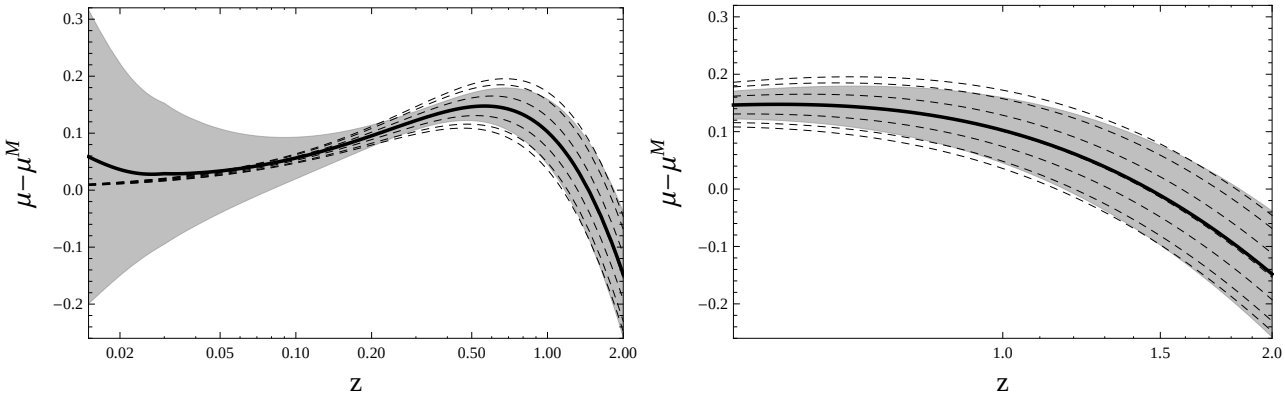

Figure 6.11: The averaged distance modulus $\overline{\langle\mu\rangle} - \mu^M$ of Eq. (5.98) (thick solid curve), and its dispersion of Eq. (5.102) (shaded region), for a perturbed ΛCDM model with $\Omega_{\Lambda 0} = 0.73$. Unlike Fig. 6.8, we have taken into account the non-linear contributions to the power spectrum given by the HaloFit model of [74] (including baryons), and used the cut-off $k_{UV} = 30\,h$ Mpc^{-1}. The averaged results are compared with the homogeneous values of μ predicted by unperturbed ΛCDM models with (from bottom to top) $\Omega_{\Lambda 0} = 0.68$, 0.69, 0.71, 0.73, 0.75, 0.77, 0.78 (dashed curves). The right panel simply provides a zoom of the same curves, plotted in the smaller redshift range $0.5 \leq z \leq 2$.

Fig. 6.11 but, for the sake of clarity, we have separately plotted our value of σ_μ in Fig. 6.12, where the thick solid curve represents the value of σ_μ obtained from Eq. (5.102), and plotted as a function of z. We can see from the figure that σ_μ has a characteristic z-dependence, with a minimal value of about 0.016 reached around $z = 0.285$. Also, the total dispersion of Eq. (5.102) nicely interpolates between the leading Doppler contribution obtained from the two last terms of Eq. (6.42) (represented by the dashed curve approaching zero at large z), and the leading lensing contribution obtained from the first term of Eq. (6.42) (represented by the dashed curve approaching zero at small z).

The total variance $\sigma_\mu^{\rm obs}$ associated with the observational data, on the other hand, can be decomposed in general as follows (see e.g. [13, 118, 119]) :

$$(\sigma_\mu^{\rm obs})^2 = (\sigma_\mu^{\rm fit})^2 + (\sigma_\mu^z)^2 + (\sigma_\mu^{\rm int})^2 \quad . \tag{6.50}$$

Here $\sigma_\mu^{\rm fit}$ is the statistical uncertainty due, for instance, to the method adopted for fitting the light curve (e.g. the so-called SALT-II method [16]), but also to the uncertainty in the modeling of the supernova process. The term σ_μ^z represents instead the uncertainty in redshift due to the peculiar velocity of the supernova as well as to the precision of spectroscopic measurements. Finally, $\sigma_\mu^{\rm int}$ is an unknown phenomenological quantity, needed to account for the remaining dispersion of the data with respect to the chosen homogeneous model. This part of the dispersion can be subsequently redefined whenever we are able to estimate some of the possible contributions it contains. The contribution we are mainly interested in here is the one originating from the lensing effect, which is dominant at large redshift. We can thus write, at large z :

$$(\sigma_\mu^{\rm int})^2 = (\widehat{\sigma_\mu^{\rm int}})^2 + (\sigma_\mu^{\rm lens})^2 \quad , \tag{6.51}$$

where $\widehat{\sigma_\mu^{\rm int}}$ is the remaining source of intrinsic dispersion.

Given the typical precision of current data [16, 120], a reasonable fit of the Hubble diagram does not seem to require a strong z-dependence of the parameter $\sigma_\mu^{\rm int}$: for instance, a nearby sample gives $\sigma^{\rm int} = 0.15 \pm 0.02$, to be compared with the value $\sigma^{\rm int} = 0.12 \pm 0.02$ obtained for distant supernovae. On the other hand, as illustrated in Fig. 6.12, the results of our computations at $z \gtrsim 0.3$ is very well captured by a linear behaviour which can be roughly fitted by $\sigma_\mu^{\rm lens}(z) = 0.056\,z$. We should also note that this contribution stays below 0.12 up to $z \sim 2$, which makes it perfectly compatible with observations so far performed.

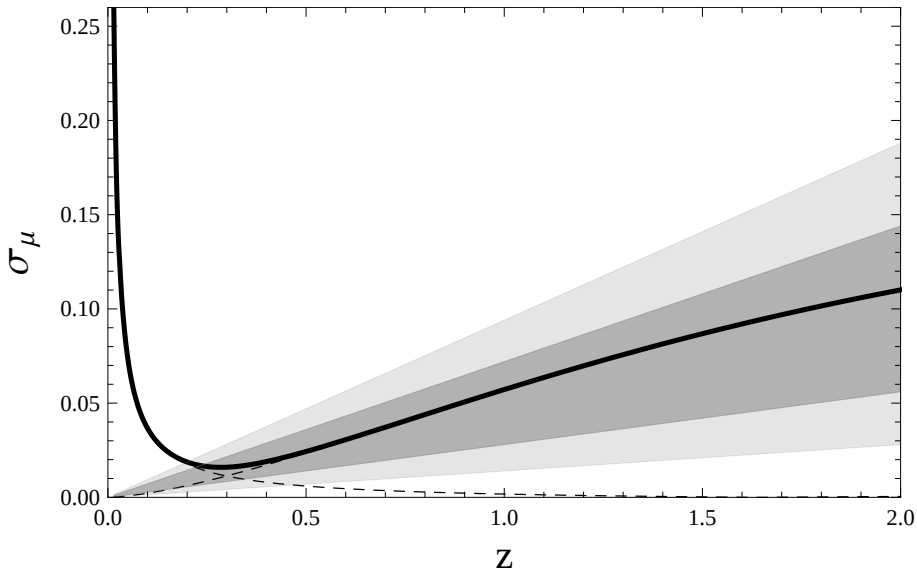

Figure 6.12: The z-dependence of the total dispersion σ_μ is illustrated by the thick solid curve, and it is separated into its "Doppler" part (dashed curve dominant at low z) and "lensing" part (dashed curve dominant at large z). The slope of the dispersion in the lensing-dominated regime is compared with the experimental estimates of Kronborg *et al.* [75] (dark shaded area), and of Jönsson *et al.* [76] (light shaded area).

It is remarkable that the (above mentioned) simple linear fit of our curve for $\sigma_\mu(z)$ at $z \gtrsim 0.3$ turns out to be very close to the experimental estimate reported in [75], namely :

$$\left(\sigma_\mu^{\rm lens}\right)_{\rm Kronborg} = (0.05 \pm 0.022)\, z \quad . \tag{6.52}$$

Also, such a fit is well compatible with the results of [76] :

$$\left(\sigma_\mu^{\rm lens}\right)_{\rm Jönsson} = (0.055\ {}^{+0.039}_{-0.041})\, z \quad . \tag{6.53}$$

These two observational estimates of the lensing dispersion, with the relative error bands, are illustrated by the shaded areas of Fig. 6.12. Our result is also in relatively good agreement with the simulations carried out in [121] which predicted an effect of $0.088\, z$. Other authors [122–124], however, have found no indication of this z-dependence of σ_μ, and such a signal certainly waits for a better observational evidence (see [125, 126] for a recent statistical approach and its applications).

It is likely that future improvements in the accuracy of SNe Ia data will detect (or disprove) this effect at a higher confidence level. In this respect, our results for $\sigma_\mu(z)$ stand out as a challenging prediction, which, we believe, could represent a further significative test of the concordance model. We finally remark, incidentally, that our prediction for the Doppler-related dispersion at small z is also consistent with previous findings [127] on the so-called Poissonian peculiar velocity contribution to σ_μ. We have checked that our result for the Doppler contribution (see Fig. 6.12) is well fitted by an inverse power law :

$$\sigma_\mu^{\rm Doppler}(z) \sim 0.00323\, z^{-1} \quad , \tag{6.54}$$

in very good agreement, shape-wise, with the corresponding result in [127]. The fact that our prediction is about a factor 1.7 larger than the one of [127] is due, presumably, to the use of somewhat different power spectra (linear or non-linear, with or without baryons).

6.4.3 Comparing theory and observations of the Union 2 data set

Taking the data of the Union 2 compilation [3], we can see the relative size of our theoretical prediction on the Hubble diagram, and especially compare our prediction on the dispersion σ_μ with the

3. We warmly thank Luigi Tedesco for giving us access to these observational data.

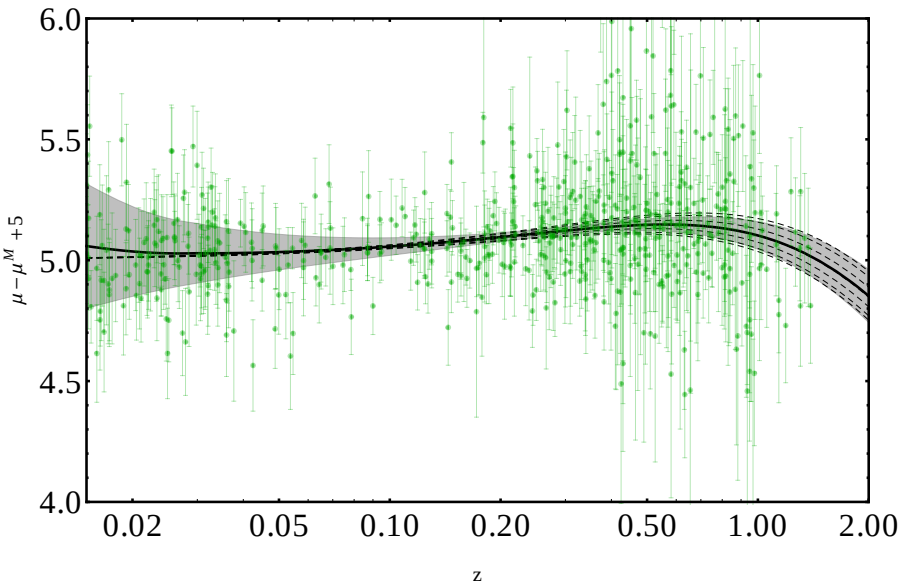

Figure 6.13: Comparison of the Union 2 data set with the theoretical prediction obtained in section 6.4.2 by the use of the non-linear power spectrum and a cut-off $k_{UV} = 30\, h\,\mathrm{Mpc}^{-1}$. We have introduced an arbitrary shift, by a value of 5, to avoid data points with $\overline{\langle\mu\rangle} - \mu^M$ reaching negative values.

data points. This comparison has been done and is presented in Fig. 6.13.

As we can see on this plot by eye, the dispersion on the data is very important compared to the theoretical dispersion that we have computed in this thesis. This difference appears especially clearly for large redshift supernovae. On the other hand, the dispersion we predict for nearby SNe Ia is in pretty good agreement with the data. This seems to indicate that the main source of dispersion in SNe Ia at small redshifts is mainly due to their peculiar velocity. On the other hand, we observe a much serious contamination of data at large redshifts which cannot be explained only by weak lensing (and subleading physical effects that we have pointed out in our calculation of the distance at second order in perturbations). This clearly means that a lot of systematic effects are still to be understood at these distances. The main source of this dispersion could be related to the supernova process itself, but a lot of other contamination effects may be involved. For example, absorption of light by some matter clouds can reduce the luminosity of SNe Ia. Another effect, not taken into account in our study, is the case of strong lensing, where a perturbative treatment breaks down.

We can nevertheless be glad to observe the relative smallness of the effect that we computed with respect to the dispersion of data. Indeed, if data would have turned out to be less dispersed than our theoretical variance, that would have meant that they could not have been used alone for studying dark energy and the whole detected shift in data to upper magnitudes would have to be considered as a statistical effect. The only hope that we would have had then would have been to remove lensing and peculiar velocity contaminations for each observed SN Ia, to disantangle the statistics from the real physical effects. As we said, it is quite fortunate that inhomogeneities do not play such a big role, that is why we discovered dark energy so easily (in practice with a lot of efforts, but from a very simple theoretical framework). Nevertheless, we should stress that the effect is not negligible and has been recently noticed in other independent studies (see [54, 110, 125, 128–130]).

We have thus proved, from our complete second order calculations and the simplifying assumptions described in the last sections, that inhomogeneities were playing a reasonably small effect on the Hubble diagram. Nevertheless, and it is important to be stressed, their effect is much bigger than it could have been thought and it depends strongly on the averaged observable. Also, the study of the induced dispersion in SNe Ia data by the inhomogeneous nature of our Universe seems to give an effect which is small enough to strengthen our confidence in the standard model of cosmology, but big enough to expect a more direct detection of its influence in the next decade. From this perspective, it looks that inhomogeneous models and their influence on observations have a major role to play in the future.

Chapter 7

Summary and conclusions

This thesis has addressed the general problem of lightcone averaging and its implications in cosmology in order to improve the understanding of the Universe in its real inhomogeneous nature.

We have first presented (in **Chapter** 1) the basic facts about the standard model of cosmology. In particular, we gave the equations used to interpret the data within the concordance ΛCDM model (the Friedmann equations). We also described one of the main experimental probes of the standard model, namely the type Ia supernovæ. These astrophysical objects are indeed at the basis of the discovery of dark energy and their conclusions are the strongest model depend ones (compared to CMB or baryonic acoustic oscillations). We also recalled the basic facts about the large scale structure in the Universe.

In **Chapter** 2 we gave the definition of the average of scalar quantities over null hypersurfaces. This definition, first inspired by Buchert's spatial averaging formalism [47, 48], shares common properties with the spatial average defined in a gauge invariant way in [82, 83]. In particular, this definition is gauge invariant, invariant under general coordinate transformations and under reparametrizations of the hypersurfaces composing it. Following this definition, we derived the equivalents of the Buchert-Ehlers commutation rule which stands at the basis of the backreaction problem. This lightcone average, whose importance has been emphasized since a long time, has never been defined in the literature before.

We then presented (in **Chapter** 3) a system of coordinates that simplifies greatly the description of physical quantities on our past light cone. We called these coordinates the "Geodesic Light-Cone" coordinates (GLC) and they turned out to be very useful for a much wider range of applications than the average. These coordinates are very close to another set known in the literature as the observational coordinates [51, 59]. Our gauge in fact corresponds to a further gauge fixing of these latter one in the sense that it only has six arbitrary functions instead of seven in the observational coordinates. It also has other differences, the main one being that the GLC coordinates use the proper time of the observer τ where the observational ones use a distance y inside the past lightcone (either null or spatial). The study of this gauge is likely to bring new interesting results for all applications of light signals in cosmology (see e.g. [131]). The GLC coordinates constitute a system where photons propagate on a constant lightcone $w = w_o$ and fixed angles $\widetilde{\theta}^a$. This nice property which consist in redefining the angles such as to follow the photon path from a source to the observer, as we saw, makes the expression of the redshift z and the luminosity distance d_L in this gauge to be very simple (and directly expressed in terms of the GLC metric components). We also discussed, as simple examples of applications, the link at first order in perturbations between these coordinates and both the synchronous gauge and a LTB model. These GLC coordinates were finally used, and are very well adapted, to the gauge invariant average on the past lightcone as they simplify greatly its expression. They also simplify the generalized Buchert-Ehlers commutation rules. We applied its definition on scalars over hypersurfaces standing at the intersection between the lightcone $w = w_o$ and the spatial $\tau = \text{cst}$ hypersurfaces but then turned to a better adapted definition for observations, i.e. in terms of $z = \text{cst}$ hypersurfaces. A first, formal, application was then made by studying the average of the redshift drift.

Backreaction, or in more common terms the effect of inhomogeneities, vanishes in an homogeneous flat FLRW spacetime and for this reason we computed in **Chapter** 4 the perturbed luminosity-redshift relation. As the inhomogeneities are assumed to be stochastic, their average disappears at first order

when we take their ensemble average. The perturbative calculation of the distance was thus pushed to second order and expressed in terms of the metric elements of the Poisson gauge, as we know the power spectrum of inhomogeneities in that gauge (and not in the GLC). The final expression for the distance is rich in physical terms, including peculiar velocities, SW and ISW effects, lensing, redshift distortions and a very large number of combined effects at second order. This result is very important for cosmology and could be used in a large set of problems. One should remark also that the GLC metric takes an important role in this calculation which is a proof of its interesting properties. Vector and tensor perturbations have not been neglected either, though considered to be of second order (because of their inflationary origin).

We then addressed, in **Chapter** 5, the question of the relative size of the influence from inhomogeneities on the luminosity distance, the flux and the distance modulus. For that we combined the lightcone average with the ensemble average over the stochastic inhomogeneities. In a first preliminary step, we did an incomplete calculation which was based only on (quadratic) first order but enough to reveal the presence of terms that we called the "induced backreaction" terms. These terms are interesting as they show the direct multiplication, within the average, between the expression of the considered scalar and the measure of integration itself. It was also enough to obtain the exact expression of the dispersion of the distance. We gave explicit examples of computation of these terms where an important intermediary result consists of the evaluation of their respective spectral coefficients. We then extended the perturbative expressions of our averaged observables and their variance to the full second order. We found that the correction to the average of the luminosity distance differs from the one of the flux by the (involving flux) contribution $\overline{\langle(\Phi_1/\Phi_0)^2\rangle}$. This correction is proportional to the average of the first order distance correction. It includes, in particular, terms which involve peculiar velocities and lensing. We then proved that vector and tensor perturbations exactly cancel under the angular (lightcone) average, which render them useless for our study. We also properly dealt with the genuine second order terms by relating them to the first order (using [104]).

Taking these theoretical results, we proceeded in **Chapter** 6 to their numerical estimation by assuming an explicit form for the transfer function of the (linear) power spectrum describing inhomogeneities (and sourced by a primordial inflationary spectrum). We first considered, as a warm up exercise, the simple case of a CDM universe with a simple transfer function involving no baryonic fraction. We applied this case to the incomplete calculation of induced backreaction terms and the variance $\overline{\langle\sigma_1^2\rangle}$. This case already showed that two effects dominate over the others in the dispersion. The first one happens at small redshifts and is related to the peculiar velocity of sources (SNe Ia) because of gravitational inhomogeneities, the second one is a lensing effect at large redshifts. This case has also proved that our integrals over the momentum of perturbations is free from both infrared (IR) and ultraviolet (UV) divergences. This result is important and is to be contrasted with the fact that spatial averages lead, in general, to UV divergences. This absence of divergence is intrinsically due to our lightcone average and its gauge invariance. Another conclusion which appeared is that the average of the distance is merely unaffected by inhomogeneities, except at small redshifts where the peculiar velocity terms are also present. However, from this incomplete calculation of quadratic contributions, one could not draw a definitive conclusion on the average.

We then presented the numerical result of the full computation of the luminosity flux, still in the CDM case. We noticed from this quantity that the flux is not affected at large redshifts and its relative correction stays at a rough order of $\sim 10^{-5}$. This revealed that the luminosity flux is a special quantity for which, when averaged over the lightcone, the lensing term in the genuine second order cancels the lensing contribution from the quadratic first order (i.e. in $\overline{\langle\sigma_1^2\rangle}$). This fact is related to the conservation of the intensity of light over the past lightcone. Nevertheless, this flux calculation also showed that inhomogeneities do not create the same effect on the flux as that of a cosmological constant : the correction is both too small and has the wrong sign at large redshifts. The effect on the distance, on the other hand, is always positive but has a characteristic shape due to the combined effects of peculiar velocity and lensing. The correction to the distance in that case can reach a value of $\sim 10^{-2}$ at $z = 2$. The consideration of the distance modulus has shown that the averaged effect is negligible (except as before at small redshifts) but the dispersion implies an equivalent error in the estimate of $\Omega_{\Lambda 0}$ of $\sim 1 - 2\,\%$.

We then addressed the more realistic ΛCDM model and added the effect of baryons (Silk damping) in the transfer function [114]. These two modifications have a direct impact on the linear power spectrum, reducing its values, and decrease the corrections of the flux and the distance by about one order of magnitude. We finally considered the non-linear regime of the power spectrum through the HaloFit model [23, 74]. This had for consequence to strengthen the effect of inhomogeneities, especially on the distance because of its sensitivity to lensing (reaching $\sim 10^{-3}$ at $z = 2$). The distance modulus then showed a shift in its average which stays negligible but a dispersion which corresponds to a possible deviation of $\sim 10\%$ in the value of $\Omega_{\Lambda 0}$. This result is important and shows that inhomogeneities cannot be neglected, especially in the dispersion of observational quantities. We finally compared our theoretical prediction of the dispersion (based on a realistic power spectrum) with the Union2 data set and the recent estimates of velocity and lensing contributions to the intrinsic dispersion of supernovæ data. Our results are found to be in amazingly good agreement with the data and should be confirmed in the next few years by surveys of high cosmological precision.

Our main conclusions, reached with the help of a convenient choice of coordinates defining the GLC gauge and by the introduction of a gauge-invariant prescription to average on the light cone, can be summarized as follows. We found that the combination of the lightcone average with a properly defined ensemble average describing stochastic inhomogeneities around a flat FLRW spacetime, applied to different observables (d_L, $\Phi \propto d_L^{-2}$ and $\mu \sim 5 \log_{10} d_L$), could not mimic a dark energy component. This result can give us trust in the robustness of the standard model of cosmology. On the other hand, averaged inhomogeneities have a much bigger impact than it was naively expected. Their influence is mainly caracterised by peculiar velocities and lensing and they affect the distance more than the flux (which is actually the least affected quantity at large z), by a factor ~ 100 at $z = 2$. This clearly selects the flux as the ideal quantity to be measured but also shows that other observables are much more sensitive to inhomogeneities. Finally we have compared our predictions to the intrinsic dispersion of SNe Ia, showing that part of this dispersion could be explained and that future experiments should be able to detect (and remove) this contaminating signal. As a consequence, this work clearly underlines that though inhomogeneities are very unlikely to explain dark energy (at least within this framework), we can strongly suspect that neglecting their effect will prevent a precise determination of the dark energy parameters in the next decade and could even lead to a misinterpretation of data, for example by the claim of a possible but in fact inhomogeneity-related spacetime dependence of dark energy.

Appendices

Appendix A

Complementary topics

We present in these appendices the detailed study of some particular topics which were too long, or not fully necessary, to be explained within the chapters of this thesis. We start by recalling technical relations of the ADM formalism and use them in a restrictive case. We then provide the basic elements relative to the linear theory of structure formation, including some recall about inflation, fluid equations and gravitational instability. The section which follows presents the main features of cosmological perturbations and their gauge invariant issues. We then present in two consecutive sections the study of the power spectrum in both its linear and non-linear regimes (through the HaloFit model). Finally we give a short derivation of the distance modulus of the Milne universe.

A.1 ADM formalism (Arnowitt-Deser-Misner)

We present here some of the basic equations related to the splitting of spacetime in spatial hypersurfaces, i.e. the so-called ADM formalism. We will mainly follow the explanations of [3] and will make use of this formalism in Sec. A.1.3.

A.1.1 The ADM metric

Let us try to build up a 4-dimensional geometry from 3-dimensional hypersurfaces in the Minkowski spacetime $\mathcal{M}_4$ (described by coordinates (τ, X^i)). One starts with a lower hypersurface at time t for which we know the inside geometry given by the 3-metric g_{ij} and the elementary distance is given by $g_{ij}(t, x^i)dx^i dx^j$. Putting an upper spatial hypersurface describing our geometry at time $t+dt$, one has a large variety of choices to fix the shape of it. One can first set this new hypersurface at a "distance above" the lower one. This is done by setting that the proper time, i.e. the time orthogonal to the spatial 3-hypersurface Σ, is equal to $\tau = N(t, x^i)dt$ where N is called the *lapse function*. Having done this first necessary step does not fix the geometry inside this upper 3-hypersurface and one needs to describe how spatial coordinates x^i change when we go from the lower to the upper hypersurfaces. This is given by introducing a 3-vector called the *shift vector* and such that $x^i_{upper}(x^k) = x^i - N^i(t, x^k)dt$. We thus obtain the line element in the upper geometry, and more generally in all hypersurface built up according to this framework:

$$ds^2_{ADM} = g^{ADM}_{\mu\nu} dx^\mu dx^\nu = -N^2 dt^2 + g_{ij}(dx^i + N^i dt)(dx^j + N^j dt) \tag{A.1}$$

$$= -\begin{pmatrix} \text{proper time from lower} \\ \text{to upper 3-geometry} \end{pmatrix}^2 + \begin{pmatrix} \text{proper distance} \\ \text{in base 3-geometry} \end{pmatrix}^2 \tag{A.2}$$

One should understand also that t is the time inside the 3-geometry (defining this hypersurface). As a consequence, the upper hypersurface inherits from the time $t + dt$ inside its hypersurface, but the proper distance used in $\mathcal{M}_4$ to set the "time distance" between the two is $d\tau = N dt$.

We thus have the metric form for $g^{ADM}_{\mu\nu}$, and its inverse $g^{\mu\nu}_{ADM}$, in (t, x^i) coordinates:

$$g^{ADM}_{\mu\nu} = \begin{pmatrix} -(N^2 - g_{ij}N^iN^j) & N_i \\ N_j & g_{ij} \end{pmatrix} \quad , \quad g^{\mu\nu}_{ADM} = \begin{pmatrix} -\frac{1}{N^2} & \frac{N^i}{N^2} \\ \frac{N^j}{N^2} & g^{ij} - \frac{N^iN^j}{N^2} \end{pmatrix} \quad , \tag{A.3}$$

where $g_{ij} = g_{ji}$ and we have used that $N_i = g_{ij}N^j$ and g^{ij} is the inverse metric of g_{ij} in the 3-hypersurface. The unit timelike covariant vector n_μ normal to the constant-t hypersurface and its contravariant counterpart n^μ are given by

$$n_\mu = (-N, \vec{0}) \quad \text{and} \quad n^\mu = (1/N, -N^i/N) \quad \text{such that} \quad n_\mu n^\mu = -1 \quad . \tag{A.4}$$

A.1.2 The extrinsic curvature

Let us illustrate now the role played by the extrinsic curvature tensor K_{ij} that we will encounter in the next section. For that we consider an elementary spatial displacement on the hypersurface given by the ADM foliation:

$$d\ell = \mathbf{e}_i \, dx^i \quad . \tag{A.5}$$

In this equation, $\mathbf{e}_i$ are the three basis tangent vectors ($\mathbf{e}_i \equiv \partial_i$) dual to the three coordinate 1-forms dx^i. A tangent vector field $\mathbf{T}$ is then defined simply by

$$\mathbf{T} = \mathbf{e}_i T^i \quad , \quad \mathbf{T} \cdot \mathbf{e}_i = T^j(\mathbf{e}_i \cdot \mathbf{e}_j) = T^j g_{ij} = T_i \quad . \tag{A.6}$$

The covariant derivative of $\mathbf{T}$ in the i-th direction is then given by the expression:

$${}^{(4)}\nabla_{\mathbf{e}_i}\mathbf{T} \equiv {}^{(4)}\nabla_i \mathbf{T} = {}^{(4)}\nabla_i(\mathbf{e}_j T^j) = \mathbf{e}_j \frac{\partial T^j}{\partial x^i} + {}^{(4)}\Gamma^\mu_{ji}\, \mathbf{e}_\mu \, T^j \quad , \tag{A.7}$$

where the last term has been obtained by using the identity: ${}^{(4)}\nabla_i \mathbf{e}_j = {}^{(4)}\Gamma^\mu_{ji}\, \mathbf{e}_\mu$. The covariant derivative of T_i in the j-th direction, intrinsic to the 3-dimensional spatial geometry, is given by

$$T_{i\,||\,j} = \mathbf{e}_j {}^{(3)}\nabla_i \mathbf{T} = \frac{\partial T_i}{\partial x^j} - {}^{(3)}\Gamma_{kji} T^k \quad , \tag{A.8}$$

where the 3-dimensional connection can be expressed in terms of the three basis vectors and the covariant 3-derivative: ${}^{(3)}\Gamma_{kji} \equiv \mathbf{e}_k {}^{(3)}\nabla_i \mathbf{e}_j$.

Let us consider the spatial hypersurface Σ on which we have a normal (timelike) vector $\mathbf{n}$. When we consider this vector at a spatial position ℓ and we do an infinitesimal transportation of this vector, parallely to itself, to another point $\ell + d\ell \in \Sigma$, the vector we obtain is not anymore orthogonal to Σ. The substraction of this transported vector to the normal vector at this new location, called $d\mathbf{n}$, is related to the extrinsic curvature by

$$d\mathbf{n} = -\mathbf{K}(d\ell) \;\; \text{(as an operator)} \quad \Rightarrow \quad {}^{(4)}\nabla_i \mathbf{n} = -\mathbf{K}(\mathbf{e}_i) = -K^j_{\ i}\mathbf{e}_j \;\; \text{(with components)} \quad . \tag{A.9}$$

One can easily show that this tensor, or more precisely $K_{ij} = K^k_{\ i}\, g_{kj} = K^k_{\ i}(\mathbf{e}_k \cdot \mathbf{e}_j)$, is symmetric, i.e. $K_{ij} = K_{ji}$. We understand by this reasoning that the extrinsic curvature of the 3-dimensional hypersurface Σ has a meaning only when it is embedded in a 4-dimensional geometry. We remark also that it is defined in such a way that it is negative when the vectors $\mathbf{n}$ at two neighbouring positions tend to point to the same future event, i.e. when the spatial hypersurfaces tend to contract (and not to expand, in which case the extrinsic curvature is positive).

The transportation of the unit vectors $\mathbf{e}_i$ can be written in terms of the extrinsic curvature and the connection inside the hypersurface, by the so-called Gauss-Weingarten equation:

$${}^{(4)}\nabla_i \mathbf{e}_j = K_{ij} \frac{\mathbf{n}}{\mathbf{n}\cdot\mathbf{n}} + {}^{(3)}\Gamma^h_{ji}\, \mathbf{e}_h \quad . \tag{A.10}$$

The parallel transportation of a vector $\mathbf{T}$ inside the 4-geometry (i.e. parallel to the geometry of the spacetime) can now be obtained directly by the expression:

$${}^{(4)}\nabla_i \mathbf{T} = T^j_{\ ||\,i}\, \mathbf{e}_j + K_{ij} T^j \frac{\mathbf{n}}{\mathbf{n}\cdot\mathbf{n}} \quad . \tag{A.11}$$

Using the covariant ADM representation of $\mathbf{n}$, where $n_\mu = (N, \vec{0})$, we can show that K_{ij} can be expressed in terms of the shift vector and the metric of the spatial hypersurface, by the ADM formula:

$$K_{ij} = \frac{1}{2N}\left[N_{i\,||\,j} + N_{j\,||\,i} - \frac{\partial g_{ij}}{\partial t} \right] \quad . \tag{A.12}$$

By the use of a self-dual basis, with the vector basis being $(\mathbf{e}_0, \mathbf{e}_i) \equiv (\mathbf{n}, \mathbf{e}_i) = (N^{-1}(\partial_t - N^m\partial_m)\ ,\ \partial_i)$ and the associated basis of 1-forms $(\mathbf{w}^0, \mathbf{w}^i) = (N\mathrm{d}t\ ,\ \mathrm{d}x^i + N^i\mathrm{d}t) = ((\mathbf{n}\cdot\mathbf{n})\mathbf{n}\ ,\ \mathrm{d}x^i + N^i\mathrm{d}t)$, one can compute the terms ${}^{(4)}\nabla_{\mathbf{e}_j}{}^{(4)}\nabla_{\mathbf{e}_k}\mathbf{e}_i$ and ${}^{(4)}\nabla_{\mathbf{e}_k}{}^{(4)}\nabla_{\mathbf{e}_j}\mathbf{e}_i$. Using now the action of the 4-dimensional Riemann curvature as an operator, we have by definition:

$$\mathcal{R}(\mathbf{e}_i, \mathbf{e}_j)\mathbf{e}_k = {}^{(4)}\nabla_i{}^{(4)}\nabla_j\mathbf{e}_k - {}^{(4)}\nabla_j{}^{(4)}\nabla_i\mathbf{e}_k - {}^{(4)}\nabla_{[\mathbf{e}_i,\mathbf{e}_j]}\mathbf{e}_k \quad , \tag{A.13}$$

where the last term is zero as $[\mathbf{e}_i, \mathbf{e}_j] = 0 \ \ \forall\ i, j$. We then obtain the expression of the 4-dimensional Riemann tensor:

$$\mathcal{R}(\mathbf{e}_j, \mathbf{e}_k)\mathbf{e}_i = \left(K_{ik\,||\,j} - K_{ij\,||\,k}\right)\frac{\mathbf{n}}{\mathbf{n}\cdot\mathbf{n}} + \left[(\mathbf{n}\cdot\mathbf{n})^{-1}(K_{jk}K_i^m - K_{ij}K_k^m) + R_{ijk}^m\right]\mathbf{e}_m \tag{A.14}$$

From this expression, one obtain the time and space components of the curvature tensor, the Gauss-Codazzi equations, by:

$$\begin{aligned} {}^{(4)}R^0_{ijk} &= \frac{1}{\mathbf{n}\cdot\mathbf{n}}{}^{(4)}R_{0ijk} = -\frac{1}{\mathbf{n}\cdot\mathbf{n}}\left(K_{ij\,||\,k} - K_{ik\,||\,j}\right) \quad , & \text{(A.15)}\\ {}^{(4)}R^m_{ijk} &= {}^{(3)}R^m_{ijk} + \frac{1}{\mathbf{n}\cdot\mathbf{n}}\left(K_{ij}K_k^m - K_{ik}K_j^m\right) \quad . & \text{(A.16)} \end{aligned}$$

One can then directly deduce the following components of the Einstein tensor:

$$\begin{aligned} -G^0{}_0 &= \frac{1}{2}R - \frac{1}{2}(\mathbf{n}\cdot\mathbf{n})^{-1}\left[(\mathrm{Tr}\,\mathbf{K})^2 - \mathrm{Tr}(\mathbf{K}^2)\right] \quad , & \text{(A.17)}\\ G^0{}_i &= -\frac{1}{\mathbf{n}\cdot\mathbf{n}}\left[K^m_{i\,||\,m} - (\mathrm{Tr}\,\mathbf{K})_{||\,i}\right] \quad , & \text{(A.18)} \end{aligned}$$

where we have:

$$\mathrm{Tr}(\mathbf{K}) = g^{ij}K_{ij} = g_{ij}K^{ij} = K^j{}_j \equiv K \qquad , \qquad \mathrm{Tr}(\mathbf{K}^2) = K_j{}^mK_m^j \quad , \tag{A.19}$$

and where the trace of K_{ij} denoted by K should not be confused with the similar symbol denoting the intrinsic (and not the extrinsic) curvature in Friedmann equations (such as Eq. (1.12)).

The component $G^0{}_0$ is a measure of curvature independent from how curved one cuts a spacelike slice, it determines how mass (or energy) fixes the curvature. $G^0{}_i$ determines the transfer of momentum by the geometry to the matter content. On the other hand, $G^i{}_j$ is hard to evaluate (except in the particular case of *Gaussian normal coordinates*) and the dynamics of the 6 components that it contains is evaluated by an Hamiltonian formalism.

A.1.3 Einstein's equations in ADM

One can address the problem of the dynamics of the Universe inside the ADM formalism and consider the coordinates (t, x^i) in a fixed gauge. Choosing a synchonous form for this gauge, i.e. taking $N = 1$ and $N^i = 0$, the line element is given by:

$$ds^2 = -dt^2 + g_{ij}dx^idx^j \quad . \tag{A.20}$$

One considers a fluid with density ρ, possibly pressure p and a velocity u^μ. We can also define a projection tensor $h_{\mu\nu}$ into the hypersuface orthogonal to $n_\mu = (-1, \vec{0}\,)$ and satisfying:

$$h_{\mu\nu} = g_{\mu\nu} + n_\mu n_\nu \quad , \quad h_{\mu\nu}n^\nu = 0 \quad . \tag{A.21}$$

One can see then that:

$$h_{00} = 0 \quad , \quad h_{0i} = 0 \quad , \quad h_{ij} = g_{ij} \quad . \tag{A.22}$$

In Sec. 2.1.1 we do the further assumption that u_μ is also orthogonal to the spatial hypersurfaces given by the foliation (static fluid), so we can also interpret $h_{\mu\nu}$ as the projection tensor on the hypersurfaces orthogonal to u_μ. Here this vector u_μ is kept general but we define a density ϵ and a pressure π (the ADM energy density and ADM pressure) which are given by the projections: $\epsilon = T_{\mu\nu}n^\mu n^\nu$ and

$\pi = \frac{1}{3}T_{\mu\nu}h^{\mu\nu}$ (see Eq. (2.73)). These quantities will thus coincide with ρ and p in the limit $u_\mu \to n_\mu$ taken in Sec. 2.1.1 (see also the discussion about the "tilt angle" in Sec. 2.1.4). We can also define the so-call extrinsic curvature tensor (or "second fundamental form" of the constant-t hypersurface) :

$$K_{ij} \equiv -h_i^\alpha h_j^\beta \nabla_\beta n_\alpha \quad . \tag{A.23}$$

One has from the considerations of Eq. (A.17), (A.18) and (A.19) that the Einstein equations (see Eq. (1.15)) and the continuity equation reduce to the constraint equations

$$\frac{1}{2}\left(\mathcal{R} + K^2 - K^i{}_j K^j{}_i\right) = 8\pi G(\epsilon + 3\pi) + \Lambda \quad , \tag{A.24}$$

$$K^i{}_{j\,||\,i} - K_{|\,j} = 0 \quad , \tag{A.25}$$

and the evolution equations

$$\dot{\rho} = K(\epsilon + \pi) \quad , \tag{A.26}$$

$$(g_{ij})^\bullet = -2\, g_{ik} K^k{}_j \quad , \tag{A.27}$$

$$(K^i{}_j)^\bullet = K K^i{}_j + \mathcal{R}^i{}_j - (4\pi G(\epsilon + 3\pi) + \Lambda)\, \delta^i{}_j \quad , \tag{A.28}$$

where $\mathcal{R} \equiv \mathcal{R}^i{}_i$ and $K \equiv K^i{}_i$ are the traces of respectively the spatial Ricci tensor $\mathcal{R}_{ij}$ and the extrinsic curvature K_{ij}.

Considering the covariant derivative of the vector $\mathbf{n}$, normal to the spatial hypersurfaces, one has in general the result :

$$n_{\mu;\nu} = \Theta_{\mu\nu} - a_\mu n_\nu \quad \text{with} \quad a_\mu = n_{\mu;\nu} n^\nu \ .$$

In the RHS of this expression, the first term is the so-called expansion tensor and the second term involves the peculiar acceleration of the world lines defined by $\mathbf{n}$. When we consider that this vector $\mathbf{n}$ describes a fluid or an observer in geodetic motion, one then has $a_\mu = n_{\mu;\nu} n^\nu = 0$. This is the case we will consider here. The quantity $n_{\mu;\nu}$ is thus equal to the expansion tensor, defined as follows :

$$\Theta_{\mu\nu} = \frac{1}{3} h_{\mu\nu}\Theta + \sigma_{\mu\nu} + \omega_{\mu\nu} \quad , \tag{A.29}$$

where the three RHS terms are the expansion scalar, the shear tensor and the vorticity tensor, defined as follows :

$$\Theta \equiv \nabla_\mu n^\mu \quad , \quad \sigma_{\mu\nu} \equiv h_\mu^\alpha h_\nu^\beta \left(\nabla_{(\alpha} n_{\beta)} - \frac{1}{3} h_{\alpha\beta}\Theta\right) \quad , \quad \omega_{\mu\nu} \equiv h_\mu^\alpha h_\nu^\beta \nabla_{[\alpha} n_{\beta]} \quad . \tag{A.30}$$

We could assume from now that the vorticity tensor is null, but we will keep this tensor in the calculations to show the similar roles played by the shear and the vorticity tensors in these calculations.

The shear tensor is symmetric and traceless as

$$\sigma^\mu{}_\mu = h^{\alpha\beta}\nabla_\alpha n_\beta - \frac{1}{3} h^\alpha{}_\alpha \Theta = \Theta - \frac{1}{3}(3\Theta) = 0 \quad , \tag{A.31}$$

where we have used the symmetry of $h^{\alpha\beta}$, $h^\alpha{}_\alpha = 3$ and $n^\beta \nabla_\alpha n_\beta = 0$. It is also the case for the vorticity tensor which is anti-symmetric, and traceless as

$$\omega^\mu{}_\mu = h^{\alpha\beta}\nabla_{[\alpha} n_{\beta]} = 0 \quad , \tag{A.32}$$

because $h^{\alpha\beta}$ is symmetric in $\alpha \leftrightarrow \beta$ whereas $\nabla_{[\alpha} n_{\beta]}$ is antisymmetric. One can obtain the vorticity vector from its tensor :

$$\omega^\mu = \frac{1}{2} n_\alpha \epsilon^{\alpha\mu\beta\gamma} \omega_{\beta\gamma} \quad . \tag{A.33}$$

In the ADM formalism, one can deal with spatial quantities only and the extrinsic curvature is directly linked to the spatial components of the expansion tensor $\Theta_{\mu\nu}$ by

$$K_{ij} = -\Theta_{ij} = -\left(\frac{1}{3} h_{ij}\Theta + \sigma_{ij} + \omega_{ij}\right) \quad . \tag{A.34}$$

Given that $\sigma^0{}_0 = 0 = h^0{}_0$ we have that the 3-dimensional trace of $\sigma_{\mu\nu}$ and $\omega_{\mu\nu}$ are also zero, leading to the result :

$$K = -\Theta \quad . \tag{A.35}$$

We will also use, in the following, the definitions

$$\sigma^2 \equiv \frac{1}{2}\sigma^i{}_j\sigma^j{}_i = \frac{1}{4}\left(\nabla_\alpha n^\beta \nabla_\beta n^\alpha + \nabla_\alpha n^\beta \nabla^\alpha n_\beta\right) - \frac{\Theta^2}{3} \quad , \tag{A.36}$$

$$\omega^2 \equiv \frac{1}{2}\omega^i{}_j\omega^j{}_i = \frac{1}{4}\left(\nabla_\alpha n^\beta \nabla_\beta n^\alpha - \nabla_\alpha n^\beta \nabla^\alpha n_\beta\right) \quad . \tag{A.37}$$

The quantity σ is called the rate of shear and represents how much a geodesic bundle is stretched out. The quantity ω similarly represents the rate of rotation of the bundle. Let us notice also that the literature employs sometimes the definition $\omega^2 \equiv \frac{1}{2}\omega_{ij}\omega^{ij}$. As ω_{ij} is an anti-symmetric tensor, this leads to a sign difference for the terms in ω^2 with respect to our notations here [1].

Taking the trace of Eq. (A.28) and making use of the expression of K_{ij} given in Eq. (A.34), we obtain the so-called *Raychaudhuri's equation*:

$$\dot{\Theta} + \frac{\Theta^2}{3} + 2\,\sigma^2 + 2\,\omega^2 + 4\pi G(\epsilon + 3\pi) - \Lambda = 0 \quad . \tag{A.38}$$

To get this expression we used the Eq. (A.24) which is the so-called *Hamiltonian constraint*:

$$\frac{1}{2}\mathcal{R} + \frac{1}{3}\Theta^2 - \sigma^2 - \omega^2 = 8\pi G(\epsilon + 3\pi) + \Lambda \quad . \tag{A.39}$$

We should notice that the Eq. (A.38) and the continuity Eq. (A.26) are analog in the Newtonian regime. The Hamiltonian constraint (A.39), however, has no Newtonian equivalent (and is at the source of the backreaction problem, as seen in Sec. 2.1). Considering also the Eq. (A.28), we can write the general result :

$$(\sigma^i{}_j + \omega^i{}_j)^{\bullet} + \Theta(\sigma^i{}_j + \omega^i{}_j) = -\left(\mathcal{R}^i{}_j - \frac{1}{3}\delta^i{}_j\mathcal{R}\right) \quad , \tag{A.40}$$

in which we can replace $\mathcal{R}$ by the use of Eq. (A.24).

The two constraint equations – Eq. (A.24), (A.25) – and the three dynamical equations – Eq. (A.26), (A.27) and (A.28) – are finally rewritten by the use of Eq. (A.34) as :

$$\frac{1}{2}\mathcal{R} + \frac{1}{3}\Theta^2 - \sigma^2 - \omega^2 = 8\pi G(\epsilon + 3\pi) + \Lambda \quad , \tag{A.41}$$

$$\sigma^i{}_{j\,||\,i} + \omega^i{}_{j\,||\,i} = \frac{2}{3}\Theta_{|\,j} \quad , \tag{A.42}$$

$$\dot{\rho} = -\Theta(\epsilon + \pi) \quad , \tag{A.43}$$

$$(g_{ij})^{\bullet} = 2g_{ik}\sigma^k{}_j + 2g_{ik}\omega^k{}_j + \frac{2}{3}\Theta g_{ij} \quad , \tag{A.44}$$

$$(\sigma^i{}_j + \omega^i{}_j)^{\bullet} = -\Theta(\sigma^i{}_j + \omega^i{}_j) - \mathcal{R}^i{}_j + \frac{2}{3}\delta^i{}_j\left[\sigma^2 + \omega^2 - \frac{\Theta^2}{3} + 8\pi G(\epsilon + 3\pi) + \Lambda\right] \tag{A.45}$$

We recall that $||i$ denotes the covariant derivative with respect to the 3-dimensional spatial metric g_{ij} and that $|i$ denotes the simple derivative ∂_i. For Θ, which is a scalar, we have $\Theta_{||i} = \Theta_{|i}$.

1. This last definition of the literature is useful to understand that the rate of shear is a quantity which gravitates, tending to gather the geodesic bundle, whereas the vorticity anti-gravitates. In our case, keeping the symmetry between ω^2 and σ^2, which play the same role, is more useful.

A.2 Linear theory of structure formation

We will give in this section the necessary elements to understand the basic principles about structure formation. For that we will mainly follow the review of [132]. These notions are important to better understand the considerations relative to the transfer function and the power spectrum.

A.2.1 Some words about inflation

General facts

The first seeds of matter fluctuations that we observe today in the large scale structure are believed to emerge from quantum fluctuations in the primordial states of the Universe. This very important fact is at the basis of the construction of the matter power spectrum. It is thus very important, in the context of this thesis, to recall some of the basic facts about inflation.

The first thing to notice is that inflation is not a precise model, but more a scenario created to solve several problems, opening the possibility of different precise realizations of this scenario. From CMB measurements, it appears that the cosmological curvature parameter today, Ω_{K0}, is very close to zero and our Universe is very close to be flat. In other words, it appears that we live in a Universe which has a curvature radius much bigger than its apparent radius. If we look back in the past, this flatness is even more puzzling. Indeed, the curvature parameter can be written as

$$\Omega_K(t) = -K\left(\frac{d_{\rm H}(t)}{R_0}\right)^2 \quad \text{with} \quad d_{\rm H}(t) \equiv \frac{c}{Ha} = \frac{c}{\dot{a}} \quad , \tag{A.46}$$

where $K = \{\ -1, 0, 1\ \}$ depending on the real nature of our Universe. $d_{\rm H}(t)$ is the "Hubble length" (roughly the observable radius of our Universe), or more commonly the *Hubble horizon*, and R_0 is the curvature radius of our Universe. If we forget about dark energy for a while, as it appeared only recently in the history of the Universe, we realize that going further in the past is going through the eras of matter and radiation domination. In these periods, the Hubble length $d_{\rm H}(t)$ is increasing with t (going from past to present), because $\dot{a}(t)$ is decreasing (the expansion is decelerating). We thus realize that our Universe needed to be very close to flatness in its earlier times. Why is that so ? This question is called the *flatness problem*.

The second problem that inflation tackles is the following one. From the expression of $d_{\rm H}$, which corresponds to the causal horizon between two points, and its value at the time of decoupling (happening for $z_{\rm dec} \sim 1100$), the angular parts of the sky that have been able to interact in their past should not exceed $1°$. Nevertheless, the relative differences in temperature over the whole sky observed in the CMB are less than $\sim 10^{-5}$. This homogeneity in temperatures cannot be explained *a priori* and this is called the *horizon problem*.

The concordance model does not give any answer to that questions and this is why we need an inflation mechanism to satisfy this observable facts. It also gives clues of why we do not observe any topological defects (such as cosmic strings) and gives the initial seeds for the formation of structures.

Inflation is a stage of the Universe where the expansion is accelerating, $\ddot{a}(t) > 0$, thus having $\dot{d}_{\rm H}(t) < 0$ leading to $\partial_t|\Omega_K(t)| < 0$. As a consequence, inflation reduces the amount of curvature of the Universe and, if it last long enough, brings it very close to zero and solves the flatness problem. It also solves the horizon problem in the following way. By definition of the comoving horizon length $d_{\rm H}$, there are no points in interaction at time t if they are separated by a spatial distance larger than $d_{\rm H}(t)$. Under this length, spatial regions are in causal contact and can thus interact. As a consequence, in the recent (matter and radiation dominated) history of the Universe, where $d_{\rm H}(t)$ is increasing, the large scale modes are the last ones to be "freed"[2]. They would have no particular reasons to keep the same properties, such as temperature, if inflation did not exist. Indeed, the fact that we observe an homogeneity in temperature at large scales in the CMB makes us believe that these modes were previously in causal contact. Again, that contact is fulfilled if inflation last long enough because

2. The dark energy period is ignored as it concerns recent times and it acts on the modes in an inflationary-like way.

inflation is a period where $d_{\rm H}(t)$ is decreasing with time and thus is big enough if it last for long. For this reason inflation is also an answer to the horizon problem.

So how long inflation should last ? It has to last long enough to satisfy observational constraints. To explain that, let us consider that the inflationary period is correctly described by a de Sitter phase (which is an approximation as, because it has H constant, such a phase cannot end by itself). Let us also consider that inflation starts at an initial time t_i where $|\Omega_K| \sim 1$ and ends at a final time $t_f > t_i$ (where $|\Omega_K|$ is minimal). The curvature can then grow again in the decelerated phase of the Universe and we assume that it grows up to $|\Omega_K| \sim 1$ today (at t_0). Assuming that strict extremal conditions, we have that all the inflaton[3] energy density ρ_ϕ is constant between t_i and t_f and is then entirely converted into radiation. We thus get that the ratio, between t_0 and t_i, of the curvature density – $\rho_K \equiv -3K/(8\pi G\, a^2)$ – is (see [133]) :

$$\left(\frac{a_i}{a_0}\right)^2 = \frac{\rho_K(a_0)}{\rho_K(a_i)} = \frac{\rho_r(a_0)}{\rho_\phi(a_i)} = \frac{\rho_r(a_0)}{\rho_\phi(a_f)} = \frac{\rho_r(a_0)}{\rho_r(a_f)} = \left(\frac{a_f}{a_0}\right)^4 \quad . \tag{A.47}$$

We can introduce a quantity called the *e-fold number* : $N \equiv \ln a$. The equality in thus recast into :

$$N_f - N_i \;=\; N_0 - N_f \quad . \tag{A.48}$$

In the general case, we can have $|\Omega_K| > 1$ at t_i and we observe that $|\Omega_K| \ll 1$ today. The consequence of this is that the second equality sign in Eq. (A.47) is an inequality sign, leading to the condition :

$$N_f - N_i \;\geq\; N_0 - N_f \quad . \tag{A.49}$$

This identity means that we need more e-folds of expansion during inflation than after to satisfy observations. We know that today $\rho_r(a_0) \simeq (10^{-4}\ \text{eV})^4$. We also know that the energy scale of inflation is $< \rho_r(a_f) \simeq (10^{16}\ \text{GeV})^4$ (otherwise observed CMB anisotropies would have already revealed gravitational waves) and this scale is also $> (1\ \text{TeV})^4$ from particle physics. These experimental constraints lead to the following condition on the time duration of inflation :

$$\Delta N \equiv N_f - N_i = \ln\left(\frac{\rho_r(a_f)}{\rho_r(a_0)}\right)^{1/4} \;\in\; [37, 67] \quad . \tag{A.50}$$

Slow-roll inflation

There are a lot of different inflation scenarios nowadays, but the simplest one to achieve the necessary behaviour is simply a single scalar field model. Indeed, if we consider an homogeneous scalar field $\phi(t)$ – the *inflaton* – described by a potential $V(\phi)$ and a kinetic energy $\dot\phi^2/2$, we can define some effective density and pressure as :

$$\rho_\phi = \frac{1}{2}\dot\phi^2 + V(\phi) \qquad , \qquad p_\phi = \frac{1}{2}\dot\phi^2 - V(\phi) \quad . \tag{A.51}$$

This field, non-interacting in an homogeneous Universe, obeys the equation of motion (EoM) :

$$\ddot\phi + 3H\dot\phi + V'(\phi) = 0 \quad . \tag{A.52}$$

We should notice the friction term $3H\dot\phi$ which shows that an expansion of space decreases $\dot\phi$, lowering at the same time the density and pressure of the field. The equation of state for this inflationary field is, by definition :

$$-1 \leq w_\phi(t) \equiv \frac{p_\phi(t)}{\rho_\phi(t)} \leq 1 \quad . \tag{A.53}$$

As we said, it is not necessary for inflation to be a really precise model. In particular, it is not necessary to give a precise expression for the potential $V(\phi)$ if it gives a long enough lasting inflationary

3. The inflaton is the particle associated to the inflation mechanism (see after).

period. A sufficient approximation is given by the slow-roll inflation description. If we assume that ϕ takes slowly varying values, i.e. that $\dot{\phi}^2$ always stays negligible with respect to $V(\phi)$, and that its varying speed is also always small – i.e. that $|\ddot{\phi}| \ll |3H\dot{\phi}|, |V'(\phi)|$ – we get that w_ϕ is close to -1 and thus we have an inflationary field which behaves like a cosmological constant (and an expansion which is exponential). Taking $K = 0$, the Friedmann equation and the EoM give us

$$H^2 = \frac{8\pi G}{3} V(\phi) \quad , \quad 3H\dot{\phi} + V'(\phi) = 0 \quad . \tag{A.54}$$

We can then define the so-called *slow-roll parameters*:

$$\epsilon \equiv \frac{1}{16\pi G}\left(\frac{V'}{V}\right)^2 = -\frac{\dot{H}}{H^2} \quad , \quad |\epsilon| \ll 1 \quad ; \quad \eta \equiv \frac{1}{8\pi G}\frac{V''}{V} = \epsilon - \frac{\ddot{\phi}}{H\dot{\phi}} \quad , \quad |\eta| \ll 1 \quad . \tag{A.55}$$

We can also notice that the condition $(\epsilon, \eta) \ll (1,1)$ is equivalent to $(|V'/V|, |V''/V|) \ll (1,1)$ and thus a flat enough potential satisfies these slow-roll conditions. More generally, the condition to have an inflationary phase is given by $w_\phi < -1/3$, which corresponds to $\dot{\phi}^2 < V(\phi)$, or equivalently $\rho_\phi + 3\,p_\phi < 0$. Consequently, a period of inflation, as the period of dark energy domination, violates the strong energy condition $\rho + 3\,p > 0$.

Inflation is a very interesting subject on its own, but it will only appear in this work through its prediction of the primordial power spectrum with especially the fact that its spectral index n_s is slightly less than 1. It also implies that perturbations are Gaussian and adiabatic.

A.2.2 Fluid equations and Newtonian approximation

In the Universe that we observe today, the density constrast for matter, namely δ, takes a very wide range of values (from very high values in neutron stars to very low ones for the voids in the Universe, taking a simple volume average). Physically, we can see this quantity in Fourier space with:

$$\delta(t, \mathbf{k}) = \delta_{\mathrm{L}}(t, \mathbf{k}) + \delta_{\mathrm{NL}}(t, \mathbf{k}) \quad , \tag{A.56}$$

where δ_{L} can be seen as the contribution to δ coming from linearized equations whereas δ_{NL} takes the rest of contributions into account, especially the contributions of different modes to the mode $\mathbf{k}$.

To obtain the general behaviour of $\delta_{\mathrm{L}}(t, \mathbf{k})$, we are now going to elaborate on the linear perturbation theory from the fluid perspective. We consider a Universe filled with an inhomogeneous fluid of matter with density $\rho(t, \mathbf{r})$, velocity field $\mathbf{v}(t, \mathbf{r})$ and pressure $p(t, \mathbf{r})$. Because this fluid is made of a massive content, it reacts and contributes to a gravitational potential $\Phi(t, \mathbf{r})$ present in this Universe, and it also has an entropy per unit mass $S(t, \mathbf{r})$. Note that we are using here a radial coordinate $\mathbf{r}$ which corresponds to a physical coordinate (in opposition to comoving coordinates, as we will see later).

In Newtonian physics, the evolution of the 7 parameters $X \equiv \{X_i\} = \{\rho, \mathbf{v}, p, \Phi, S\}$ describing the fluid of matter, is given by:

$$\partial_t \rho + \nabla \cdot (\rho \mathbf{v}) = 0 \qquad \text{(continuity eq.)} \quad , \tag{A.57}$$

$$\partial_t \mathbf{v} + (\mathbf{v} \cdot \nabla)\mathbf{v} = -\frac{\nabla p}{\rho} - \nabla \Phi \qquad \text{(Euler eq.)} \quad , \tag{A.58}$$

$$\nabla^2 \Phi = 4\pi G\, \rho \qquad \text{(Poisson eq.)} \quad , \tag{A.59}$$

$$\partial_t S + (\mathbf{v} \cdot \nabla) S = 0 \qquad \text{(entropy conservation)} \quad . \tag{A.60}$$

This system of equations is actually not closed and for this reason we need to add up an extra equation given by the (general) equation of state:

$$p = p\,(\rho, S) \quad . \tag{A.61}$$

From now on, the 7 unknown functions can be found, at least in principle. We can notice that these equations are non-relativistic equations and, consequently, implicitly assume that $|\mathbf{v}| \ll c$ and $p \ll \rho c^2$. It is also assumed that there are no bifurcations in this fluid. In other words, we say that the fluid is in a single stream regime, i.e. fluid particles that are close to each other at a certain time, stay

close in time (let say heuristically that the distance that separate them is always much less than the distance they traveled). This is a very good approximation for dark matter particles which interact very weakly with baryonic matter and radiation.

Splitting the 7 quantities X_i in background plus first order perturbations:

$$X_i = \overline{X_i} + \delta X_i \quad , \tag{A.62}$$

we can solve this system perturbatively and find, at zeroth order and assuming $\overline{p} = 0$:

$$\dot{\overline{\rho}} + 3H\overline{\rho} = 0 \quad , \quad \partial_t \overline{\mathbf{v}} + (\overline{\mathbf{v}} \cdot \nabla)\overline{\mathbf{v}} = -\nabla\overline{\Phi} \quad , \quad \nabla^2\overline{\Phi} = 4\pi G\,\overline{\rho} \quad , \quad \partial_t \overline{S} + (\overline{\mathbf{v}} \cdot \nabla)\overline{S} = 0 \quad . \tag{A.63}$$

Taking the divergence of the second relation above and using the Hubble relation at zeroth order:

$$\overline{\mathbf{v}} = H(t)\,\mathbf{r} \quad \text{gives rise to} \quad \dot{H} + H^2 = -\frac{4\pi G}{3}\overline{\rho} \quad , \tag{A.64}$$

where we have used the Poisson equation (A.59). This last equation is the Friedmann equation for a pressureless matter background fluid. In order to take into account a fluid with pressure, we need to study more closely the situation we have. Indeed, if in the Universe that we are studying there are other energy contributions interacting with our matter fluid only through gravitation, and if these contributions are homogeneous, they will only enter as an homogeneous term in the Poisson equation. They will thus enter only at the unperturbed level and will not affect orders in perturbations. On the other hand, they will modify the expansion of the Universe and could bring some relativistic pressure. It turns out that we can consider our Newtonian system of equations to be correct at zeroth order and just assume that the evolution is given by the relativistic Friedmann equation (involving pressure).

We can thus eliminate the background and write the equations at first order in perturbations:

$$\partial_t \delta\rho + \overline{\rho}\,\nabla \cdot \delta\mathbf{v} + \nabla \cdot (\delta\rho\,\overline{\mathbf{v}}) = 0 \quad , \tag{A.65}$$

$$\partial_t \delta\mathbf{v} + (\delta\mathbf{v} \cdot \nabla)\overline{\mathbf{v}} + (\overline{\mathbf{v}} \cdot \nabla)\delta\mathbf{v} = -\tfrac{1}{\overline{\rho}}\nabla(c_s^2\delta\rho + \tau\delta S) - \nabla\delta\Phi \quad , \tag{A.66}$$

$$\nabla^2\delta\Phi = 4\pi G\,\delta\rho \quad , \tag{A.67}$$

$$\partial_t S + (\mathbf{v} \cdot \nabla)S = 0 \quad , \tag{A.68}$$

where we have used the expansion involving $c_s^2 \equiv (\partial\overline{p}/\partial\overline{\rho})_{\overline{S}}$, the speed of sound and $\tau \equiv \left(\partial\overline{p}/\partial\overline{S}\right)_{\overline{\rho}}$:

$$\delta p = c_s^2\delta\rho + \tau\delta S \quad . \tag{A.69}$$

As a final step, we can introduce the comoving coordinates $(t, \mathbf{x})$, linked to the physical ones by:

$$\mathbf{r} = a\,\mathbf{x} \quad , \quad \nabla_{\mathbf{r}} = \frac{1}{a}\nabla_{\mathbf{x}} \quad , \quad \left.\frac{\partial}{\partial t}\right|_{\mathbf{r}} = \left.\frac{\partial}{\partial t}\right|_{\mathbf{x}} - \frac{1}{a}(\mathbf{v} \cdot \nabla_{\mathbf{x}}) \quad . \tag{A.70}$$

Taking now the Fourier expansion of this system of equations and defining the comoving momentum $\tilde{\mathbf{k}} \equiv \mathbf{k}/a$ (and $\tilde{k} = |\tilde{\mathbf{k}}|$), we obtain:

$$\partial_t \delta\rho + 3H\delta\rho + i\tilde{\mathbf{k}} \cdot \delta\mathbf{v} = 0 \quad , \tag{A.71}$$

$$\partial_t \delta\mathbf{v} + H\delta\mathbf{v} = -\tfrac{i\tilde{\mathbf{k}}}{\overline{\rho}}\nabla(c_s^2\delta\rho + \tau\delta S) - i\tilde{\mathbf{k}}\delta\Phi \quad , \tag{A.72}$$

$$\tilde{k}^2\delta\Phi = -4\pi G\delta\rho \quad , \tag{A.73}$$

$$\partial_t \delta S = 0 \quad , \tag{A.74}$$

where we used $\nabla \cdot \mathbf{v} = 3H$ and $(\delta\mathbf{v} \cdot \nabla)\overline{\mathbf{v}}/a = \delta v\,H$. We see that these relations do not contain pressure and we are left with 5 coupled linear first order differential equations and one algebraic equation.

The solution of this system is then a superposition of 5 linear independent modes: 2 vortical modes, 2 adiabatic modes, and one entropy mode. The *entropy mode* is a static entropy perturbation $\delta S(t, \mathbf{k}) = \delta S(\mathbf{k})$, with other functions $\delta\rho$, $\delta\mathbf{v}$ and $\delta\Phi$ chosen appropriately, and can only appear in a multi-component fluid. As dark matter is an almost non-interacting field and that this entropy mode

is not predicted by simple inflationary models, we can neglect it. Furthermore, we can see for a static universe ($H = 0$ and $\overline{\rho} = \text{cst}$) that the density fluctuation does not grow and this entropy mode thus has no impact on structure formation. The *vortical modes* are obtained by setting $\delta\rho = \delta\Phi = \delta S = 0$ and $\mathbf{k} \cdot \delta\mathbf{v} = 0$. In that case, the Euler equation is equivalent to

$$\partial_t \delta\mathbf{v} + H\delta\mathbf{v} = 0 \qquad \Rightarrow \qquad \delta\mathbf{v} \propto 1/a \quad . \tag{A.75}$$

That explains the well-known statement that vortical modes are negligible as they decay with time as the inverse of the scale factor. The last ones, the *adiabatic modes*, are obtained by $\delta S = 0$ and $\mathbf{k} \parallel \delta\mathbf{v}$ (so $\mathbf{k} \cdot \delta\mathbf{v} = k\delta v$). Indeed, these conditions and the continuity equation at zeroth and first order give :

$$\dot{\delta} + i\tilde{k}\delta v = 0 \quad \text{with} \quad \delta(t, \mathbf{k}) \equiv \frac{\delta\rho(t, \mathbf{k})}{\overline{\rho}(t)} \quad . \tag{A.76}$$

Differentiating this equation with respect to cosmic time t, we can eliminate $\partial_t \delta v$ from the Euler equation and then use Eq. (A.76) and the Poisson equation to get

$$\ddot{\delta} + 2H\dot{\delta} + (c_s^2 \tilde{k}^2 - 4\pi G\overline{\rho})\delta = 0 \quad . \tag{A.77}$$

This equation is a linear second order differential equation and it has in general two independent solutions which can be either stable or evolving in time.

A.2.3 Gravitational instability and growth of structures

We can notice that the stability of a mode of comoving momentum $\tilde{k}$ in Eq. (A.77) is determined by the sign of the last term in this equation, i.e. by the sign of $c_s^2 \tilde{k}^2 - 4\pi G\overline{\rho}$. Indeed, when this term is positive, we have two oscillatory modes and, when this term is negative, we have exponentially growing/decaying modes. As we can notice, these two different regimes happen at different wavelengths, due to the fact that this coefficient is $\tilde{k}$-dependent. Consequently, we have exponential solutions when the mode we consider has a comoving wavelength $\tilde{\lambda}$ such that :

$$\tilde{\lambda} = \frac{2\pi}{\tilde{k}} \quad > \quad \tilde{\lambda}_{\text{J}} = c_s \sqrt{\frac{\pi}{G\overline{\rho}}} \quad . \tag{A.78}$$

This critical value for the wavelength is called the *Jeans length* and it says that a structure of matter larger than this length is not stable, so it either grows or decays.

Considering a sphere of density ρ, we understand that this structure will collapse or grow if its density is too high, in other words if its mass exceeds a certain mass, called the *Jeans mass*, given by :

$$M_{\text{J}} = \frac{4\pi}{3} \left(\frac{\lambda_{\text{J}}}{2}\right)^3 \overline{\rho} = \frac{\pi}{6} \lambda_{\text{J}}^3 \, \overline{\rho} \quad . \tag{A.79}$$

To give an example, we can notice that the speed of sound of baryonic matter during the radiation era is $c_s = c/\sqrt{3} \simeq 0.6\ c$ as baryons are tightly coupled to photons. So the Jeans length is large and baryons cannot start forming structures. After the decoupling, however, the baryonic matter is decoupled from photons and its speed of sound is very close to zero. Baryons can then start to form structures. On the other hand, dark matter is only interacting gravitationally and has a very small speed of sound even in the radiation dominated phase of the Universe. That explains why after decoupling baryons start to fall in the potential wells created by dark matter and why baryonic structures form in a faster way than it would have been expected in a Universe without dark matter.

For a very large wavelength mode, the equation (A.77) is approximated by

$$\ddot{\delta} + 2H\dot{\delta} - 4\pi G\,\overline{\rho}\,\delta = 0 \quad , \tag{A.80}$$

which has for general solution :

$$\delta(t, \mathbf{k}) = \delta_+(\mathbf{k}) D_+(t) + \delta_-(\mathbf{k}) D_-(t) \quad . \tag{A.81}$$

Here, $D_+(t) \equiv D(t)$ is the *linear growth function*. When our Universe is matter dominated, we then have $H(t) = 2/3t$. We can then use the Friedmann equation $4\pi G\overline{\rho} = 3H^2/2$ and look for solutions of $\delta(t, \mathbf{k})$ of the type $\delta(t, \mathbf{k}) = \delta(\mathbf{k})\, t^\alpha$ (with $\alpha \in \mathbb{R}$). We find easily that only two values are authorized : $\alpha = 2/3, -1$. Hence $D_+ \propto t^{2/3}$ and $D_- \propto t^{-1}$. Compared to the growth of perturbations going as an exponential when the Universe is static, we have structures that form only as a power law in the realistic matter era. During the radiation era, the growth of dark matter structures is even slower, and we can show under reasonable conditions that the growing mode does not grow more than by a factor 2.5 during that period. This is called the *Meszaros effect* : dark matter pertubations of wavelength much longer than the Jeans length are almost frozen during the radiation era.

To conclude on this subsection, we should notice that there is no analytical solution of Eq. (A.80) in the case of a flat ΛCDM model. Nevertheless, a very good approximation is given by [134] :

$$D(z) = \frac{1}{1+z}\frac{g(z)}{g(0)} \quad \text{with} \quad g(z) \propto \Omega_m(z)\left[\Omega_m^{4/7}(z) - \Omega_\Lambda(z) + \left(1 + \frac{\Omega_m(z)}{2}\right)\left(1 + \frac{\Omega_\Lambda(z)}{70}\right)\right]^{-1} \tag{A.82}$$

$$\text{where} \qquad \Omega_m(z) = \frac{\Omega_{m0}(1+z)^3}{\Omega_{m0}(1+z)^3 + \Omega_{\Lambda 0}} \quad , \quad \Omega_\Lambda(z) = \frac{\Omega_{\Lambda 0}}{\Omega_{m0}(1+z)^3 + \Omega_{\Lambda 0}} \quad . \tag{A.83}$$

A.2.4 Reentering of the modes, the transfer function

The discussion made above, leading to the expression of $D(z)$, is valid for perturbations well inside the Hubble horizon. For modes larger than this horizon, a general relativistic treatment is needed and we must deal with gauge invariance complications. Qualitatively, what happens is that modes reentering the horizon, during radiation or matter domination, have grown in amplitude. We can show that the density contrast of a mode reentering at $t_{\rm in}$ scales as

$$\delta(t_{\rm in}, \mathbf{k}(t_{\rm in})) \propto \frac{1}{H^2(t_{\rm in})a^2(t_{\rm in})} \propto \begin{cases} a^2(t_{\rm in}) & \text{for } t_{\rm in} \in \text{ Radiation Era} \quad , \\ a(t_{\rm in}) & \text{for } t_{\rm in} \in \text{ Matter Era} \quad . \end{cases} \tag{A.84}$$

We thus have matter perturbations growing like a both outside and inside the horizon during matter domination, and super-horizon pertubations growing like a^2 when sub-horizon perturbations are frozen during the radiation dominated era. We can hence use the modes reentering the horizon as references for the inside horizon modes. Thus, we can understand how these modes have been modified during the radiation domination. This is the role of the *transfer function*, which is defined as :

$$T(k) \equiv \frac{\delta(t, \mathbf{k})}{\delta(t_{\rm in}, \mathbf{k})}\frac{D(t_{\rm in})}{D(t)} \quad . \tag{A.85}$$

This function has by definition the limit $\lim_{k\to 0} T(k) = 1$ as super-horizon modes are not affected by radiation domination (they reenter during the Matter Era). We also understand that $T(k)$ has to include all physical effects changing the amplitude of perturbations during radiation domination. These effects are numerous and a precise determination of $T(k)$ is only possible by solving the full relativistic Boltzmann equation. Nevertheless, the main physical effects that we can retain are the overall suppression due to evolution, the Silk damping effect, and baryonic oscillations.

The main effect building $T(k)$ is the overall suppression from evolution. Indeed, super-horizon perturbations are frozen and passively grow as a^2 in radiation domination. When they reenter the horizon during matter domination, they have a larger size than if they had reentered some time before. On the other hand, a perturbation reentering during radiation domination stays almost frozen due to the Meszaros effect and only starts to grow like $D \propto a$ after matter-radiation equality ($t = t_{\rm eq}$). The consequence is a suppression of all the modes reentering at a time $t_{\rm in} < t_{\rm eq}$ by a factor $(a(t_{\rm eq})/a(t_{\rm in}))^2$. During radiation, we also know that modes reentering have a momentum $k \propto H(t_{\rm in})a(t_{\rm in}) \propto 1/a(t_{\rm in})$, so we have the ratio with respect to the matter-radiation equality : $k/k_{\rm eq} = a(t_{\rm eq})/a(t_{\rm in})$. The suppression of modes is thus going like $(k/k_{\rm eq})^{-2}$ and we have the important scaling limit :

$$\lim_{k\to\infty} T(k) \sim (k/k_{eq})^{-2} \quad . \tag{A.86}$$

The Newtonian description of perturbations is valid well within the Hubble horizon. For super-horizon perturbations, we must use the full relativistic perturbation theory.

A.3 Gauge invariance and perturbation theory

We will mainly use here the considerations and notations of [135] and [136] to explain the basic notions on gauge invariance. We will nevertheless use the opposite signature for the metric. We first mention a subtlety of language that we will avoid to address in this section. One should in principle make the distinction between "gauge independent" and "gauge invariant". Indeed, the first notion implies the second, but not the converse. To avoid any complication, we will only speak of gauge invariance, gathering hence both concepts in the same term.

A.3.1 General considerations

The study of the evolution of perturbations within the set up of general relativity consists in the linearization of Einstein's equations around a certain background. The problem we then have to face is that general relativity does not assume a preferred system of coordinates and there is a non-physical freedom associated to these coordinates that we call the gauge freedom. We will describe in these sections different gauges and will give the elements describing the formulation of perturbation theory in a gauge invariant way, i.e. keeping only physically relevant quantities.

We should notice first of all that the linearized gravitational perturbation theory that we will describe here is only valid around a homogeneous and isotropic FLRW background. So most of the equations that we will present in this section will be valid at first order in perturbations only. This assumption is reasonable if we consider observations and it is enforced by the fact that in a FLRW Universe the solution of the linearized equations is also the linearization of the solution of the full (i.e. non-perturbative) equations. Let us decompose the metric of the perturbed universe as "background plus pertubations" in a given system of coordinates $\{x^\mu\}$:

$$g_{\mu\nu}(x) = g^{(0)}_{\mu\nu} + \delta g_{\mu\nu} \quad , \tag{A.87}$$

and let us choose the background to be isotropic and homogeneous so its line element is

$$ds^2_{b.g.} = g^{(0)}_{\mu\nu} dx^\mu dx^\nu = -dt^2 + a^2(t)\gamma_{ij}(|\mathbf{x}|)dx^i dx^j = a(\eta)^2(-d\eta^2 + \gamma_{ij}(|\mathbf{x}|)dx^i dx^j) \quad . \tag{A.88}$$

Choosing this background geometry to be FLRW, we take:

$$\gamma_{ij}(|\mathbf{x}|) = \delta_{ij}\left[1 + \frac{1}{4}K|\mathbf{x}|^2\right]^{-2} \qquad \text{with} \quad K = -1, 0, 1 \quad , \tag{A.89}$$

depending on whether the $\eta = \text{cst}$ spatial hypersurfaces are closed, flat or opened [4].

Using the Einstein equations:

$$G^\mu{}_\nu = R^\mu{}_\nu - \frac{\delta^\mu{}_\nu}{2}R = 8\pi G\, T^\mu{}_\nu \quad , \tag{A.90}$$

where $R \equiv R^\mu{}_\mu$, we get only two independent equations

$$(0,0) \quad : \quad (a')^2 + Ka^2 = -\tfrac{8\pi G}{3}\, T^0_0 a^4 \quad , \tag{A.91}$$

$$(\text{i,i}) \quad : \quad a'' + Ka = -\tfrac{4\pi G}{3}\, T a^3 \quad , \tag{A.92}$$

with $a' \equiv da/d\eta$ and $T \equiv T^\mu{}_\mu$. In the second of these equations, we used that $T^i{}_i = (T - T^0_0)/3$ (with no summation over i) and used the first equation. We should notice that these equations only involve time and because we choosed an isotropic background, we got that $R^i{}_j \propto \delta^i{}_j$. This leads to the conclusion that $T^i{}_j \propto \delta^i{}_j$.

The equation of matter conservation, namely $\nabla_\mu T^\mu{}_0 \equiv T^\mu{}_{0;\mu} = 0$, can be written as:

$$dT^0_0 = -(4T^0_0 - T)d\ln a \quad . \tag{A.93}$$

4. We can directly show that this definition of the FLRW metric in Eq. (A.89) is equivalent to the definition given in Eq. (1.3) by setting $r = |\mathbf{x}|/\left(1 + \frac{K}{4}|\mathbf{x}|^2\right)$.

The metric perturbations at first order can be decomposed in three independent types of perturbations [5] : scalar, vector and tensor. We will see that scalar perturbations are the only ones to grow in an expanding universe : vector perturbations then decay and tensor perturbations do not couple to density and pressure perturbations. It turns out that the 10 degrees of freedom (dofs) present in Einstein's equations describing a general universe are decomposed in 4 scalar dofs, $2 \times (3-1) = 4$ vector dofs and $6-(3+1) = 2$ tensor dofs.

The most general form of the metric scalar perturbations at first order is

$$\delta g_{\mu\nu}^{(s)} = -a^2(\eta) \begin{pmatrix} 2\phi & -B_{|i} \\ -B_{|i} & 2(\psi\gamma_{ij} - E_{|ij}) \end{pmatrix} \quad , \tag{A.94}$$

where $|i$ denotes the simple derivative with respect to the spatial metric inside the constant-η hypersurface, i.e. $B_{|i} = \partial_i B$. The vector perturbations can be written as :

$$\delta g_{\mu\nu}^{(v)} = a^2(\eta) \begin{pmatrix} 0 & -S_i \\ -S_i & F_{i|j} + F_{j|i} \end{pmatrix} \quad , \tag{A.95}$$

with $S_i^{|i} = F_i^{|i} = 0$. This divergenceless condition imposes that S_i and F_i have no contribution coming from the gradient of a scalar quantity. Last, the vector perturbations contribute only to the spatial part of the metric :

$$\delta g_{\mu\nu}^{(t)} = a^2(\eta) \begin{pmatrix} 0 & 0 \\ 0 & h_{ij} \end{pmatrix} \quad , \tag{A.96}$$

where h_{ij} is a transverse contribution : it is trace-free ($h_i{}^i = 0$) and divergence-free ($h_{ij}{}^{|j} = 0$), i.e. it has neither vector nor scalar contributions.

The total metric perturbation can thus be written as

$$\delta g_{\mu\nu} = a^2(\eta) \begin{pmatrix} -2\phi & B_{|i} - S_i \\ B_{|i} - S_i & -2(\psi\gamma_{ij} - E_{|ij}) + F_{i|j} + F_{j|i} + h_{ij} \end{pmatrix} \quad . \tag{A.97}$$

and the most general line element of the "background + perturbation" metric is

$$ds^2 = a^2(\eta)\big(-(1+2\phi)d\eta^2 + 2(B_{|i} - S_i)d\eta dx^i + [(1-2\psi)\gamma_{ij} - E_{|ij} + F_{i|j} + F_{j|i} + h_{ij}]dx^i dx^j\big) \ . \tag{A.98}$$

This line element is often rewritten in the following way :

$$ds^2 = a^2(\eta)\left[-(1+2\phi)d\eta^2 + 2B_i dx^i d\eta + (\gamma_{ij} + 2C_{ij})dx^i dx^j\right] \tag{A.99}$$

with the following definitions of metric perturbations :

$$\begin{cases} \delta g_{00}^{(n)} = -2a^2\phi^{(n)} \\ \delta g_{0i}^{(n)} = a^2 B_i^{(n)} \\ \delta g_{ij}^{(n)} = 2a^2 C_{ij}^{(n)} \end{cases} \quad , \qquad \text{with} \qquad \begin{cases} B_i = B_{,i} - S_i \quad , \quad B_{[,ij]} = 0 \text{ (curl-free)} \\ C_{ij} = -\psi\delta_{ij} + E_{,ij} + F_{(i,j)} + \frac{1}{2}h_{ij} \end{cases} \quad \text{for n=1} \quad , \tag{A.100}$$

where (n) is the order in perturbations. In the following, the equations we will derive will concern only the first order. We recall that we have 4 scalar dofs (ϕ, ψ, B, E), 4 vector dofs (S_i and F_i), and 2 tensor dofs (h_{ij}).

A.3.2 Passive and active approaches of gauge transformations

There are at least two different ways to consider the meaning of gauge transformations : the passive and the active descriptions. In the passive approach, one specifies two systems of coordinates and then evaluate how geometrical quantities change under the transformation of coordinates, staying at the same physical point. In the active approach, one sees how the geometrical quantities change under a mapping of coordinates (including the transformation of geometrical quantities), staying at the same coordinate point.

5. They will not be independent anymore at second order as for example we can have vector and tensor perturbations generated by spatial derivatives of scalar perturbations, this if no mechanism like inflation comes into play.

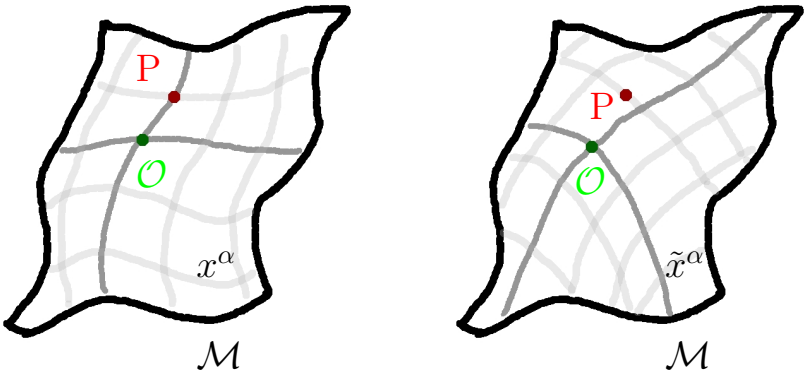

Figure A.1: Illustration of the passive approach of gauge transformations.

Passive approach : We consider a 4-dimensional manifold $\mathcal{M}$ and a fixed point $\mathrm{P} \in \mathcal{M}$. We can parametrize $\mathcal{M}$ by two different systems of coordinates x^α and $\tilde{x}^\alpha$, as illustrated in Fig. A.1 . We suppose that we have a backgound function $Q^{(0)}(x^\alpha)$ which is attached to the point P and is not a geometrical quantity (i.e. we are not interested by the displacement of this quantity as we could be for a scalar or a vector). We thus have the perturbation defined as

$$\delta Q(\mathrm{P}) = Q(x^\alpha(\mathrm{P})) - \mathrm{Q}^{(0)}(\mathrm{x}^\alpha(\mathrm{P})) \quad \text{with the } x^\alpha\text{-parametrization of } \mathcal{M} \ , \tag{A.101}$$

$$\delta \widetilde{Q}(\mathrm{P}) = \widetilde{Q}(\tilde{x}^\alpha(\mathrm{P})) - \mathrm{Q}^{(0)}(\tilde{\mathrm{x}}^\alpha(\mathrm{P})) \quad \text{with the } \tilde{x}^\alpha\text{-parametrization of } \mathcal{M} \ , \tag{A.102}$$

where it is important to notice that $Q^{(0)}(x^\alpha(\mathrm{P}))$ has the same value as $Q^{(0)}(\tilde{x}^\alpha(\mathrm{P}))$ though we have $x^\alpha(\mathrm{P}) \neq \tilde{\mathrm{x}}^\alpha(\mathrm{P})$ in general. On the other hand $Q(x^\alpha(\mathrm{P})) \neq \widetilde{\mathrm{Q}}(\tilde{\mathrm{x}}^\alpha(\mathrm{P}))$ and thus $\delta Q(\mathrm{P}) \neq \delta\widetilde{\mathrm{Q}}(\mathrm{P})$. We can thus speak about a change of variables $x^\alpha(\mathrm{P}) \to \tilde{\mathrm{x}}^\alpha(\mathrm{P})$ for each $\mathrm{P} \in \mathcal{M}$ and the corresponding change $\{\delta Q(\mathrm{P}) \to \delta\widetilde{\mathrm{Q}}(\mathrm{P}),\ \mathrm{P} \in \mathcal{M}\}$ is called the gauge transformation associated to this change of variables.

Active approach : In this approach, we consider a background manifold $\mathcal{N}$ with a rigid system of coordinates $\{X^\alpha\}$ on it and two diffeomorphisms $\mathcal{D}$ and $\widetilde{\mathcal{D}}$ giving rise to different systems of coordinates $\{x^\alpha\}$ and $\{\tilde{x}^\alpha\}$ on the manifold $\mathcal{M}$, as illustrated in Fig. A.2. Because these two diffeomorphisms are different, a point $\mathrm{P} \in \mathcal{M}$ is the image of two different points (R_1 and R_2) of $\mathcal{N}$ through $\mathcal{D}$ and $\widetilde{\mathcal{D}}$. We thus have two different perturbations at the point $\mathrm{P} \in \mathcal{M}$ simply because of the different diffeomorphisms that has been used :

$$\delta Q(\mathrm{P}) = Q(\mathrm{P}) - \mathrm{Q}^{(0)}(\mathcal{D}^{-1}(\mathrm{P})) \quad \text{with the diffeomorphism } \mathcal{D} \ , \tag{A.103}$$

$$\delta \widetilde{Q}(\mathrm{P}) = \widetilde{Q}(\mathrm{P}) - \mathrm{Q}^{(0)}(\widetilde{\mathcal{D}}^{-1}(\mathrm{P})) \quad \text{with the diffeomorphism } \tilde{\mathcal{D}} \ , \tag{A.104}$$

where $Q(\mathrm{P}) = \widetilde{\mathrm{Q}}(\mathrm{P})$ because we want the total perturbation at $\mathrm{P} \in \mathcal{M}$ to be independent on the parametrization. We thus have $Q^{(0)}(\mathcal{D}^{-1}(\mathrm{P})) \neq \mathrm{Q}^{(0)}(\widetilde{\mathcal{D}}^{-1}(\mathrm{P}))$, which is consistent with the fact that these quantities correspond to the evaluation of $Q^{(0)}$ on two different points of the manifold $\mathcal{N}$. To conclude that case, we see that the change $\mathcal{D} \to \widetilde{\mathcal{D}}$ induces a change in the size of the perturbations that we can call the gauge transformation : $\delta Q(\mathrm{P}) \to \delta\widetilde{\mathrm{Q}}(\mathrm{P})$.

Comparison : To explain things in a simple form, the passive approach considers a point on $\mathcal{M}$ and move this point in two different places by two different choices of coordinates. The final perturbation $Q(x^\alpha(\mathrm{P}))$ is thus different from the perturbation in the other system of coordinates, namely $\widetilde{Q}(\tilde{x}^\alpha(\mathrm{P}))$ and this because they correspond to a different point on the perturbed manifold whereas the non-perturbed positions of these two points were the same. The active approach does the converse

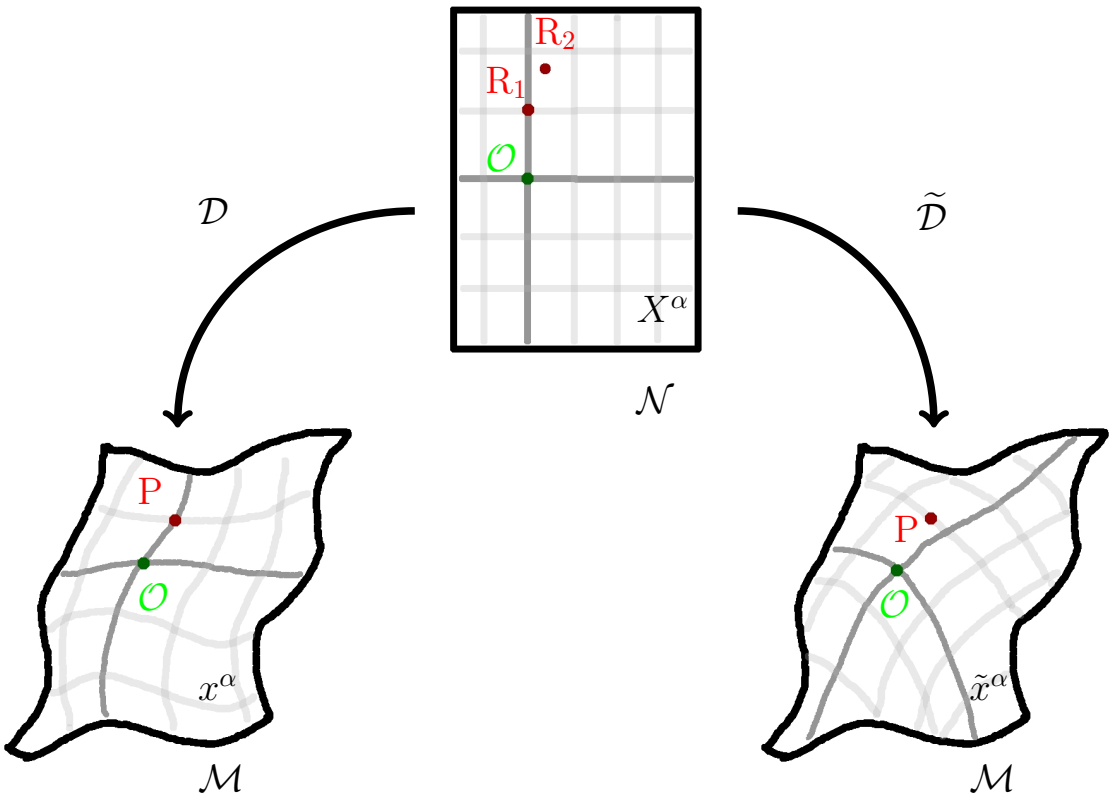

Figure A.2: Illustration of the active approach of gauge transformations.

consideration. It starts with two different points on the unperturbed manifold $\mathcal{N}$, but the diffeomorphims that we choose both lead to the same perturbed point. Consequently, the values of Q in the unperturbed manifold are different, but the final value on $\mathcal{M}$ is the same (because we are at the same physical point). The important thing is that in both cases we can trace back the change in Q due to the change in coordinates and keep track of this change to avoid any non-physical value of perturbations coming from the choice of coordinates themselves.

Lie derivation : To be more precise on these aspects of independence of physical quantities from the choice of a gauge, let us now consider an infinitesimal change of coordinates given by :

$$x^\mu \to \tilde{x}^\mu = x^\mu + \xi^\mu \quad , \tag{A.105}$$

where ξ^μ is an infinitesimal change in coordinates (considered here to be first order in perturbations). From the explanations given above, we know that a quantity Q defined on the manifold $\mathcal{M}$ vary by an amount which is also the Lie derivative of Q in the direction of ξ^μ :

$$\Delta Q = \widetilde{\delta Q} - \delta Q = \mathscr{L}_\xi Q \quad . \tag{A.106}$$

These infinitesimal gauge tranformations form a group, the Lie group of infinitesimal transformations.

In general terms, one can decompose a tensorial quantity $\mathbf{T}$ (scalar, vector, tensor, ...), as follows :

$$\mathbf{T}(\eta, x^i) = \mathbf{T}_0(\eta) + \delta\mathbf{T}(\eta, x^i) \quad \text{with} \quad \delta\mathbf{T}(\eta, x^i) = \sum_{n=1}^{\infty} \frac{\epsilon^n}{n!} \delta\mathbf{T}_n(\eta, x^i) \quad , \tag{A.107}$$

where ϵ an infinitesimal parameter. In this equation, the background quantity $\mathbf{T}_0(\eta)$ is gauge invariant and we need to choose a gauge to describe the perturbations. The generator of the gauge

transformation ξ^μ can be decomposed in perturbations as :

$$\xi^\mu \equiv \epsilon\xi_1^\mu + \frac{1}{2}\epsilon^2\xi_2^\mu + \mathcal{O}(\epsilon^3) \quad . \tag{A.108}$$

We then have the transformed tensor :

$$\widetilde{\mathbf{T}} = e^{\mathscr{L}_\xi}\mathbf{T} \quad \text{with} \quad e^{\mathscr{L}_\xi} = 1 + \epsilon\mathscr{L}_\xi + \frac{1}{2}\epsilon^2[\mathscr{L}_{\xi_2} + \mathscr{L}_{\xi_1}^2] + \mathcal{O}(\epsilon^3) \quad , \tag{A.109}$$

which defines the perturbed quantities :

$$\begin{aligned} \widetilde{\mathbf{T}}_0 &= \mathbf{T}_0 \quad , \\ \delta\widetilde{\mathbf{T}}_1 &= \delta\mathbf{T}_1 + \mathscr{L}_{\xi_1}\mathbf{T}_0 \quad , \\ \delta\widetilde{\mathbf{T}}_2 &= \delta\mathbf{T}_2 + 2\mathscr{L}_{\xi_1}\delta\mathbf{T}_1 + \mathscr{L}_{\xi_2}\mathbf{T}_0 + \mathscr{L}_{\xi_1}^2\mathbf{T}_0 \quad . \end{aligned} \tag{A.110}$$

In the case of a vector quantity $\mathbf{T}$, with covariant components T^μ, the Lie derivative gives the following transformation :

$$\mathscr{L}_\xi T^\mu = \xi^\nu\partial_\nu T^\mu - T^\nu\partial_\nu\xi^\mu \quad . \tag{A.111}$$

For a more general tensorial quantity, this last relation is generalized to the following transformation :

$$\mathscr{L}_\xi\, T^{\mu_1\ldots\mu_m}_{\nu_1\ldots\nu_n} = \xi^\alpha\partial_\alpha T^{\mu_1\ldots\mu_m}_{\nu_1\ldots\nu_n} - \sum_{i=1}^{m} T^{\mu_1\ldots\alpha\ldots\mu_m}_{\nu_1\ldots\nu_n}\partial_\alpha\xi^{\mu_i} + \sum_{j=1}^{n} T^{\mu_1\ldots\mu_m}_{\nu_1\ldots\alpha\ldots\nu_n}\partial_{\nu_j}\xi^\alpha \quad . \tag{A.112}$$

The Lie derivative is an important notion to study the symmetries of Riemannian spacetimes. Moreover, one can show that the derivative of the metric tensor is :

$$\mathscr{L}_\xi\, g_{\mu\nu} = \nabla_\mu\xi_\nu + \nabla_\nu\xi_\mu \quad , \tag{A.113}$$

and thus we have that $g_{\mu\nu}$ is invariant under the change of coordinates of Eq. (A.105) when we have $\mathscr{L}_\xi g_{\mu\nu} = 0$ (called *Killing's equation* and where ξ^μ is then called a Killing vector).

We finally have the general mapping between the two systems of coordinates $\{x^\mu(p)\}$ and $\{x^\mu(q)\}$:

$$x^\mu(q) = e^{\xi^\lambda\frac{\partial}{\partial x^\lambda}|_p}x^\mu(p) = x^\mu(p) + \epsilon\xi^\mu(p) + \frac{1}{2}\epsilon^2(\xi^\mu_{1,\nu}\,\xi_1^\nu + \xi_2^\mu)(p) \quad . \tag{A.114}$$

and the 3-vector part of ξ^μ can be decomposed in two contributions

$$\xi^i = \xi^i_{tr} + \gamma^{ij}\xi_{|j} \quad \text{where} \quad \xi^i_{tr|i} = 0 \quad \text{and} \quad \xi^{|i}{}_{|i} = \xi^i{}_{|i} \quad , \tag{A.115}$$

that is to say in a transverse vector part and a scalar part. The most general transformation which preserve the scalar nature of perturbations is thus given by the condition $\xi^i_{tr} = 0$:

$$\eta \to \tilde{\eta} = \eta + \xi^0(\eta, \mathbf{x}) \quad , \quad x^i \to \tilde{x}^i = x^i + \gamma^{ij}\xi_{|j}(\eta, \mathbf{x}) \quad , \tag{A.116}$$

where we recall that γ^{ij} is the inverse background metric of spatial coordinates.

Gauge invariant perturbations : The infinitesimal transformation of the coordinates $x^\mu \to x^\mu + \xi^\mu$ changes the perturbation of the metric $g_{\mu\nu}$ by $\Delta g_{\mu\nu}$:

$$\delta g_{\mu\nu} \to \widetilde{\delta g}_{\mu\nu} = \delta g_{\mu\nu} + \Delta g_{\mu\nu} \quad . \tag{A.117}$$

Let us consider an example and take the transformation of the scalar contribution ϕ of the component g_{00}. We have by definition $\tilde{g}_{\mu\nu}(\tilde{x}) = g^{(0)}_{\mu\nu}(\tilde{\eta}) + \widetilde{\delta g}_{\mu\nu}(\tilde{x})$ where

$$\widetilde{\delta g}^{(s)}_{\mu\nu} = -a^2(\tilde{\eta})\begin{pmatrix} 2\tilde{\phi} & -\tilde{B}_{|i} \\ -\tilde{B}_{|i} & 2(\tilde{\psi}\gamma_{ij} - \tilde{E}_{|ij}) \end{pmatrix} \quad , \tag{A.118}$$

and where $x = (\eta, \mathbf{x})$, $\tilde{x} = (\tilde{\eta}, \tilde{\mathbf{x}})$, and we have :

$$\widetilde{g}_{\mu\nu}(\tilde{x}) = \frac{\partial \tilde{x}^\alpha}{\partial x^\mu}\frac{\partial \tilde{x}^\beta}{\partial x^\nu} g_{\alpha\beta}(x) \quad \text{and} \quad \left\{ \begin{array}{l} \eta = \tilde{\eta} - \xi^0(\tilde{\eta}, \tilde{\mathbf{x}}) \\ x^i = \tilde{x}^i - \gamma^{ij}\xi_{|j}(\tilde{\eta}, \tilde{\mathbf{x}}) \end{array} \right. \quad . \tag{A.119}$$

In principle we should also add a tilde over γ_{ij} and γ^{ij} in both equations above as we must express this tensor in terms of $\tilde{x}$. Nevertheless, this tensor multiplies $\tilde{\psi}$ and $\xi_{|j}$ respectively, which are first order quantities. Consequently it is not necessary to go to that level of specification at the infinitesimal level we are considering here. The transformation between the two metrics, with the expansion of $a(\tilde{\eta})$ as $a(\eta)(1 + \mathcal{H}(\tilde{\eta})\xi^0)$, leads us to

$$\tilde{\phi} = \phi - \partial_{\tilde{\eta}}\xi^0 - \mathcal{H}(\tilde{\eta})\xi^0 \quad . \tag{A.120}$$

We could also have added tildes over ξ^0 but for simplity we kept the same notation for $\xi^0(\tilde{\eta}, \tilde{\mathbf{x}})$. Also, the derivative $\partial_{\tilde{\eta}}$ can be replaced by ∂_η at this order, or more simply denoted by a prime. Similarly, we can replace $\mathcal{H}(\tilde{\eta})$ by $\mathcal{H}(\eta)$ at this order.

Proceeding in the same way for the other scalar dofs, we get the transformations :

$$\tilde{\psi} = \psi + \mathcal{H}\xi^0 \quad , \quad \tilde{B} = B + \xi^0 - \xi' \quad , \quad \tilde{E} = E - \xi \quad . \tag{A.121}$$

From these expressions, we can also build up gauge invariant combinations. Bardeen indeed showed that we can form two quantities having this property and defined as :

$$\Phi = \phi + \frac{[(B - E')a]'}{a} \quad , \quad \Psi = \psi - \mathcal{H}(B - E') \quad . \tag{A.122}$$

These are called the Bardeen potentials [6] and they have been extensively used in the literature. We should add that every combination of these variables is also gauge invariant but that Φ and Ψ are the simplest gauge invariant quantities that we can write down. These two quantities are invariant under all infinitesimal scalar coordinate transformations, but we should keep in mind that they are not invariant under all finite coordinate transformations.

If we consider a 4-scalar $q(\eta, \mathbf{x})$ on $\mathcal{M}$, we can decompose this scalar into a background and a perturbed contribution. From homogeneity, the background contribution is only time dependent and the perturbation is of first order :

$$q(\eta, \mathbf{x}) = q^{(0)}(\eta) + \delta q(\eta, \mathbf{x}) \quad . \tag{A.123}$$

As a consequence, this scalar quantity is modified under infinitesimal coordinate transformations and its variation is given by :

$$\delta q(\eta, \mathbf{x}) \quad \rightarrow \quad \widetilde{\delta q}(\eta, \mathbf{x}) = \delta q(\eta, \mathbf{x}) - q^{(0)}(\eta)'\,\xi^0(\eta, \mathbf{x}) \quad , \tag{A.124}$$

and thus δq is gauge invariant only if $q^{(0)}$ is time independent. Otherwise, we can build up a gauge invariant quantity by combining δq and gauge perturbations, namely :

$$\delta q^{g.i.} = \delta q + (q^{(0)})'\,(B - E') \quad . \tag{A.125}$$

Explicit formulation of gauge transformations : Let us summarize the effect of an infinitesimal transformation of the coordinates defined by the first order quantity $\xi^\mu = (\alpha\,,\, \beta^{|i} + \gamma^i)$. Using the notations for perturbations introduced at the end of Sec. A.3.1, one has :

– For scalar perturbations :

$$\left\{ \begin{array}{l} \tilde{\phi} = \phi + \mathcal{H}\alpha + \alpha' \\ \tilde{\psi} = \psi - \mathcal{H}\alpha \\ \tilde{B} = B - \alpha + \beta' \\ \tilde{E} = E + \beta \end{array} \right. \tag{A.126}$$

6. In fact, Bardeen potentials were Φ_A and Φ_H such that $\Phi_A = \Phi$ and $\Phi_H = -\Psi$, cf. [137].

– For vector perturbations :

$$\begin{cases} \widetilde{S^i} = S^i - (\gamma^i)' \\ \widetilde{F^i} = F^i + \gamma^i \end{cases} \tag{A.127}$$

– For tensor perturbations :

$$\tilde{h}_{ij} = h_{ij} \quad . \tag{A.128}$$

We recall that tensorial metric perturbations are not gauge invariant at second order in perturbations but they are at first. We can also introduce the transformation of quantities which are not metric elements such as the scalar shear potential $\sigma = E' - B$ and the spatial velocity perturbation of a fluid velocity $u^\mu = (u^0, u^i)$ which is given at first order by $u^0 = a^{-1}(1-\phi)$ and $u^i = a^{-1}v^i$, with v^i that can be split into scalar and vector parts : $v^i = \delta^{ij}\, v_{,j} + v^i_{\rm vec}$. These two quantities change, under the previous coordinate transformations, in the following way :

$$\begin{cases} \tilde{\sigma} = \sigma + \alpha \\ \tilde{v} + \tilde{B} = v + B - \alpha \\ \tilde{v}_i + \tilde{B}_i = v_i + B_i - \alpha_{,i} \end{cases} \quad . \tag{A.129}$$

A.3.3 Different gauges : synchronous & longitudinal

We have seen that only two scalar quantities are necessary to fully describe the infinitesimal scalar coordinate transformations : ξ^0 and ξ. We can thus impose two conditions on the four scalar degrees of freedom (dofs) of first order metric perturbations. Different conditions impose different gauges and different transformations of the coordinates (which involve these dofs). Choosing a gauge is thus equivalent to choosing the system of coordinates in which we want to describe perturbations. We will now present the two important gauges for this thesis : the synchronous and longitudinal gauges. We emphasize the point that expressions presented here, i.e. in particular the functions $\psi, \phi, B, E, \ldots$, are all first order relations that are more involved at second order (see e.g. Eq. (A.110)).

Synchronous gauge (SG) : It is defined by

$$\tilde{\phi} = 0 \quad , \quad \tilde{B} = 0 \qquad \text{(synchronous gauge condition)} \quad . \tag{A.130}$$

We can understand from $\tilde{\phi} = 0$ that an observer at a fixed position x^i_s in the synchronous gauge has a proper time which coincide with the cosmic time of the FLRW background (i.e. $d\tau = a d\eta \equiv dt$).

One can see that Eq. (A.120) and (A.121) give in that case :

$$0 = \phi - \partial_{\tilde{\eta}}\xi^0 - \mathcal{H}\xi^0 \quad , \quad \tilde{\psi} = \psi + \mathcal{H}\xi^0 \quad , \quad 0 = B + \xi^0 - \xi' \quad , \quad \tilde{E} = E - \xi \quad , \tag{A.131}$$

and so we can choose the functions (ξ^0, ξ), i.e. the transformation of coordinates which set a general perturbed background (i.e. in an arbitrary system of coordinates), in such a way that these properties are satisfied and so that the system of coordinates $\{\tilde{x}^\mu\}$ has the desired properties. The solution to be used is

$$\eta \to \eta_s = \eta + \frac{1}{a}\int a\phi\, d\eta \quad , \quad x^i \to x^i_s = x^i + \gamma^{ij}\left(\int B d\eta + \int \frac{1}{a} d\eta \int a\phi d\eta\right)_{|j} \quad . \tag{A.132}$$

These coordinates (η_s, x^i_s) are the very popular synchronous gauge coordinates [7].

We can see nevertheless that synchronous coordinates are not totally fixed : there is a residual gauge freedom under the transformation :

$$\eta \to \eta_s = \eta + \frac{1}{a}C_1(\mathbf{x}) \quad , \quad x^i \to x^i_s = x^i + \gamma^{ij}C_{1|j}(\mathbf{x})\int \frac{1}{a}d\eta + \gamma^{ij}C_{2|j}(\mathbf{x}) \quad , \tag{A.133}$$

7. Note that the subscript "s" here means "synchronous" and not the source position as it was employed in the main body of this thesis.

where $C_1(\mathbf{x})$ and $C_2(\mathbf{x})$ are arbitrary functions of the spatial coordinates. It was thus realized historically that this gauge can lead to ambiguities : the so called gauge-modes which are not physical but only due to this arbitrary freedom in the coordinates. For that reason the synchronous gauge is less used nowadays, especially for the interpretation of super-horizon perturbations.

One way out to this problem of residual gauge freedom is to impose the further condition that $\widetilde{v}_{cdm} = 0$. One then has that $C_1(\mathbf{x}) = a(v_{cdm} + B)$.

Longitudinal gauge : This gauge is also called conformal **Newtonian gauge (NG)** (or the *orthogonal zero-shear gauge*). It is defined by

$$\tilde{B} = 0 \quad , \quad \tilde{E} = 0 \qquad \text{(longitudinal gauge condition)} \quad . \tag{A.134}$$

This condition thus implies that the scalar shear potential is zero in the longitudinal gauge : $\sigma_\ell = E'_\ell - B_\ell = 0$.

We can see from Eq. (A.121) that these conditions fix ξ^0 and ξ, as B and E are given in our starting system of coordinates $\{x^\mu\}$. We then find the infinitesimal transformation of coordinates which write this metric in the longitudinal form :

$$\eta \to \eta_\ell = \eta - (B - E') \quad , \quad x^i \to x^i_\ell = x^i + \gamma^{ij} E_{|j}(\mathbf{x}) \quad , \tag{A.135}$$

We can also see from Eq. (A.122) that the gauge invariant Bardeen potentials are simply equal to the variables ϕ and ψ in the longitudinal gauge : $\Phi = \phi_\ell$ and $\Psi = \psi_\ell$ [8]. It is thus very interesting to derive the EoM in the longitudinal gauge as these EoMs are the gauge invariant EoMs after we replace (ϕ_ℓ, ψ_ℓ) by (Φ, Ψ). If the stress-energy tensor has a spatial part which is diagonal, we then have $\Phi = \Psi$ which is a generalization of the Newtonian gravitational potential ϕ.

We can do a transformation of coordinates to write the synchronous coordinates in the longitudinal gauge. For this we apply the transformation of Eq. (A.135) which writes a general metric in the longitudinal gauge, and we fix this general metric to actually be the synchronous metric, i.e. we set $\phi = B = 0$ (and specifying $E = E_s$, $\psi = \psi_s$). The general transformation to go from the synchronous gauge to the longitudinal one is thus :

$$\eta_s \to \eta_\ell = \eta_s + E'_s \quad , \quad x^i_s \to x^i_\ell = x^i_s + \gamma^{ij} E_{s|j}(\mathbf{x}) \quad . \tag{A.136}$$

We find that the functions ϕ and ψ in both gauges are related by the following relations :

$$\phi_\ell = -\mathcal{H} E'_s - E''_s \quad , \quad \psi_\ell = \psi_s + \mathcal{H} E'_s \quad . \tag{A.137}$$

Using Eq. (A.124), one can show that the energy-density perturbations in synchronous and longitudinal gauges are linked by

$$\delta\epsilon_\ell = \delta\epsilon_s - \epsilon'_0 E'_s \quad . \tag{A.138}$$

Conversely, we can also write the longitudinal gauge in a synchronous gauge form (see [136], p. 217).

We should note also that the instability implied by $\sigma_\ell = 0$ is known to make the use of the longitudinal gauge difficult in the super-horizon limit.

A.3.4 Other interesting gauges

We have presented until now the synchronous gauge and the longitudinal gauge. Other gauges are commonly used in the literature and we intend to give a short review of them here.

8. We remark that the longitudinal gauge, given simply by the line element

$$ds^2 = -(1 + 2\Phi)dt^2 + (1 - 2\Psi)\gamma_{ij} dx^i dx^j \quad ,$$

is sometimes also written, with clearly different definitions of the Bardeen potentials Φ and Ψ, in the following way :

$$ds^2 = -e^{2\Phi} dt^2 + e^{-2\Psi} \gamma_{ij} dx^i dx^j \quad .$$

Poisson gauge : The Poisson gauge is an extension of the Newtonian gauge to the case of vector and tensor modes. One can define this gauge by the following line element (presented in Eq. (4.1)) :

$$ds^2 = a^2(\eta)\left[-(1+2\Phi)d\eta^2 + 2\omega_i dx^i d\eta + ((1-2\Psi)\delta_{ij} + h_{ij})dx^i dx^j\right] \tag{A.139}$$

where $h^i{}_i = 0$, $h_{ij}{}^{|i} = 0$ and $\omega_i{}^{,i} = 0$.

One obtain the definition of this gauge by taking the gauge conditions of the Newtonian gauge, Eq. (A.134), and by adding to them the further conditions :

$$\widetilde{B}^i_l = 0 \quad \text{and} \quad \widetilde{S}^i_l = 0 \quad . \tag{A.140}$$

This defines the vectorial part of the spatial gauge transformation :

$$\gamma^i_{1l} = \left[\int S^i_1 \mathrm{d}\eta\right] + \hat{C}^i_1(\mathbf{x}) \tag{A.141}$$

where $\hat{C}^i_1(\mathbf{x})$ is an arbitrary 3-vector which depends on the choice of the spatial coordinates on the initial hypersurface.

Spatially flat gauge : It is also called the *Uniform curvature gauge* or the *Off-diagonal gauge* and it is defined by the gauge conditions :

$$\widetilde{\psi} = \widetilde{E} = 0 \qquad \text{and} \qquad \widetilde{F}_i = 0 \tag{A.142}$$

This gauge is sometimes more practical than the longitudinal gauge, e.g. in calculations involving collapsing Pre-Big Bang scenarios.

Comoving orthogonal gauge : We can choose the spatial coordinates such that the 3-velocity of the fluid cancels :

$$\widetilde{v}_i = 0 \quad . \tag{A.143}$$

The orthogonality of the constant-η hypersurfaces with the 4-velocity u^μ imposes :

$$\widetilde{v}_i + \widetilde{B}_i = 0 \quad . \tag{A.144}$$

One then has α_{com} which is fixed but β_{com} depends on an arbitrary function $\hat{C}(x^i)$ corresponding to a translation of spatial coordinates.

Total matter gauge : It is also called the *velocity orthogonal isotropic gauge*. One fixes the temporal part of this gauge by imposing that the *total momemtum potential* cancels :

$$\widetilde{v} + \widetilde{B} = 0 \quad . \tag{A.145}$$

The spatial part is fixed by the following :

$$\widetilde{E} = \widetilde{F}_i = 0 \quad . \tag{A.146}$$

Uniform density gauge : One fixes the temporal part of this gauge by imposing the following conditions on the density :

$$\widetilde{\delta\rho} = 0 \quad . \tag{A.147}$$

It remains a liberty which is the liberty of the spatial part of the gauge. One fixes it by choosing that either $\tilde{B}$, $\tilde{E}$, or $\tilde{v}$ is zero in order to fix β.

A.3.5 Perturbations of Einstein's equations

Now we have described the gauge issue and the proper way to deal with it through gauge invariant quantities, we come back on Einstein's equations (A.90) and explain the basic elements to deal with perturbations of these equations. We attach ourself in particular to describe the properties of the stress-energy tensor as it is important for this thesis.

Let us decompose the Einstein tensor and the stress-energy tensor as

$$G^{\mu}{}_{\nu} = G^{(0)\mu}{}_{\nu} + \delta G^{\mu}{}_{\nu} \quad , \quad T^{\mu}{}_{\nu} = T^{(0)\mu}{}_{\nu} + \delta T^{\mu}{}_{\nu} \quad , \tag{A.148}$$

where the background FLRW universe implies

$$G^{(0)0}{}_{0} = 3\frac{\mathcal{H}^2 + K}{a^2} \quad , \quad G^{(0)0}{}_{i} = 0 \quad , \quad G^{(0)i}{}_{j} = \frac{2\mathcal{H}' + \mathcal{H}^2 + K}{a^2}\delta^i{}_j \quad . \tag{A.149}$$

and to respect the symmetry we must have

$$T^{(0)i}{}_{0} = T^{(0)0}{}_{i} = 0 \quad , \quad T^{(0)i}{}_{j} \propto \delta^i{}_j \quad . \tag{A.150}$$

Using that

$$G^{(0)\mu}{}_{\nu} = 8\pi G\, T^{(0)\mu}{}_{\nu} \quad , \tag{A.151}$$

we get at first order in perturbations:

$$\delta G^{\mu}{}_{\nu} = 8\pi G\, \delta T^{\mu}{}_{\nu} \quad . \tag{A.152}$$

Nevertheless $\delta G^{\mu}{}_{\nu}$ is not gauge invariant in general and thus the RHS and LHS of these last perturbed Einstein equations are not both invariant under gauge transformations.

Under scalar perturbations given by Eq. (A.116), $\delta G^{\mu}{}_{\nu}$ transforms as:

$$\begin{aligned}
\delta G^0{}_0 &\rightarrow \widetilde{\delta G}^0{}_0 = \delta G^0{}_0 - (G^{(0)0}{}_0)'\,\xi^0 \quad , \\
\delta G^0{}_i &\rightarrow \widetilde{\delta G}^0{}_i = \delta G^0{}_i + (G^{(0)0}{}_0 - \frac{1}{3}\delta G^k{}_k)\xi^0{}_{|i} \quad , \\
\delta G^i{}_j &\rightarrow \widetilde{\delta G}^i{}_j = \delta G^i{}_j - (G^{(0)i}{}_j)'\,\xi^0 \quad ,
\end{aligned} \tag{A.153}$$

where $\delta G^0{}_0$, $\delta G^0{}_i$ and $\delta G^i{}_j$ are complicated expressions of ϕ, ψ, B and E. Nevertheless, it is possible to build up gauge invariant perturbations of $\delta G^{\mu}{}_{\nu}$ by

$$\begin{aligned}
\delta G^{(g.i.)0}{}_0 &= \delta G^0{}_0 + (G^{(0)0}{}_0)'(B - E') \quad , \\
\delta G^{(g.i.)0}{}_i &= \delta G^0{}_i + (G^{(0)0}{}_0 - \frac{1}{3}\delta G^k{}_k)(B - E')_{|i} \quad , \\
\delta G^{(g.i.)i}{}_j &= \delta G^i{}_j + (G^{(0)i}{}_j)'(B - E') \quad ,
\end{aligned} \tag{A.154}$$

and where

$$\begin{aligned}
\delta G^0{}_0 &= 2a^{-2}\left[-3\mathcal{H}(\mathcal{H}\Phi + \Psi') + \nabla^2\Psi + 3K\Psi + 3\mathcal{H}(-\mathcal{H}' + \mathcal{H}^2 + K)(B - E')\right] \quad , \\
\delta G^0{}_i &= 2a^{-2}\left[\mathcal{H}\Phi + \Psi' + (\mathcal{H}' - \mathcal{H}^2 - K)(B - E')\right]_{,i} \quad , \\
\delta G^i{}_j &= -2a^{-2}\Bigg[\left([2\mathcal{H}' + \mathcal{H}^2]\Phi + \mathcal{H}\Phi' + \Psi'' + 2\mathcal{H}\Psi' - K\Psi + \frac{1}{2}\nabla^2 D\right)\delta^i_j \\
&\qquad + \left(\mathcal{H}'' - \mathcal{H}\mathcal{H}' - \mathcal{H}^3 - K\mathcal{H}\right)(B - E')\delta^i_j - \frac{1}{2}\gamma^{ik}D_{|kj}\Bigg] \quad , \\
D &\equiv \Phi - \Psi \quad .
\end{aligned} \tag{A.155}$$

We can define, in the same way as in Eq. (A.154), gauge invariant perturbations of the stress-energy tensor. The same relations hold in the case where $(G^{\bullet}{}_{\bullet}, \delta G^{\bullet}{}_{\bullet})$ is replaced by $(T^{\bullet}{}_{\bullet}, \delta T^{\bullet}{}_{\bullet})$. Doing so, we get the equality

$$\delta G^{(g.i.)\mu}{}_{\nu} = 8\pi G\, \delta T^{(g.i.)\mu}{}_{\nu} \quad , \tag{A.156}$$

where both the LHS and the RHS are now gauge invariant. We can also write down this last equation in an explicit form. In that case, we can easily see by going to the longitudinal gauge that the general gauge invariant expression $\delta G^{(g.i.)\mu}{}_{\nu}$ is just given by Eq. (A.155) where we set $B = E = 0$. The perturbation $\delta T^{(g.i.)\mu}{}_{\nu}$ is on the other hand given by its (A.154)-like form. Finally, we need to close the system by writing the EoMs of the universe content in a gauge invariant way.

A.3.6 Gauge invariant EoMs

The most general expression of the first order scalar perturbation of the stress-energy tensor involves 4 scalar $\delta\rho$, δp, v and σ :

$$\delta T^{\mu}_{\nu} = \begin{pmatrix} \delta\rho & -(\rho_0 + p_0)a^{-1}v_{,i} \\ (\rho_0 + p_0)a^{-1}v_{,i} & -\delta p\delta_{ij} + \sigma_{|ij} \end{pmatrix} \quad . \tag{A.157}$$

If we are only dealing with a perfect fluid, σ which corresponds to the anisotropic stress is zero and if the fluid is dissipationless we have the general expression for T^{μ}_{ν} :

$$T^{\mu}_{\nu} = (\rho + p)u^{\mu}u_{\nu} - p\,\delta^{\mu}_{\nu} \quad . \tag{A.158}$$

where in general $p = p(\rho, S)$ (the equation of state), with S is the entropy per baryon ratio, and :

$$\delta p = \left(\frac{\partial p}{\partial \rho}\right)_S \delta\rho + \left(\frac{\partial p}{\partial S}\right)_\rho \delta S \equiv c_s^2\delta\rho + \tau\delta S \quad . \tag{A.159}$$

In conformal time, the scalar perturbations δT^{μ}_{ν} can thus be written as

$$\delta T^{0}_{0} = \delta\rho \quad , \quad \delta T^{0}_{i} = (\rho_0 + p_0)a^{-1}\delta u_i \quad , \quad \delta T^{i}{}_{j} = -\delta p\,\delta^{i}_{j} \quad . \tag{A.160}$$

To find the gauge invariant perturbations $\delta T^{\mu}{}_{\nu}$, we use the gauge invariant expressions of $\delta\rho$, δp and δu_i :

$$\begin{aligned} \delta\rho^{(g.i.)} &= \delta\rho + \rho_0'(B - E') \quad , \\ \delta p^{(g.i.)} &= \delta p + p_0'(B - E') \quad , \\ \delta u_i^{(g.i.)} &= \delta u_i + a(B - E')_{|i} \quad . \end{aligned} \tag{A.161}$$

We can notice that these gauge invariant expressions correspond to the expressions of $\delta\rho$, δp and δu_i in the longitudinal gauge, as expected. We thus have

$$\delta T^{(g.i.)0}{}_{0} = \delta\rho^{(g.i.)} \quad , \quad \delta T^{(g.i.)0}{}_{i} = (\rho_0 + p_0)a^{-1}\delta u_i^{(g.i.)} \quad , \quad \delta T^{(g.i.)i}{}_{j} = -\delta p^{(g.i.)}\delta^{i}{}_{j} \quad . \tag{A.162}$$

We find the gauge invariant perturbed Einstein equations to be equivalent to :

$$\begin{aligned} -3\mathcal{H}(\mathcal{H}\Phi + \Psi') + \nabla^2\Psi + 3K\Psi &= 4\pi G a^2\delta\rho^{(g.i.)} \quad , \\ \left(\mathcal{H}\Phi + \Psi'\right)_{,i} &= 4\pi G(\rho_0 + p_0)\delta u_i^{(g.i.)} \quad , \\ \left([2\mathcal{H}' + \mathcal{H}^2]\Phi + \mathcal{H}\Phi' + \Psi'' + 2\mathcal{H}\Psi' - K\Psi + \frac{1}{2}\nabla^2 D\right)\delta^{i}{}_{j} - \frac{1}{2}\gamma^{ik}D_{|kj} &= 4\pi G a^2\delta p^{(g.i.)}\delta^{i}{}_{j} \quad . \end{aligned} \tag{A.163}$$

From the $(i, j \neq i)$ component of $T^{\mu}{}_{\nu}$, one can show that we need the condition $\Phi = \Psi$ (and thus $D = 0$) [9]. We hence obtain

$$\begin{aligned} \nabla^2\Phi - 3\mathcal{H}\Phi' - 3(\mathcal{H}^2 - K)\Phi &= 4\pi G a^2\delta\rho^{(g.i.)} \quad , \\ (a\Phi)'_{,i} &= 4\pi G(\rho_0 + p_0)\delta u_i^{(g.i.)} \quad , \\ \Phi'' + 3\mathcal{H}\Phi' + (2\mathcal{H}' + \mathcal{H}^2 - K)\Phi &= 4\pi G a^2\delta p^{(g.i.)} \quad . \end{aligned} \tag{A.164}$$

9. See [136], p. 223, for more details on this statement. We should notice that the notion of the vanishing of averaging over a spatial hypersurface at first order is mentioned to justify this condition.

We notice that the first of these equations is the generalization of the Poisson equation in the case of an expanding background. Another important fact about this equation is that it is valid only in its linear regime, i.e. for $|\Phi| \ll 1$, which does not imply $|\delta\rho/\rho| \ll 1$ and so this equation can be valid even for high density contrasts (such as in clusters of galaxies or on super-horizon scales). We directly get the general expression of the gauge invariant perturbations of the matter density and its peculiar velocity (for dust matter, the pressure is negligible and so not interesting) :

$$\begin{aligned} \frac{\delta\rho^{(g.i.)}}{\rho_0} &= 2\frac{\nabla^2\Phi - 3\mathcal{H}\Phi' - 3(\mathcal{H}^2 - K)\Phi}{3(\mathcal{H}^2 + K)} \quad , \\ \delta u^{(g.i.)i} &= -\frac{(a\Phi)'_{,i}}{a^2(\mathcal{H}^2 - \mathcal{H}' + K)} \quad . \end{aligned} \tag{A.165}$$

A.4 The power spectrum in the linear regime

A.4.1 Basic facts

Let us recall here the notions that we presented in Sec. 1.4.2 in order to illustrate and complete them. We will then, in Sec. A.5, extend these notions to the non-linear spectrum.

In synchronous gauge, the Poisson equation gives a relation between the gravitational (Bardeen) potential and the matter density contrast which is given by:

$$\nabla^2\psi(x) = 4\pi G\rho(t)\,\delta(x)\ . \tag{A.166}$$

When we go in Fourier space, assuming a flat FLRW model, this equation becomes:

$$|\psi_k|^2 = \left(\frac{3}{2}\right)^2 \frac{\Omega_m^2(z)\mathcal{H}^4}{k^4}|\delta_k|^2 \qquad \text{where} \qquad \Omega_m(z) = \Omega_{m0}(1+z)\left(\frac{\mathcal{H}_0}{\mathcal{H}}\right)^2\ . \tag{A.167}$$

The dimensionless power spectrum for the potential is defined by

$$\mathcal{P}_\psi(k,\eta) \equiv \frac{k^3}{2\pi^2}|\psi_k(\eta)|^2\ , \tag{A.168}$$

and effectively built up from the primordial inflationary spectrum $\left(\frac{3}{5}\right)^2\Delta^2_{\mathcal{R}}$ and the addition of a transfer function $T(k)$, to describe the sub-horizon evolution of the gravitational potential during the radiation era, and a growth factor $g(z)$ to account for its evolution during the (recent) dark energy dominated era. Consequently, one has the expression for the primordial inflationary spectrum:

$$\Delta^2_{\mathcal{R}} = A\left(\frac{k}{k_0}\right)^{n_s-1} \qquad \text{and} \qquad (A, n_s, k_0/a_0) = \left(2.45\ 10^{-9}\ ,\ 0.96\ ,\ 0.002\ \text{Mpc}^{-1}\right)\ , \tag{A.169}$$

and the linear power spectrum is finally given by

$$\mathcal{P}_\psi(k) = \left(\frac{3}{5}\right)^2 \Delta^2_{\mathcal{R}} T^2(k)\left(\frac{g(z)}{g_\infty}\right)^2\ . \tag{A.170}$$

A.4.2 Transfer function

From the study of Eisenstein & Hu [68], we can approximate the true transfer function $T(k)$ with an effective shape in the case of density perturbations with no baryonic effects involved (such as Silk damping or acoustic oscillations). In other words, all the baryonic matter is considered as being dark matter. We then write $T(k) = T_0(k)$ with:

$$T_0(q) = \frac{L_0}{L_0 + q^2 C_0(q)}\ , \quad L_0(q) = \ln(2e{+}1.8q)\ , \quad C_0(q) = 14.2{+}\frac{731}{1+62.5q}\ , \quad q = \frac{k}{13.41k_{\rm eq}}\ , \tag{A.171}$$

where $k_{\rm eq} = (\Omega_{m0}h^2/13.41)\,\text{Mpc}^{-1}$ is the scale corresponding to matter-radiation equality and $h \equiv H_0/(100\,\text{km}\,\text{s}^{-1}\text{Mpc}^{-1})$. In the following we will use $h = 0.7$ and set $a_o = 1$. The numerical value of $k_{\rm eq}$ is then $k_{\rm eq} \simeq 0.036$ Mpc^{-1} for $\Omega_{m0} = 1$ (CDM) and $k_{\rm eq} \simeq 0.010$ Mpc^{-1} for $\Omega_{m0} = 0.27$ (ΛCDM). We can easily check that the above transfer function goes to 1 for $k \ll k_{\rm eq}$, while it falls like $k^{-2}\log k$ for $k \gg k_{\rm eq}$.

We can complicate the description of the transfer function by including the effect of a baryonic fraction in Ω_{m0}. In that case the transfer function is suppressed by the so-called Silk damping, leading to a decrease of 10-40% of the transfer function in the range $k \gtrsim 0.01h\,\text{Mpc}^{-1}$. In order to take into account this baryonic contribution we have to replace the value of q used in the previous section, i.e.

$q = k/(13.41 k_{\rm eq})$, with the more accurate value given by [68] :

$$\begin{aligned} q &= \frac{k \times \mathrm{Mpc}}{h\Gamma} \quad , \\ \Gamma &= \Omega_{m0} h \left(\alpha_\Gamma + \frac{1-\alpha_\Gamma}{1+(0.43ks)^4} \right) \quad , \\ \alpha_\Gamma &= 1 - 0.328 \ln(431 \Omega_{m0} h^2) \frac{\Omega_{b0}}{\Omega_{m0}} + 0.38 \ln(22.3 \Omega_{m0} h^2) \left(\frac{\Omega_{b0}}{\Omega_{m0}} \right)^2 \quad , \\ s &= \frac{44.5 \ln(9.83/\Omega_{m0} h^2)}{\sqrt{1+10(\Omega_{b0} h^2)^{3/4}}} \, \mathrm{Mpc} \quad . \end{aligned} \tag{A.172}$$

Here Ω_{b0} is the baryon density parameter, s is the sound horizon and Γ is the k-dependent effective shape parameter. For the numerical values, we can take $\Omega_{\Lambda 0} = 0.73$, $\Omega_{m0} = 0.27$, $\Omega_{b0} = 0.046$, and $h = 0.7$.

We could go further in complexifying the expression of this transfer function by including the effect of baryonic oscillations. Nevertheless, to avoid unnecessary complications, and because we have not used it in our work, they are neglected here. Above considerations regarding the two different transfer functions can easily be verified in Fig. A.3.

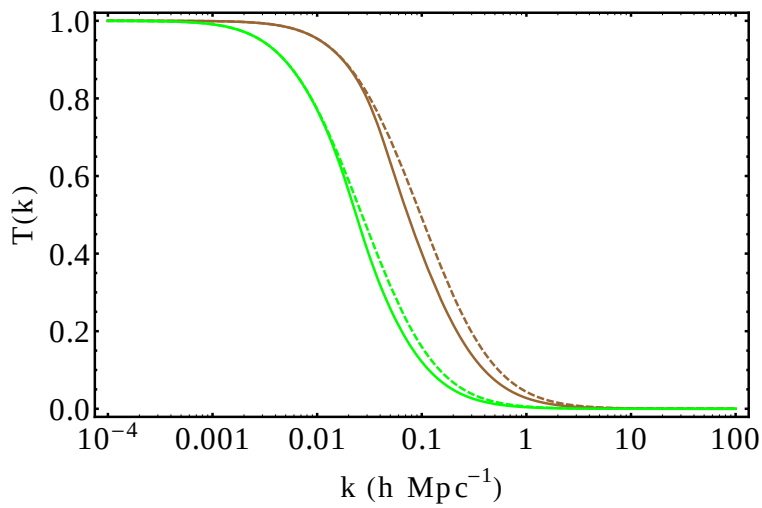

Figure A.3: The transfer function used in the elaboration of the linear power spectrum $\mathcal{P}_\psi(k)$ in different situations : in CDM for $\Omega_{m0} = 1$ (brown) and in ΛCDM with $(\Omega_{m0}, \Omega_{\Lambda 0}) = (0.27, 0.73)$ (green). There is no z-dependence in $T(k)$. Plots are represented in the simple case of dark matter only (dashed), Eq. (A.171), and in the case including a baryonic contribution (solid), Eq. (A.172).

A.4.3 The growth factor g(z)

In the expression (A.170), the growth factor $g(z)$ is taking into account the time dependence of ψ_k due to the late dark energy phase of expansion, i.e. :

$$\psi_k(z) = \frac{g(z)}{g(0)} \psi_k(0)$$

and its general expression in the case of ΛCDM is (see [134, 138]) :

$$g(z) = \frac{5}{2} \Omega_m(z) \, g_\infty \left[\Omega_m(z)^{4/7} - \Omega_\Lambda(z) + \left(1 + \frac{\Omega_m(z)}{2}\right) \left(1 + \frac{1}{70} \Omega_\Lambda(z)\right) \right]^{-1} \tag{A.173}$$

$$\text{with} \quad \Omega_m(z) = \frac{\Omega_{m0}(1+z)^3}{\Omega_{m0}(1+z)^3 + \Omega_{\Lambda 0}} \quad \text{and} \quad \Omega_\Lambda(z) = \frac{\Omega_{\Lambda 0}}{\Omega_{m0}(1+z)^3 + \Omega_{\Lambda 0}} \quad , \tag{A.174}$$

where the limit $z \to 0$ gives $g(0) = 0.7584\ g_\infty$. In the limiting case ($\Omega_{m0} \to 1, \Omega_{\Lambda 0} \to 0$), that is to say a CDM model, we get $g(z) = g_\infty\ \forall\ z$. We can thus take $g_\infty = 1$ if we want, the important thing being that $g(z)/g(0) = 1$.

A.4.4 Plot of the linear power spectrum

We have all the elements to draw the power spectrum for the gravitational potential, in the linear regime of perturbations, for different redshifts. This is what is done in Fig. A.4. We remark from these plots that $\mathcal{P}_\psi(k)$ decreases in magnitude when z decreases (a modulation entirely due to the factor $g(z)$ as it can be seen in Eq. (A.170)). In the case of the matter density spectrum, it would be the contrary and this change in behavior is due to the $(1+z)^2$ factor, coming from $\Omega_m^2(z)$, in Eq. (A.167).

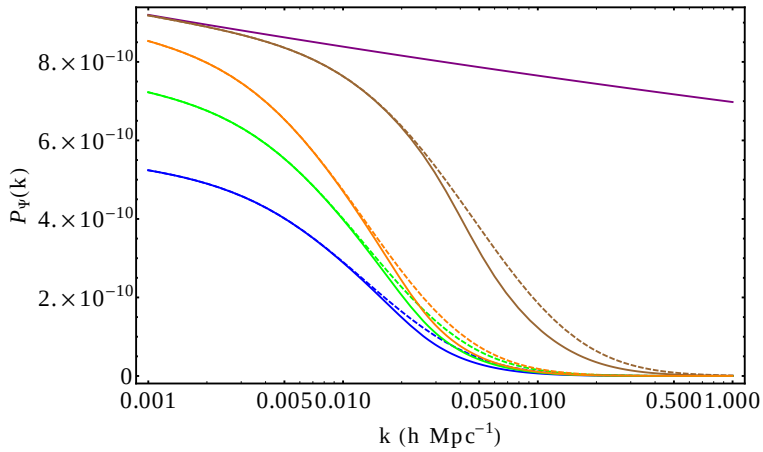

Figure A.4: The linear gravitational power spectrum in different situations : CDM (brown) ; ΛCDM for $z = 0$ (blue), $z = 0.5$ (green), and $z = 1.5$ (orange). It can be compared to the primordial power spectrum from inflation (purple). Dotted (solid) lines correspond to the use of the transfer function without (with) baryonic effect.

A.5 The HaloFit model

In this section we will describe the HaloFit model which brings an effective description of the power spectrum in its non-linear regime. This model was first established by [23] and recently revisited in [74] in the case of more accurate N-body simulations.

A.5.1 General considerations : density power spectrum

Let us recall here the basic considerations about the density power spectrum, already shown in Sec. 1.4.3. The density spectrum is defined by the density variance :

$$\sigma^2 \equiv \overline{\delta(x)\delta(x)} = \int \frac{d^3k}{(2\pi)^3}|\delta_{\vec{k}}|^2 = \int \frac{k^2 dk}{2\pi^2}|\delta_k|^2 = \int \Delta^2(k)\ d\ln k \quad . \tag{A.175}$$

This expression leads to the direct definition in Fourier space :

$$\Delta^2(k,z) = \frac{k^3}{2\pi^2}|\delta_k(z)|^2 = \frac{d\sigma^2}{d\ln k} \quad , \tag{A.176}$$

showing that $\Delta(k,z)$ is a dimensionless quantity.

This density spectrum is related to the gravitational potential spectrum by the Poisson equation (A.167) which is valid both in the linear and non-linear regimes :

$$\mathcal{P}_\psi^{\mathrm{L,NL}}(k) = \frac{9}{4}\frac{\Omega_{m0}^2\mathcal{H}_0^4}{k^4}(1+z)^2\Delta^2_{\mathrm{L,NL}}(k) \quad . \tag{A.177}$$

Using the linear power spectrum given by Eq. (A.170), one gets the expression for the density spectrum in the linear regime :

$$\Delta^2_{\rm L}(k) = \frac{4}{9}\frac{k^4}{\Omega^2_{m0}\mathcal{H}_0^4(1+z)^2}\mathcal{P}^{\rm L}_\psi(k) = \frac{4}{25}\frac{A\Omega^{-2}_{m0}\mathcal{H}_0^{-4}}{(1+z)^2}\,\frac{k^{n_s+3}}{k_0^{n_s-1}}\left(\frac{g(z)}{g_0}\right)^2 T^2(k) \quad . \tag{A.178}$$

We will now use the HaloFit model to generate from $\Delta^2_{\rm L}(k)$ the density power spectrum in its non-linear regime, i.e. $\Delta^2_{\rm NL}(k)$. As a last step, we will use the Poisson equation in the non-linear regime to obtain $\mathcal{P}^{\rm NL}_\psi(k)$, the quantity of interest for our work.

A.5.2 The NLPS from the LPS : the HaloFit Model

The HaloFit model decomposes the matter density spectrum into a sum of two contributions:

$$\Delta^2_{\rm NL}(k) = \Delta^2_{\rm Q}(k) + \Delta^2_{\rm H}(k) \quad , \tag{A.179}$$

where roughly one settles the linear behaviour and the other deals with the non-linear regime of inhomogeneities. Indeed, the first term in the RHS of Eq. (A.179), $\Delta^2_{\rm Q}(k)$, is called the two-halo term and is taking into account matter correlations at large distances (low k). The other one, $\Delta^2_{\rm H}(k)$, is the one-halo term and it describes the non-linear behaviour of matter inside the halo region. These two contributions are parametrized [23] by :

$$\begin{aligned}
\Delta^2_{\rm Q}(k) &= \Delta^2_{\rm L}(k)\left[\frac{(1+\Delta^2_{\rm L}(k))^{\beta_n}}{1+\alpha_n\Delta^2_{\rm L}(k)}\right]e^{-f(y)} \quad , \\
\Delta^2_{\rm H}(k) &= \frac{\Delta^2_{\rm H}{}'(k)}{1+\mu_n y^{-1}+\nu_n y^{-2}} \quad \text{with} \quad \Delta^2_{\rm H}{}'(k) = \frac{a_n\ y^{3f_1(\Omega_{m0})}}{1+b_n y^{f_2(\Omega_{m0})}+[c_n f_3(\Omega_{m0})\ y]^{3-\gamma_n}} \quad ,
\end{aligned} \tag{A.180}$$

where $y \equiv k/k_\sigma$ and $f(y) = y/4 + y^2/8$. We can easily understand from its expression that $\Delta^2_{\rm Q}(k)$ is made to fit the linear power spectrum $\Delta^2_{\rm L}(k)$ when it takes small values (i.e. at large scales) and change it when it becomes of order 1 (i.e. when it reaches the weak non-linear regime). It is then rapidly negligible at $k > k_\sigma$ (defined later) because of its exponential suppression factor. The other contribution $\Delta^2_{\rm H}(k)$ is taking into account the non-linear aspect of the power spectrum in a way which is more difficult to analyse analytically, but which is physically expected to raise the power spectrum (to enhance the strength of non-linear scales).

We can see in these expressions of Eq. (A.180) that a lot of parameters come into play. The first parameters that we can notice are functions of the cosmology in $\Delta^2_{\rm H}{}'(k)$, namely $\{f_i\}_{i=1,2,3}$. These Ω_{m0}-dependent functions are parametrized as follows (see [23]) :

$$\left.\begin{aligned}
f_{1a}(\Omega_{m0}) &= (\Omega_{m0})^{\ -0.0732} \\
f_{2a}(\Omega_{m0}) &= (\Omega_{m0})^{\ -0.1423} \\
f_{3a}(\Omega_{m0}) &= (\Omega_{m0})^{\ 0.0725}
\end{aligned}\right\} \text{ for } \Omega_{m0} \leq 1\,, \quad
\left.\begin{aligned}
f_{1b}(\Omega_{m0}) &= (\Omega_{m0})^{\ -0.0307} \\
f_{2b}(\Omega_{m0}) &= (\Omega_{m0})^{\ -0.0585} \\
f_{3b}(\Omega_{m0}) &= (\Omega_{m0})^{\ 0.0743}
\end{aligned}\right\} \text{ for } \Omega_{m0}+\Omega_{\Lambda 0} = 1\,. \tag{A.181}$$

We naturally choose this last (b) case where $\Omega_{m0}+\Omega_{\Lambda 0} = 1$ to be consistent with the ΛCDM model [10]. This is also the case adopted by [74].

We can see that the Eq. (A.180) includes an additional parameter which is k_σ. In fact this parameter is involved in the function $e^{-f(y)}$ and it basically sets the non-linear scale. It is also present in all the other parameters that we will describe in the next subsection. It is thus a very important quantity. For this we redefine the variance of the density perturbation presented in Eq. (A.175), applying to it a Gaussian filtering at a physical scale $R_{\rm G}$:

$$\sigma^2(R_{\rm G}) \equiv \int \Delta^2_{\rm L}(k,z)\ \exp(-k^2R^2_{\rm G})\ d\ln k \quad , \tag{A.182}$$

10. For models in which $\Omega_{\Lambda 0}$ is neither zero nor $1-\Omega_{m0}$, [23] suggests to interpolate the functions f_i linearly in $\Omega_{\Lambda 0}$ between the open and flat cases. This is not our case.

we then define k_σ by normalizing this variance to 1 :

$$\sigma^2(R_{\rm G}=k_\sigma^{-1},z)\equiv\int\Delta^2_{\rm L}(k,z)\,\exp(-(k/k_\sigma)^2)\,d\ln k\equiv 1\quad . \tag{A.183}$$

In practice we compute this integral by incrementing the value of k_σ until we reach a value for σ^2 which is close enough to unity. It is also obvious that the ΛCDM case will produce a linear spectrum $\Delta^2_{\rm L}(k,z)$ that depends on the redshift. As a consequence k_σ will also be a redshift dependent quantity and so will be the X_n parameters of the fit that we are now going to present.

A.5.3 Two parametrizations : Smith *et al.* & Takahashi *et al.*

The other coefficients, namely $X_n\equiv\{a_n,b_n,c_n,\gamma_n,\alpha_n,\beta_n,\mu_n,\nu_n\}$, are found by fitting simulations and give a really accurate effective description. They are expressed as polynomials of two quantities : an effective spectral index $n_{\rm eff}$ and a parameter C controling the curvature of the spectral index.

This effective spectral index is given by

$$3+n_{\rm eff}\equiv-\left.\frac{d\ln\sigma^2(R)}{d\ln R}\right|_{\sigma=1}\quad , \tag{A.184}$$

and it basically describes the deviation of the linear power spectrum $\Delta^2_{\rm L}(k)$ from a power law $\sim k^{n+3}$. In our case, we start with a linear density spectrum given by Eq. (A.178) and it will clearly not be a power law.

The curvature of the spectral index C is by definition [11] :

$$\begin{aligned} C &\equiv -\left.\frac{d^2\ln\sigma^2(R)}{d\ln R^2}\right|_{\sigma=1}=\left\{-\frac{d}{d\ln R}\left[\frac{R}{\sigma^2}\frac{d\sigma^2(R)}{dR}\right]\right\}_{R=k_\sigma^{-1}} \\ &= \left\{-\frac{R}{\sigma^2}\frac{d\sigma^2}{dR}+\frac{R^2}{(\sigma^2)^2}\left(\frac{d\sigma^2}{dR}\right)^2-\frac{R^2}{\sigma^2}\frac{d^2\sigma^2}{dR^2}\right\}_{R=k_\sigma^{-1}}\quad . \end{aligned} \tag{A.186}$$

We understand that both $n_{\rm eff}$ and C will have a dependence on z, for the simple reason that they depend on k_σ. Their value is computed numerically after having computed the d/dR derivatives analytically (these derivatives acting only in the exponential of Eq. (A.182)) and replaced $\Delta^2_{\rm L}(k,z)$ by its explicit form of Eq. (A.178).

In [23], the X_n coefficients are evaluated for a certain set of initial power spectra (which, we recall, are taken as power laws of k) and are found to be [12] :

$$\begin{aligned} \log_{10}a_n &= 1.4861+1.8369\,n_{\rm eff}+1.6762\,n_{\rm eff}^2+0.7940\,n_{\rm eff}^3+0.1670\,n_{\rm eff}^4-0.6206\,C\quad , \\ \log_{10}b_n &= 0.9463+0.9466\,n_{\rm eff}+0.3084\,n_{\rm eff}^2-0.9400\,C\quad , \\ \log_{10}c_n &= -0.2807+0.6669\,n_{\rm eff}+0.3214\,n_{\rm eff}^2-0.0793\,C\quad , \\ \gamma_n &= 0.8649+0.2989\,n_{\rm eff}+0.1631\,C\quad , \\ \alpha_n &= 1.3884+0.3700\,n_{\rm eff}-0.1452\,n_{\rm eff}^2\quad , \\ \beta_n &= 0.8291+0.9854\,n_{\rm eff}+0.3401\,n_{\rm eff}^2\quad , \\ \log_{10}\mu_n &= -3.5442+0.1908\,n_{\rm eff}\quad , \\ \log_{10}\nu_n &= 0.9589+1.2857\,n_{\rm eff}\quad . \end{aligned} \tag{A.187}$$

11. We can show that $C=0$ when the linear matter spectrum is a power law ($\Delta^2_{\rm L}(k)\sim k^{n+3}$). In this case we get :

$$C\equiv-2(n+3)G(n)+4G(n)^2\quad\text{with}\quad G(n)\equiv\Gamma\left(\frac{n+5}{2}\right)\Big/\Gamma\left(\frac{n+3}{2}\right)=\frac{n+3}{2}\quad , \tag{A.185}$$

and that is actually zero.

12. We should note that [23] study $\Delta^2_{\rm L}\sim k^{n+3}$ with a wide range of values for n, between 0 and −2, as they are believed to bring a self-similarity behaviour. Spectra outside this range are not well tested and thus not considered. Also, the fact that we (will) obtain values of $n_{\rm eff}$ which are between 0 and −2, by the use of $\Delta^2_L(k)$ given in Eq. (A.178), is a confirmation that we are indeed authorized to use these expressions for X_n in our study. From [23] we also learn that terms up to n^4 in the fit of a_n are especially required in order to describe the rapid rise in amplitude of the halo term for $n<-2$.

With these parameters (and others previously described), [23] obtain a deviation between the model and N-body simulations at scales $k < 10\,h\,\mathrm{Mpc}^{-1}$ which is always $< 3\%$, up to $z < 3$.

In a recent paper, Takahashi *et al.* [74] have reconsidered the halo model with a greater accuracy in simulations. This new study found the following parametrization of these parameters:

$$\begin{aligned}
\log_{10} a_n &= 1.5222 + 2.8553\, n_{\rm eff} + 2.3706\, n_{\rm eff}^2 + 0.9903\, n_{\rm eff}^3 + 0.2250\, n_{\rm eff}^4 - 0.6038\, C \\
&\quad +0.1749\, \Omega_{DE}(z)(1+w_{DE}) \\
\log_{10} b_n &= -0.5642 + 0.5864\, n_{\rm eff} + 0.5716\, n_{\rm eff}^2 - 1.5474\, C \\
&\quad +0.2279\, \Omega_{DE}(z)(1+w_{DE}) \\
\log_{10} c_n &= 0.3698 + 2.0404\, n_{\rm eff} + 0.8161\, n_{\rm eff}^2 + 0.5869\, C \\
\gamma_n &= 0.1971 - 0.0843\, n_{\rm eff} + 0.8460\, C \\
\alpha_n &= |6.0835 + 1.3373\, n_{\rm eff} - 0.1959\, n_{\rm eff}^2 - 5.5274\, C| \\
\beta_n &= 2.0379 - 0.7354\, n_{\rm eff} + 0.3157\, n_{\rm eff}^2 + 1.2490\, n_{\rm eff}^3 + 0.3980\, n_{\rm eff}^4 - 0.1682\, C \\
\mu_n &= 0 \quad , \\
\log_{10} \nu_n &= 5.2105 + 3.6902\, n_{\rm eff} \quad ,
\end{aligned} \tag{A.188}$$

where a new parameter, namely the dark energy density parameter $\Omega_{DE}(z)$, has been introduced. These $\Omega_{DE}(z)$-terms are redshift dependent and represent a possible deviation from a cosmological-constant nature of the acceleration. In our case (i.e. ΛCDM), it is naturally set to zero as $w_{DE} = -1$. This new parametrization is believed to be accurate up to very small scales: $k \leq 30\,h\,\mathrm{Mpc}^{-1}$. More precisely, [74] estimates its precision to be $\sim 5\%$ for $0 \leq z \leq 10$ and $k \leq 1\,h\,\mathrm{Mpc}^{-1}$, and to be $\sim 10\%$ for $0 \leq z \leq 3$ and $1 \leq k \leq 10\,h\,\mathrm{Mpc}^{-1}$.

A.5.4 Results on the density spectrum

We will present in the following three subsections (the current one, and the next two) the results of the computation of the power spectra at the non-linear level, using the first expression for the tranfer function $T(k)$, i.e. $T_0(k)$ which does not include any baryonic effect.

The different contributions $\{\Delta^2_{\rm L}(k), \Delta^2_{\rm H}(k), \Delta^2_{\rm Q}(k), \Delta^2_{\rm NL}(k)\}$ can be seen in Fig. A.5 for the case of Smith *et al.* parametrization. It confirms the different properties that have been described previously. We could also obtain the same quantities from the parametrization of Takahashi *et al.*, but the plots would basically be the same. Nevertheless, this latter parametrization is not adapted to the CDM case. For these two reasons, we do not present the plot from Takahashi *et al.* parametrization. However, we will present its results on the final gravitational power spectrum. One may be astonished by the color ordering in Fig. A.5 as it was the blue spectrum for gravitational potential which was the lowest one. Nevertheless, this tendency of the ΛCDM case is changed when we go to the spectrum of density contrast, and is due to the factor $(1+z)^2$ in the Poisson equation.

We present in Fig. A.6 the plot of the ratio $\Delta^2_{\rm NL}(k)/\Delta^2_{\rm L}(k)$ obtained from above's method. The results are given for ΛCDM and give a first element of comparison between [23] and [74]. Takahashi's parametrization is not presented but rather similar to the one of Smith *et al.*.

A.5.5 Final result: the gravitational spectrum

Using back the Poisson equation to get the power spectrum for the gravitational potential, we have:

$$\mathcal{P}^{\rm NL}_{\psi}(k) = \frac{9}{4}\frac{\mathcal{H}_0^4 \Omega_{m0}^2}{k^4}(1+z)^2 \Delta^2_{\rm NL}(k) \quad . \tag{A.189}$$

We should not think however that the $(1+z)^2$ factor completely cancels out because $\Delta^2_{\rm L}(k)$ is proportional to $1/(1+z)^2$. Indeed, first the parameters necessary to build up $\Delta^2_{\rm Q}(k)$ and $\Delta^2_{\rm H}(k)$ depend on the model and, for the case of ΛCDM, the redshift too. But secondly, $\Delta^2_{\rm Q}(k)$ is a non-trivial function of $\Delta^2_{\rm L}(k)$ and consequently still depends on z. Thus the three spectra now intersect each other in the NL regime. We can indeed check that comments in Fig. A.7 and A.8.

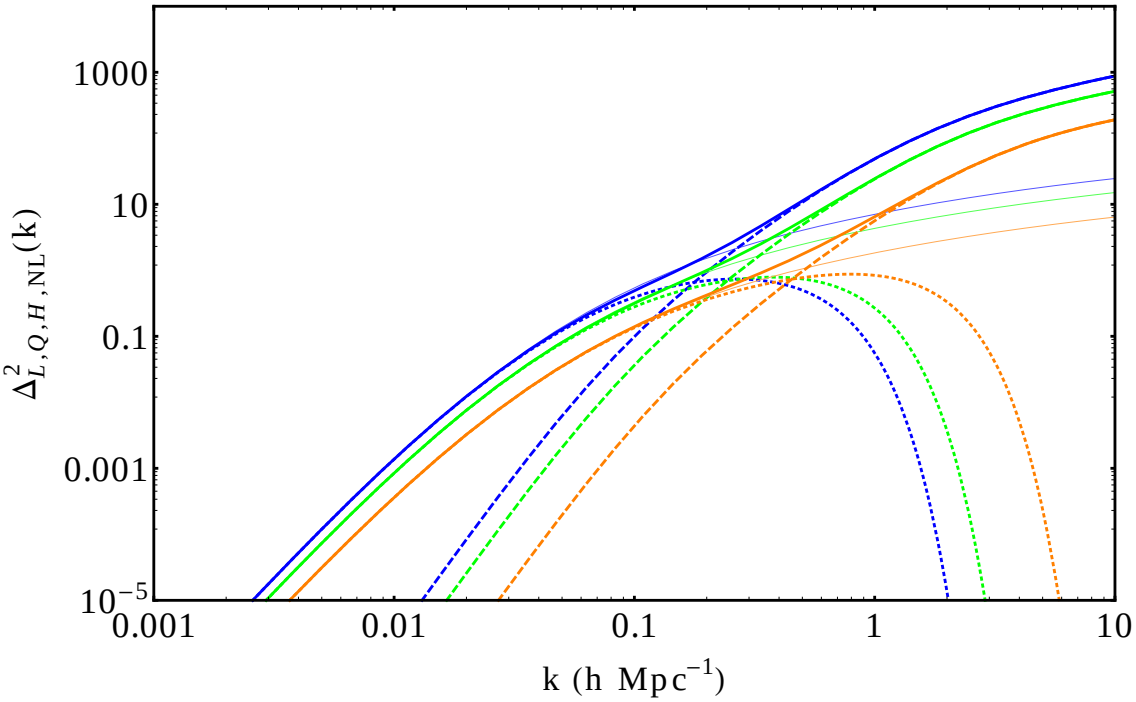

Figure A.5: The linear and non-linear density spectra deduced from Smith's method is shown for ΛCDM at 3 different redshifts (z=0 : blue ; z=0.5 : green ; z = 1.5 : orange). For each of them, $\Delta^2_{\mathrm{L}}(k)$ is in thin light color (always increasing with k and increasing when z decreases, as expected), $\Delta^2_{\mathrm{Q}}(k)$ is in dotted line (dominant at small k and exponentially suppressed at $k \sim 1 - 10\,h\,\mathrm{Mpc}^{-1}$), $\Delta^2_{\mathrm{H}}(k)$ is in dashed line and contributes only to the NL regime (dominant at large k), $\Delta^2_{\mathrm{NL}}(k)$ is in solid line. These plots should be compared with Fig. 14 & 15 in [23].

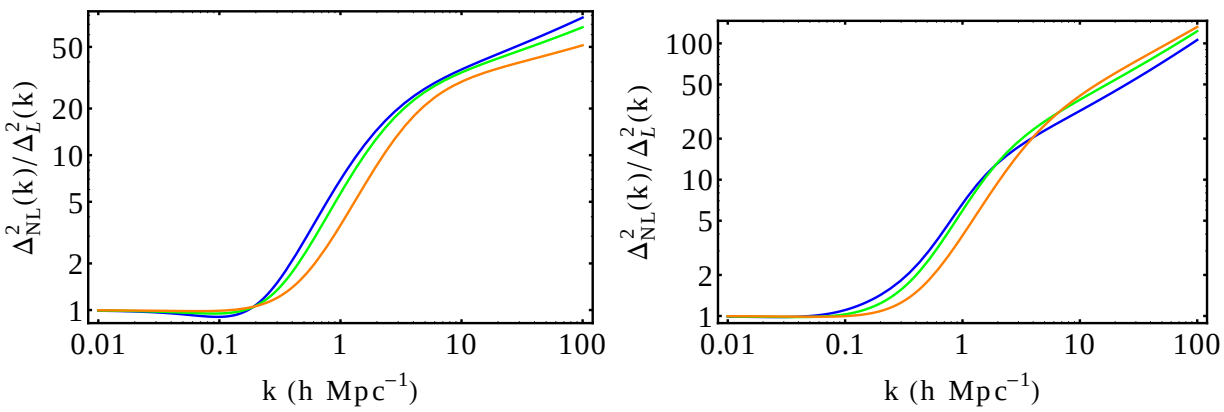

Figure A.6: Ratio $\Delta^2_{\mathrm{NL}}(k)/\Delta^2_{\mathrm{L}}(k)$ computed from Smith's method (left panel) and Takahashi's (right panel) for ΛCDM at 3 different redshifts (z=0 : blue ; z=0.5 : green ; z = 1.5 : orange). The CDM case is not represented. These plots can be compared with Fig. 16 in [23].

As a last result, we present in Fig. A.9 the computation of

$$\mathrm{DiffP}(k) \equiv \frac{\mathcal{P}^{\mathrm{NL}}_{\psi}(\mathrm{Takahashi;k}) - \mathcal{P}^{\mathrm{NL}}_{\psi}(\mathrm{Smith;k})}{\mathcal{P}^{\mathrm{NL}}_{\psi}(\mathrm{Smith;k})} \quad ,$$

for the 3 redshifts of the ΛCDM model already addressed. We can see that the two parametrizations differ only during the non-linear transition and at very small scales (large k). The difference, however, stays less than 40% for the redshifts under study.

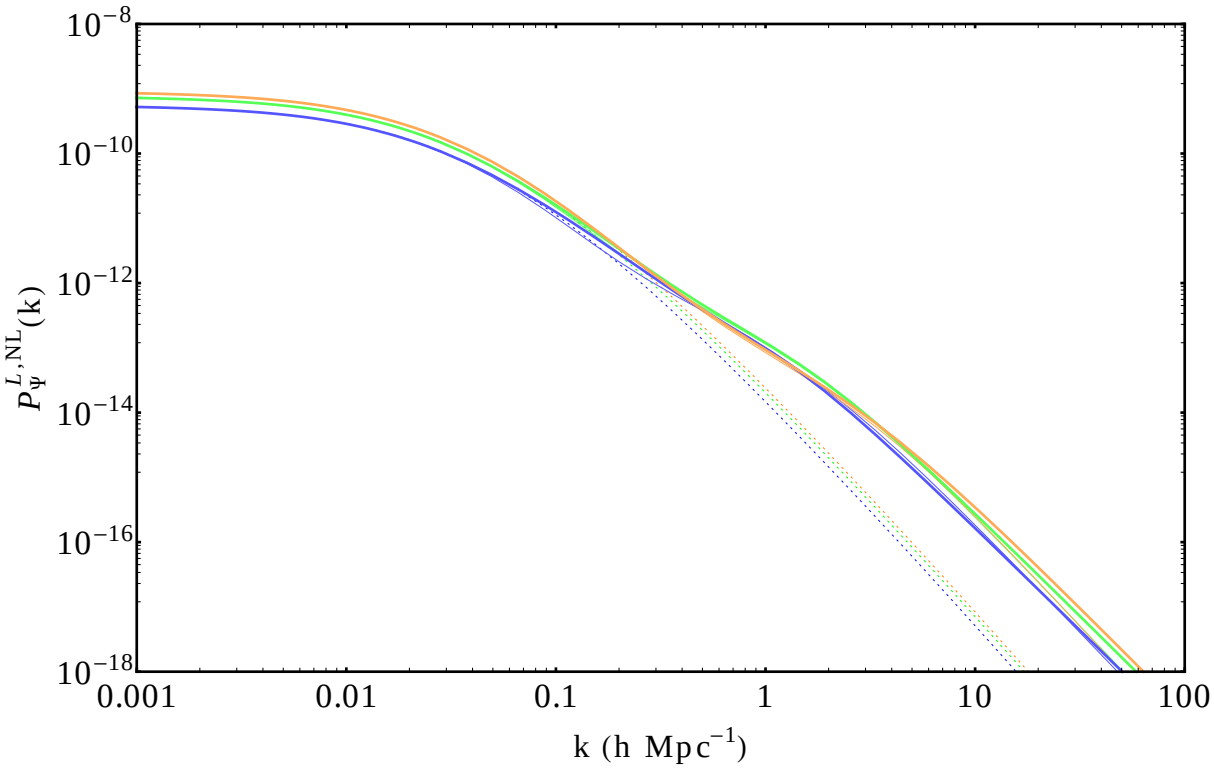

Figure A.7: The linear spectrum and the non-linear spectrum for the gravitational potential in ΛCDM at 3 different redshifts (z=0 : blue ; z=0.5 : green ; z = 1.5 : orange). For each of them, $\mathcal{P}_{\psi}^{\mathrm{L}}(k)$ is in dotted line, $\mathcal{P}_{\psi}^{\mathrm{NL}}(k)$ is in solid thin line (Smith) or solid thick line (Takahashi). The difference is very hard to read, and it is better to look at Fig. A.8 in order to compare both parametrizations.

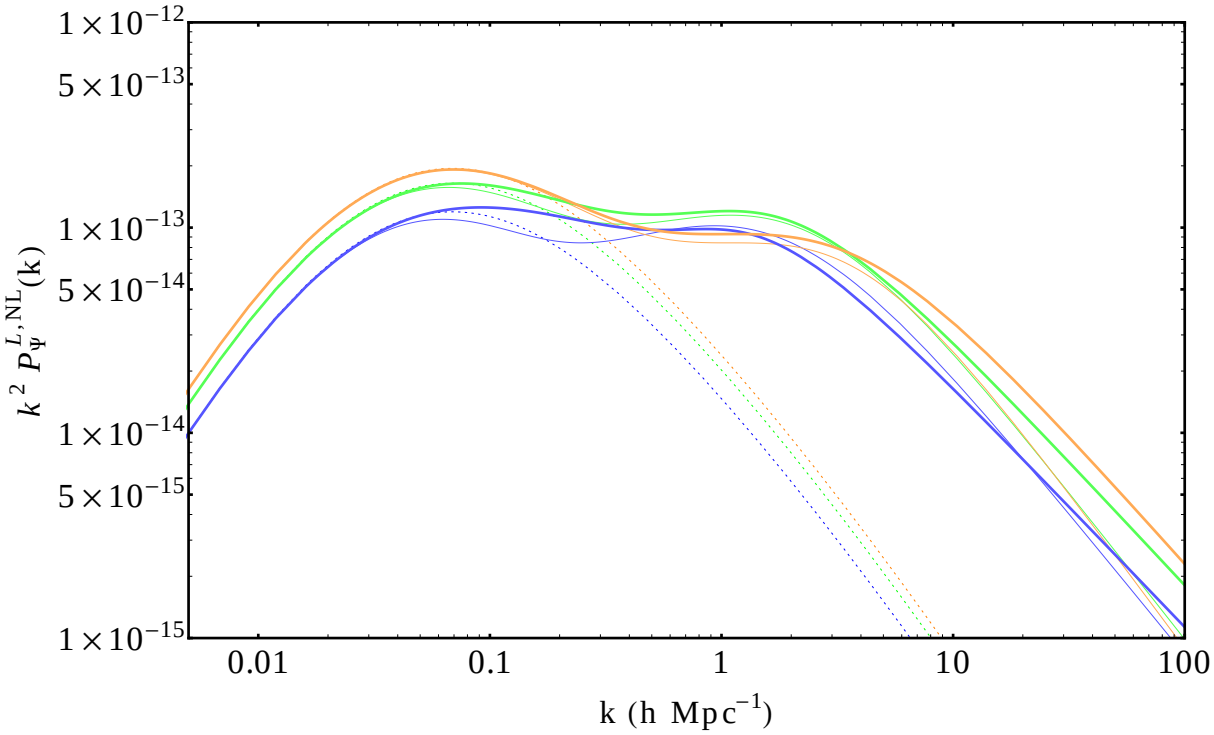

Figure A.8: Same as in Fig. A.7 except that spectra are multiplied by k^2 in order to have a better understanding of their non-linear behaviour.

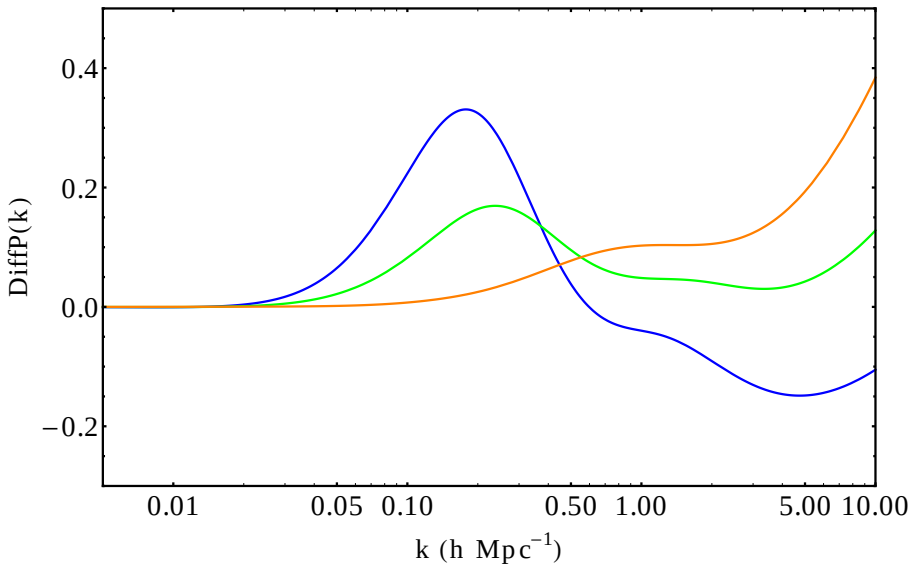

Figure A.9: Relative difference for the NLPS : DiffP(k) ; for the 3 different redshifts in the ΛCDM model we considered. The NLPS by Smith *et al.* cannot be much trusted at large k.

A.5.6 Deflection

Another quantity that we can compute is the variance of density perturbations at a radius of $R_8 = 8\,h^{-1}$Mpc. Using a top-hat spatial window function to compute it, we have [13] :

$$\sigma_8^2 \equiv \int_0^\infty \frac{dk}{k} \Delta_{\rm L}^2(k) \left(3\frac{j_1(kR_8)}{kR_8}\right)^2 \quad \text{with} \quad j_1(kR_8) = \frac{\sin(kR_8) - (kR_8)\cos(kR_8)}{(kR_8)^2} \ . \tag{A.190}$$

The value obtained from this expression gives a good test of the calculations we are doing. We have computed it, and the relevant physical quantities described before, in the case of ΛCDM and in the Smith *et al.* parametrization. These results are given in Table A.1. As we can see, the ΛCDM-values for σ_8^2 have the good order of magnitude.

Table A.1: Parameters deduced from the identification of the non-linear spectrum of Smith *et al.*. We give the estimation of the parameters for ΛCDM at 3 different redshifts. The quantity σ_8^2 appears as a by-product of the estimation of other parameters. It is thus used to test the validity of the NL power spectrum.

	$\Lambda CDM(z=0)$	$\Lambda CDM(z=1.5)$	$\Lambda CDM(z=1.5)$
k_σ	0.158	0.223	0.447
$n_{\rm eff}$	-1.502	-1.648	-1.888
C	0.444	0.387	0.296
σ_8^2	1.269	0.777	0.330

13. We could also use a Gaussian window and use $\sigma_8^2 \equiv \sigma^2(R_8) = \int \Delta_{\rm L}^2(k) \exp(-k^2 R_8^2)\, d\ln k$.

A.6 Distance modulus for a Milne model

We briefly describe here how the expression of the distance modulus for a Milne-type geometry can be derived, i.e. :

$$\mu^M = 5\log_{10}\left[\frac{(2+z_s)z_s}{2H_0}\right] \quad . \tag{A.191}$$

In the Milne Universe, homogeneity and isotropy are assumed in their strict sense. The metric has thus the general form of a Robertson-Walker Universe (taking $c = 1$) :

$$ds^2 = -dt^2 + a^2(t)\left[\frac{dr^2}{1-Kr^2} + r^2 d\Omega^2\right] \quad , \tag{A.192}$$

and the Milne geometry consists in taking $a(t) = t$. One can then show that the associated curvature of this metric only cancels if $K = -1$, i.e. if the spatial 3-hypersurfaces have an hyperbolic geometry. In that case, we prove by the transformation (see [139]) :

$$t = \sqrt{\bar{t}^2 - \bar{r}^2} \quad , \quad r = \frac{\bar{r}}{\sqrt{\bar{t}^2 - \bar{r}^2}} \quad , \tag{A.193}$$

that this metric indeed takes the flat Minkowski form $ds^2 = -d\bar{t}^2 + d\bar{r}^2 + \bar{r}^2 d^2\Omega$.

The luminosity distance is then related to the angular distance by $d_L = (1+z)^2 d_A$ and this last distance is given by :

$$d_A(z_s) = a(t_s)\sinh\left(\int_{t_s}^{t_o}\frac{dt}{a(t)}\right) = t_s \sinh\left(\ln\left(\frac{t_o}{t_s}\right)\right) = \frac{H_0^{-1}}{1+z_s}\sinh\left(\ln(1+z_s)\right) \quad , \tag{A.194}$$

where we have used that $H(t) = 1/t$ and $1 + z_s = a(t_o)/a(t_s)$. Using finally that :

$$\sinh\left(\ln(1+z_s)\right) = \frac{(2+z_s)z_s}{2(1+z_s)} \quad , \tag{A.195}$$

and the expression of the distance modulus being $\mu = 5\log_{10} d_L$, we obtain the result announced in Eq. (A.191).

Appendix B

Résumé (en français)

Nous présentons dans cette section un résumé de cette thèse en langue française. La majorité des notions de la thèse est abordée. Néanmoins, certaines discussions qui concernent moins notre travail sont significativement réduites de manière à laisser à ce chapitre une taille raisonnable. La plupart des équations importantes sont présentées et le nombre de références a été réduit de manière à ce que la lecture de ce chapitre puisse se faire sans avoir besoin de revenir souvent au document.

B.1 Introduction, motivations et plan de la thèse

B.1.1 Le modèle standard de la cosmologie

Les observations effectuées depuis plusieurs décennies en cosmologie ont amené à un modèle d'Univers qui semble expliquer avec une grande précision les données collectées. Dans ce modèle dit *Modèle Standard* de la cosmologie, la géométrie de l'Univers est celle d'un espace homogène et isotrope, décrite de manière générale par la métrique de Friedmann-Lemaître-Robertson-Walker (FLRW) :

$$\begin{aligned} ds^2_{\text{FLRW}} &= -dt^2 + \gamma_{ij}(|\mathbf{x}|)dx^i dx^j \\ &= -dt^2 + a^2(t)\left[d\chi^2 + \left(\frac{1}{\sqrt{K}}\sin\left(\sqrt{K}\chi\right)\right)^2 d\Omega^2\right] \quad , \\ \text{avec} \qquad d\Omega^2 &= d\theta^2 + (\sin\theta)^2 d\phi^2 \quad . \end{aligned} \tag{B.1}$$

Dans cette métrique, exprimée en fonction du temps cosmique t et des coordonnées sphériques $(\mathbf{x}) = (\chi, \theta, \phi)$, la constante K détermine la courbure des sections spatiales et vaut $\{1, 0, -1\}$ selon que l'Univers est fermé, plat, ou ouvert. Sous une telle forme, le facteur d'échelle $a(t)$, introduit ci-dessus, possède la dimension d'une distance [1]. Cette métrique se réécrit en coordonnées sphériques comme :

$$ds^2_{\text{FLRW}} = -dt^2 + a(t)^2\left(\frac{1}{1-Kr^2}dr^2 + r^2 d\Omega^2\right) \quad , \tag{B.2}$$

et on peut redonner ici à r la dimension d'une distance et considérer $a(t)$ comme une grandeur sans dimension. Le temps cosmique peut être remplacé par le temps conforme η tel que $d\eta = dt/a(t)$.

Sous ces hypothèses d'homogénéité et d'isotropie, le tenseur énergie impulsion d'un fluide de matière s'écrit comme

$$T^{\mu\nu} = (\rho + p)u^\mu u^\nu + p\, g^{\mu\nu} \quad , \tag{B.3}$$

avec $\rho(t)$ la densité d'énergie du fluide, $p(t)$ sa pression (relativiste), et u^μ sa 4-vitesse. Les 10 équations d'Einstein indépendantes (dont 4 peuvent être éliminée par un choix dit de « jauge ») :

$$G_{\mu\nu} + \Lambda g_{\mu\nu} \equiv R_{\mu\nu} - \frac{1}{2}Rg_{\mu\nu} + \Lambda g_{\mu\nu} = 8\pi G\, T_{\mu\nu} \quad , \tag{B.4}$$

1. Nous avons également imposé à la vitesse de la lumière d'être égale à $c = 1$ dans ces unités.

se réduisent alors à deux équations indépendantes que sont les équations de Friedmann :

$$H^2 = \frac{8\pi G}{3}\rho - \frac{K}{a^2} + \frac{\Lambda}{3} \quad , \tag{B.5}$$

$$\frac{\ddot{a}}{a} = -\frac{4\pi G}{3}(\rho + 3p) + \frac{\Lambda}{3} \quad , \tag{B.6}$$

avec $H(t) \equiv \dot{a}(t)/a(t)$ le paramètre de Hubble, et l'équation de conservation :

$$\dot{\rho} + 3H(\rho + p) = 0 \quad . \tag{B.7}$$

Nous avons introduit ici un terme de constante cosmologique $\propto \Lambda$ et nous voyons que cette composante en énergie peut être écrite comme un fluide ayant les propriétés suivantes :

$$\rho_\Lambda = \frac{\Lambda}{8\pi G} \quad , \quad p_\Lambda = -\frac{\Lambda}{8\pi G} \quad \text{et l'équation d'état} \quad w_\Lambda \equiv \frac{p_\Lambda}{\rho_\Lambda} = -1 \quad . \tag{B.8}$$

Seules deux de ces trois dernières équations sont indépendantes et elles déterminent les évolutions respectives du facteur d'échelle $a(t)$ et de la densité de matière $\rho(t)$ après que $p(t)$ eut été choisi en fonction de $\rho(t)$ par l'imposition d'une équation d'état $p(t) = w\,\rho(t)$. L'équation (B.5) peut se réécrire en terme des paramètres de densité suivants :

$$\Omega_m = \frac{8\pi G\,\rho}{3H^2} \quad , \quad \Omega_\Lambda = \frac{\Lambda}{3H^2} \quad , \quad \Omega_K = -\frac{K}{H^2 a^2} \quad , \tag{B.9}$$

qui donnent lieu à :

$$\Omega_m + \Omega_\Lambda + \Omega_K \equiv \Omega_{\text{tot}} + \Omega_K = 1 \quad . \tag{B.10}$$

On notera que dans le cas d'un Univers contenant plusieurs types de matière (ou de radiation), il suffit de remplacer ρ par $\sum_i \rho_i$ avec ρ_i les densités de matière respectives des différents fluides. Si certains de ces fluides ont une pression, on doit aussi poser $p = \sum_i p_i$. Enfin, chacun des fluides suit une équation de conservation qui est $\dot{\rho}_i + 3H(\rho_i + p_i) = 0$ et le système est fermé par le choix d'une équation d'état $p_i = p_i(\rho_i)$ pour chacun de ces fluides.

Le modèle standard de la cosmologie, dit modèle ΛCDM, est lui composé de différents paramètres (entre 6 et 12 selon les interprétations) qui, entre autres, définissent la composition de matière de l'Univers. Les mesures expérimentales, que nous allons brièvement décrire maintenant, donnent une composition faite de $\sim 73\%$ d'énergie sombre (prise comme une constante cosmologique Λ), $\sim 26\%$ de matière noire froide (CDM) dont 4.6% de matière baryonique, et des densités de radiation et de courbure négligeables aujourd'hui.

B.1.2 Les Supernovæ de type Ia

Les supernovæ sont des phénomènes très rares qui se caractérisent par l'explosion d'une naine blanche ayant accrétée de la matière d'une étoile compagnon jusqu'à atteindre la masse de Chandrashekar ($\sim 1.4\,M_\odot$). On observe la progression de leur intensité sur une période de l'ordre de la centaine de jours, qu'on appelle la courbe de lumière (Fig. 1.1), et on les observe sur des distances aussi grandes que la moitié de notre Univers observable. On en distingue plusieurs types dont le plus intéressant est celui des Supernovæ Ia (SNe Ia) caractérisé par l'absence d'Hydrogène (et d'Hélium) et la présence de silicium dans son spectre (Fig. 1.2). C'est aussi celui des supernovæ les plus lumineuses.

Les SNe Ia sont intéressantes du fait de l'homogénéité des conditions qui leur donnent naissance mais sont néanmoins le résultat d'un processus complexe et encore mal compris. Elles sont toutefois « standardisables » (Fig. 1.3) et deviennent alors des étalons de distance en cosmologie. C'est en réalisant leur intérêt que l'on a pu mesurer des distances se rapportant à une dizaine de milliards d'années lumières et mettre en exergue l'existence de l'énergie sombre. Leur mesure se fait dans différentes bandes spectrales et leur analyse permet d'extraire deux quantités très utiles pour leur standardisation : le facteur de *stretch* (étirement) s et le paramètre de couleur c.

Comme pour tout autre objet astrophysique, la question de la magnitude est importante dans le cas des SNe Ia. On peut montrer que le module de distance, après un choix d'unité appropriée (ici le parsec pc), est définit par

$$\mu(\mathrm{pc}) = m - M = -2.5 \log_{10} \left(\frac{\Phi(\mathrm{pc})}{\Phi(10\,\mathrm{pc})} \right) \quad , \tag{B.11}$$

avec m la magnitude apparente de la SN Ia, M sa magnitude absolue (i.e. à une distance de 10 pc) et Φ le flux lumineux de l'étoile. Ce module de distance est relié à la distance de luminosité selon

$$\mu(\mathrm{Mpc}) = 25 + 5 \log_{10}(d_L(\mathrm{Mpc})) = 43.16 + 5 \log_{10} \left(H_0(\mathrm{Mpc}^{-1}) d_L(\mathrm{Mpc}) \right) \quad . \tag{B.12}$$

C'est par le tracé de cette quantité μ en fonction du redshift (ou « décalage vers le rouge ») des SNe Ia, soit autrement dit du diagramme de Hubble (Fig. 1.4), et l'estimation de H_0 que le modèle de matière CDM (pour *cold dark matter*) a été mis en défaut et que le modèle ΛCDM fut introduit. Dans ce modèle d'univers de type FLRW et plat (i.e. $K = 0$), contenant de la matière (noire et baryonique) ainsi qu'une constante cosmologique, la distance de luminosité s'écrit :

$$d_L^{\Lambda\mathrm{CDM}}(z_s) = \frac{1 + z_s}{H_0} \int_0^{z_s} \frac{dz'}{[\Omega_{\Lambda 0} + \Omega_{m0}(1 + z')^3]^{1/2}} \quad . \tag{B.13}$$

C'est par le fit (l'ajustement) des données des SNe Ia, et leur combinaison avec d'autres mesures cosmologiques (cf. Fig. 1.5), que les paramètres cosmologiques ont été évalués à $(\Omega_{\Lambda 0}, \Omega_{m0}) = (0.73, 0.27)$.

B.1.3 L'Univers inhomogène

Les relevés d'observations aux grandes échelles, tels que SDSS et le 2dFGRS, ont révélé une structure très filamenteuse de la matière aux petites échelles et une bonne homogénéité statistique aux plus grandes (cf. Fig. 1.6). Néanmoins plusieurs complications se présentent à nous lorsque l'on cherche à déduire de ces observations la vraie distribution de matière dans l'Univers. Premièrement, ce que nous observons se situe sur notre cône de lumière passé et la vraie distribution que nous voyons est celle des galaxies (qui émettent de la lumière). Le contraste de densité des galaxies est relié au contraste de matière par la relation suivante :

$$\delta_{\mathrm{gal}}(t, \mathbf{x}) = b\, \delta\,(t, \mathbf{x}) \qquad \text{avec} \qquad \delta(t, \mathbf{x}) = \frac{\rho(t, \mathbf{x}) - \rho(t)}{\rho(t)} \equiv \frac{\delta\rho(t, \mathbf{x})}{\rho(t)} \quad , \tag{B.14}$$

et où $\rho(t)$ est la partie homogène de la densité de matière, $\rho(t, \mathbf{x})$ le champ de matière complet. Le paramètre $b(t, \mathbf{x})$ est appelé le biais et a été étudié en détail dans la littérature. Une deuxième complication, de taille, est que les galaxies ne sont en fait pas observées dans l'espace réel, mais bien dans l'espace des redshifts, i.e. par deux angles dans le ciel et le redshift z qui peut être relié à la « distance » sur le cône de lumière, telle que la combinaison $\eta - r$, mais ceci seulement après le choix d'un modèle d'Univers. La conséquence à cela est que les effets de vitesse (dont l'effet caractéristique nommé *fingers of God*) affectent directement la mesure de la distance.

Quoi qu'il en soit, la combinaison de plusieurs méthodes, et les mesures par effet de lentilles gravitationnelles faibles (indépendantes du biais), ont permis de reconstruire le spectre de puissance de la matière $\delta(t, \mathbf{x})$. On peut alors se placer dans l'espace de Fourier et, supposant un principe ergodique, prendre la moyenne de volume des fonctions de corrélation à 2 points et considérer que ceci correspond à la moyenne stochastique $\overline{\delta_{\mathbf{k}} \delta_{\mathbf{k}}}$ [2]. On obtient ensuite la valeur expérimentale du spectre de matière par sa définition :

$$\Delta^2(t, \mathbf{k}) = \frac{k^3}{2\pi^2} |\delta_{\mathbf{k}}(t)|^2 \quad , \tag{B.15}$$

et ses valeurs expérimentales présentée en Fig. 1.7.

2. Notons que cette moyenne est habituellement dénotée par des crochets angulaires, $\langle \ldots \rangle$, dans la littérature. Néanmoins, cette dernière notation sera pour nous la moyenne sur le ciel, d'où notre choix pour la moyenne stochastique.

Toutefois, nous ne saurions utiliser directement ce spectre pour nos calculs. En effet, les inhomogénéités que nous décrirons dans le reste de ce travail seront représentées par leur champ gravitationnel et non la densité de matière. Il nous faut par conséquent utiliser l'équation de Poisson qui relie ces deux grandeurs. Dans la jauge synchone (voir Sec. A.3.3), cette équation s'écrit comme :

$$\nabla^2\psi(t,\mathbf{x}) = 4\pi G\rho(t)\,\delta(t,\mathbf{x}) \quad , \tag{B.16}$$

avec $\rho(t)$ la densité de fond (i.e. homogène). La relation entre $|\delta_k|^2$ et $|\psi_k|^2$ est alors donnée par :

$$|\psi_{\mathbf{k}}(z)|^2 = \left(\frac{3}{2}\right)^2 \frac{\Omega_m^2(z)\mathcal{H}^4}{k^4}|\delta_{\mathbf{k}}(z)|^2 = \left(\frac{3}{2}\right)^2 \frac{\Omega_{m0}^2\mathcal{H}_0^4}{k^4}(1+z)^2|\delta_{\mathbf{k}}(z)|^2 \quad , \tag{B.17}$$

où nous avons fait l'hypothèse d'une matière de type poussière (i.e. sans pression) et avons utilisé la relation qui en découle : $\Omega_m(z) = \Omega_{m0}(1+z)\left(\frac{\mathcal{H}_0}{\mathcal{H}}\right)^2$.

D'autre part, le spectre de puissance (sans dimension) du champ gravitationnel est relié à $|\psi_{\mathbf{k}}|^2$ par la définition :

$$\mathcal{P}_\psi(\mathbf{k},\eta) \equiv \frac{k^3}{2\pi^2}|\psi_{\mathbf{k}}(\eta)|^2 \ , \tag{B.18}$$

et où la dépendance en temps η peut être convertie en redshift (de manière analytique dans un Univers CDM, sous forme intégrale dans le cas ΛCDM). On sait aussi relier ce spectre au spectre de puissance inflationnaire (i.e. produit par les fluctuations quantiques à la fin de l'inflation) où sa valeur est de $\left(\frac{3}{5}\right)^2\Delta_{\mathcal{R}}^2$, avec :

$$\Delta_{\mathcal{R}}^2 = A\left(\frac{k}{k_0}\right)^{n_s-1} \quad \text{et} \quad A = 2.45\ 10^{-9} \quad , \quad n_s = 0.96 \quad , \quad k_0/a_0 = 0.002\ \mathrm{Mpc}^{-1} \quad . \tag{B.19}$$

Il est nécessaire d'ajouter à cette contribution initiale une fonction de transfert dont le rôle est de prendre en compte l'évolution des modes sub-horizon (i.e. de taille plus petite que l'horizon cosmologique) réentrant dans la période de domination par la radiation. Nous ajoutons enfin un « facteur de croissance » (*growth factor* dans la suite) qui a pour rôle de décrire l'évolution de ces modes depuis et entre autre durant la période récente de domination par l'énergie sombre. Nous aboutissons alors à l'expression du spectre de puissance dans son régime linéaire :

$$\mathcal{P}_\psi(k) = \left(\frac{3}{5}\right)^2 \Delta_{\mathcal{R}}^2 T^2(k)\left(\frac{g(z)}{g_\infty}\right)^2 \quad . \tag{B.20}$$

Finissons enfin cette section en décrivant brièvement la manière dont est calculée le spectre de puissance dans son régime non-linéaire. En effet, ce régime nous est nécessaire car c'est celui qui décrit la matière aux petites échelles (typiquement celles des amas de galaxies et moindres). Pour cela, il est nécessaire de repasser à une description en terme de densité de matière, la raison étant que le régime non-linéaire a été étudié au travers des simulations à N-corps où cette densité est directement mesurable. Ces simulations nous fournissent alors une paramétrisation du spectre de matière jusque dans son régime non-linéaire $\Delta_{\mathrm{NL}}(k)$, dit le modèle du HaloFit, en fonction de son spectre linéaire $\Delta_{\mathrm{L}}(k)$ et de paramètres de fit (cf. [23]). En utilisant le fait que l'équation de Poisson est valable à la fois dans les régimes linéaire et non-linéaire :

$$\mathcal{P}_\psi^{\mathrm{L,NL}}(k) = \frac{9}{4}\frac{\Omega_{m0}^2\mathcal{H}_0^4}{k^4}(1+z)^2\Delta_{\mathrm{L,NL}}^2(k) \quad , \tag{B.21}$$

nous obtenons directement le spectre de matière linéaire correspondant à (B.20) :

$$\Delta_{\mathrm{L}}^2(k) = \frac{4}{9}\frac{k^4}{\Omega_{m0}^2\mathcal{H}_0^4(1+z)^2}\mathcal{P}_\psi^{\mathrm{L}}(k) = \frac{4}{25}\frac{A\Omega_{m0}^{-2}\mathcal{H}_0^{-4}}{(1+z)^2}\frac{k^{n_s+3}}{k_0^{n_s-1}}\left(\frac{g(z)}{g_0}\right)^2 T^2(k) \quad , \tag{B.22}$$

et il est alors possible d'obtenir le spectre non-linéaire $\Delta_{\mathrm{NL}}^2(k)$. Par une utilisation directe de (B.21) cette fois, on obtient finalement la valeur de $\mathcal{P}_\psi^{\mathrm{NL}}(k)$. Cette méthode et les détails de la parametrisation du HaloFit sont expliqués en Sec. A.4 et A.5.

B.1.4 Introduction à la thèse

Le modèle de concordance (ou ΛCDM), basé sur l'association commune de l'énergie sombre, des matières noire et baryonique, est devenu le paradigme de référence pour la description de notre Univers dans son époque récente (cf. e.g. [27]). Il rend compte à la fois des observations du CMB, des grandes structures et des données de SNe Ia [10,11]. Néanmoins, ces dernières sont plus directement affectées par leur dépendance à un modèle théorique qui est choisi comme étant le modèle de Friedmann-Lemaître-Robertson-Walker (FLRW), homogène et isotrope. Il a ainsi été suggéré que la prise en compte des inhomogénéités pourrait significativement altérer ces conclusions. Par exemple, les modèles inhomogènes dans lesquels nous occupons une position privilégiée ont démontré la possibilité de simuler une énergie sombre, i.e. une accélération de l'expansion (cf. [25]). Ils nécessitent néanmoins trop d'ajustements pour être réalistes. On ne peut toutefois contredire le fait que la dispersion dans les données du diagramme de Hubble est très importante et, bien que sa source principale soit probablement en grande partie due à la variabilité des SNe elles-mêmes, on ne peut s'empêcher de se demander quelle est la part de dispersion qui est causée par la présence d'inhomogénéités de matière. Au final, on peut résumer le but de la cosmologie à l'étude de deux choses : le contenu de l'Univers et la dynamique de ce contenu. Il apparaît ainsi très important de comprendre comment la matière, et sa structure, affectent la mesure des distances en cosmologie. Il est aussi clair qu'un traitement plus complet de l'accélération de l'Univers est nécessaire, au moins de manière perturbative autour d'un modèle homogène, pour aboutir à des considérations précises et établir notre entière confiance dans la capacité du modèle ΛCDM à expliquer les diverses observations.

Il est de plus bien établi (cf. e.g. [28]) que les solutions moyennées des équations d'Einstein complètes (et inhomogènes) sont, en général, différentes de celles obtenues en résolvant les équations d'Einstein moyennes (homogènes, i.e. les équations de Friedmann). En particulier, la procédure de moyenne ne commute pas avec les opérateurs différentiels agissant dans les équations d'Einstein qui sont fondamentalement de nature non-linéaire. Par conséquent, la dynamique des géométries moyennées est affectée par des contributions dites de "backreaction" (« rétro-action ») engendrées par les inhomogénéités. Ces effets ont donc suscité un intérêt grandissant ces dernières années (voir [6, 26, 29, 30]). Pour certains auteurs [38–44], les inhomogénéités de matière pourraient expliquer l'accélération que nous observons aujourd'hui, rendant inutile l'introduction de l'énergie sombre et répondant en même temps au « problème de coincidence ». Pour d'autres [31, 33–35, 45, 46], l'effet est complètement négligeable. La vraie réponse à ce problème pourrait se trouver à mi-chemin entre ces différentes interprétations et révéler l'importance des inhomogénéités lors de l'établissement de contraintes précises sur les paramètres de l'énergie sombre.

Si les inhomogénéités ont en effet une influence importante, cela signifie que les observations actuelles correspondent à une certaine mesure de quantités moyennes. Un accent particulier a donc été porté ces dernières années à la définition de moyennes pour correctement prendre en compte les effets des inhomogénéités. Dans la quasi-totalité de ces travaux, suivant l'exemple des articles fondateurs de T. Buchert [47–50], la géométrie homogène résultante de la procédure de moyenne a été déterminée par l'intégration sur des hypersurfaces spatiales à 3 dimensions. Néanmoins, et comme suggéré depuis longtemps [51, 52], une reconstruction effective de la métrique d'espace-temps et de son évolution aux échelles cosmologiques (révélée expérimentalement par la mesure de la distance et du redshift [10,11]), ne peut se faire que par la considération d'observations sur le cône de lumière passé (l'hypersurface sur laquelle se propagent tous les signaux lumineux). La procédure de moyenne doit donc être faite sur une hypersurface de genre lumière, plutôt que sur des hypersurfaces spatiales. Cette procédure de moyenne dont l'importance a été soulignée plusieurs fois dans la litérature (cf. [6, 51–57]), n'avait jamais été mise en oeuvre en pratique.

Nous présentons dans cette thèse une définition générale, invariante de jauge, pour la définition de quantités scalaires sur des hypersurfaces de type lumière, résolvant ainsi le problème de la moyenne sur le cône de lumière. Nous appliquons aussi cette moyenne au cas d'un observateur générique au sein d'un univers inhomogène et nous établissons les relations analogues à la règle de commutation de Buchert-Ehlers [58] dans le cas de la dérivation des moyennes sur ce cône. Nous mettons aussi à profit l'invariance de jauge de ces moyennes par l'introduction d'un système de coordonnées adapté à leur simplification, que nous avons appelé coordonnées « géodésiques sur le cône de lumière » (GLC).

Ces coordonnées correspondent à une fixation de jauge des coordonnées dites « observationelles » (cf. [51, 59]) et ne sont pas totalement équivalentes. Notre définition de la moyenne se simplifie alors tout en gardant le nombre de degrés de liberté nécessaire pour son application à des métriques inhomogènes générales. Ces coordonnées GLC se révèlent aussi utiles pour le calcul de nombreuses quantités sur le cône de lumière et ont donc une application qui dépasse largement le problème de la moyenne. Entre autre, on observe que le redshift et la distance de luminosité prennent une expression très simple dans ces coordonnées.

Nous portons ensuite notre attention sur le cas d'un modèle de type FLRW et plat en présence d'inhomogénéités scalaires d'origine primordiale (inflationnaire). Ce modèle est réaliste du point de vue des observations et assez simple pour une approche analytique. Ce genre de perturbation est en général définit dans la jauge longitudinale (ou Newtonienne, [60]) et nous établissons pour cela la transformation de coordonnées entre les jauges GLC et Newtonienne. Du fait de la stochasticité des inhomogénéités considérées, les effets de ces dernières n'apparaissent qu'au second ordre en perturbation. Nous calculons ainsi, à l'aide de notre transformation, la relation de distance-redshift jusqu'au second ordre. Ce résultat très général a un intérêt en lui-même, indépendant des considérations de moyennes, et pourrait aboutir à de nombreuses applications en cosmologie de précision. De plus, ce résultat pour d_L est valable quelque soit la géométrie de fond considérée (sauf en présence de caustiques où la distance est modifiée).

Associant ces deux résultat théoriques, nous étudions ensuite la moyenne de quantités scalaires S développées au second ordre autour d'une géométrie de fond du type FLRW plat. Nous introduisons une moyenne d'ensemble sur les inhomogénéités et un spectre de puissance des perturbations stochastiques. La combinaison de la moyenne angulaire sur le cône de lumière et de cette moyenne stochastique amène à des contributions caractéristiques désignées comme « backreaction induite » du fait de la corrélation qu'elles contiennent entre les pertubations de S et la mesure d'intégration de la moyenne. L'application de cette procédure à des quantités telles que le flux et la distance de luminosité nous permet d'étudier l'effet des inhomogénéités de nature stochastiques sur la détermination des paramètres de l'énergie sombre en cosmologie de précision. Contrairement à d'autres études utilisant des moyennes spatiales (cf. [36, 37]), nos résultats sont exempts aussi bien de divergences infrarouges que de divergences ultraviolettes. Toutefois, les termes de backreaction induite n'englobent pas tout les effets des inhomogénéités et un calcul complet au second ordre est établi. En commençant par un modèle simple de type CDM, nous trouvons que le flux $\Phi \sim d_L^{-2}$ n'est quasiment pas affecté par les inhomogénéités tandis que les grandeurs plus communément utilisées (comme d_L ou le module de distance $\mu \sim 5 \log_{10} d_L$) recoivent des corrections plus significatives (et bien plus grandes qu'on aurait pu le penser naïvement). Ceci prouve, au moins en principe, qu'il existe une ambiguité dans la mesure des paramètres de l'énergie sombre lorsque l'on ne prend correctement en compte l'effet des inhomogénéités. La faible dépendence du flux, déjà remarquée dans le contexte différent de l'étude du binning en z des données [67], est très surement à rapprocher de la conservation de la quantité de lumière le long du cône passé. Les premières conclusions de notre analyse, basées sur un spectre de puissance dans son régime linéaire dans un modèle CDM [68], sont les suivantes. D'un côté, les inhomogénéités ne peuvent simuler une fraction conséquente d'énergie sombre, leur contribution étant à la fois trop faible et ne possède pas la dépendance en z adéquate. D'un autre, ces fluctuations stochastiques apportent une dispersion relativement importante aux prédictions du modèle FLRW homogène et isotrope. Cette dispersion est indépendante de l'appareil expérimental, de la procédure d'observation ou de la dispersion dans la luminosité des sources observées. Elle pourrait, si non prise en compte, empêcher la détermination du paramètre cosmologique $\Omega_\Lambda(z)$ en dessous du pourcent. Une autre conclusion importante à souligner est que la moyenne sur le cône de lumière de différentes fonctions de la même observable sont affectées différemments, avec le flux qui apparaît comme la quantité la mieux conservée.

Nous avons ensuite étendu notre étude par la considération d'un modèle ΛCDM, en ajoutant l'effet des baryons, et en considérant deux paramétrisations du modèle du HaloFit [23, 74] décrivant le spectre de densité de matière dans son régime non-linéaire (i.e. aux petites échelles). Nous avons calculé l'effet des inhomogénéités de la même manière que précédemment tout en ne considérant toutefois que les termes dominants qui ont été indentifiées dans le cas CDM. Nous trouvons que

l'effet des inhomogénéités est renforcé aux grands redshifts du fait du terme dominant de lentille gravitationnelle. En dépit de cet effet, les inhomogénéités ne parviennent toujours pas à simuler une fraction importante de l'énergie sombre. La dispersion quant à elle est fortement augmentée et correspond à une possible déviation statistique de $\sim 10\%$ sur $\Omega_{\Lambda 0}$. Ce résultat suggère fortement de considérer l'effet des inhomogénéités de matière dans l'interprétation des données des SNe Ia. Nous trouvons de plus que cette dispersion est en très bon accord avec les données du Union2 aux petits redshifts (où les effets de vitesse particulière dominent) mais est bien trop petite aux larges redshifts. Ceci démontre la robustesse des conclusions du modèle standard en soulignant toutefois la nécessité de considérer l'aspect non-négligeable des inhomogénéités. Enfin, nous comparons de manière précise la dispersion due à l'effet de lentille avec les tentatives récentes d'évaluation d'un signal de lentille au sein des SNe Ia [75, 76]. Nous trouvons notre prédiction en parfait accord avec ces études et pouvons donc espérer une confirmation expérimentale de cette prédiction dans les prochaines années.

B.2 Moyennes sur le cône de lumière

B.2.1 Approche historique à la Buchert

Le formalisme de Buchert considère l'Univers comme statistiquement homogène à partir d'une certaine échelle de distance (conformément aux observations), rempli de matière sans pression et d'une constante cosmologique (de pression négative), et cherche à dériver – à partir des équations d'Einstein – des équations effectives et non-perturbatives pour la cosmologie. Les observations présentes, encore peu précises et toutes de nature astrophysique (objets locaux au centre des inhomogénéités de matière), consistent en effet en des moyennes spatiales (plus justement sur le cône de lumière passé) et ne garantissent pas que les équations homogènes de Friedmann soient, stricto sensu, les bonnes pour interpréter ces observations.

Dans ce formalisme, nous considérons donc un domaine compact $\mathcal{D}(t)$ au sein d'un espace folié par des hypersurfaces à temps $t = \text{cst}$, dit formalisme ADM (Arnowitt-Deser-Misner). L'élément de distance dans ce formalisme est donné par :

$$ds^2 = -N^2 dt^2 + g_{ij}(dx^i + N^i dt)(dx^j + N^j dt) \quad , \tag{B.23}$$

où N est appelée la *lapse function* et N^i le *shift vector* et $n_\mu = (-N, \vec{0})$ (ou $n^\mu = (1/N, -N^i/N)$) est le vecteur normal aux hypersurfaces à t constant. Nous pouvons aussi travailler (en imposant $N = 1$ et $N^i = 0$) dans la jauge dite synchrone :

$$ds^2_{\text{SG}} = -dt^2 + g_{ij} dx^i dx^j \quad . \tag{B.24}$$

Le volume $\mathcal{D}(t)$ est choisi de manière à conserver la masse $M_\mathcal{D}$ qu'il contient à l'instant initial t_0 et la moyenne d'une quantité scalaire S est définie en terme d'une moyenne de volume Riemannienne (i.e. pondérée par la métrique) :

$$\langle S(t,\mathbf{x})\rangle_\mathcal{D}(t) = \frac{1}{V_\mathcal{D}} \int_\mathcal{D} S(t,\mathbf{x})\, d\mu_g \quad \text{avec} \quad V_\mathcal{D} = \int_\mathcal{D} d\mu_g \quad \text{et} \quad d\mu_g \equiv J\, d^3\mathbf{x} = \sqrt{\det g_{ij}}\, d^3\mathbf{x} \quad . \tag{B.25}$$

La dérivée temporelle de cette moyenne donne alors la *règle de commutation* de Buchert-Ehlers :

$$\langle S\rangle^{\dot{}}_\mathcal{D} - \langle \dot{S}\rangle_\mathcal{D} = \langle S\Theta\rangle_\mathcal{D} - \langle S\rangle_\mathcal{D} \langle \Theta\rangle_\mathcal{D} \quad , \tag{B.26}$$

qui montre que la moyenne spatiale et la dérivation temporelle ne peuvent être simplement échangées dans un univers dont le facteur d'expansion Θ dépend de l'espace. On peut aussi définir un facteur d'échelle effectif $a_\mathcal{D}$ et un paramètre de Hubble effectif $H_\mathcal{D}$ en fonction du volume de ce domaine :

$$a_\mathcal{D}(t) \equiv \left(\frac{V_\mathcal{D}(t)}{V_\mathcal{D}(t_i)}\right)^{1/3} \quad \text{et donc} \quad \frac{\dot{V}_\mathcal{D}}{V_\mathcal{D}} = 3\frac{\dot{a}_\mathcal{D}}{a_\mathcal{D}} \equiv 3H_\mathcal{D} \quad . \tag{B.27}$$

Il convient toutefois d'être prudent avec cette définition qui redonne bien $a_\mathcal{D}(t) = a(t)$ dans le cas homogène mais qui, dans le cas non-homogène, voit $a_\mathcal{D}(t)$ correspondre à des volumes d'intégration $\mathcal{D}(t)$ bien différents.

Equations d'Einstein dans ADM : On introduit plusieurs quantités que sont le tenseur de projection sur une hypersurface à t constant, qui est aussi orthogonal à la 4-vitesse du fluide (supposé statique et donc pour lequel on peut choisir $u^\mu = n^\mu$) :

$$h_{\mu\nu} \equiv g_{\mu\nu} + n_\mu n_\nu \quad , \quad h_{\mu\nu} n^\nu = 0 \quad \text{et donc ici :} \quad h_{00} = 0 \quad , \quad h_{0i} = 0 \quad , \quad h_{ij} = g_{ij} \quad , \tag{B.28}$$

ainsi que le tenseur de courbure extrinsèque

$$K_{ij} \equiv -h_i^\alpha h_j^\beta \nabla_\beta \, n_\alpha \quad . \tag{B.29}$$

On peut alors montrer que les équations d'Einstein et l'équation de conservation se réduisent à des équations de contrainte :

$$\frac{1}{2}\left(\mathcal{R} + K^2 - K^i{}_{ij} K^j{}_i\right) = 8\pi G\rho + \Lambda \quad , \tag{B.30}$$

$$K^i{}_{j\,||\,i} - K_{|j} = 0 \quad , \tag{B.31}$$

et les équations d'évolution suivantes :

$$\dot{\rho} = K\rho \quad , \tag{B.32}$$

$$(g_{ij})^\bullet = -2\, g_{ik} K^k{}_j \quad , \tag{B.33}$$

$$(K^i{}_j)^\bullet = K K^i{}_j + \mathcal{R}^i{}_j - (4\pi G\rho + \Lambda)\delta^i{}_j \quad . \tag{B.34}$$

La notation $||i$ désigne la dérivée covariante par rapport à la métrique spatiale tridimensionnelle g_{ij} (et $|i$ est une simple dérivée ∂_i). Nous avons aussi utilisé la trace K de K_{ij} ainsi que celle du tenseur de Ricci spatial $\mathcal{R} \equiv \mathcal{R}^i{}_i$ qui représente la courbure locale à l'intérieur d'une hypersurface à t constant.

On peut aussi définir le tenseur d'expansion d'un faisceau de lignes géodésiques :

$$\Theta_{\mu\nu} = \frac{1}{3} h_{\mu\nu}\Theta + \sigma_{\mu\nu} + \omega_{\mu\nu} \quad , \tag{B.35}$$

qui fait intervenir respectivement le scalaire d'expansion, le tenseur symétrique de cisaillement, et le tenseur anti-symétrique de vorticité :

$$\Theta \equiv \nabla_\mu n^\mu \quad , \quad \sigma_{\mu\nu} \equiv h_\mu^\alpha h_\nu^\beta \left(\nabla_{(\alpha} n_{\beta)} - \frac{1}{3} h_{\alpha\beta}\Theta\right) \quad , \quad \omega_{\mu\nu} \equiv h_\mu^\alpha h_\nu^\beta \nabla_{[\alpha} n_{\beta]} \quad . \tag{B.36}$$

Ces deux tenseurs sont sans trace ($\sigma^\mu{}_\mu = 0 = \omega^\mu{}_\mu$) et leurs carrés, $\sigma^2 \equiv \sigma^\mu{}_\nu \sigma^\nu{}_\mu/2$ et $\omega^2 \equiv \omega^\mu{}_\nu \omega^\nu{}_\mu/2$, représentent les taux de cisaillement et de rotation des lignes géodésiques.

Dans la jauge ADM, le tenseur de courbure extrinsèque est directement lié au tenseur d'expansion par $K_{ij} = -\Theta_{ij}$ et on a directement que sa trace est $K = -\Theta$. Les équations de contrainte et dynamiques se réécrivent alors comme

$$\frac{1}{2}\mathcal{R} + \frac{1}{3}\Theta^2 - \sigma^2 - \omega^2 = 8\pi G\rho + \Lambda \quad , \tag{B.37}$$

$$\sigma^i{}_{j\,||\,i} + \omega^i{}_{j\,||\,i} = \frac{2}{3}\Theta_{|j} \quad , \tag{B.38}$$

$$\dot{\rho} = -\Theta\rho \quad , \tag{B.39}$$

$$(g_{ij})^\bullet = 2 g_{ik}\sigma^k{}_j + 2 g_{ik}\omega^k{}_j + \frac{2}{3}\Theta g_{ij} \quad , \tag{B.40}$$

$$(\sigma^i{}_j + \omega^i{}_j)^\bullet = -\Theta(\sigma^i{}_j + \omega^i{}_j) - \mathcal{R}^i{}_j + \frac{2}{3}\delta^i{}_j \left[\sigma^2 + \omega^2 - \frac{\Theta^2}{3} + 8\pi G\rho + \Lambda\right] \quad . \tag{B.41}$$

Nous avons utilisé dans l'Eq. (B.41) la trace de l'Eq. (B.34), appelée l'*équation de Raychaudhuri* :

$$\dot{\Theta} + \frac{\Theta^2}{3} + 2\sigma^2 + 2\omega^2 + 4\pi G\rho - \Lambda = 0 \quad , \tag{B.42}$$

et remplacé $\mathcal{R}$ par son expression (B.37) qui est dénommée *contrainte Hamitonienne*. Ces deux équations, bien que plus générales ici, gardent la même forme en gravité Newtonienne.

Moyennes spatiales de ces equations : On peut remarquer que le tenseur de courbure extrinsèque peut aussi s'écrire comme $K^i{}_j = -\frac{1}{2}g^{ik}(g_{kj})^{\bullet}$. En définissant alors $J(t,\mathbf{x}) \equiv \sqrt{\det g_{ij}}$, nous avons :

$$(\ln J)^{\bullet} = \frac{1}{2}g^{ik}(g_{ki})^{\bullet} = -K \quad \text{et donc} \quad \dot{J} = -KJ = \Theta J \quad , \tag{B.43}$$

et cette dernière égalité nous montre que

$$\langle\Theta\rangle_{\mathcal{D}} = \frac{1}{V_{\mathcal{D}}}\int_{\mathcal{D}} \frac{\dot{J}}{J}\, J\, d^3\mathbf{x} = \frac{1}{V_{\mathcal{D}}}\left(\int_{\mathcal{D}} J\, d^3\mathbf{x}\right)^{\bullet} = \frac{\dot{V}_{\mathcal{D}}}{V_{\mathcal{D}}} = 3H_{\mathcal{D}} \quad . \tag{B.44}$$

L'équation de conservation (B.39) s'écrit aussi simplement comme

$$(\rho J)^{\bullet} = 0 \quad , \quad \text{de solution générale} \quad \rho(t,\mathbf{x}) = \frac{\rho(t_0,\mathbf{x})J(t_0,\mathbf{x})}{J(t,\mathbf{x})} \quad . \tag{B.45}$$

Ce résultat implique que la masse conservée dans $\mathcal{D}(t)$ est constante au cours du temps :

$$M_{\mathcal{D}} = \int_{\mathcal{D}} \rho J\, d^3\mathbf{x} = \text{cst} \quad \text{et donc} \quad \langle\rho\rangle_{\mathcal{D}} = \frac{1}{V_{\mathcal{D}}}\int_{\mathcal{D}} \rho J\, d^3\mathbf{x} = \frac{M_{\mathcal{D}}}{V_{\mathcal{D}}} = \frac{M_{\mathcal{D}}}{V_{\mathcal{D}(t_0)}a_{\mathcal{D}}^3} \quad . \tag{B.46}$$

L'équation de Rauchaudhuri (B.42), moyennée et en utilisant $S = \Theta$ dans l'Eq. (B.26), vaut :

$$\langle\Theta\rangle_{\mathcal{D}}^{\bullet} - \frac{2}{3}\left\langle\Theta^2\right\rangle_{\mathcal{D}} + \langle\Theta\rangle_{\mathcal{D}}^2 + 2\left\langle\sigma^2\right\rangle_{\mathcal{D}} + 2\left\langle\omega^2\right\rangle_{\mathcal{D}} + 4\pi G\langle\rho\rangle_{\mathcal{D}} - \Lambda = 0 \quad . \tag{B.47}$$

Elle peut s'écrire aussi :

$$3\frac{\ddot{a}_{\mathcal{D}}(t)}{a_{\mathcal{D}}(t)} + 4\pi G\frac{M_{\mathcal{D}}}{V_{\mathcal{D}_0}a_{\mathcal{D}}^3} + \Lambda = \mathcal{Q}_{\mathcal{D}} \quad , \tag{B.48}$$

avec

$$\mathcal{Q}_{\mathcal{D}} \equiv \frac{2}{3}\left[\left\langle\Theta^2\right\rangle_{\mathcal{D}} - \langle\Theta\rangle_{\mathcal{D}}^2\right] - 2\left\langle\sigma^2\right\rangle_{\mathcal{D}} - 2\left\langle\omega^2\right\rangle_{\mathcal{D}} \quad . \tag{B.49}$$

La contrainte Hamiltonienne (B.37) moyennée s'écrit quant à elle comme

$$\frac{1}{2}\langle\mathcal{R}\rangle_{\mathcal{D}} + \frac{1}{3}\left\langle\Theta^2\right\rangle_{\mathcal{D}} - 8\pi G\langle\rho\rangle_{\mathcal{D}} - \Lambda = \left\langle\sigma^2\right\rangle_{\mathcal{D}} + \left\langle\omega^2\right\rangle_{\mathcal{D}} \quad , \tag{B.50}$$

et se révèle équivalente à

$$3\left(\frac{\dot{a}_{\mathcal{D}}}{a_{\mathcal{D}}}\right)^2 + \frac{1}{2}\langle\mathcal{R}\rangle_{\mathcal{D}} - 8\pi G\frac{M_{\mathcal{D}}}{V_{\mathcal{D}_0}a_{\mathcal{D}}^3} - \Lambda = -\frac{\mathcal{Q}_{\mathcal{D}}}{2} \quad . \tag{B.51}$$

On a donc trois équations qui généralisent le cas homogène et qui, lorsque l'on rajoute une courbure constante au modèle FLRW, s'écrivent :

$$3\frac{\ddot{a}_{\mathcal{D}}(t)}{a_{\mathcal{D}}(t)} = -4\pi G\langle\rho\rangle_{\mathcal{D}} + \mathcal{Q}_{\mathcal{D}} + \Lambda \quad , \tag{B.52}$$

$$3H_{\mathcal{D}}^2 = 8\pi G\langle\rho\rangle_{\mathcal{D}} - \frac{3k_{\mathcal{D}_i}}{a_{\mathcal{D}}^2} - \frac{1}{2}\left(\mathcal{W}_{\mathcal{D}} + \mathcal{Q}_{\mathcal{D}}\right) + \Lambda \quad , \tag{B.53}$$

$$\langle\rho\rangle_{\mathcal{D}}^{\bullet} = -3H_{\mathcal{D}}\langle\rho\rangle_{\mathcal{D}} \quad . \tag{B.54}$$

On a définit ici la déviation de courbure à la courbure constante $K_{\mathcal{D}_i}$ selon :

$$\mathcal{W}_{\mathcal{D}} = \langle\mathcal{R}\rangle_{\mathcal{D}} - 6\,\frac{K_{\mathcal{D}_i}}{a_{\mathcal{D}}^2} \quad . \tag{B.55}$$

On peut vérifier que deux seulement de ces équations sont indépendantes si et seulement si nous avons la *condition* nécessaire dite *d'intégrabilité* :

$$\dot{\mathcal{Q}}_{\mathcal{D}} + 6H_{\mathcal{D}}\mathcal{Q}_{\mathcal{D}} + \dot{\mathcal{W}}_{\mathcal{D}} + 2H_{\mathcal{D}}\mathcal{W}_{\mathcal{D}} = 0 \iff a_{\mathcal{D}}^{-6}\left(a_{\mathcal{D}}^6\mathcal{Q}_{\mathcal{D}}\right)^{\bullet} + a_{\mathcal{D}}^{-2}\left(a_{\mathcal{D}}^2\mathcal{W}_{\mathcal{D}}\right)^{\bullet} = 0 \quad . \tag{B.56}$$

C'est par l'étude de ce système d'équations qu'à été proposée l'idée que les inhomogénéités puissent entrainer une accélération apparente en cosmologie et ce du fait que les vraies quantitées observées sont des quantités moyennes. On voit que cette condition d'intégrabilité impose une relation entre la moyenne sur le domaine spatial $\mathcal{D}$ de la courbure tridimensionnelle, au sein de $\mathcal{W}_{\mathcal{D}}$, et le terme dit de rétroaction (« backreaction ») $\mathcal{Q}_{\mathcal{D}}$ qui contient les effets géométriques d'une distribution inhomogène de matière. L'étude de ces équations peut aussi être développée en fonction d'un champ scalaire effectif $\Phi_{\mathcal{D}}$, dépendant du domaine étudié, et nommé le champ de *morphon* (cf. Sec 2.1.1).

B.2.2 Moyenne sur le cône de lumière

La moyenne sur le cône de lumière est une généralisation de la moyenne sur une hypersurface spatiale au cas d'hypersurfaces nulles. Réexprimons brièvement cette première de manière invariante de jauge[3]. On considère une hypersurface spatiale déterminée par l'équation $A(x) = A_0$ où A est un scalaire dans $\mathcal{M}_4$. Le vecteur normal à cette hypersurface est de type temps et se définit comme

$$n_\mu = -\frac{\partial_\mu A}{\sqrt{-\partial_\nu A \partial^\nu A}} \quad \text{avec} \quad n_\mu n^\mu = -1 \quad . \tag{B.57}$$

On prend alors pour définition de la moyenne d'une quantité scalaire S sur un domaine $\mathscr{D} \subset \mathcal{M}_4$:

$$\langle S \rangle_{\mathscr{D}} = \frac{I(S;\mathscr{D})}{I(1;\mathscr{D})} \quad \text{où} \quad I(S;\mathscr{D}) = \int_{\mathcal{M}_4} d^4x \sqrt{-g(x)}\; W_{\mathscr{D}}(x) S(x) \quad . \tag{B.58}$$

$W_{\mathscr{D}}$ est une fonction fenêtre qui sélectionne le domaine d'intégration. Dans le cas d'une intégration sur un domaine $\mathscr{D}$ de l'hypersurface $A = A_0$, délimité par la condition radiale $B(x) < r_0$ avec $B > 0$ (cf. Fig. 2.1), on peut (avec δ_D la distribution de Dirac et Θ celle de Heaviside) prendre la fonction :

$$W_{\mathscr{D}}(x) = n^\mu \nabla_\mu \Theta(A(x) - A_0)\Theta(r_0 - B(x)) = \sqrt{-\partial_\mu A \partial^\mu A}\; \delta_{\mathrm{D}}(A(x) - A_0)\Theta(r_0 - B(x)) \quad . \tag{B.59}$$

Si l'on veut en revanche intégrer sur toute l'hypersurface $A(x) = A_0$, il suffit de prendre $r_0 \to \infty$. Le coefficient $\sqrt{-\partial_\mu A \partial^\mu A}$ qui apparaît dans la fonction $W_{\mathscr{D}}$ garantit l'invariance de jauge de cette moyenne. Il faut aussi pour cela que $B(x)$ soit un scalaire. Cette définition est de plus invariante sous les reparametrisations du type $A(x) \to A'(x)$ (à condition que les surfaces physiques soient inchangées).

On voit pourtant que transformer $A(x)$ en un scalaire de genre lumière (ou nul) ne suffit pas pour décrire la moyenne de S sur une surface nulle. On a en effet $\sqrt{-\partial_\mu A \partial^\mu A} = 0$ et la moyenne précédente est non-définie. Pour définir alors cette moyenne, on introduit un scalaire V définissant une hypersurface nulle et un scalaire A définissant une hypersurface spatiale (analogues de w et τ dans la jauge GLC). La moyenne sur un volume d'espace-temps à 4 dimensions délimité par ces deux surfaces est alors donnée par l'utilisation de l'intégrale :

$$I(S;-;A_0,V_0) = \int_{\mathcal{M}_4} d^4x \sqrt{-g}\; \Theta(V_0 - V)\Theta(A - A_0)\; S(x) \quad . \tag{B.60}$$

Appliquée à $S = \nabla_\mu n^\mu$, on obtient par une simple intégration par parties que :

$$\begin{aligned} \int_{\mathcal{M}_4} d^4x \sqrt{-g}\; \Theta(V_0 - V)\Theta(A - A_0)\nabla^\mu n_\mu \;&=\; -\int_{\mathcal{M}_4} d^4x \sqrt{-g}\, \Theta(V_0 - V)\delta_{\mathrm{D}}(A - A_0)\sqrt{-\partial_\mu A \partial^\mu A} \\ &+\; \int_{\mathcal{M}_4} d^4x \sqrt{-g}\, \delta_{\mathrm{D}}(V_0 - V)\Theta(A - A_0)\frac{-\partial_\mu V \partial^\mu A}{\sqrt{-\partial_\nu A \partial^\nu A}} \quad . \end{aligned} \tag{B.61}$$

Ce résultat est instructif car il contient à droite de l'égalité, d'une part une moyenne spatiale sur la base du 4-cône (tronqué) considéré (Fig. 2.2 (b)), d'autre part une moyenne sur la surface nulle du cône elle-même (Fig. 2.2 (a)). De plus, le coefficient qui apparaît dans l'intégrande de cette dernière quantité se révèle être la bonne normalisation pour définir la moyenne sur la surface nulle.

3. J'écris *invariante de jauge* pour traduire le terme *gauge invariant*, ce que d'autres appèlent *covariante de jauge* en français. J'utilise ainsi *indépendante de jauge* pour traduire *gauge independent*, ce que d'autres appellent *invariant de jauge*, mais nous éviterons d'entrer dans ces complications.

Physiquement, il n'est pas vraiment intéressant d'intégrer sur cette surface nulle car cela revient à extraire un nombre unique pour toute les observations effectuées sur le cône. La perte d'information est donc considérable. Il est plus judicieux de découper ce cône en sphères à valeurs de A constantes et d'intégrer sur chacune de ces sphères. On obtient alors, en prenant $W_{\mathscr{D}} \propto \delta_{\mathrm{D}}(V_0 - V)\delta_{\mathrm{D}}(A - A_0)$:

$$I(S; V_0, A_0; -) = \int_{\mathcal{M}_4} d^4x\sqrt{-g}\ \delta_{\mathrm{D}}(V_0 - V)\delta_{\mathrm{D}}(A - A_0)\ |\partial_\mu V \partial^\mu A| S(x) \quad , \tag{B.62}$$

ce qui correspond à la bonne manière – invariante de jauge – d'intégrer sur la 2-sphère topologique contenue dans les hypersurfaces $V(x) = V_0$ et $A(x) = A_0$ (Fig. 2.2 (c)). On peut enfin regrouper ces trois définitions dans des notations distinctes :

$$\langle S\rangle_{V_0,A_0} = \frac{I(S; V_0, A_0; -)}{I(1; V_0, A_0; -)} \quad , \quad \langle S\rangle_{V_0}^{A_0} = \frac{I(S; V_0; A_0)}{I(1; V_0; A_0)} \quad , \quad \langle S\rangle_{A_0}^{V_0} = \frac{I(S; A_0; V_0)}{I(1; A_0; V_0)} \quad , \tag{B.63}$$

où l'indice du bas correspond à une distribution δ_D et celui du haut à Θ. De manière plus générale, la définition de l'intégrale utilisée peut être résumée par l'Eq. (2.95) et le tableau Tab. 2.1.

B.2.3 Généralisation des règles de Buchert-Ehlers

Il est possible de montrer que les définitions données dans la section précédente amènent elles aussi à des règles de commutation. En effet, la dérivation de la moyenne sur la surface du cône de lumière par rapport aux paramètres A_0 et V_0 donne :

$$\frac{\partial}{\partial A_0}\langle S\rangle_{V_0}^{A_0} = \left\langle \frac{k\cdot\partial S}{k\cdot\partial A}\right\rangle_{V_0}^{A_0} + \left\{ \frac{1}{k\cdot\partial A}\left[\nabla\cdot k - \frac{1}{2}\frac{k^\mu\partial_\mu\left((\partial A)^2\right)}{(\partial A)^2}\right] \middle| S\right\}_{V_0}^{A_0} \quad , \tag{B.64}$$

$$\begin{aligned}\frac{\partial}{\partial V_0}\langle S\rangle_{V_0}^{A_0} &= \left\langle \frac{\partial A\cdot\partial S}{k\cdot\partial A}\right\rangle_{V_0}^{A_0} - \left\langle k\cdot\partial S\frac{(\partial A)^2}{(k\cdot\partial A)^2}\right\rangle_{V_0}^{A_0} + \left\{ \frac{\left[\Box A - \partial^\mu A\partial_\mu \ln\left((\partial A)^2\right)\right]}{k\cdot\partial A} \middle| S\right\}_{V_0}^{A_0} \\ &\quad - \left\{ \left[\nabla\cdot k\frac{(\partial A)^2}{(k\cdot\partial A)^2} + \frac{1}{2}k^\mu\partial_\mu\left(\frac{(\partial A)^2}{(k\cdot\partial A)^2}\right)\right] \middle| S\right\}_{V_0}^{A_0} \quad .\end{aligned} \tag{B.65}$$

La dérivation de la moyenne sur la 2-sphère donne quant à elle :

$$\frac{\partial}{\partial A_0}\langle S\rangle_{V_0,A_0} = \left\langle \frac{k\cdot\partial S}{k\cdot\partial A}\right\rangle_{V_0,A_0} + \left\{ \frac{\nabla\cdot k}{k\cdot\partial A} \middle| S\right\}_{V_0,A_0} \quad , \tag{B.66}$$

$$\frac{\partial}{\partial V_0}\langle S\rangle_{V_0,A_0} = \left\langle \frac{\partial A\cdot\partial S}{k\cdot\partial A}\right\rangle_{V_0,A_0} - \left\langle k\cdot\partial S\frac{(\partial A)^2}{(k\cdot\partial A)^2}\right\rangle_{V_0,A_0} + \left\{ \frac{\Box A - \nabla_\mu\left(k^\mu\frac{(\partial A)^2}{k\cdot\partial A}\right)}{k\cdot\partial A} \middle| S\right\}_{V_0,A_0} \tag{B.67}$$

Nous avons ici introduit les notations simplifiées suivantes :

$$\{A \mid B\}_{V_0,A_0} \equiv \langle A\ B\rangle_{V_0,A_0} - \langle A\rangle_{V_0,A_0}\ \langle B\rangle_{V_0,A_0} \quad , \tag{B.68}$$

$$\{A \mid B\}_{V_0}^{A_0} \equiv \langle A\ B\rangle_{V_0}^{A_0} - \langle A\rangle_{V_0}^{A_0}\ \langle B\rangle_{V_0}^{A_0} \quad , \tag{B.69}$$

$$k^\mu\partial_\mu S = k\cdot\partial S \quad , \quad k^\mu\partial_\mu A = k\cdot\partial A \quad , \quad \partial_\mu A\,\partial^\mu S = \partial A\cdot\partial S \quad , \tag{B.70}$$

$$\partial_\mu A\,\partial^\mu A = (\partial A)^2 \quad , \quad \nabla_\mu k^\mu = \nabla\cdot k \quad , \quad \Box = \nabla^\mu\nabla_\mu \quad . \tag{B.71}$$

B.3 Jauge géodésique sur le cône de lumière (GLC)

B.3.1 Définition de la jauge géodésique sur le cône de lumière

Les équations d'Einstein ne privilégient aucun système de coordonnées et possèdent une liberté dite de jauge. Cette liberté est similaire à celle que l'on observe en électromagnétisme lorsque l'on

redéfinit le potentiel électrique ou le potentiel vecteur sans en changer les champs. On peut alors, sans changer la physique, choisir une jauge dans laquelle nos équations sont les plus simples.

Dans le cas de calculs sur le cône de lumière passé, on définit la métrique GLC (pour *geodesic lightcone gauge* [140]) qui dépend de 6 fonctions arbitraires (un scalaire Υ, un 2-vecteur U^a, et une matrice 2×2 symétrique γ_{ab} avec $a,b=1,2$). L'élément de distance est alors défini par

$$ds^2_{GLC} = \Upsilon^2 dw^2 - 2\Upsilon dw d\tau + \gamma_{ab}(d\widetilde{\theta}^a - U^a dw)(d\widetilde{\theta}^b - U^b dw) \quad , \tag{B.72}$$

où la coordonnée w est de type nulle (i.e. $\partial_\mu w\, \partial^\mu w = 0$) et elle spécifie un cône de lumière passé au sommet duquel se trouve un observateur. Le temps τ définit le temps propre de cet observateur et est égal au temps t de la jauge synchrone (quelque soit la métrique). On peut vérifier que le vecteur $\partial_\mu \tau$ définit son flot géodésique, soit :

$$(\partial^\nu \tau)\, \nabla_\nu\, (\partial_\mu \tau) = 0 \quad . \tag{B.73}$$

Quant aux angles $\widetilde{\theta}^a$, ils paramétrisent la surface compacte topologiquement équivalente à une 2-sphère située à l'intersection des hypersurfaces $\tau = \text{cst}$ et $w = \text{cst}$. Sous forme matricielle, et en terme des coordonnées $(\tau, w, \widetilde{\theta}^a)$, la métrique et son inverse s'écrivent :

$$g^{GLC}_{\mu\nu} = \begin{pmatrix} 0 & -\Upsilon & \vec{0} \\ -\Upsilon & \Upsilon^2 + U^2 & -U_b \\ \vec{0}^T & -U_a^T & \gamma_{ab} \end{pmatrix} \quad , \quad g^{\mu\nu}_{GLC} = \begin{pmatrix} -1 & -\Upsilon^{-1} & -U^b/\Upsilon \\ -\Upsilon^{-1} & 0 & \vec{0} \\ -(U^a)^T/\Upsilon & \vec{0}^T & \gamma^{ab} \end{pmatrix} \quad , \tag{B.74}$$

avec $\vec{0} = (0,0)$, $U_b = (U_1, U_2)$, et où γ_{ab} (resp. γ^{ab}) est une matrice 2×2 qui sert à descendre (resp. monter) les indices angulaires. Cette matrice γ_{ab} paramétrise la géométrie de la 2-sphère. On peut aussi montrer la relation simple suivante :

$$\sqrt{-g} = \Upsilon \sqrt{|\gamma|} \qquad \text{avec} \qquad \gamma \equiv \det \gamma_{ab} \quad . \tag{B.75}$$

Dans la limite d'un Univers FLRW, les coordonnées et les éléments de métrique se réduisent à :

$$\tau = t \quad , \quad w = r + \eta \quad , \quad \Upsilon = a(t) \quad , \quad U^a = 0 \quad , \quad \gamma_{ab} d\tilde{\theta}^a d\tilde{\theta}^b = a^2(t) r^2 (d\theta^2 + (\sin\theta)^2 d\phi^2) \quad . \tag{B.76}$$

La métrique GLC possède de fortes similitudes avec la métrique ADM. En effet, la comparaison des Eqs. (B.72) et (B.23) montre que l'on peut interpréter Υ comme une *lapse function*, définissant la « distance » entre deux cônes de lumière $w = w_0$ et $w = w_1$. Le vecteur U^a est alors similaire à un *shift vector* et définit le changement des coordonnées angulaires lorsque l'on passe d'une 2-sphère $\Sigma(w_0, \tau_0)$ à une autre $\Sigma(w_1, \tau_1)$. Enfin, γ_{ab} est la métrique définissant la géométrie au sein de la 2-sphère.

Il convient aussi de noter que cette métrique, dans sa forme générale, correspond à la fixation de jauge d'un système de coordonnées dites *observationelles* (*observational coordinates*, [59]) pour lesquelles nous avons employé une coordonnée de type temps (i.e. τ) à la place d'une coordonnée radiale (qui peut être choisie de différentes manières). D'autres différences peuvent également être relevées (cf. Sec. 3.2.3).

B.3.2 Applications

Redshift et distance de luminosité

On comprend aisément que cette métrique GLC est parfaitement adaptée aux observations. Ceci se voit d'autant plus par la considération du redshift et de la distance de luminosité calculés dans ces coordonnées. Considérons en effet une source située sur le cône $w = w_o$ et à un temps τ_s en dénotant par "o" une quantité évaluée au niveau de l'observateur et par "s" une quantité située au niveau de la source. Les photons émis par cette source ont un moment $k_\mu = \partial_\mu w$ orthogonal à lui même ($k_\mu k^\mu = 0$) et à la 2-sphère ($\partial_\mu \widetilde{\theta}^a k^\mu = 0$). Le produit scalaire de k_μ avec le vecteur $n^\mu = -\partial_\mu \tau$ normal à l'hypersurface spatiale $\tau = \text{cst}$ donne alors simplement

$$k_\mu n^\mu = g^{w\tau}_{GLC} = -\Upsilon^{-1} \quad . \tag{B.77}$$

Le redshift est alors donné par le rapport de ces quantités aux positions de la source et de l'observateur,

$$(1+z_s) = \frac{(k^\mu u_\mu)_s}{(k^\mu u_\mu)_o} = \frac{\Upsilon(w_o, \tau_o, \widetilde{\theta}^a)}{\Upsilon(w_o, \tau_s, \widetilde{\theta}^a)} \quad , \tag{B.78}$$

et ne dépend que de Υ. La distance de luminosité d_L d'une source ayant un redshift z_s est elle obtenue à travers la distance angulaires d_A selon l'expression :

$$d_L(z_s) = (1+z_s)^2 d_A(z_s) \tag{B.79}$$

qui découle du théorème de réciprocité d'Etherington [18]. On peut alors écrire, d'après l'équation de convergence de Sachs, que

$$\frac{d}{d\lambda}(\ln d_A) = \frac{\hat{\Theta}}{2} \equiv \frac{1}{2}\nabla_\mu k^\mu \quad , \tag{B.80}$$

où λ est un paramètre affine allant de la source ($\lambda = 0$) à l'observateur ($\lambda = 1$) le long du chemin parcouru par le photon. De l'égalité $k^\mu = dx^\mu/d\lambda = -\delta^\mu_\tau \Upsilon^{-1}$ nous déduisons :

$$\nabla_\mu k^\mu = -\Upsilon^{-1}\partial_\tau(\ln\sqrt{\gamma}) = \frac{d}{d\lambda}(\ln\sqrt{\gamma}) \quad \text{avec } \gamma \equiv \det\gamma_{ab} \quad . \tag{B.81}$$

L'intégration de (B.80) donne alors

$$d_A^2(\lambda) = c\sqrt{\gamma(\lambda)} \quad , \tag{B.82}$$

où c est une constante vis-à-vis du paramètre affine λ. En prenant la limite $d_A \to 0$ (ou $\lambda \to 0$) pour laquelle $\widetilde{\theta}^a \to \theta^a$ (i.e. les angles homogènes θ, ϕ), nous obtenons que $\lim_{\lambda\to 0}\left[\sqrt{\gamma}/d_A^2\right] = \sin\widetilde{\theta}^1 = \sin\theta^1_o$ et donc $c = 1/\sin\tilde{\theta}^1$. Nous avons ainsi montré que la distance de luminosité pouvait s'écrire :

$$d_L(z_s) = (1+z_s)^2\ \gamma^{1/4}(z_s, w_o, \widetilde{\theta}^a)\left(\sin\tilde{\theta}^1\right)^{-1/2} \quad . \tag{B.83}$$

Cette relation simple et non-perturbative donne la distance de luminosité dans un Univers quelconque et ne fait intervenir que le déterminant de la métrique sur la 2-sphère à $w = w_o$ et $\tau_s = \tau(w_o, z_s, \widetilde{\theta}^a)$.

Règles de Buchert-Ehlers

L'utilisation de la jauge GLC pour les coordonnées $\{x^\mu\}$ des intégrales présentes dans les règles de commutation établies en Sec. B.2.3 révèle une propriété intéressante. En effet, les choix naturels $A(\tau, w, \widetilde{\theta}^a) = \tau$ et $V(\tau, w, \widetilde{\theta}^a) = w$ nous permettent de montrer que les expressions précédentes sont équivalentes à :

$$\partial_{\tau_s}\langle S\rangle = \langle\partial_\tau S\rangle + \left\langle S\partial_\tau \ln\sqrt{|\gamma|}\right\rangle - \left\langle\partial_\tau\ln\sqrt{|\gamma|}\right\rangle\langle S\rangle \quad , \tag{B.84}$$

$$\begin{aligned}\partial_{w_o}\langle S\rangle \quad = \quad & \langle\partial_w S + U^a\partial_a S\rangle + \left\langle\left[\partial_w\ln\sqrt{|\gamma|}\right]S\right\rangle - \left\langle\partial_w\ln\sqrt{|\gamma|}\right\rangle\langle S\rangle \\ & + \left\langle\left[\partial_a U^a + U^a\partial_a\ln\sqrt{|\gamma|}\right]S\right\rangle - \left\langle\partial_a U^a + U^a\partial_a\ln\sqrt{|\gamma|}\right\rangle\langle S\rangle \quad .\end{aligned} \tag{B.85}$$

Ces expressions sont valides à la fois pour $\langle\ldots\rangle^{\tau_s}_{w_o}$ (surface nulle) et $\langle\ldots\rangle = \langle\ldots\rangle_{w_o,\tau_s}$ (2-sphère). C'est une des nombreuses propriétés remarquables de cette métrique GLC dont un autre exemple est le calcul du *redshift drift* (cf. Sec. 3.6.3).

On peut enfin montrer qu'il n'y a pas d'effet de rétroaction dans un espace homogène et isotrope. Les équations de Friedmann généralisées à un domaine $\mathscr{D}$ se réduisent alors aux équations de Friedmann présentées en Eqs. (B.5) et (B.6) (cf. Sec. 2.4). Le scénario le plus proche du modèle standard que l'on puisse trouver et qui fasse intervenir un effet de rétroaction est l'Univers FLRW plat et perturbé.

B.4 La distance de luminosité au second ordre en perturbations

B.4.1 Au premier ordre

Nous allons calculer la distance de luminosité au second ordre dans les perturbations de métrique autour d'un Univers de type FLRW. Pour cela, nous profitons des relations simples que nous offre le choix de la métrique GLC. Néanmoins, les perturbations de métrique sont souvent exprimés dans la jauge Newtonienne (ou plus généralement de Poisson). De plus, nous connaissons le spectre de puissance des inhomogénéités dans la jauge Newtonienne, et non dans la métrique GLC. Il nous est par conséquent nécessaire de trouver la transformation entre la métrique GLC, utile pour nos calculs, et la métrique de Poisson qui définit les inhomogénéités. Nous verrons que la nature de ces inhomogénéités, considérées comme des quantités stochastiques, impose d'évaluer cette transformation jusqu'au deuxième ordre en perturbations. On utilise donc :

$$g^{\alpha\beta}_{GLC}(x) = \frac{\partial x^\alpha}{\partial y^\mu}\frac{\partial x^\beta}{\partial y^\nu} g^{\mu\nu}_{PG}(y) \quad , \tag{B.86}$$

avec $\{x^\mu\} = (\tau, w, \widetilde{\theta}^a)$, $\{y^\mu\} = (\eta, r, \theta, \phi)$ et la métrique de Poisson (*Poisson Gauge*) :

$$g^{\mu\nu}_{PG} = a(\eta)^{-2}\mathrm{diag}(-1+2\tilde{\Phi}, 1+2\tilde{\Psi}, (1+2\tilde{\Psi})\gamma^{ab}_0) \quad , \tag{B.87}$$

où, de manière cohérente avec les Eqs. (4.1) et (4.2), nous avons :

$$\tilde{\Phi} = \psi + \frac{1}{2}\phi^{(2)} - 2\psi^2 \quad , \quad \tilde{\Psi} = \psi + \frac{1}{2}\psi^{(2)} + 2\psi^2 \quad , \quad \gamma^{ab}_0 = \mathrm{diag}\left(r^{-2}, r^{-2}\sin^{-2}\theta\right) \quad . \tag{B.88}$$

Les champs $\tilde{\Phi}$ et $\tilde{\Psi}$ sont appelés *potentiels de Bardeen* et généralisent la notion du potentiel gravitationnel Newtonien. Nous les prenons égaux au premier ordre car nous supposons le cisaillement de la distribution de matière nul à cet ordre [4].

Les composantes (τ,τ), (w,w) et $(w,\widetilde{\theta}^a)$ de $g^{\alpha\beta}_{GLC}$ nous permettent d'écrire $\{\tau, w, \widetilde{\theta}^a\}$ comme un ensemble de fonctions de (η, r, θ, ϕ) (voir Eqs. (4.8) à (4.13)). Pour rendre la discussion plus simple, nous ne présenterons que les résultats au premier ordre de cette transformation. On obtient donc :

$$\tau = \int_{\eta_{in}}^{\eta} d\eta' a(\eta')\left[1+\psi(\eta', r, \theta^a)\right] \quad , \tag{B.89}$$

$$w = \eta_+ + \int_{\eta_+}^{\eta_-} dx\, \hat{\psi}(\eta_+, x, \theta^a) \quad , \tag{B.90}$$

$$\widetilde{\theta}^a = \theta^a + \frac{1}{2}\int_{\eta_+}^{\eta_-} dx\, \hat{\gamma}^{ab}_0(\eta_+, x, \theta^a)\int_{\eta_+}^{x} dy\, \partial_b\hat{\psi}(\eta_+, y, \theta^a) \quad , \tag{B.91}$$

où $\hat{\psi}(\eta_+, \eta_-, \theta^a) \equiv \psi(\eta, r, \theta^a)$, $\hat{\gamma}^{ab}(\eta_+, \eta_-, \theta^a) \equiv \gamma^{ab}(\eta, r, \theta^a)$ et η_{in} représente un temps assez reculé pour que l'intégrande considérée soit négligeable. Nous avons aussi introduit les variables d'ordre zero sur le cône de lumière :

$$\eta_\pm = \eta \pm r \quad \text{avec :} \quad \partial_\eta = \partial_+ + \partial_- \quad , \quad \partial_r = \partial_+ - \partial_- \quad , \quad \partial_\pm = \frac{\partial}{\partial\eta_\pm} = \frac{1}{2}\left(\partial_\eta \pm \partial_r\right) \quad . \tag{B.92}$$

Les autres composantes (τ, w), $(\tau, \widetilde{\theta}^a)$ et $(\widetilde{\theta}^a, \widetilde{\theta}^b)$ donnent alors $\{\Upsilon, U^a, \gamma^{ab}\}$ en terme de $(\psi, \psi^{(2)}, \phi^{(2)})$ (voir Eqs. (4.14) à (4.23)), avec au premier ordre :

$$\Upsilon = a(\eta)\left[1+\hat{\psi}(\eta_+, \eta_+, \theta^a) - \int_{\eta_+}^{\eta_-} dx\, \partial_+\hat{\psi}(\eta_+, x, \theta^a)\right] + \int_{\eta_{in}}^{\eta} d\eta' a(\eta')\partial_r\psi(\eta', r, \theta^a) \quad , \tag{B.93}$$

$$\begin{aligned} U^a = {} & \frac{1}{2}\hat{\gamma}^{ab}_0\int_{\eta_+}^{\eta_-} dx\, \partial_b\hat{\psi}(\eta_+, x, \theta^a) - \frac{1}{a(\eta)}\gamma^{ab}_0\int_{\eta_{in}}^{\eta} d\eta' a(\eta')\,\partial_b\psi(\eta', r, \theta^a) \\ & + \frac{1}{2}\int_{\eta_+}^{\eta_-} dx\, \partial_+\left[\hat{\gamma}^{ab}_0(\eta_+, x, \theta^a)\int_{\eta_+}^{x} dy\, \partial_b\hat{\psi}(\eta_+, y, \theta^a)\right] - \frac{1}{2}\lim_{x\to\eta_+}\left[\hat{\gamma}^{ab}_0(\eta_+, x, \theta^a)\int_{\eta_+}^{x} dy\, \partial_b\hat{\psi}(\eta_+, y, \theta^a)\right] \quad , \end{aligned} \tag{B.94}$$

$$\gamma^{ab} = \frac{1}{a(\eta)^2}\left\{\left[1+2\psi(\eta, r, \theta^a)\right]\gamma^{ab}_0 + \frac{1}{2}\left[\hat{\gamma}^{ac}_0\int_{\eta_+}^{\eta_-} dx\, \partial_c\left(\hat{\gamma}^{bd}_0(\eta_+, x, \theta^a)\int_{\eta_+}^{x} dy\, \partial_d\hat{\psi}(\eta_+, y, \theta^a)\right) + a \leftrightarrow b\right]\right\} \quad . \tag{B.95}$$

4. Autrement, les termes de propagation du photon au premier ordre dépendent de la combinaison $\tilde{\Phi} + \tilde{\Psi}$.

On obtient par l'Eq. (B.83), après considération de certaines subtilités entre autre liées au développement perturbatif du terme $a(\eta_s)r_s$ contenu dans $\gamma \equiv \det \gamma_{ab}$ (cf. Sec. 4.2.1 au second ordre ou, plus simplement, en Sec. 5.1), l'expression de la distance de luminosité au second ordre :

$$\frac{d_L(z_s,\theta^a)}{d_L^{\rm FLRW}(z_s)} = \frac{d_L(z_s,\theta^a)}{(1+z_s)a_o(\eta_o-\eta_s)} = 1 + \delta_S^{(1)}(z_s,\theta^a) + \delta_S^{(2)}(z_s,\theta^a) \quad , \tag{B.96}$$

où seules les perturbations scalaires ont été considérées. Nous introduisons les grandeurs suivantes :

$$\Xi_s = 1 - \frac{1}{\mathcal{H}_s \Delta\eta} \quad , \quad \Delta\eta = \eta_o - \eta_s^{(0)} \quad , \tag{B.97}$$

$$Q(\eta_+,\eta_-,\theta^a) = \int_{\eta_+}^{\eta_-} dx\ \hat{\psi}(\eta_+,x,\theta^a) \quad , \quad P(\eta,r,\theta^a) = \int_{\eta_{in}}^{\eta} d\eta' \frac{a(\eta')}{a(\eta)} \psi(\eta',r,\theta^a) \quad . \tag{B.98}$$

En définissant maintenant les quantités physiques qui suivent :

$$J = ([\partial_+ Q]_s - [\partial_+ Q]_o) - ([\partial_r P]_s - [\partial_r P]_o) \quad , \tag{B.99}$$

$$J_2^{(1)} = \frac{1}{2}\nabla_a \tilde{\theta}^{a(1)} = \frac{1}{2}\left(\cot\theta\ \tilde{\theta}^{(1)} + \partial_a \tilde{\theta}^{a(1)}\right) = \int_{\eta_s^{(0)}}^{\eta_o} \frac{d\eta}{\Delta\eta}\ \frac{\eta-\eta_s^{(0)}}{\eta_o-\eta} \Delta_2 \psi(\eta,\eta_o-\eta,\theta^a) \quad , \tag{B.100}$$

la correction au premier ordre $\delta_S^{(1)}$ s'écrit comme :

$$\delta_S^{(1)}(z_s,\theta^a) \quad = \quad \Xi_s J - \frac{Q_s}{\Delta\eta} - \psi_s^{(1)} - J_2^{(1)} \quad . \tag{B.101}$$

Ces termes à l'ordre 1 sont bien connus dans la littérature et sont aisément interprétables. Les contributions du type $\partial_r P$ correspondent au produit scalaire $\mathbf{v}\cdot\mathbf{n}$ du vecteur vitesse (de la source ou de l'observateur) avec un vecteur unitaire $\mathbf{n}$ parallèle au chemin du photon et pointant en direction de l'observateur. La vitesse $\mathbf{v}$ s'écrit, dans la jauge Newtonienne :

$$\mathbf{v} = -\int_{\eta_{in}}^{\eta} d\eta' \frac{a(\eta')}{a(\eta)} \nabla\psi(\eta',r,\theta^a) \quad . \tag{B.102}$$

Les termes du type :

$$\partial_+ Q_s - \partial_+ Q_o \sim \psi_o - \psi_s - 2\int_{\eta_s}^{\eta_o} d\eta\ \partial_\eta \psi(\eta,r,\theta^a) \quad , \tag{B.103}$$

correspondent aux effets Sachs-Wolfe (SW) et Sachs-Wolfe intégré (ISW). Enfin, le terme

$$J_2 = \int_{\eta_s^{(0)}}^{\eta_o} \frac{d\eta}{\Delta\eta}\ \frac{\eta-\eta_s^{(0)}}{\eta_o-\eta} \Delta_2 \psi(\eta,\eta_o-\eta,\theta^a) + \mathcal{O}(2) \quad , \tag{B.104}$$

est un terme de lentille gravitationnelle.

B.4.2 Au second ordre

On obtient la correction à la distance de luminosité au deuxième ordre dans les perturbations scalaires $\delta_S^{(2)}(z_s,\theta^a)$ de la même manière qu'au premier ordre, i.e. en développant $\gamma^{1/4}(z_s,w_o,\widetilde{\theta}^a)$ et $(\sin\tilde{\theta}^1)^{-1/2}$ dans l'Eq. (B.83). L'expression de d_L obtenue est alors du type $(1+z_s)^2(a_s r_s)\big(1+\mathcal{O}(1)+\mathcal{O}(2)\big)$ avec $a_s \equiv a(\eta_s)$ le facteur d'échelle au niveau de la source et r_s sa distance radiale (cf. Eq. (4.36)). Ces deux termes doivent ensuite être développés en perturbations. Le premier est obtenu en considérant la relation $1+z_s = \Upsilon_o/\Upsilon_s$ que l'on développe d'après l'expression perturbée de Υ. On obtient alors une égalité du type $1+z_s = a(\eta_o)/a(\eta_s)(1+\mathcal{O}(1)+\mathcal{O}(2))$ et on peut développer $a(\eta_s)$ comme $a(\eta_s^{(0)})\left(1+\eta_s^{(1)}\mathcal{H}_s+\mathcal{O}(2)\right)$. L'utilisation de l'indentité $1+z_s = a(\eta_o)/a(\eta_s^{(0)})$ impose

d'annuler toutes les perturbations présentes et donne les corrections de $\eta_s = \eta_s^{(0)} + \eta_s^{(1)} + \eta_s^{(2)}$. On peut alors calculer les corrections à r_s en utilisant la transformation : $w_s = \eta_o = \eta_s + r_s + \mathcal{O}(1) + \mathcal{O}(2)$. Bien sûr toutes ces opérations, dont le détail rigoureux est présenté en Sec. 4.2.1, génèrent de nombreux termes au second ordre à partir du premier ordre (termes quadratiques).

Les termes obtenus et résumés en Eqs. (4.60), (4.61) et (4.50), (4.51), sont de toutes les sortes possibles. On trouve en effet des combinaisons du premier ordre, du type :

$$\begin{aligned} &\psi_s^2 \quad , \quad (\psi_s, Q_s) \times (\text{Lent. Grav., ISW, Doppler}) \quad , \quad (\text{ISW})^2 \quad , \\ &(\text{Doppler})^2 \quad , \quad \text{ISW} \times \text{Doppler} \quad , \quad (\text{Lent. Grav.})^2 \quad . \end{aligned} \tag{B.105}$$

On y trouve aussi des termes intrinsèques à l'ordre 2 :

$$\psi_s^{(2)} \quad , \quad (\text{Lent. Grav.})^{(2)} = \frac{1}{2}\nabla_a \tilde{\theta}^{a(2)} \quad , \quad Q_s^{(2)} \quad , \tag{B.106}$$

de nouveaux termes intégrés tels que :

$$\frac{1}{4\Delta\eta}\int_{\eta_s^{(0)+}}^{\eta_s^{(0)-}} dx \ \left[4\hat{\psi}\ \partial_+ Q + \hat{\gamma}_0^{ab}\ \partial_a Q\ \partial_b Q\right](\eta_s^{(0)+}, x, \theta^a) \quad , \tag{B.107}$$

et des termes de déformation angulaire :

$$(\gamma_0)_{ab}\partial_+\tilde{\theta}^{a(1)}\partial_-\tilde{\theta}^{b(1)} \quad , \quad \partial_a\tilde{\theta}^{b(1)}\partial_b\tilde{\theta}^{a(1)} \quad , \tag{B.108}$$

avec $\widetilde{\theta}^{a(1)}$ donné en Eq. (B.91). Enfin, les perturbations de redshift engendrent un grand nombre de nouvelles contributions, e.g. :

$$\gamma_0^{ab}\left(\partial_a P\ \partial_b P\ ,\ \partial_a Q\ \partial_b Q\ ,\ \partial_a Q\ \partial_b P\right) \quad , \quad \partial_+ \int_{\eta_+}^{\eta_-} dx \ \left[4\hat{\psi}\ \partial_+ Q + \hat{\gamma}_0^{ab}\partial_a Q\ \partial_b Q\right] \quad , \tag{B.109}$$

$$\int_{\eta_{in}}^{\eta} d\eta' \ \frac{a(\eta')}{a(\eta)}\partial_r\left[(\partial_r P)^2 + \gamma_0^{ab}\partial_a P\ \partial_b P\right] \quad , \tag{B.110}$$

dont la dernière contient la partie transverse $\partial_a P$ de la vitesse particulière de la source.

Il est possible de généraliser ces calculs à des perturbations de métrique vectorielles et tensorielles. On utilise dans ce cas la jauge de Poisson au lieu de la jauge Newtonienne :

$$ds_{PG}^2 = a^2(\eta)\left(-d\eta^2 + 2v_i d\eta dx^i + [(\gamma_0)_{ij} + \chi_{ij}]dx^i dx^j\right) \ , \ \{x^i\} = (r, \theta, \phi) \quad , \tag{B.111}$$

avec v^i et χ^{ij} qui vérifient :

$$\nabla_i v^i = \nabla_i \chi^{ij} = 0 \qquad (\text{sans divergence}) \quad , \quad (\gamma_0)_{ij}\chi^{ij} = 0 \qquad (\text{sans trace}) \quad . \tag{B.112}$$

Les résultats de la transformation des coordonnées et des éléments de métrique, en supposant les perturbations vectorielles et tensorielles nulles au premier ordre (prédit par l'inflation), sont analogues et font intervenir la combinaison radiale $\frac{v^r}{2} - \frac{\chi^{rr}}{4}$ (cf. Eqs. (4.26) à (4.29)). On obtient aussi des corrections à la distance de luminosité (cf. Eq. (4.78)). Néanmoins, la moyenne de ces corrections sur la 2-sphère (Sec. 5.3.6) est symétriquement nulle et il n'est pas nécessaire de les décrire plus.

B.5 Moyenne stochastique sur le cône de lumière

B.5.1 Considérations générales

Dans le but d'évaluer l'effet des inhomogénéités sur les observations cosmologiques de l'énergie sombre, nous allons effectuer la moyenne d'observables scalaires, une moyenne sur la 2-sphère qui se situe dans notre cône de lumière passé à un redshift z_s, mais aussi stochastique, de manière à s'affranchir d'une distribution particulière de matière et à la place ne considérer que le spectre de

puissance de ces inhomogénéités. On décompose le champ gravitationnel au premier ordre en modes de Fourier :

$$\psi(\eta, \mathbf{x}) = \frac{1}{(2\pi)^{3/2}} \int d^3k \; \mathrm{e}^{i\mathbf{k}\cdot\mathbf{x}} \; \psi_k(\eta) E(\mathbf{k}) \quad , \tag{B.113}$$

où E est une variable aléatoire unitaire vérifiant :

$$E^*(\mathbf{k}) = E(-\mathbf{k}) \quad \text{(homogénéité statistique)} \quad , \tag{B.114}$$

$$\overline{E(\mathbf{k})} = 0 \quad , \quad \overline{E(\mathbf{k}_1)E(\mathbf{k}_2)} = \delta_{\mathrm{D}}(\mathbf{k}_1 + \mathbf{k}_2) \quad \text{(moyenne d'ensemble)} \quad . \tag{B.115}$$

Cette variable aléatoire E rend les fluctuations statistiquement homogènes et isotropes.

Le spectre de puissance du champ gravitationnel est donné dans son régime linéaire par :

$$\mathcal{P}_\psi(k, \eta) \quad \equiv \quad \frac{k^3}{2\pi^2} |\psi_k(\eta)|^2 = g^2(z) T^2(k) \frac{9}{25} A \left(\frac{k}{k_0}\right)^{n_s - 1} \quad . \tag{B.116}$$

C'est une quantité sans dimension qui dépend du spectre primordial (issu de l'inflation) $A\,(k/k_0)^{n_s-1}$ dont les paramètres numériques sont connus :

$$A = 2.45 \; 10^{-9} \quad , \quad n_s = 0.96 \quad \text{(indice spectral)} \quad , \quad \frac{k_0}{a_0} = 0.002 \; \mathrm{Mpc}^{-1} \quad . \tag{B.117}$$

Il dépend aussi d'une fonction $T(k)$, la fonction de transfert, qui tient compte de l'évolution de la matière entre la fin de l'inflation et la période de matière (autrement dit, dans l'ère de radiation). Grossièrement, cette fonction décrit l'effet de réentrée progressive de ces modes et leur perte de puissance aux courtes longueurs d'onde due à la dispersion par radiation (*Silk damping*) et l'oscillation (BAO) des modes de grande longueur d'onde (mais plus courte que l'horizon causal). Ce dernier phénomène n'ajoute qu'une faible modulation à l'amplitude de $T(k)$ et n'est pas considéré dans notre étude. Enfin, le spectre de puissance fait intervenir la fonction du redshift z (ou du temps η) :

$$g(z) = \frac{5 g_\infty}{2} \Omega_m(z) \left[\Omega_m(z)^{4/7} - \Omega_\Lambda(z) + \left[1 + \frac{\Omega_m(z)}{2}\right] \left[1 + \frac{\Omega_\Lambda(z)}{70}\right] \right]^{-1} \quad , \tag{B.118}$$

qui a déjà été décrite en Sec. B.1.3. Cette fonction fait intervenir l'expression des paramètres cosmologiques dans un Univers de type ΛCDM :

$$\Omega_m(z) = \frac{\Omega_{m0}(1+z)^3}{\Omega_{m0}(1+z)^3 + \Omega_{\Lambda 0}} \quad , \quad \Omega_\Lambda(z) = \frac{\Omega_{\Lambda 0}}{\Omega_{m0}(1+z)^3 + \Omega_{\Lambda 0}} \quad . \tag{B.119}$$

B.5.2 Termes quadratiques : backreaction induite

Le but de notre étude, liée aux observations des SNe Ia, est de calculer des corrélations du type $\overline{\langle d_L(z, \mathbf{n}) \rangle}$ ou e.g. $\overline{\langle d_L(z, \mathbf{n}) d_L(z, \mathbf{n}) \rangle}$ et non $\overline{\langle d_L(z, \mathbf{n}) d_L(z, \mathbf{n}') \rangle}$ ou encore $\overline{\langle d_L(z, \mathbf{n}) d_L(z', \mathbf{n}) \rangle}$ (cf. [63] pour ces dernières). On considère donc des perturbations aux quantités présentes dans le modèle FLRW et dont l'origine est le fond stochastique des perturbations primordiales. Ces perturbations vérifient les conditions présentées en Eq. (B.114) : $\overline{\psi} = 0$ et $\overline{\psi^2} \neq 0$. Par conséquent, la moyenne au premier ordre d'une quantité scalaire S donne $\overline{S} = S^{\mathrm{FLRW}}$. Pour obtenir une correction au modèle homogène, il est donc nécessaire d'aller à l'ordre quadratique ou des ordres supérieurs (ou, encore une fois, de considérer des quantités du type $\overline{S(z, \theta^a) S(z', \theta'^a)}$). Dans cette étude toutefois, nous allons considérer la moyenne stochastique, non pas directement d'une quantité scalaire S, mais de sa moyenne sur le cône de lumière $\langle S \rangle$. Nous allons voir qu'il est alors possible d'obtenir des corrections à partir du simple premier ordre de S et ce du fait du couplage, dans la moyenne, entre cette quantité scalaire et la mesure d'intégration sur le cône (amenant ainsi $\overline{\langle S \rangle} \neq S^{\mathrm{FLRW}}$). C'est cet effet généré par la combinaison des deux moyennes, sur le cône de lumière et stochastique, que nous allons ici décrire. Il convient de rappeler aussi que cette combinaison avait déjà été étudiée dans le cas d'une moyenne spatiale (cf. [37, 110, 111]), mais jamais avec la moyenne sur le cône.

Considérons une moyenne typique sur une surface compacte Σ (topologiquement équivalente à une 2-sphère) plongée dans le cône de lumière passé $w = w_o$ et à un redshift constant z_s. Nous écrivons cette moyenne simplement comme :

$$\langle S \rangle_\Sigma = \frac{\int_\Sigma d^2\mu \, S}{\int_\Sigma d^2\mu} \quad , \tag{B.120}$$

où $d^2\mu$ est la mesure d'intégration adéquate obtenue par notre approche invariante de jauge (voir Eq. (3.67)) et S est une observable scalaire (possiblement non locale). On peut séparer la contribution homogène de la perturbation au premier ordre dans ces deux quantités :

$$d^2\mu = (d^2\mu)^{(0)}(1+\mu) \qquad , \qquad S = S^{(0)}(1+\sigma) \quad , \tag{B.121}$$

et renormaliser nos intégrales de sorte que $\int (d^2\mu)^{(0)} = 1$. On obtient alors :

$$\left\langle \frac{S}{S^{(0)}} \right\rangle = \frac{\int (d^2\mu)^{(0)}(1+\mu)(1+\sigma)}{\int (d^2\mu)^{(0)}(1+\mu)} = \frac{\langle (1+\mu)(1+\sigma) \rangle_0}{1 + \langle \mu \rangle_0} \quad , \tag{B.122}$$

où nous avons omis le symbole Σ et avons désigné les moyennes relatives à la mesure $(d^2\mu)^{(0)}$ par la notation $\langle \ldots \rangle_0$. Ce dernier indice sera oublié dans les considérations qui font suite.

Considérons maintenant la moyenne d'ensemble (stochastique) en gardant à l'esprit que celle-ci ne se factorise pas, i.e. $\overline{AB} \neq \overline{A}\ \overline{B}$. On trouve par cette moyenne de l'Eq. (B.122) que :

$$\overline{\langle S/S^{(0)} \rangle} = 1 + \overline{(\langle \sigma \rangle + \langle \mu\sigma \rangle)(1 + \langle \mu \rangle)^{-1}} \quad . \tag{B.123}$$

Cette relation devient particulièrement intéressante lorsque l'on developpe μ et σ en séries :

$$\mu = \sum_i \mu_i \qquad , \qquad \sigma = \sum_i \sigma_i \quad , \tag{B.124}$$

et que l'on fait l'hypothèse que μ_1 et σ_1 s'annulent sous l'effet de la moyenne d'ensemble (comme toute perturbation d'origine inflationnaire). Notre résultat peut alors se développer selon :

$$\overline{\langle S/S^{(0)} \rangle} = 1 + \overline{\langle \sigma_2 \rangle} + \mathrm{IBR}_2 + \overline{\langle \sigma_3 \rangle} + \mathrm{IBR}_3 + \ldots \tag{B.125}$$

où, par l'utilisation de $\overline{\langle \mu_1 \rangle \langle \sigma_1 \rangle} \neq \overline{\langle \mu_1 \rangle}\ \overline{\langle \sigma_1 \rangle}$, nous avons :

$$\mathrm{IBR}_2 = \overline{\langle \mu_1\sigma_1 \rangle} - \overline{\langle \mu_1 \rangle \langle \sigma_1 \rangle} \quad , \tag{B.126}$$

$$\mathrm{IBR}_3 = \overline{\langle \mu_2\sigma_1 \rangle} - \overline{\langle \mu_2 \rangle \langle \sigma_1 \rangle} + \overline{\langle \mu_1\sigma_2 \rangle} - \overline{\langle \mu_1 \rangle \langle \sigma_2 \rangle} - \overline{\langle \mu_1 \rangle \langle \mu_1\sigma_1 \rangle} + \overline{\langle \mu_1 \rangle \langle \mu_1 \rangle \langle \sigma_1 \rangle} \quad . \tag{B.127}$$

On observe que ce résultat de la combinaison des deux moyennes dépend, à un ordre donné, à la fois de termes provenants directement du développement de S et d'autres venant de la combinaison des fluctuations de S et de celles de la mesure d'intégration $d^2\mu$. Ces derniers termes sont dit termes de « backreaction induite » (*Induced Backreaction*, IBR) du fait de leur capacité à engendrer des corrections au modèle homogène à partir du premier ordre de S. Lorsque S et $d^2\mu$ ne sont pas corrélées, ces contributions sont nulles et seules les contributions ne dépendant que de S (et de la mesure homogène $d^2\mu^{(0)}$) subsistent, i.e. $\overline{\langle \sigma_i \rangle}$ avec $i \geq 2$.

Abordons finalement le calcul de la variance, i.e. de la largeur de la distribution des valeurs de $S/S^{(0)}$ autour de la valeur moyenne $\overline{\langle S/S^{(0)} \rangle}$. Cette dispersion est due, en même temps, aux fluctuations de la surface spatiotemporelle sur laquelle est faite la moyenne et à celles dues à la moyenne d'ensemble. On la définit donc en considérant les deux opérations communément :

$$\mathrm{Var}[S/S^{(0)}] \equiv \overline{\left\langle \left(S/S^{(0)} - \overline{\langle S/S^{(0)} \rangle} \right)^2 \right\rangle} = \overline{\langle (S/S^{(0)})^2 \rangle} - \left(\overline{\langle S/S^{(0)} \rangle} \right)^2 \quad . \tag{B.128}$$

Par l'introduction des développements de l'Eq. (B.121) et quelque calculs, cette variance devient :

$$\mathrm{Var}[S/S^{(0)}] = \overline{\langle \sigma^2(1+\mu) \rangle (\langle 1+\mu \rangle)^{-1}} - \left(\overline{\langle \sigma(1+\mu) \rangle (1 + \langle \mu \rangle)^{-1}} \right)^2 \quad . \tag{B.129}$$

On montre alors que les développements en séries de μ et σ imposent au second terme de l'Eq. (B.129) d'être au moins d'ordre quatre. Par conséquent, on trouve qu'à l'ordre dominant (ordre 2) :

$$\mathrm{Var}[S/S^{(0)}] = \overline{\langle \sigma_1^2 \rangle} \quad . \tag{B.130}$$

Comme pour le terme IBR_2, nous avons un résultat qui ne dépend que de l'ordre quadratique. De plus ici le résultat ne dépend pas des fluctuations de métrique, mais seulement du scalaire moyenné.

Notons enfin que nous aurions pu opter pour une autre définition de la variance, en considérant la dispersion stochastique de la moyenne $\langle S/S^{(0)} \rangle$. Cette définition de la variance donne l'expression suivante :

$$\mathrm{Var}'[S/S^{(0)}] \equiv \overline{\left(\langle S/S^{(0)} \rangle - \overline{\langle S/S^{(0)} \rangle} \right)^2} = \overline{\left(\langle S/S^{(0)} \rangle \right)^2} - \left(\overline{\langle S/S^{(0)} \rangle} \right)^2 \quad , \tag{B.131}$$

qui après des considérations similaires à celles déjà présentées, a pour résultat :

$$\mathrm{Var}'[S/S^{(0)}] = \overline{\langle \sigma_1 \rangle^2} \quad . \tag{B.132}$$

On verra dans le cas $S \equiv d_L$ que cette dispersion est beaucoup plus petite que la première. La raison intuitive qui explique ce fait est la suivante. $\mathrm{Var}'[S]$ définit la variation de la moyenne spatiale $\langle S \rangle$ par la considération de différentes réalisations de notre Univers inhomogène (décrit par le spectre du puissance). On comprend que pour une sphère assez grande devant la taille des inhomogénéités, et pour l'ordre en k des termes considérés, cette variation doit être petite. D'un autre côté, la variance $\mathrm{Var}[S]$ exprime la dispersion de l'observable S autour de la valeur moyenne $\overline{\langle S \rangle}$, et c'est cette quantité qui fluctue de manière importante. La vraie dispersion se trouve donc dans la moyenne angulaire et non dans la moyenne stochastique (non moins nécessaire pour autant) et par conséquent nous oublierons la définition de $\mathrm{Var}'[S]$ pour ne garder que $\mathrm{Var}[S]$.

B.5.3 Application à l'ordre quadratique

Nous décrirons brievement ici l'élaboration du calcul des termes composant IBR_2 dans le cas où S est une observable physique. Pour des SNe Ia, cette observable est normalement le flux lumineux, $S \propto d_L^{-2}$, mais on peut également penser à moyenner la distance de luminosité $S = d_L$. En effet, le calcul de ces termes de backreaction induite permet une première évaluation de la moyenne de ces quantités, bien qu'incomplète, à partir de la transformation des coordonnées au premier ordre. Ces termes apparaissent de la manière suivante :

$$(\overline{\langle d_L^{-2} \rangle})^{-1/2} = d_L^{\mathrm{FLRW}} \left(1 + \overline{\langle \sigma_2 \rangle} + \mathrm{IBR}_2 - \frac{3}{2} \overline{\langle \sigma_1^2 \rangle} \right) \quad , \quad \overline{\langle d_L \rangle} = d_L^{\mathrm{FLRW}} \left(1 + \overline{\langle \sigma_2 \rangle} + \mathrm{IBR}_2 \right) \quad , \tag{B.133}$$

et seul un calcul complet au second ordre (dont nous présenterons les résultats par la suite) permet la détermination de $\overline{\langle \sigma_2 \rangle}$. Toutefois, les expressions des termes de backreaction induite IBR_2 et de la variance au second ordre $\overline{\langle \sigma_1^2 \rangle}$ ne dépendent que du premier ordre. Ces quantités peuvent donc déjà être évaluées exactement par un calcul au premier ordre. On peut aussi remarquer qu'il n'est pas nécessaire de connaître μ_2 pour le calcul au second ordre.

D'après l'Eq. (B.101), nous avons :

$$\sigma_1 = A_1 + A_2 + A_3 + A_4 + A_5 \quad , \tag{B.134}$$

$$A_1 = -\psi_s \quad , \quad A_2 = -Q_s/\Delta\eta \quad , \quad A_3 = \Xi_s I_+ \quad , \quad A_4 = -\Xi_s I_r \quad , \quad A_5 = -J_2 \quad , \tag{B.135}$$

avec I_+ et I_r définis en Eqs. (5.8) et (5.9). D'autre part, puisque nous intégrons sur le ciel à un certain redshift dans notre cône de lumière passé, la mesure $d^2\mu$ est donnée par l'Eq. (3.67) :

$$d^2\mu = d^2\widetilde{\theta} \sqrt{\gamma(w_o, \tau(z_s, w_o, \tilde{\theta}^a), \tilde{\theta}^a)} \quad . \tag{B.136}$$

Il nous faut transformer l'intégration sur $d^2\widetilde{\theta}$ (i.e. sur la 2-sphère Σ) en une intégration sur les coordonnées polaires usuelles $d^2\theta = d\theta d\phi$ de la jauge Newtonienne. On vérifie aisément (en considérant le Jacobien de la transformation $\theta^a \to \widetilde{\theta}^a$, cf. Eq. (B.91)) que l'on a au premier ordre :

$$\int d^2\widetilde{\theta} \sqrt{\gamma} = \int d\phi d\theta \sin\theta \left([a_s r_s](z_s, \theta^a) \right)^2 (1 - 2\psi_s) \ . \tag{B.137}$$

La mesure non perturbée est donc donnée par $(d^2\mu)^{(0)} = d^2\Omega/4\pi$ avec $d^2\Omega = d\phi d\theta \sin\theta$. L'utilisation du développement du produit $a_s r_s$ présenté en Eq. (5.21) (ou (4.55)) donne ensuite :

$$\mu_1 = -2\psi_s - 2Q_s/\Delta\eta + 2\Xi_s J(z_s, \theta^a) = 2\left(A_1 + A_2 + A_3 + A_4\right) \quad . \tag{B.138}$$

Il nous est donc possible d'obtenir la contribution IBR_2, ainsi que la variance de d_L/d_L^{FLRW}, en insérant les résultats de (B.134) et (B.138) dans les Eqs. (B.126) et (B.130). Les contributions à calculer sont bilinéaires dans le champ gravitationnel ψ et apparaissent toutes sous la forme $\overline{\langle A_i A_j\rangle}$ ou bien $\overline{\langle A_i\rangle\langle A_j\rangle}$ et où les A_i ont été définis en Eq. (B.135).

L'exemple le plus simple est celui de $A_1 = -\psi_s$. En utilisant la notation $\overline{\langle\ldots\rangle}$ pour la moyenne présentée en Eq. (B.120), et dénotant par $d^2\Omega/4\pi$ la mesure d'intégration homogène (et normalisée), nous obtenons :

$$\begin{aligned}
\overline{\langle\psi_s\psi_s\rangle} &= \int \frac{d^3k\ d^3k'}{(2\pi)^3}\overline{E(\mathbf{k})E(\mathbf{k}')}\int\frac{d^2\Omega}{4\pi}\left[\psi_k(\eta_s^{(0)})e^{ir\mathbf{k}\cdot\hat{\mathbf{x}}}\right]_{r=\eta_o-\eta_s^{(0)}}\left[\psi_{k'}(\eta_s^{(0)})e^{ir\mathbf{k}'\cdot\hat{\mathbf{x}}}\right]_{r=\eta_o-\eta_s^{(0)}} \\
&= \int\frac{d^3k}{(2\pi)^3}\ |\psi_k(\eta_s^{(0)})|^2\int_{-1}^{1}\frac{d(\cos\theta)}{2}\left[e^{ik\Delta\eta\cos\theta}\right]\left[e^{-ik\Delta\eta\cos\theta}\right] \\
&= \int\frac{d^3k}{(2\pi)^3}\ |\psi_k(\eta_s^{(0)})|^2 = \int_0^\infty\frac{dk}{k}\ \mathcal{P}_\psi(k,\eta_s^{(0)}) \quad ,
\end{aligned} \tag{B.139}$$

$$\begin{aligned}
\overline{\langle\psi_s\rangle\,\langle\psi_s\rangle} &= \int \frac{d^3k\ d^3k'}{(2\pi)^3}\overline{E(\mathbf{k})E(\mathbf{k}')}\left[\int\frac{d^2\Omega}{4\pi}\psi_k(\eta_s^{(0)})e^{ir\mathbf{k}\cdot\hat{\mathbf{x}}}\right]_{r=\eta_o-\eta_s^{(0)}}\left[\int\frac{d^2\Omega'}{4\pi}\psi_{k'}(\eta_s^{(0)})e^{ir\mathbf{k}'\cdot\hat{\mathbf{x}}'}\right]_{r=\eta_o-\eta_s^{(0)}} \\
&= \int\frac{d^3k}{(2\pi)^3}\ |\psi_k(\eta_s^{(0)})|^2\left[\int_{-1}^{1}\frac{d(\cos\theta)}{2}e^{ik\Delta\eta\cos\theta}\right]\left[\int_{-1}^{1}\frac{d(\cos\theta')}{2}e^{-ik\Delta\eta\cos\theta'}\right] \\
&= \int\frac{d^3k}{(2\pi)^3}\ |\psi_k(\eta_s^{(0)})|^2\left(\frac{\sin(k\Delta\eta)}{k\Delta\eta}\right)^2 = \int_0^\infty\frac{dk}{k}\ \mathcal{P}_\psi(k,\eta_s^{(0)})\left(\frac{\sin(k\Delta\eta)}{k\Delta\eta}\right)^2 \quad .
\end{aligned} \tag{B.140}$$

Dans la seconde ligne de ces deux résultats, nous avons utilisé l'isotopie (i.e. $\psi_{\mathbf{k}}$ ne dépend que de $k = |\mathbf{k}|$) et avons définit les angles θ et θ' comme les angles respectifs entre $\mathbf{k}$ et $\mathbf{x} \equiv r\hat{\mathbf{x}}$ et entre $\mathbf{k}'$ et $\mathbf{x}' \equiv r\hat{\mathbf{x}}'$. Nous avons aussi introduit le spectre de puissance donné par l'Eq. (B.18).

Un cas légèrement plus compliqué de terme qui combine moyenne angulaire et moyenne stochastique, avec $\mathcal{P}_\psi$ supposé indépendant de η (cas vérifié dans le modèle CDM), est donné par :

$$\begin{aligned}
\overline{\left\langle\psi_s\frac{Q_s}{\Delta\eta}\right\rangle} &= -\frac{2}{\Delta\eta}\int\frac{d^3k_1d^3k_2}{(2\pi)^3}\psi_{k_1}\psi_{k_2}\overline{E(\mathbf{k}_1)E(\mathbf{k}_2)}\left\langle e^{i\mathbf{k}_1\cdot\hat{\mathbf{x}}\Delta\eta}\int_{\eta_s}^{\eta_o}d\eta\ e^{i\mathbf{k}_2\cdot\hat{\mathbf{x}}(\eta_o-\eta)}\right\rangle \\
&= -\frac{2}{\Delta\eta}\int_0^\infty\frac{dk}{4\pi k}\mathcal{P}_\psi(k)\int_{\eta_s}^{\eta_o}d\eta\left\langle e^{ik(\eta_s-\eta)\cos\theta}\right\rangle \\
&= \int_0^\infty\frac{dk}{k}\mathcal{P}_\psi(k)\ \left[-\frac{2}{k\Delta\eta}\mathrm{SinInt}(k\Delta\eta)\right] \quad ,
\end{aligned} \tag{B.141}$$

$$\overline{\langle\psi_s\rangle\left\langle\frac{Q_s}{\Delta\eta}\right\rangle} = \int_0^\infty\frac{dk}{k}\mathcal{P}_\psi(k)\ \left[-\mathrm{Sinc}(k\Delta\eta)\frac{2}{k\Delta\eta}\mathrm{SinInt}(k\Delta\eta)\right] \quad . \tag{B.142}$$

On remarque la différence dans les résultats et le fait que le calcul effectué sur le cône de lumière a une influence directe sur la nature des intégrandes finales où interviennent le sinus cardinal et le sinus intégral :

$$\mathrm{Sinc}(x) \equiv \frac{\sin(x)}{x} \quad , \quad \mathrm{SinInt}(x) = \int_0^x dy\ \mathrm{Sinc}(y) \quad . \tag{B.143}$$

On a supposé dans ces deux derniers calculs que l'on avait un Univers CDM, et ce pour avoir ψ_k indépendant du temps η et ainsi pouvoir factoriser le spectre de puissance $\mathcal{P}_\psi(k)$.

Dans le calcul complet de IBR_2 ou de la variance, de nombreux termes apparaissent et ont des dépendances différentes. Dans le cas d'une géométrie de fond décrite par un modèle CDM, cette dépendance est simplifiée par le fait que les perturbations ψ, ou le spectre de puissance $\mathcal{P}_\psi$, sont

indépendantes du temps (i.e. $\partial_\eta \psi_k = 0$). Dans ce cas, toutes les contributions peuvent être écrites de la manière suivante :

$$\overline{\langle A_i A_j \rangle} = \int_0^\infty \frac{dk}{k}\, \mathcal{P}_\psi(k)\, \mathcal{C}_{ij}(k, \eta_o, \eta_s) \quad , \tag{B.144}$$

$$\overline{\langle A_i \rangle \langle A_j \rangle} = \int_0^\infty \frac{dk}{k}\, \mathcal{P}_\psi(k)\, \mathcal{C}_i(k, \eta_o, \eta_s)\, \mathcal{C}_j(k, \eta_o, \eta_s) \quad , \tag{B.145}$$

où les $\mathcal{C}_{ij}$ et $\mathcal{C}_i$ sont appelés coefficients spectraux. Dans ces conditions, le terme de backreaction induite IBR_2, résultant du développement (B.125) de $\overline{\langle d_L \rangle}/d_L^{\mathrm{FLRW}}$, peut s'écrire comme :

$$\begin{aligned} \mathrm{IBR}_2 &= 2 \sum_{i=1}^{4} \sum_{j=1}^{5} \left[\overline{\langle A_i A_j \rangle} - \overline{\langle A_i \rangle \langle A_j \rangle} \right] \\ &= \int_0^\infty \frac{dk}{k}\, \mathcal{P}_\psi(k) \times 2 \sum_{i=1}^{4} \sum_{j=1}^{5} \left[\mathcal{C}_{ij}(k, \eta_o, \eta_s) - \mathcal{C}_i(k, \eta_o, \eta_s)\, \mathcal{C}_j(k, \eta_o, \eta_s) \right] \quad . \end{aligned} \tag{B.146}$$

La variance quant à elle, exprimée par l'Eq. (B.130), s'écrit comme :

$$\begin{aligned} \left(\mathrm{Var} \left[\frac{d_L}{d_L^{\mathrm{FLRW}}} \right] \right)^{1/2} &= \sqrt{\overline{\langle \sigma_1^2 \rangle}} = \left[\sum_{i=1}^{5} \sum_{j=1}^{5} \overline{\langle A_i A_j \rangle} \right]^{1/2} \\ &= \left[\int_0^\infty \frac{dk}{k}\, \mathcal{P}_\psi(k) \sum_{i=1}^{5} \sum_{j=1}^{5} \mathcal{C}_{ij}(k, \eta_o, \eta_s) \right]^{1/2} \quad . \end{aligned} \tag{B.147}$$

Les valeurs obtenues pour ces coefficients $\mathcal{C}_{ij}$ et $\mathcal{C}_i$ sont données en Table 5.1 et Table 5.2. Cette première table contient également la limite aux petits k ($k\Delta\eta \ll 1$) de $\mathcal{C}_{ij}$ et $\mathcal{C}_i\mathcal{C}_j$. Nous avons utilisé par simplicité la variable sans dimension $l = k\Delta\eta$.

Certains des termes nécessitent l'utilisation du facteur d'échelle. Dans ce cas nous avons supposé le cas CDM, i.e. dominé par une matière de type poussière implicant $a(\eta) = a(\eta_o)(\eta/\eta_o)^2$, et défini :

$$f_{o,s} \equiv \int_{\eta_{in}}^{\eta_{o,s}} d\eta \frac{a(\eta)}{a(\eta_{o,s})} = \frac{\eta_{o,s}^3 - \eta_{in}^3}{3\eta_{o,s}^2} \simeq \frac{1}{3}\eta_{o,s} \qquad \text{avec} \qquad \eta_{in} \ll \eta_{o,s} \quad . \tag{B.148}$$

L'utilisation du modèle CDM impose également la relation entre la durée $\Delta\eta$ et z_s à l'ordre zéro :

$$\Delta\eta = \frac{2}{a_o H_0} \left[1 - \frac{1}{\sqrt{1+z_s}} \right] \simeq \frac{z_s}{a_o H_0} \qquad \text{pour} \qquad z_s \ll 1 \quad . \tag{B.149}$$

B.5.4 Distance et flux lumineux à l'ordre 2 (complet)

Bien que le choix soit large, l'une des quantités les plus intéressantes à moyenner est le flux lumineux envoyé par différentes sources au redshift z_s le long de notre cône passé. Il se révèle aussi être la quantité qui subit le moins l'effet des inhomogénéités. Considérons donc la définition classique du flux et sa décomposition perturbative (implicant une luminosité intrinsèque L constante) :

$$\Phi = L/(4\pi d_L^2) = \Phi_0 + \Phi_1 + \Phi_2 \quad . \tag{B.150}$$

On peut moyenner ce flux sur la 2-sphère à redshift constant. On trouve :

$$\langle d_L^{-2} \rangle (z_s, w_o) = (1+z_s)^{-4} \left[\int \frac{d^2\tilde{\theta}^a}{4\pi} \sqrt{\gamma}(w_o, \tau_s(z_s, \tilde{\theta}^a), \tilde{\theta}^b) \right]^{-1} \equiv I_\phi(w_o, z_s)^{-1} (d_L^{\mathrm{FLRW}})^{-2} \quad , \tag{B.151}$$

avec $I_\phi(w_o, z_s)^{-1}$ la correction au cas homogène et dont l'inverse vaut :

$$I_\phi(w_o, z_s) \equiv \frac{\mathcal{A}(w_o, z_s)}{4\pi (d_A^{\rm FLRW})^2} = (d_A^{\rm FLRW})^{-2} \int \frac{d^2\tilde{\theta}^a}{4\pi} \sqrt{\gamma}(w_o, \tau_s(z_s, \tilde{\theta}^a), \tilde{\theta}^b) \quad , \tag{B.152}$$

$$= \frac{\mathcal{A}(w_o, z_s)}{4\pi (a(\eta_s^{(0)})\Delta\eta)^2} = \int \frac{d^2\tilde{\theta}^a}{4\pi} \sin\tilde{\theta}\,(1 + \mathcal{I}_1 + \mathcal{I}_{1,1} + \mathcal{I}_2) \quad . \tag{B.153}$$

Nous avons dans cette dernière égalité définit les corrections qui interviennent dans la moyenne du flux (différentes de celles du flux par des termes de dérivées totales angulaires) et qui regroupent respectivement des termes d'ordre $\mathcal{O}(1)$, $\mathcal{O}(1)^2$ et $\mathcal{O}(2)$ en perturbations. Ces contributions ont des expressions très compliquées qui ont été regroupées au sein des Eqs. (5.89), (5.90) et (5.91) et d'une manière plus pratique par les décompositions :

$$\mathcal{I}_1 = \sum_{i=1}^{3} \mathcal{T}_i^{(1)} \quad , \quad \mathcal{I}_{1,1} = \sum_{i=1}^{23} \mathcal{T}_i^{(1,1)} \quad , \quad \mathcal{I}_2 = \sum_{i=1}^{7} \mathcal{T}_i^{(2)} \quad , \tag{B.154}$$

et où le détail de ces 33 termes a été donné en Eqs. (5.82), (5.83) et (5.84). Nous avons aussi montré les relations :

$$\mathcal{I}_1 = 2\bar{\delta}_S^{(1)} + (\text{t. d.})^{(1)} \quad , \quad \mathcal{I}_{1,1} + \mathcal{I}_2 = 2\bar{\delta}_{\rm S}^{(2)} + (\bar{\delta}_{\rm S}^{(1)})^2 + (\text{t. d.})^{(2)} \quad , \tag{B.155}$$

où il est intéressant de constater que la dérivée totale $(\text{t. d.})^{(1)}$ est égale à $2J_2^{(1)}$ et que bien que ce terme de lentille gravitationnelle soit présent dans le flux $\Phi \propto d_L^{-2}$, il disparait totalement de sa moyenne au premier ordre. Les coefficients spectraux de chacun de ces termes présentés en Eqs. (5.81-5.84) ont été évalués en Sec. 5.3.4. Prenons la moyenne stochastique de $\langle d_L^{-2}\rangle(z_s, w_o)$, nous obtenons alors :

$$\overline{\langle d_L^{-2}\rangle}(z) = (d_L^{\rm FLRW})^{-2}\overline{(I_\Phi(z))^{-1}} \equiv (d_L^{\rm FLRW})^{-2}\,[1 + f_\Phi(z)] \quad , \tag{B.156}$$

où

$$f_\Phi(z) \equiv \overline{\langle \mathcal{I}_1\rangle^2} - \overline{\langle \mathcal{I}_{1,1} + \mathcal{I}_2\rangle} \tag{B.157}$$

est la correction au flux due aux effets des inhomogénéités par rapport au cas homogène.

On obtient la correction à la distance, sans refaire le calcul de toutes ses contributions, simplement par un développement de Taylor des quantités moyennées. En effet, la moyenne d'une fonction F d'une quantité scalaire $S = S_0 + S_1 + S_2$ peut se décomposer comme

$$\overline{\langle F(S)\rangle} = F(S_0) + F'(S_0)\overline{\langle S_1 + S_2\rangle} + F''(S_0)\overline{\langle S_1^2/2\rangle} \quad , \tag{B.158}$$

et de manière générale $\overline{\langle F(S)\rangle} \neq F(\overline{\langle S\rangle})$ du fait de l'aspect non-linéaire de la procédure de moyenne. Aussi, on a vu que $\overline{\langle S_1\rangle}$ n'était pas toujours égal à zéro, comme dans le cas des contributions de backreaction induite. En prenant $S = \Phi$ et en considérant $F(\Phi) = \Phi^{-1/2} \sim d_L$, on obtient :

$$\overline{\langle d_L\rangle}(z) = d_L^{\rm FLRW}\,[1 + f_d(z)] \quad , \tag{B.159}$$

avec f_d relié à f_Φ selon la relation importante :

$$f_d = -\frac{1}{2} f_\Phi + \frac{3}{8}\,\overline{\langle (\Phi_1/\Phi_0)^2\rangle} \quad . \tag{B.160}$$

On peut aussi montrer que $\overline{\langle (\Phi_1/\Phi_0)^2\rangle} = 4\,\overline{\langle (\bar{\delta}_S^{(1)})^2\rangle}$. Nous verrons que ce terme se révèle capital et qu'il contient à la fois un terme Doppler et un terme de lentille gravitationnelle qui dominent par rapport aux autres effets physiques. D'une manière plus générale, on montre que :

$$f_{d^\beta} = -\frac{\beta}{2} f_\phi + \frac{(2+\beta)\beta}{2}\,\overline{\left\langle (\bar{\delta}_S^{(1)})^2\right\rangle} \quad \forall \quad \beta \neq 0 \quad , \tag{B.161}$$

ce qui montre que toute puissance $\beta \neq -2$ dépend de ce dernier terme.

On peut aussi appliquer le développement de Taylor à la fonction $F(\Phi) = -2.5\log_{10}\Phi + \text{cst}$, soit le module de distance μ, on obtient alors :

$$\overline{\langle\mu\rangle} = \mu^{\text{FLRW}} - 1.25(\log_{10} e)\Big[\,2f_\Phi - \overline{\langle(\Phi_1/\Phi_0)^2\rangle}\,\Big] \quad . \tag{B.162}$$

Encore une fois, la déviation au modèle homogène est donnée par une fonction de $\overline{\langle(\bar{\delta}_S^{(1)})^2\rangle}$.

La deuxième notion intéressante que l'on peut définir est la variance d'une quantité scalaire S. On a vu en Sec. B.5.2 que deux cas sont possibles selon que l'on considère les deux moyennes (spatiale et stochastique) comme deux opérations successives ou comme une seule opération :

$$\text{Var}'[S] \equiv \overline{\Big(\langle S\rangle - \overline{\langle S\rangle}\Big)^2} = \overline{(\langle S\rangle)^2} - \Big(\overline{\langle S\rangle}\Big)^2 \quad , \quad \text{Var}[S] \equiv \overline{\Big\langle\Big(S - \overline{\langle S\rangle}\Big)^2\Big\rangle} = \overline{\langle S^2\rangle} - \Big(\overline{\langle S\rangle}\Big)^2 \quad . \tag{B.163}$$

Nous avons en fait montré, par des considérations sur les termes d'ordre $\mathcal{O}(1)^2$ (suffisantes pour la variance), que la première de ces variances est très petite devant la seconde et moins intéressante du point de vue physique. Nous choisissons donc d'utiliser cette dernière et définissons l'écart-type (ou « dispersion ») :

$$\sigma_S \equiv \sqrt{\overline{\Big\langle\Big(S - \overline{\langle S\rangle}\Big)^2\Big\rangle}} = \sqrt{\overline{\langle S^2\rangle} - \Big(\overline{\langle S\rangle}\Big)^2} \quad . \tag{B.164}$$

Appliquée au flux lumineux, cette définition de la dispersion donne :

$$\sigma_\Phi = \sqrt{\overline{\langle(\Phi/\Phi_0)^2\rangle} - \Big(\overline{\langle\Phi/\Phi_0\rangle}\Big)^2} = \sqrt{\overline{\langle(\Phi_1/\Phi_0)^2\rangle}} \quad . \tag{B.165}$$

Pour le module de distance, nous avons :

$$\sigma_\mu = \sqrt{\overline{\langle\mu^2\rangle} - \Big(\overline{\langle\mu\rangle}\Big)^2} = 2.5(\log_{10} e)\sqrt{\overline{\langle(\Phi_1/\Phi_0)^2\rangle}} \quad . \tag{B.166}$$

La quantité $\overline{\langle(\Phi_1/\Phi_0)^2\rangle}$ est positive et inférieure à 1, on peut donc s'attendre à observer une dispersion significativement plus grande que la moyenne dans les cas du flux et du module de distance.

Toutes ces contributions peuvent être écrite de manière similaire à ce qui a été présenté pour l'ordre quadratique, en Eqs. (B.144) et (B.145), i.e. sous la forme :

$$\overline{\langle X\rangle} = \int_0^\infty \frac{dk}{k}\,\mathcal{P}_\psi(k,\eta_o)\,\mathcal{C}_X(k,\eta_o,\eta_s^{(0)}) \quad , \tag{B.167}$$

$$\overline{\langle X'\rangle\langle Y'\rangle} = \int_0^\infty \frac{dk}{k}\,\mathcal{P}_\psi(k,\eta_o)\,\mathcal{C}_{X'}(k,\eta_o,\eta_s^{(0)})\,\mathcal{C}_{Y'}(k,\eta_o,\eta_s^{(0)}) \quad . \tag{B.168}$$

Ici, X' et Y' (X) sont des fonctions générales du premier (second) ordre dépendantes de (η, r, θ^a) et les $\mathcal{C}$ leurs coefficients spectraux. Cette intégration sur k est faite numériquement et un cut-off doit être choisi sur des bases physiques (bien que les intégrales soient, comme nous le verrons en Sec. B.6.1, convergentes dans l'UV et l'IR). Notons maintenant qu'une complication importante émerge lorsque l'on ne considère pas le simple cas CDM. Dans celui-ci, le spectre de puissance est factorisable selon l'ordre des équations ci-dessus et les coefficients spectraux ne dépendent pas du spectre. On utilisera d'ailleurs dans la section suivante ce cas simple pour identifier les effets physiques dominants parmi les nombreux termes évalués. Dans le cas d'un Universe ΛCDM, en revanche, le spectre de puissance apparaît aussi dans les expressions des coefficients $\mathcal{C}$ car il est directement dépendant du temps $\eta_s^{(0)}$ et donc non-factorisable. Il intervient aussi généralement au sein d'intégrales sur η qui doivent donc être déterminées numériquement. Il faut alors en général procéder à des approximations sur le spectre lui-même.

Une deuxième complication est que nous connaissons uniquement le spectre de puissance du champ gravitationnel ψ, i.e. l'ordre linéaire. Pour les termes intrinsèques à l'ordre 2, tels que ceux qui

mettent en jeu $\phi^{(2)}$ et $\psi^{(2)}$, nous n'avons pas de spectre associé. Pour remédier à cela, nous utilisons les équations développées par [104] pour relier le second ordre au premier. On a pour le cas CDM :

$$\phi^{(2)} = 2\psi^2 - 6\,\mathcal{O}^{ij}\partial_i\psi\partial_j\psi + \frac{\eta^2}{14}\,\mathcal{O}_2^{ij}\partial_i\psi\partial_j\psi \quad , \tag{B.169}$$

$$\psi^{(2)} = -2\psi^2 + 4\,\mathcal{O}^{ij}\partial_i\psi\partial_j\psi + \frac{\eta^2}{14}\,\mathcal{O}_2^{ij}\partial_i\psi\partial_j\psi \quad , \tag{B.170}$$

avec les opérateurs suivants :

$$\mathcal{O}^{ij} = \nabla^{-2}\left(\frac{\partial^i\partial^j}{\nabla^2} - \frac{1}{3}\delta^{ij}\right) \quad , \quad \mathcal{O}_2^{ij} = \frac{10}{3}\frac{\partial^i\partial^j}{\nabla^2} - \delta^{ij} \quad . \tag{B.171}$$

Il nous est alors possible de calculer tous les termes, aux approximations du spectre près, au prix d'une augmentation du nombre de termes par la conversion de ceux à l'ordre 2 intrinsèque. La conversion est encore plus compliquée dans le cas ΛCDM, cf. (5.109) et (5.110), mais encore une fois réalisable.

B.6 Résultats pour le spectre non-linéaire et un Univers ΛCDM

Nous allons ici présenter les résultats principaux de cette thèse liés à l'estimation numérique de l'effet des inhomogénéités sur les observables cosmologiques. Pour cela, nous utiliserons une expression explicite du spectre de puissance. Nous commencerons par donner l'estimation de la taille des termes quadratiques présents dans IBR_2 et $\overline{\langle\sigma_1^2\rangle}$, ceci dans le cas CDM. Nous avons déjà vu que cette dernière quantité permet une estimation complète de la variance. Nous calculerons ensuite l'effet des inhomogénéités par un calcul complet au deuxième ordre, dans un premier temps dans le cas CDM, où nous évaluerons les contributions dominantes, puis dans le cas ΛCDM. Nous traiterons d'abord le cas d'un spectre de puissance linéaire, puis celui du régime non-linéaire donné par le modèle du HaloFit.

B.6.1 Termes dominants dans CDM à l'ordre quadratique, convergence UV et IR

Fonction de transfert

Nous avons présenté en Sec. B.5.1 l'expression du spectre de puissance dans son régime linéaire. Nous nous sommes toutefois gardé de donner une expression de la fonction de transfert $T(k)$. Nous utiliserons dans le cas présent, où nous évaluons les termes d'ordre quadratique décrits en Secs. B.5.2 et B.5.3, la fonction de transfert en l'absence de contribution baryonique, dénotée par $T(k) = T_0(k)$ et simplement donnée par [68] :

$$T_0(q) = \frac{L_0}{L_0 + q^2 C_0(q)} \quad , \quad L_0(q) = \ln(2e + 1.8q) \quad , \quad C_0(q) = 14.2 + \frac{731}{1 + 62.5q} \quad , \quad q = \frac{k}{13.41 k_{\mathrm{eq}}} \quad . \tag{B.172}$$

Ici $k_{\mathrm{eq}} \simeq 0.07\,\Omega_{m0}\,h^2\mathrm{Mpc}^{-1}$ est le moment correspondant à l'échelle d'égalité matière-radiation, avec $h \equiv H_0/(100\,\mathrm{km\,s^{-1}Mpc^{-1}})$. Il est facile de voir que $T_0(k)$ tend vers 1 pour $k \ll k_{\mathrm{eq}}$ tandis qu'elle décroit comme $k^{-2}\log k$ pour $k \gg k_{\mathrm{eq}}$. Nous utiliserons les valeurs $h = 0.7$, $a_o = 1$ et $\Omega_m = 1$ dans le cas de nos estimations numériques, ici dans le modèle CDM. Dans ce cas, nous avons $k_{\mathrm{eq}} \simeq 0.036\,\mathrm{Mpc}^{-1}$ et on peut définir le régime asymptotique de la fonction de transfert comme suit : $T_0 \simeq 1$ pour $k \lesssim 10^{-3}\,\mathrm{Mpc}^{-1}$ et $T_0 \sim k^{-2}\log k$ pour $k \gtrsim 2.5\,\mathrm{Mpc}^{-1}$. Notons que cette deuxième échelle se trouve déjà profondément ancrée dans le régime non-linéaire. De plus amples détails sont donnés en Secs. A.2.4 et A.4.2.

Contributions dominantes, convergence IR et UV

Les intégrales que nous estimons sont à la fois fonction du spectre de puissance et des coefficients spectraux correspondants aux observables calculées. L'étude des termes présentés dans les Tables 5.1 et 5.2, de leur dépendance en k, nous montre que les coefficients spectraux $\mathcal{C}_{ij}$ et $\mathcal{C}_i\mathcal{C}_j$ de IBR_2 et $\overline{\langle\sigma_1^2\rangle}$ sont d'ordre $\mathcal{O}(1)$, mais que leur combinaison $\mathcal{C}_{ij} - \mathcal{C}_i\mathcal{C}_j$ est d'ordre $\mathcal{O}(k^2\Delta\eta^2)$ dans la limite

infrarouge (IR) : $k\Delta\eta \ll 1$. D'autre part le spectre de puissance est quasi constant dans cette limite ($\mathcal{P}_\psi(k) \sim k^{n_s-1} \simeq k^{-0.04}$). On a par conséquent que les termes IBR_2 et $\overline{\langle\sigma_1^2\rangle}$ donnent une contribution négligeable dans la limite IR et on peut sans crainte poser le cut-off IR de nos intégrales comme étant $k = H_0$ (i.e. en intégrant sur tous les modes sub-horizon). De plus, les coefficients $\mathcal{C}_{ij}$ et $\mathcal{C}_i\mathcal{C}_j$ n'augmentent pas plus rapidement que $\mathcal{O}(k^3\Delta\eta^3)$ dans la limite ultraviolette (UV) : $k\Delta\eta \gg 1$. Le comportement de la fonction de transfert au carré, allant comme $k^{-4}(\log k)^2$ dans cette limite, fait donc que les intégrales que nous calculons convergent aussi dans la limite UV. On comprend donc que l'essentiel de l'effet des inhomogénéités vient du domaine des moments donné par $1/\Delta\eta \ll k \leq 2.5\,\mathrm{Mpc}^{-1}$, là où la fonction de transfert ne décroit pas encore significativement. On peut en fait constater que seules deux contributions dominent sur les autres dans la Table 5.1 et que les termes $\mathcal{C}_i\mathcal{C}_j$ donnent lieu à des contributions inférieures en général à celles de $\mathcal{C}_{ij}$. Ces deux contributions dominantes sont $\mathcal{C}_{44}$ et $\mathcal{C}_{55}$. En effet, dans la limite UV, nous avons ces deux termes qui valent :

$$\mathcal{C}_{44} \simeq \left(1 - \frac{1}{\mathcal{H}_s\Delta\eta}\right)^2 \frac{(f_0^2 + f_s^2)}{\Delta\eta^2}\frac{k^2\Delta\eta^2}{3} \quad , \tag{B.173}$$

$$\mathcal{C}_{55} \simeq \frac{k^3\Delta\eta^3}{15}\mathrm{SinInt}(k\Delta\eta) \quad . \tag{B.174}$$

On comprend aussi à partir de la dépendance temporelle de ces deux expressions que $\overline{\langle A_4A_4\rangle}$ est la contribution la plus importante lorsque $z_s \ll 1$ tandis que $\overline{\langle A_5A_5\rangle}$ domine pour $z_s \gg 1$ (voir Fig. 6.1). Cette première correspond à un terme de vitesse particulière (effet Doppler) tandis que la seconde correspond à un terme de lentille gravitationnelle. Notons aussi que les intégrales calculées ici, bien que convergentes dans l'IR et dans l'UV, convergent plus rapidement dans ce premier cas de figure, du fait des puissances en k relevées ci-dessus. La contribution IBR_2, dominée par $2\overline{\langle A_4A_4\rangle}$ (et n'ayant pas $\overline{\langle A_5A_5\rangle}$), dépend donc très faiblement du cut-off k_{UV}. La contribution à la dispersion donnée par l'Eq. (B.147), dominée par $\overline{\langle A_5A_5\rangle}$ (mais ayant aussi $\overline{\langle A_4A_4\rangle}$), y est plus sensible. Nous présentons en Fig. 6.1 l'évaluation numérique de ces deux termes $\overline{\langle A_4A_4\rangle}$ et $\overline{\langle A_5A_5\rangle}$ en fonction du redshift (dans un domaine correspondant à celui des SNe Ia observées actuellement) et pour différents cutoffs ($k_{UV} = 0.1\,\mathrm{Mpc}^{-1}$ à $k_{UV} = +\infty$). On notera finalement, pour insister, le rôle primordial de la fonction de transfert dans la détermination de la taille de l'effet des inhomogénéités. L'absence de divergence qui découle aussi de cette fonction est illustrée en Fig. 6.2.

Finalement, il est possible de calculer l'effet de l'ensemble des contributions IBR_2 et $\overline{\langle\sigma_1^2\rangle}$ dans le cas CDM, i.e. en supposant qu'il n'est pas de constante cosmologique, et de comparer ce résultat de $\overline{\langle d_L\rangle} \pm d_L^{CDM}\sqrt{\overline{\langle\sigma_1^2\rangle}}$ (incluant la dispersion autour de la moyenne) avec la distance de luminosité du modèle ΛCDM. On est contraint pour cela de ne pas considérer la contribution $\overline{\langle\sigma_2\rangle}$ dans cette expression de $\overline{\langle d_L\rangle}$ (cf. Eq. (B.126)), i.e. que nous prenons $\overline{\langle d_L\rangle} = d_L^{CDM}(1 + \mathrm{IBR}_2)$. La contribution manquante ne peut être calculée que par un calcul complet au second ordre, ce qui sera effectué par la suite. Nous avons établi cette comparaison du cas homogène et du cas CDM avec perturbations en traçant le module de distance $\mu(\overline{\langle d_L\rangle}) \equiv m - M = 5\log_{10}(\overline{\langle d_L\rangle})$ auquel a été soustrait le module de distance de l'Univers de Milne dans lequel l'expansion est linéaire (cf. Appendice A.6) :

$$\Delta(m - M) \equiv \mu(\overline{\langle d_L\rangle}) - \mu^M = 5\log_{10}\left[\overline{\langle d_L\rangle}\right] - 5\log_{10}\left[\frac{(2 + z_s)z_s}{2H_0}\right] \quad . \tag{B.175}$$

Notons que la manière rigoureuse d'évaluer cet effet est de prendre la moyenne du module de distance, i.e. $\overline{\langle\mu\rangle}$, et non $5\log_{10}(\overline{\langle d_L\rangle})$. C'est ce que nous ferons en Sec. B.6.3, en nous basant sur les Eqs. (B.162) et (B.166). Les résultats de ce tracé sont présentés en Fig. 6.3 pour des cut-offs de $k_{UV} = 0.1\,\mathrm{Mpc}^{-1}$ et $k_{UV} = 1\,\mathrm{Mpc}^{-1}$. Ils sont à comparer avec les tracés de l'Univers ΛCDM pour $\Omega_\Lambda = 0.1$ et $\Omega_\Lambda = 0.73$. L'utilisation d'un cut-off plus grand aurait pour effet d'augmenter légèrement le résultat final, toutefois, le spectre de puissance adéquat à ces échelles entre dans son régime non-linéaire et ne saurait être celui utilisé jusqu'à présent.

Conclusions sur IBR$_2$ et $\overline{\langle\sigma_1^2\rangle}$

Il apparaît clairement sur la Fig. 6.3 que les corrections induites par IBR$_2$ sur la distance de luminosité dans le cas d'un modèle homogène CDM ne peuvent simuler le phénomène que nous nommons énergie sombre, ceci même lorsque l'on prend en compte la dispersion autour de la moyenne $\overline{\langle d_L\rangle}$. On voit dans ces figures que l'utilisation d'un cut-off de $1\,\mathrm{Mpc}^{-1}$ impose une dispersion assez grande pour expliquer une constante cosmologique de paramètre $\Omega_\Lambda \sim 0.1$ comme une fluctuation statistique. Cependant même ce résultat, si on le veut utile pour expliquer une partie de la constante cosmologique que l'on observe aujourd'hui, doit être réinterprété dans le cadre d'un calcul au sein d'un modèle ΛCDM ayant une part d'énergie sombre. C'est ce que nous ferons en Sec. B.6.3 et B.6.4.

Il y a donc différentes raisons pour effectuer ce calcul de manière complète au second ordre en perturbations. Premièrement, et comme déjà mentionné, un calcul définitif de l'effet des inhomogénéités se doit d'inclure $\overline{\langle\sigma_2\rangle}$. A priori, cette contribution peut contenir des termes similaires à ceux de la dispersion, entre autre un terme de lentille $\overline{\langle A_5 A_5\rangle}$. Dans ce cas, la moyenne $\overline{\langle d_L\rangle}$ serait significativement affectée, en particulier aux grand redshifts. Nous verrons que ce terme n'apparaît pas dans $\overline{\langle\sigma_2\rangle}$, par une annulation quasi-miraculeuse qui est en fait liée à la conservation du flux lumineux. Ensuite, il est certain que l'effet des inhomogénéités est renforcé par la considération du spectre de puissance dans son régime non-linéaire qui autorise une intégration allant à des cut-offs plus grands que $1\,\mathrm{Mpc}^{-1}$. Enfin, la détermination la plus précise possible de l'effet des inhomogénéités a une conséquence très importante pour les observations futures. En effet, cette estimation précise peut être comparée aux relevés observationels et constituer une signature des inhomogénéités qui ne saurait être confondue avec une dépendance spatiotemporelle de l'énergie sombre. Ce calcul est donc nécessaire également pour pouvoir enveler la contribution, même faible, des inhomogénéités dans les données.

Remarquons enfin que certaines combinaisons de puissances de d_L ne dépendent pas de $\overline{\langle\sigma_2\rangle}$ mais seulement de $\overline{\langle\sigma_1^2\rangle}$. C'est le cas des combinaisons suivantes :

$$\overline{\left\langle \left(d_L/d_L^{\mathrm{FLRW}}\right)^\alpha\right\rangle} - \alpha\overline{\left\langle d_L/d_L^{\mathrm{FLRW}}\right\rangle} = 1-\alpha+\frac{\alpha(\alpha-1)}{2}\,\overline{\langle\sigma_1^2\rangle} \qquad \forall\,\alpha\in\mathbb{R}\ . \tag{B.176}$$

On peut tracer cette quantité pour un modèle inhomogène donné et différentes valeurs de α et comparer ces courbes à leurs équivalentes dans le cas d'un modèle ΛCDM, de manière potentiellement discriminante pour ce dernier. Néanmoins, nous ne mesurons en pratique que le flux des SNe Ia et il n'est pas exclu que les deux modèles (inhomogène et ΛCDM) donnent le même résultat pour cette observable particulière.

B.6.2 Calcul complet dans CDM

Nous allons ici évaluer numériquement les moyennes de $\mathcal{I}_1$, $\mathcal{I}_{1,1}$ et $\mathcal{I}_2$ dans le cas du modèle CDM. Nous étudierons les termes dominants, retrouvant entre autres ceux déjà présentés pour IBR$_2$ et $\overline{\langle\sigma_1^2\rangle}$, qui nous seront utiles pour le calcul plus général (et plus complexe) dans le cas d'un modèle ΛCDM.

Les contributions $\overline{\langle\mathcal{I}_1\rangle^2}$ et $\overline{\langle\mathcal{I}_{1,1}\rangle}$

Nous calculons ici ces deux termes qui contribuent à l'expression de la correction du flux présentée en Eq. (B.157). On commence par $\overline{\langle\mathcal{I}_1\rangle^2}$ qui, par les Eqs. (5.81) et (5.82), vaut :

$$\overline{\langle\mathcal{I}_1\rangle^2} = \sum_{i=1}^{3}\sum_{j=1}^{3}\overline{\left\langle\mathcal{T}_i^{(1)}\right\rangle\left\langle\mathcal{T}_j^{(1)}\right\rangle} = \int_0^\infty \frac{dk}{k}\,\mathcal{P}_\psi(k,\eta_o)\,\sum_{i=1}^{3}\sum_{j=1}^{3}\mathcal{C}_{\mathcal{T}_i^{(1)}}(k,\eta_o,\eta_s)\,\mathcal{C}_{\mathcal{T}_j^{(1)}}(k,\eta_o,\eta_s)\ , \tag{B.177}$$

où nous substituons dès lors η_s à $\eta_s^{(0)}$. Encore une fois, le cas CDM impose que $\partial_\eta\psi_k = 0$ et $a(\eta) = a(\eta_o)(\eta/\eta_o)^2$. On peut aussi définir (avec $\eta_{in} \ll \eta_{o,s}$) :

$$f_{o,s} \equiv \int_{\eta_{in}}^{\eta_{o,s}} d\eta\,\frac{a(\eta)}{a(\eta_{o,s})} = \frac{\eta_{o,s}^3-\eta_{in}^3}{3\eta_{o,s}^2} \simeq \frac{1}{3}\eta_{o,s}\ . \tag{B.178}$$

Les coefficients de l'Eq. (B.177) peuvent ainsi être calculés et leurs résultats sont présentés en Table 6.1, qui est équivalent (dans ces nouvelles notations) à la Table 5.2.

De la même manière, on estime les contributions à $\overline{\langle \mathcal{I}_{1,1} \rangle}$ par :

$$\overline{\langle \mathcal{I}_{1,1} \rangle} = \int_0^\infty \frac{dk}{k} \, \mathcal{P}_\psi(k, \eta_o) \, \sum_{i=1}^{23} \mathcal{C}_{\mathcal{T}_i^{(1,1)}}(k, \eta_o, \eta_s) \quad , \tag{B.179}$$

avec les formes explicites des coefficients $\mathcal{C}(\mathcal{T}_i^{(1,1)})$ pour le cas CDM qui sont présentées en Sec. 5.3.4.

En rassemblant les contributions de $\overline{\langle \mathcal{I}_1 \rangle^2}$ et $\overline{\langle \mathcal{I}_{1,1} \rangle}$ selon l'expression (B.157), il apparaît que les termes dominants appartiennent à $\overline{\langle \mathcal{I}_{1,1} \rangle}$ et non $\overline{\langle \mathcal{I}_1 \rangle^2}$. Il sont caractérisés par la dépendance en k^2 de leurs coefficients spectraux et se révèlent être les $\mathcal{T}_i^{(1,1)}$ tels que $\{i = 2, 4, 5, 7, 8, 12, 14, 18, 20\}$ (cf. les termes encadrés en Sec. 5.3.4). En ne retenant que ces contributions, soit l'ordre dominant (*Leading order*), on trouve :

$$\begin{aligned} \left[\sum_{i=1}^{23} \mathcal{C}_{\mathcal{T}_i^{(1,1)}} \right]_{\text{Lead}} &= \aleph_s \frac{f_s^2 + f_o^2}{3} k^2 + \frac{2(\Xi_s - 3)}{\mathcal{H}_s} \frac{f_s}{3} k^2 + \Xi_s \frac{f_s^2}{3} k^2 - \Xi_s \frac{f_o^2}{3} k^2 \\ &= f_o^2 k^2 \left(\frac{\aleph_s}{3} - \frac{\Xi_s}{3} \right) + f_s^2 k^2 \left(\frac{\aleph_s}{3} + \frac{4\Xi_s}{3} - 3 \right) \quad = \quad - \frac{k^2}{\mathcal{H}_0^2} \, \widetilde{f}_{1,1}(z) \quad , \end{aligned} \tag{B.180}$$

où nous avons défini :

$$\aleph_s \equiv \Xi_s^2 - \frac{1}{\mathcal{H}_s \Delta\eta} \left(1 - \frac{\mathcal{H}_s'}{\mathcal{H}_s^2} \right) \quad , \tag{B.181}$$

et utilisé $\mathcal{H}_s \simeq 2/(3 f_s)$ (valide pour le modèle CDM). La fonction $\widetilde{f}_{1,1}(z)$ contient toute la dépendance en z de ces contributions et vaut :

$$\widetilde{f}_{1,1}(z) = \frac{10 - 12\sqrt{1+z} + 5z \left(2 + \sqrt{1+z} \right)}{27 \, (1+z) \left(-1 + \sqrt{1+z} \right)^2} \quad . \tag{B.182}$$

Elle change de signe pour une valeur $z^* = 0.205$, comme présenté en Fig. 6.4 et visible en Fig. 6.5.

La contribution intrinsèque au second ordre : $\overline{\langle \mathcal{I}_2 \rangle}$

Le calcul de $f_\Phi(z)$ est complet une fois la quantité $\overline{\langle \mathcal{I}_2 \rangle}$ évaluée. Pour cela, il nous faut estimer les coefficients $\mathcal{C}(\mathcal{T}_i^{(2)})$ définis en terme des potentiels de Bardeen dans l'Eq. (5.84). Les résultats de la Sec. 5.3.5, en particulier les Eqs. (5.109) et (5.110) montrent que les seules contributions en k^2 contenues dans ces termes $\mathcal{C}(\mathcal{T}_i^{(2)})$ sont celles venant des termes $B_3(\eta) \nabla^{-2} \partial_i \partial^j (\partial^i \psi_o \partial_j \psi_o)$ et $B_4(\eta) \partial^i \psi_o \partial_i \psi_o$. Par conséquent, nous avons que $\phi^{(2)} \simeq \psi^{(2)}$ à l'ordre dominant. Dans le cas CDM considéré ici, nous avons $l(\eta) = 1$ et $B_1(\eta) = B_2(\eta) = 0$ (cf. Eqs. (5.112) et (5.113)). De plus, les modèles d'inflation usuels nous encouragent à poser $a_{nl} = 1$ (absence de non-Gaussiannités). Les Eqs. (5.109) et (5.110) se réduisent alors à :

$$\psi^{(2)} = -2\psi_o^2 - \frac{4}{3} \, \mathcal{O}^{ij} \partial_i \psi_o \partial_j \psi_o + B_3(\eta) \, \mathcal{O}_3^{ij} \partial_i \psi_o \partial_j \psi_o + B_4(\eta) \, \mathcal{O}_4^{ij} \partial_i \psi_o \partial_j \psi_o \quad , \tag{B.183}$$

$$\phi^{(2)} = 2\psi_o^2 + 2 \, \mathcal{O}^{ij} \partial_i \psi_o \partial_j \psi_o + B_3(\eta) \, \mathcal{O}_3^{ij} \partial_i \psi_o \partial_j \psi_o + B_4(\eta) \, \mathcal{O}_4^{ij} \partial_i \psi_o \partial_j \psi_o \quad , \tag{B.184}$$

et nous utilisons $a(\eta) = a(\eta_o) \, (\eta/\eta_o)^2$ pour obtenir de l'Eq. (5.114) :

$$B_3(\eta) = \frac{20}{21} \frac{1}{\mathcal{H}^2} \quad , \quad B_4(\eta) = -\frac{2}{7} \frac{1}{\mathcal{H}^2} \quad . \tag{B.185}$$

On peut calculer alors les termes du second ordre tels que ceux présentés en Eqs. (5.120), (5.122) et (5.123) et voir que les termes $\mathcal{C}(\mathcal{T}_1^{(2)})$ et $\mathcal{C}(\mathcal{T}_2^{(2)})$ s'annulent. Les contributions $\mathcal{C}(\mathcal{T}_3^{(2)})$ et $\mathcal{C}(\mathcal{T}_4^{(2)})$ sont

quant à elles nulles par symétrie sphérique de notre intégration. La contribution $\mathcal{T}_5^{(2)}$ ne s'annule pas du fait d'une dérivée ∂_η agissant sur les coefficients $B_A(\eta)$:

$$\mathcal{C}(\mathcal{T}_5^{(2)}) = \frac{\Xi_s}{126}(\eta_s^2 - \eta_o^2)k^2 \quad . \tag{B.186}$$

Enfin les deux termes $\mathcal{C}(\mathcal{T}_6^{(2)})$ et $\mathcal{C}(\mathcal{T}_7^{(2)})$ valent :

$$\begin{aligned}
\mathcal{C}(\mathcal{T}_6^{(2)}) &= -2 - \frac{k^2\eta_s^2}{126} + \frac{32k}{45}\frac{\psi_k\partial_k\psi_k^*}{|\psi_k|^2} + \frac{8k^2}{45}\frac{\psi_k\partial_k^2\psi_k^*}{|\psi_k|^2} \quad , \\
\mathcal{C}(\mathcal{T}_7^{(2)}) &= \frac{\eta_o^3 - \eta_s^3}{189\Delta\eta}k^2 + \frac{16k}{45}\frac{\psi_k\partial_k\psi_k^*}{|\psi_k|^2} + \frac{4k^2}{45}\frac{\psi_k\partial_k^2\psi_k^*}{|\psi_k|^2} \quad .
\end{aligned} \tag{B.187}$$

La somme de toute ces contributions donne enfin :

$$\sum_{i=1}^{7}\mathcal{C}(\mathcal{T}_i^{(2)}) = -2 + \frac{1}{7}\left[\frac{\Xi_s}{2}(f_s^2 - f_o^2) - \frac{f_s^2}{2} - \frac{f_s^3 - f_o^3}{\Delta\eta}\right]k^2 + \frac{16k}{15}\frac{\psi_k\partial_k\psi_k^*}{|\psi_k|^2} + \frac{4k^2}{15}\frac{\psi_k\partial_k^2\psi_k^*}{|\psi_k|^2} \quad , \tag{B.188}$$

et sa contribution dominante peut s'écrire comme :

$$\left[\sum_{i=1}^{7}\mathcal{C}(\mathcal{T}_i^{(2)})\right]_{\text{Lead}} = \frac{1}{7}\left[\frac{\Xi_s}{2}(f_s^2 - f_o^2) - \frac{f_s^2}{2} - \frac{f_s^3 - f_o^3}{\Delta\eta}\right]k^2 = -\frac{k^2}{\mathcal{H}_o^2}\widetilde{f}_2(z) \quad , \tag{B.189}$$

avec :

$$\widetilde{f}_2(z) = -\frac{1}{189}\frac{2 - 2\sqrt{1+z} + z\left(9 - 2\sqrt{1+z}\right)}{(1+z)(\sqrt{1+z} - 1)} \quad . \tag{B.190}$$

Le point intéressant ici est que cette contribution $\overline{\langle\mathcal{I}_2\rangle}$ est d'un ordre de grandeur inférieure aux contributions décrites pour $\overline{\langle\mathcal{I}_{1,1}\rangle}$, pour des redshifts $z \sim 0.1 - 2$, et ce à cause d'une annulation partielle des termes présents. Ce fait est apparent lorsque l'on compare $\widetilde{f}_{1,1}$ et $\widetilde{f}_2$, comme en Fig. 6.4. Ceci répond donc à la question de la taille relative du terme $\overline{\langle\sigma_2\rangle}$ par rapport au terme de backreaction induite IBR_2 qui avait été soulevée à partir de la transformation au premier ordre en perturbations.

Résultat complet dans le modèle CDM

Nous avons donc trouvé la contribution totale à la correction du flux lumineux (cf. Eq. (B.157)) :

$$f_\Phi(z) = \int_0^\infty \frac{dk}{k}\mathcal{P}_\psi(k, z=0)\Big[f_{1,1}(k,z) + f_2(k,z)\Big] \quad , \tag{B.191}$$

avec $f_{1,1}$ et f_2 des fonctions compliquées mais connues analytiquement dans le modèle CDM. Nous avons aussi remarqué que les contributions majeures à ces termes sont du type $f(k,z) \sim (k/\mathcal{H}_o)^2\widetilde{f}(z)$, permettant d'écrire avec une très bonne approximation que :

$$f_\Phi(z) \simeq \left[\widetilde{f}_{1,1}(z) + \widetilde{f}_2(z)\right]\int_0^\infty \frac{dk}{k}\left(\frac{k}{\mathcal{H}_o}\right)^2\mathcal{P}_\psi(k, z=0) \quad , \tag{B.192}$$

avec $\widetilde{f}_{1,1}(z)$ et $\widetilde{f}_2(z)$ donnés par les Eqs. (B.182) et (B.190). Les résultats obtenus, en prenant les bornes d'intégrations similaires à celles décrites dans les sections précédentes, sont présentés en Fig. 6.5. On y voit la très bonne approximation due aux termes dominants de l'Eq. (B.192). On voit aussi que le flux ne reçoit pas de correction importante aux grands redshifts, du fait de l'absence de terme de lentille gravitationnelle (l'origine de ceci étant liée à la conservation du flux lumineux le long du cône de lumière). Notons aussi que cette correction a une dépendance en z caractéristique et n'a pas le bon signe aux larges redshifts pour simuler une composante, même petite, d'énergie sombre.

B.6.3 Le cas ΛCDM avec spectre linéaire

Nous généraliserons ici les résultats présentés dans la section précédente au cas du modèle de concordance en cosmologie, i.e. le modèle ΛCDM, et ce en utilisant le spectre de puissance dans son régime linaire. Nous changerons néanmoins l'expression de la fonction de transfert pour la remplacer par une expression plus réaliste. La Sec. 6.3.2 suivante utilisera quant à elle le spectre dans son régime non-linéaire. Nous nous attacherons à ne considérer que les termes dominants d'ordre k^2 et k^3 déjà identifiés dans la section précédente. Nous considérerons aussi les cas de la distance de luminosité et du module de distance. Nous utiliserons dans la suite les valeurs numériques suivantes : $\Omega_{\Lambda 0} = 0.73$, $\Omega_{m0} = 0.27$, $\Omega_{b0} = 0.046$, $h = 0.7$.

Corrections du flux au second ordre

Dans le cas d'un modèle ΛCDM, le spectre de puissance dépend du temps et peut s'écrire dans son régime linéaire comme :

$$\mathcal{P}_\psi(k,\eta) = \left[\frac{g(\eta)}{g(\eta_o)}\right]^2 \mathcal{P}_\psi(k,\eta=\eta_o) \quad , \tag{B.193}$$

où nous avons utilisé le *growth factor* $g(\eta)$ pour décrire l'évolution temporelle des perturbations du champ gravitationnel.

Il nous est donc possible à partir de ce nouveau spectre d'évaluer les contributions dominantes du flux déjà décrites dans les sections précédentes pour le calcul de $\overline{\langle \mathcal{I}_{1,1}\rangle}$. Les contributions dominantes à la correction du flux I_ϕ, du type k^2, sont issues des termes rappelés en Eq. (6.27). Notons que pour la plupart de ces contributions – $\mathcal{T}^{(1,1)}_{2,L}$, $\mathcal{T}^{(1,1)}_{4,L}$, $\mathcal{T}^{(1,1)}_{5,L}$, $\mathcal{T}^{(1,1)}_{7,L}$, $\mathcal{T}^{(1,1)}_{12,L}$, $\mathcal{T}^{(1,1)}_{14,L}$ et $\mathcal{T}^{(1,1)}_{20,L}$ – la dépendance temporelle peut être factorisée car elle n'apparaît pas dans les facteurs exponentiels $\exp(i\,\mathbf{k}\cdot\mathbf{x})$ (cf. e.g. Eq. (5.60)). C'est le cas des contributions qui dépendent de l'intégrale $P(\eta, r, \widetilde{\theta}^a)$. On évalue donc aisément ces contributions en (i) insérant un facteur $g(\eta_s)/g(\eta_o)$ pour chaque terme ψ_s présent, et (ii) en remplaçant les facteurs $f_{o,s}$ par :

$$\widetilde{f}_{o,s} \equiv \int_{\eta_{in}}^{\eta_{o,s}} d\eta \frac{a(\eta)}{a(\eta_{o,s})}\frac{g(\eta)}{g(\eta_o)} \quad . \tag{B.194}$$

Pour les deux termes dominants qui restent, à savoir $\mathcal{T}^{(1,1)}_{8,L}$ et $\mathcal{T}^{(1,1)}_{18,L}$, nous effectuons les intégrales le long du chemin $r = \eta_o - \eta$ et la dépendance temporelle ne peut être factorisée. Il faut donc calculer les intégrales selon η et k numériquement. Toutefois, on peut approximer ces termes en remplaçant $\psi(\eta', \eta_o - \eta', \tilde{\theta}^a)$ par $\psi(\eta_s, \eta_o - \eta', \tilde{\theta}^a)$ du fait que la composante principale de ces intégrales émerge à partir de temps proches de η_s. On obtient ainsi :

$$\mathcal{C}(\mathcal{T}^{(1,1)}_{8,L}) = \frac{2}{3}\Xi_s \frac{\widetilde{f}_s}{\mathcal{H}_s} k^2 \quad , \quad \mathcal{C}(\mathcal{T}^{(1,1)}_{18,L}) = -\frac{4}{3}\frac{\widetilde{f}_s}{\mathcal{H}_s} k^2 \quad , \tag{B.195}$$

identique à celui établi dans le cas CDM mais avec f_s remplacé par $\widetilde{f}_s$.

Les contributions à $\overline{\langle \mathcal{I}_2\rangle}$ doivent aussi être estimées dans le cas ΛCDM. On se limite encore une fois aux opérateurs $\mathcal{O}^{ij}_3$ et $\mathcal{O}^{ij}_4$ donnés en Eqs. (5.109), (5.110) et (5.111). On trouve que les contributions $\mathcal{T}^{(2)}_1$ et $\mathcal{T}^{(2)}_2$ donnent un effet négligeable et que les termes $\mathcal{T}^{(2)}_3$ et $\mathcal{T}^{(2)}_4$ s'annulent comme avant (par symétrie). On obtient les trois contributions restantes par l'utilisation des Eqs. (5.122) et (5.123) :

$$\mathcal{C}(\mathcal{T}^{(2)}_{5,L}) = -\Xi_s\left[\frac{1}{3}\left(B_3(\eta_o) - B_3(\eta_s)\right) + \left(B_4(\eta_o) - B_4(\eta_s)\right)\right] k^2 \quad , \tag{B.196}$$

$$\mathcal{C}(\mathcal{T}^{(2)}_{6,L}) = -\left(\frac{1}{3}B_3(\eta_s) + B_4(\eta_s)\right) k^2 \quad , \tag{B.197}$$

$$\mathcal{C}(\mathcal{T}^{(2)}_{7,L}) = \frac{2}{\Delta\eta}\int_{\eta_s}^{\eta_o} d\eta' \left(\frac{1}{3}B_3(\eta') + B_4(\eta')\right) k^2 \quad . \tag{B.198}$$

Ces contributions sont évaluées alors en utilisant les Eqs. (5.114) et (5.115) et en changeant la variable η au profit du redshift, avec :

$$\mathcal{H}(z) = \frac{\mathcal{H}_0}{1+z}\left[\Omega_{m0}(1+z)^3 + \Omega_{\Lambda 0}\right]^{1/2} \quad , \tag{B.199}$$

$$\Omega_m(z) = \frac{\Omega_{m0}(1+z)^3}{\Omega_{m0}(1+z)^3 + \Omega_{\Lambda 0}} \quad , \quad \Omega_\Lambda(z) = \frac{\Omega_{\Lambda 0}}{\Omega_{m0}(1+z)^3 + \Omega_{\Lambda 0}} \quad , \tag{B.200}$$

On trouve, comme dans le cas CDM, que ces contributions intrinsèques au deuxième ordre sont d'un ou deux ordres de grandeur inférieures aux termes quadratiques de $\overline{\langle \mathcal{I}_{1,1} \rangle}$.

Commentons enfin sur le spectre de puissance. Dans le cas ΛCDM, le spectre s'écrit d'après l'Eq. (B.193) comme :

$$\mathcal{P}_\psi(k,z) = \left(\frac{3}{5}\right)^2 \Delta^2_{\mathcal{R}} T^2(k) \left(\frac{g(z)}{g_\infty}\right)^2 \quad , \tag{B.201}$$

où nous avons inclus la dépendance temporelle des perturbations gravitationnelles. Il faut aussi noter que l'échelle d'équilibre entre la période de radiation et celle de matière est réduite (ceci à cause de la diminution de Ω_{m0} lors du passage de CDM à ΛCDM). Cet effet de la réduction de puissance dans le cas ΛCDM est illustré en Fig. 6.6. On remarque dans cette figure que la fonction de transfert $T(k) = T_0(k)$ (en trait tireté) déjà présentée ne dépend pas d'une composante baryonique de matière. Le cas où cette composante baryonique est présente est représenté en trait plein. On constate que le manque de considération de la fraction baryonique de Ω_{m0} entraine une surestimation de la puissance du spectre de près de 40% dans le domaine $k \gtrsim 0.01\, h\,\mathrm{Mpc}^{-1}$, et ce du fait de l'effet de *Silk damping* (cf. [68]). Nous considérons donc cet effet en remplaçant la valeur de q précédemment utilisée, $q = k/(13.41\, k_{\mathrm{eq}})$, par [68] :

$$q = \frac{k \times \mathrm{Mpc}}{h\Gamma} \quad , \tag{B.202}$$

$$\Gamma = \Omega_{m0} h \left(\alpha_\Gamma + \frac{1-\alpha_\Gamma}{1+(0.43ks)^4}\right) \quad , \tag{B.203}$$

$$\alpha_\Gamma = 1 - 0.328 \ln(431\Omega_{m0}h^2)\frac{\Omega_{b0}}{\Omega_{m0}} + 0.38\ln(22.3\Omega_{m0}h^2)\left(\frac{\Omega_{b0}}{\Omega_{m0}}\right)^2 \quad , \tag{B.204}$$

$$s = \frac{44.5\ln(9.83/\Omega_{m0}h^2)}{\sqrt{1+10(\Omega_{b0}h^2)^{3/4}}}\,\mathrm{Mpc} \quad . \tag{B.205}$$

Ω_{b0} est le paramètre de densité baryonique, s l'horizon du son (*sound horizon*) et Γ le paramètre de forme effectif (*effective shape parameter*) qui dépend de k. L'effet des oscillations acoustiques de baryons (BAO) se révèle négligeable pour nos calculs. En effet, celui-ci a pour effet de superposer au spectre de puissance une oscillation qui est quasiment annulée par notre intégration sur k.

Les résultats de l'intégration des termes dominants contribuants à la correction du flux lumineux sont présentés en Fig. 6.7. On voit que l'effet obtenu pour $|f_\Phi|$ est inférieur à celui qui avait été obtenu en Fig. 6.5. Les raisons à cela sont la présence du *growth factor* dans le spectre, le changement d'expression de la fonction de transfert et la diminution du moment k_{eq}. Le flux, en tant que quantité minimalement affectée par les inhomogénéités, apparaît donc comme la grandeur la plus adaptée pour extraire des informations sur les paramètres cosmologiques. Ce n'est pas le cas de la distance d_L ou du module de distance μ que nous allons décrire maintenant.

Correction aux autres observables et dispersions

Considérons les autres observables que le flux et qui ont été présentées en Sec. B.5.4, à savoir la distance d_L et le module μ. Les corrections à ces deux grandeurs diffèrent de celle du flux f_Φ par des fonctions de la moyenne de $(\Phi_1/\Phi_0)^2$. En prenant $d_L = d_L^{(0)} + d_L^{(1)} + d_L^{(2)}$ et en tenant compte des explications données en Sec. B.4.1 et B.4.2, nous pouvons montrer que :

$$\frac{\Phi_1}{\Phi_0} = -2\frac{d_L^{(1)}}{d_L^{(0)}} = -\mathcal{I}_1 + (\mathrm{t.d.})^{(1)} = 2\left(-\Xi_s J + \frac{Q_s}{\Delta\eta} + \psi_s + J_2^{(1)}\right) \quad . \tag{B.206}$$

Nous avons aussi montré que la contribution principale (*Leading contribution*) à la moyenne de ce terme, dans le cas CDM, est donnée par :

$$\overline{\left\langle \left(\frac{\Phi_1}{\Phi_0}\right)^2 \right\rangle}_L = 4\left\{ \overline{\left\langle \left(J_2^{(1)}\right)^2 \right\rangle} + \Xi_s^2 \left[\overline{\langle ([\partial_r P]_s)^2 \rangle} + \overline{\langle ([\partial_r P]_o)^2 \rangle} \right] \right\} \quad . \tag{B.207}$$

Nous avons déjà vu que les termes faisant intervenir $\partial_r P$ étaient des termes de vitesse particulière et qu'ils peuvent être calculés dans le modèle ΛCDM sans approximation. Leur intégrandes sont du type $k^2\mathcal{P}_\psi(k,\eta_o)$. Le premier terme de ce résultat, le terme de lentille gravitationnelle (du type $k^3\mathcal{P}_\psi(k,\eta_o)$), est en revanche plus difficile à évaluer. Il est en effet nécessaire de remplacer $\psi(\eta',\eta_o-\eta',\tilde{\theta}^a)$ par $\psi(\eta_s,\eta_o-\eta',\tilde{\theta}^a)$ dans ce dernier terme. On obtient au final le coefficient spectral dominant :

$$\mathcal{C}((\Phi_1/\Phi_0)_L^2) \simeq \frac{4}{3}\Xi_s^2\left(\tilde{f}_s^2+\tilde{f}_o^2\right)k^2 + \frac{4}{15}\left[\frac{g(\eta_s)}{g(\eta_o)}\right]^2 \Delta\eta^3 k^3\,\mathrm{SinInt}(k\Delta\eta) \quad . \tag{B.208}$$

Du fait de l'existence de ce terme dans μ et d_L et son abscence dans Φ (le terme de lentille, du moins), on peut s'attendre à avoir une correction plus grande pour ces quantités que pour le flux. C'est en effet ce que l'on observe en Fig. 6.7 où est présentée la contribution f_d et où il apparaît clairement que $|f_\Phi| \ll f_d$ aux larges redshifts. Nous constatons donc encore une fois que l'effet des inhomogénéités est dominé par les vitesses particulières aux petits redshifts et dominé par les effets de lentille aux grands redshifts. Mais là ou le flux n'est pas affecté dans ce dernier cas, la distance l'est significativement.

En applicant ce même résultat au module de distance $\overline{\langle\mu\rangle} - \mu^M = \overline{\langle\mu\rangle} - 5\log_{10}[(2+z)z/(2H_0)]$, nous estimons directement l'effet des inhomogénéités de matière sur le diagramme de Hubble, à la fois sur la moyenne (cf. Eq. (B.162)) et sur la dispersion (cf. Eq. (B.166)). Nous présentons en Fig. 6.8 le résultat de cette estimation de $\overline{\langle\mu\rangle} - \mu^M$ et sa dispersion, pour $\Omega_{\Lambda 0} = 0.73$, et le comparons aux résultats homogènes pour différentes valeurs de $\Omega_{\Lambda 0}$. Nous trouvons que la moyenne de μ n'est modifiée par l'effet des inhomogénéités, avec le spectre linéaire, qu'à la troisième décimale. Nous pouvons aussi constater sur la Fig. 6.8 que la dispersion du module de distance, aux larges redshifts, est comparable à une erreur de 2% sur le paramètre d'énergie sombre $\Omega_{\Lambda 0}$. Nous allons voir dans la section suivante comment ces faits sont modifiés dans le cas de l'utilisation d'un spectre non-linéaire.

B.6.4 Le cas ΛCDM avec spectre non-linéaire

Spectre de puissance

Nous avons pu voir que le calcul de la moyenne ou de la dispersion se résument, modulo quelque approximations, au calcul d'une intégrale sur les moments k des perturbations de matière. Cette intégrale sur $[0,\infty[$ doit être restreinte, pour des raisons physiques, en remplaçant 0 par $\sim H_0$ (aucun mode ayant une longueur d'onde plus grande que l'horizon H_0^{-1} de l'Univers observable) et ∞ par un cut-off n'exédant pas le moment où la description du spectre devient inappropriée. Pour le spectre linéaire (cf. Eq. (B.116)) ce cut-off correspond à une échelle de l'ordre de 1 Mpc^{-1}. Si on veut utiliser des échelles plus petites, il nous faut considérer l'aspect non-linéaire de la distribution de matière.

Le modèle effectif le plus simple pour décrire le régime non-linéaire est celui du HaloFit (voir [23] et plus récemment [74]). Pour le comprendre, il faut définir le spectre (sans dimension) de la densité de matière :

$$\Delta^2(k) = \frac{k^3}{2\pi^2}|\delta_k|^2 \quad , \tag{B.209}$$

et utiliser l'équation de Poisson dans un Univers de type ΛCDM :

$$\nabla^2\psi(x) = 4\pi G\rho(t)\,\delta(x) \quad \Rightarrow \quad \mathcal{P}_\psi^{\mathrm{L,NL}}(k) = \frac{9}{4}\frac{\Omega_{m0}^2\mathcal{H}_0^4}{(1+z)^{-2}k^4}\,\Delta^2_{\mathrm{L,NL}}(k) \quad . \tag{B.210}$$

Cette dernière relation est valide dans les deux régimes. Ceci nous permet d'écrire le spectre de la densité de matière en fonction de celui du champ gravitationnel dans le régime linéaire :

$$\Delta^2_{\mathrm{L}}(k) = \frac{4}{25}\frac{A\Omega_{m0}^{-2}\mathcal{H}_0^{-4}}{(1+z)^2}\,\frac{k^{n_s+3}}{k_0^{n_s-1}}\left(\frac{g(z)}{g_0}\right)^2 T^2(k) \quad . \tag{B.211}$$

Le modèle du HaloFit, basé sur les résultats de simulations à N-corps, donne alors l'expression du spectre de la matière dans le régime non-linéaire. Cette expression est une paramétrisation effective, somme d'un terme représentant la corrélation entre deux halos séparés et d'un autre représentant la matière à l'intérieur d'un halo donné :

$$\Delta^2_{\rm NL}(k) = \Delta^2_{\rm Q}(k) + \Delta^2_{\rm H}(k) \quad , \tag{B.212}$$

$$\text{avec} \quad \Delta^2_{\rm Q}(k) = \Delta^2_{\rm L}(k) \left[\frac{(1+\Delta^2_{\rm L}(k))^{\beta_n}}{1+\alpha_n \Delta^2_{\rm L}(k)} \right] e^{-f(y)} \quad , \quad y \equiv \frac{k}{k_\sigma} \quad , \quad f(y) = \frac{y}{4} + \frac{y^2}{8} \quad , \tag{B.213}$$

$$\text{et} \quad \Delta^2_{\rm H}(k) = \frac{\Delta^2_{\rm H}{}'(k)}{1+\mu_n y^{-1} + \nu_n y^{-2}} \quad , \quad \Delta^2_{\rm H}{}'(k) = \frac{a_n \; y^{3 f_1(\Omega)}}{1 + b_n y^{f_2(\Omega)} + [c_n f_3(\Omega) \; y]^{3-\gamma_n}} \quad , \tag{B.214}$$

où $\{\alpha_n, \beta_n, \gamma_n, \mu_n, \nu_n, a_n, b_n, c_n\}$ sont des paramètres déterminés par trois grandeurs (cf. Eq. (A.187)).

Le premier de ces trois paramètres est le moment k_σ correspondant à l'échelle d'entrée dans le régime non-linéaire. Il est obtenu en normalisant à 1 la variance de la densité de matière :

$$\sigma^2(k_\sigma^{-1}) \equiv \int \Delta^2_{\rm L}(k,z) \; \exp\left(-(k/k_\sigma)^2\right) \; d\ln k \equiv 1 \quad . \tag{B.215}$$

Les deux autres grandeurs sont l'indice spectral effectif du spectre et la courbure de cet indice :

$$n_{\rm eff} \equiv -\left[3 + \frac{d\ln\sigma^2(R)}{d\ln R}\right]_{R=k_\sigma^{-1}} \quad , \quad C \equiv -\left.\frac{d^2\ln\sigma^2(R)}{d\ln R^2}\right|_{R=k_\sigma^{-1}} \quad . \tag{B.216}$$

La première de ces grandeurs, et par conséquent les deux autres ainsi que les paramètres du modèle du HaloFit, dépendent du redshift (autrement dit du temps) et ce de manière non-triviale. On a donc une paramétrisation du spectre jusque dans le régime non-linéaire. Pour [23], le spectre est physiquement valide jusque $k \sim 1 \; h \; \mathrm{Mpc}^{-1}$, tandis que [74] donne une confiance sur le résultat allant jusque $k \sim 30 \; h \; \mathrm{Mpc}^{-1}$. Le spectre non-linéaire obtenu par l'implémentation de ces deux paramétrisations du modèle du HaloFit, [23] et [74], est illustré en Fig. 6.9.

B.6.5 Résultats numériques et comparaison avec le régime linéaire

Nous avons déjà mentionné la dépendance temporelle du spectre de puissance dans le cas ΛCDM. Il faut maintenant comprendre que le spectre non-linéaire dépend d'autant plus du temps (ou du redshift) que chacun des paramètres cités dans la section précédente a aussi une dépendance en temps. Il devient alors impossible de calculer l'effet des différents termes inhomogènes sans recourir à de nouvelles approximations. Pour cela, nous avons utilisé l'approximation du spectre suivante :

$$\mathcal{P}^{\rm NL}_\psi(k,z) = \frac{g^2(z)}{g^2(z^*)} \mathcal{P}^{\rm NL}_\psi(k,z^*) \quad , \tag{B.217}$$

où nous avons choisi $z^* = z_s/2$ pour essayer de minimiser les imprécisions. En effet, notre étude porte sur des redshifts tels que $0.015 \leq z \leq 2$ et cette approximation ne devient discutable que lorsque $z_s = 2$ (i.e. $z^* = 1$) et que l'on estime nos termes en $z = 0.015$ et $z = 2$. Dans ce cas, nous sous-estimons le spectre de 40% pour $z = 0.015$ et le surestimons d'environ 80% pour $z = 2$. Ces erreurs sont néanmoins présentes seulement pour deux étroites bandes de moment centrées sur $k = 1\,h\,\mathrm{Mpc}^{-1}$ et $k = 2\,h\,\mathrm{Mpc}^{-1}$. On estime donc la précision globale de notre evaluation à $\sim 10\%$. Il est alors possible d'estimer les intégrales des diverses quantités d_L^{-2}, d_L, μ comme précédemment, pour chaque redshift, en intégrand numériquement sur k. Le résultat final de nos calculs est donné en Figs. 6.10 et 6.11, et ce en utilisant le spectre de puissance donné par le modèle du HaloFit de [74] et incluant une contribution baryonique. On constate que la distance d_L reçoit une correction de l'ordre de 10^{-3} autour de $z = 2$ alors que la correction au flux est deux ordres de grandeur moindre. La comparaison de ces résultats avec les Figs. 6.7 et 6.8 montre que le spectre de puissance considéré dans son régime non-linéaire a augmenté l'effet des inhomogénéités sur les moyennes des observables. Ces effets restent

néanmoins très difficiles à observer expérimentalement. On peut aussi voir sur la partie droite de la Fig. 6.11 que la considération du spectre non-linéaire ne rend l'effet sur la moyenne que difficilement identifiable visuellement. En revanche, la dispersion théorique due aux inhomogénéités est augmentée significativement. En effet, la dispersion sur μ est de l'ordre de 10% à $z = 2$, ce qui montre que les modèles homogènes ayant une valeur de $\Omega_{\Lambda 0}$ entre 0.68 et 0.78 se situent à moins d'une déviation standard ($1\,\sigma$) de notre prédiction pour un modèle inhomogène avec $\Omega_{\Lambda 0} = 0.73$.

B.6.6 Comparaison avec la dispersion intrinsèque des SNe Ia

Attachons nous ici à comparer notre prédiction théorique de la dispersion σ_μ avec la dispersion intrinsèque estimée par les données des SNe Ia. Pour ne présenter que cette dispersion σ_μ, nous l'avons tracé en Fig. 6.12 (et déjà visible en Fig. 6.11). Dans ce tracé, le trait plein représente la contribution totale de σ_μ obtenue par l'Eq. (B.166) en fonction de z. Cette dispersion tolale est dans une très bonne approximation donnée par la somme des termes de vitesse et de lentille gravitationnelle (comme déjà évoqués dans l'étude de l'Eq. (B.207)). Cette dispersion possède une évolution en z bien caractéristique avec une valeur minimale proche de 0.016 pour $z = 0.285$.

La variance totale $\sigma_\mu^{\rm obs}$ associée aux observations peut quant à elle être décomposée en diverses composantes (cf. e.g. [13,118,119]) :

$$(\sigma_\mu^{\rm obs})^2 = (\sigma_\mu^{\rm fit})^2 + (\sigma_\mu^{z})^2 + (\sigma_\mu^{\rm int})^2 \quad , \tag{B.218}$$

où $\sigma_\mu^{\rm fit}$ est la dispersion liée à la méthode utilisée pour ajuster les courbes de lumière (e.g. la méthode SALT-II [16]) mais aussi la modélisation du processus amenant à la supernova. σ_μ^{z} représente l'incertitude sur la vitesse particulière des SNe Ia et la précision des mesures spectroscopiques. Enfin, $\sigma_\mu^{\rm int}$ représente toutes les autres sources d'incertitudes non prises en compte par le modèle homogène. Cette dernière quantité peut donc être redéfinie, par la connaissance de la dispersion due à l'effet de lentille gravitationnelle que nous avons estimé précédemment, de la manière suivante :

$$(\sigma_\mu^{\rm int})^2 = (\widehat{\sigma_\mu^{\rm int}})^2 + (\sigma_\mu^{\rm lens})^2 \quad . \tag{B.219}$$

Ici $\widehat{\sigma_\mu^{\rm int}}$ est la dispersion intrinsèque restante des SNe Ia. La précision actuelle des données (cf. [16,120]) et du diagramme de Hubble ne permet pas de mettre en lumière une forte dépendance en z de $\sigma_\mu^{\rm int}$: nous avons $\sigma^{\rm int} = 0.15 \pm 0.02$ pour les SNe Ia les plus proches et $\sigma^{\rm int} = 0.12 \pm 0.02$ pour les plus éloignées. D'un autre côté, on voit dans le résultat de nos calculs, présenté en Fig. 6.12, que notre prédiction pour le terme de lentille est linéaire pour $z \gtrsim 0.3$. On trouve en effet que cette prédiction est très bien approximée par $\sigma_\mu^{\rm lens}(z) = 0.056\,z$, ce qui la rend parfaitement compatible avec les observations (elle est < 0.12 jusque $z \sim 2$).

Il est aussi encore plus intéressant de noter que cette prédiction est en parfait accord avec les tentatives récentes de mesure de cet effet de lentille au sein des SNe Ia, par [75] :

$$\left(\sigma_\mu^{\rm lens}\right)_{\rm Kronborg} = (0.05 \pm 0.022)\,z \quad , \tag{B.220}$$

ou encore [76] :

$$\left(\sigma_\mu^{\rm lens}\right)_{\rm Jönsson} = (0.055^{+0.039}_{-0.041})\,z \quad . \tag{B.221}$$

Cette compatibilité de notre calcul avec ces mesures exprimentales est clairement identifiable dans la Fig. 6.12. Les simulations de lentille (cf. [121]) ont aussi apporté une estimation de $0.088\,z$, en parfait accord avec notre prédiction. Remarquons toutefois que d'autres auteurs n'ont pas relevé d'effet de lentille significatif avec la précision actuelle des données (cf. [122–124]). Il est plus que probable que les prochaines données sur les supernovae permettront de confirmer ou d'infirmer la présence de cet effet de lentille dans la dispersion du diagramme de Hubble. Ceci constitue donc un test du modèle de concordance. Notons enfin que notre prédiction de la dispersion liée à la vitesse particulière (cf. Fig. 6.12) est très bien approximée par la loi de puissance suivante :

$$\sigma_\mu^{\rm Doppler}(z) \sim 0.00323\,z^{-1} \quad . \tag{B.222}$$

Ce résultat est en très bon accord avec ceux de [127].

B.6.7 Dispersion et comparaison aux données expérimentales

Nous avons finalement effectué la comparaison entre nos prédictions sur le module de distance et les données issues de la compilation « Union 2 », comme présenté en Fig. 6.13. Comme il est possible de le voir à l'oeil nu, la dispersion théorique que nous avons calculé est moins importante que la dispersion des données, en particulier aux grands redshifts. Il apparait donc que la composante principale de la dispersion des données aux petits redshifts est essentiellement due aux vitesses particulières et que notre prédiction en terme de perturbations inhomogènes est une bonne explication à cela. D'un autre côté, notre dispersion calculée aux grands redshifts et due essentiellement au terme de lentille gravitationnelle ne suffit absolument pas à expliquer la dispersion des données, révélant des sources de dispersion non prises en compte dans notre calcul. Il est en fait logique d'aboutir à une telle conclusion. Les SNe Ia sont des phénomènes physiques très complexes et notre calcul ne prend en compte que l'effet des inhomogénéités, celui qui nous intéresse dans cette étude. Des effets comme l'absorption de la lumière par le milieu interstellaire ou encore des effets de lentilles fortes sont possible. De plus, et il s'agit probablement d'un facteur important, les supernovae ont une dispersion intrinsèque dans leur luminosité qui est très difficile à estimer.

On peut en fait se réjouir d'un tel résultat car il montre que le modèle standard de la cosmologie est robuste aux effets des inhomogénéités présentés ici et que le décalage dans le diagramme de Hubble qui a donné lieu à la découverte de l'accélération de l'Univers n'est pas une simple fluctuation statistique. Dans le cas d'une dispersion plus petite que notre prédiction, nous serions forcés de soustraire les effets de dispersion pour chacune des sources avant de pouvoir conclure à l'existence de l'énergie sombre. Nous avons donc montré par nos calculs au second ordre que les inhomogénéités ne pouvaient pas jouer le rôle de cette énergie sombre. Toutefois, il est très important de remarquer que l'effet que nous avons obtenu est plus grand que celui qui était naïvement attendu, il dépend sensiblement de l'observable physique considérée et est susceptible d'être détecté dans les prochaines années, donnant ainsi un autre test des inhomogénéités et de meilleures contraintes sur les propriétés de l'énergie sombre.

B.7 Résumé et Conclusions

Nous avons étudié dans cette thèse le problème général de la moyenne sur le cône de lumière et ses implications en cosmologie de manière à améliorer notre compréhension de l'Univers et de sa nature inhomogène.

En premier lieu, nous avons décrit le modèle standard de la cosmologie en donnant en particulier les équations utilisées pour interpréter les données expérimentales dans le cadre du modèle de concordance ΛCDM (les equations de Friedmann). Nous avons aussi décrit l'utilisation des supernovæ de type Ia qui sont à la base de la découverte de l'énergie sombre et les considérations de base relatives aux grandes structures.

Nous avons ensuite donné la définition de la moyenne de quantités scalaires sur des hypersurfaces de type lumière. Cette définition, inspirée par la moyenne spatiale du formalisme de Buchert [47, 48], possède des caractéristiques communes avec leur généralisation invariante de jauge [82, 83]. En particulier, cette définition est invariante sous les transformations de coordonnées, de jauge et sous les reparamétrisations de ses hypersurfaces. On a ainsi pu écrire les relations équivalentes à la règle de commutation de Buchert-Ehlers qui est à la base des questions de backreaction. Cette moyenne sur le cône de lumière, longtemps soulignée comme importante, n'avait jamais été définie dans la littérature.

Ensuite, nous avons introduit un système de coordonnées qui simplifie grandement la description de quantités physiques sur notre cône de lumière passé. Nous les avons appelées coordonnées « géodésiques sur le cône de lumière » ("Geodesic Light-Cone" coordinates) et celles-ci se sont révélées utiles pour une gamme d'applications bien plus large que la moyenne. Elles sont aussi assez proches d'un autre système de coordonnées dites « observationelles » [51, 59] et correspondent à une fixation de jauge de ces dernières qui contiennent un degré de liberté supplémentaire. D'autres différences sont à noter, comme le fait que nos coordonnées contiennent le temps τ de l'observateur tandis que les coordonnées observationnelles utilisent une distance y sur le cône passé (qui est nulle ou de type spatial). L'étude de cette jauge est fortement susceptible d'apporter des résultats pour toutes les

applications liées aux signaux lumineux en cosmologie. Ces coordonnées GLC forment un système dans lequel les photons se propagent à coordoonées $w = w_o$ et $\widetilde{\theta}^a$ constantes. Cette redéfinition des angles le long de la propagation fait que les expressions du redshift z et de la distance de luminosité d_L sont très simples dans cette jauge (et directement exprimées en terme de ses éléments de métrique). Nous avons aussi décrit l'exemple de la transformation entre les coordonnées GLC et les métriques synchrone et LTB. Ces coordonnées ont enfin été utilisées pour simplifier l'expression générale de la moyenne sur le cône de lumière passé et les relations de commutation de Buchert-Ehlers et ont été appliquées par l'exemple de la moyenne du redshift drift.

Les effets de backreaction disparaissent dans le cas particulier d'un modèle FLRW et il nous a donc été nécessaire d'évaluer la distance de luminosité dans le cas d'un modèle perturbé. Du fait de l'aspect stochastique des inhomogénéités introduites, la moyenne de leurs effets disparaît au premier ordre lorsque l'on prend leur moyenne d'ensemble. Le calcul perturbatif de la distance a donc dû être poussé jusqu'au second ordre et a été exprimé en terme des éléments de métrique de la jauge de Poisson du fait que le spectre de puissance des inhomogénéités est connu dans cette jauge (et non dans la jauge GLC). L'expression finale de cette distance est riche de sense physique et inclut des termes de vitesse particulière, les effets SW et ISW, l'effet de lentille, les distortions de redshift et un grand nombre de combinaisons relatives à ces effets. Ce résultat est donc très intéressant pour la cosmologie et pourrait être utilisé dans un grand nombre de problèmes. Encore une fois, la métrique GLC joue un rôle capital pour l'établissement de ce résultat. Les perturbations vectorielles et tensorielles n'ont pas été oubliées, mais considérées seulement au second ordre (du fait de leur origine inflationnaire).

Nous avons ensuite abordé la question de la taille relative de l'effet des inhomogénéités sur la distance de luminosité, le flux lumineux et le module de distance. Pour cela nous avons dû combiner la moyenne sur le cône de lumière avec la moyenne d'ensemble sur les perturbations stochastiques. Dans une premier temps, nous avons effectué un calcul partiel basé sur l'ordre quadratique mais suffisant pour mettre en lumière la présence de termes dit de « backreaction induite ». Ces termes sont intéressants car il regroupent les expressions des scalaires moyennés et de la mesure d'intégration. Ils permettent aussi l'évaluation exacte de la dispersion de ces grandeurs. Nous avons donné l'expression des coefficients spectraux relatifs à ces termes et avons ensuite considéré le cas complet au second ordre. Nous avons trouvé que la moyenne de la distance de luminosité différait de celle du flux lumineux par une contribution (de flux) : $\overline{\langle(\Phi_1/\Phi_0)^2\rangle}$. Cette contribution est proportionnelle à la moyenne du carré de la correction au premier ordre de la distance. Elle contient entre autres les termes de vitesse particulière et de lentille gravitationnelle. Nous avons aussi montré que les perturbations vectorielles et tensorielles disparaissent sous l'effet de notre moyenne (et ce par symétrie). Quant aux contributions intrinsèques au second ordre, elles ont été reliées par l'utilisation de [104] à celles du premier ordre.

Faisant usage de ces résultats théoriques, nous sommes passés à l'évaluation numérique de leurs effets en choisissant une forme explicite pour la fonction de transfert du spectre de puissance linéaire (produit par le spectre primordial). Nous avons tout d'abord considéré le cas simple d'un univers CDM avec une fonction de transfert ne contenant pas de contribution baryonique. Nous avons utilisé ce cas pour l'évaluation des termes de backreaction induite et de la variance $\overline{\langle\sigma_1^2\rangle}$. Nous avons constaté, comme prévu, que l'effet dominant qui agit sur les SNe Ia à petits redshifts est celui de leur vitesse particulière (due aux inhomogénéités) et aux grands redshifts celui de lentille gravitationnelle. Ce cas nous a aussi aidé à voir que nos intégrales sont libres de toute divergence, ultraviolette ou infrarouge. Ce résultat est à comparer avec celui des moyennes spatiales où des divergences UV existent et il est dû à la construction de notre moyenne, sur le cône de lumière et de manière invariante de jauge. Une autre conclusion a été que la moyenne de la distance de luminosité est très faiblement affectée par les inhomogénéités, sauf par l'effet de vitesse à petits redshifts. Toutefois, ce calcul était imcomplet et donc incertain.

Nous avons donc établi le résultat numérique du calcul complet au second ordre, dans le cas du flux et encore au sein d'un modèle CDM. Nous avons pu constater que le flux est très faiblement affecté aux large redshifts, sa correction relative restant de l'ordre de $\sim 10^{-5}$, ce qui fait du flux une quantité très spéciale pour laquelle les effets de lentille s'annulent lorsque l'on prend la moyenne sur le cône de lumière. Ceci est bien sûr relié à la conservation du flux le long du cône. Ce calcul a aussi montré que les inhomogénéités ne pouvaient simuler une constante cosmologique : la correction à la moyenne est

trop faible et ne possède par le bon signe aux grand redshifts. L'effet sur la distance est quant à lui toujours positif mais possède une variation bien caractéristique du fait des deux effets de vitesse et de lentille. La correction à la distance peut atteindre la valeur de $\sim 10^{-2}$ à $z = 2$. La considération du module de distance a montré que l'effet sur la moyenne reste négligeable (hormis aux petits redshifts) mais que la dispersion des inhomogénéités entraine une erreur de $\sim 1 - 2\,\%$ sur $\Omega_{\Lambda 0}$.

Nous avons ensuite considéré le cas réaliste d'un modèle ΛCDM et ajouté l'effet des baryons (*Silk damping*) dans la fonction de transfert [114]. Ces deux modifications ont une conséquence directe sur le spectre de puissance linéaire, en réduisant ses valeurs, et font donc décroître les corrections du flux et de la distance d'environ un ordre de grandeur. Nous avons ensuite considéré le régime non-linéaire du spectre à travers le modèle du HaloFit [23, 74]. Ceci a eu pour conséquence de renforcer l'effet des inhomogénéités et ce en particulier sur la correction à la distance du fait de sa sensibilité aux effets de lentille (atteignant ainsi $\sim 10^{-3}$ à $z = 2$). Le module de distance a quant à lui révélé un changement négligeable sur sa moyenne mais a vu sa dispersion augmenter et correspondre à une erreur de $\sim 10\%$ sur la valeur de $\Omega_{\Lambda 0}$. Ce résultat est donc très important et démontre que les inhomogénéités ne peuvent être négligées, en particulier au sein de la dispersion des quantités observables. Nous avons finalement comparé notre prédiction théorique avec la dispersion des données du Union2 et les récentes tentatives d'estimation des contributions de vitesse et de l'effet de lentilles dans la dispersion des SNe Ia. Notre résultat se révèle être en parfait accord avec les données et devrait être confirmé dans les prochaines observations de cosmologie de précision.

Nos conclusions, élaborées à l'aide d'un système de coordonnées dites GLC et l'introduction d'une prescription invariante de jauge pour la moyenne sur le cône de lumière passé, peuvent être résumées comme suit. Nous avons trouvé que la combinaison de la moyenne sur le cône avec une moyenne d'ensemble sur des perturbations stochastiques autour d'un modèle d'Univers FLRW plat, appliquée à différentes observables (d_L, $\Phi \propto d_L^{-2}$ et $\mu \sim 5 \log_{10} d_L$) ne pouvait simuler l'énergie sombre. Ce résultat peut nous donner confiance en la robustesse du modèle standard de la cosmologie. D'un autre côté, les inhomogénéités moyennées ont un impact bien plus grand que ce qui était naïvement attendu. Leur influence est principalement caractérisée par la vitesse particulière et l'effet de lentille gravitationnelle et elles affectent la distance plus que le flux (qui est la quantité minimalement affectée aux grands redshifts) par un facteur ~ 100 à $z = 2$. Cela montre que le flux est bel-et-bien la quantité idéale à mesurer et que les autres observables sont bien plus sensibles aux inhomogénéités. Enfin, nous avons comparé nos prédictions avec la dispersion intrinsèque des SNe Ia et montré qu'une part de cette dispersion devrait être explicables dans les futures observations capables de détecter (et de soustraire) ce signal de contamination. Par conséquent, notre travail souligne que, bien que les inhomogénéités ne puissent expliquer l'énergie sombre (du moins dans le cadre de notre calcul), nous pouvons avec confiance croire que l'absence de considération de leur effet rendra impossible une détermination des paramètres de l'énergie sombre en dessous du pourcent et pourrait même aboutir à une mauvaise interprétation des données comme, par exemple, la possible découverte d'une dépendence spatiotemporelle de cette énergie qui ne serait enfin que le reflet des inhomogénéités.

List of Figures

1.1 Idealized light curves for different types of supernovæ 9
1.2 Spectra of different types of supernovæ 9
1.3 SNe Ia light curves of the Calán-Tololo survey and the stretch correction 10
1.4 Hubble diagram with binned data 14
1.5 Cross plot from the Union 2 data set. 14
1.6 The 2dF Galaxy Redshift Survey (2dFGRS) 15
1.7 The matter power spectrum as measured from different sources 16
1.8 Illustration of the backreaction problem 19

2.1 Spatial averaging and introduction of a spatial boundary 32
2.2 Three averaging prescriptions : light-cone, spatial hypersurface and embedded 2-sphere 38

3.1 Illustration of the GLC coordinates 46
3.2 Illustration of the comparative forms of the ADM and GLC metrics 54
3.3 A graphic illustration of the redshift drift effect 57

6.1 Doppler contribution $\overline{\langle A_4 A_4 \rangle}$ with non-baryonic transfer function and different cut-offs 97
6.2 Illustration of the absence of IR and UV divergences 97
6.3 Distance-modulus and dispersion for an inhomogeneous CDM model, $k_{UV} = 0.1\,\mathrm{Mpc}^{-1}$ 98
6.4 Plot of the redshift functions $\widetilde{f}_{1,1}(z)$ and $\widetilde{f}_2(z)$. 102
6.5 Flux correction f_Φ in CDM, with non-baryonic $T(k)$ in $\mathcal{P}_{\mathrm{L}}(k)$, with $k_{UV} = 1\mathrm{Mpc}^{-1}$ . . 103
6.6 Linear power spectra $\mathcal{P}_{\mathrm{L}}(k)$ in CDM and ΛCDM, with baryonic and non-baryonic $T(k)$ 106
6.7 Flux f_Φ and distance f_d corrections in ΛCDM, using $\mathcal{P}_{\mathrm{L}}(k)$ with/without baryon $T(k)$ 107
6.8 Average $\overline{\langle\mu\rangle} - \mu^M$ and dispersion, in CDM with $\mathcal{P}_{\mathrm{L}}(k)$ up to $k_{UV} = 1\,h\ \mathrm{Mpc}^{-1}$ 109
6.9 Linear and non-linear spectra $k^2\ \mathcal{P}_\psi^{\mathrm{L,NL}}$ within the HaloFit model, for $z = 0\ ,\ 1.5$ . . . 110
6.10 Flux f_Φ and distance f_d corrections in ΛCDM, using $\mathcal{P}_{\mathrm{NL}}(k)$ up to $k_{UV} = 10\ ,\ 30\,h\,\mathrm{Mpc}^{-1}$ 111
6.11 Average $\overline{\langle\mu\rangle} - \mu^M$ and dispersion, in ΛCDM with $\mathcal{P}_{\mathrm{NL}}(k)$ up to $k_{UV} = 30\,h\ \mathrm{Mpc}^{-1}$ . . 112
6.12 The z-dependence of the total dispersion σ_μ compared with experimental estimates . . 113
6.13 Comparison of the Union 2 data set with our theoretical prediction 114

A.1 Illustration of the passive approach of gauge transformations. 134
A.2 Illustration of the active approach of gauge transformations. 135
A.3 The transfer function $T(k)$ 145
A.4 The linear gravitational power spectrum $\mathcal{P}_{\mathrm{L}}(k)$ 146
A.5 The linear and non-linear density spectra deduced from the HaloFit model 150
A.6 Ratio $\Delta^2_{\mathrm{NL}}(k)/\Delta^2_{\mathrm{L}}(k)$ computed from Smith and Takahashi parametrizations 150
A.7 The linear spectrum and the non-linear spectrum for the gravitational potential 151
A.8 Same as in Fig. A.7 except that spectra are multiplied by k^2 151
A.9 Relative difference DiffP(k) 152

List of Tables

2.1 Different normalizations to be used to recover the four average definitions 38

5.1 The spectral coefficients $\mathcal{C}_{ij}(k, \eta_o, \eta_s^{(0)})$ for the $\overline{\langle A_i A_j \rangle}$ terms. 80
5.2 The spectral coefficients $\mathcal{C}_i$ for the $\overline{\langle A_i \rangle \langle A_j \rangle}$ terms 80

A.1 Parameters deduced from the identification of the non-linear spectrum of Smith *et al.*. 152

PhD publications

We present here a brief description of the different papers that have been published during the elaboration of this manuscript, in chronological order between 2011 and 2013.

1. ***Light-cone averaging in cosmology: Formalism and applications***,
   M. Gasperini, G. Marozzi, F. Nugier and G. Veneziano,
   JCAP **1107** (2011) 008, [arXiv:1104.1167 [astro-ph.CO]]. Reference [140].

   We give in this paper the first definition of the average on the past lightcone of a geodetic observer. This average is gauge invariant and invariant under reparametrization and coordinates transformations. Generalizations of Ehlers-Buchert commutation relations are derived. The average is applied to different scalars : the luminosity distance (formally) and the redshift drift.

2. ***Backreaction on the luminosity-redshift relation from gauge invariant light-cone averaging***,
   I. Ben-Dayan, M. Gasperini, G. Marozzi, F. Nugier and G. Veneziano,
   JCAP **1204** (2012) 036, [arXiv:1202.1247 [astro-ph.CO]]. Reference [107].

   This paper stands as a first attempt to apply lightcone averaging to the luminosity distance, making use of the average on a topological 2-sphere embedded on the past lightcone and a constant redshift hypersurface. The transformation between the GLC coordinates and the Poisson gauge is derived only at first order and the estimation of the backreaction effect, intrinsically a second order effect in inhomogeneities, is only partial. It nevertheless gives a first sight on the calculation features. We introduce the linear power spectrum of inflationary origin which describes inhomogeneities. It is found that the integrals computed to estimate this effect are both free from IR and UV divergences. Terms coming from Doppler effect and weak lensing of light signals are identified. It is not known at this time if the backreaction effect is big or small.

3. ***Do stochastic inhomogeneities affect dark-energy precision measurements?***,
   I. Ben-Dayan, M. Gasperini, G. Marozzi, F. Nugier and G. Veneziano,
   PRL **110**, 021301 (2013), [arXiv:1207.1286 [astro-ph.CO]]. Reference [141].

   In this PRL letter, we describe the results of a full computation of the luminosity distance at second order in perturbations, using the linear power spectrum to describe inhomogeneities. The effect on the average of the luminosity distance is found to be small, corrections are $\sim 10^{-5}$ for the luminosity flux, but $\sim 10^{-3}$ for the distance itself, this because of the presence of a lensing term in this latter quantity. Hence some observables in cosmology are more sensitively dependent on inhomogeneities than others, the flux being the minimalized observable. The effect of the variance is important, equivalent to a 2% change in Ω_Λ with a linear matter power spectrum.

4. ***The second-order luminosity-redshift relation in a generic inhomogeneous cosmology***,
   I. Ben-Dayan, G. Marozzi, F. Nugier and G. Veneziano,
   JCAP **1211** (2012) 045, [arXiv:1209.4326 [astro-ph.CO]]. Reference [142].

The detailed derivation of the expression of the luminosity distance at second order in perturbations is given, including scalar, vector and tensor inhomogeneities. This expression is interesting on its own and have a large range of applications in cosmology, independently from the question of the backreaction of inhomogeneities. Among the effects encountered, we have normal and integrated Sachs-Wolfe effects, peculiar velocity effects (Doppler), weak lensing and almost all their possible combinations at second order (including integrated effects).

5. ***Average and dispersion of the luminosity-redshift relation in the concordance model***,
I. Ben-Dayan, M. Gasperini, G. Marozzi, F. Nugier and G. Veneziano,
JCAP **06** (2013) 002, [arXiv:1302.0740 [astro-ph.CO]]. Reference [143].

The full calculation is produced. The average of the luminosity distance is found to be small as indicated in our previous studies. Details of the PRL letter on the average (both over the sky and stochastically) are given. A non-linear power spectrum elaborated from the HaloFit model is used. The effect is enhanced by small scales, but the order of magnitude stays the same. We find that the variation of Ω_Λ can go up to 10%. We also find that this non-linear power spectrum prediction is in very good agreement with SNe Ia measurements, for the Doppler effect (at small redshifts) and the lensing dispersion (at large redshifts). Our work hence gives a clear theoretical prediction which could be compared with data in the next couple of years.

This thesis has lead me to give a certain number of seminars, in Europe and United States. Here is a list of seminars that I gave concerning its content.

Journée des doctorants du LPT ENS 2011,
LPT ENS, Paris, France – 26 October 2011
String, Cosmology & Gravity Student Conference 2011,
London Mathematical Society, London, England – 2-4 November 2011
Backreaction: Where do we stand?,
IAP, Paris, France – 22-23 November 2011
Séminaire INformel des JEunes (SINJE),
LPT Orsay, Paris-Sud 11, France – 27 Feb. 2011
Summer School on Cosmology,
ICTP, Trieste, Italy – 16-27 July 2012
Journée des doctorants du LPT ENS 2012,
LPT ENS, Paris, France – 7 November 2012
Particle and Astrophysics Seminar,
ITP, University of Zurich, Switzerland – 14 Nov. 2012
Cosmology & Particle Phys. Sem.,
Geneva Cosmology Group, Univ. Geneva – 16 Nov. 2012
Cosmology Lunch Discussion,
Dep. Astrophysical Sciences, Princeton Univ. – 10 Dec. 2012
High Energy Theory Seminar,
Center for Particle Cosmology, UPenn, USA – 11 Dec. 2012
HEP Informal Talk,
Center for Cosmology & Particle Physics, New York Univ. – 13 Dec. 2012
APC Colloquium,
Laboratoire AstroParticule & Cosmologie, Paris – 5 March 2012
Video Conference Seminar,
Los Alamos National Laboratory – 5 July 2013
Student Talk at Les Houches,
École de Physique des Houches, France – 26 July 2013

Bibliography

[1] S. Weinberg, *Cosmology*. Cosmology. OUP Oxford, 2008. http://books.google.fr/books?id=nqQZdg020fsC.

[2] S. Weinberg, *Gravitation and cosmology: principles and applications of the general theory of relativity*. Wiley, 1972. http://books.google.fr/books?id=XLbvAAAAMAAJ.

[3] C. Misner, K. Thorne, and J. Wheeler, *Gravitation: Charles W. Misner, Kip S. Thorne, John Archibald Wheeler*. Gravitation. W. H. Freeman, 1973. http://books.google.fr/books?id=w4Gigq3tY1kC.

[4] J. Peacock, *Cosmological Physics*. Cambridge Astrophysics Series. Cambridge University Press, 1999. http://books.google.fr/books?id=t8O-yylU0j0C.

[5] E. J. Copeland, M. Sami, and S. Tsujikawa, "Dynamics of Dark Energy," *International Journal of Modern Physics D* **15** (2006) 1753–1935, arXiv:hep-th/0603057.

[6] T. Buchert, "Toward physical cosmology: focus on inhomogeneous geometry and its non-perturbative effects," *Class. Quant. Grav.* **28** (2011) 164007, arXiv:1103.2016 [gr-qc].

[7] M. Gasperini, *Elements of String Cosmology*. Cambridge University Press, 2007. http://books.google.fr/books?id=d0izBJTl7b4C.

[8] P. Peter and J. Uzan, *Primordial Cosmology*. Oxford Graduate Texts. OUP Oxford, 2013. http://books.google.fr/books?id=WlgLgUfZaTwC.

[9] E. Hubble, "A Relation between Distance and Radial Velocity among Extra-Galactic Nebulae," *Proceedings of the National Academy of Science* **15** (Mar., 1929) 168–173.

[10] **Supernova Search Team** Collaboration, A. G. Riess *et al.*, "Observational evidence from supernovae for an accelerating universe and a cosmological constant," *Astron. J.* **116** (1998) 1009–1038, arXiv:astro-ph/9805201 [astro-ph].

[11] **Supernova Cosmology Project** Collaboration, S. Perlmutter *et al.*, "Measurements of Omega and Lambda from 42 high redshift supernovae," *Astrophys. J.* **517** (1999) 565–586, arXiv:astro-ph/9812133 [astro-ph].

[12] N. Fourmanoit, *Analyse des 5 ans de données de l'expérience SuperNova Legacy Survey*. These, Université Pierre et Marie Curie - Paris VI, Sept., 2010. http://tel.archives-ouvertes.fr/tel-00587450.

[13] A. Conley, J. Guy, M. Sullivan, N. Regnault, P. Astier, *et al.*, "Supernova Constraints and Systematic Uncertainties from the First 3 Years of the Supernova Legacy Survey," *Astrophys. J. Suppl.* **192** (2011) 1, arXiv:1104.1443 [astro-ph.CO].

[14] B. Carroll and D. Ostlie, *An Introduction to Modern Galactic Astrophysics And Cosmology*. Pearson Addison Education, 2006. http://books.google.fr/books?id=9VKiAAAACAAJ.

[15] N. Palanque-Delabrouille and on behalf of the SNLS collaboration, "SNIa photometric studies in SNLS," *ArXiv e-prints* (May, 2010) , arXiv:1005.1890 [astro-ph.CO].

[16] J. Guy, P. Astier, S. Baumont, D. Hardin, R. Pain, *et al.*, "SALT2: Using distant supernovae to improve the use of Type Ia supernovae as distance indicators," *Astron. Astrophys.* **466** (2007) 11–21, arXiv:astro-ph/0701828 [ASTRO-PH].

[17] J. Frieman, M. Turner, and D. Huterer, "Dark Energy and the Accelerating Universe," *Ann. Rev. Astron. Astrophys.* **46** (2008) 385–432, arXiv:0803.0982 [astro-ph].

[18] I. Etherington, "On the definition of distance in general relativity," *Phil. Mag. ser. 7 15, 761–773* (1933) .

[19] R. P. Kirshner, "Hubble's diagram and cosmic expansion," *Proceedings of the National Academy of Sciences* **101** no. 1, (2004) 8–13, http://www.pnas.org/content/101/1/8.full.pdf+html. http://www.pnas.org/content/101/1/8.abstract.

[20] **Planck Collaboration** Collaboration, P. Ade *et al.*, "Planck 2013 results. XVI. Cosmological parameters," arXiv:1303.5076 [astro-ph.CO].

[21] R. Amanullah, C. Lidman, D. Rubin, G. Aldering, P. Astier, *et al.*, "Spectra and Light Curves of Six Type Ia Supernovae at $0.511 < z < 1.12$ and the Union2 Compilation," *Astrophys. J.* **716** (2010) 712–738, arXiv:1004.1711 [astro-ph.CO].

[22] **SDSS Collaboration** Collaboration, M. Tegmark *et al.*, "The 3-D power spectrum of galaxies from the SDSS," *Astrophys. J.* **606** (2004) 702–740, arXiv:astro-ph/0310725 [astro-ph].

[23] **Virgo Consortium** Collaboration, R. Smith *et al.*, "Stable clustering, the halo model and nonlinear cosmological power spectra," *Mon. Not. Roy. Astron. Soc.* **341** (2003) 1311, arXiv:astro-ph/0207664 [astro-ph].

[24] C. Clarkson, G. F. Ellis, A. Faltenbacher, R. Maartens, O. Umeh, *et al.*, "(Mis-)Interpreting supernovae observations in a lumpy universe," *Mon. Not. Roy. Astron. Soc.* **426** (2012) 1121–1136, arXiv:1109.2484 [astro-ph.CO].

[25] M.-N. Celerier, "Do we really see a cosmological constant in the supernovae data?," *Astron. Astrophys.* **353** (2000) 63–71, arXiv:astro-ph/9907206 [astro-ph].

[26] C. Clarkson, G. Ellis, J. Larena, and O. Umeh, "Does the growth of structure affect our dynamical models of the universe? The averaging, backreaction and fitting problems in cosmology," *Rept. Prog. Phys.* **74** (2011) 112901, arXiv:1109.2314 [astro-ph.CO].

[27] **Particle Data Group** Collaboration, K. Nakamura *et al.*, "Review of particle physics," *J. Phys.* **G37** (2010) 075021.

[28] G. Ellis, "Republication of: Relativistic cosmology," *General Relativity and Gravitation* **41** (2009) 581–660. http://dx.doi.org/10.1007/s10714-009-0760-7.

[29] G. F. Ellis, "Inhomogeneity effects in Cosmology," arXiv:1103.2335 [astro-ph.CO].

[30] T. Buchert and S. Rasanen, "Backreaction in late-time cosmology," *Ann. Rev. Nucl. Part. Sci.* **62** (2012) 57–79, arXiv:1112.5335 [astro-ph.CO].

[31] E. E. Flanagan, "Can superhorizon perturbations drive the acceleration of the universe?," *Phys. Rev.* **D71** (2005) 103521, arXiv:hep-th/0503202 [hep-th].

[32] G. Geshnizjani, D. J. Chung, and N. Afshordi, "Do large-scale inhomogeneities explain away dark energy?," *Phys. Rev.* **D72** (2005) 023517, arXiv:astro-ph/0503553 [astro-ph].

[33] C. M. Hirata and U. Seljak, "Can superhorizon cosmological perturbations explain the acceleration of the Universe?," *Phys. Rev.* **D72** (2005) 083501, arXiv:astro-ph/0503582 [astro-ph].

[34] A. Ishibashi and R. M. Wald, "Can the acceleration of our universe be explained by the effects of inhomogeneities?," *Class. Quant. Grav.* **23** (2006) 235–250, arXiv:gr-qc/0509108 [gr-qc].

[35] A. Paranjape and T. Singh, "Cosmic Inhomogeneities and the Average Cosmological Dynamics," *Phys. Rev. Lett.* **101** (2008) 181101, arXiv:0806.3497 [astro-ph].

[36] E. W. Kolb, "Backreaction of inhomogeneities can mimic dark energy," *Class. Quant. Grav.* **28** (2011) 164009.

[37] C. Clarkson and O. Umeh, "Is backreaction really small within concordance cosmology?," *Class. Quant. Grav.* **28** (2011) 164010, arXiv:1105.1886 [astro-ph.CO].

[38] T. Buchert, "On average properties of inhomogeneous cosmologies," arXiv:gr-qc/0001056 [gr-qc].

[39] T. Buchert and M. Carfora, "Cosmological parameters are dressed," *Phys. Rev. Lett.* **90** (2003) 031101, arXiv:gr-qc/0210045 [gr-qc].

[40] S. Rasanen, "Dark energy from backreaction," *JCAP* **0402** (2004) 003, arXiv:astro-ph/0311257 [astro-ph].

[41] S. Rasanen, "Accelerated expansion from structure formation," *JCAP* **0611** (2006) 003, arXiv:astro-ph/0607626 [astro-ph].

[42] E. Barausse, S. Matarrese, and A. Riotto, "The Effect of inhomogeneities on the luminosity distance-redshift relation: Is dark energy necessary in a perturbed Universe?," *Phys. Rev.* **D71** (2005) 063537, arXiv:astro-ph/0501152 [astro-ph].

[43] E. W. Kolb, S. Matarrese, A. Notari, and A. Riotto, "The Effect of inhomogeneities on the expansion rate of the universe," *Phys. Rev.* **D71** (2005) 023524, arXiv:hep-ph/0409038 [hep-ph].

[44] E. W. Kolb, S. Matarrese, and A. Riotto, "On cosmic acceleration without dark energy," *New J. Phys.* **8** (2006) 322, arXiv:astro-ph/0506534 [astro-ph].

[45] D. Baumann, A. Nicolis, L. Senatore, and M. Zaldarriaga, "Cosmological Non-Linearities as an Effective Fluid," *JCAP* **1207** (2012) 051, arXiv:1004.2488 [astro-ph.CO].

[46] S. R. Green and R. M. Wald, "A new framework for analyzing the effects of small scale inhomogeneities in cosmology," *Phys. Rev.* **D83** (2011) 084020, arXiv:1011.4920 [gr-qc].

[47] T. Buchert, "On average properties of inhomogeneous fluids in general relativity. 1. Dust cosmologies," *Gen. Rel. Grav.* **32** (2000) 105–125, arXiv:gr-qc/9906015 [gr-qc].

[48] T. Buchert, "On average properties of inhomogeneous fluids in general relativity: Perfect fluid cosmologies," *Gen. Rel. Grav.* **33** (2001) 1381–1405, arXiv:gr-qc/0102049 [gr-qc].

[49] T. Buchert, "On Average Properties of Inhomogeneous Fluids in General Relativity: Dust Cosmologies," *General Relativity and Gravitation* **32** (Jan., 2000) 105–126, arXiv:gr-qc/9906015.

[50] T. Buchert, "On Average Properties of Inhomogeneous Fluids in General Relativity: Perfect Fluid Cosmologies," *General Relativity and Gravitation* **33** (Aug., 2001) 1381–1405, arXiv:gr-qc/0102049.

[51] R. Maartens, *PhD Thesis.* PhD thesis, University of Cape Town, 1980.

[52] R. Maartens and D. Matravers *Class. Quant. Grav.* **11** *(1994) 2693* (1994) .

[53] V. Marra, E. W. Kolb, and S. Matarrese, "Light-cone averages in a swiss-cheese Universe," *Phys. Rev.* **D77** (2008) 023003, arXiv:0710.5505 [astro-ph].

[54] N. Li, M. Seikel, and D. J. Schwarz, "Is dark energy an effect of averaging?," *Fortsch. Phys.* **56** (2008) 465–474, arXiv:0801.3420 [astro-ph].

[55] S. Rasanen, "Light propagation in statistically homogeneous and isotropic dust universes," *JCAP* **0902** (2009) 011, arXiv:0812.2872 [astro-ph].

[56] S. Rasanen, "Light propagation in statistically homogeneous and isotropic universes with general matter content," *JCAP* **1003** (2010) 018, arXiv:0912.3370 [astro-ph.CO].

[57] E. W. Kolb and C. R. Lamb, "Light-cone observations and cosmological models: implications for inhomogeneous models mimicking dark energy," arXiv:0911.3852 [astro-ph.CO].

[58] T. Buchert and J. Ehlers, "Averaging inhomogeneous Newtonian cosmologies," *Astron. Astrophys.* **320** (1997) 1–7, arXiv:astro-ph/9510056 [astro-ph].

[59] G. F. R. Ellis, S. D. Nel, R. Maartens, W. R. Stoeger, and A. P. Whitman, "Ideal observational cosmology.," *Phys.Rep.* **124** (1985) 315–417.

[60] V. F. Mukhanov, H. Feldman, and R. H. Brandenberger, "Theory of cosmological perturbations. Part 1. Classical perturbations. Part 2. Quantum theory of perturbations. Part 3. Extensions," *Phys. Rept.* **215** (1992) 203–333.

[61] M. Sasaki, "The Magnitude - Redshift relation in a perturbed Friedmann universe," *Mon. Not. Roy. Astron. Soc.* **228** (1987) 653–669.

[62] M. Kasai and M. Sasaki, "The number count – redshift relation in a perturbed Friedmann Universe," *Mod. Phys. Lett.* **A2** (1987) 727.

[63] C. Bonvin, R. Durrer, and M. A. Gasparini, "Fluctuations of the luminosity distance," *Phys. Rev.* **D73** (2006) 023523, arXiv:astro-ph/0511183 [astro-ph].

[64] T. Pyne and M. Birkinshaw, "The luminosity distance in perturbed flrw spacetimes," *Mon. Not. Roy. Astron. Soc.* **348** (2004) 581, arXiv:astro-ph/0310841 [astro-ph].

[65] O. Umeh, C. Clarkson, and R. Maartens, "Nonlinear general relativistic corrections to redshift space distortions, gravitational lensing magnification and cosmological distances," arXiv:1207.2109 [astro-ph.CO].

[66] G. Ellis, B. Bassett, and P. Dunsby, "Lensing and caustic effects on cosmological distances," *Class. Quant. Grav.* **15** (1998) 2345–2361, arXiv:gr-qc/9801092 [gr-qc].

[67] Y. Wang, "Flux-averaging analysis of type ia supernova data," *Astrophys. J.* **536** (2000) 531, arXiv:astro-ph/9907405 [astro-ph].

[68] D. J. Eisenstein and W. Hu, "Baryonic features in the matter transfer function," *Astrophys. J.* **496** (1998) 605, arXiv:astro-ph/9709112 [astro-ph].

[69] J. A. Frieman, "Weak lensing and the measurement of q(0) from type Ia supernovae," arXiv:astro-ph/9608068 [astro-ph].

[70] D. E. Holz, "Lensing and high-z supernova surveys," arXiv:astro-ph/9806124 [astro-ph].

[71] R. B. Metcalf, "Gravitational lensing of high redshift type Ia supernova: A Probe of medium scale structure," *Mon. Not. Roy. Astron. Soc.* **305** (1999) 746, arXiv:astro-ph/9803319 [astro-ph].

[72] C. Porciani and P. Madau, "On the Association of gamma-ray bursts with massive stars: implications for number counts and lensing statistics," *Astrophys. J.* **548** (2001) 522–531, arXiv:astro-ph/0008294 [astro-ph].

[73] K. Bolejko, C. Clarkson, R. Maartens, D. Bacon, N. Meures, *et al.*, "Anti-lensing: the bright side of voids," *Phys. Rev. Lett.* **110** (2013) 021302, arXiv:1209.3142 [astro-ph.CO].

[74] R. Takahashi, M. Sato, T. Nishimichi, A. Taruya, and M. Oguri, "Revising the Halofit Model for the Nonlinear Matter Power Spectrum," *Astrophys. J.* **761** (2012) 152, arXiv:1208.2701 [astro-ph.CO].

[75] T. Kronborg, D. Hardin, J. Guy, P. Astier, C. Balland, *et al.*, "Gravitational lensing in the Supernova Legacy Survey (SNLS)," arXiv:1002.1249 [astro-ph.CO].

[76] J. Jonsson, M. Sullivan, I. Hook, S. Basa, R. Carlberg, *et al.*, "Constraining dark matter halo properties using lensed SNLS supernovae," arXiv:1002.1374 [astro-ph.CO].

[77] R. Zalaletdinov, "Towards a theory of macroscopic gravity," *Gen.Rel.Grav.* **25** (1993) 673–695.

[78] R. M. Zalaletdinov, "Averaging problem in general relativity, macroscopic gravity and using Einstein's equations in cosmology," *Bull.Astron.Soc.India* **25** (1997) 401–416, arXiv:gr-qc/9703016 [gr-qc].

[79] A. Coley, N. Pelavas, and R. Zalaletdinov, "Cosmological solutions in macroscopic gravity," *Phys.Rev.Lett.* **95** (2005) 151102, arXiv:gr-qc/0504115 [gr-qc].

[80] A. Paranjape, "The Averaging Problem in Cosmology," arXiv:0906.3165 [astro-ph.CO].

[81] T. Buchert, N. Obadia, and X. Roy, "Effective Inhomogeneous Cosmologies and Emerging Scalar Fields," arXiv:1012.3083 [gr-qc].

[82] M. Gasperini, G. Marozzi, and G. Veneziano, "Gauge invariant averages for the cosmological backreaction," *JCAP* **0903** (2009) 011, arXiv:0901.1303 [gr-qc].

[83] M. Gasperini, G. Marozzi, and G. Veneziano, "A Covariant and gauge invariant formulation of the cosmological 'backreaction'," *JCAP* **1002** (2010) 009, arXiv:0912.3244 [gr-qc].

[84] N. Li, T. Buchert, A. Hosoya, M. Morita, and D. J. Schwarz, "Relative information entropy and Weyl curvature of the inhomogeneous Universe," *Phys.Rev.* **D86** (2012) 083539, arXiv:1208.3376 [gr-qc].

[85] F. Finelli, G. Marozzi, G. Vacca, and G. Venturi, "Backreaction during inflation: A Physical gauge invariant formulation," *Phys. Rev. Lett.* **106** (2011) 121304, arXiv:1101.1051 [gr-qc].

[86] G. Marozzi, "The cosmological backreaction: gauge (in)dependence, observers and scalars," *JCAP* **1101** (2011) 012, arXiv:1011.4921 [gr-qc].

[87] C. Clarkson and R. Maartens, "Inhomogeneity and the foundations of concordance cosmology," *Class. Quant. Grav.* **27** (2010) 124008, arXiv:1005.2165 [astro-ph.CO].

[88] P. Schneider, J. Ehlers, and E. Falco, *Gravitational Lenses*. Astronomy and Astrophysics Library. Springer, 1999. http://books.google.fr/books?id=sPAIgy9QGBsC.

[89] J. Kristian and R. K. Sachs, "Observations in Cosmology," *Astrophys. J.* **143** (Feb., 1966) 379.

[90] R. A. Vanderveld, E. E. Flanagan, and I. Wasserman, "Systematic corrections to the measured cosmological constant as a result of local inhomogeneity," *Phys. Rev.* **D76** (2007) 083504, arXiv:0706.1931 [astro-ph].

[91] R. A. Sussman, "Back-reaction and effective acceleration in generic LTB dust models," *Class. Quant. Grav.* **28** (2011) 235002, arXiv:1102.2663 [gr-qc].

[92] L. Cosmai, G. Fanizza, M. Gasperini, and L. Tedesco, "Discriminating different models of luminosity-redshift distribution," *Class. Quant. Grav.* **30** (2013) 095011, arXiv:1303.5484 [gr-qc].

[93] G. Lemaître, "The expanding universe," *Gen. Rel. Grav.* **29** (1997) 641–680.

[94] R. C. Tolman, "Effect of imhomogeneity on cosmological models," *Proc. Nat. Acad. Sci.* **20** (1934) 169–176.

[95] H. Bondi, "Spherically symmetrical models in general relativity," *Mon. Not. Roy. Astron. Soc.* **107** (1947) 410–425.

[96] A. Sandage, "The Change of Redshift and Apparent Luminosity of Galaxies due to the Deceleration of Selected Expanding Universes.," *APJ* **136** (Sept., 1962) 319.

[97] A. Loeb, "Direct Measurement of Cosmological Parameters from the Cosmic Deceleration of Extragalactic Objects," *Astrophys. J.* **499** (1998) L111–L114, arXiv:astro-ph/9802122 [astro-ph].

[98] C. Quercellini, L. Amendola, A. Balbi, P. Cabella, and M. Quartin, "Real-time Cosmology," *Phys. Rept.* **521** (2012) 95–134, arXiv:1011.2646 [astro-ph.CO].

[99] J.-P. Uzan, C. Clarkson, and G. F. Ellis, "Time drift of cosmological redshifts as a test of the Copernican principle," *Phys. Rev. Lett.* **100** (2008) 191303, arXiv:0801.0068 [astro-ph].

[100] L. Pasquini, S. Cristiani, H. Dekker, M. Haehnelt, P. Molaro, F. Pepe, G. Avila, B. Delabre, S. D'Odorico, J. Liske, P. Shaver, P. Bonifacio, S. Borgani, V. D'Odorico, E. Vanzella, F. Bouchy, M. Dessauges-Lavadsky, C. Lovis, M. Mayor, D. Queloz, S. Udry, M. Murphy, M. Viel, A. Grazian, S. Levshakov, L. Moscardini, T. Wiklind, and S. Zucker, "CODEX: Measuring the Expansion of the Universe (and beyond)," *The Messenger* **122** (Dec., 2005) 10–14.

[101] E. Bertschinger, "Cosmological dynamics," *NASA STI/Recon Technical Report N* **96** (Jan., 1995) 22249, arXiv:astro-ph/9503125.

[102] L. Bombelli, W. E. Couch, and R. J. Torrence, "Perfect fluid perturbations of cosmological spacetimes in Stewart's variables," *Classical and Quantum Gravity* **11** (Jan., 1994) 139–155.

[103] S. Matarrese, S. Mollerach, and M. Bruni, "Second order perturbations of the Einstein-de Sitter universe," *Phys. Rev.* **D58** (1998) 043504, arXiv:astro-ph/9707278 [astro-ph].

[104] N. Bartolo, S. Matarrese, and A. Riotto, "The full second-order radiation transfer function for large-scale cmb anisotropies," *JCAP* **0605** (2006) 010, arXiv:astro-ph/0512481 [astro-ph].

[105] E. Di Dio and R. Durrer, "Vector and Tensor Contributions to the Luminosity Distance," *Phys. Rev.* **D86** (2012) 023510, arXiv:1205.3366 [astro-ph.CO].

[106] S. Dodelson, E. W. Kolb, S. Matarrese, A. Riotto, and P. Zhang, "Second order geodesic corrections to cosmic shear," *Phys. Rev.* **D72** (2005) 103004, arXiv:astro-ph/0503160 [astro-ph].

[107] I. Ben-Dayan, M. Gasperini, G. Marozzi, F. Nugier, and G. Veneziano, "Backreaction on the luminosity-redshift relation from gauge invariant light-cone averaging," *JCAP* **1204** (2012) 036, arXiv:1202.1247 [astro-ph.CO].

[108] R. Durrer, *The Cosmic Microwave Background*. Cambridge University Press, 2008. http://books.google.fr/books?id=WZkN1QDOD1sC.

[109] **WMAP Collaboration** Collaboration, E. Komatsu *et al.*, "Seven-Year Wilkinson Microwave Anisotropy Probe (WMAP) Observations: Cosmological Interpretation," *Astrophys. J. Suppl.* **192** (2011) 18, arXiv:1001.4538 [astro-ph.CO].

[110] N. Li and D. J. Schwarz, "Scale dependence of cosmological backreaction," *Phys. Rev.* **D78** (2008) 083531, arXiv:0710.5073 [astro-ph].

[111] C. Clarkson, K. Ananda, and J. Larena, "The influence of structure formation on the cosmic expansion," *Phys. Rev.* **D80** (2009) 083525, arXiv:0907.3377 [astro-ph.CO].

[112] A. Wiegand and D. J. Schwarz, "Inhomogeneity-induced variance of cosmological parameters," arXiv:1109.4142 [astro-ph.CO].

[113] G. Marozzi and J.-P. Uzan, "Late time anisotropy as an imprint of cosmological backreaction," *Phys. Rev.* **D86** (2012) 063528, arXiv:1206.4887 [astro-ph.CO].

[114] D. J. Eisenstein, "An Analytic expression for the growth function in a flat universe with a cosmological constant," *Astrophys. J.* (1997) , arXiv:astro-ph/9709054 [astro-ph].

[115] G. Marozzi and G. P. Vacca, "Isotropic Observers and the Inflationary Backreaction Problem," *Class. Quant. Grav.* **29** (2012) 115007, arXiv:1108.1363 [gr-qc].

[116] R. E. Smith, R. K. Sheth, and R. Scoccimarro, "An analytic model for the bispectrum of galaxies in redshift space," *Phys. Rev.* **D78** (2008) 023523, arXiv:0712.0017 [astro-ph].

[117] A. Lewis, A. Challinor, and A. Lasenby, "Efficient computation of CMB anisotropies in closed FRW models," *Astrophys. J.* **538** (2000) 473–476, arXiv:astro-ph/9911177 [astro-ph].

[118] M. March, R. Trotta, P. Berkes, G. Starkman, and P. Vaudrevange, "Improved constraints on cosmological parameters from SNIa data," *Mon. Not. Roy. Astron. Soc.* **418** (2011) 2308–2329, arXiv:1102.3237 [astro-ph.CO].

[119] R. G. Vishwakarma and J. V. Narlikar, "A Critique of Supernova Data Analysis in Cosmology," *Res. Astron. Astrophys.* **10** (2010) 1195–1198, arXiv:1010.5272 [physics.gen-ph].

[120] **Supernova Cosmology Project** Collaboration, M. Kowalski *et al.*, "Improved Cosmological Constraints from New, Old and Combined Supernova Datasets," *Astrophys. J.* **686** (2008) 749–778, arXiv:0804.4142 [astro-ph].

[121] D. E. Holz and E. V. Linder, "Safety in numbers: Gravitational lensing degradation of the luminosity distance-redshift relation," *Astrophys. J.* **631** (2005) 678–688, arXiv:astro-ph/0412173 [astro-ph].

[122] L. L. Williams and J. Song, "Weak lensing of the high redshift SNIa sample," *Mon. Not. Roy. Astron. Soc.* **351** (2004) 1387, arXiv:astro-ph/0403680 [astro-ph].

[123] B. Menard and N. Dalal, "Revisiting the magnification of Type Ia supernovae with SDSS," *Mon. Not. Roy. Astron. Soc.* **358** (2005) 101–104, arXiv:astro-ph/0407023 [astro-ph].

[124] N. Karpenka, M. March, F. Feroz, and M. Hobson, "Bayesian constraints on dark matter halo properties using gravitationally-lensed supernovae," arXiv:1207.3708 [astro-ph.CO].

[125] V. Marra, M. Quartin, and L. Amendola, "Accurate Weak Lensing of Standard Candles, Part 1: Flexible Cosmological Fits," arXiv:1304.7689 [astro-ph.CO].

[126] M. Quartin, V. Marra, and L. Amendola, "Accurate Weak Lensing of Standard Candles, Part 2: Measuring sigma8 with Supernovae," arXiv:1307.1155 [astro-ph.CO].

[127] L. Hui and P. B. Greene, "Correlated Fluctuations in Luminosity Distance and the (Surprising) Importance of Peculiar Motion in Supernova Surveys," *Phys. Rev.* **D73** (2006) 123526, arXiv:astro-ph/0512159 [astro-ph].

[128] P. Fleury, H. Dupuy, and J.-P. Uzan, "Can all cosmological observations be accurately interpreted with a unique geometry?," arXiv:1304.7791 [astro-ph.CO].

[129] P. Fleury, H. Dupuy, and J.-P. Uzan, "Interpretation of the Hubble diagram in a nonhomogeneous universe," *Physical Review D 87,* **123526** (2013) , arXiv:1302.5308 [astro-ph.CO].

[130] V. Marra, L. Amendola, I. Sawicki, and W. Valkenburg, "Cosmic variance and the measurement of the local Hubble parameter," *Phys. Rev. Lett. 110,* **241305** (2013) , arXiv:1303.3121 [astro-ph.CO].

[131] G. Fanizza, M. Gasperini, G. Marozzi, and G. Veneziano, "An exact Jacobi map in the geodesic light-cone gauge," arXiv:1308.4935 [astro-ph.CO].

[132] C. Knobel, "An introduction into the theory of cosmological structure formation," arXiv:1208.5931 [astro-ph.CO].

[133] J. Lesgourgues, "Inflationary cosmology." Personal web page, March, 2006. http://lesgourg.web.cern.ch/lesgourg/Inflation_EPFL.pdf. EPFL.

[134] S. M. Carroll, W. H. Press, and E. L. Turner, "The Cosmological constant," *Ann. Rev. Astron. Astrophys.* **30** (1992) 499–542.

[135] K. A. Malik and D. Wands, "Cosmological perturbations," *Phys. Rept.* **475** (2009) 1–51, arXiv:0809.4944 [astro-ph].

[136] V. F. Mukhanov, H. A. Feldman, and R. H. Brandenberger, "Theory of cosmological perturbations," *Phys. Rep.* **215** (June, 1992) 203–333.

[137] J. M. Bardeen, "Gauge-invariant cosmological perturbations," *PRD* **22** (Oct., 1980) 1882–1905.

[138] O. Lahav, P. B. Lilje, J. R. Primack, and M. J. Rees, "Dynamical effects of the cosmological constant," *Mon. Not. Roy. Astron. Soc.* **251** (1991) 128–136.

[139] R. G. Vishwakarma, "A curious explanation of some cosmological phenomena," *Phys. Scripta* **05** (2013) 055901, arXiv:1306.1809 [astro-ph.CO].

[140] M. Gasperini, G. Marozzi, F. Nugier, and G. Veneziano, "Light-cone averaging in cosmology: Formalism and applications," *JCAP* **1107** (2011) 008, arXiv:1104.1167 [astro-ph.CO].

[141] I. Ben-Dayan, M. Gasperini, G. Marozzi, F. Nugier, and G. Veneziano, "Do stochastic inhomogeneities affect dark-energy precision measurements?," *Phys. Rev. Lett.* **110** (2013) 021301, arXiv:1207.1286 [astro-ph.CO].

[142] I. Ben-Dayan, G. Marozzi, F. Nugier, and G. Veneziano, "The second-order luminosity-redshift relation in a generic inhomogeneous cosmology," *JCAP* **1211** (2012) 045, arXiv:1209.4326 [astro-ph.CO].

[143] I. Ben-Dayan, M. Gasperini, G. Marozzi, F. Nugier, and G. Veneziano, "Average and dispersion of the luminosity-redshift relation in the concordance model," *JCAP* **1306** (2013) 002, arXiv:1302.0740 [astro-ph.CO].

Glossary

A

absolute magnitude . 11
adiabatic modes . 130
ADM Arnowitt-Deser-Misner. 33, 53, 121
ADM energy density . 34, 123
ADM formula . 122
ADM pressure . 34, 123
angular distance . 12, 48, 49
apparent magnitude . 10
averaging problem . 19, 25

B

backreaction . 75
backreaction parameter . 27
backreaction problem . 19
BAO Baryonic Acoustic Oscillations. 13, 106
Bardeen potentials . 137
bias . 15
Born approximation . 67

C

Chandrasekhar mass . 8
Christoffel symbols . 5
CMB Cosmic Microwave Background. 13, 126
coincidence problem . 4
color parameter . 10
commutation rule . 27, 33, 39
Copernican principle . 4
cosmological constant problem . 7
cosmological principle . 4
curvature of the spectral index . 109, 148

D

DE dark energy. 4
deceleration parameter . 11
decoupling . 126, 130
density variance . 17, 109, 146
distance modulus . 11, 153
DM dark matter. 3
dofs degrees of freedom. 133, 138
Doppler effect . 65, 70, 79, 84, 96

E

e-fold number . 127
effective shape parameter . 106, 145
effective spectral index . 109, 148
Einstein equations . 19, 124, 132
Einstein tensor . 6
ensemble-average conditions . 74
entropy mode . 129
EoM equation of motion. 127
equation of state . 7, 128
Etherington law . 12
expansion scalar . 26, 33, 124
expansion tensor . 26, 124
extrinsic curvature . 26, 28, 122

F

fitting problem . 19
flatness problem . 126
FLRW Friedmann-Lemaître-Robertson-Walker. 5, 41, 45, 132
Frame dragging . 70

G

gauge freedom . 132
gauge invariance . 30
Gauss-Codazzi equations . 123
Gauss-Weingarten equation . 122
GCT General Coordinate Transformation. 30
geodesic light-cone . 45
growth factor . 90
GT Gauge Transformation. 30

H

HaloFit model . 108
Hamiltonian constraint . 27, 125
horizon problem . 126
Hubble diagram . 13
Hubble horizon . 126

I

IBR induced backreaction. 76, 87
inflationary spectrum . 17
inflaton . 127
integrability condition . 28
ISW integrated Sachs-Wolfe effect. 65, 66, 70, 84

J

Jeans length . 130
Jeans mass . 130

K

Kullback-Leibler entropy . 30

L

lapse function . 53, 121
large scale structure . 3, 126
lens-lens coupling . 67
lensing . 70, 79, 96, 108, 112
lensing dispersion . 113
Lie derivative . 135
light curve . 8
linear growth function . 131
LTB Lemaître-Tolman-Bondi. 51, 58
luminosity distance . 48, 67, 87, 111
luminosity flux . 10, 83

M

Meszaros effect . 131
Milne . 97, 108, 153
morphon . 29

N

N-body simulations . 17, 28
NG Newtonian gauge. 60, 71
non-linearity scale . 109

O

observational coordinates . 43
one-halo term . 147

P

peculiar velocity . 65, 107, 113
Perturbed trajectories . 70
PG Poisson gauge. 59
Poisson equation . 16

R

Raychaudhuri's equation . 26, 27, 125
RD redshift drift. 57
Ricci tensor . 6
Riemann tensor . 6
RP redshift perturbations. 65, 66, 70
RSD redshift space distortions. 66, 70

S

scalar shear potential . 138
shear tensor . 26, 28, 41, 124
shift vector . 53, 121
Silk damping . 105, 144
slow-roll parameters . 17, 128
SMC standard model of cosmology. 3
sound horizon . 106
spectral coefficients . 78
speed of sound . 129, 130
standard candels . 8
statistical homogeneity condition . 74
stress energy tensor . 6
stretch factor . 10
strong energy condition . 128
SW Sachs-Wolfe effect. 65, 66, 70, 84

T

transfer function . 74, 95, 106, 131, 144
two-halo term . 147

V

virial equilibrium . 29
vortical modes . 130
vorticity tensor . 26, 28, 41, 124

W

window function . 31

Fabien Nugier

Moyennes sur le Cône de Lumière et Cosmologie de Précision

Lightcone Averaging and Precision Cosmology

Résumé :

Le premier objectif de cette thèse est de répondre au manque en cosmologie de description sur le cône de lumière passé : hypersurface nulle où se propagent tous les signaux observés. Son deuxième est d'évaluer l'importance des inhomogénéités dans la détermination des paramètres de l'énergie sombre, de nature encore inconnue et pour laquelle l'influence des structures de matière a été proposée comme une alternative cosmologique. Nous définissons une jauge «géodésique sur le cône de lumière » qui simplifie grandement l'étude de la propagation lumineuse dans l'Univers. Nous établissons ensuite une moyenne, invariante de jauge, pour les quantités scalaires sur le cône et calculons l'effet des inhomogénéités sur le flux lumineux en considérant leur spectre de puissance jusque son régime non-linéaire. Leur effet sur le flux est négligeable tandis que des observables comme la distance de luminosité, évaluée jusqu'au second ordre en perturbations, sont bien plus affectées. Nous étudions aussi le module de distance à la base de la découverte de l'énergie sombre par les supernovæ (SNe) Ia. La moyenne de ce module est peu affectée par les inhomogénéités mais sa variance l'est sensiblement. Ces résultats montrent, dans leur cadre, qu'une alternative à l'énergie sombre par un effet des structures est impossible mais, en même temps, soulignent leur importance sur la dispersion des données du diagramme de Hubble. Les effets physiques dominants sont la vitesse des SNe et l'effet de lentille faible. Nos prédictions sur la dispersion se révèlent en très bon accord avec les premières analyses de SNe visant à détecter un signal de lentilles et seront vérifiables dans les années futures.

Mots-Clés : Cosmologie, Relativité Générale, Energie Sombre, Univers Inhomogènes, Supernovæ, Lentilles Gravitationnelles.

Summary :

The first objective of this thesis is to fill the lack in cosmology of a description on the past light cone : the null hypersurface on which observed signals propagate. Its second goal is to evaluate the importance of inhomogeneities in the determination of dark energy parameters, whose real nature is still unknown and for which the influence of matter structures has been proposed as a cosmological alternative. We start with the definition of a "geodesic lightcone" gauge simplifying greatly the study of light propagation in the Universe. We then define a gauge invariant average of scalars on the past light cone and compute the effect of inhomogeneities on the luminosity flux by considering their power spectrum up to its non-linear regime. The effect on the flux is negligible whereas observables like the luminosity distance, computed at second order in perturbations, are much more affected. We also study the distance modulus at the basis of the discovery of dark energy from type Ia supernovæ (SNe). The average of this modulus is only slightly affected by inhomogeneities but its variance sensitively depends on them. These results show, within their hypotheses, that an alternative to dark energy by an effect of structures is impossible but, at the same time, emphasize their importance on the dispersion of data in the Hubble diagram. The dominating physical effects turn out to be peculiar velocity of SNe and weak lensing. Our predictions on the dispersion are in very good agreement with first analyses carried out so far to detect a signal of lensing among SNe Ia data and will be testable in the near future.

Keywords : Cosmology, General Relativity, Dark Energy, Inhomogeneous Universes, Supernovæ, Gravitational Lensing.